

The Development of Activated Carbon from Biomass Precursors

A thesis submitted to the University of Nottingham in the degree of Doctor of Engineering

Andrew Gill

Supervisors: Prof. Colin Snape, Prof. John Patrick

30/09/16

Abstract

The focus of this paper is to investigate the production of activated carbon from biomass on laboratory (lab) and pilot scales. Different biomass sources (> 30) were pyrolysed and steam activated on a lab scale to assess final quality. These were reduced to six based on potential, which were then activated under different temperatures and residence times to develop an analysis matrix. From this and other set criteria, olive stone and pine wood - a granular and powder carbon respectively - were chosen. The biomass chars were tested and compared under many production variables in lab and pilot scale production.

Further novel findings: Linear burn off rates were seen by increasing activation temperature residence time, and an exponential burn off by increasing water flow. In both lab and pilot scale there was direct linear correlation between burn off percentage and CTC (carbon tetrachloride activity) values for both biomasses proving scalability, this was maintained as porosity changed with increasing burn off. The maximum CTC value for olive stone was found to be 84.5 at 74% burn off using activation conditions of 775 ^{o}C, 120 minutes and 1.125 ml/min water flow rate. Pine wood produced a peak CTC value of 120 at 80% to 82% burn off using activations conditions of 800 ^{o}C, 90 minutes and 1.5 ml/min water flow rate. Both carbons produced a higher CTC than a tested commercial carbon (60). The CTC values curtailed after > 80% and > 85% burn off for olive stone and pine wood respectively due to destruction and high ash to carbon ratios. Methylene blue numbers were seen up to 22 (330 mg/g) and 25 (375 mg/g) for olive stone and pine wood respectively. Olive stone produced surface areas up to (1157 m^2/g) micropore volumes (0.458 cm^3/g), mesopore volumes (0.317 cm^3/g) and total pore volumes up to (0.753 cm^3/g) with this surface area, mesopore volume and total pore volumes were the highest found in literature for steam activation. Pine wood produced surface areas up to (1190 m^2/g), micropore volumes (0.472 cm^3/g), mesopore volumes (0.589 cm^3/g) and total pore volume to (1.061 cm^3/g), all higher than any current reported values using steam activation. Production variable limits prior to excessive burn off were found for both biomasses: Activation temperatures over 850 ^{o}C and 825 ^{o}C for olive stone and pine wood respectively, olive stone with a residence time of > 6 hours and steam flow rate of > 1.875 ml/min whereas there proved to be no adverse effects to long residence times and high steam flow rates with pine wood. This was deduced to be due to a higher mass transfer limitation seen with the higher density olive stone resulting in external particle ablation. Single step production was carried out on lab and pilot scale with no negative effects seen to adsorption properties and pore structures. The produced carbons was comparable to the products produced by the usual two-step process. Calcium oxide ash component in pine wood is lost during production proved by ion chromatography analysis. Hot water washing biomass had no effect on the burn off percentage, CTC correlation only on the individual burn off percentage and total yields of the carbons. An OPEX/CAPEX cost analysis was completed and showed that both carbons are potentially profitable products.

Acknowledgements

Gratitude goes to my full supervision team who have been involved with and aided the research: Prof. Colin Snape who has been the main supervisor throughout the project and provided guidance and broad knowledge around the research project. Prof. John Patrick who has been the secondary supervisor and offered guidance and advice over the last 4 years. Paul Rodgers who was the industrial supervisor for the 1st year followed by Juan Turrion-Gomez who took over where Paul left off and offered guidance and support for the three remaining years spent at CPL industries.

Appreciation also goes to the lab staff at CPL industries Melvyn Duckmanton, Dave Elliot, Dave Lowther, Ron Dean, Steve Martin, Darren Burrows and Liz Balch who have always been available to help sort out and fix equipment. Great thanks goes towards Carl Wood who was the lead technician under Juan Turrion-Gomez who provided assistance on pilot scale by sorting out the biomass and being there for support if anything went wrong. Additionally, other technicians at CPL industries and Adrian Quinn, Dr. Hui Deng, Dr. Lee Stevens and Dr. Emily Smith at the University of Nottingham who went out of their way to help me during the last 4 years. I would also like to thank Tim Minett and Andy Bishop for making the project a possibility and for their interest throughout.

Also, away from work, a big thank you goes to my parents and friends (both inside and outside the EFET centre) who have always been supportive through the ups and downs. I would also like to thank the centre management, Anup Patel and Diane Vincent who have helped the centre to run smoothly and be a success.

Finally, I would like to thank the Research Councils UK (RCUK) and CPL Industries for the financial support that made this research project a possibility.

Potential Publications and Conference Presentations

"**Butane Adsorption and Burn Off Correlations for Biomass Derived Activated Carbons**"

- Burn off and yield /CTC correlation across six biomasses
- High: Surface areas, micropore volumes, mesopore volumes and mesopore % (lab scale)
- CTC correlations to pore analysis and methylene blue numbers
- The benefits of a CTC test compared to other analysis techniques

"**Physical Activation Production Variables and Production Limits Impacts on Porosity for Olive Stone and Pine Wood Derived Activated Carbons**"

- Pore analysis of production variables
- Production limits
- Difference between pine wood and olive stone (porosity, adsorption, physical characteristics, mass transfer limitations, etc)
- Ash analysis
- Burn off rates with by changing variables

"**Single Step Carbon Production with Washed and Unwashed Olive Stone and Pine Wood Biomass**"

- Pore analysis two-step vs single step
- CTC analysis
- Pyrolysis and activation yields
- Fast and slow heating rates

"**Pilot Scale Two-Step and Single Step Production and Analysis of Olive Stone Derived Activated Carbons**"

- Pore analysis
- CTC analysis
- Changes in production
- Optimum kiln operating conditions
- Single step vs two-step differences
- High CTC, surface area values

Presentation at PACS 33rd Activated Carbon Conference Florida February 2014 – Activated Carbon from Biomass Precursors

Contents

1 Chapter 1 Background 1

1.1 The Move Away From Fossil Fuels 1

1.2 Activated Carbon 2

1.2.1 Brief History of Activated Carbon 3

1.3 Activated Carbon Characteristics 4

1.3.1 Activated Carbon Production 4

1.3.2 Activated Carbon Supply and Demand 5

1.3.3 Project Novelty 6

1.4 Introduction to Chapters 6

1.4.1 Chapter 2 - Literature Review 6

1.4.2 Chapter 3 – Methods 7

1.4.3 Chapter 4 – Preliminary Tests 7

1.4.4 Chapter 5 - Lab Scale Activation 7

1.4.5 Chapter 6 – Pilot Scale Activation 8

1.4.6 Chapter 7 – Financial and Process Cost Model 8

1.4.7 Chapter 8 – Conclusions and Future Work 8

1.5 References 9

2 Chapter 2 Literature Review 10

2.1 Background- The Move Away from Fossil Fuels 10

2.2 Precursors 11

2.3 Activated Carbon Structure 13

2.4 Activated Carbon Production 14

2.5 Pyrolysis 15

2.6 Activation of Char 17

2.7 Steam Activation 17

2.8 Activation Using Both Steam and Carbon Dioxide 18

2.8.1 Comparison of Carbon Dioxide and Steam Activation 21

2.8.2 Single and Two-Step Production of Activated Carbon 23

2.8.3 Chemical versus Physical Activation 24

2.9 The Use of Activated Carbon in Liquid and Gas Phase Applications 25

2.9.1 Gas Adsorption 25

2.9.2 Liquid Adsorption 26

2.10 Adsorption Mechanism- London Dispersion Forces 28

2.11 Analytical Techniques Used in Activated Carbon Production 28
2.11.1 CTC Analysis 28
2.11.2 Methylene Blue Analysis 29
2.11.3 BET Surface Area and Pore Analysis 29
2.11.4 Iodine Number 31
2.11.5 Transitional Electron Microscopy and Scanning Electron Microscopy (TEM/SEM) 31
2.11.6 TGA 32
2.11.7 Proximate and Ultimate Analysis 32
2.12 Pore Structure 32
2.13 Surface Groups 33
2.14 BET Surface Area, Burn Off and Yield 34
2.15 Precursors Used for Activated Carbon Production with Optimal Activation Conditions 37
2.15.1 Olive Stones and Walnut Shell 38
2.15.2 Chicken Waste 39
2.15.3 Date Stones 40
2.15.4 Almond Shell 41
2.15.5 Eucalyptus 41
2.15.6 Algarroba Wood 42
2.15.7 Apricot Stones 42
2.15.8 Coconut Shell 42
2.15.9 Palm Kernel Shell 43
2.15.10 Pistachio Nut Shells 44
2.15.11 Acorn Shell 45
2.15.12 Polyethyleneterephthalate (PET) wastes 45
2.15.13 Olive bagasse 46
2.15.14 Soybean Oil Cake 46
2.15.15 Sewage Sludge 46
2.15.16 Waste Newspaper 46
2.15.17 Agricultural Waste: 47
2.15.18 Rubber Seed Shell 48
2.15.19 Waste Tyres 49
2.15.20 Peach Stone 49

2.16 Regeneration of Activated Carbon 50
2.17 How to Minimise the Cost of Production of Activated Carbon 52
2.18 Problems Using Biomass for Activated Carbon Production 53
2.19 Recent Olive Stone and Pine Wood Carbon Literature 54
2.20 Aim, Objectives and Initial Plan 55
2.21 Conclusion and Literature Gaps 56
2.22 References 57
3 Chapter 3 - Methods 63
3.1 Raw Materials 63
3.2 Lab Scale Trials 63
3.3 Pyrolysis Step 65
3.4 Activation Step 66
3.5 Peristaltic Water Pumps 69
3.6 Single Step Lab Scale 71
3.7 Analysis Techniques 72
3.7.1 Proximate/Ultimate Analysis 72
3.7.2 Carbon tetrachloride (CTC) Activity 73
3.7.3 Methylene Blue Number 74
3.7.4 Iodine Number 74
3.7.5 Hardness Test 75
3.7.6 Bulk Density 76
3.7.7 BET Surface Area and Pore Analysis 76
3.7.8 Non Local Density Function Theory 79
3.7.9 pH Tests 79
3.7.10 Hot Water Washing 79
3.7.11 Ion Chromatography 80
3.7.12 XPS Analysis 80
3.7.13 Acid Washing –Fe Analysis 80
3.7.14 SEM/TEM Imaging 80
3.8 Pilot Scale 81
3.9 Main Analysis Repeats and Errors 83
3.9.1 CTC Error 83
3.9.2 Pore Analysis Error 85
3.9.3 Methylene Blue Error 88

3.10 References 89
4 Chapter 4 Preliminary Tests. 90
4.1 Introduction- Preliminary Trials 90
4.2 Pyrolysis 90
4.3 Steam Activation 91
4.4 TEM Images 94
4.5 Biomass Database (Appendix Table A-1) 94
4.6 Selected Biomass Analysis 95
4.6.1 Pyrolysis of the Six Biomasses 96
4.6.2 Activation of Chosen Biomass 97
4.6.3 Pore Analysis 101
4.7 Carbon Dioxide Activation - Olive Stone 104
4.8 Carbon Dioxide and Steam Combination 108
4.9 Pore Analysis of CO_2 Activation Trials 110
4.10 Changing the Nitrogen Flow 111
4.11 Conclusion 113
4.12 References 114
5 Chapter 5 Lab Scale Olive Stone and Pine Wood Analysis 116
5.1 CTC, Burn Off Percentage Correlations 117
5.1.1 Olive Stone 118
5.1.2 Pine Wood 120
5.2 Overall Pore Analysis 122
5.2.1 Olive Stone 122
5.2.2 Pine Wood 123
5.3 Overall Methylene Blue Results 125
5.3.1 Olive Stone 125
5.3.2 Pine Wood 125
5.4 SEM Images 126
5.4.1 Olive Stone Char 126
5.4.2 Olive Stone Activated Carbon 126
5.4.3 Pine Wood Char 127
5.4.4 Pine Wood Activated Carbon 127
5.5 Primary Production Variables – Activation Temperature 128
5.5.1 Temperature - Olive Stone 128

5.5.2 Temperature – Pine Wood 133
5.5.3 Comparison of Olive Stone and Pine Wood 135
5.5.4 Methylene Blue Adsorption 139
5.5.5 High Temperature Trials 141
5.6 The Effect of Residence Time on Olive Stone Activated Carbons 146
5.6.1 Change in Activation Residence Time with Constant Water Flow 146
5.6.2 Pore Analysis of Residence Time Trials 148
5.6.3 Residence Time Pine Wood 150
5.6.4 Comparison of Olive Stone and Pine Wood Derived Carbons 151
5.6.5 Change in Residence Time with Altered Water Flow to Allow Same Total Water Volume Flow into the System 152
5.6.6 Long Residence Time Trials 155
5.6.7 Steam Flow 159
5.6.8 Methylene Blue Results 161
5.6.9 Pore Analysis of Two Hour Residence Time Trials. 161
5.6.10 Methylene Blue and Pore Analysis 165
5.6.11 Two Hour Residence Time Trials Conclusion 169
5.7 Steam Percentage Reacting During Activation 169
5.7.1 Olive Stone Trials 169
5.7.2 High Water flow Rate Trials 173
5.8 Secondary Production Variables 178
5.8.1 Steam Carbon Contact 178
5.8.2 Reaction Rates- Changing Char Mass 179
5.8.3 Burn Off Rates 184
5.8.4 Single Step Lab Trials 186
5.8.5 Fast Pyrolysis Vs Slow Pyrolysis 189
5.8.6 Impact of Ash with Ion Chromatography Analysis 194
5.8.7 Acid Washing to Reduce Iron Content 199
5.8.8 XPS Analysis 200
5.8.9 Hot Washing Biomass 202
5.8.10 Single Step Process Using Washed Biomass. 209
5.8.11 Pore Analysis of Single Step and Washed Biomass 213
5.8.12 Carbon Dioxide Isotherms 214
5.9 Conclusions 218

5.10 References 220
6 Chapter 6 Pilot Scale Activation 223
6.1 Pilot Scale Kiln Introduction 223
6.2 Lab and Pilot Scale Differences. 223
6.2.1 Reynolds Number 223
6.3 Reference Trial with Coconut Shell 226
6.4 Olive Stone Pilot Scale Activation 226
6.5 Pilot Scale Activation of Pine Wood Char 228
6.6 Single Step Pilot Scale 230
6.6.1 Olive Stone Single Step Activation 230
6.6.2 Pine Wood Single Step Activation 231
6.7 Additional Analysis 232
6.8 The Importance of Steam Carbon Contact 232
6.8.1 A Single Step Process Kiln Concept. 234
6.9 Pore Analysis on Pilot Scale Material 235
6.10 Conclusions 236
6.11 References 237
7 Chapter 7 Cost Analysis Model 238
7.1 Process Overview 238
7.2 Introduction 239
7.3 Application Examples 239
7.4 Option 1 Drying and Pyrolysis 239
7.5 Option 2 Pyrolysis 245
7.6 Activation Stage 248
7.6.1 Energy Balance for Activation 252
7.7 Pore and Methylene Blue number Estimates 254
7.8 Energy Recovery 255
7.8.1 Boiler Potential 255
7.8.2 Heat Exchanger and De-Superheater 261
7.9 Part 4 Raw Material Costs 265
7.10 Part 5 Additional OPEX Costs and Selling Price 267
7.11 Selling Price 268
7.12 Summary of OPEX and Profitability 269
7.13 Capital Costs 273

7.14 Sensitivities 275
7.15 Break Even Analysis 280
7.16 Conclusions 282
7.17 References 283
8 Chapter 8 Key Conclusions and Future Work 285
8.1 Key Conclusions 285
8.2 Future Work 287
A. Appendix 288
A.1 Gibbs Free Energy Analysis of Reaction 1 and Reaction 2 288
Reaction 1 288
Reaction 2 289
A.2 Equilibrium Rate constant 290
A.3 Tables and Figures 290

Chapter 1 Background

The project was completed in collaboration between the University of Nottingham and CPL Industries. CPL Industries is a company that mainly develops coal based fuels for domestic heating. The project entails investigating the production of activated carbon from biomass, with the aim of producing a commercially viable carbon whilst also lowering the carbon footprint of CPL Industries. Using an EU sourced biomass as an alternative to coal can reduce the carbon footprint of the process: firstly because it is a renewable material and, secondly, a locally (EU) sourced biomass reduces transportation associated emissions. Currently CPL imports coal from places such as China and Columbia.

1.1 The Move Away From Fossil Fuels

In November 2015 an agreement was put in place at the 2015 United Nations Climate Change Conference held in Paris. The agreement is partly legally binding and partly voluntary. The main agreement was to keep global temperature increase "well below" 2 ^{o}C and to pursue efforts to limit temperature rise to 1.5 ^{o}C [BBC, 2015]. The 1.5 °C goal will require zero emissions sometime between 2030 and 2050, according to some scientists.

Globally there is a consensus that moving away from fossil fuels is one of the main ways to reduce anthropogenic CO_2 and greenhouse gas (GHG) emissions. Biomass is one alternative to fossil fuels that this project focuses on. Biomass can be seen to be carbon neutral (argued in Chapter 2) as, during growth, biomass uses carbon dioxide from the atmosphere via photosynthesis. This means when biomass is used to produce energy, or for other purposes where CO_2 is released, the CO_2 released was present in the atmosphere to begin with, so theoretically there is no net gain in carbon emissions as Figure 1:1 shows. Currently, many activated carbons are formed from brown and anthracitic coals whilst bituminous coals are used less for carbon production due to the melting effect they experience upon heating that can lead to a reduction of internal porosity [Marsh and Reinoso, 2006]. However, coals can be said to be the worst culprit in terms of unwanted emissions as Höök and Tang [2013] state ‘A better handling of coal is crucial, as it accounts for both the largest amounts of remaining fossil fuels as well as the largest CO_2 emissions’. This is where using a renewable source such as biomass can be of advantage. Many biomass precursors for activated carbon production have been and are currently being researched today as a coal alternative. The main biomass used today for producing commercial carbons is coconut shell. Activated carbon derived from coconut shell was used in gas marks as far back as in World War 1 and is highly microporous (proved in this project) which is advantageous in gas purification. However, coconut shell is becoming more expensive and is

starting to be used more in other industries and by developing countries from whence the shells originate. Coconut shell was seen as a waste. However, recently there has been a push to use coconut shells for heating and cooking in developing countries as an article by Kyizom, [2014] explains, in that coconut shell is no longer seen as a waste that used to be littering the streets. Coconut shell has a high relative calorific value, 20.8 MJ/kg [Zafar, 2014] and people across many developing countries are now using this cheap 'fuel' for other purposes. This means that alternate biomass must be found to start replacing coconut shell activated carbon. Further studies have demonstrated the significant potential of other biomasses to be a precursor in activated carbon production.

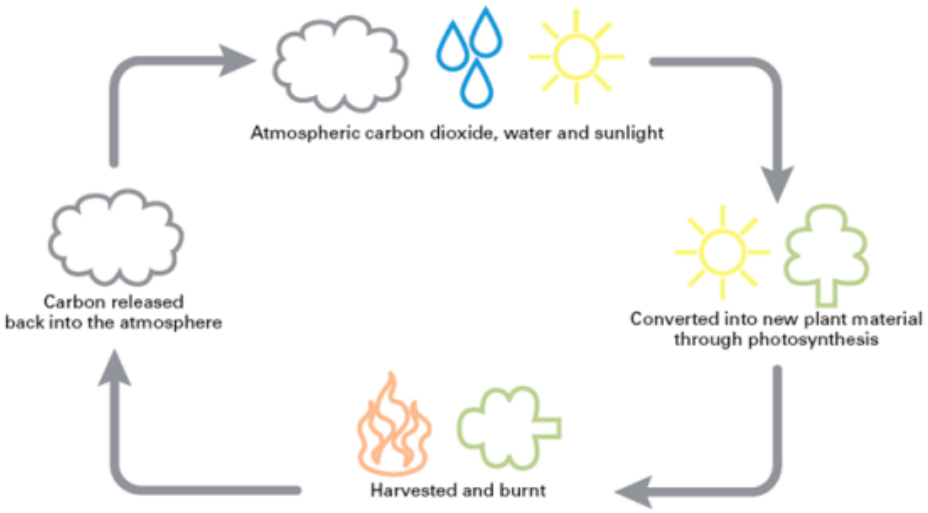


Figure 1:1 Biomass carbon cycle [Carbon Trust, 2009].

1.2 Activated Carbon

Activated carbon is a carbonaceous material that contains porosity (space) that is within and surrounded by carbon atoms - typically an activated carbon has a large surface area approx. 600 m^2/g to 1200 m^2/g and a pore volume between 0.2 cm^3/g and 0.6 cm^3/g [Weber and Vliet, 1980]. Pore volume has been reported to go up to 1 cm^3/g [Bansal, 2005]. This porosity comes in many different shapes and sizes with each pore being slightly different. The pore sizes can be categorised by their diameter: micropores with a pore size diameter smaller than 2 nm, mesopores between 2 nm and 50 nm and macropores which are greater than 50 nm in diameter.

Activated carbons are versatile adsorbents; adsorption occurs mainly through physical adsorption via London dispersion forces (LDF) but can also occur through chemical adsorption depending on the compounds present in the carbon. Bansal [2005] states 'Activated carbons have a large surface area with a high degree of surface reactivity. Activated carbons are used

industrially and domestically to purify, decolourise, deodorise, de-chlorinate, separate, concentrate for recovery and to filter remove, or modify the harmful constituents from gas and liquid phases'. Typical industries where carbons are used are: food, chemical, automobile, petroleum and pharmaceutical,

Activated carbon usually comes in the form of either a powder, granular or pelletised form as shown in Figure 1:2



Figure 1:2 Different physical forms of activated carbon [Desotec, 2015].

Activated carbon produced from biomass attempts to meet two main separate targets:

1. Lowering the producer's and user's carbon footprint by reducing the use of fossil fuel.

2. The carbon product is then used to further reduce harmful substances.

1.2.1 Brief History of Activated Carbon

Activated carbon has been around for many years. It was described as early as 3750 B.C with it being used by the Egyptians and Sumerians [Bansal 2005]. Wood chars were used to reduce zinc, copper and tin ores in bronze production. In 1550 BC there is the first recorded use of charcoal for medicinal purposes. It was used to adsorb odorous vapours from purifying wounds and from within the intestinal tract. In the 18th century carbons were made from blood, wood and animals and were used for the purification of liquids [Charcoal house 2006]. At this point the precursors used produced only powdered activated carbons. The applications used for these carbons were in the form of batch treatment, where a known quantity of carbon was mixed with a certain volume of liquid with a set contact time. The resulting solution was then subject to filtration or sedimentation. In the 19th century the decolourisation using bone char was used in the sugar industry in England. The bone char was a granular carbon that allowed continuous purification through a column. The bone char was made up of mainly calcium phosphate with little carbon and for this reason was only used in the sugar industry. During the 20th century the first carbons

were designed with defined properties for use in industry. However at this point steam and chemical activation could only produce powdered carbons, yet carbons started to appear in every hospital, clinic, research department, poison control centre and many other varied applications across the world. Activated carbon growth continues in many industries with current research being done to increase the use further. Today there is a shift towards granular activated carbon as it can be regenerated and used in a continuous fashion [Chemviron 2015].

1.3 Activated Carbon Characteristics

There is still no 'one' way to currently describe the structure of activated carbons. Marsh and Reinoso, [2006] states numerous times how activated carbons are essentially all assemblies of defective graphene layers and an emphatic 'no' to the assumption they are amorphous materials. However, Bansal, [2005] describes activated carbons by calling them processed amorphous carbon based materials and, whilst not truly amorphous, the material contains microcrystalline structures. What is certain though is that by investigating numerous sources each view point and terminology can be both backed up and dismissed. Further details of this will be discussed in Chapter 2.

Activated carbon consists mainly of carbon to the extent of 85% to 95%. In addition activated carbons contain elements such as hydrogen, nitrogen, sulphur and oxygen. The heteroatoms and quantities present are linked to the raw material used and how the carbon is formed: whether with a physical or chemical activation method. According to Bansal, [2005] a typical carbon is found to contain 88% C, 0.5% H, 0.5% N, 1% S, and 6% to 7% O, the balance being inorganic ash content which contain alkali alkaline metals. The oxygen percentage can vary between 1% and 20% depending on the raw material and activation procedure used.

1.3.1 Activated Carbon Production

The project investigates the differences between the pore sizes listed above that form within the carbon structure, and how pore characteristics are dependent on the both the precursor and production conditions chosen. An important part of the project was to focus on the production of activated carbon. The usual two-step process is shown in Figure 1:3. The project shows how different production variables affect the carbon porosity and thus, in turn, the given quality. These physical activation variables are oxidising agent flow/concentration, activation temperature, residence time and steam carbon contact. Another objective is to produce carbons on pilot scale to meet required specifications for industrial applications. To do this scalability of carbons had to be investigated from lab to pilot scale production.

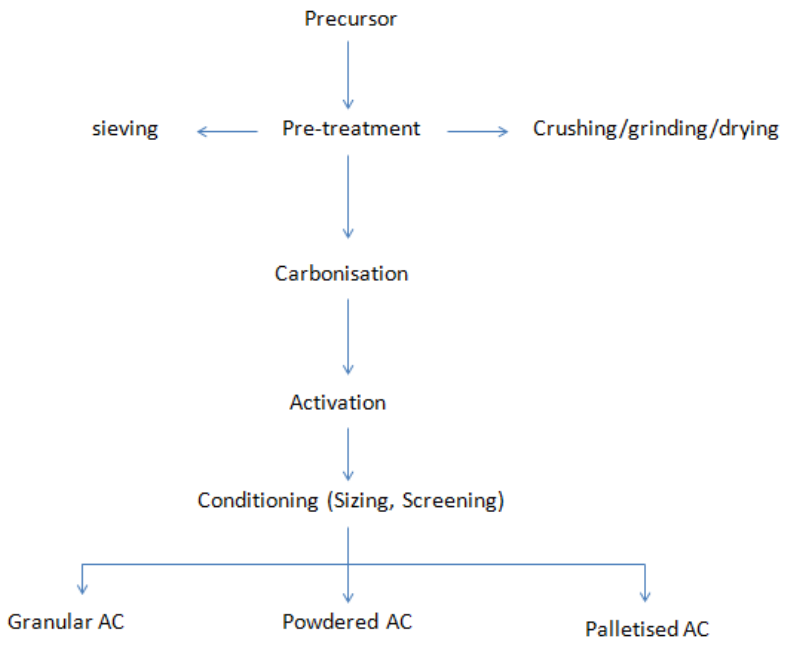


Figure 1:3 Activated carbon production flow diagram [Marsh, 2006].

Pyrolysis usually occurs at temperatures < 800 ^{o}C. During pyrolysis liquid and gaseous volatiles from the raw material are released and onset of pore formation is initiated.

Activation then follows - either physical activation (H_2O, CO_2) usually between 700 ^{o}C and 1000 ^{o}C, or by chemical activation where there are many different methods used such as using zinc chloride, phosphoric acid or potassium hydroxide etc.

1.3.2 Activated Carbon Supply and Demand

Forecasted activated carbon demand is set to rise 8.1% from 2014 to 2018. This increase means a production of 2.1 million metric tonnes of carbon will be required in 2018. In the US alone demand is expected to rise by 11% through 2017 with a market value of $1.35 billion [Freedonia group 2014]. The Freedonia group report [2014] state this is driven by the forever tightening pollution regulations and rising manufacturing activity. The increase in 2017 in America is put down to the implementation of the US environmental protection agency's (EPA) new mercury removal standards. Activated carbon demand could rise exponentially if China start putting stricter regulations in place and Bansal [2005] back this up by stating 'This is due to the fact that Asian countries, by and large, have not started using active carbons for water and air pollution control purposes in large quantities.' However, the group study indicated that North America will remain the largest activated carbon market, at least for now, whilst the Asia/Pacific region will slightly outpace and overtake North America by 2023.

1.3.3 Project Novelty

Whilst many biomasses were initially tested the main novelty comes from the in-depth review of two precursors in particular both on lab and pilot scale. The results found will significantly extend the knowledge in terms of physical activation, which in this study mainly involves steam used as the oxidising agent. Olive stone was one of the chosen precursors that was investigated in depth. Whilst there is published material on olive stone and it has been used as a carbon previously, this report greatly extends this knowledge with over 350 experiments conducted to get a real understanding of the potential of this precursor for certain applications. Pine wood was the other chosen biomass. Less literature is found on this precursor especially relating to pure physical activation. Again many trials have been conducted to investigate pine wood's potential as a commercially viable activated carbon. Both carbons are compared with production boundaries and peak porosities found for each using pore analysis and CTC (carbon tetrachloride) tests, which are currently not reported on in literature. Many trends and correlations are found between burn off, CTC values, methylene blue numbers, surface areas and micropore/mesopore volumes. Activation was carried out using biomass char with manipulated char reactivities. The char reactivity was changed by hot washing to remove alkali alkaline metals and/or changing pyrolysis conditions and procedures. Single step production was also carried out on both biomass types with the standard and manipulated chars. The other main area of novelty comes from scalability of the activated carbon production using a pilot scale rotary kiln in which single and two-step production techniques are studied.



Figure 1:4 Pine wood and olive stone biomass feedstock used for part of this project.

1.4 Introduction to Chapters

1.4.1 Chapter 2 - Literature Review

This chapter covers current literature for activated carbon production using a number of biomass precursors. The chapter expands on current gaps in knowledge within the carbon industry. During the literature review it is quite evident how activated carbon is a growing product that can be used for an increasing number of applications. The literature review shows that demand for carbons within industry, which is forever increasing, is not being met and thus leaving gaps

and opportunities for a new carbon product to enter the market. The review covers precursor selection to final technical analysis and use.

1.4.2 Chapter 3 – Methods

This chapter covers all production and analysis methods used. Numerous items of equipment and procedures have been used during this project conducted at CPL Industries and the University of Nottingham. This involves methods for pyrolysis, activation both lab and pilot scale, changing the variables during activation, CTC analysis, hardness testing, iodine numbers, carbon pH, proximate and ultimate analysis, methylene blue numbers, bulk density tests, hot water and acetic acid washing, BET surface areas, pore analysis, ion chromatography, X-ray photoelectron spectroscopy (XPS), scanning electron microscopy (SEM) and transmission electron microscopy (TEM). The chapter also covers the experimental errors and repeats for lab scale trials.

1.4.3 Chapter 4 – Preliminary Tests

A wide range of biomasses (over 30) were initially tested under certain conditions. Using this information five biomasses (olive stone, pine wood, eucalyptus wood, almond shell, grape cake) and coconut shell (used as a reference) were selected based upon their potential of producing a commercially viable carbon. The carbons were also chosen by using an additional selection criteria consisting of costs, availability and location etc. The chosen biomasses fell in to other categories: nut shells, fruit stone, fruit waste residue and wood producing either powdered or granular carbon. These biomasses are then tested under a range of different conditions and from this the selection was narrowed down to the final two chosen biomasses. The decision is based upon results from the trials and also additional selection criteria. The initial trials are executed to become familiar with the pyrolysis and activation technique in addition to equipment set up. It was important that a standard procedure was put in place. Both pyrolysis and activation was conducted on the small scale horizontal tube furnace (HTF).

Carbon dioxide and simultaneous carbon dioxide and steam activation are investigated and how the products compared to solely steam activation. Nitrogen flow rates and the impacts are also investigated.

1.4.4 Chapter 5 - Lab Scale Activation

The three main variables (classed as primary variables in this report) for physically activated, activated carbon production are activation temperature, residence time and oxidising agent quantity and flow rate. The impacts of altering the variables are investigated. This included their effect on carbon burn off and porosity, which are tested using a number of analytical techniques. The chapter considers trade-offs between the variables and the production limits of these

variables for both olive stone and pine wood before a drop off in performance is seen for a given yield.

The chapter evaluates pore development for both carbons and how activation reaction rates differ between the two. The pore structure of the carbons is analysed. The main areas of focus are the micro and mesoporosities of the carbons. Each application suits a different type of carbon and pore sizes play a significant role in deciding which carbon should be used.

Single step, pre washing and slow and fast pyrolysis are investigated and show what different production techniques have on the end carbon products in yield and porosity.

Decolouring potential was tested by methylene blue adsorption and gas adsorption by CTC analysis. Other tests in this chapter, in addition to the three main analysis tests mentioned above, include ion chromatography, XPS, pH, SEM and proximate and ultimate analysis.

1.4.5 Chapter 6 – Pilot Scale Activation

This chapter focuses on pilot scale production for olive stone and pine wood carbons. Pilot scale production and products are compared to carbons produced on lab scale using CTC and pore analysis. Further tests are conducted including hardness, iron and iodine tests. Single step production trials are completed along with the standard two-step process. The chapter examines how the contact between steam and carbon differs in different systems and is crucial in carbon development.

1.4.6 Chapter 7 – Financial and Process Cost Model

A production and cost analysis model has been made to evaluate the procedure and costs associated from raw biomass to end product with application examples. The model uses results acquired throughout the project in a theoretical process plant. The model covers the procedure and cost of drying, pyrolysis, and activation stages, with associated OPEX, CAPEX costs. Other areas include selling prices, energy recovery, cost sensitivities and potential investment required with break-even analysis. The model has been created for use with both olive stone and pine wood activated carbons.

1.4.7 Chapter 8 – Conclusions and Future Work

This chapter concludes the findings from all previous chapters and shows how the project objectives were met.

1.5 References

Anon. (2015). Retrieved Nov 2015, from Chemviron: http://www.chemvironcarbon.com/en/activated-carbon/history-of-activated-carbon

Anon. (2015). *Activated Carbon*. Retrieved Nov 2015, from Desotec: http://www.desotec.com/carbonology/activated-carbon-carbonology/what-is-activated-carbon/3549/

Anon. (2006). *Anon,* . Retrieved Nov 2015, from Charcoal house : http://www.buyactivatedcharcoal.com/activated_charcoal_history

Anon. (2009). *Biomass Carbon Dioxide cycle Biomass heating A practical guide for potential users* . Retrieved 2013, from Carbon Trust: https://www.carbontrust.com/media/31667/ctg012_biomass_heating.pdf

Anon. (2014). *Freedonia Group*. Retrieved Nov 2015, from http://www.freedoniagroup.com/World-Activated-Carbon.html accessed

Anon. (2015, Nov). *Science & Environment*. Retrieved May 2016, from BBC News: http://www.bbc.co.uk/news/science-environment-35084374

Höök, M. and X. Tang. . (2013). Depletion of fossil fuels and anthropogenic climate change—A review. *Energy Policy 52(0)* , 797-809.

Kyizom, L. (2014). *Cooking Fuel From Elneer Shells Coming.* India: New Indian Express.

Marsh H and Reinoso FR. (2006). "*Activated Carbon."* Elsevier Science & Technology Books.

Roop Chand Bansal and Meenakshi Goyal, 2005 . (2005). "*Activated Carbon Adsorption"*. Boca Raton London New York Singapore: A CRC.

W. Weber, B. V. (1980). "*Activated Carbon Adsorption of Organics from the Aqueous Phase"*. Science Publishers, Inc, Ann Arbor, MI .

Zafar, S. (2014). "*Energy Potential of Coconut Biomass"*. Bio Energy Consult.

Chapter 2 Literature Review

2.1 Background- The Move Away from Fossil Fuels

Globally there is a general consensus that we need to move away from using fossil fuels as burning fossil fuels to produce energy is the highest anthropogenic source of CO_2. Burning fossil fuels releases large amounts of GHGs which cause climate change. The three fossil fuels of coal, oil and gas all have different properties and compositions. For instance, coal contains a higher percentage of sulphur than oil and gas, whereas natural gas contains a higher amount of hydrogen than coal and oil. Reduction in the usage of fossil fuels is seen as one solution to meet future emission targets [EIA, 2009]. Reduction in fossil fuel use cannot be done instantly but the goal can be achieved by taking small steps at a time [IPCC, 2010]. A review undertaken by Höök and Tang [2013] reports that limits on fossil fuel usage need to be set in order to limit anthropogenic CO_2. Conversely, they also state that this may not be the case as other studies have reached quite different conclusions regarding future atmospheric CO_2 concentrations caused by fossil fuel limitations in that other climate mechanisms can have greater effects on climate change and limiting fossil fuel production has little impact on the overall picture [Etheridge, D. M *et al*., 1984].

What is clear from this study is that coal is seen as the worst of the three fossil fuels in regards to its impacts on the environment with GHG emissions as mentioned in Chapter 1. Moving away from coal may prove to be difficult. Coal is the cheapest and most abundant fossil fuel and for this reason is being used in large quantities by developing countries. Jin-ke, *et al.,* [2009] report that although developing countries are fully aware of the need to try and cut down CO_2 emissions, they see economic growth as a more important issue and coal is the cheapest way to produce energy needed for economic growth. The results in the study show a clear relationship between economic growth and coal consumption in developing countries. This means that due to forever changing supply and demand the coal market can be unpredictable. Due to this uncertainty and the harmful emissions given off during combustion many industries are looking for other carbonaceous alternatives to coal.

Biomass is a possible alternative to coal in energy production and additional uses which includes activated carbon production. Unfortunately, biomass has a lower fixed carbon percentage and requires larger mass and volume to produce the same amount of energy when compared to coal, although it can still be burnt or used in a similar manner. Biomass can be considered carbon neutral as shown in Figure 1:1 Chapter 1. However, there is a worldwide debate whether biomass is actually carbon neutral - in some instances reports show that biomass can be far more carbon positive than fossil fuels [Johnson 2009]. This is because of the fact that the required transportation and harvesting can be quite energy intensive. According to the EPA [2011], at the

smokestack, large-scale biomass produces up to 50% more carbon emissions than coal fired power stations to generate the same amount of electricity.

However, using biomass in order to cut net CO_2 emissions required for the agreed targets set at the UN climate change conference [2015], can be seen as a step in the right direction. Using biomass is also more beneficial from a social and economic perspective than capturing and sequestering CO_2 [Hall, 1997], meaning that using biomass as a fuel is cheaper than using coal and capturing and storing CO_2. It must be noted that Hall's report was written in 1997 but this is still the case today backed up by Mckinsey, [2010] who has been looking for the most cost effective methods of power production and general fossil fuel usage in view of the current financial crisis still affecting many parts of the world. Biomass production can also be beneficial by creating jobs and being financially rewarding for the local community [Mckinsey, 2010].

This brief background shows why the move away from fossil fuels can be environmentally beneficial, albeit it is not something that can be carried out instantly and will be a slow process. The use of biomass is a possible solution but carries with it many associated uncertainties in respect of its actual environmental impact, yet using biomass can still be considered an overall greener alternative resource than using coal - especially if the selected biomass is locally sourced with transportation kept to a minimum. This can be crucial as most of the coal used by the U.K. is currently being imported from countries such as China, Australia and America making the associated carbon footprint significant.

2.2 Precursors

Most organic materials rich in carbon do not fuse upon carbonisation and can be used as precursors for the manufacture of activated carbon.

Table 2-1 shows how biomass composition differs from hard and soft coal and coals shown in Table 2-2

Table 2-1 Typical biomass and coal composition [Zarifah Nadiah 2010].

Raw materials	Carbon %	Volatile %	Density (kg/m^3)	Ash %	Texture of AC
Softwood	40-45	55-60	0.4-0.5	0.3-1.1	Soft, large pore volume
Hardwood	40-42	55-60	0.55-0.8	0.3-1.2	Soft, large pore volume
Lignin	35-40	58-60	0.3-0.4	/	Soft, large pore volume
Nut Shells	40-45	55-60	1.4	0.5-0.6	Hard large multi pore volume
Lignite	55-70	25-40	1.0-1.35	5-6	Hard small pore volume

Soft coal	65-80	25-30	1.25-1.50	2.12	Medium hard, medium micropore volume
Petroleum coke	70-85	15-20	1.35	0.5-0.7	Medium hard, medium micropore volume
Semi hard wood	70-75	1-15	1.45	5-15	Hard large pore volume
Hard coal	85-95	5-10	1.5-2.0	2.15	Hard large volume

Table 2-2 Proximate analysis results taken from three types of coal [Green and Perry, 1997].

Coal Rank	Proximate Analysis (wt % ar)				Ultimate Analysis (wt % maf)					Net Heating Value (maf) (MJ/kg)
	Fixed carbon	Volatile matter	Moisture	Ash	C	H	O	N	S	
Anthracite	81.8	7.7	4.5	6.0	91.8	3.6	2.5	1.4	0.7	36.2
Bituminous	54.9	35.6	5.3	4.2	82.8	5.1	10.1	1.4	0.6	36.1
Subbituminous	43.6	34.7	10.5	11.2	76.4	5.6	14.9	1.7	1.4	31.8
Lignite	27.8	24.9	36.9	10.4	71.0	4.3	23.2	1.1	0.4	26.7

The first significant difference is that coal consists of a superior fixed carbon content with anthracite at around 80% down to 25/30% with brown coal. This is larger than the measured values for biomass. Although moisture content can vary by external factors, there is a clear lower volatile to fixed carbon ratio with coals. Biomass has a much larger volatile to carbon ratio; this suggests that the production yields for biomasses will be much lower than coal when producing activated carbon. However, with an increased volatile content theoretically there should be a larger potential for porosity formation from early stages of pyrolysis.

The ash contents found in coal are generally higher than in biomass. This is backed up in many published sources - for example Ciolkosz, [2010] who states 'Coal has a much higher ash content than biomass' However, the report goes on to say 'biomass ash is also more prone to forming deposits within the combustor, called "slagging" and "fouling." This is due to the fact that biomass ash contains relatively reactive salt compounds (especially K_2O), rather than the more stable silicates found in coal ash'. The fouling and slagging is less of a concern during activated carbon production due to the fact the carbon is not being combusted in the same way as, for example, a co-firing plant as the ash remains in the carbon product. Nonetheless high ash (inorganic material) content is an unwanted property in the final activated carbon product as it can reduce the efficiency of the carbon and lower the surface area [Gaspard and Ncibi, 2014]; [Schröder *et al*., 2011]. It also must be noted that high ash content also reduces efficiency of regeneration [Carbochem, 2015]. This is an important consideration when producing a regeneratable granular carbon.

Lignocellulosic materials constitute the more commonly used precursor and account for around 45% of total raw materials used in activated carbon manufacture. Coconut and fruit stones are popular for many types of activated carbon because of their high density, hardness and volatile content. These types of biomass are ideal to produce granular activated carbon. Coconut, peach stones and olive stones are good precursors to produce an activated carbon with a high microporosity and so useful for a wide range of applications. These precursors produce around 20% to 30% yield depending on process conditions [Schuth, 2002]; [Marsh and Reinoso, 2006].

Coal is used in many countries for activated carbon production as it is currently readily available and cheap. However, this situation may change with coal demand on the increase due to countries such as China and India using large amounts to fuel their economic growth. The rank of coal is key as coal's microporosity increases with increasing rank of coal, so anthracite coal is the best to use if one is looking for high microporosity [Marsh and Reinoso, 2006].

2.3 Activated Carbon Structure

Marsh and Reinoso, [2006] review the structure of activated carbons. Each carbon is different and each carbon atom has an associated reactivity. Carbons are considered as a continuing decrease in the degree or order from single crystal hexagonal graphite. The layers of hexagonal carbon layers are known as graphene layers. In activated carbon these layers can be disordered and not directly above and below each other. Within the graphene layers the bonding is trigonal sp^2-hybrid a-bonds with delocalized π-bonds within the layers. The interlayer spacing of 0.335 nm, being larger than the 0.142 nm of the C—C bond, indicates no chemical bonding between layers, with forces of attraction being limited to van der Waals forces.

During carbonisation carbon atoms move short distances (< 1 nm) within the network to positions of increased stability. Each precursor decomposes in their own way to form their own unique structures. From the release of volatile components and the movements of carbon atoms void space is created and this is the onset of porosity [Marsh and Reinoso, 2006].

Activated carbon can be considered as molecular space. The space surrounded by three dimensional continuous network of carbon atoms arranged in imperfect layers. Marsh and Reinoso, [2006] report how carbons are disordered but not amorphous unlike how Bansal, [2005] describes the carbon structures- that they are considered amorphous.

Modelling has proved difficult with many attempts being conducted to model a microporous carbon. In Marsh and Reinoso's review they state 'Models designed to describe the microporous nature of carbons have been compared leading to an assessment of the requirements of a comprehensive model to account for the properties of microporous systems'. No comprehensive model has, as yet, been created. This statement shows how predicting the porosity structure of

carbons is difficult due to the possibilities each precursor brings. The conclusion found in this review states that a maze like model fits best with given criteria.

There are about 10^{18} adsorption sites per gram of activated carbon with no identical sites, the adsorption potential in each being a function of the location of the adsorbate molecule within the confines of the graphene layers [Marsh and Reinoso, 2006].

2.4 Activated Carbon Production

Activated carbon can theoretically be produced from nearly all carbon containing organic materials e.g. wood, nutshells, fruit stones, peat, lignite, coal, petroleum, coke etc. The use of a given precursor depends on cost and availability, but also main application and type of installation present. Activated carbon production can be split into two main areas, these being physical and chemical activation. Within this project the physical activation will be studied in greater detail. Within physical activation either steam or/and carbon dioxide are used for the required oxidising atmosphere.

Production occurs in two stages or, as discussed later, studies have begun for a single step production. Usually a pyrolysis step is then followed by activation.

Conditions for these processes can vary depending on precursor. Optimum conditions should be found to maximise efficiency, cost, quality of process and final product. For a successful production of activated carbon there is an optimum balance between cost and quality that must be found. Pyrolysis usually occurs around 500 ºC to 800 ºC. This process leaves a char behind and this is then activated at higher temperatures of around 800 ºC to 1000 ºC. During this stage is when the main pore network is produced [Bansal 1988]. A flow diagram of production is shown in Figure 1:3 in Chapter 1 and Figure 2:1

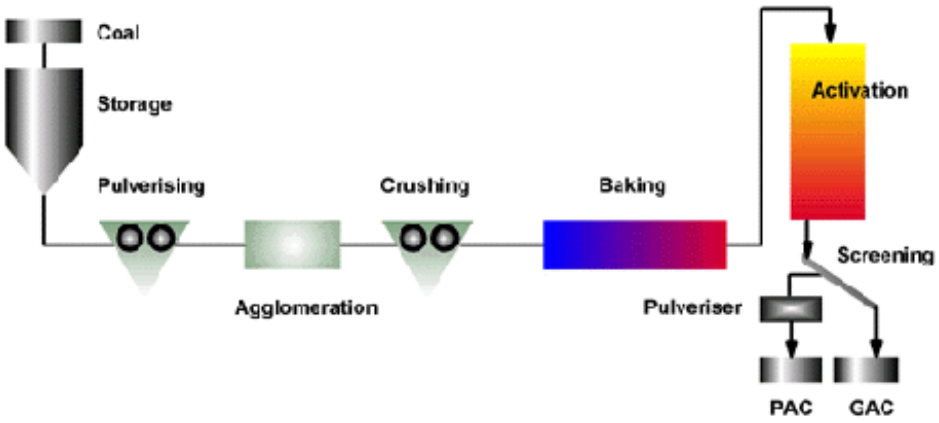


Figure 2:1 Flow diagram of a typical activated carbon production process using coal [Chemvironcarbon, 2013].



Figure 2:2 Three main sizes of activated carbon - powder, granular and pellets [Finne Zhang, 2008].

2.5 Pyrolysis

Pyrolysis is the first of the two main steps in the production process. This is the stage where the majority of volatiles are emitted and the resultant char formed.

Carbonisation of coal is simply heating the coal to high temperatures in the absence of oxygen to distil out tars and light oils. The process can also be used to produce metallurgical coke for use in iron-making blast furnaces and other smelting processes. The extra products given off during carbonisation include oven/coal gas along with ammonia, sulphur compounds and water. During this process bituminous coal tar, ammoniac, light oils and coal-gas are produced [James L Johnson, 1981].

The process is irreversible and a chemical composition change occurs in the coal structure. Pyrolysis is a type of thermolysis and is most commonly observed in organic materials exposed to high temperatures. Pyrolysis of organic substances emit gas and liquid products leaving a solid residue. In coal this leaves a char which is rich in carbon content and is called carbonisation [Krevelen D.W. 1993]. The process is used heavily in industry to produce a variety of things such as charcoal, activated carbon and methanol.

Pyrolysis differs from other processes that are also undertaken at high temperatures, like combustion and hydrolysis, in that it does not usually involve reactions with water, oxygen or any other reactants. However, a small amount of oxidation occurs as it is impossible to achieve a 100% free oxygen atmosphere [Krevelen D.W. 1993].

There have been studies around the carbonisation/pyrolysis stage and to what effects this process has on the final activated carbon product.

Li, Yang *et al.*, [2008] conducted a series of experiments studying the effects of pyrolysis temperature on porosity of coconut shell char and the activated carbon produced from the char. The temperatures used in these pyrolysis experiments were 400 ^{o}C, 600 ^{o}C, 800 ^{o}C and 1000 ^{o}C. The results show that a higher pyrolysis temperature the activated carbon derived produced a

higher BET surface area, total volume, and micropore volume (**Error! Reference source not ound.**). Higher carbonisation temperatures caused the evolution of more volatiles and this led to more micropores being formed. However, this also gave a reduction in yield. Conversely, Huang, Jin *et al.*, [2008] reports the opposite and that in their study with chicken waste as the precursor, carbonisation temperature change had insignificant effect on BET surface area.

Table 2-3 Coconut char porosity characteristics under different carbonisation temperatures. [Li, Yang *et al.,* 2008].

Carbonization temperature (°C)	S_{BET} (m^2/g)	V_{tot} (cm^3/g)	V_{micro} (cm^3/g)	$D_{average}$ (nm)
400	130	0.19	0.03	5.93
600	186	0.27	0.04	5.78
800	576	0.44	0.28	3.07
1000	702	0.53	0.35	3.03

Bouchelta, Medjram *et al.*, [2008] experimental work on date stones show the percentage yield decreasing with increasing pyrolysis temperature and hold time. Temperature ranges were from 500 ^oC to 800 ^oC for the pyrolysis process and maintained for 1 hour. Nitrogen to produce an inert atmosphere was used with a flow rate of 100 cm^3 min^{-1} and heating rate of 10 ^oC per minute.

Optimum pyrolysis temperature was found to be 700 ^oC with a 1 hour hold time, a 10 ^oC min^{-1} heating rate and 100 cm^3 min^{-1} nitrogen flow rate. Using SEM analysis it was evident that porosity increase occurred after the pyrolysis stage but more significantly after activation. The main conclusion from their study was that optimisation of pyrolysis conditions can lead to a higher number of micropores formed after activation has taken place.

Bansal, [1988] reports that a pyrolysis temperature of approx. 500 ^oC is the temperature at which the porosity in the char begins to initiate. However, at this temperature there was limited porosity development due to only partial volatile evolution. A higher pyrolysis temperature and activation is required before a full pore network can be developed.

M C Blanco Lopez *et al.*, [2002] looked into olive stone pyrolysis with the three main components: char, liquid and gas. The gas released was composed of CO, CO_2, CH_4, $C2H_4$, C_2H_6 and H_2. The major components being CO and CO_2 at 350 ^oC with CH_4 devolatilisation increasing with temperature.

To summarise - the pyrolysis is an important stage in char formation. However there are conflicting reports as to how significant it actually is. This is an area that will be looked into during the project to see just how much an impact pyrolysis has by carrying out single step production.

2.6 Activation of Char

Char activation is the final step in producing the activated carbon before screening takes place. Activation, whether physical or chemical, is seen as the key parameter to activated carbon quality. Other parameters include the raw precursors, particle size, reaction temperature, heating rate, gas flow rate and residence time [Rashidi, Yusup *et al.,* 2012].

Activation is the most studied area surrounding activated carbon production. Literature focuses on how the aspects associated with activation affect the activated carbon - this being the yield, pore structure and pore volume. In this project physical activation will be used and so the literature below focuses on either steam or carbon dioxide activation. These are the two main oxidising agents used within physical activation. Physical activation consists of oxidising the char at high temperatures with the oxidising agents mentioned. Activation is an endothermic reaction and so requires a constant high temperature to be generated around 700 ^{o}C to 1200 ^{o}C. The temperature will vary depending on the raw material selection [Claimex, 2013].

2.7 Steam Activation

Steam activation is the most widely used process to activate carbonaceous materials and steam activation is known as physical activation within industry even though chemical reactions are taking place. The chemical reaction between carbon and steam producing hydrogen and carbon monoxide takes place at the internal surface of the carbon, removing carbon from the pore walls and thereby enlarging the pores.

The steam activation process allows manipulation of pore structure and distribution to suit specific end uses. The pore structure has to be opened up more for the adsorption of small molecules from a solution, as in water purification, than for the adsorption of large colour molecules as in sugar decolourisation. Activated carbon for gas phase use is more expensive than activated carbons produced for liquid phases due to it requiring a longer activation time inside the furnace [Haycarb, 2013].

Basic chemistry along with the kinetic data (see Appendix section A.1 and A.2) shows that an in increase in temperature kinetically favours the forward reaction. It is noted that there possibly needs to be on average 10^7 collisions between a H_2O molecule and a carbon atom before there is successful reaction and the carbon atom is released [Marsh and Reinoso, 2006]. At higher temperature, the H_2O molecule will have more kinetic energy and collide more frequently with carbon surface. If the collision has the required activation energy then the reaction will occur. Taking into account the information provided by Marsh and Reinoso, [2006] then only a small amount of collisions have the required activation energy. This can be directed back to the

statement that each carbon atom is of different reactivity. The trend follows the Maxwell and Boltzmann distribution curve shown below.

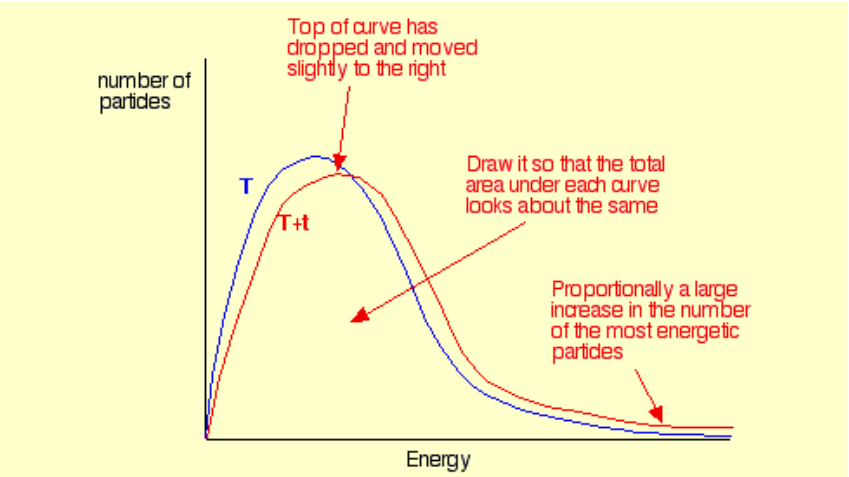


Figure 2:3 Maxwell and Boltzmann distribution curve [Clark, 2002].

The area under the curve represents the number of particles of the required specified energy. Depending on the reactivity of the carbon atoms within the graphene layers the energy requirement change. A carbon atom with lower reactivity will require a higher activation energy to react and a fewer number of H_2O molecules will possess this, so a reaction is less likely. Increasing the temperature changes the shape of the graph as shown by the red line in Figure 2:3 - this now means that collisions are more likely to result in a successful reaction.

2.8 Activation Using Both Steam and Carbon Dioxide

Molina-Sabio, Gonzalez *et al*., [1996] looks into the effect of steam and carbon dioxide during activation of the char sample and how this reaction develops the pore structure. The results showed a wide range of burn off of 8% to 70%. Carbon dioxide mainly caused the creation of the microporosity, however steam widened the microporosity from early stages of the activation process. Carbon dioxide produced a larger micropore volume and a narrower micropore size distribution, yet micropore widening was the predominant effect from activation with steam. Larger development of narrow microporosity produced by carbon dioxide and widening by steam is paralleled by the evolution of carbon monoxide from oxygen surface groups decomposing. The porous structure created was in relation to oxygen surface groups. Oxygen surface groups decomposed at different temperatures producing CO and CO_2, with CO producing surface groups decomposing at higher temperatures. Activation by carbon dioxide created larger number of groups emitted as carbon monoxide but the groups were also thermally more stable than those

produced by steam. The increase in micropore volume with a burn off of over 40% for steam activation is less than with carbon dioxide activation.

Rodríguez-Reinoso, Molina-Sabio *et al.*, [1995] also looked at steam and carbon dioxide activation using olive stones. The gasification was carried out in the same manner for both samples of char obtained from olive stones by carbonisation at 850 ^{o}C within a nitrogen atmosphere for 2 hours. Carbon dioxide was found to open and widen narrow microporosity, whereas steam widened from early stages but in the end resulted in a lower micropore volume. This coincides with the Molina-Sabio, Gonzalez *et al.*, [1996] report.

Carbon dioxide and steam develop microporosity in char with different effects, however these differences are minimised at lower temperatures. This is mainly due to the lower reactivity of both CO_2 and H_2O at lower temperatures. However, the H_2O molecule is smaller and presumably may have favourable access to entrance of micropores; additionally diffusion of water across the porous network is greater than for carbon dioxide. Activating gas reacts with exterior and interior of the particle, with interior reaction requiring gas diffusion.

Water molecules diffuse quickly into the particle from start of the activation reaction. This produced a wide range of porosity. Carbon monoxide and hydrogen are produced during the reaction and can act as inhibitors to the forward reaction, [Marsh and Reinoso, 2006] report this can promote exterior reaction as interior inhibited by inhibitors. This can lead to destruction of porosity and destruction occurred at burn off higher than 20% especially in the micropore region.

With a too high activation temperature the C-H_2O reaction rate increases rapidly and the control of reaction is more influenced by pore and bulk diffusion. i.e the speed at which the steam can diffuse through the char particle to react with the internal surface carbon atoms. Activation temperature optimum was found around 850 ^{o}C. Literature is very consistent on this point with all reports mentioning optimum activation temperature ranging from 800 ^{o}C to 1200 ^{o}C for a range of biomass.

H_2O reacts less selectively with carbon atoms than CO_2 does, this results in additional micropore widening [Marsh and Reinoso, 2006]. This can be attributed to CO_2 being linear and water molecule being angular with oxygen in the middle, which has been suggested in previous work [Rodríguez-Reinoso, Molina-Sabio *et al*., 1995]. Activation with CO_2 produces more oxygen surface groups than activation with steam. These surface groups, in early stages where pores are narrow, may act as constrictors of the micropore, reducing the width of the pores. At larger burn off and higher temperatures these effects disappear as pore size is larger. However, further research is required to confirm this. Carbon dioxide was found to produce widening effect of

narrow micropores and steam widens the micropores from early stages of activation, even when the removal rate of carbon atoms from both chars is equal.

For the common gasification rate, activation with steam produces activated carbon with a lower micropore volume as opposed to carbon dioxide. Steam activation produces a larger development of mesopores and macropores and subsequently means a wider distribution of pore size is present compared to carbon dioxide. Demiral, Demiral *et al.*, [2011] also found that with an increase in activation time and temperature micropore volume increased. In this case the activated carbon produced a maximum of 1106 m^2/g at an activation temperature of 900 ^oC and an activation time of 45 minutes. The activated carbons were tested similarly to other studies and according to pore size distribution the activated carbons prepared via steam activation were mainly microporous.

Increasing activation residence time to a certain limit increases micropore formation, with shorter reaction times more mesopores are formed. However, with further extended activation residence times mesopores and even macropores form from micropore widening [Yang and Lua, 2003]. This shows how important it is to get the optimum dwell time in order to deliver the highest quality activated carbon possible, whilst at the same time taking into consideration that a longer dwell time will usually be a more expensive process due to more energy being required for heating. Yang and Lua, [2003] found 2 to 2.5 hours as the optimum dwell time.

Activation times are important and many reports have looked into this such as Li, Yang *et al.*, [2008] who conducted activation trials by running a series of experiments for 30, 60, 90 and 120 minutes. The activation temperature was kept constant at 900 ^oC. Activated carbons derived from different activation times showed how pore size and pore diameters decreased whilst BET surface area, total pore volume and micropore volume increased with increasing residence time.

Carbon dioxide activation leads to continuous evolution of ultra micropore volumes. At higher temperatures, the decrease of micropore volume is due to external burn off [Zhu, Gao *et al.*, 2012]. This conflicts with other reports that micropore volume decrease is down to a 'melt' inside the pore network. However, Zhu, Gao *et al.*, [2012] go on to say how micropore volumes of steam activated carbons are always larger than those for CO_2 activation with the exception of the samples with over 70% burn off.

The effects of activation temperature and the amount of char burn off on the physio-chemical properties of the two series were studied [Zhu, Gao *et al.*, 2012]. The findings were that micropore volume alone does not ensure optimal SO_2 adsorption, rather the pore size and pore size distribution should be considered more important factors. An increase in temperature leads to an increase in CO_2-C activation rate. To achieve a suitable CO_2-C activation rate the temperature must be over 800 ^oC. For steam, the activation temperature has a slight influence on

activation rate when temperature precedes 850 °C. To achieve a similar gasification rate to the steam activation, the sample activated by CO_2 had to have a temperature of 950 °C. This leads to the assumption that steam is a more reactive agent than CO_2 for taixi-anthracite as a precursor [Zhu, Gao *et al.*, 2012]. Activation with steam at 850 °C produces a development of total porosity. However, with carbon dioxide used as an activating agent, the micropore development continues right through the activation process. Too high an activation temperature caused external burn off only due to the reaction rate being too high. Too high an activation temperature also lead to an increase in median pore diameter, which suggests the average size of the micropore will be larger. With carbon dioxide used as the oxidising agent at a high activation temperature (900 °C to 950 °C), the median pore diameter is larger than that of steam activation which means that as temperature rises from 850 °C to 950 °C, CO_2 activated carbons present greater difference in pore structure. Activated carbons produced at lower temperatures (850 °C) have larger quantities of basic surface sites than ones produced at higher temperatures (950 °C) [Marsh and Reinoso, 2006].

2.8.1 Comparison of Carbon Dioxide and Steam Activation

González, Molina-Sabio *et al.,* [1994]; Román, González *et al.,* [2008] compared both carbon dioxide and steam as oxidising agents for the activation process. The results were that they produced different porous structure in olive stones. Carbon dioxide activation caused mainly micropores to be formed, whilst for steam at a given burn off the porosity development was higher. Steam activation also caused wider pore distributions and a higher amount of macropores are formed.

Researchers have been studying the optimal temperature at which activation should take place. Economically, the lower the temperature the less energy required - meaning a cheaper process. However, optimisation of conditions is important to produce a high quality, economically favourable activated carbon. The final temperature of activated carbon is when the most effects on the pore network take place. Throughout literature it is reported that the increase in activation temperature decreases the yield of the product as more is 'burnt off' examples are shown in Figure 2:4 and Table 2-4. The temperature of carbonisation does not need to go above 800 °C [Zarifah Nadiah, 2010]. Additionally, this study found that materials with higher carbon and ash content meant that during carbonisation more volatiles were given off, thus leaving behind more stable carbon and ash forming materials.

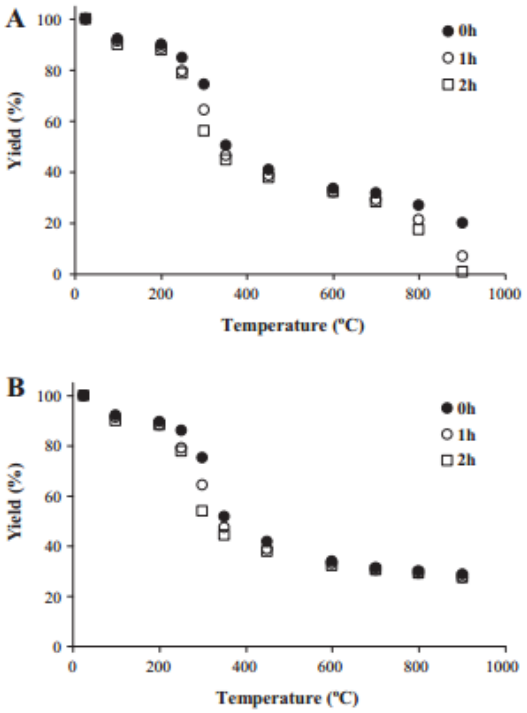


Figure 2:4 Product yield against activation temperature [Matos, Nahas *et al.,* 2011].

Table 2-4 Activation temperature effect on product yield [Bouchelta, Medjram *et al.,* 2008].

Parameters	Yield (%)
Temperature °C	
500	28.39
600	25.22
650	24.25
700	23.37
800	23.08
Hold time (h)	
0.5	24.51
1	23.09
2	21.44
3	14.29
6	13.62

An increase in activation temperature can give rise to an increase in surface area [Román, González *et al.*, 2008] but it may only be a slight increase. For example, in their experiments with olive stone using CO_2, there was shown to be a slight increase in surface area from an activation temperature of 850 °C to 900 °C. More significant was that a higher activation temperature resulted in an increased mesopore fraction due to pore widening. During experiments mesopore percentage increased from 10% to 19% with these two activation temperatures. This was also experienced with little rise of burn off [Román, González *et al.*,

2008]. This coincides with the endothermic reaction of CO_2-C, which creates micropores but also causes pore widening: turning these sized pores into mesopores.

R González *et al.*, [2008] also looked into the effect on activation temperature during steam activation. Higher temperatures caused a higher porosity and wider pore size until a maximum BET surface area was reached, after which destruction of micropores occurs when activation temperature goes too high. In these particular experiments with olive stones this temperature was found to be 900 ^oC.

[Toles, Marshall *et al.*, 2000] investigated almond shells comparing the estimated costs of production of using carbon dioxide and steam. Each biomass precursor requires different process conditions for surface area and yield optimisation, as shown later in the report. When looking into the different precursors, Zarifah Nadiah, [2010] shows that it requires 3 hours activation time for palm kernel shell compared to almond shell which Toles, Marshall *et al.*, [2000] report requires 2 hours activation time. The main findings proved the notion that steam activation is the most cost effective method in terms of production due to the current price of carbon dioxide. It also made the most economical sense in respect to the adsorption of copper metal ions. Another point that was found was pyrolysis at 800 ^oC instead of 700 ^oC improved organic adsorption regardless of activation conditions.

Overall steam activated carbons were found to be better adsorbers of organic substances than carbon dioxide derived activated carbons. Oxidation had no clear cut effect on adsorption of polar and non-polar organics.

Table 2-5 Cost comparisons for steam and CO_2 activation [Toles, Marshall *et al.*, 2000].

Treatment[b]	Production ($/kg)	Cu^{2+} adsorption ($/mol Cu^{2+})	Organics adsorption ($/mol)
Steam activation			
1–7–2–8 (7.0 ml/min)	1.54	4.16	2.96
1–7–2–8 (7.0 ml/min-ox.)	1.91	3.67	3.60
1–8–2–8 (7.0 ml/min)	1.54	4.40	2.40
1–8–2–8 (7.0 ml/min-ox.)	1.91	4.78	3.14
CO_2 activation			
1–7–2–8 (75% CO_2)	2.56	6.74	4.63
1–7–2–8 (75% CO_2-ox.)	2.93	5.05	5.59

2.8.2 Single and Two-Step Production of Activated Carbon

So far discussed is two-step production: pyrolysis followed by activation. Recent reports, however, have looked into a single step process that theoretically could save time and money for industry. However more research in this area is needed and single step with steam activation could alter volatile release. Rashidi, Yusup *et al.*, [2012] looked into pyrolysis and physical activation using carbon dioxide as opposed to steam. The study showed that single step process can be accomplished with high quality carbon being produced, with single step production being

comparable with two stage production in coconut shell porosity. The precursors used were coconut shell and palm kernel shell. The process conditions: CO_2 flow rate (100 to 300 cm^3/min), reaction temp 500 to 900 ^oC, and residence time 15 to 90 minutes.

Single step production has limited scientific research the paper reports. The optimum process conditions included an activation temperature of 900 ^oC with a CO_2 flow rate of 200 cm^3/min and 140 minutes residence time.

2.8.3 Chemical versus Physical Activation

This research project mainly focuses on physical activation. However, understanding the difference between physical and chemical activation is important. Activated carbons can be impregnated with certain chemicals to increase carbon adsorption performance for given applications. Reports in this review mention how chemical activation has been used and compared to physical activation with physically activated carbon performing better than chemically activated carbons and vice versa. Song, Jin *et al.,* [2013] conducted a study that involves looking at biomass precursors for activated carbon and the difference in the two activation techniques (physical and chemical). In this instance iodine numbers for physical activation were 665.23 mg/g and for chemical activation 1262.25 mg/g. For physical activation, pyrolysis temperature and activation temperature was 450 ^oC and 800 ^oC and dwell time 1 and 2 hours respectively. For chemical activation, pyrolysis temperature and activation temperature was 400 ^oC and 800 ^oC respectively and dwell time 1 and 2 hours respectively. Chemical activation produced higher pore volume and BET surface area and showed the highest CO_2 adsorption capacity (1.5 mmol g^{-1}) at 298 K with the pressure of 100 kPa. For physical activation, CO_2 adsorption capacity varies with the different pyrolysis and activation parameters. However, during chemical activation harmful gases were given off which can be seen as a disadvantage during production. The chemically activated carbons for CO_2 adsorption outperform physically activated carbons and this was similar to findings by Okada, Yamamoto *et al.,* [2003] who also found the surface area was higher using chemical activation. This again is backed up by Maciá-Agulló, Moore *et al.,* [2004] who reported higher surface area and yield with chemical activation over physical activation. However, one disadvantage of using chemical activation is that companies who want to go down this route require further licenses and staff training which may add to costs. Physical activation has also been found to be more effective at reducing the moisture content [Matthew E. Kuchta1 *et al.,* 2010]

2.9 The Use of Activated Carbon in Liquid and Gas Phase Applications

Activated carbon has numerous usages and can be used in many industries. Examples of its uses are as follows: in food production for the removal of odours, colours and unwanted material; in the production of alcoholic beverages in distilleries; in the sugar industry by decolourising the sugar during the refining process; in the chemical and pharmaceutical industries- organic compounds decolourised and clarified. Activated carbon can also be used to recover wanted material, for example the recovery of gold and silver in amongst other metals. It can also be used in liquid fuels to remove sulphur including mercaptans [Taylor and Francis, 2005].

Activated carbon can be used in both gas and liquid phases. In the gas phase activated carbons are usually used for a wide variety of applications that include recovery of organic solvents, removal of sulphur dioxide, hydrogen sulphide and carbon disulphide. In the liquid phase activated carbon is used to remove unwanted compounds and metals.

Activated carbon can be used in nuclear technology for purification of exhaust and circulating gases, in vacuum technology to remove oil and mercury in laboratories, medicinal applications, gas storage, where any methane given off can be adsorbed. The above are just a few examples of uses for activated carbon.

2.9.1 Gas Adsorption

Significant quantities of hazardous gases and vapours are being released into the air by numerous types of industry such as chemical, pharmaceutical, power etc. These emissions contain volatile organic compounds (VOCs). The flue gases also contain oxides of nitrogen and sulphur which can combine with VOCs to create smog. Activated carbons can go a long way to provide an answer to these emission problems [Bansal, 2005].

Activated carbon can adsorb low concentration VOCs from gas streams. These low concentration VOCs can be found in the paint, printing and automotive assembly plants. The major VOCs in this case tend to be alcohols and acetates. The flow rates tend to be approx. 10,000 kg/hr to 14,000 kg/hr. Granular activated carbon adsorption rate is low due to the inter-particulate diffusion process, powdered is therefore preferred [Bansal 2005].

Activated carbon can also be used in the Carbon Capture and Storage (CCS) industry for carbon dioxide adsorption, and it is one of a number of solids and liquids being researched for carbon capture. Hao, Björkman *et al.*, [2013] have looked into both physical and chemical activation of waste biomass for use as activated carbon in CCS. Activated carbons produced had a high

number of micropores and a high capacity to adsorb CO_2. The capacity to adsorb CO_2 from both of the activated carbons was studied with regard to their microporosity. The microporosity was measured by N_2 adsorption. Physically activated carbons (PACS) exhibited a large adsorption of CO_2 (1.45 mmol/g) at a small pressure of CO_2 (10 kPa) at a temperature of 0 ^oC. These PACS were prepared by activation in a stream of CO_2. PAC from hydrothermally carbonised grass cuttings and from horse manure had the largest ultra micropore volume. Generally, PAC showed excellent adsorption and regeneration capabilities. The CO_2 uptake was also considered rapid, which is crucial for such an application. The PACs had a highest adsorption of CO_2 over chemically activated carbons (CAC). The CACs displayed higher selectivity for CO_2 over N_2. However, the CACs only had half the amount of micropore volume compared to the PACs. This information shows how the micropore region is the dominant factor in CO_2 adsorption.

2.9.2 Liquid Adsorption

Waste effluent is a huge problem and comes from a various number of sources such as industrial, manufacturing, urban and rural run-off that contains chemicals, fertilizers, pesticides etc. This water is then unfit for human consumption and so has to be purified. The demand for clean water is increasing especially in city areas. To add to this problem, industries are developing and using more chemicals in their processes and disposing of them in the liquid effluent streams. The organic and inorganic compounds found in waste water can be toxic and carcinogenic. Bansal, [2005] reports that more than 800 organic and inorganic chemicals have been identified in various drinking waters. Old methods for 'cleaning' such as filtration, coagulation and ion exchange are becoming inefficient and even ineffective due to the continuing increase in variety and amount of hazardous chemicals present in our lakes and rivers. Activated carbon operations carried out in several countries have shown that it can be used to remove inorganic and organic compounds from water. The smaller the particle size the faster the adsorption, but this is more difficult to use on fixed beds so granular activated carbon is preferred. In addition powdered activated carbon causes high pressure drop and regeneration issues due to blockage on the fixed bed. Granular activated carbons sizes are usually around 0.6 to 4.0 mm and are usually hard, abrasive and dense meaning high mechanical strength to withstand harsh operating conditions. However, granular activated carbons are more expensive to produce than the powdered type but they have the advantage of lasting much longer [Bansal, 2005].

The parameters on which activated carbon adsorption quality is centred have been discussed, but it is also dependant on the surface chemistry of the activated carbon. Most activated carbons are hydrophobic and contain carbon-oxygen surface groups. Such activated carbons adsorb neutral or non-polar organic compounds and show low adsorption for ionic or polar pollutants - an example of this is phenol for which the surface chemistry is more important than the regular parameters such as surface area.

Activated carbon for water treatment can be placed in three main categories. One treatment is for drinking water, and must meet certain requirements. These requirements are in place to remove odour, bad taste and contaminants hazardous to health and involve large scale treatment of rivers, lakes and reservoirs. The second category is water treatment in industry such as from heat exchangers, steam generators and cooling towers. This treatment removes contaminants that cause corrosion. The third category involves treatment of effluent streams from industry that contain many hazardous substances and is important as this water is usually discarded into ground water. Activated carbon can play an important role here in removing organic and inorganic compounds [Bansal, 2005].

Activated carbon can play two different roles in effluent 'cleaning'. It can remove heavy metals but also can trap valuable gold and silver which can be recovered. Chemically activated carbons can also be used as catalysts for the decomposition of gases and vapours in industrial effluent streams.

The ability of activated carbon to adsorb inorganic material and specifically metal cations is through their ion exchange properties due to heteroatoms such as oxygen, nitrogen, sulphur and halogens on the surface. These elements are then bonded to carbon to produce surface functional groups.

These surface groups influence adsorption of inorganics from aqueous phase. However, the carbon-oxygen surface groups exert the most influence. Surface oxidation can increase carbon-oxygen surface groups significantly. This produces two types of carbon–oxygen surface groups, one being acidic and one being neutral. The acidic surface group are polar and enhance ion exchange properties, thereby increasing adsorption of metal cations. A few examples of cations that activated carbon can remove are barium, iron, vanadium, selenium and also several chlorine, fluorine and cyanide compounds. Other compounds activated carbons are used for include sulphides, nitrates, chlorides, chlorites, chlorates, cyanides, boric acid, borax, and borates and other metals such as, copper, lithium, iron, cerium dysprosium and strontium.

Activated carbons are used in the water treatment industry where they can decontaminate phenolic compounds [Sekirifa, Hadj-Mahammed *et al.,* 2013]. Tay, Ucar *et al.,* [2009] also report that activated carbons produced from waste biomass can be made to the specification required to be used as adsorbents for various environmental applications such as removing hazardous compounds from industrial waste liquids/gases.

2.10 Adsorption Mechanism- London Dispersion Forces

London dispersion forces (LDF) are the main adsorption mechanism occurring with physically activated carbons - the main focus of this project. LDF are the weakest of intermolecular forces and occur when electrons in two adjacent atoms occupy positions that cause the formation of temporary dipoles [Marsh and Reinoso, 2006].

This intermolecular interaction exists between all molecules both polar and non-polar but is extremely short ranged.

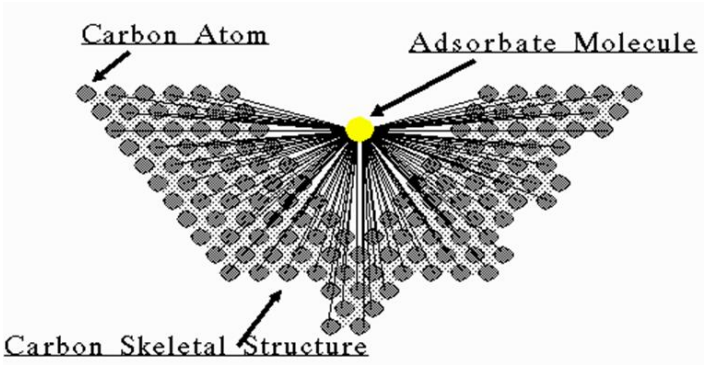


Figure 2:5 Adsorption of adsorbate [Greenbank, 2006].

The adsorption force present at the adsorption site is the sum of all individual interactions between the carbon atoms and the adsorbate molecule. LDF are independent of temperature from -273 ºC to 1000 ºC. The force strength is also sensitive to separation of the molecules. These characteristics means that LDF are analogous to gravitational forces but are shorter ranged. Stronger dispersion forces occur in larger and heavier molecules as temporary dipole can form easier due to valence electrons being further from the nucleus. In the narrow micropore region is where dispersion forces are at their strongest [Marsh and Reinoso, 2006].

2.11 Analytical Techniques Used in Activated Carbon Production

2.11.1 CTC Analysis

The Carbon Tetrachloride Activity (ASTM D3467) measures the loading of carbon tetrachloride within the carbon. The method is a measure of the pore volume generally accepted within the micropore region. The test is designed to be a quality assurance test for carbons. Carbon Tetrachloride Activity has been replaced by the Butane Activity (ASTM D5742) test due to the ban on carbon tetrachloride. CCl_4 activity = 2.55 × the Butane Activity [Desotec, 2013]. CTC value is still the used as reference in industry and for this reason the butane number is converted.

2.11.2 Methylene Blue Analysis

Methylene blue adsorption is a liquid phase adsorption test designed to test the capacity of activated carbon for the methylene blue molecule and other molecules of similar size. The molecule is bigger than butane and therefore can only fit within larger pores. Methylene blue is used as a test for activated carbon in literature by [Wu *et al.,* 2009];[Sayed *et al.,* 2014];[Nunes and Guerreiro, 2011];[Wang *et al.,* 2005].

2.11.3 BET Surface Area and Pore Analysis

The BET surface area equation:

$$\frac{p}{V(p^0 - p)} = \frac{1}{V_m c} + \frac{(c-1)p}{V_m c p^0}$$

Equation 2-1 [Marsh and Reinoso, 2006]

Brunauer–Emmett–Teller (BET) theory aims to explain the physical adsorption of gas molecules on a solid surface and serves as the basis for an important analysis technique for the measurement of the specific surface area of a material. In literature almost all reports use BET surface area to determine the quality of the activated carbon as the higher the surface area the more theoretical adsorption sites available. The BET surface area is measured using various assumptions and these are as follows:-

1. Surface is flat.
2. Surface is energetically (chemically) uniform, so all adsorption sites are equivalent.
3. No lateral interactions between adsorbed molecules.
4. Heat of adsorption is the same as latent heat of vaporisation for all layers above the first.

[S Rigby, 2013]

There are limitations with BET surface area and these assumptions may mean that the BET value isn't a true value - for example not all surfaces are flat and it is thought BET analysis could possibly overestimate the surface area. However, this can be misconceived as [Gauden, Terzyk *et al.,* 2010] state 'results show that the BET method underestimates and not, as it was usually postulated, overestimates the surface areas of microporous carbons'.

A microporous carbon (1000 m^2/g) adsorbs nitrogen at 0.1 MPA (77 K) to the extent of 10 mmol/g; 1 g of carbon is equivalent to 80 mmol of carbon atoms. This means that eight carbon atoms are used to adsorb one nitrogen molecule as Figure 2:6 shows.

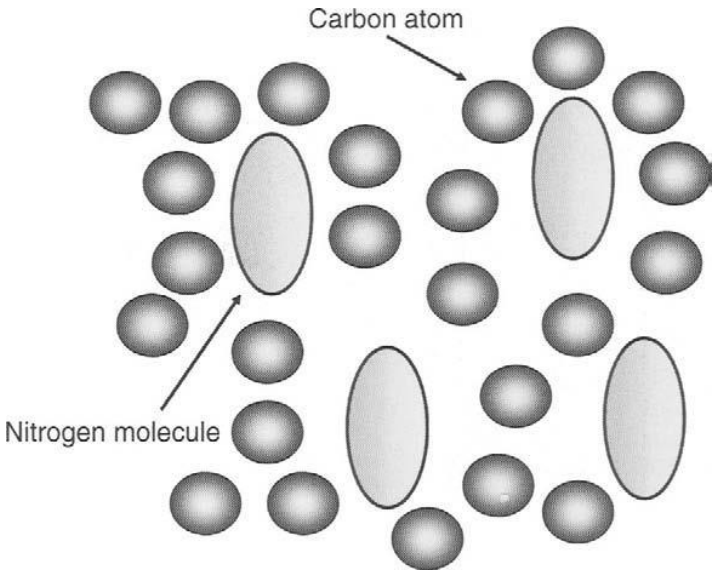


Figure 2:6 Nitrogen molecule adsorbed to eight carbon atoms [Marsh and Reinoso, 2006].

Marsh and Reinoso, [2006] state that nitrogen provides volumes of microporosity of 0.7 nm to 2 nm and carbon dioxide isotherms are required to measure the narrow micropore volumes of < 0.7 nm. To get an overall detailed analysis it is ideal that both isotherms are produced and joined together. Nitrogen isotherms also provide information regarding mesopore volumes (2 nm to 50 nm).

Surface areas can provide misleading perceptions of activated carbons. A large surface area does not necessary give an overall indication of carbon quality as it depends on the adsorbate molecule. For example, butane will adsorb differently to nitrogen and give different values.

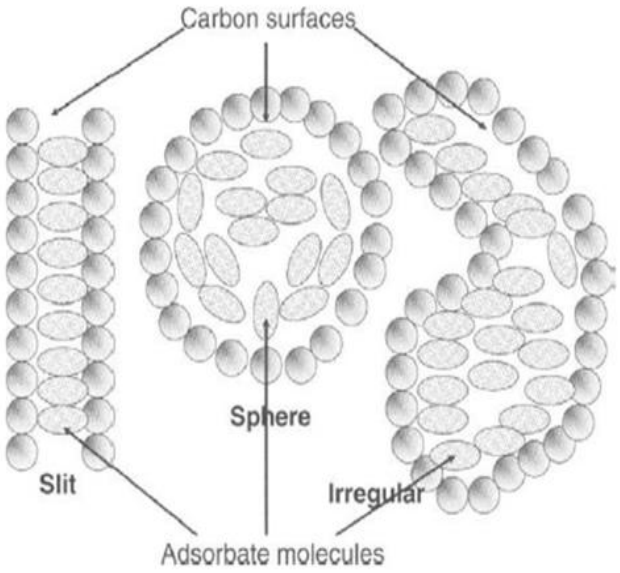


Figure 2:7 Surface area available for adsorption is different dependant on type of adsorbate [Marsh and Reinoso, 2006].

Whilst BET surface area is not an accurate description of a carbon it is well known parameter in industry and helps give an indication of the type of carbon present. Although it can be deemed inaccurate and misleading a larger surface area indicates a high quality highly microporous carbon.

2.11.3.1 Isotherms and pore analysis

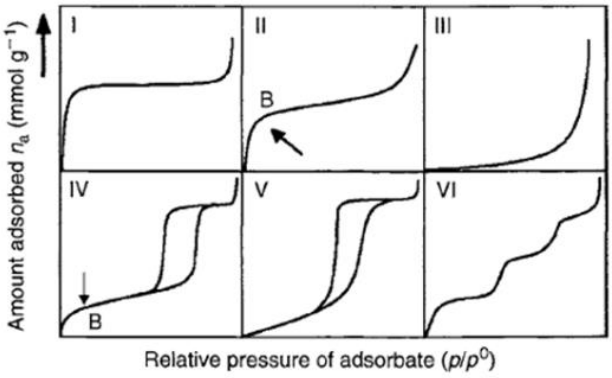


Figure 2:8 Types of adsorption isotherms [Sing *et al.,* 1985].

Type-I and Type-IV are the two main isotherms seen with activated carbons. Type-I isotherms are indicative of microporous carbons with a levelling off after p/p^0 approx. 0.2 which signals mesopore volume filling. Type-IV isotherms are more inflections of mesoporous carbons with increased mesopore filling after p/p^0 approx. 0.2. Type-IV isotherms usually exhibit hysteresis loops which are produced due to capillary condensation in which the adsorbate is then trapped in bottle necked mesopores [Marsh and Reinoso 2006]; [Tascon, 2012].

2.11.4 Iodine Number

Iodine number is one of the most fundamental and common parameters used to characterize activated carbon performance. It is a measure of activity level (higher number indicates higher degree of activation), often reported in mg/g (typical range 500–1200 mg/g). CPL Industries are preferably looking for an activated carbon to have over 700 mg/g, as this is seen as the boundary for commercially viable activated carbon [CPL Industries 2013]. However, activated carbons with lower iodine numbers still have specific markets. Iodine number is a measure of the micropore content of the activated carbon (0 to 20 Å, or up to 2 nm) by adsorption of iodine from solution. Iodine number is the standard measure for liquid phase applications [Aygün, Yenisoy-Karakaş *et al.,* 2003].

2.11.5 Transitional Electron Microscopy and Scanning Electron Microscopy (TEM/SEM)

TEM can achieve very high resolutions; it is a microscopy technique that involves a beam of electrons being transmitted through an ultra-thin specimen. An image is formed from the

interaction of electrons that have been transmitted through the specimen. The image is then focused onto an imaging device such as a fluorescent screen on photographic film or detected by a sensor such as a CCD camera. Scanning electron microscopy (SEM) is a type of electron microscope that produces images of a sample by scanning it with a focused beam of electrons. The electrons interact with atoms in the sample, producing various signals that can be detected and which contain information about the sample's surface topography and composition. TEM can achieve resolution better than 1 nm, which means that the micropore region can be observed. Pré, Huchet *et al.,* [2013] studied TEM for activated carbon analysis and reached a resolution of 0.24 nm showing the resolution is high enough to see all size of pores.

2.11.6 TGA

Thermogravimetric analysis (TGA) is a method of thermal analysis in which changes in physical and chemical properties of materials are measured as a function of increasing temperature (with constant heating rate), or as a function of time (with constant temperature and/or constant mass loss) [Zhang, Resende *et al.*, 2012].

2.11.7 Proximate and Ultimate Analysis

The ultimate analysis gives the percentage of the composition in regards to carbon, hydrogen, oxygen, nitrogen and sulphur content.

The proximate analysis provides information about moisture content, volatile content, consisting of gases and vapours driven off during pyrolysis (when heated to 950 ^{o}C), the fixed carbon and ash.

Proximate and ultimate analysis are required for precursor composition, it is important to conduct elemental analysis of the precursor used as it can help predict activated carbon quality [Gillespie, Everard *et al.*, 2013].

2.12 Pore Structure

Micro, meso and macro sized pores allow for a wide range of molecules of different dimensions to be adsorbed.

Micropore structure has been studied throughout literature and their shape is best described to be slit like. This has been tested by adsorption of both round and slit shaped molecules. It was found that the slit shaped molcules had a much higher adsorption rate. This was because they could be adsorbed into the narrow slit shaped micropores that provide the highest binding energy sites for adsorption due to the LDF attraction discussed above [H. Nowicki, 2014].

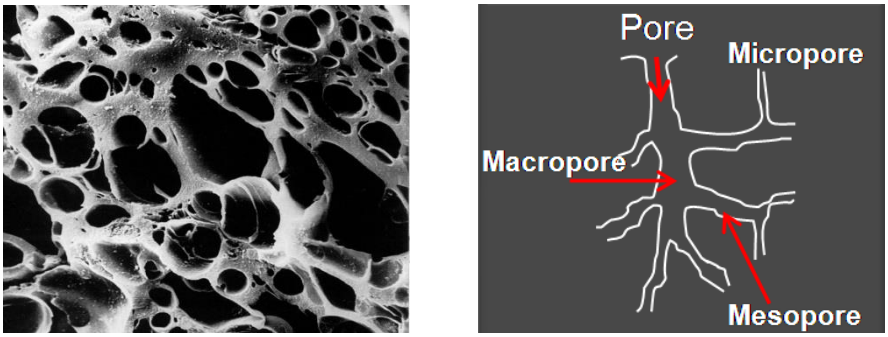


Figure 2:9 Pores under SEM (Scanning Electron Microscopy) along with labelled diagram of pore network [Alarco, 2010].

Over 90% of the molecules are adsorbed in the micropore region of the activated carbon. However, mesopores and macropores are also important as they facilitate the access of the molecules to the micropores. Surface area and microporosity are the usual parameters in defining the quality of activated carbon however, surface chemistry plays an important role in adsorption properties [Bansal, 2005].

The surface of an activated carbon can bind molecules from gaseous and liquid phases by predominantly physical forces of VDW type, causing high concentration at the surface. Chemisorption is also possible with stronger bonds on activated carbon active sites. This makes activated carbon suitable for industrial applications.

During adsorption macropores and mesopores allow rapid transport of the adsorbate into microporous areas. Without macro and mesopores it would be hard for the adsorbate to reach the microporous region. A well-developed porous network containing all three sizes aids adsorption properties. Martínez, Torres *et al.*, [2006] report carbons obtained with walnut shells contained a predominance of macropores. Olive stone activated carbon gave a greater variety of randomly distributed pore size. Olive stone and walnut shells differ in their microscopic characteristics and adsorptive properties but with both as particle size decreased surface area increased. This report shows that each precursor and each change in process condition can have a big effect on the pore network. The pore network needs to be developed specifically relevant to the application it is to be used for.

2.13 Surface Groups

Surface groups are seen as an important factor to consider with activated carbons. Carbons contain heteroatoms (H, S, O, and N) in addition to carbon and inorganic matter. Sulphur, nitrogen and oxygen can be bonded to edge atoms or in within the graphene layers. These atoms can affect carbon properties, in particular edge bonded oxygen [Marsh and Reinoso, 2006]. Many oxygen surface groups can be present as shown below:

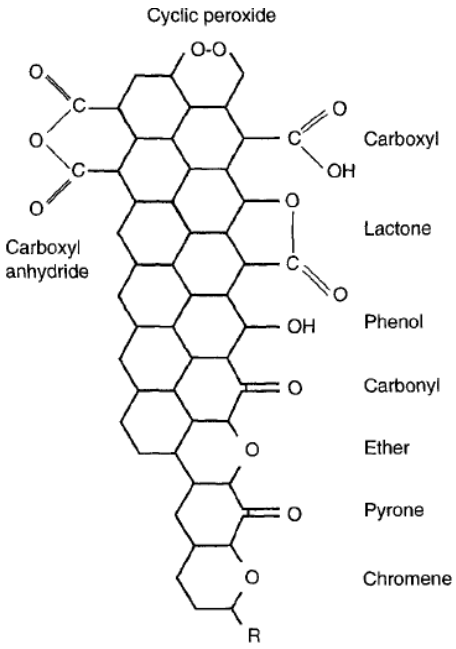


Figure 2:10 Oxygen surface groups found in carbons [M Sabio, 1998].

Different precursors and oxidising agents can affect which groups and quantities are present. The surface groups can also have an impact on the pH of the carbon. However, according to Reinoso, [1998]; Reinoso and Sabio, [1998] basicity is not entirely associated with surface groups. Carbon exhibits basic characteristics on equilibrium with water and the carbon basicity is still being investigated [Marsh and Reinoso, 2006]. Marsh and Reinoso, [2006] also summarise that oxygen surface groups did not offer advantages to the adsorption process from both gas and liquid phases. However, in terms of polarity created, the increased adsorption of polar molecules may be minimized by pore blockages.

2.14 BET Surface Area, Burn Off and Yield

Burn off is the term given to the amount of material lost during activation - it is given in terms of percentage and affects the percentage yield of the product. It is impossible to produce activated carbon without any burn off, as without burn off, a porous structure is impossible to make. Burn off percentage is related to temperature and time whilst the precursor also plays a large part [Yang and Lua, 2003].

Surface area is a crucial parameter for optimised porous carbons, however no single experimental technique will give the exact surface area due to the complexity within a micro and mesoporous carbon, Brunauer-Emmett-Teller (BET) is the technique usually used [Tascon, 2012].

BET surface area and burn off are linked together, as a higher burn off up until a point produces a higher BET surface area, but at the cost of the yield of the activated carbon. Bouchelta, Medjram *et al.*, [2008] investigated date stones as a precursor using SEM, X-ray diffraction and

Fourier transform infrared to analyse the pore structure along with Nitrogen adsorption to calculate the BET surface area. BET surface area allows one to see the total surface area of the activated carbon. In this case the surface area was recorded to be 635 m^2/g when the date stones were ground and pyrolysed at 700 ^oC under 100 cm^3/min flow of nitrogen. The biomass char was then subjected to steam activation at 700 ^oC for 6 hours. However, a 6 hour activation time meant yield decreased from 24.51% to 13.62%

Studies have also been conducted on the differences in BET surface areas for steam and CO_2 activation. Toles, Marshall *et al.,* [2000] discovered their carbons produced a higher BET surface area with steam when compared to CO_2 activation. The study also deduced that the higher the activation temperature usually meant BET surface area increased up until a certain point where external surface burn off commenced. Zarifah, [2010] also backed this up by reporting BET surface area increased with an increase in activation temperature, but a large BET surface area does not specifically mean that the carbon is of higher quality than a carbon with a lower surface area as it depends of pore size distribution [Marsh and Reinoso, 2006].

Increasing the activation temperature enhances existing pores and also forms new pores, due to de-volatilisation and carbon burn off. This is backed up by studies conducted by Demiral, Demiral *et al.,* [2011] who report as activation temperature was increased from 750 ^oC to 900 ^oC the weight loss of the sample also increased. This happened due to volatile release and carbon burn off through carbon-steam oxidation. Increase in burn off also increases surface area as Nabais, Laginhas *et al.,* [2011] add, with their higher burn off samples producing higher BET surface areas.

There is a compromise that must be met. A large burn off percentage can mean a very well developed porous activated carbon, but burn off percentage can be very important in relation to economics as well as to activated carbon quality. It is important that a happy medium is met i.e. the process should produce a high enough yield to be profitable but also one that can produce a sufficiently high quality product. High burn off allows larger pore volume but too high and it can damage the activated carbon by widening pores causing collapse. The collapse or 'melt', was also seen by Yang and Lua [2003] who studied two-step physical activation with olive stones used as the precursor. Activation temperature and residence time were found to be key parameters that affect activated carbon. In addition carbon dioxide flow rate and heating rate were studied. Initial pore increase occurs with increasing dwell time to a point. This point is known as a 'melt', and when this point is reached a melt occurred and closed some pores. Additionally too long a dwell time results in micropore widening and pore structural collapse. A severe C-CO_2 reaction was seen when activation temperature increased over 850 ^oC and BET surface area was found to peak 0.5 hours later than when micropore volume peaked testing with

olive stones [González, Molina-Sabio *et al.,* 1994]. Increased flow rates of carbon dioxide enhanced the reaction and burn off which resulted in a decreased yield. Flow rate should be increased to maximise BET surface area but after that is not necessary to increase further. Too high a flow rate can affect diffusion rates, decrease contact time and lead to a reduced BET surface area. Heating rate can affect BET surface area, with higher heating rates usually aiding diffusion due to higher thermal gradient across char, with resultant pore widening. Too high a heating rate and the BET surface area decreased due to a shorter contact time for C-CO_2 reaction causing a reduction in pore formation. Heating rate of 10 ^oC/min was used. [González, Molina-Sabio *et al.,* 1994].

Demiral, Demiral *et al.,* [2011] Activated carbons produced had BET surface area from 523 m^2/g to 1106 m^2/g. This coincides with Bansal, [2005] who reports that these values are in the typical range of BET surface area size within activated carbon. Adsorption was demonstrated with iodine numbers. Microporosity was measured by scanning electron microscopy. The iodine number increased with increasing BET surface area - the iodine number is an indication of the adsorption capacity in micropore region.

Martínez, Torres *et al.,* [2006] also looked into iodine numbers and what are the main conditions that affect adsorption. The results showed that the characteristics of the starting materials, activating agent concentration and carbon particle size influenced the iodine adsorption capacity. In addition to these conditions, weight loss during the carbonisation stage also influenced iodine adsorption. The study involved the use of olive stones and walnut shell and the results were that olive stone activated carbon was more effective in iodine adsorption than walnut shell. However, this was also dependant on carbon particle size as particle size reduction (granular to power) increases adsorption capacity due to surface area increase; the standard method used for iodine tests requires the granular carbon to be crushed.

Zhu, Gao *et al.,* [2012] compared both carbon dioxide and steam activation and found that at higher burn off for both series (CO_2 and H_2O) nitrogen adsorption increased as micropores widened. With steam activation an increase of adsorption was found up to 50% burn off, after which a decrease occurred. With carbon dioxide, above 50% burn off the adsorption increase slowed a little. This was down to pore size distribution and functional properties of the activated carbons. Microporous regions fill first with nitrogen at very low pressures and as pressure increases the mesoporous regions start to fill [Bouchelta, Medjram *et al.,* 2008].

Table 2-6 Residence time and activation temperature effect on yield of activated carbon [Yang and Lua, 2003].

Effect of activation dwell time[a]						
Dwell time	0.5 h	1.0 h	1.5 h	2.0 h	2.5 h	3.0 h
Yield (%) (series A)	24.3	22.7	19.8	14.4	12.5	10.5
Yield (%) (series B)	23.8	22.1	19.3	14.3	12.2	10.3
Effect of activation temperature[b]						
Temperature	725 °C	750 °C	775 °C	800 °C	825 °C	
Yield (%) (series A)	23.9	23.3	19.8	14.4	8.2	
Yield (%) (series B)	20.9	20.0	18.1	12.2	7.2	

2.15 Precursors Used for Activated Carbon Production with Optimal Activation Conditions

Lignocellulosic materials are good and cheap precursors for the production of activated carbon [Tay, Ucar *et al.*, 2009]**.** A wide range of biomass precursors have been studied and below are examples of the types of biomass used for activated carbon production. This section covers the activation conditions in which the best quality carbon was produced.

Table 2-7 Biomass studied

Biomass	**Reference**
Coconut shell	[Li, Yang et al., 2008]
Palm kernel shell	[Rashidi, Yusup et al., 2012]
Olive stones	[Rodríguez-Reinoso, Molina-Sabio et al., 1995]
Walnut shells and olive stone	[Martínez, Torres et al., 2006]
Pistachio nut shells	[Yang and Lua, 2003]
Olive bagasse	[Demiral, Demiral et al., 2011]
Date stone	[Sekirifa, Hadj-Mahammed et al., 2013]
Waste Algerian date stones	[Bouchelta, Medjram et al., 2008]
Soybean oil cake	[Tay, Ucar et al., 2009]
Apricot stones	[Gergova and Eser, 1996], [Şentorun-Shalaby, Uçak-Astarlıog˘lu *et al.*, 2006]
Rubber seed	[Sun and Jiang, 2010]
Agricultural waste	[Aworn, Thiravetyan et al., 2008]
Waste newspaper	[Okada, Yamamoto et al., 2003]
Sewage sludge	[Chen, Jeyaseelan et al., 2002]
Palm oil wastes	[Dias, Alvim-Ferraz et al., 2007]
Eucalyptus wood	[Amaya, Medero et al., 2007]
Waste tyres	[Mui, Cheung et al., 2010]
Acorn shell	[Şahin and Saka, 2013]
Waste plastics	[Esfandiari, Kaghazchi et al., 2012]

These are just a few examples of different types of biomass that have been studied. There is a vast amount of different biomass that has been used as precursors with specific biomass performing much better than others. The performance of each precursor is usually down to a number of factors, such as structure and the many process conditions. In this section the basic structure of the precursor is considered.

There are two basic categories of biomass and these are 'hard' biomass and 'soft' biomass. Each category is defined by the structure of the biomass and mainly to do with moisture and carbon content. Hard biomass tends to have much lower moisture content and higher carbon content. This means hard biomass is seen as the preferred choice when it comes to activated carbon production and this is backed up by many literature sources, for example by Soleimani and Kaghazchi, [2008]. 'Hard shell of fruit stones such as apricot stones and pistachio are very hard materials, a property that makes them an alternative precursor for granular activated carbons since loss due to attrition of the particle is undesirable'. This was in relation to hard shells being better for activated carbon production as opposed to agricultural waste that can mostly be classed as soft biomass. Acharjee, Coronella *et al.,* [2011] reports that hard biomass is preferred due to cost of pre-treatment. Biomass should be as dry as possible when being carbonised as otherwise 'wet' biomass can mean longer pyrolysis time which in turn means more energy required for the process. Biomass should be kept dry during storage and go through a drying process if already wet, this can help prevent mould growth that can lower the calorific value, and can add additional cost of drying the biomass in the pre-treatment stage.

2.15.1 Olive Stones and Walnut Shell

Studies such as Martínez, Torres *et al.,* [2006] compare precursors and their effectiveness as activated carbons. In this case olive stones were compared to walnut shells. Iodine adsorption was used to test porosity and, under the same conditions, olive stone was found to be more porous. However, this was dependent upon particle size. Particle size reduction of the precursor char (granular to powder) was found to increase adsorption rate. Walnut shells contained a predominance of macropores whereas olive stone activated carbon gave a variety of randomly distributed pore size. This all meant that olive stone and walnut shell differed in their microscopic characteristics and adsorptive properties. Behaviour of these materials seemed to be in relation to their external surface texture. Samples were pyrolysed at 600 ^{o}C for 1 hour in inert atmosphere (N_2) activation temperature carried out at 900 ^{o}C for 1 hour.

González, Molina-Sabio *et al.,* [1994] studied physical activation (steam). The temperature of this was 800 ^{o}C to 850 ^{o}C, with a steam flow rate of 100 to 300 ml/min. The steam flow rate was seen to affect macroporosity as opposed to micro and mesoporosity, especially at low burn offs. Low activation temperature (800 ^{o}C) was seen to favour widening of pores and higher

activation temperature (850 ºC) was seen to increase general porosity. Above this temperature pore size started to decrease, again due to pore deformation caused by high reaction rates.

Román, González *et al.*, [2008] Olive stones were shredded to 1 mm to 1.6 mm and were carbonised at 600 ºC for 1 hour. Activation was conducted by steam and carbon dioxide. Activation temperatures were between 650 ºC and 950 ºC and residence times between 20 to 120 minutes.

Table 2-8 Burn off, surface area and pore volumes [Román, González *et al.*, 2008].

Series	Sample	Burn-off (%)	S_{BET} ($m^2 g^{-1}$)	V_{miG} ($cm^3 g^{-1}$)	V_{meG} ($cm^3 g^{-1}$)	$S_{ex\,(t)}$ ($m^2 g^{-1}$)	$V_{mi\,(t)}$ ($cm^3 g^{-1}$)
Char		79	209	0.089	0.016	114	0.094
CO_2	C-850-30	19.3	446	0.243	0.021	56	0.223
	C-850-60	36.5	572	0.319	0.036	90	0.287
	C-850-90	45.9	761	0.406	0.059	124	0.361
	C-850-120	65.3	778	0.406	0.068	177	0.342
	C-900-60	37.9	603	0.300	0.072	139	0.266
Steam	S-800-30 (2.4)	46.9	808	0.426	0.067	166	0.366
	S-850-30 (2.4)	49.5	813	0.427	0.076	174	0.363
	S-850-20 (1.6)	28.1	589	0.312	0.042	101	0.276
	S-850-20-F (3)	68.7	713	0.358	0.091	233	0.301
	S-900-30 (2.4)	53.4	437	0.216	0.067	155	0.161
	S-850-60 (4.8)	82.5	1074	0.525	0.124	417	0.377
CO_2/steam	CS-850-30	37.1	674	0.357	0.057	125	0.312
	CS-850-60	76.5	1187	0.553	0.148	469	0.384

Zabaniotou, Stavropoulos *et al.*, [2008] investigated olive kernels which were pyrolysed at 800 ºC for 45 minutes in an inert (N_2) atmosphere. Chars were then subsequently activated with carbon dioxide and steam at 970 ºC producing the maximum BET surface area of 1000 m^2/g to 1200 m^2/g. BET surface area with steam activation increases with residence time, the maximum time was 2.5 hours, after which pore destruction occurred. An increased BET surface area meant an increased burn off, negatively affecting the product yield.

2.15.2 Chicken Waste

Yang Zhang *et al.*, [2007] activated carbons were made from chicken waste and coal blended at different ratios from 100% chicken waste to 100% coal. Pyrolysis took place at 430 ºC for 60 minutes with a nitrogen flow rate of 300 ml/min. Physical activation took place at 650 ºC for 60

minutes with a nitrogen flow rate of 100 ml/min and water flow rate of 0.1 ml/min. Chicken waste has low sulphur content but high volatile content (55 wt%). Activated carbons produced had high surface areas when mixed with coal.

Table 2-9 Coal and chicken waste ratio with BET surface area using nitrogen and carbon dioxide as adsorbent [Yang Zhang *et al.,* 2007].

	N_2		CO_2	
coal fraction	specific surface area: SSA_{BET} (m^2/g)	pore diameter (nm)	specific surface area: SSA_{BET} (m^2/g)	pore diameter (nm)
0	128	2.78	164.2	1.04
0.2	203	2.27	203.6	1.27
0.5	235	2.23	230.0	1.30
0.8	248	1.30	247.0	1.30
1	250	1.68	263.9	1.35

Another study on chicken waste was conducted by Huang, Jin *et al.,* [2008] their chicken waste was dried at 200 ^oC before it was subject to pyrolysis in N_2 atmosphere at 400 ^oC to 600 ^oC. Activation was carried out using carbon dioxide as the oxidising agent at 700 ^oC to 900 ^oC with a residence time of 1 to 2.5 hours. Results showed that chicken waste activated carbon has the same mercury capacity as commercial activated carbon, although the total surface area of this activated carbon is 10 times smaller than typical commercial activated carbon. The maximum BET surface area was recorded at 89.5 m^2/g at 800 ^oC with a holding time of 2 hours. Macropores have very low surface areas compared to micropores. A highly macroporous carbon therefore is likely to have a small surface area. This explains why Huang, Jin *et al.,* [2008] chicken waste carbons can still perform as other commercial carbons for mercury adsorption despite a lower surface area as mercury is adsorbed into the macropore region.

2.15.3 Date Stones

Bouchelta, Medjram *et al.,* [2008] studied precursor composition using date stones. Results show cellulose and hemi-cellulose in raw material and predominance of carbon and graphite after pyrolysis. Pyrolysis yield becomes constant during activation when temperatures increased over 700 ^oC due to all cellulose and hemicellulose being decomposed at these temperatures, whereas the other component lignin decomposes at higher temperatures. The removal of cellulose and hemi-cellulose produces pores; lignin then reacts with the oxidising agent (CO_2 or H_2O). The optimum conditions to achieve the highest surface area of 635 m^2/g and a microporous volume of 0.716 cm^3/g are obtained with grinded date stones pyrolysed at 700 ^oC under a nitrogen flow of 100 cm^3/min followed by steam activation at 700 ^oC for 6 hours.

Sekirifa, Hadj-Mahammed *et al.,* [2013] used carbon dioxide as opposed to steam. The BET surface area recorded was 604 m^2/g with a micropore volume of 0.29 cm^3/g. Pyrolysis was carried out in the range of 700 ^oC to 900 ^oC. With a heating rate 150 $^oC/min$ and under a nitrogen

flow of 250 ml/min. Activation was carried out at 900 ºC. Data shows date stones can be used for activated carbon production as they produced a well-developed pore structure by pyrolysis and physical activation with steam. The key points to note were that date stones required a low cost operation to form adequate activated carbon and when the process conditions were optimised date stones proved to be a very good precursor.

2.15.4 Almond Shell

Nabais, Laginhas *et al.,* [2011] conducted thorough studies on almond shell with physical activation. The results showed that almond shell, using carbon dioxide as the oxidising agent, proved to produce a high quality activated carbon with good physical and chemical properties in terms of adsorption, mechanical strength and surface chemistry. A low temperature pyrolysis took place at 400 ºC to lower costs. Final product was comparable to other literature showing low temperature pyrolysis can work. 800 ºC was seen as the optimal activation temperature as this produced the highest BET surface area of up to 1138 m^2/g with a micropore volume of 0.24 cm^3/g to 0.49 cm^3/g.

Toles, Marshall *et al.,* [2000] investigated almond shell as a precursor and found that optimum conditions, when using carbon dioxide as the oxidising agent, were a pyrolysis of 1 hour at 700 ºC followed by 2 hours activation at 800 ºC using 75% CO_2 and 25% N_2. For steam activation, a pyrolysis of 1 hour at either 700 ºC or 800 ºC followed by 2 hours activation at 800 ºC with a water flow rate of 7.0 ml/min.

2.15.5 Eucalyptus

Amaya, Medero *et al.*. [2007] show how carbon briquettes can be made when high mechanical strength is needed in a continuous or cyclic process. Activated carbon produced by eucalyptus in previous studies showed low mechanical strength even after briquetting. Therefore eucalyptus should not be used for high mechanical strength applications. However, using a mixture of eucalyptus, rice husk (10%) and grape must as a binder significantly improved mechanical strength. Even so, under very harsh conditions other alternatives should be considered. This type of study shows how precursors can be enhanced by mixing with other types of biomass to increase the quality of activated carbon produced that can then be used to meet specific requirements.

Pyrolysis was carried out at 500 º C with a heating rate of 1.4 ºC/min. Once the temperature had reached 500 ºC it was held for 2 hours. The chars were then uniformly sized to make sure all were smaller than 0.18 mm. Briquettes were then made by mixing in mortar. Steam then was used as the activating agent and temperature ranged from 880 ºC to 920 ºC with either 1.7 g or 2.5 g of steam per g of char. The residence time was between 105 minutes and 150 minutes.

2.15.6 Algarroba Wood

Matos, Nahas *et al.,* [2011] used algarroba wood, the maximum surface area was found with activation conditions of 800 ^{o}C under CO_2 and N_2 gaseous flow and a heating rate of 10 ^{o}C. Ultra microporous activated carbon with pore diameters of 6.7 Å were obtained at 900 ^{o}C. Pore structure could easily be altered by changing activation temperature. Pyrolysis was conducted at ranges between 200 ^{o}C and 900 ^{o}C with a heating rate also at 10 ^{o}C/min.

2.15.7 Apricot Stones

Şentorun-Shalaby, Uçak-Astarlıogˇlu *et al*., [2006] showed that activated carbons produced by apricot stones exhibited large nitrogen adsorption showing a well-developed micropore structure. These specific activated carbons were produced via a one-step mechanism of both pyrolysis and physical activation. The micropore volumes of activated carbons varied in the range of 0.02 cm^3/g to 0.037 cm^3/g. Yields were found to be 25.7% to 5.2% with activation temperature at 650 ^{o}C to 800 ^{o}C for 1,2, and 4 hours. For optimum process conditions, and to achieve a high surface area, the temperature of activation should be kept within the range of 750 ^{o}C to 800 ^{o}C and soak time for around 3 to 4 hours. Activation at 800 ^{o}C and 4 hours gave highest pore volume (0.63 cm^3/g) and micropore volume at (0.37cm^3/g).

2.15.8 Coconut Shell

Li, Yang *et al.,* [2008] used coconut as a precursor for activated carbon production. The optimum conditions that produced the highest BET surface area, total volume and micropore volume of activated carbon prepared from the char, was a carbonisation temperature of 1000 ^{o}C, activation (steam) temperature of 900 ^{o}C and a dwell time of 120 minutes. However, at these temperatures and dwell times the yield was low. Therefore one has to balance porosity with yield, taking into account the economic viability of the process.

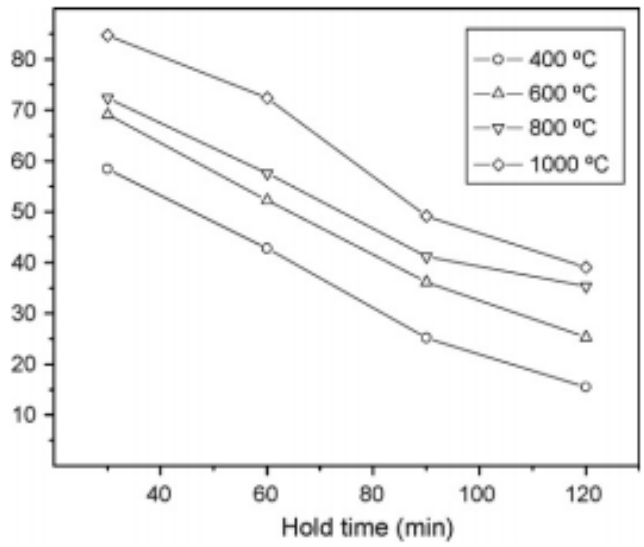


Figure 2:11 Yield (%) against hold time (mins) [Li, Yang *et al.,* 2008].

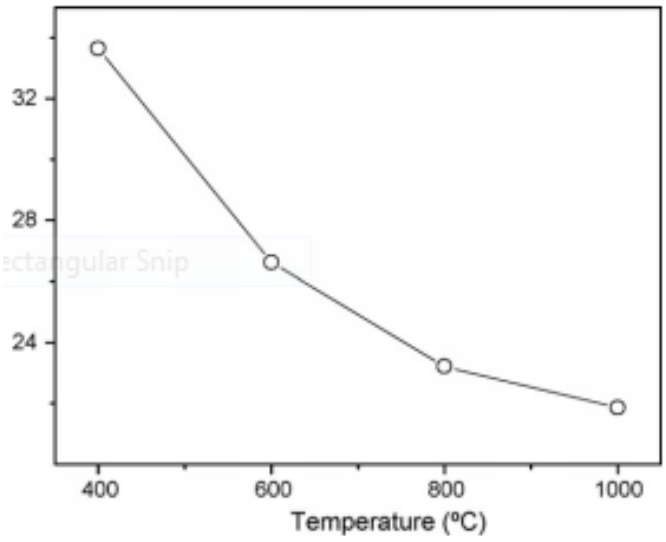


Figure 2:12 Yield (%) against activation temperature (°C) [Li, Yang *et al.*, 2008].

2.15.9 Palm Kernel Shell

Zarifah Nadiah, [2010] used palm kernel shell for activated carbon production and showed that 1000 °C is the optimum temperature to carbonise and an activation time 1 to 3 hours at 800 °C to achieve maximum surface area.

Arami-Niya, Daud *et al*.. [2011] also used palm shell, carbonised for 1 hour at 900 °C, heating rate of 10 °C/min, carbon dioxide flow rate of 100 ml/min, activation temperature of 850 °C for 1 to 7 hours. BET surface areas along with pore and micropore volume are shown in Table 2-10 below

Table 2-10 Results at different burn off percentage on BET surface area, total pore and micropore volume [Arami-Niya, Daud *et al.*, 2011].

Sample	Burn-off (%)	S_{BET} (m^2/g)	V_{Micro} (cm^3/g)	V_{Total} (cm^3/g)	D (nm)
CZ1	0	728	0.35	0.36	1.9
CZ3	7.2	737	0.36	0.38	1.95
CZ5	11.6	863	0.43	0.44	2.01
CZ7	12.61	1118	0.42	0.51	2.24
CP1	21.75	1066	0.56	0.57	1.95
CP3	38.25	1542	0.78	0.8	1.99
CP5	61.75	1653	0.89	0.94	2.27
CP7	73	1035	0.54	0.69	2.67
C1	5.75	554	0.26	0.27	1.95
C3	30.5	707	0.35	0.37	2.09
C5	36.5	896	0.44	0.48	2.11
C7	51.25	1213	0.58	0.66	2.13

2.15.10 Pistachio Nut Shells

Yang and Lua, [2003] looked into pistachio nuts. The process conditions were as follows: The shells required drying at 110 °C for 12 hours to reduce moisture content. Particle size in the range of 1 mm to 2 mm. Nitrogen gas at a flow rate of 150 cm^3/min flowed over a 10 g sample. A 10 °C/min heating rate was selected during pyrolysis to reach a final temperature of 500 °C with a dwell time for 2 hours. Optimum activation conditions for this experiment were an activation temperature of 800 °C with a dwell time of 2.5 hours. Carbon dioxide was used as the oxidising agent and had a flow rate of 100 cm^3/min. The maximum BET surface area under these conditions was found to be 1064.2 m^2/g.

In another study by Yang and Lua, [2004] the effects of pyrolysis temperature was studied on pistachio nut shells and the char composition. The optimum pyrolysis conditions were found to be a temperature of 500 °C with a 2 hour hold time, heating rate of 10 °C/min, and a nitrogen flow rate of 150 cm^3/min. This char went onto produce the carbon with the highest surface area.

Table 2-11 Pyrolysis temperature effects on pistachio nut composition [Lua, Yang *et al*. 2004].

Pyrolysis temperature (°C)	Char (wt.%)			Activated carbon (wt.%)		
	Volatile content	Fixed carbon	Ash	Volatile content	Fixed carbon	Ash
250	64.8	34.2	1.0	21.3	77.0	1.7
300	43.0	55.9	1.1	18.0	80.1	1.9
400	34.5	64.4	1.1	16.5	81.6	1.9
500	25.4	73.5	1.1	15.7	82.2	2.1
600	22.7	76.1	1.2	12.7	84.9	2.4
700	20.1	78.1	1.8	12.1	85.1	2.8
800	16.4	81.7	1.9	12.3	84.2	3.5
900	11.8	86.2	2.0	10.4	85.7	3.9
1000	9.5	88.4	2.1	8.1	88.4	3.5

[a] Pyrolysis conditions: hold time = 2 h, nitrogen flow rate = 150 cm^3/min, heating rate = 10 °C/min.
[b] Dry basis means that the proximate analyses were based on the sample without moisture content.

The final conclusion from the two studies was that moderate BET surface area activated carbons can be produced by pistachio nut shells.

2.15.11 Acorn Shell

Şahin and Saka, [2013] investigated activated carbons prepared using acorn shell with physical activation. Carbon dioxide was used first by being passed through water with a flow rate of 100 cm^3/min. The activation temperature used was 850 ^oC. The maximum BET surface area was found to be 1779 m^2/g. Adsorption capacity was demonstrated with iodine numbers with the maximum found at 825 mg/g. Maximum yield found at a pyrolysis temperature of 600 ^oC for 30 minutes with at 10 ^oC heating rate under nitrogen atmosphere found in a previous report [Saka 2012].

2.15.12 Polyethyleneterephthalate (PET) wastes

The optimum conditions were found for PET wastes. This included carbonisation at 800 ^oC for 1 hour, activation temperature 975 ^oC, 4 hours dwell time, heating rate of 10 ^oC/min, N_2 flow rate of 200 ml/min and a CO_2 flow rate of 100 ml/min. A burn off of 65% occurred during this point. Iodine number for these activated carbons was recorded at 630 mg/g with a BET surface area of 790 m^2/g [Esfandiari, Kaghazchi *et al.*, 2012].

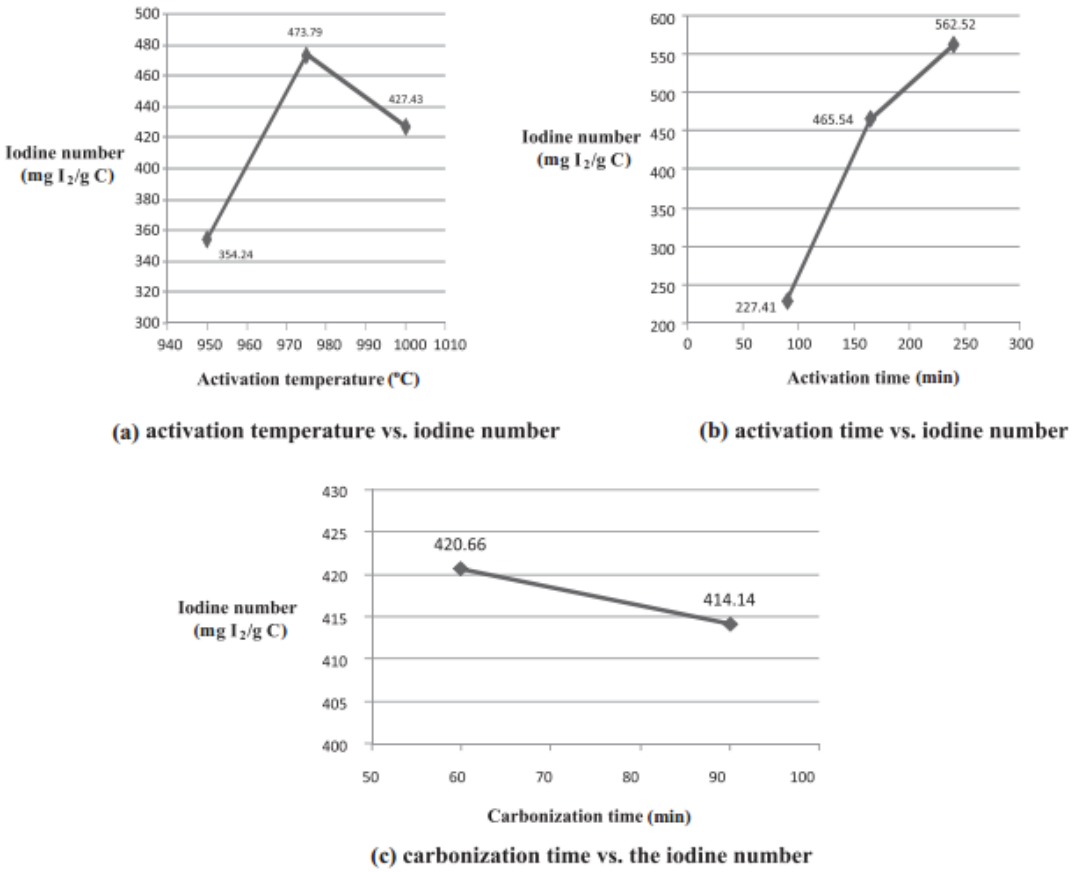


Figure 2:13 Iodine numbers against activation temperature (a), activation time (b) and carbonisation time (c) [Esfandiari, Kaghazchi *et al.*. 2012].

2.15.13 Olive bagasse

Demiral, Demiral *et al.*, [2011] investigated olive bagasse as an activated carbon precursor. Here the physical activated carbon produced a maximum BET surface area of 1106 m^2/g at an activation temperature of 900 ^oC with an activation time of 45 minutes. The carbonisation temperature was carried out at 500 ^oC due to it being the optimum temperature for maximum yield whilst still developing the pore network. Olive bagasse was found to produce a mainly microporous activated carbon. The activation temperature ranged from 750 ^oC to 900 ^oC. Weight loss increased with increasing activation temperature due to more volatile loss and carbon burn off.

Table 2-12 Olive bagasse activation time and the effects this has on surface area and pore volume [Demiral, Demiral *et al.*, 2011].

ID	T (°C)	Activation time (min)	S_{BET} (m^2/g)	S_{micro} (m^2/g)	V_T[a] (cm^3/g)	V_{micro} (cm^3/g)	V_{meso} (cm^3/g)
C750/30	750	30	523	397	0.2757	0.1989	0.0768
C800/30	800	30	679	585	0.3197	0.2697	0.0500
C850/30	850	30	714	550	0.3927	0.2730	0.1197
C900/30	900	30	947	619	0.4916	0.3635	0.1211
C750/45	750	45	584	357	0.3501	0.2639	0.0862
C800/45	800	45	692	425	0.3925	0.2790	0.1195
C850/45	850	45	803	520	0.4723	0.3002	0.1721
C900/45	900	45	1106	659	0.6067	0.4012	0.2055
C750/60	750	60	617	452	0.3816	0.2839	0.0977
C800/60	800	60	735	504	0.4084	0.2981	0.1103
C850/60	850	60	824	516	0.4886	0.3313	0.1573
C900/60	900	60	915	608	0.4695	0.3684	0.1011
Olive bagasse char	15	–	0.0095	0.0061	0.0033		

2.15.14 Soybean Oil Cake

Tay, Ucar *et al.*, [2009] produced activated carbon by chemical activation (K_2CO_3) with soybean oil cake. The maximum surface area was obtained at 800 ^oC activation temperature and was recorded at 1352.86 $m^{2/}g$.

2.15.15 Sewage Sludge

Chen, Jeyaseelan *et al.*, [2002] used sewage sludge which was first dried (103 ^oC, 24 to 36 hours), made into uniform size 0.5 mm to 2 mm and impregnated with 25 ml of 5 M $ZnCl_2$. A 10 g sample was carbonised at 500 ^oC for 2 hours under a nitrogen atmosphere and heating rate of 15 ^oC/min. Sewage sludge was found to have 'remarkable' micropore and mesopore surface areas and adsorption capacities for carbon tetrachloride and phenols.

2.15.16 Waste Newspaper

Okada, Yamamoto *et al.*, [2003] produced activated carbon from waste newspaper. The study involved both physical and chemical activation. The maximum value of BET surface area was 1090 m^2/g. The optimum conditions for physical activation were as follows:- Carbonisation was first carried out at 600 ^oC for 2 hours in inert atmosphere (N_2). Physical activation took place using steam at 850 ^oC for 2 hours with N_2 gas at 20 mol% and a water flow rate of 0.5 ml/min.

This was done via both a single step (carbonisation and activation simultaneously) and a two-step process. The single step process showed slightly better properties in regards to pores but a lower yield than the two-step process. The paper retained its shape after activation.

Table 2-13 Single and two-step activation process for waste newspaper and the effects this has on yield, surface area and pore volume [Okada, Yamamoto *et al.,* 2003].

Method	Temp. (°C)	H_2O/gas (mol%)	Flow rate (l/min)	Time (h)	Supplied H_2O (g)	Yield (%)	S_{BET} (m^2/g)	V_P (ml/g)
Single-step	850	20	0.5	2	9.64	10.6	1086	1.01
Two-step	850	20	0.5	2	9.64	11.2	1008	0.90
Single-step	900	31	1	0.5	7.47	10.2	1043	0.98
Two-step	900	31	1	0.5	7.47	12.5	945	0.80
Single-step	900	31	0.25	1	3.74	9.6	957	1.01
Two-step	900	31	0.25	1	3.74	10.1	940	0.97

2.15.17 Agricultural Waste:

Macadamia nut shell, corncob, bagasse bottom ash, pistachio nuts, sawdust fly ash and rice husk fly ash.

Aworn, Thiravetyan *et al*., [2008] tested agricultural waste and the optimum conditions depended on the raw material used (see Table 2-14). The volatile matter in the material that provided an activated carbon with the largest surface area was in the region of 17% to 25% (see Table 2-14). For a microporous carbon the study found that when using Macadamia nut shell steam activation was preferred and, when using corncob, carbon dioxide activation was preferred. Mesoporous activated carbon, suitable for larger molecule adsorption due to larger sized pores, was found to be produced by bagasse bottom ash by steam and sawdust by carbon dioxide activation. Rice husk fly ash was not suitable for activated carbon due to less volatile matter, low fixed carbon and high ash content resulting in low surface area.

Table 2-14 Five types of agricultural waste compositions [Aworn, Thiravetyan *et al.*, 2008].

Chars	Proximate analysis (dry basis wt.%)		
	Volatile matter	Fixed carbon	Ash
Corncob			
300 °C	39.7	57.5	2.8
400 °C	27.6	69.6	2.8
500 °C	20.7	76.0	3.3
600 °C	16.5	80.7	2.8
800 °C	14.3	81.9	3.8
Bagasse bottom ash			
300 °C	18.1	57.5	24.4
400 °C	15.8	59.7	24.5
500 °C	15.4	59.1	25.5
600 °C	15.1	59.0	25.9
800 °C	10.5	60.7	28.8
Sawdust fly ash			
400 °C	31.9	55.7	12.4
500 °C	24.7	61.7	13.6
600 °C	17.7	66.9	15.4
800 °C	16.1	67.9	16.0
Macadamia nut-shell			
400 °C	28.3	70.6	1.1
500 °C	17.4	81.8	0.8
600 °C	11.8	87.4	0.8
800 °C	8.4	90.5	1.1
Rice husk fly ash			
500 °C	14.9	39.7	45.4

Optimum temperatures and residence time can be seen in the table below, with pistachio nut shell having the largest surface area.

Table 2-15 Agricultural waste carbonisation and activation conditions along with surface area [Aworn, Thiravetyan *et al.*, 2008].

Material	Carbonization conditions	Activation conditions	S_{BET} ($m^3 g^{-1}$)	V_T ($cm^3 g^{-1}$)
Corncob	500 °C in N_2 (2 h)	–	39	0.075
	500 °C in N_2 (2 h)	Steam at 850 °C (1 h)	607	0.296
	Pre-heated to 350 °C	Steam at 350 °C continued up to 600 °C (2 h)	618	0.321
	Pre-heated to 350 °C	Steam at 350 °C continued up to 700 °C (2 h)	786	0.430
Sawdust	500 °CiuN_2 (1 h)	Steam at 800 °C (1 h)	516	–
Bagasse	450 °C in N_2	Steam at 750 °C (2 h)	446	0.287
	450 °C in N_2	Steam at 780 °C (2 h)	545	0.342
	450 °C in N_2	Steam at 810 °C (2 h)	593	0.401
	450 °C in N_2	Steam at 840 °C (2 h)	607	0.445
Pistachio nut-shell	500 °C in N_2 (2 h) (series A)	CO_2 (200 cm^3 mm^1) at 800 °C (1 h)	884	–
	500 °C in N_2 (2 h) (series B)	CO_2 (200 cm^3 min^{-1}) continued up to 800 °C (2.5 h)	964	–
Macadamia nut-shell	700 °C in N_2 (2 h)	CO_2 at 500 °C (4 h)	750	–
Bagasse	Impregnated with HCl (4:3 w w^{-1}). Heated at 160 °C (2 h)	CO_2 at 900 °C (1 h)	614	0.31

2.15.18 Rubber Seed Shell

Sun and Jiang, [2010] used rubber seed as a raw material for activated carbon. Results showed that rubber seed shell is a good precursor for activated carbon. The optimal conditions for steam activation: activation temperature of 880 °C, water flow of 6 kg/h, residence time of 60 minutes. The yield produced in this instance was 30.5% with a BET surface area measurement of 948

m^2/g and total volume of 0.988 m^3/kg. An iodine number was given to be 1.326 g/g. Carbonisation temperature was carried out in the range of 450 °C to 600 °C.

Table 2-16 Activation of rubber seed shell at different temperatures and durations, with the row highlighted showing optimum conditions chosen for production [Sun and Jiang, 2010].

Sample	Temp. (°C)	Time (min)	Steam ($kg\,h^{-1}$)	Q_{iodine} ($mg\,g^{-1}$)	Q_{mb} ($mg\,g^{-1}$)	Yield (%)	Hardness (%)
1	820	40	4	742	75	64.0	95.4
2	820	60	6	913	90	52.6	94.8
3	820	80	8	905	105	52.0	94.3
4	850	40	8	867	150	48.5	94.7
5	850	60	6	996	195	43.0	94.0
6	850	80	4	979	120	50.2	94.4
7	880	40	8	1026	240	40.5	94.2
8	880	60	4	1141	255	30.5	92.8
9	880	60	6	1326	265	30.5	94.7
10	880	60	4	1043	255	26.7	91.2
11	880	80	8	1048	235	20.7	92.4
12	880	80	6	1268	245	17.6	91.0
13	880	80	8	1149	235	15.7	90.1

2.15.19 Waste Tyres

Mui, Cheung *et al.*, [2010] used waste tyres. Waste tyres can be a very cheap biomass to obtain due to the fact they are truly waste with little or no value and they are a concern to the environment in respect of their disposal. However, waste tyres can be used to produce activated carbon because of their high carbon content. Chemicals (acids) are needed in the process to remove unwanted materials, but the product can still be produced by physical activation. BET surface areas were measured up to 1000 m^2/g which are comparable to commercial activated carbons. However, it must be noted that these surface area recordings were in relation to the tyres that had gone through heavy chemical treatment using nitric acid. The activated carbons produced also possessed high mesopore volumes and so more suited to liquid adsorption. Pyrolysis was conducted at 500 °C with a 5 °C heating rate for two hours in an inert atmosphere (N_2). Activation took place from temperatures ranging from 750 °C to 1050 °C for 2 hours using CO_2 as oxidising agent. At a temperature of 1050 °C the BET surface area reached its maximum which was recorded at 483 m^2/g, but in reaching the maximum surface area yield dropped 63.2% at 950 °C to 20.2% at 1050 °C. Thus from an economical point of view the lower temperature may well be preferred if it meets required standards.

Betancur, Martínez *et al.*, [2009] also looked into waste tyres as precursors. Activation temperature in this study was conducted between 800 °C to 900°C and a reaction time of 1, 1.5, 2, 2.5 and 3 hours. The main findings were that activated carbon produced has a higher surface area the longer the activation lasted.

2.15.20 Peach Stone

Arriagada, García *et al.*, [1997]) used peach stones as the precursor for activated carbon and these were pyrolysed at 930 °C under nitrogen flow of 200 ml/min. Chars obtained were crushed

to a particle size of 1 mm to 2 mm and then activated with steam with a flow rate of 140 ml/min. Peach stones were found to produce a very microporous activated carbon in which macroporosity was almost absent.

Table 2-17 Precursor, activation method, BET surface area, pore volume and micropore volume of other selected precursors.[Li, Yang *et al.*, 2008].

References	Precursor	Activation method	S_{BET} (m^2/g)	V_{tot} (cm^3/g)	V_{micro} (cm^3/g)
Present work	Coconut shells	Physical (steam)	1926	1.260	0.931
Çiğdem et al. (2006)	Apricot stones	Physical (steam)	1092	0.51	0.37
Su et al. (2003)	Coconut shells	Physical (without activation agent)	663	0.23	
Achaw and Afrane (2007)	Coconut shells	Physical (35% steam, 65% N_2)	524	0.226	0.210
Gañán et al. (2006)	Almond tree pruning	Physical (CO_2)	840	0.55	0.39
Boonamnuayvitaya et al. (2005)	Coffee residue	Physical (steam)	469	0.362	0.170
Lua et al. (2006)	Oil-palm-shell	Physical (CO_2)	519		0.215
Bouchelta et al. (2008)	Date stones	Physical (steam)	635		0.716
Suzuki et al. (2007)	Rice bran	Physical (CO_2)	652	0.137	0.057
Azevedo et al. (2007)	Coconut shells	Chemical ($ZnCl_2$)	1266	0.731	0.676
Azevedo et al. (2007)	Coconut shells	Chemical activation with $ZnCl_2$ followed by physical activation	2114	1.307	1.142
Yang and Lua (2003)	Pistachio-nut shells	Physical (steam)	1064		0.21

Many different biomass samples have been studied for activated carbon production. The studies above have looked into different pyrolysis and activation conditions for producing activated carbons that exhibit a well-developed pore structure in most cases. The above information shows the temperatures to achieve maximum BET surface area. These may have to be altered to increase product yield but show an understanding of the temperature ranges required for such types of Biomass.

2.16 Regeneration of Activated Carbon

The project will cover both granular and powdered carbons. However it is granular carbon that is regenerated within industry and, therefore, is cheaper than producing fresh carbon.

Thermal regeneration is the most commonly used regeneration technique. There are others such as chemical, supercritical fluid, wet oxidation and solvent regeneration but thermal regeneration is used because it is cheaper than producing freshly made activated carbon and is seen as a more environmentally friendly approach. Activated carbon can be regenerated roughly 10 times before it incurs significant efficiency loses.

The process involves:

1. Adsorbent drying at approximately 105 °C.
2. High temperature desorption and decomposition (500 °C to 900 °C) under an inert atmosphere.
3. Residual organic gasification by an oxidising gas (steam or carbon dioxide) at elevated temperatures (800 °C).

The adsorbed volatile compounds are released when temperatures rise to the upper temperature set.

Characteristics of the activated carbon are determined by parameters of thermal regeneration process. If the regeneration conditions barely meet the requirements, activated carbon will lose some adsorption capacity and if conditions are too harsh the adsorption can be heavily altered for the worse. In addition to this, too harsh conditions cause burn off and leads to loss of activated carbon. Make-up carbon is used to replenish activated carbon lost, this usually equates to around (10% to 12%) of total mass. However, it can equal 20% to 40% to the cost of regeneration showing how freshly made new carbon is more expensive than regenerating used activated carbon.

Adsorption capacity, mass loss and regeneration granular strength are the main indicators as to how effective the regeneration process is. However these three indicators have antagonistic relations [Guo and Du, 2012]. More than 90% of granular activated carbon (GAC) surface is formed by carbon planes but there are heterogeneous functional groups also on the surface that can affect adsorption capacity along with the pore structure and pore surface area. For example, studies showed acidic functional groups on the surface show an increase in water adsorption. It is believed that the effect on functional groups in relation to adsorption bond formation is caused by three mechanisms, the π-π dispersion mechanism, hydrogen bond formation and electronic mechanism of complex formation. The π- π dispersion is where the oxygen containing functional groups act as an electron withdrawing group and can reduce electron density on the carbon skeleton. This weakens the role between adsorbate and adsorbent which leads to a decreasing adsorption rate. Hydrogen bonds can form with oxygen containing functional groups and adsorbents forming relatively strong bonds [Gup and Du, 2012].

Román, Ledesma *et al*., [2013] also looks into regeneration of activated carbon and the type of gases that are emitted during the regeneration process. The heating rate was found to have little effect on regeneration - even though a slower heating rate had a slight increase in porosity it was small, albeit it did in fact show a wider pore size. The temperature for regeneration is the major factor and was required to be at least 500 ^{o}C for maximum regeneration to take place. Between 500 ^{o}C and 700 ^{o}C a narrower pore size distribution occurred compared to 700 ^{o}C to 900 ^{o}C due to the fact that at higher temperature external burning may take place.

The higher the temperature, the improved decomposition of materials. However, higher temperature results in an increased cost of the process. Up to 79% efficiency was recovered simply from old activated carbon. According to Guo and Du, [2012] it is actually possible to achieve 100% of performance but this means a huge loss of activated carbon that would have to be replaced, leading to the process not making economic sense. It is best to strike a balance, i.e.

to keep the activated carbon quality high enough for the required application but not unnecessarily high that results in the costs rising enormously.

2.17 How to Minimise the Cost of Production of Activated Carbon

The cost of producing an activated carbon is key when going through all the stages in the process - from selecting the precursor, through pyrolysis and activation to the final product. Stavropoulos and Zabaniotou, [2009] look into ways of minimizing the cost of activated carbon. The report produced shows an economic evaluation of the activated carbon production process. The main findings from the report were that a raw material should be selected for highest yield possible whilst still producing a good activated carbon that meets specific requirements. The raw material takes up a large percentage of the cost and the cheaper the precursor the better, and if the precursor is a free-of-charge waste material even better still. Chemical activation was found to be slightly more cost effective than physical activation but requires licensing and chemical training. Product price should be based upon product surface area and adsorption capacity as opposed to weight of the product. Process conditions can be optimised to make savings. A precursor that requires low activation temperatures may be favoured even though the initial material price is higher. The whole process costs should be evaluated, not just the cost of individual sectors. Some raw materials may also need pre-treatments that can add to the cost both in OPEX and CAPEX (operational and capital expenditure) forms, so ideally the selected precursor would not need large amounts of pre-treatment.

Table 2-18 price of activated carbon produced from biomass feedstocks and activated by both physical and chemical methods [Stavropoulos and Zabaniotou, 2009].

Raw material	Heating value, kcal/kg	Raw material cost, $/kg	Product price, $/kg, (physical activation)	Product price, $/kg, (chemical activation)
Diesel oil	10,250	1.26	–	–
Wood	4541	0.808	1.54	1.54
Used tires	8760	1.558	0.96	1.34
Pet coke	7833	1.394	1.92	5.76
Carbon black	8202	1.459	0.96	0.96
Charcoal	6667	1.186	1.72	3.84
Lignite	4156	0.739	1.54	4.22

Table 2-19 Cost and economic evaluation of produced carbons [Stavropoulos and Zabaniotou, 2009].

	Used tires	Wood	Pet coke	Carbon black	Charcoal	Lignite
Total investment cost	7,301,682	8,145,760	3,086,328	3,656,307	3,777,027	7,130,948
Total operating cost	2,762,118	3,088,436	1,324,303	1,498,209	1,535,940	2,697,561
Total production cost	3,306,734	3,691,853	1,606,124	1,812,264	1,856,967	3,230,516
Production cost (US$/kg)	2.23	2.49	1.08	1.22	1.25	2.18
Production cost (10^{-2} US$/m^2)	*44.5*	*31.1*	*10.8*	*24.4*	*13.9*	*27.2*
Income	4,482,720	2,851,200	2,850,858	2,850,994	2,851,200	2,850,592
Income	3,057,120	2,280,960	2,850,858	1,425,497	2,566,080	2,280,473
Return on investment (ROI), %	16.1	<0	40.3	28.4	26.3	<0
Return on investment (ROI) %[a]	*<0*	*<0*	*40.3*	*<0*	*18.8*	*<0*
Net present value (NPV), $	<0	<0	2,415,412	934,893	617,493	<0
Net present value (NPV $)	*<0*	*<0*	*2,415,412*	*<0*	*<0*	*<0*
Discounted pay-back (DPB), %	–	<0	5.59	9.27	10.5	<0
Discounted pay-back (DPB)	*<0*	*<0*	*5.59*	*<0*	*22.9*	*<0*
Pay-out period (POT), years	12.8	<0	3.12	4.97	5.55	<0
Pay-out period (POT, years)	*<0*	*<0*	*3.12*	*<0*	*9.55*	*<0*

Capacity: 4.5 t/day, physical activation, zero raw materials cost.
[a] Items in italics refer to costs per m^2 of carbon BET surface area.

The process costs of any precursor must be considered, as it is obviously necessary to get a return on investment. If this is impossible to achieve with a particular precursor then that precursor should in no way be selected for activated carbon production for an industrial company. However, the costs can be brought down in many instances when large capacity production is undertaken, but with this larger financial risk also is present.

2.18 Problems Using Biomass for Activated Carbon Production

Using biomass as a precursor can be seen as a more carbon neutral approach. However, using biomass also has its own associated problems that must be considered. The Environmental Agency has two main concerns in respect to biomass and these are as follows:-

1. 'Biomass energy should be developed in a way that provides the greatest reductions in greenhouse gas emissions possible at an acceptable financial cost.'

2. 'Biomass should be produced sustainably in order that negative environmental impacts, such as on soils, groundwater, air quality, forests and water resources, are reduced as far as possible' [Environmental agency, 2012]

These two points show that, whilst organisations such as the Environmental Agency are in favour of the use of biomass, they also have concerns about what impacts biomass usage could potentially have on the environment. Everything needs to be considered when growing and processing biomass. Finding a way to optimise the efficiency of the process is key, along with reducing greenhouse gases at a commercially acceptable cost whilst still minimising environmental impacts. The message the Environmental Agency send out is that if biomass is developed in a sustainable manner and not just for quick profit, and if it is thought out and planned carefully, then it can be a leading alternative to fossil fuel.

An important area to consider when using biomass is that it contains a much higher moisture content than coal and also has the tendency to absorb moisture during storage and can start to grow mould and fungus. Coal does not have this problem. Therefore biomass needs to kept as dry as possible during storage and be dried prior to use as a high moisture content can affect pyrolysis as reports [Rashidi, Yusup *et al.*, 2012], who go into depth about moisture associated with biomass both intrinsic and extrinsic. Intrinsic moisture is influenced by the material itself whilst the extrinsic moisture is influenced by the environment and weather. The report states that both moisture contents can affect pyrolysis rates.

2.19 Recent Olive Stone and Pine Wood Carbon Literature

As olive stone and pine wood biomass feedstocks were the main focus during the project for producing activated carbons the literature below is continuously updated with the latest research conducted with these two precursors.

[Bohli *et al.,* 2015] studied physically activated olive stone for removal of NO_2 at ambient temperature. The loading was found to be approx. 131 mg/g. 2g of olive stone was carbonised at 600 ^oC for 60 minutes. The carbons were activated at 750 ^oC for 6 hours with 70 % vol H_20 in N_2 with an N_2 flow rate of 10 NL/hr. The carbons were found to have a surface area of 807 m^2/g and micropore volume of 0.3 cm^3/g.

Bohli *et al*., [2015] in another study looked into olive stones for heavy metal removal. The olive stones were chemically activated using phosphoric acid. Raw olive stones were impregnated with the acid solution (50%) at 100 ^oC for 9 hours. Thermal activation was then used at 380 ^oC for 2.5 hours. The carbon was then washed to remove impurities and dried. The results showed that olive stone is a promising precursor for removing heavy metals but adsorption was governed by pH.

Hazzaa and Hussein, [2015] Studied olive stone use for cationic dye adsorption (methylene blue) The carbons were prepared by "thermal activation" at 400, 500, 600, 700, 800 and 900 ^oC and times of 30, 60 and 120 minutes. No oxidising agents are given and the author states carbonisation temperature and activation temperature for the same procedure leading to the conclusion that the olive stones were only carbonised at varying times and temperatures. The results tie in with this conclusion with the resultant char yields and the very low maximum methylene blue adsorption seen (16 mg/g).

Larous and Meniai, [2016] looked into Diclofenac adsorption using olive stone activated carbon. The olive stones were washed with slightly acidified water and then dried. An aqueous solution of 10% H_2SO_4 was mixed in the ratio 1:1with the olive pits for 24 h. The sorbent was washed with distilled water, dried at room temperature for more than 6 h, then at 110 °C for 24 h. The treated material was carbonised at 550 °C in a programmable oven. The surface area was very low (83.7 m^2/g). The adsorption was stated as high given the low surface area with the reason pointing towards present functional groups.

M C Tonucci *et al.,* [2015] studied pine wood activated carbon along with coconut shell, carbon nano tubes and coal for removal of sulfamethoxazole. Pine wood was found to be the best performer adsorbing approx. 131 mg/g at 25 ^oC which was ~4.6 times higher than the observed value for the carbon nano tubes. The pine wood carbon was activated at 800 ^oC.

M Galhetas *et al*., [2014] investigated coal and pine wood activated with potassium carbonate for the adsorption of caffeine. The surface area was found to be approx. 1500 m^2/g. Chars were mixed with ground K_2CO_3 in a 1:1 and 1:3 ratio and activated in a HTF under N_2 flow (5 cm^3/s). Temperatures used were 700 ^oC to 900 ^oC with a residence time of 0.5 hrs to 2 hrs. Samples were washed till a pH of 7 was seen and dried at 100 ^oC. Pine wood produced a higher porosity carbon than coal. 800 ^oC produced mainly micropores whilst 900 ^oC a higher mesopore volume. Adsorption characteristics were found to be governed by surface chemistry.

2.20 Aim, Objectives and Initial Plan

The main aim of the project is to produce a high quality activated carbon product from biomass feedstocks, whilst achieving novel scientific findings. Initially a wide range of biomass feedstocks are to be carbonised and activated. From the literature review it is evident whilst many biomass feedstocks have been investigated for activated carbon production many types of carbonaceous material remains untested. However, the biomass feedstocks used must be readily available and available at a low enough price to make the product financially viable. From this wide range of initial tests, biomass feedstocks that show the highest potential (highest CTC, highest yield) will be taken forward for further more in depth analysis to observe and compare carbon performance. Carbons produced from coconut shell will be used as a reference as stated in the literature review coconut shell carbon has been used for many years. Evidence from the literature review points to pore analysis and other analysis techniques that can be used to determine carbon performance. The carbon must be able to meet industrial application requirements and able to be produced on large scale and will be tested using these analysis techniques. To do this production is to be proven both on lab and pilot scale. Information gathered on lab scale will be used to scale up production using a pilot scale rotary kiln. Additionally using data from a combination of lab and pilot scale production activation conditions will be tailored to manipulate carbon pore structures and improve production efficiency. A cost analysis is to be produced that shows the carbons potential as a future product for CPL industries.

2.21 Conclusion and Literature Gaps

1. Biomass seen as a suitable alternative to coal in activated carbon production.
2. Many different biomass feedstocks used for activated carbon production. Still many more to be investigated. This gap in research enables new novel carbons to be produced and tested.
3. Any carbonaceous material can theoretically be turned into activated carbon resulting in many precursors being a viable option for activated carbon production.
4. Activation stage governs the quality of activated carbon produced. Pyrolysis appears less significant in the pore network development. However, during this stage pores begin to develop.
5. Changing the activation conditions alters the pore size distribution
6. Activation conditions reported in literature, with certain biomasses, that yield the highest quality activated carbons found during the author's investigations.
7. Steam and CO_2 activation produce different pore size distributions with CO_2 producing a more ultra-microporous carbon. Using both N_2 and CO_2 adsorption isotherms to get a full pore size analysis with CO_2 adsorption isotherms being more suited for determining ultra micropore volume.
8. Trade-off between porosity and yield is seen but lack of information in possible ways to maximise porosity whilst reducing yield loss by physical activation methods
9. Modelling of activated carbon porosity still not fully understood.
10. Gaps in literature regarding large scale production and improving production efficiency.
11. Currently no real confidence in predicting porosity by changing activation conditions and the trade-off between all the production variables.
12. Production limits are scarcely reported for most biomasses, the maximum activation temperature, residence time and steam flow rate is not researched in depth.
13. Current literature does not state the most energy efficient way, therefore minimizing carbon footprint to achieve the best carbons derived from biomass feedstocks.
14. Current literature has minimal information and results centred on single step pyrolysis and activation using biomass precursors on both lab and pilot scale.

2.22 References

Acharjee, T. C., C. J. Coronella, et al. (2011). "*Effect of thermal pretreatment on equilibrium moisture content of lignocellulosic biomass*." Bioresource Technology **102**(7): 4849-4854.

Amaya, A., N. Medero, et al. (2007). "*Activated carbon briquettes from biomass materials*." Bioresource Technology **98**(8): 1635-1641.

Alarco, (2010) "*Water filters*." http://www.alarco.gr/filtra-nerou/en/photo, Accessed July 2013

Anon, 2015. *Carbochem.* [Online]
Available at: http://carbochem.com/activated-carbon/activated-carbon-101
[Accessed November 2015].

Anon, 2013. *Desotec.* [Online]
Available at: http://www.desotec.com/activated-carbon/types-of-activated-carbon/properties/carbon-tetrachloride-activity
[Accessed June 2013].

Arami-Niya, A., W. M. A. W. Daud, et al. (2011). "*Comparative study of the textural characteristics of oil palm shell activated carbon produced by chemical and physical activation for methane adsorption*." Chemical Engineering Research and Design **89**(6): 657-664.

Aworn, A., P. Thiravetyan, et al. (2008). "*Preparation and characteristics of agricultural waste activated carbon by physical activation having micro- and mesopores*." Journal of Analytical and Applied Pyrolysis **82**(2): 279-285.

Aygün, A., S. Yenisoy-Karakaş, et al. (2003). "*Production of granular activated carbon from fruit stones and nutshells and evaluation of their physical, chemical and adsorption properties*." Microporous and Mesoporous Materials **66**(2–3): 189-195.

Bansal, R. C. G., Meenakshi (2005). "*Activated Carbon and Its Surface Structure*." Activated Carbon Adsorption, CRC Press**:** 1-65.

Bansal R, J Baptiste Donnet, Fritz Stoeckli, (1998). "*Active carbon."* New York and Basel: Marcel Dekker inc..

Betancur, M., J. D. Martínez, et al. (2009). "*Production of activated carbon by waste tire thermochemical degradation with CO_2*." Journal of Hazardous Materials **168**(2–3): 882-887.

Blanco Lopez, C.G. Blanco, A. Martinez-Alonso, J.M.D. Tascon (2002) "*Composition of gases released during olive stones pyrolysis*" Journal of Analytical and Applied Pyrolysis 65 (2002) 313–322 www.elsevier.com/locate/jaap

Bohli T , Abdelmottaleb Ouederni , Nuria Fiol, Isabel Villaescusa (2015) "*Evaluation of an activated carbon from olive stones used as an adsorbent for heavy metal removal from aqueous phases*." International Chemical Engineering Congress

Bouchelta, C., M. S. Medjram, et al. (2008). "*Preparation and characterization of activated carbon from date stones by physical activation with steam*." Journal of Analytical and Applied Pyrolysis **82**(1): 70-77.

Carbon Trust., (2009). *Biomass Carbon Dioxide cycle.* [Online]
Available at: http://www.masenv.co.uk/Biomass
[Accessed July 2013].

Chemvironcarbon, (2013). *Activated Carbon Manufacture.* [Online]
Available at: http://www.chemvironcarbon.com/en/activated-carbon
[Accessed July 2013].

Chen, X., S. Jeyaseelan, et al. (2002). "*Physical and chemical properties study of the activated carbon made from sewage sludge*." Waste Management **22**(7): 755-760.

Clark, J., (2002). *chemguide.* [Online]
Available at: http://www.chemguide.co.uk/physical/basicrates/introduction.html
[Accessed March 2016].

Cleiton A. Nunes, Mário C. Guerreiro (2010) "*Estimation of Surface Area and Pore Volume of Activated Carbons by Methylene Blue and Iodine Numbers.*"
Departamento de Química, Universidade Federal de Lavras, CP 3037, 37200-000 Lavras - MG, Brasil

Ciolkosz, D., (2010). "*Renewable and Alternative Energy Fact Sheet." ,* Pennsylvania State University: Green Buildings and Bioenergy.

Demiral, H., İ. Demiral, et al. (2011). "*Production of activated carbon from olive bagasse by physical activation*." Chemical Engineering Research and Design **89**(2): 206-213.

Don W. Green and Robert H Perry, (1997). In: *Perry's chemical Engineers handbook 6th edition.* Mcgraw-Hill.

Dias, J. M., M. C. M. Alvim-Ferraz, et al. (2007). "*Waste materials for activated carbon preparation and its use in aqueous-phase treatment: A review*." Journal of Environmental Management **85**(4): 833-846.

EIA, (2009). "*Future Targets in relation to Carbon Emissions."* [Online]
Available at: http://www.eia.gov/environment/emissions/ghg_report/ghg_overview.cfm
[Accessed June 2013].

EIA, (2012). "*Biomass Selection Criteria."*[Online]
Available at: http://www.eia.gov/energyexplained/?page=biomass_environment
[Accessed June 2013].

Etheridge, D. M. L. P. Steele,R. L. Langenfelds,R. J. Francey,J.-M. Barnola,V. I. Morgan, (1996). "*Natural and anthropogenic changes in atmospheric CO2 over the last 1000 years from air in Antarctic ice and firn"*. *Journal of Geophysical Research: Atmospheres,* (1984–2012)(101.D2 4115-4128.).

Esfandiari, A., T. Kaghazchi, et al. (2012). "*Preparation and evaluation of activated carbons obtained by physical activation of polyethyleneterephthalate (PET) wastes*." Journal of the Taiwan Institute of Chemical Engineers **43**(4): 631-637.

Finne Zhang, (2008) "*Coal based activated carbon.*" http://www.alibaba.com/product-gs/250146187/coal_based_activated_carbon.html accessed July 2013

Galhetas Margarida, Ana S. Mestre , Moisés L. Pinto , Ibrahim Gulyurtlu , Helena Lopes , Ana P. Carvalho, (2014). "*Chars from gasification of coal and pine activated with K2CO3: Acetaminophen and caffeine adsorption from aqueous solutions*". *Journal of Colloid and Interface Science*.

Gamal O.El-Sayed, Mohamed M.Yehia, Amany A Saad (2014) "*Assessment of activated carbon prepared from corncob by chemical activation with phosphoric acid.*" Water Resources and Industry7-8 66–75

Gaspard and Ncibi, (2014). "*Biomass for sustainable application pollution and remediation energy".* RSC Green Chemistry.

Gauden, P. A., A. P. Terzyk, et al. (2010). "BET surface area of carbonaceous adsorbents—Verification using geometric considerations and GCMC simulations on virtual porous carbon models." Applied Surface Science **256**(17): 5204-5209.

Gergova, K. and S. Eser (1996). "*Effects of activation method on the pore structure of activated carbons from apricot stones."*. Carbon **34**(7): 879-888.

Gillespie, G. D., C. D. Everard, et al. (2013). "*Prediction of quality parameters of biomass pellets from proximate and ultimate analysis"*. Fuel **111**(0): 771-777.

González, M. T., M. Molina-Sabio, et al. (1994). "*Steam activation of olive stone chars, development of porosity*." Carbon **32**(8): 1407-1413

Greenbank M October 20th, (2006) "*Surface Chemist Calgon Carbon Corporation A New Line of Palm Kernel Activated Carbons*" 18th international conference

Guo, J., Y. Luo, et al. (2007). "*Adsorption of hydrogen sulphide (H2S) by activated carbons derived from oil-palm shell*." Carbon **45**(2): 330-336.

Guo, Y. and E. Du (2012). "*The Effects of Thermal Regeneration Conditions and Inorganic Compounds on the Characteristics of Activated Carbon Used in Power Plant*." Energy Procedia **17, Part A**(0): 444-449.

Hall, D. O. (1997). "*Biomass energy in industrialised countries—a view of the future*." Forest Ecology and Management **91**(1): 17-45.

Hazzaa R , Hussein M 2015 "*Adsorption of cationic dye from aqueous solution onto activated carbon prepared from olive stones*" Environmental Technology & Innovation

Höök, M. and X. Tang (2013). "*Depletion of fossil fuels and anthropogenic climate change—A review.*" Energy Policy **52**(0): 797-809.

Huang, Y., B. Jin, et al. (2008). "*Characteristic and mercury adsorption of activated carbon produced by CO2 of chicken waste*." Journal of Environmental Sciences **20**(3): 291-296

IPCC, (2010). *Working Group III: Mitigation.* [Online]
Available at: https://www.ipcc.ch/pdf/assessment-report/ar5/wg3/ipcc_wg3_ar5_full.pdf
[Accessed May 2013].

Jin-ke, L., W. Feng-hua, et al. (2009). "*Differences in coal consumption patterns and economic growth between developed and developing countries*." Procedia Earth and Planetary Science **1**(1): 1744-1750.

Johnson, E. (2009). "*Goodbye to carbon neutral: Getting biomass footprints right.*" Environmental Impact Assessment Review **29**(3): 165-168

Krevelen D, W., (1993). "*Coal- physics-chemistry-constitution."* third edition ed. s.l.:Elsevier Science.

Larous Soumaya , Meniai Abdeslam-Hassen, 2016. Adsorption of Diclofenac from aqueous solution using activated carbon prepared from olive stone. *International Journal of Hydrogen Energy*

Li, W., K. Yang, et al. (2008). "*Effects of carbonization temperatures on characteristics of porosity in coconut shell chars and activated carbons derived from carbonized coconut shell chars*." Industrial Crops and Products **28**(2): 190-198.

Lua, A. C., T. Yang, et al. (2004). "*Effects of pyrolysis conditions on the properties of activated carbons prepared from pistachio-nut shells*." Journal of Analytical and Applied Pyrolysis **72**(2): 279-287

Marsh H and Reinoso FR. (2006). "*Activated Carbon."* Elsevier Science & Technology Books

Martínez, M. L., M. M. Torres, et al. (2006). "*Preparation and characteristics of activated carbon from olive stones and walnut shells*." Industrial Crops and Products **23**(1): 23-28.

Matos, J., C. Nahas, et al. (2011). "*Synthesis and characterization of activated carbon from sawdust of Algarroba wood. 1. Physical activation and pyrolysis*." Journal of Hazardous Materials **196**(0): 360-369.

Mckinsey, (2010). "*Impact of the financial crisis on carbon economics."* Version 2.1 of the Global Green House Gas Abatement Cost Curve.

Mui, E. L. K., W. H. Cheung, et al. (2010). "*Mesoporous activated carbon from waste tyre rubber for dye removal from effluents.*" Microporous and Mesoporous Materials **130**(1–3): 287-294.

Nabais, J. M. V., C. E. C. Laginhas, et al. (2011). "*Production of activated carbons from almond shell*." Fuel Processing Technology **92**(2): 234-240.

Okada, K., N. Yamamoto, et al. (2003). "*Porous properties of activated carbons from waste newspaper prepared by chemical and physical activation*." Journal of Colloid and Interface Science **262**(1): 179-193.

Pré, P., G. Huchet, et al. (2013). "*A new approach to characterize the nanostructure of activated carbons from mathematical morphology applied to high resolution transmission electron microscopy images.*" Carbon **52**(0): 239-258.

Rashidi, N. A., S. Yusup, et al. (2012). "*Activated Carbon from the Renewable Agricultural Residues Using Single Step Physical Activation: A Preliminary Analysis*." APCBEE Procedia **3**(0): 84-92.

Rodríguez-Reinoso, F., M. Molina-Sabio, et al. (1995). "*The use of steam and CO2 as activating agents in the preparation of activated carbons.*" Carbon **33**(1): 15-23.

Román, S., J. F. González, et al. (2008). "*Control of pore development during CO2 and steam activation of olive stones.*" Fuel Processing Technology **89**(8): 715-720.

Román, S., B. Ledesma, et al. (2013) "*Two stage thermal regeneration of exhausted activated carbons. Steam gasification of effluents."* Journal of Analytical and Applied Pyrolysis(0)

Şahin, Ö. and C. Saka (2013). "*Preparation and characterization of activated carbon from acorn shell by physical activation with H2O–CO2 in two-step pretreatment*." Bioresource Technology **136**(0): 163-168.

Saka, C. (2012). "*BET, TG–DTG, FT-IR, SEM, iodine number analysis and preparation of activated carbon from acorn shell by chemical activation with ZnCl2."* Journal of Analytical and Applied Pyrolysis **95**(0): 21-24

Schröder E, Klaus Thomauske, Benjamin Oechsler, Sabrina Herberger, Sabine Baur and Andreas Hornung, (2011). "*Activated Carbon from Waste Biomass."* Croatia: Janeza Trdine

Schuth, F, Kenneth S. W. Sing, and Jens Weitkamp, (2002) "*Handbook of Porous Solids."* Volume

Sekirifa, M. L., M. Hadj-Mahammed, et al. (2013). "*Preparation and characterization of an activated carbon from a date stones variety by physical activation with carbon dioxide*." Journal of Analytical and Applied Pyrolysis **99**(0): 155-160.

Şentorun-Shalaby, Ç. d., M. G. Uçak-Astarlıogˇlu, et al. (2006). "*Preparation and characterization of activated carbons by one-step steam pyrolysis/activation from apricot stones*." Microporous and Mesoporous Materials **88**(1–3): 126-134

Sing KSW, Everett DH, Haul RA, Moscou L, Pierotti RA, Rouquerol J, Siemieniewska T. (1985) "*Reporting physisorption data for gas/solid systems with special reference to the determination ofsurface area and porosity*." *PureAppl Chem*;57(4):603.

Soleimani, M. and T. Kaghazchi (2008). "*Activated Hard Shell of Apricot Stones: A Promising Adsorbent in Gold Recovery*." Chinese Journal of Chemical Engineering **16**(1): 112-118

Stavropoulos, G. G. and A. A. Zabaniotou (2009). "*Minimizing activated carbons production cost.*" Fuel Processing Technology **90**(7–8): 952-957.

Sun, K. and J. c. Jiang (2010). "*Preparation and characterization of activated carbon from rubber-seed shell by physical activation with steam*." Biomass and Bioenergy **34**(4): 539-544

Tay, T., S. Ucar, et al. (2009). "*Preparation and characterization of activated carbon from waste biomass*." Journal of Hazardous Materials **165**(1–3): 481-485

Tonucci M C, L Vinícius Alves Gurgel, S F de Aquino (2015) "*Activated carbons from agricultural byproducts (pine tree and coconut shell), coal, and carbon nanotubes as adsorbents for removal of sulfamethoxazole from spiked aqueous solutions: Kinetic and thermodynamic studies.*" Industrial Crops and Products 74

Toles, C. A., W. E. Marshall, et al. (2000). "*Steam- or carbon dioxide-activated carbons from almond shells: physical, chemical and adsorptive properties and estimated cost of production*." Bioresource Technology **75**(3): 197-203

Tascon Juan M.D (2012) "*Novel Carbon Adsorbents"*, Oviedo Spain, Elsevier pg 54, 119, 12

US Environmental Protection Agency (2011) "*Carbon Emissions*." U.S. Environmental Protection Agency 1200 Pennsylvania Ave., N.W. Washington, DC 2046

Wang S a,∗, Z.H. Zhua, Anthony Coomes b, F. Haghseresht c, G.Q. Luc (2005) "*The physical and surface chemical characteristics of activated carbons and the adsorption of methylene blue from wastewater*" Journal of Colloid and Interface Science 284 (2005) 440–446
Elsevier

Wu Feng-Chin, Ru-Ling Tseng,∗, Ruey-Shin Juang, (2009) "*Initial behavior of intraparticle diffusion model used in the description ofadsorption kinetics.*" Chemical Engineering Journal 153 1–8

Yang, T. and A. C. Lua (2003). "*Characteristics of activated carbons prepared from pistachio-nut shells by physical activation.*" Journal of Colloid and Interface Science **267**(2): 408-417

Yang Zhang et.al, (2007) "*Characterization of Activated Carbon prepared from Chicken waste and Coal*" Institute for combustion science and environmental technology, Western Kentucky University

Zarifah Nadiah, (2010),"*To Produce the Activated Carbon from Matured Palm Kernel Shell*" Engineering. Universiti Malaysia Pahang

Zhu, Y., J. Gao, et al. (2012). "*Preparation of activated carbons for SO2 adsorption by CO2 and steam activation.*" Journal of the Taiwan Institute of Chemical Engineers **43**(1): 112-119.

Chapter 3 - Methods

3.1 Raw Materials

Raw materials were, in the main, sourced via the Procurement Department at CPL industries. The two main biomasses used were olive stone and pine wood. Olive stone was sourced from Spain through Garcia-Munte Energia, and pine wood sourced through Forest Fuels.

The olive stones were used as received with a crushed particle size of approx. 1 to 4 mm. Raw pine wood chips were milled using a 3 mm mesh for lab scale trials. However, the pine wood was not milled before being placed in the pilot kiln and was in the form of chips as shown in Figure 3:1. The char from the pilot kiln was then milled using a 3 mm sieve mesh used for activation trials on lab scale and kept as produced for pilot scale trials.



Figure 3:1 Raw material and char used for lab scale (1- 4) and pilot scale (1, 2 and 5, 6) activated carbon production.

3.2 Lab Scale Trials

Lab scale production experiments were conducted on two horizontal tube furnaces (HTF). The first HTF, at the University of Nottingham, was used for a small amount of preliminary trials and the second, at CPL industries, for all remaining trials. The HTFs were very similar apart from the fact that the one at the University of Nottingham had a removable lid as Figure 3:2 shows.



Figure 3:2 HTF at the University of Nottingham.



Figure 3:3 HTF at CPL industries.

The equipment set up contained the following:

1. HTF furnace.
2. Control HMI (human machine interface).
3. Peristaltic water pump (continuous flow).
4. Quartz tube (length 120 mm, diameter 40 mm) with outer insulation with rubber bungs at each end.
5. Two water vessels to aid tar removal/ condense water.
6. Extraction.
7. Pitot tube for nitrogen gas and water entry to furnace.

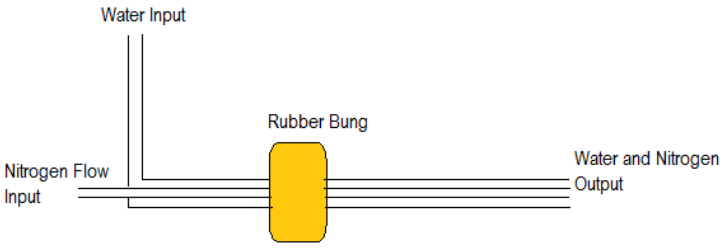


Figure 3:4 Pitot tube diagram.

Using a pitot tube allowed both nitrogen gas and water to enter the furnace via one piece of equipment, whilst preventing mixing prior to entry. This was important for design purposes i.e. inserting water into a nitrogen line is not ideal and this way allowed both flows to be adjusted independently. The nitrogen flow was through the inner tube whilst water through the outer tube. This was so the water would get maximum heat from the furnace for rapid steam production. The rubber bung was placed on the tube to create a seal with the quartz tube.

3.3 Pyrolysis Step

The first part of producing activated carbon is the pyrolysis stage. The selected initial temperature and time used for pyrolysis was determined by looking at published literature. The target, when deciding on a suitable temperature and residence time, was to produce a char that has a relatively low volatile percentage to aid activation by the onset of pore formation and also, high char uniformity for repeatability. The reported temperatures and times used for pyrolysis were between 600 ^{o}C to 800 ^{o}C and with a residence time of between 10 minutes and 1 hour. Therefore, the initial chosen temperature was 700 ^{o}C with a residence time of 1 hour as this has been found to be the optimum temperature for porosity development during carbonisation [Bouchelta, Medjram *et al*., 2008]

Further on, after the preliminary trials in Chapter 4, it was seen that by reducing the pyrolysis time to 30 minute the same char was produced as with a residence time of 1 hour. Therefore 700 ^{o}C and 30 minutes was used throughout the rest of the project both on small and large scale in order that the activation step could be focused upon. Proximate analysis was carried out on samples produced on lab scale under these conditions that showed a consistent volatile percentage (4% to 6%) over several materials, as shown in Chapter 4.

The heating rate was selected to be 15 ^{o}C per minute using ‘middle ground’ figures reported in literature and recommended by colleagues with experience on the HTF furnace. This heating rate has been used throughout the project on small scale unless stated. Heating rates, when studying

activation, is not a significant area of interest with large scale production as material will be added straight into a furnace at around 700 ^{o}C. Heating rate becomes more important when considering the time taken for the material to go from the initial temperature at which the steam is added to the final set activation temperature as discussed in Chapter 6. 1 L/min of nitrogen gas was added on lab scale to act as a carrier gas and produce an inert atmosphere.

A stainless steel crucible was filled with raw biomass. The mass for each biomass differed due to density differences. For example olive stone (20 g) and pine wood (6.5 g) filled approximately the same volume of the crucible. The wide range of biomasses initially tested (see Appendix Table A-1) were all pyrolysed in the HTF as stated within the table.

The crucible was placed within the furnace at room temperature. A flow of 1 L/min of Nitrogen was used as a carrier gas and for an inert atmosphere. Once 700 ^{o}C and 30 minutes had passed the furnace heater was turned off. The furnace was left to cool to around 200 ^{o}C when the char could be safely removed. The char was then quickly placed into a sample tube and sealed (to prevent moisture adsorption), left to cool further for 2 minutes and then weighed.

3.4 Activation Step

A significant decision was taken during this point and was carried on throughout the project. The peristaltic water pump would be turned on once the furnace reached the peak pyrolysis temperature (700 ^{o}C). This was the case for all activations except high activation temperature trials (Chapter 5) where steam flow began at 800 ^{o}C to make sure the final activation temperature was reached within the given residence time of the test. The furnace was then heated up to the final activation temperature chosen for each trial. The residence time stated is the time the water pump was on and not the residence time at the final activation temperature. This was decided for the following reasons;

1. This method facilitates the data to be used for a single step system where activation immediately follows pyrolysis and comparison between a two-step and single step process which can be seen in Chapters 5 and 6, with any burn off (mass loss) linked to activation and not higher pyrolysis temperature.
2. The objective for this project is to consider and conduct large scale production. This procedure takes into consideration that the initial section of the rotary kiln would be cooler than the following sections where the final activation temperature is reached. The reason for this is the cooling effect that the char and steam provide upon entering the system. This procedure best replicates a large scale system on a small scale furnace as opposed to starting the pump when the final activation temperature is reached.

The time spent at the final activation temperature can still be calculated by using:

Equation 3-1

$$A_{rt} - \left(\frac{AT_f - 700}{15}\right)$$

A_{rt} = Activation residence time i.e. the time the water pump is on in minutes

AT_f= final activation temperature

For this purpose the residence stated refers to the amount of time that water is entering the system.

Initially before production variables were altered testing began using a "standard activation" set of conditions. These were 800 ^oC, 1 hour residence time and 1.5 ml/min water flow. This was roughly in line with conditions used across literature for a wide range of biomass types. This was the first set of conditions used for each trial and conditions altered from associated results.

First char was weighed and placed into the stainless steel crucible. The mass of char was dependant on which biomass was used. For the olive stone and pine wood char this weight was 10 g and 3.5 g respectively. The crucible with char was placed into the furnace at < 200 ^oC. The final activation temperature and heating rate was set using the HMI. Nitrogen flow was turned on and set to 1 L/min using the flow meter. Once the furnace temperature reached 700 ^oC the water pump was started with the pre-set flow rate for the trial. When the stop start peristaltic pump system was used, the on off timer was set prior the experiment beginning. The water pump was turned on simultaneously with the countdown timer for the desired residence time. Once the required time had passed the water pump was immediately turned off. The furnace was then turned off and left to cool to approx. 200 ^oC. The crucible, now containing activated carbon, was taken out of the furnace and the activated sample then placed into a sealed glass sample tube which was left to cool for a further 3-5 minutes. This sample was then weighed using the same method discussed above with pyrolysis.

During the preliminary tests (Chapter 4) the first variable considered was activation temperature. Three different temperatures were used. The chosen activation temperatures used were based upon published literature and kinetic and thermodynamic information (provided in Appendix section A.1 and A.2). The residence time was selected to be 1 hour and the chosen temperatures were 750 ^oC, 800 ^oC and 850 ^oC for palm kernel shell and almond shell. A slightly lower temperature range was used for wood due to lower yields reported, for example by Tancredi, [1996] who studied steam activation of eucalyptus wood. In this case, 700 ^oC, 750 ^oC and 800 ^oC were chosen. For olive cake a wider range was chosen from 700 ^oC to 850 ^oC. Nitrogen flow

of 1 L/min was used to create an inert atmosphere within the quartz tube. The flows were reduced to 1 L/min in future experiments as such a high flow proved unnecessary. The water flow at 1.5 ml/min was the speed of the peristaltic pump supplied for these trials and it was not possible to change this flow at this stage.

Three different residence times and temperatures were used. Each time a sample of 10 g of coconut shell char was placed into the crucible. Roughly the same volume of the crucible was filled each time. The water carbon molar ratio was also calculated:

Example, for a residence time of 1 hour:

$$\text{Moles carbon} = \frac{mass\ C\ (g)}{molar\ mass\ C\ (g/mol)} = \frac{10}{12} = 0.833 \text{ moles C} \qquad \textbf{Equation 3-2}$$

$$\text{Moles water} = \frac{mass\ H_2O\ (g)}{molar\ mass\ H_2O\ (g/mol)} = \frac{90}{18} = 5 \text{ moles } H_2O \qquad \textbf{Equation 3-3}$$

$$\text{Ratio} = \frac{Moles\ H_2O}{Moles\ C} = 6{:}1 \qquad \textbf{Equation 3-4}$$

Again, for each of these trials the water flow was kept constant at 1.5 ml/min due to the limitations of the water pump at this stage.

During the preliminary trials carbon dioxide activation was investigated. The maximum carbon dioxide flow used was 1 L/min as this was the maximum flow rate possible through the carbon dioxide flow meter. The carbon dioxide line was added to the pitot tube by swapping it with the water inlet tube shown in Figure 3:4. The temperatures used for the carbon dioxide trials were also increased to achieve a higher burn off percentage. With the exception of the addition of carbon dioxide, the experimental procedure was carried out the same way as steam activation. During the simultaneous steam and carbon dioxide trials the nitrogen line was replaced with the carbon dioxide line.

In addition to carbon dioxide trials nitrogen flow rates were altered by adjusting the nitrogen flow meter during activation. The rest of the procedure remained the same. The flow rates were altered from 0.5 L/min to 4 L/min for both olive stone and pine wood chars. Water/nitrogen molar ratios were calculated by:

Moles Nitrogen

$$PV = nRT \qquad \textbf{Equation 3-5}$$

Moles Water

$$Moles = Mass/Mr \qquad \textbf{Equation 3-6}$$

Moving on to trials completed in Chapter 5, the biomasses studied were olive stone and pine wood. The first stage was to investigate the main variables during production. These were temperature, residence time and steam flow rate.

During these trials a wider range of temperatures were used: 600 ^{o}C up to 1000 ^{o}C. Residence time range increased: 15 minutes up to 8 hours. With a new peristaltic pump the flow rate range also changed from between 0.375 ml/min up to 3 ml/min. The older peristaltic pump was operated on a stop-start system which is explained in section 3.5.

During chapter 5 and chapter 7 the percentage steam reacted from the total amount entering the system was required. This was calculated using:

$$H_2O + C \rightarrow CO + H_2 \qquad \textbf{Reaction 1}$$

1 mole of steam reacts with 1 mole of carbon. In respect of comparing burn off percentages, it is assumed that burn off from the char is 100% carbon. Therefore moles carbon burn off equals moles steam reacted. Moles carbon burn off is calculated by:

$$\text{Moles carbon} = \frac{mass\ C\ burn\ off\ (g)}{molar\ mass\ C\ (g/mol)} \qquad \textbf{Equation 3-7}$$

The mass of water entering the system is known and therefore the mass reacted was calculated by:

$$\text{Steam reacted (\%)} = \frac{moles\ steam\ reacted \times molar\ mass}{Total\ Water\ mass\ (g)} \times 100 \qquad \textbf{Equation 3-8}$$

3.5 Peristaltic Water Pumps

Two water peristaltic water pumps were used during the trials. The first water pump could only operate under a set flow rate of 1.5 ml/min. This was used for the preliminary trials and it is stated when this was used during the project. The second pump flow rate could be altered and is used for all remaining trials. (If not stated then this pump was used). The first pump's flow could be altered by using a stop-start system. During the two hour trials in Chapter 5 the flow

was altered on a minute basis so the desired ml/min could be used. This was done with the pump being turned on for either 15, 30, 45 or 60 seconds per minute and therefore off for 45, 30, 15 or 0 seconds per minute respectively.

The continuous flow pump was set by adjusting the rpm of the pump - the calibration curve can be seen in Figure 3:5. The stop-start and continuous flows were compared and no difference was found as shown in Figure 3:6 below. With the burn off results being identical between the two systems (stop-start and continuous flow), the results can be compared as the different flow characterises are not affecting the end product

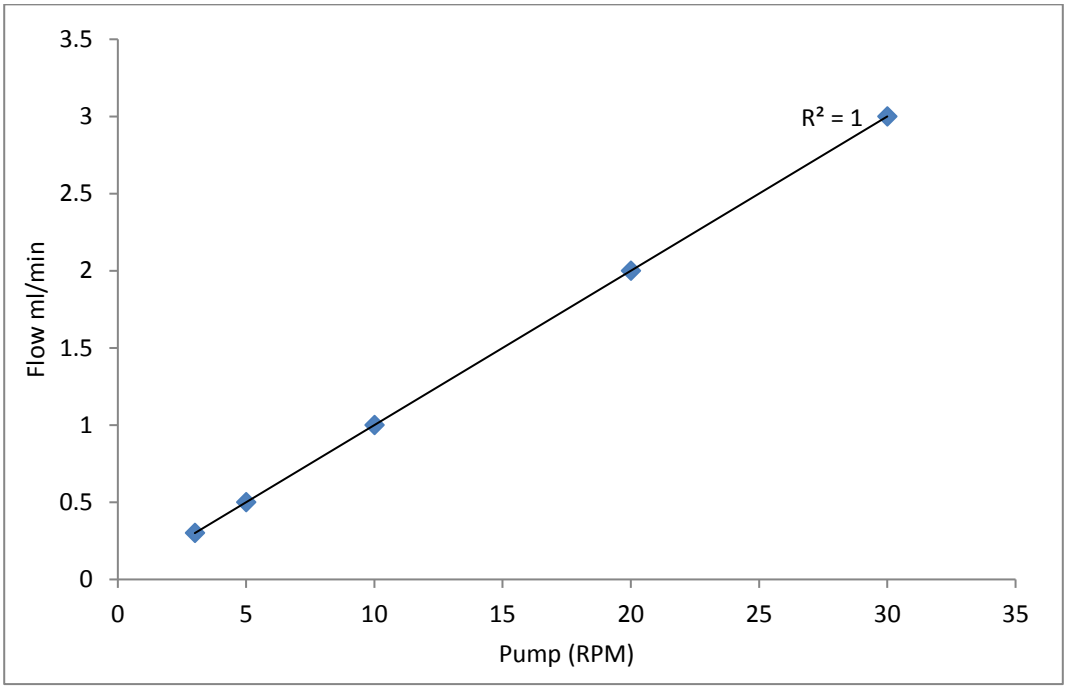


Figure 3:5 Peristaltic pump calibration curve.

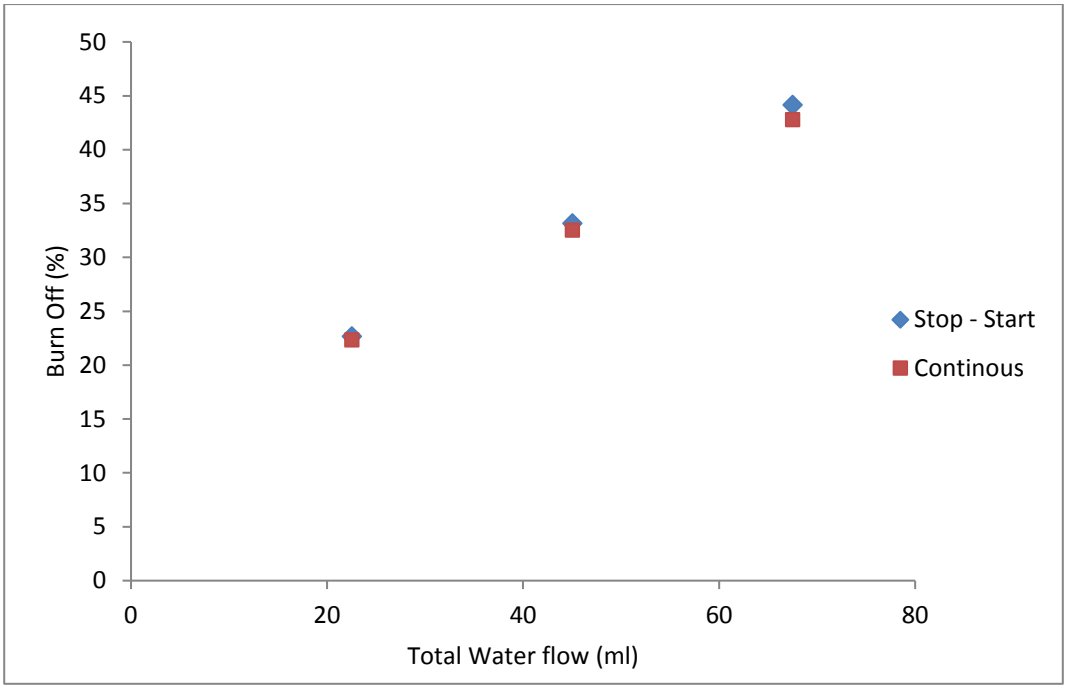


Figure 3:6 Showing trials comparing stop start and continuous flow for an activation time of 1 hour and 800 °C.

3.6 Single Step Lab Scale

Single step lab scale trials were conducted with both olive stone and pine wood. Firstly, for comparative purposes a two-step process was carried out. This was done by placing 20 g of olive stone and 6.5g of pine wood into a crucible. Unlike previous pyrolysis experiments the biomass was added into the furnace when 700 °C was reached. This is classed as fast pyrolysis in the thesis. This was done so the yield between fast and slow pyrolysis could be measured and also a burn off percentage obtained for the single step process between the char and activated carbon. The char was then weighed after cooling to 200 °C; after the furnace was again heated initially up to 700 °C.

When the char was placed back into the furnace, the water pump was turned on and then the final activation temperature reached at 15 °C/min, as previously conducted. The activation was left to continue under the desired residence time and water flow rate. The furnace was allowed to cool and the final activated carbon yield was recorded. In this instance the burn off percentage was known because the char was taken out the furnace and weighed before activation.

The main single step process was carried out by placing olive stone (20 g) or pine wood (6.5 g) into the furnace at 700 °C. At this point the water pump was turned on along with the timer. The furnace continued to increase to the final activation temperature at 15 °C/min. The furnace was then left to cool before the carbon was weighed. The burn off (%) was recorded by using the

average fast pyrolysis value as the individual char yield cannot be known on the single step production.

3.7 Analysis Techniques

3.7.1 Proximate/Ultimate Analysis

Proximate analysis was carried in accordance to international standard organisation ISO 17246:2010. The tests were carried out in a series of muffle furnaces at different temperatures moisture (105 ^{o}C), volatile (900 ^{o}C) and ash contents (815 ^{o}C). The standard methods followed were from BS-1016-1 and BS- 1016-3 which covers procedures for both moisture and proximate analysis tests.

3.7.1.1 Moisture

Moisture content was calculated by weighing around 1 g to 1.1 g of material into an aluminium plate with individual and total mass recorded. This plate was then placed into an air oven for 90 minutes. The plates were then removed from the oven with a lid quickly placed over them before being transferred into an oxygen free cooler (7 minutes). The samples were then removed to a desiccator for a further 7 minutes before being weighed.

Moisture content calculation:

$$Moisture\ (\%) = \frac{M_{Int} - M_{fin}}{M_{Int}} \times\ 100 \qquad \textbf{Equation 3-9}$$

Where, M_{int} and M_{fin} are the initial and final masses, respectively.

3.7.1.2 Volatile Content

Volatile content was calculated by weighing around 1 g to 1.1 g of material into silica crucibles with attached lids, the individual and total masses recorded. The crucibles were fitted with lids to prevent combustion taking place with air entry. The crucibles were then placed into the muffle furnace for 7 minutes followed by being removed and placed into a desiccator for 7 minutes to cool. The sample was then reweighed and volatile content calculated:

$$Volatile\ (\%) = \frac{M_{Int} - M_{fin}}{M_{Int}} \times\ 100 \qquad \textbf{Equation 3-10}$$

3.7.1.3 Ash Content

Ash content was calculated by weighing around 1 g to 1.1 g of material into an open silica crucible to allow combustion. The crucibles were transferred to the furnace once the temperature was cooled to approx. 200 °C. The furnace temperature was then gradually increased to 815 °C and left for 2 hours. The samples were then removed and cooled in a desiccator. After cooling the samples were weighed with the ash content calculated by:

$$Ash\ (\%) = \frac{M_{Int} - M_{fin}}{M_{Int}} \times\ 100 \qquad \textbf{Equation 3-11}$$

3.7.1.4 Fixed Carbon Content

Fixed carbon content was calculated by difference:

$$Fixed\ carbon\ (\%) = 100 - Volatile\ \ (\%) -\ Ash\ (\%) \qquad \textbf{Equation 3-12}$$

3.7.1.5 Elemental Analysis

Ultimate analysis was completed on a LECO ea at the University of Nottingham by lab technicians. This was to see the Carbon, nitrogen, hydrogen with oxygen (calculated by difference) contents of the char and activated carbon. Sulphur content was also measured.

3.7.2 Carbon tetrachloride (CTC) Activity

CTC analysis was carried out following ASTM D 5742 method with the only difference being a water bath was not used. However, the lab in which the testing took place was kept at a constant temperature.

Depending on how much sample was produced after activation, at least half was used to determine the CTC value. This was done by weighing out the mass of dry activated carbon sample into a designed sintered test tube that allowed the gas to pass through but prevent any carbon loss. Butane was then passed through the carbon sample for 20 minutes to make sure full saturation point was reached. The sample was then reweighed. Using the correlation factor provided in ASTM D 5742 the following calculation was used:

$$\frac{saturated\ (g) - unsaturated(g)}{unsaturated\ (g)} \times\ 100 = \%\ Butane \qquad \textbf{Equation 3-13}$$

$$\%\ Butane\ \times\ 2.55 = CTC$$

The CTC value is reported to the nearest 0.5 throughout the project.

3.7.3 Methylene Blue Number

Methylene blue was conducted in line with the method provided by CEFIC European council of chemical manufacture federations, test methods for activated carbons.

Methylene blue dye 1.5 g was dissolved in exactly 1 L of ultrapure water and sealed in a volumetric flask. This was left to stand for 24 hours.

Dry carbon samples were ground up to a fine powder of which 0.1 g was added to a stoppered conical flask. Methylene blue solution was added 1 ml at a time to the flask. The flask was swirled until the solution became colourless. Methylene blue was continuously added 1 ml at a time until the solution eventually did not become colourless after a maximum of 5 minutes of swirling. If the solution did not become colourless after 5 minutes the previous volume of methylene blue used was recorded.

3.7.4 Iodine Number

Following ASTM D 4607:

The carbon was first crushed and dried for 12 hours at 110 ^{o}C. The sample was then removed from the oven and cooled in a desiccator. During the drying stage the iodine sample was prepared, 12.7 g of iodine and 19.1 g of potassium iodide were placed into a beaker. Whilst stirring, distilled water was added in small increments until the solution level reached approx. 50 ml. The solution was left for 4 hours to ensure full dissolution. This solution was then transferred into a 1 L amber volumetric flask and filled to the 1 L mark with distilled water. Sodium thiosulphate and Hydrochloric acid were purchased with the correct concentrations (0.1 N and 5 % by weight respectively). The next step was to standardise the solutions: 25 ml of iodine solution with a few drops of starch solution was titrated against sodium thiosulphate until a colourless solution was observed. The iodine solution normality was calculated by:

$$N_1 = (S.N_2)/I \qquad \textbf{Equation 3-14}$$

Where,

N_1 = Sodium thiosulphate Normality

S = Sodium thiosulphate volume (ml)

N_2 = Iodine Normality

I = Iodine volume (ml)

Around 1 g of carbon was weighed into a conical flask and 10 ml of HCl acid was then added. This solution was brought to the boil for 30 ± 2 seconds to remove any sulphur present in the

carbon and then cooled. Next, 100 ml of the iodine solution was added to the flask containing the carbon and was shaken vigorously for 30 ± 2 seconds before filtering to remove the carbon from the iodine solution. 50 ml of the filtered solution was transferred to a clean conical flask and was titrated against the sodium thiosulphate. When the solution turned yellow a couple drops of starch indicator was added. The titration continued until the solution turned colourless. The sodium thiosulphate volume required for this was recorded.

The following calculations were then completed to calculate mg/g iodine adsorbed:

$$A = (N_2)\,(12693) \qquad \textbf{Equation 3-15}$$

N_2 = Iodine Normality

$$B = (N_1)\,(126.93) \qquad \textbf{Equation 3-16}$$

N_1 = Sodium thiosulphate Normality

$$DF = I + H/F \qquad \textbf{Equation 3-17}$$

DF = dilution factor

I = Iodine volume (ml)

H = 5% (w/w%) HCL used

F = filtrate volume (ml)

$$mg/g = [A - (DF)(B)(S)]/M \qquad \textbf{Equation 3-18}$$

M = carbon used (g)

S = Sodium thiosulphate (g)

3.7.5 Hardness Test

The hardness tests were completed following ASTM D 3802:

The hardness test is geared towards granular activated carbon. To begin the char was screened. The mesh size containing the majority of the particles is used following ASTM D 2862 where the nominal particle size is found. To make sure there was enough sample for the test the screened sample was placed into a 100 ml measuring cylinder. If the sample did not come close to the 100 ml mark more sample had to be screened. This sample was then weighed. The material was transferred to the hardness pan along with 15 steel balls and placed at the bottom of the sieve stack in the shaker as shown in Figure 3:7. The extra sieves serve only to form the stack that fills

the shaker. The sieve shaker was then turned on for 30 minutes. At the end, the hardness pan was removed from the bottom of the stack and the steel balls taken out. The content was then emptied into the mesh size used to find the nominal particle size and placed on top of the stack. The sieve shaker was then turned on for a further 10 minutes. When completed the remaining sample left in this sieve was weighed. The carbon hardness number is calculated by:

$$H = 100\, B/A \qquad \textbf{Equation 3-19}$$

H = Hardness number

B = Weight of sample retained on hardness test sieve

A = Weight of sample loaded onto the hardness pan



Figure 3:7 Sieve shaker similar to the one used in this project [Laval Lab, 2016].

3.7.6 Bulk Density

Bulk density was tested on biomass and resultant chars. The bulk density is the mass for a given volume. It was calculated using a 1 L bucket for pilot scale and a 100 ml measuring cylinder for lab scale. The bucket/measuring cylinder was knocked three times to level out the biomass and topped up to the marker line. The density was recorded in grams per decimetre cubed.

3.7.7 BET Surface Area and Pore Analysis

The BET surface area and pore analysis was conducted on a micrometrics ASAP 2420 surface area and pore analyser.

The carbon sample was left in granular form unless the particle size was too big to fit into the round bottomed analysis tubes provided, this was only the case with almond and coconut shell. First the tube and stopper was weighed. Roughly 0.1 g of material was then placed into the tube. This was altered slightly depending on the predicted surface area with slightly more added if the predicted surface area was smaller. The tube with stopper and the inserted carbon sample was

weighed. The analysis tubes were screwed into place for degassing; the step before the actual analysis takes places.

Degassing took place under vacuum to make sure the sample was fully dry. The process lasted 14 hours at 120 ^{o}C. The samples were then reweighed with small decrease in weight expected. Once the new weights had been inputted into the micro active 1.01 software the samples were set up for pore analysis. For nitrogen isotherms the samples were analysed in liquid nitrogen (77 K). For this the dewars were filled to the mark with liquid nitrogen. Once the covers and isothermal jackets had been placed on the analysis tubes the procedure could begin. This lasted between 8 and 24 hours depending on sample. Once the samples were completed the tubes were unscrewed, cleaned, and the carbon kept or disposed accordingly. CO_2 isotherms were completed in the same way except using CO_2 and conducted a 273 K with lower pressures used to get more detailed analysis of the ultra micropore region: dewars were filled with ice as opposed to liquid nitrogen. Diffusion of the CO_2 molecule is much faster than N_2 at their respective temperatures meaning CO_2 can be adsorbed into ultra micropores relatively quickly compared to using N_2. This allowed detailed analysis in micropore region by looking at the ultra micropores (< 0.7 nm). Additionally with CO_2 being a linear molecule it can fit into these smaller pores more easily. The two isotherms were joined together for a selection of samples using non local density functional theory (NLDFT) plots.

3.7.7.1 Brunauer, Emmett and Teller (BET) Analysis

BET surface area (m^2/g) is a measurement used across industry for activated carbon. Whilst higher surface areas would usually lead to the conclusion of a higher quality carbon, it is not necessarily the case, as a highly mesoporous carbon whilst having a smaller surface area can outperform a microporous carbon in some applications [Marsh, Reinoso, 2006]. The surface area is determined by adsorption of a gas (N_2) on the internal surface of the carbon. It is calculated by the quantity of adsorbate gas corresponding to a monomolecular layer on the surface.

BET surface area:

$$\frac{p}{V(p^0 - p)} = \frac{1}{V_m c} + \frac{(c-1)p}{V_m c p^0} \qquad \textbf{Equation 3-20}$$

Where p = partial vapour pressure of adsorbate gas, p^o = saturated pressure of adsorbate gas, V = amount adsorbed in volume (mmol/g), Vm = monolayer capacity (mmol/g), c = dimensionless constant related to enthalpy of adsorption of adsorbate gas,

The BET theory is an extension of Langmuir theory, of monolayer molecular adsorption and multiplayer adsorption:

1. Gas molecules physically adsorb on a solid in layers infinitely;
2. There is no interaction between each adsorption layer; and
3. The Langmuir theory can be applied to each layer.

[Marsh and Reinoso, 2006]

As discussed in Chapter 2 there are limitations to the BET theory. The BET surface area was processed using MicroActive software version 1.01. The BET surface area was calculated by selecting the first four data points on the BET plot produced (< 0.2 p/p_0). This was carried out in accordance to MicroActive interactive methods and Tascon, [2012] using the Rouquerol *et al.*, [1964] transform maxima making sure the C value and Y intercept were positive. This method has been adopted by international organisation for standardisation for determination of the specific surface area of solids for gas adsorption (ISO FDIS 9277) [Tascon 2012].

3.7.7.2 Dubinin and Radushkevich

Dubinin and Radushkevich (DR) method was used to determine the micropore volume (cm^3/g), it has been used in this instance across literature. The DR equation (Equation 3-21) is not based upon an adsorption model but is a derivative of the mathematics of Rayleigh, Gaussian or Lorenztain distributions [Marsh and Reinoso, 2006]. The Dubinin–Radushkevich equation is widely used for description of adsorption in microporous materials, especially those of a carbonaceous origin. The equation has a semi-empirical origin and is based on the assumptions of a change in the potential energy between the gas and adsorbed phases and a characteristic energy of a given solid [Nguyen, 2000].

$$W = W_0 \exp[(-\mathrm{RT}\ln(\mathrm{x})/\mathrm{E})^2] \qquad \textbf{Equation 3-21}$$

Where W = volume of adsorbate filling micropores, W_0 = total volume of micrpore system, x = p/p^0 and E =the characteristic energy E for a given fluid–solid system. The micropore volume via the DR method was calculated using MicroActive software by selecting the same end five data points on linear section of Dubinin-Radushkevich plot ignoring the two last points.

3.7.7.3 Total Pore Volume

Total pore volume (cm^3/g) was taken directly from the isotherm which includes both micropore and mesopore volumes, some macropore volumes are also likely to be added here although they make up such a small percentage in these carbons they are simply regarded as, and added to the mesopore volumes.

3.7.7.4 Mesopore Volume and Mesopore Percentage

Mesopore volume (cm^3/g) was calculated following the Gurvitsch rule where all pores are filled at approx. p/p_0 0.95 [Tascon, 2012]:

$$Total\ pore\ V\ (cm^3/\mathrm{g}) - \text{Micropore V}\ (cm^3/\mathrm{g}) \qquad \textbf{Equation 3-22}$$

And Mesopore %:

$$\frac{Mesopore\ V\ (cm^3/\mathrm{g})}{Total\ pore\ V\ (cm^3/\mathrm{g})} \times 100 \qquad \textbf{Equation 3-23}$$

3.7.8 Non Local Density Function Theory

NLDFT (carbon slit pores) an adaption of the DFT model was used to join together the N_2 and CO_2 isotherms and was done on MicroActive 4.03 software. The slit pore model is based upon uniform flat surfaced walls of infinite extent [Jagiello and Olivier, 2013]. The carbon slit model is widely used for carbons to determine pore size distribution (PSD). NLDFT allowed an accurate PSD of the micropore region with ultra micropores considered to be of pore diameters of < 0.7 nm. The cumulative pore volume produced by this model was used to obtain the values.

3.7.9 pH Tests

The pH test was carried out in accordance to the method provided by CEFIC European council of chemical manufacture federations, test methods for activated carbons.

First the pH probe was calibrated using standard solutions of specific pH values. The carbon was ground into a powder and 4 g of carbon material was placed into 100 ml of water boiling within a 250 ml beaker. The water was pre boiled to remove any carbon dioxide. The water, with the carbon, was then boiled for a further 5 minutes. A thermometer was placed in the solution as it was left to cool slightly. Before the solution reached 60 ^{o}C the supernatant liquid was poured off. The decanted portion was left to reach room temperature, at which the pH was measured using the pH probe. This was repeated using the same sample carbon to see the effect of a second "wash".

3.7.10 Hot Water Washing

Hot washing of the biomass was carried out two times. The raw biomass approx. 100 g was placed into a beaker with 500 ml of ultrapure water. The water with the biomass was boiled for 5 minutes. The water was decanted and replaced with fresh (500 ml). The biomass was then again boiled for 5 minutes. Once complete and cooled the biomass was recovered by filtration. The biomass was left in oven at 110 ^{o}C to dry for around 24 hours. The washed samples were pyrolysed and activated in the same way as the two-step and single step process shown in section 3.6

3.7.11 Ion Chromatography

Samples for ion chromatography were produced using the pH method in 3.6.10, using samples from both one and two "washes". The samples were filtered a second time to assure that all carbon had been removed.

Based on literature ash composition the main alkali alkaline cationic metals wanting to be observed were magnesium (Mg^{+2}), sodium (Na^{+}), potassium (K^{+}) and calcium (Ca^{+2}). For this standard solutions had to be made. The standards solutions were made using ultra-pure water at concentrations 10, 20, 30, 40 and 50 ppm. 1 ml of these solutions were injected into an ICS 5000+ using 6 mmol methane sulfonic acid (MSA) as the eluent. The sample was passed through at 0.25 ml/min and the test ran for 20 minutes per sample. The results were generated using Chromeleon 7.2 software.

3.7.12 XPS Analysis

X-ray photoelectron spectroscopy (XPS) analysis was carried out on a Kratos Analytical Ultra-2008 XPS system by Dr. Emily Smith at the University of Nottingham. The results were then generated using CasaXPS software.

3.7.13 Acid Washing –Fe Analysis

Prior to starting all equipment was washed with ultra-pure water to prevent contamination. Carbon (approx. 400 g) was weighed out into a 1 L beaker. This was filled to the mark with 2 M acetic acid and heated on a hot plate to 80 ^{o}C for 30 minutes. The acid was decanted and ultra-pure water added back to the 1 L mark. The sample was placed back onto the hot plate and heated for a further 30 minutes at boiling point. The beaker was then left to cool for 10 minutes before being filtered. The carbon was washed three times with 500 ml of ultra-pure water whilst being filtered. The sample was then put into a clean beaker before being placed into an oven for 12 hours for drying (110 ^{o}C). The sample was then taken out and cooled before being sealed in a sample bag. The sample was sent to Warwick Analytical for analysis.

3.7.14 SEM/TEM Imaging

Scanning Electron Microscopy (SEM) analysis of the char samples was carried out with a FEI XL30 FEG-ESEM, equipped with an energy dispersive x-ray (EDX) detection system. The accelerating voltage used was 10 kV, for the scattered electron and back scattered electron modes the spot size was 3.0. The working distance ranged between 9.2 -11.8 mm. Samples approx. 0.3g were stuck on to sticky back tabs and all analysis was carried out in vacuum secondary electron mode.

Transmission Electron Microscopy (TEM) was conducted at the University of Nottingham with help provided by TEM technicians from the Faculty of Engineering department. High resolution

TEM was carried out using a JEOL 2100F microscope (JEOL, Japan) at an acceleration voltage of 200kV.

3.8 Pilot Scale

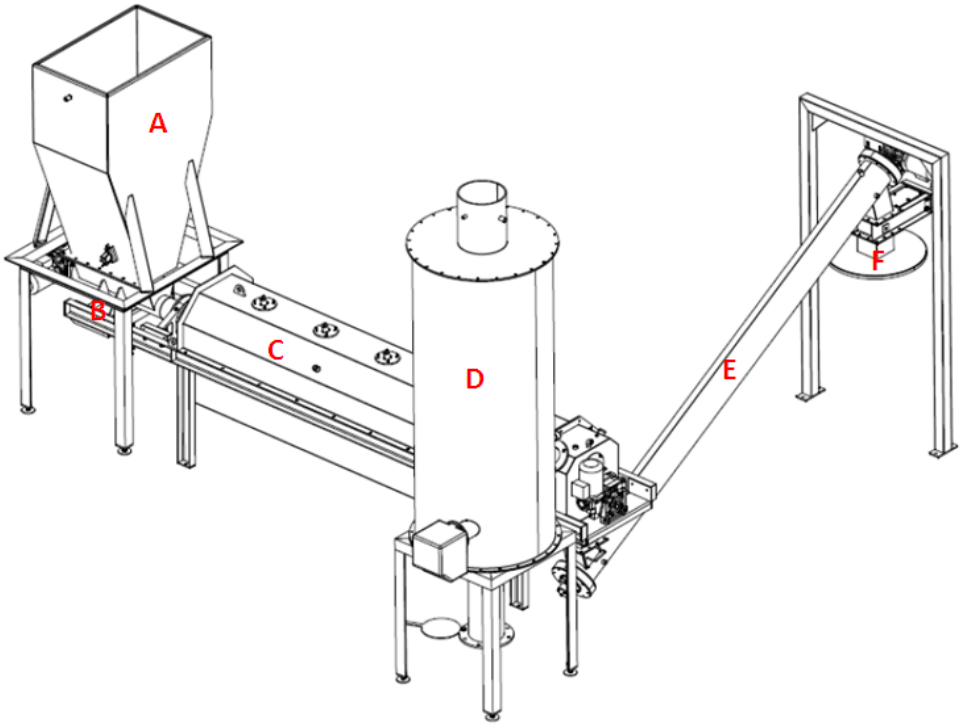


Figure 3:8 Ansac HK250E pyrolysis kiln. A = feed hopper; B = feed screw; C = rotating heat tube; D = after burner; E = cooling screw; F = discharge slide gate [J Lenthall, 2012].

3.8.1.1 Pyrolysis

A know mass of coconut shell, olive stone or pine wood was deposited into the feed hopper (A) (0.67 m^3). The kiln is switched on and heated to the final pyrolysis temperature (700 ^oC) across the three heating elements. At 700 ^oC the temperature fluctuation inside the rotary kiln was found to be a very stable, at lower temperatures this was not the case. Nitrogen flow of approx. 5 L/min was passed through the kiln (C) and cooling screw (E) to produce an inert atmosphere. The after burner (D) was turned on at this stage to heat up - using natural gas. Once the temperature (700 ^oC) was reached the feed screw (B) (length = 1 m) was turned on at a set percentage: the higher the percentage the faster the feed screw rpm, meaning increased feed rate. The material then enters the heat tube (C) (length = 3 m, diameter 0.25 m, incline of 1.5 ^{o}) again the percentage set on the HMI (see Figure 3:9) increases or decreases the rpm of the heat tube and affects residence time. The rpm was configured to give approx. 30 minutes residence time. At this point (D) the natural gas was turned off as the pyrolysis volatiles were now used as the fuel source; any exhaust fumes were sent up a 6 m vertical chimney. Once the material had traversed the heat tube it fell into the water cooled cooling jacket. At the bottom of the cooling jacket the water cooled cooling

screw (E) beings. The hot char passed up through this screw cooling as it went before being deposited (F) into an air tight steel drum.

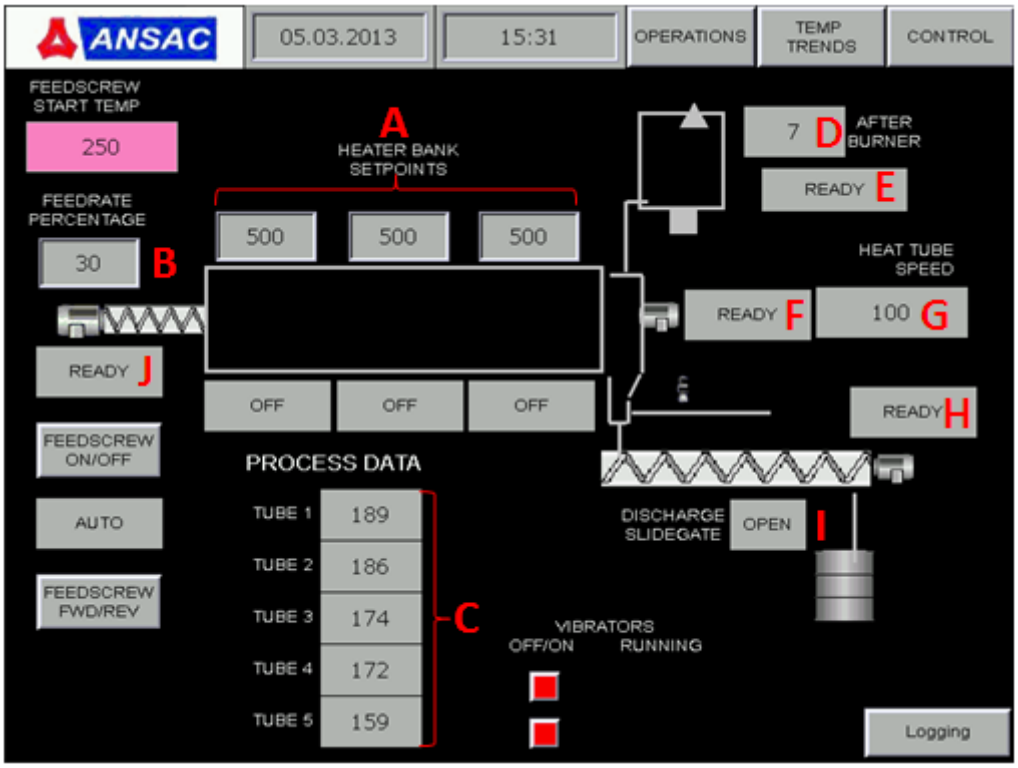


Figure 3:9 Main screen of the HMI used to operate the pyrolysis equipment. A = heater bank set-points; B = feed screw rate (%); C = rotary kiln thermocouple outputs; D = afterburner thermocouple output; E = afterburner status; F = rotary kiln status; G = heat tube rate (%); H = cooling screw status; I = discharge gate status; and J = feed screw status [J.Lenthall, 2013].

3.8.1.2 Activation

In the pilot activation tests the residence time had to be increased more than usual to allow sufficient steam to enter the system and the time for steam – carbon contact to take place. Although the Reynolds number was higher on pilot scale, without heat tube lifters present a large space remains above the carbon bed where steam will potentially pass without contacting the biomass char. Residence time was altered by adjusting the heat tube speed (rpm). Average residence time was calculated by placing 20 kg of char into the feed hopper and running the kiln cold. Feed rate was then calculated by measuring the time until the feed hopper was empty. At this point the heat tube was switched off with just the cooling screw left running. Once the cooling screw had been emptied, the material was weighed. By knowing the weight of this char, the weight inside the kiln could be calculated by subtraction from the weight of the original mass. This weight was then divided by the feed rate:

$$\text{Average residence time} = \frac{Mass\ in\ heat\ tube\ (kg)}{Feed\ rate\ (kg/\text{hr})} \qquad \textbf{Equation 3-24}$$

Average residence time is calculated as each particle will have a slightly different residence time until a steady state is reached when the kiln heat tube is full.

Temperature ranges were based on the boundaries found in Chapter 5, taking into consideration the thermocouples read the temperature just outside the heat tube which will be slightly higher than the carbon bed. Water flow rate was adjusted between 50 ml and 300 ml and system pressure was kept as close to 0 inH_2O as possible by opening and closing the valve to the after burner when necessary. This was for safety reasons and for an open system comparison to lab scale.

The kiln was prepared as with pyrolysis stage. The temperatures were set and the steam generator tuned on to the chosen flow rate. The kiln was allowed to reach 50 ^oC under the final chosen activation temperatures before the feed screw was turned on. This was to allow for any over shoot in temperature of the kiln. The kiln was set to automatically alarm and turn off at 950 ^oC. If the calculated residence time was 3 hours the first sample was taken from the discharge barrel at the 4 hour mark followed by the 5^{th}, 6^{th} hour or until the heat tube was empty. This allowed the carbon enough time to traverse the cooling screw and drop into the discharge barrel. Each sample was placed on a tray and left in a drying oven for 12 hours at 125 ^oC. The kiln was switched off 3 hours after the feed hopper emptied. The cooling screw was left on to recover any remaining material. The following day any material deposited in the discharge barrel was dried as with previous collected samples for 12 hours (125 ^oC). Once the individual samples had been dried they were deposited in sample buckets and weighed. The total weight of the samples was added to calculate the total burn off percentage. The middle two samples were then used for CTC analysis as they were activated during steady state (when the heat tube was full). The CTC test was carried out three times for each sample.

3.9 Main Analysis Repeats and Errors

3.9.1 CTC Error

As so many experiments were conducted due to the amount of possible variables only select experiments were repeated numerous times. This set of repeats come from different production sample batches produced under the same conditions. The main standard two-step steam activation repeats can be seen below and were repeated at least six times each (tables shown in Appendix A-5, A-6) for both olive stone and pine wood carbons. This was to find the variability in burn off and associated CTC values, methylene blue numbers and pore analysis from the optimum ratio trend lines. The error bars (Standard deviation) can be seen below.

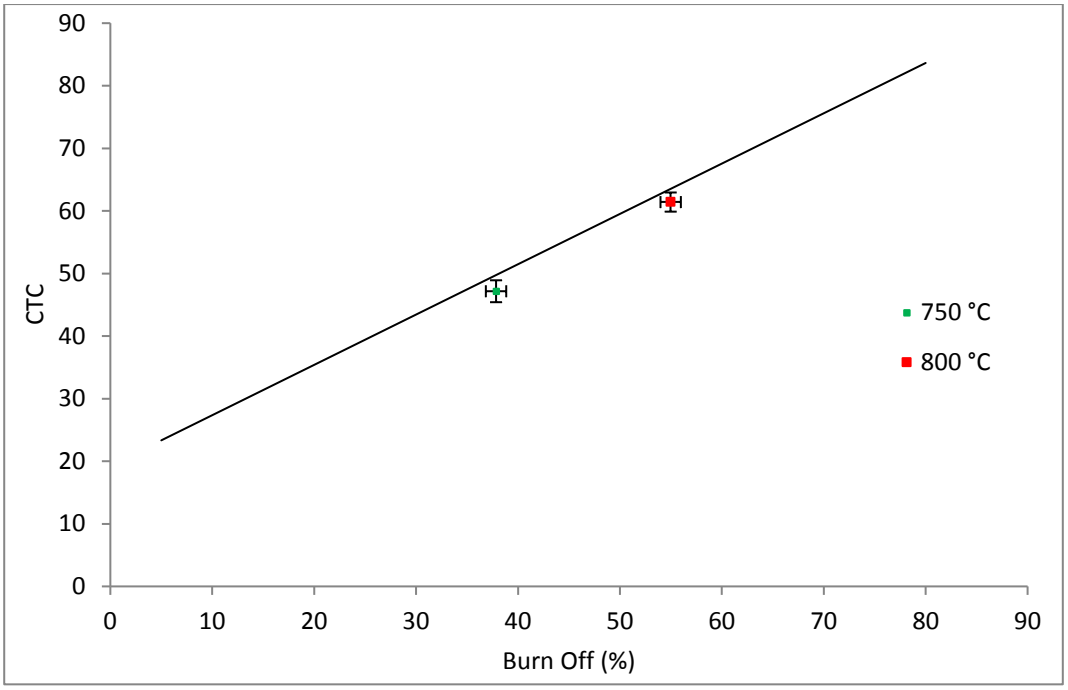


Figure 3:10 Different production batch repeats with error bars (SD) against optimum CTC, burn off ratio linear correlation taken from Figure 5:2 for olive stone activated carbons

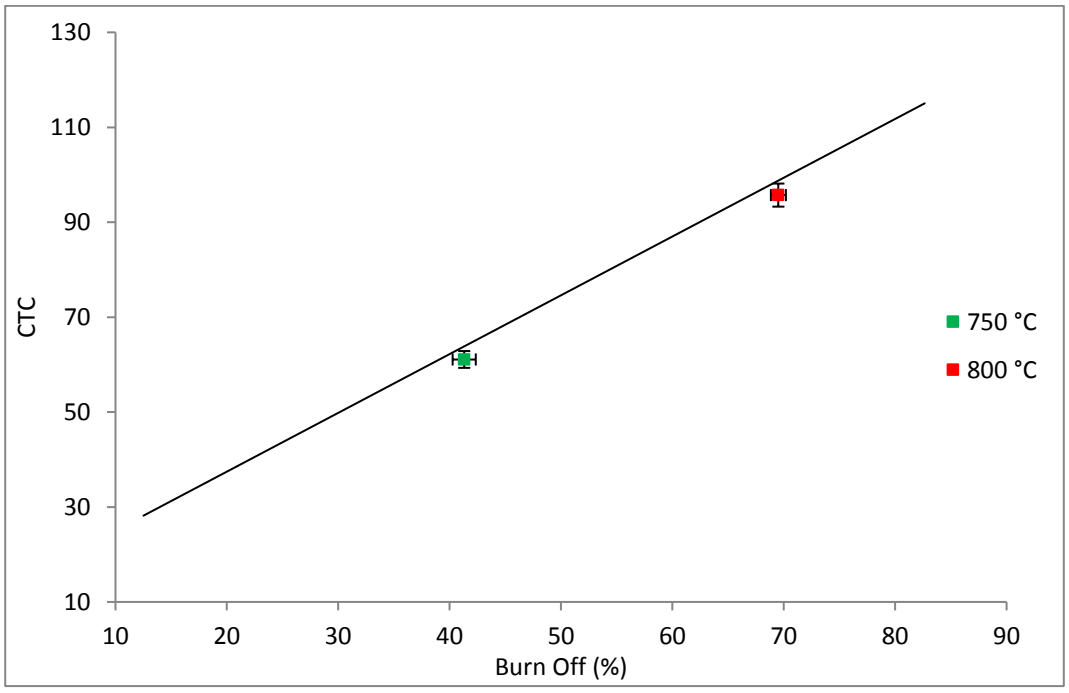


Figure 3:11 Different production batch repeats with error bars (SD) against optimum CTC, burn off ratio linear correlation taken from Figure 5:4 for pine wood activated carbons.

The repeats from both the raw data tables (Appendix Tables A-5 and A-6) and the error bars in Figure 3:10 and Figure 3:11 show the error is relatively small across both olive stone and pine wood lab trials. As stated the pine wood char is milled to a mesh of 3 mm and the olive stone particle size is unaltered ranging from 1 mm to 4 mm and so product uniformity is high.

3.9.2 Pore Analysis Error

The repeat samples used above were then used for numerous pore analysis runs to see the associated error with regards to porosity. Five runs at 750 °C and 850 °C were conducted for both olive stone and pine wood carbons. Table 3-1 shows an example of how the repeats were carried out. Three different production samples batches (produced under the same conditions) were repeated along with three repeats of the same sample batch.

Table 3-1 Example (olive stone) of how the repeats were carried out for BET analysis.

No.	Temperature (°C)	Residence Time (mins)	BET (m^2/g)	Vmi (cm^3/g)	Vme (cm^3/g)	Vtot (cm^3/g)	Vme (%)	Burn Off (%)	CTC
1	750	60	712.2	0.2791	0.1462	0.4253	34.38	36.54	45.0
2	750	60	715.9	0.2800	0.1361	0.4161	32.71	37.45	46.5
3	750	60	724.0	0.2839	0.1441	0.4280	33.67	37.79	46.0
3(2)	750	60	709.0	0.2782	0.1467	0.4249	34.53	37.79	46.0
3(3)	750	60	692.3	0.2710	0.1140	0.3850	29.61	37.79	46.0
	Average		**710.7**	**0.2784**	**0.1374**	**0.4157**	**32.98**	**37.47**	**45.9**
	Standard Deviation		**11.7**	**0.0047**	**0.0138**	**0.0178**	**2.01**	**0.54**	**0.5**

Other tables can be found in the Appendix Table A-7

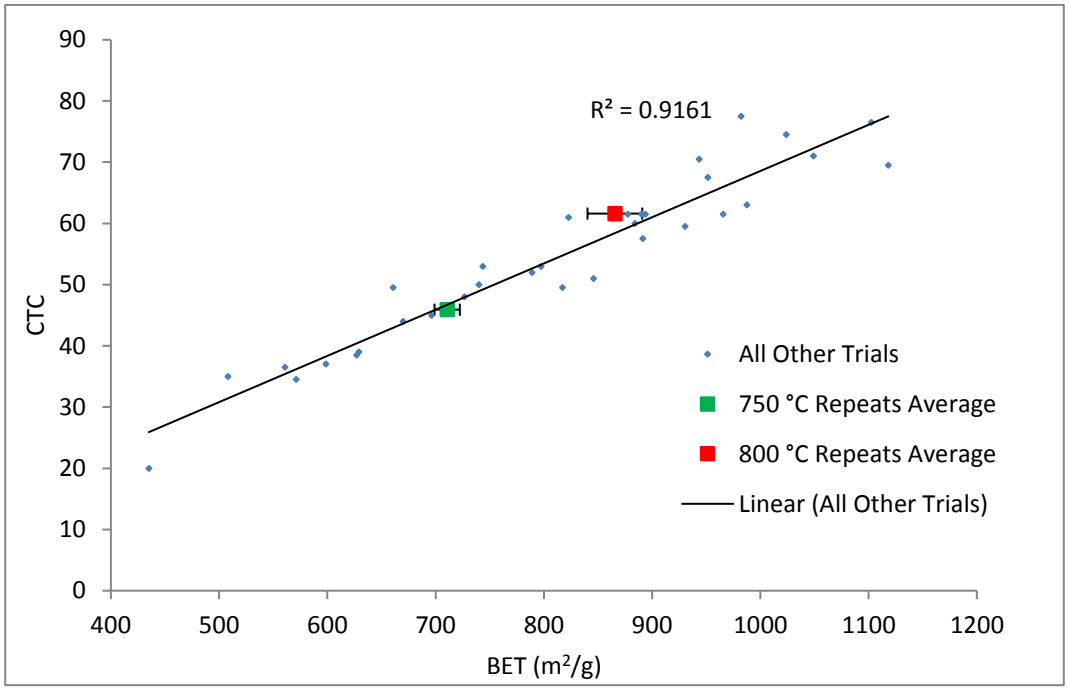


Figure 3:12 Different batch samples and same batch repeats shown with associated error (SD) for BET surface area (m^2/g) against CTC, olive stone.

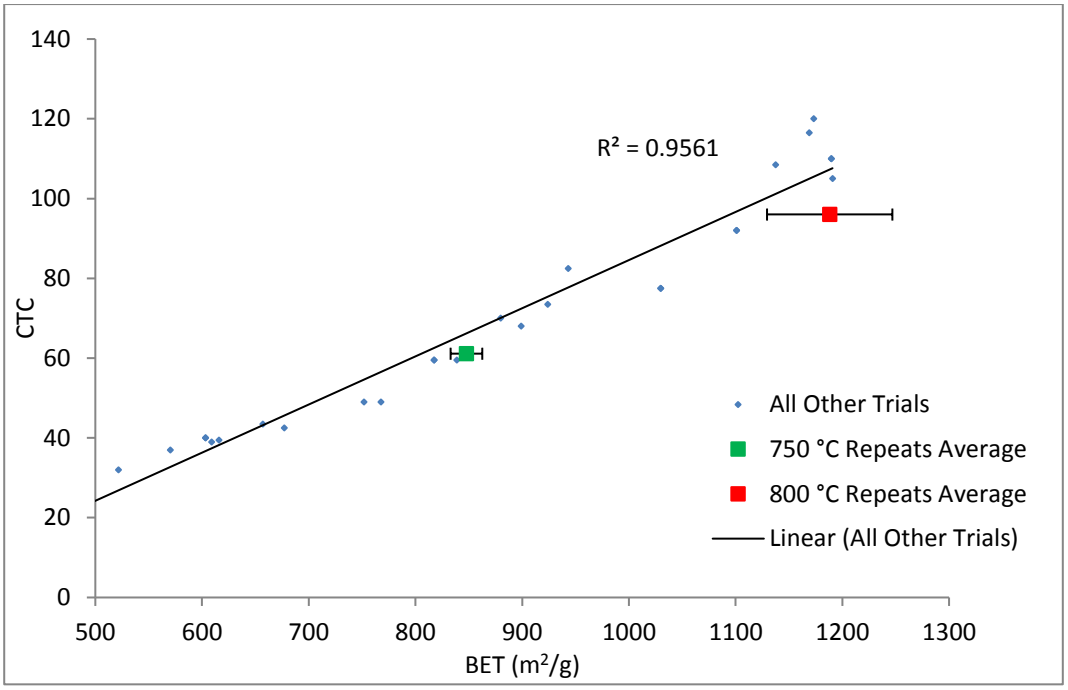


Figure 3:13 Different batch samples and same batch repeats shown with associated error (SD) for BET surface area (m^2/g) against CTC, pine wood.

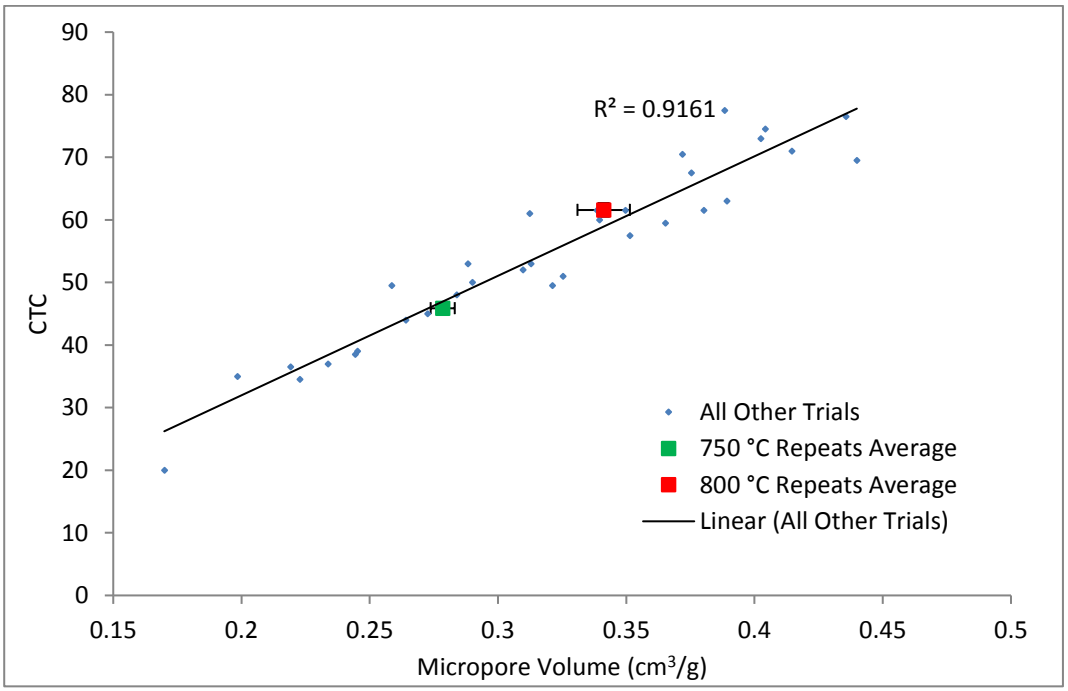


Figure 3:14 Different batch samples and same batch repeats shown with associated error (SD) for micropore volume (cm^3/g) against CTC, olive stone.

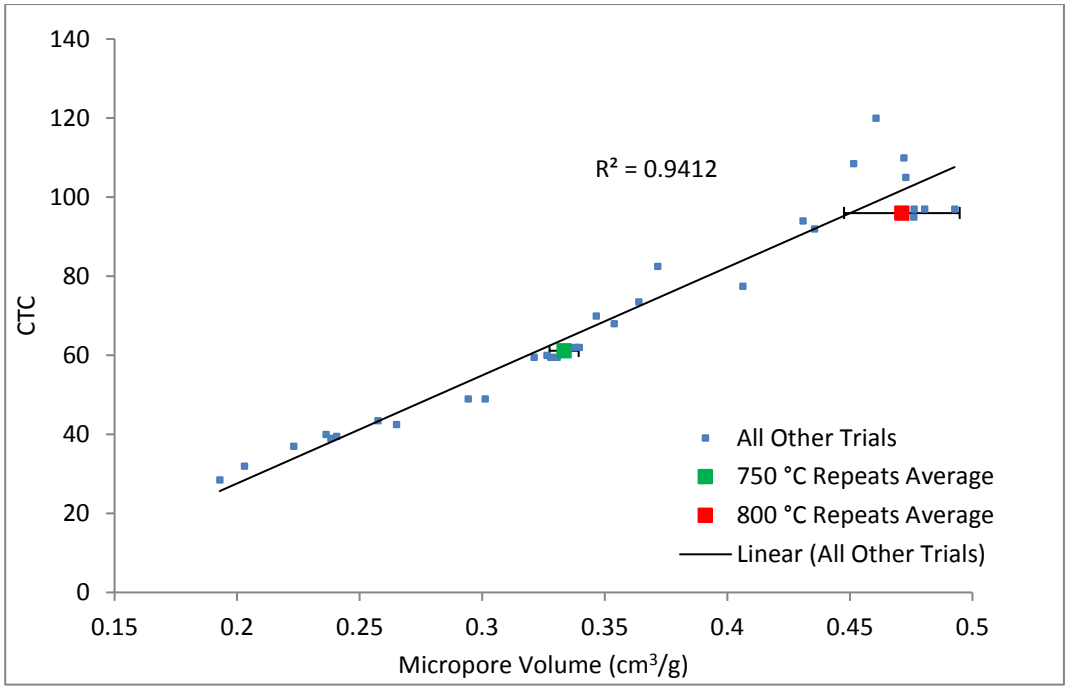


Figure 3:15 Different batch samples and same batch repeats shown with associated error (SD) for micropore volume (cm^3/g) against CTC, pine wood.

Figure 3:12 to Figure 3:15 show the standard deviation of repeats in graphical form for both BET surface area and micropore volume against CTC values taken from samples produced from different and the same batch. The error is relatively small (see Table A-7 in Appendix) meaning results can be taken with confidence however, this also points towards changing the variables in addition to activation temperature is having a slight influence on surface area, porosity and associated CTC values as data points fall outside the error range seen for these repeats.

3.9.3 Methylene Blue Error

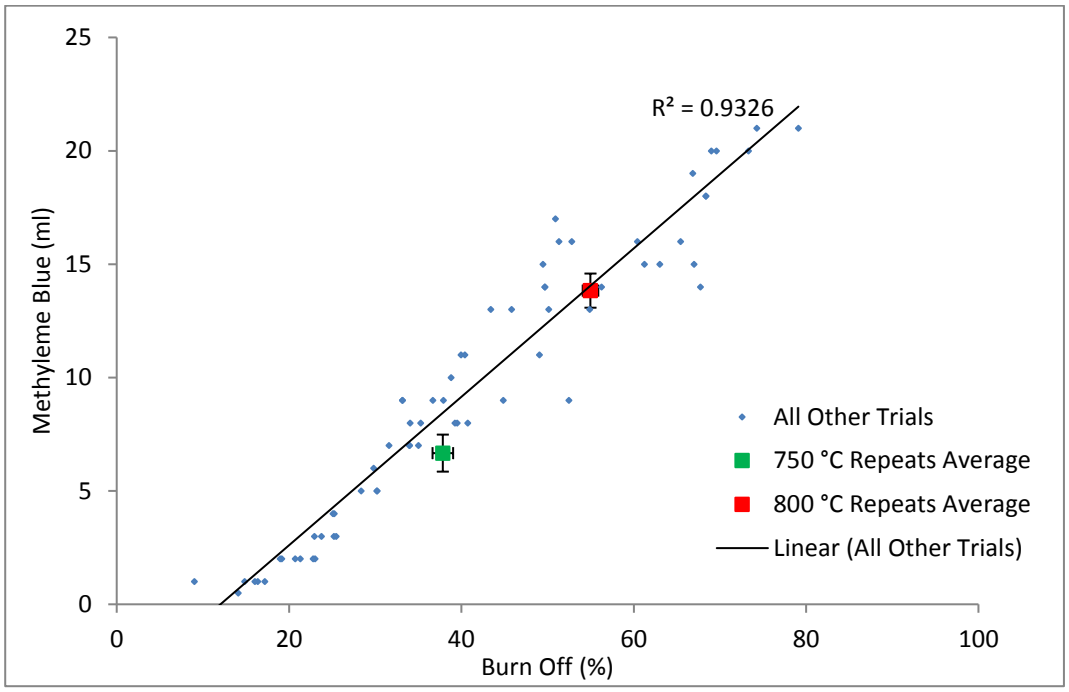


Figure 3:16 Different sample batch repeats with associated error (SD) for burn off (%) against methylene blue (ml), olive stone.

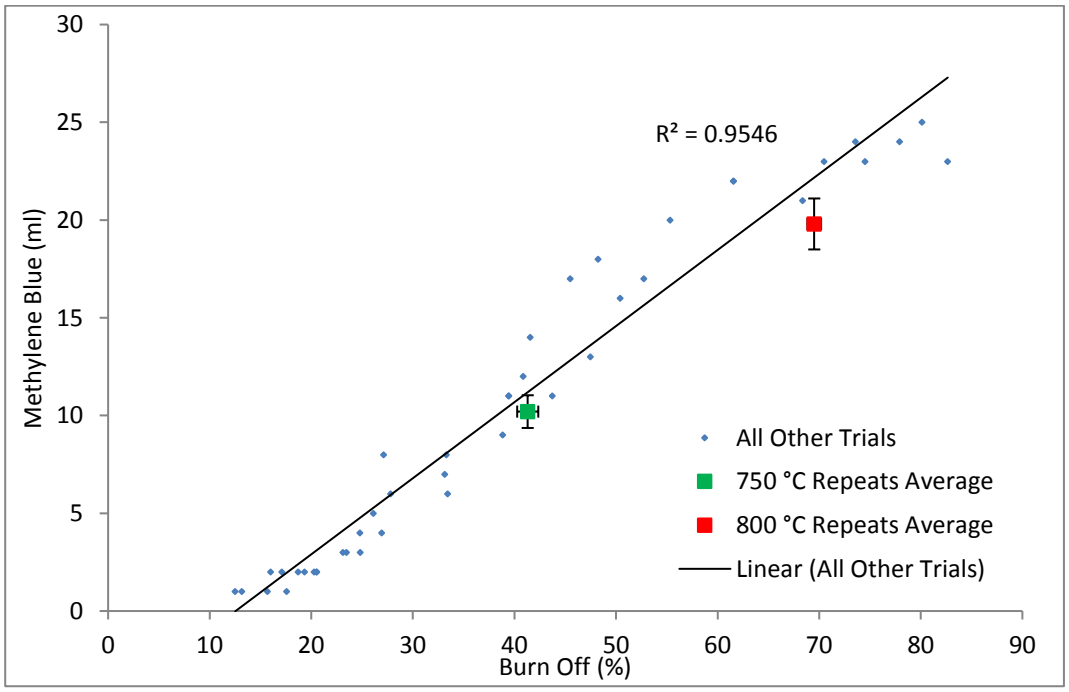


Figure 3:17 Different sample batch repeats with associated error (SD) for Burn off (%) against methylene blue (ml), pine wood.

Figure 3:16 and Figure 3:17 show the standard deviation errors for the burn off and methylene blue correlation for both olive stone and pine wood (see Appendix Tables A-5 and A-6). As before the error is smaller than the range seen, whilst the correlation is strong there is some further influence on results by altering the activation conditions as shown in Chapter 5.

3.10 References

Anon, Laval Lab http://test-sieve.com/ro-tap-sieve-shaker/ 2016 [accessed July 2016]

J Jagiello and J Olivier "*2D-NLDFT adsorption models for carbon slit-shaped pores with surface energetical heterogeneity and geometrical corrugation"* Carbon Vol 55 pg 70-80

Joanne Lenthall 2013 "*The Development of Solid Fuels With Reduced CO_2 Emissions"* 2014, University of Nottingham

Marsh H and Reinoso FR. 2006. "*Activated Carbon."* Elsevier Science & Technology Books.

Nguyen, D.D. 2000 "*The Dubinin–Radushkevich equation and the underlying microscopic adsorption description*" Carbon 39 (2001) 1327–1336 Department of Chemical Engineering, The University of Queensland, St. Lucia, Qld 4072, Australia

Rouquerol F Rouquerol J, Imelik B, 1964 "*Validite de la loi BET dans le cas de l'adsorption d'azote d'argon et de butane sur des adsorbants poreux*" Bull soc. Chim France 635-639

Tascon Juan M.D (2012) "*Novel Carbon Adsorbents"*, Oviedo Spain, Elsevier pg 120

Chapter 4 Preliminary Tests.

4.1 Introduction- Preliminary Trials

Preliminary trials commenced on a horizontal tube furnace (HTF) at the University of Nottingham shown in Chapter 3. Four biomasses were acquired. These were palm kernel shell, almond shell, olive cake pellets and mixed wood waste. The first three were taken from CPL industries whilst wood waste sample was taken from the University of Nottingham.

The following proximate analysis was conducted for the four biomasses as shown in Table 4-1

Table 4-1 Proximate analysis results for given biomass feedstocks.

Biomass	Moisture (%)	Ash (Dry Basis, %)	Volatile (Dry Basis, %)	Fixed Carbon (Dry Basis, %)
Almond Shell	7.9	1.0	87.0	12.0
Palm Kernel Shell	7.7	1.4	82.1	16.5
Waste Wood Chips	9.9	2.3	84.2	13.5
Olive Cake Pellets	12.3	5.7	84.4	9.9

As expected, the four biomass types show how they are dominated by volatiles and have roughly the same proportion of moisture, ash and fixed carbon with a relatively low fixed carbon percentage compared to coal (see Chapter 2 Table 2-2).

4.2 Pyrolysis

Table 4-2 Average results of pyrolysis for the given biomass feedstocks.

Biomass	Pyrolysis Temperature (^{o}C)	Residence Time (mins)	N2 flow (L/m)	Char Yield + Ash (Dry basis, %)
Palm Kernel Shell	700	60	1	30.7
Almond Shell	700	60	1	24.5
Waste Wood Chips	700	60	1	26.1
Olive Cake Pellets	700	60	1	27.7

To get enough material for activation charring was conducted three times. The results above indicate the average percentage yield for the three repeats.

The yield (dry basis) is calculated for a direct comparison between the four chars, although it must be noted moisture content can affect char yields [P Brownsort, 2009]. The yield follows the fixed carbon content with the first three raw materials, with palm kernel shell having the highest yield followed by waste wood chips and almond shell. Olive cake pellets has the lowest fixed carbon content but this is negated by the high ash content which should also be left behind in the char. The alkali alkaline metals in the ash can also increase char yields as reported throughout literature such as by Maty, *et al*., [2015] who look into the zinc and calcium metals as flame

retardants which increase in char yields and DeMartini *et al*., [2013] who looked into the effect of removing alkali/alkaline metals from pine wood which decreased pyrolysis yield. If the ash and fixed carbon content is added together for all four biomasses the pattern observed is that the total ash and carbon content relate to the pyrolysis yield as shown in Table 4-3.

Table 4-3 Total ash and carbon contents compared to their corresponding char yields.

Biomass	Total Ash and Carbon (dry basis, %)	Pyrolysis Char Yield + Ash (dry basis, %)
Palm Kernel Shell	17.9	30.7
Almond Shell	13.0	24.5
Waste Wood Chips	15.8	26.1
Olive Cake Pellets	15.6	27.7

Almond shell has the highest volatile content and it is therefore expected that the resultant char has the lowest yield of the four. The biomass char yields fall between the stated "20% and 30%", [Marsh and Reinoso, 2006].

4.3 Steam Activation

$$H_2O_{(g)} + C_{(s)} \rightarrow CO_{(g)} + H_{2\,(g)} \qquad \textbf{Reaction 1}$$

Reaction 1 shows the chemical reaction between steam and carbon during steam activation.

The main results are shown in Table 4-4 below

Table 4-4 Preliminary trial results for the four biomass precursors, 5g char used each time.

Biomass	Temperature (°C)	Residence Time (mins)	Flow rate (ml/min)	Nitrogen flow rate (L/min)	Carbon + Ash yield (%)
PKS	750	60	1.5	2	84.4
	800	60	1.5	2	74.6
	850	60	1.5	2	60.5
Almond Shell	750	60	1.5	2	58.4
	800	60	1.5	2	52.1
	850	60	1.5	2	22.6
Mixed Wood	700	60	1.5	2	83.4
	750	60	1.5	2	67.2
	800	60	1.5	2	56.0
Olive Cake	700	60	1.5	2	57.4
	725	60	1.5	2	43.1
	750	60	1.5	2	35.2
	800	60	1.5	2	20.3
	850	60	1.5	2	16.1

Table 4-4 shows that the yield decreases as temperature increases. Palm kernel shell (pks) achieved the highest yield in both pyrolysis and activation. Mixed wood again achieved a slightly higher yield with pyrolysis and activation, compared to almond shell under the same conditions. However, olive cake had the second highest pyrolysis yield, yet conversely now had the lowest yield after activation. As shown in Table 4-1 olive cake pellets contain the highest ash content by a significant margin. Ash contents have been covered in the Chapter 2 and Chapter 5 and it is known ash can act as a catalyst during activation as Marsh and Reinoso, [2006] stated 'Of these inorganic materials it is the salts, oxides and metals of the series of alkali metals, alkali earth metals and transition metals which are particularly effective as catalysts'. High alkali metal content in olive cake is reported by Atimtay and Varol, [2008], who investigated olive cake for fuel in a combustor, who report high alkali metal content, in particular, K_2O, CaO and Na_2O compared to coal and other biomass types. Looking at the data presented it looks like this is occurring with the olive cake during activation and is the reason for the enhanced burn off. Conversely high alkali alkaline metal content can increase pyrolysis yields, which is discussed in Chapter 5.

Two values were acquired for these preliminary tests - these were the CTC value using standard (ASTM D 5742) which proves throughout this project a very good test for overall activity in carbons, and BET surface area (m^2/g) on the highest burn off samples, (pks, almond shell and, waste wood) to provide a quick but effective analysis of these three biomass types.

Table 4-5 CTC and BET surface area results from the preliminary test data.

Biomass	Temperature (°C)	Carbon Yield + Ash (%)	CTC	BET (m^2/g)
PKS	750	84.4	31.0	
	800	74.6	44.0	
	850	60.5	47.0	948
Almond Shell	750	58.4	37.5	
	800	52.1	55.0	
	850	22.6	62.5	1137
Waste Wood	700	83.4	30.5	
	750	67.2	46.5	
	800	56.0	55.5	959
Olive cake pellets	700	57.4	20.0	
	725	43.1	25.0	
	750	35.2	21.5	
	800	20.3	8.5	
	850	16.1	6.0	

For the first three biomasses, as the temperature is increased CTC value also increases. The highest CTC value is obtained with almond shell at 850 °C. This is also at the point of the highest burn off between the three biomasses. When the burn off is approx. 15% for both pks at 750 °C

and waste wood at 700 ºC the CTC value is the lowest (30/31). These results begin to indicate that the higher the burn off, the higher the resultant CTC and therefore the higher the temperature the higher the CTC. The results can be seen in graphical form:

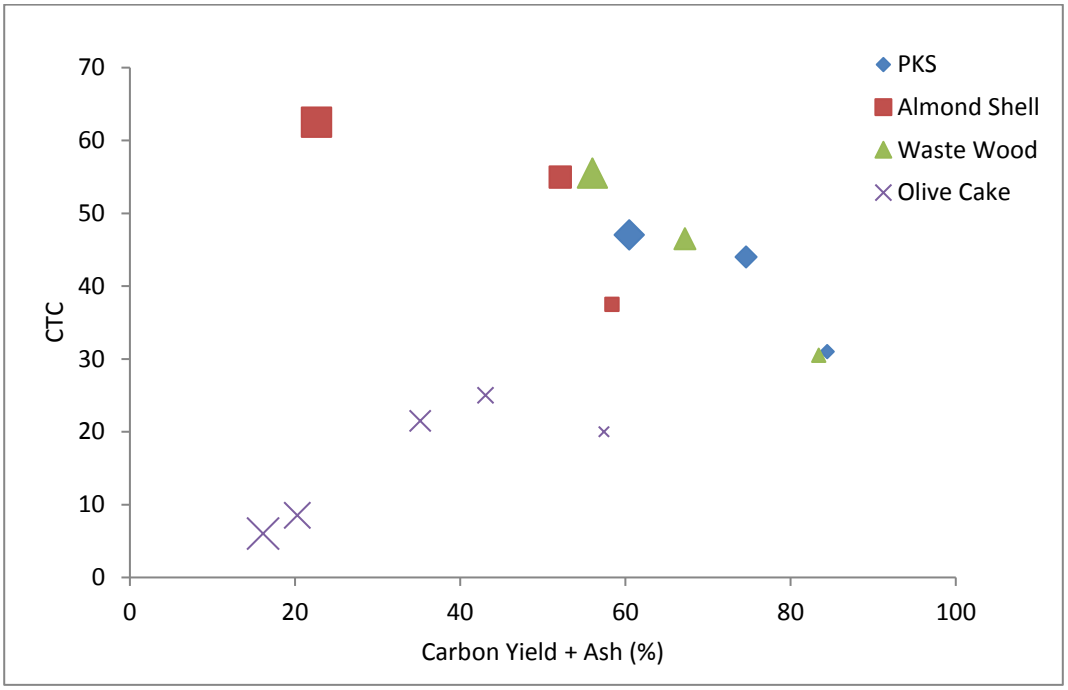


Figure 4:1 Carbon yield against CTC. The marker size increase represents an increase in activation temperature.

Figure 4:1 shows a clearer representation of all four biomasses. Although there are only three experimental data points for pks, almond shell and waste wood there is a clear indication of a large initial increase in CTC as yield decreases for pks and almond shell. This increase in CTC then begins to plateau as burn off increases further. Waste wood has not reached this point as yet as the increase in CTC is still linear. However, olive cake differs greatly from the other biomasses with a much lower CTC for a given yield. Peak performance is seen during activation conducted at 725 ºC with a 43% carbon yield, yielding a CTC of 25. After this peak there is a drop off and is likely to be due to pore destruction and/or a high ash to carbon ratio. As mentioned olive cake has the lowest fixed carbon percentage along with the highest ash content and as reported by Varol, [2006] olive cake contains a high alkali metal content. This means the ratio between catalyst (alkali metals) that enhance the reaction rate [Wen-Yang Wen, 2006] and fixed carbon is high. This enhanced catalytic effect appears to be having a negative impact on the pore development of the olive cake carbon. In terms of physical appearance of the olive cake, carbon ash could be clearly seen on the carbon surface at higher burn off as Figure 4:2 shows.



Figure 4:2 Olive cake pellets high burn off leaving high ash to carbon ratio, sample conducted at 800 ^{o}C, 60 minutes.

4.4 TEM Images

TEM images were also taken for the three biomasses (pks, almond shell and mixed wood)

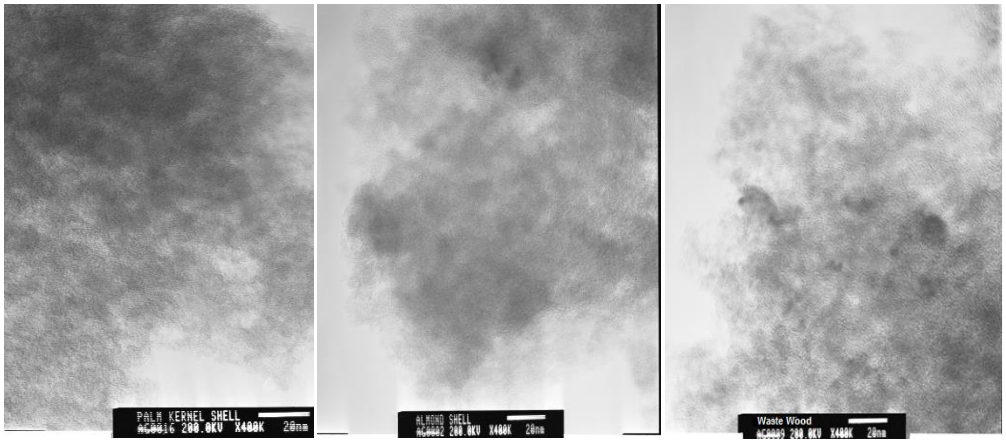


Figure 4:3 TEM images (from left to right) of PKS, Almond Shell and Waste Wood.

From Figure 4:3 the graphene layers and the porous nature is evident across the three carbons. The lighter parts of the images indicate 'open space' porous regions within the deformed graphene layer. Due to the high resolution both micropores and mesopores should be shown, whilst the grey areas shows the disordered graphene layers surrounded by porosity.

4.5 Biomass Database (Appendix Table A-1)

Following trials began at CPL industries using a similar HTF and procedure. Pyrolysis and activation was carried out on a large number of biomasses. The objective of this was to get a quick overall understanding of many different types of biomass (see Appendix Table A-1).

Results Table A-1 shows most of the over 30 biomasses that were tested during the early stages of this project. The biomasses went through pyrolysis (700 ^{o}C, 30 minutes) followed by the chosen standard activation (800 ^{o}C, 1 hour and 1.5 ml/min steam flow). The activation conditions were only changed if the carbon yield was too low for analysis and in this case the activation

temperature was then reduced. Proximate analysis of the biomasses (when enough material was available) was completed, and can be found in the Appendix Table A-2.

The majority of biomasses in this list produced char yields of between 20% and 30%, the usual expected [Marsh and Reinoso, 2006]. The two coals (brown coal and anthracite) produced yields of around 45% and 78% respectively. This is, of course, an expected occurrence with the volatile content of brown and anthracitic coals being much lower than biomass.

Comparing the other biomass types, the yield differences can be attributed to the makeup of the biomass, i.e. the cellulose, hemicellulose and lignin content. Cellulose and hemicellulose decomposes at 'low' temperatures, typically below 400 ^{o}C. In comparison, lignin decomposes over a much wider range up to 900 ^{o}C. Therefore, it can be said that generally the higher lignin content, the higher the yield of produced char [Demirbas, 2006]. It must be stressed that the results shown for pyrolysis yields are for biomass on an 'as received' basis and so have varying moisture contents. Dry basis values are looked at when the list is narrowed down to six biomasses shown in section 4.6

The resultant char from each biomass was weighed and placed back into the furnace for activation. There are now two yields presented: char yield and the carbon yield which can also be represented by burn off percentage which is calculated by:

$$100\% - (\text{Carbon} + \text{Ash yield } \%) \qquad \textbf{Equation 4-1}$$

The final total yield takes into account both char and carbon yield. In depth analysis of burn off and burn off rates are covered in Chapter 5.

4.6 Selected Biomass Analysis

The criteria listed below were used when narrowing down the biomass selection to six.

1. A relatively high CTC to burn off ratio.
2. If the material is readily available in large quantities.
3. Potential cost of raw material.
4. A reasonable overall yield taking number 3 above into account.
5. Location of raw material (transport cost and carbon footprint with long distances).
6. A least two of each granular and powdered activated carbon for comparison.
7. Low ash content.
8. The potential to become a viable commercial activated carbon.

From this list the aim was to reduce the number of potential biomasses to around five, along with coconut shell that was to be used as a reference material to make up the six possible biomasses. The selection:-

1. Coconut Shell:
   As the reference material
2. Olive Stone:
   High CTC for given burn off, Best overall yield to CTC. Cost and availability good but dependant on harvest, EU sourced, low ash content. Granular carbon.
3. Pine Wood:
   Low overall yield offset by cheap price and year round availability. Can be UK or EU sourced, low ash content. Powdered carbon.
4. Eucalyptus Wood:
   Similar to pine wood, however, slightly more expensive due to being hard wood and slower growing properties, sourced within EU and not UK. Powdered carbon.
5. Grape Seed:
   Very low cost, high CTC potential, EU sourced. Powdered carbon.
6. Almond Shell:
   Low yield but high surface area and high CTC values, sourced from southern Europe, readily available, low ash high volatile. Granular carbon.

4.6.1 Pyrolysis of the Six Biomasses

As discussed previously, lignin content is seen by many as the key parameter to pyrolysis yields. The lignin content has not been tested with these specific biomasses used in these trials. However, literature values are shown below. It must be stressed how each biomass can vary depending on where it has originated.

PKS 50% [E.C. Okoroigwe, 2012]

Olive stone = 39%, Coconut shell = 44.0% [Mendu, 2011]

Eucalyptus wood = 31.3%, Pine wood= 27.7% [Klemn *et al*., 1998]

Almond shell = 27.20% [Antal *et al*., 2000]

The pyrolysis yields (dry basis) of these biomasses are shown in Table 4-6:

Table 4-6 Pyrolysis yields (dry basis).

Biomass	Char yield + Ash (dry basis, %)
Almond Shell	24.5
Palm Kernel Shell	30.7
Olive Stone	31.5
Coconut Shell	28.5
Eucalyptus Wood	21.2
Pine Wood	20.2

When comparing these values to the literature values for lignin content there is no direct correlation for each specific individual biomass. Nonetheless, the three biomasses with the highest lignin percentages have the highest pyrolysis yields. The woods and almond shell have a significantly lower lignin percentage than the previous three biomasses and it can be seen that the pyrolysis yields of these three biomasses are significantly lower.

4.6.2 Activation of Chosen Biomass

Activation was then completed for each biomass. An example of the production matrix is shown in Table 4-7

Table 4-7 Example of the matrix completed for the six biomass types, (example shown: Coconut Shell).

Coconut Shell	Dwell Time (mins)	Temperature (°C)	Mass sample (g)	Water flow (ml/min)	Burn Off (%)	Carbon +Ash Yield (Dry Basis, %)	CTC
	30	750	10	1.5	7.5	26.4	19.0
	45	750	10	1.5	15.5	24.1	36.5
	60	750	10	1.5	20.5	22.7	38.0
	30	800	10	1.5	16.3	23.9	36.5
	45	800	10	1.5	27.1	20.8	50.0
	60	800	10	1.5	34.3	18.7	53.5
	30	850	10	1.5	27.0	20.8	41.5
	45	850	10	1.5	34.3	18.7	53.5
	60	850	10	1.5	48.6	14.7	63.5

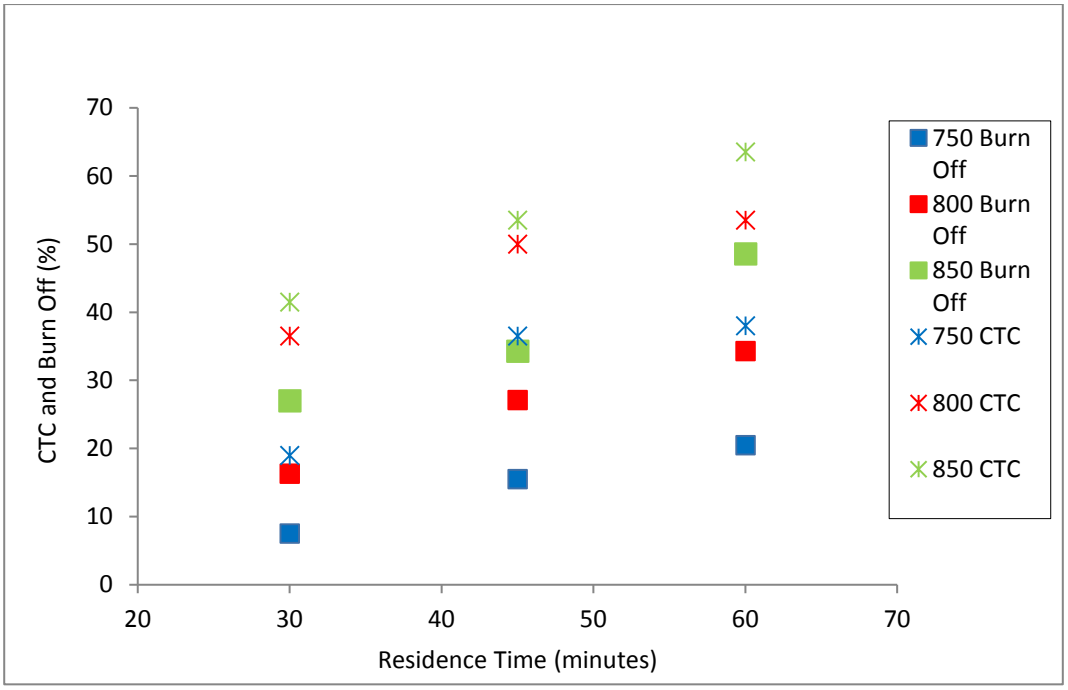


Figure 4:4 CTC, temperature and burn off (%) relationship for coconut shell activated carbon.

In Figure 4:4 as residence time increases carbon burn off also increases with coconut shell char. The same trend is observed with an increase in activation temperature. As the activation temperature increases from 750 ^{o}C to 850 ^{o}C and the residence time increases from 30 minutes to 60 minutes there becomes a larger burn off difference between the burn off percentage value from the trial conducted at 750 ^{o}C compared to the trial conducted at 850 ^{o}C. This increases in burn off produces an increase in CTC.

The other biomass types produced similar figures as Figure 4:4 above (see Appendix Figures A:2 to A:6) with the exception of grape cake (see Appendix A:4). It must be noted that grape cake was used as a substitute for grape seed as additional grape seed could not be sourced. Grape cake trials produced a similar trend observed with olive cake in that CTC remained relatively low compared to the other biomass types and high burn off leaving mainly ash was produced at an activation temperature of 850 ^{o}C and a residence time of 1 hour.

An increase in burn off due to longer residence time and higher activation temperatures has been reported throughout literature and reported in Chapter 2: For example by Yang and Lua, [2003] who studied two-step physical activation with olive stones as the precursor. Activation temperature and residence time were found to be key parameters that affect activated carbon. A longer residence time facilitates an increase in the amount of steam carbon contact. Higher temperature increases the rate of reaction between H_2O and C via Reaction 1 and therefore kinetically favours the forward reaction (see Appendix A.1 and A.2).

CTC values are rarely looked at in literature but this project proves how this relatively quick analysis technique gives very good indication as to the overall quality of the activated carbon across many tests. The correlations made between the CTC results and other carbon characteristics are very strong.

With the individual burn off and CTCs shown for each biomass, the biomasses can be compared in terms of their overall total yield.

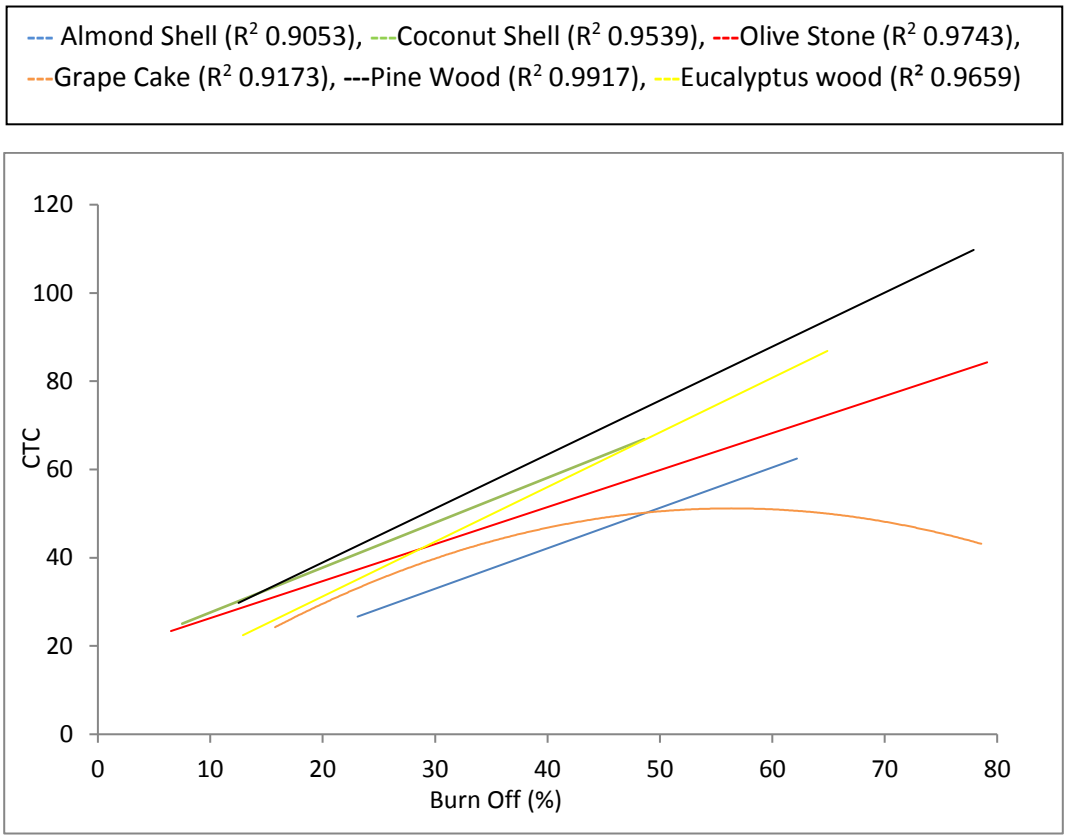


Figure 4:5 Biomass char burn off (%) and CTC relationship.

Figure 4:5 shows the relationship between burn off percentage and the CTC values. The biomass types produce a linear trend between burn off percentage and CTC with the exception of grape cake that had the significant reduction in CTC value. The initial char moisture content and volatile percentage of all chars were relatively similar with moisture below 1.5% and volatiles between 3% and 6%. All trend lines fall in a similar range to one another but there are significant differences. The highest ratio between CTC to burn off is associated to pine wood. Pine wood achieves a higher CTC at a lower specific burn off compared to the other five biomass precursors. Just beneath pine wood is both coconut shell and eucalyptus wood. The lowest ratio is obtained for almond shell and grape cake.

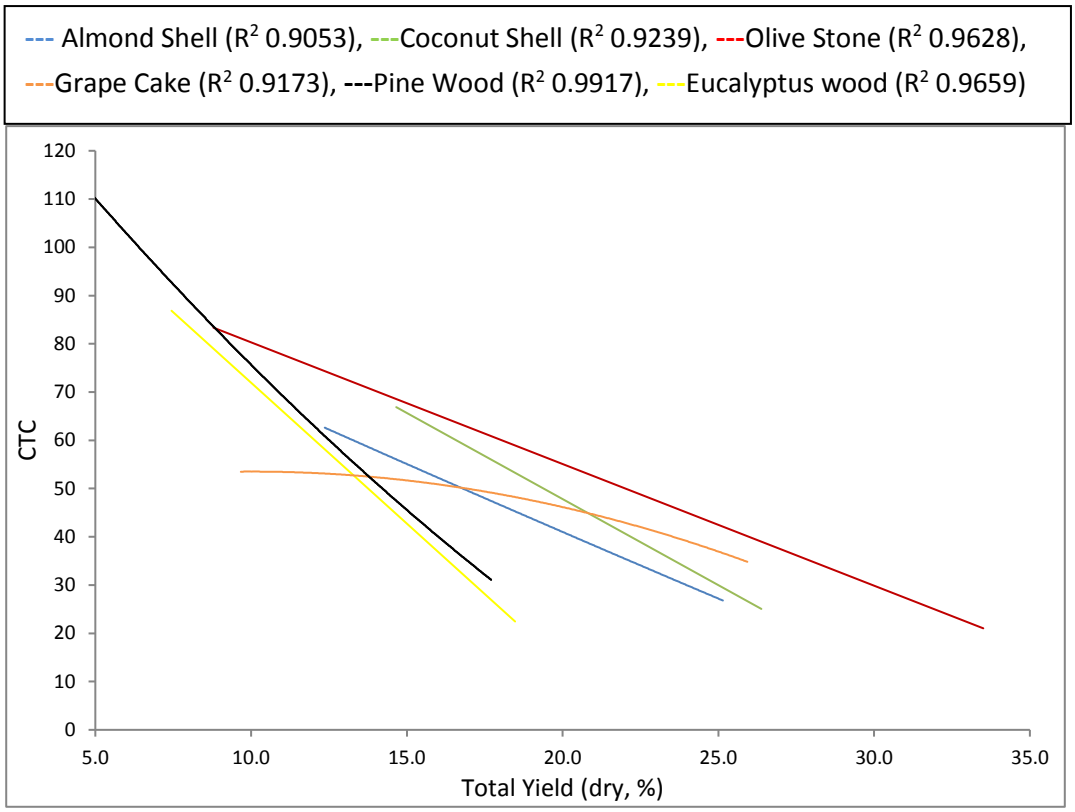


Figure 4:6 Biomasses final yield (dry basis, %) and CTC.

The yield results have been shown on a dry basis to negate the varying moisture levels between each biomass and also to take into account the pyrolysis yield. The six biomass types can be categorised into four categories. These are woods (eucalyptus and pine wood), nut shells (coconut and almond shell), fruit stones (olive stone) and waste residue (grape). There are three granular carbons (olive stone, coconut and almond shell) and three powdered carbons (grape cake, pine and eucalyptus wood).

What is noticeable is that similar biomasses are very similar in terms of yield and CTC results. Coconut and almond shell, and eucalyptus and pine wood are very close together and show similar correlation trend lines. The woods show an exceptionally close relationship between yield and CTC as do, to a slightly lesser extent, the nut shells.

When comparing the yield to CTC for the six biomasses it can be seen how olive stone has the highest CTC for a given yield by being above the other precursors in Figure 4:6.

Comparing Figure 4:5 and Figure 4:6 the woods have the highest CTC to burn off ratio. This essentially means that less carbon from the char is burnt off to produce certain porosity. Pine wood and eucalyptus being woods are naturally porous materials and not much carbon removal is required for micropore and mesopore formation. In contrast in Figure 4:6 they have the overall

lowest yield to CTC ratio. This is because their pyrolysis yield is much lower than that of the other biomass types.

4.6.3 Pore Analysis

Pore analysis was conducted on the six biomasses using samples produced from the standard activating conditions. Each isotherm in Figure 4:7, therefore, is corresponding to these carbons at varying degrees of activation and porosity. However, the shapes of the isotherms provide interesting information.

Table 4-8 Pore analysis results.

Biomass	Vmi (cm^3/g)	Vme (cm^3/g)	Vtot (cm^3/g)	Vme (%)	BET (m^2/g)	Burn off (%)	CTC
Almond Shell	0.3197	0.1137	0.4334	26.2	815	42.9	55.0
Olive Stone	0.3192	0.0918	0.411	22.3	814	49.0	61.0
Eucalyptus Wood	0.335	0.3116	0.6466	48.2	847	64.9	81.5
Coconut Shell	0.391	0.0461	0.4371	10.5	992	37.9	54.5
Grape Cake	0.2886	0.0737	0.3623	20.3	731	51.8	54.0
Pine Wood	0.4355	0.3929	0.8284	47.4	1101	61.6	92.0

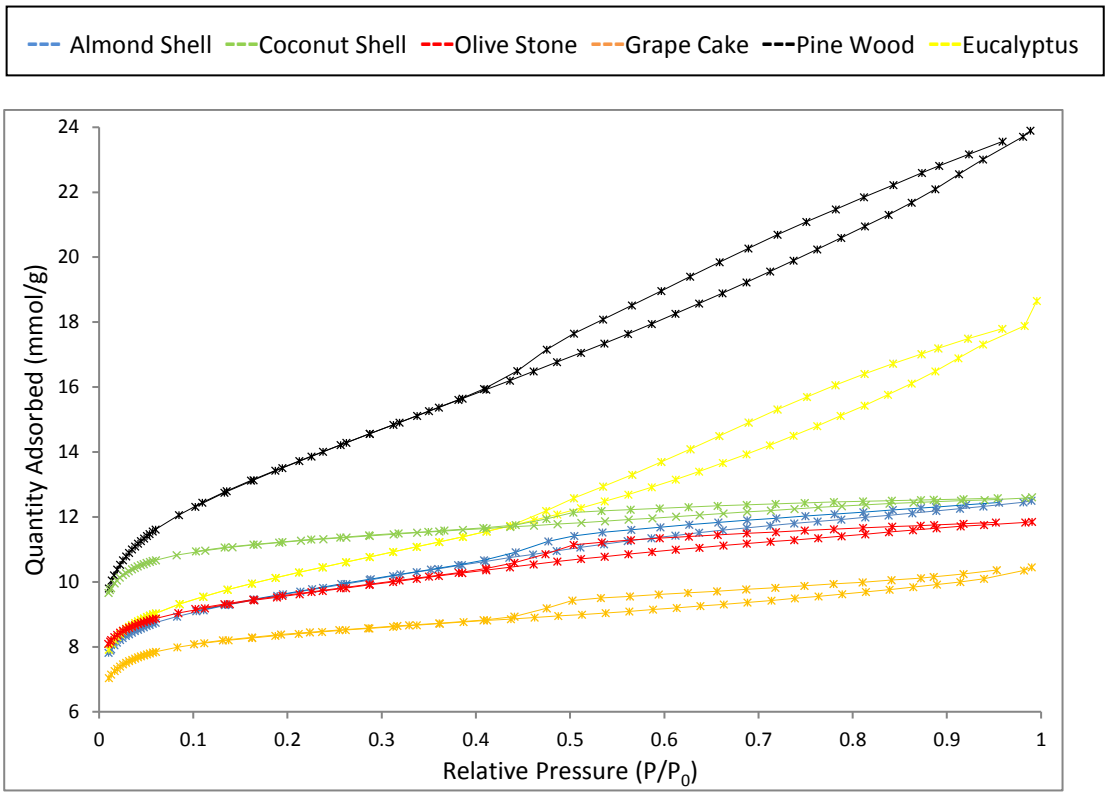


Figure 4:7 Nitrogen isotherms for the carbons derived from the biomass precursors activated at standard conditions (800 °C 1 hour residence time and a flow rate of 1.5ml/min).

Where the isotherms are positioned on the y-axis across to p/p_0 =1 on the x-axis shows the total quantity of nitrogen (mmol/g) adsorbed at the given pressure and relates to the overall pore volume. The shapes of the isotherms in Figure 4:7 provide significant information regarding the characteristics of the carbon. A Type-I isotherm is shown by almond shell, olive stone, grape cake and coconut shell. Type-I indicates that the carbons are mainly microporous [Marsh and Reinoso, 2006)]. The two woods show a Type-IV isotherm which indicates high mesoporosity as Marsh and Reinoso, [2006] state 'With mesoporosity present, the isotherms of activated carbons adopt the Type-IV shape, usually terminating without a plateau' which is seen for both pine and eucalyptus wood. The increased mesoporosity also leads to a larger hysteresis loop which are more prevalent with both woods, this is caused by capillary condensation in "ink bottled" shape pore that can block the release of the adsorbate. Pine wood and eucalyptus wood mesopore regions account for 47% and 48% of the overall porosity, the highest in Table 4-8 this also coincides with the higher burn off showing how an increase in burn off can also increase mesopore volume. The initial rise to around < 0.2 p/p_0 shows the micropore region - the steeper the initial rise the more micropore filling (volume) is occurring in the high energy adsorption sites, this again will be affected by the level of activation and the type of precursor used. Pine wood and coconut shell have the two highest micropore volumes and thus their isotherms (N_2) start above the other biomass. The next stage as pressure increases the mesopore region (> 0.2 p/p_0) filling begins. Here the two wood precursors show a continued rise. This is showing that the woods contain a high amount of mesopores typical of the Type-IV isotherm. Coconut shell isotherm levels off almost completely at this stage, indicating that is it almost entirely made up of pores that fall in the microporous region and this is proved by data in Table 4-8 with mesopores only accounting for 10% of the overall porosity.

The desorption curves will be discussed in more detail in Chapter 5 but evidence from these curves and the appearance of hysteresis loops can be used to show mesoporosity. It is very unusual to get a fully microporous carbon [Marsh and Reinoso, 2006]; coconut shell is known to be one of the highest microporous carbons in the market yet still contains 10% of its pore volume in the mesoporous region. All carbons are at a varying degree of activation (burn off) as shown in Table 4-8 so comparisons at the same burn off cannot be made at this stage.

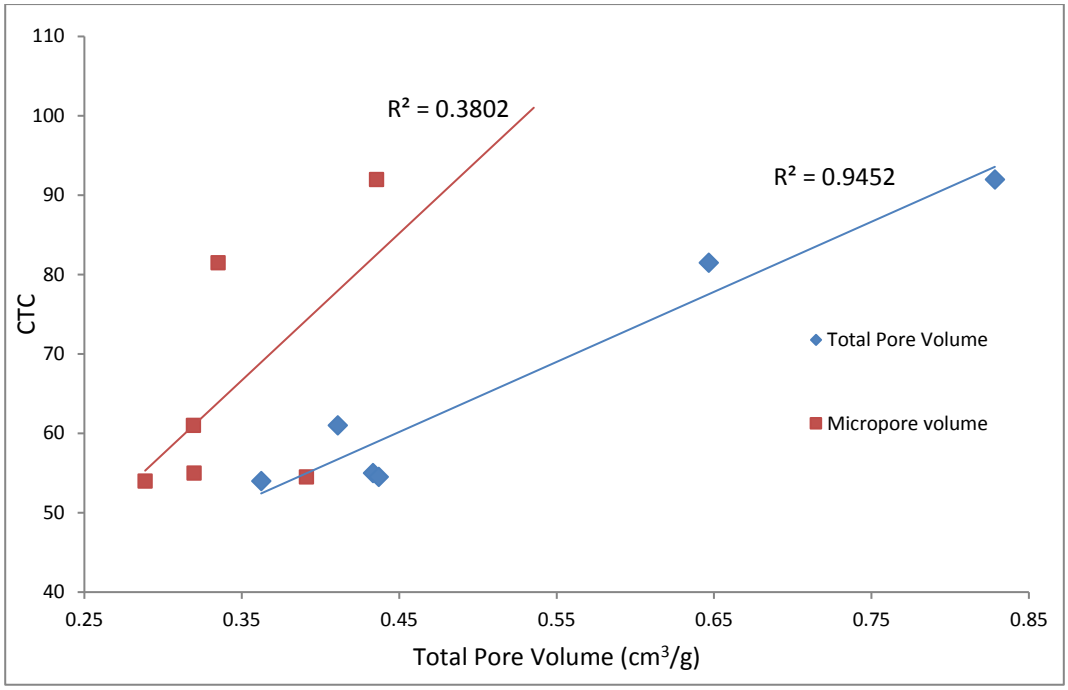


Figure 4:8 CTC correlation with micropore and total pore volume (cm^3/g).

Figure 4:8 shows that CTC value correlates better to the overall pore volume and not the micropore volume across the varying biomass types. ASTM D 5742 states 'The butane activity is an indication of the micropore volume of the activated carbon sample'. Results throughout this project suggest that CTC values for individual biomasses agree with this statement, however, CTC values also offer a satisfactory gauge to overall porosity as shown in Chapter 5. This is a significant finding, as being able to conduct a quick and cheap analysis technique such as a CTC test that allows an accurate estimate of a carbon's overall quality is of great advantage.

The relationship between micropore volume and BET surface area can be seen in Figure 4:9. The total area of micropores far outweighs the surface area provided by mesopores as reported in Chapter 2. Figure 4:9 shows a direct correlation between the micropore volume and BET surface area across the different types of precursor.

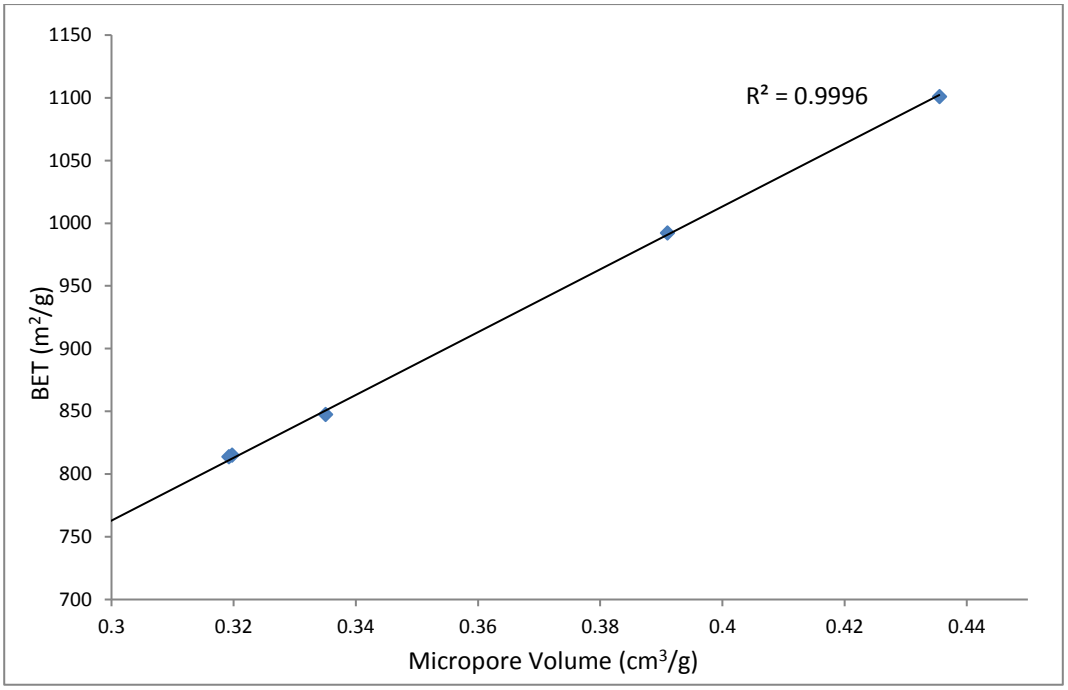


Figure 4:9 Correlation between micropore volume (cm^3/g) and BET surface area (m^2/g).

4.7 Carbon Dioxide Activation - Olive Stone

$$CO_{2\,(g)} + C_{(s)} \rightarrow 2CO_{(g)} \qquad \textbf{Reaction 2}$$

Reaction 2 shows the chemical reaction between carbon dioxide and carbon.

The next stage in the preliminary tests involved the introduction of small scale carbon dioxide trials. The carbon dioxide trials were conducted on olive stone char to see how this oxidising agent differed from steam activation in this system. González, Molina-Sabio *et al*. [1994]; Román, González *et al*. [2008] have conducted work in this area, these tests were carried out to expand on this knowledge, to see if similar results were observed and to see if carbon dioxide activation would be beneficial for commercial scale production.

Table 4-9 Results from the carbon dioxide trials including repeats.

No.	CO_2 flow L/minute	Temperature (°C)	Residence Time (mins)	Nitrogen flow (L/mins)	Carbon Yield + Ash (%)	CTC
1	0.2	800	60	1	89.5	12.0
1	0.2	800	60	1	89.1	13.0
2	0.6	800	60	1	81.3	17.0
2	0.6	800	60	1	81.1	17.0
3	1.0	800	60	1	81.2	24.0
3	1.0	800	60	1	80.0	25.0
4	1.0	800	60	0	74.7	22.0
4	1.0	800	60	0	75.3	22.5
5	1.0	900	60	1	67.0	35.5
5	1.0	900	60	1	68.0	36.0
6	1.0	1000	60	1	24.5	34.0
6	1.0	1000	60	1	27.0	32.0

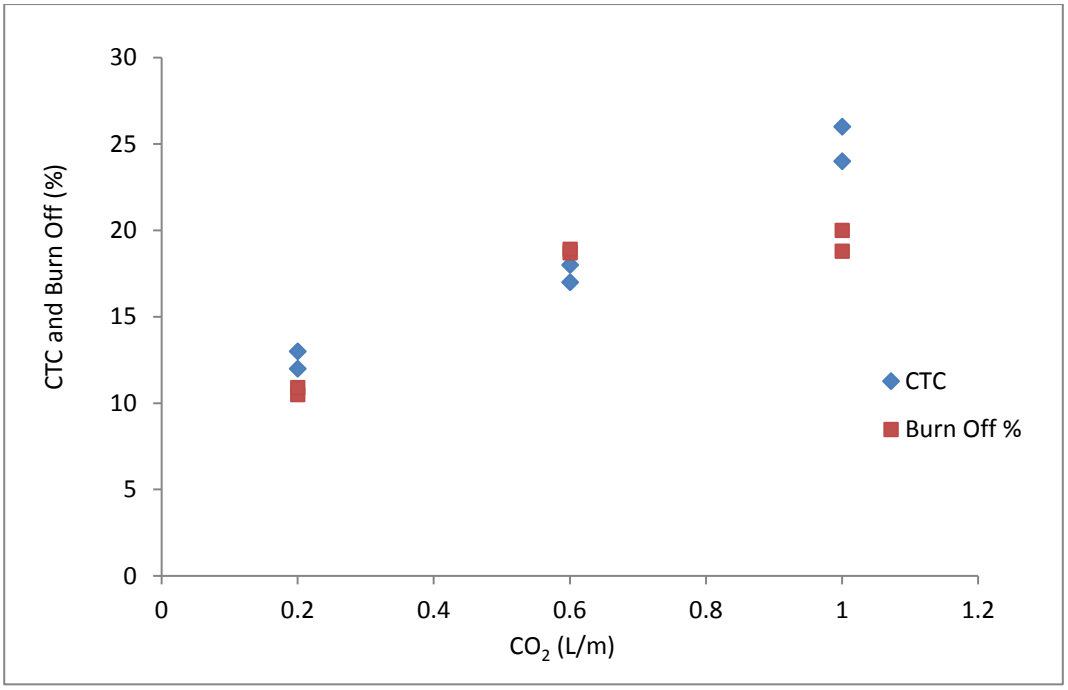


Figure 4:10 How an increase in CO_2 flow effects the CTC and burn off (%), 800 (°C).

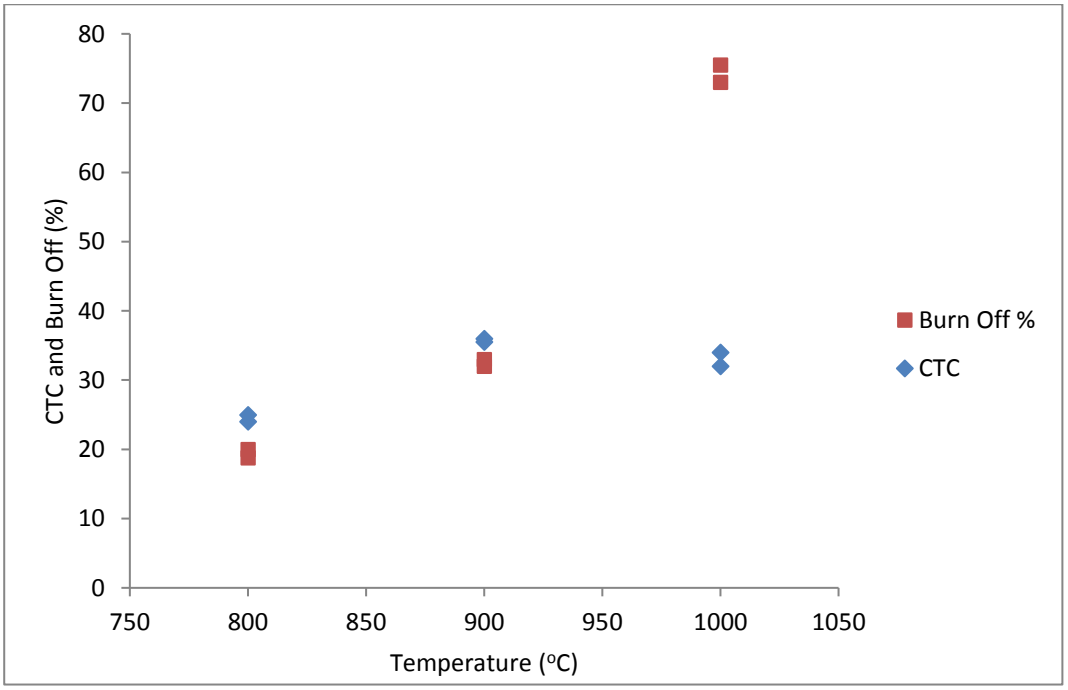


Figure 4:11 Effect of increasing the temperature from 800 °C to 1000 °C.

The figures show that as CO_2 flow increases the yield shows a sudden decrease from 0.2 L/min to 0.6 L/min but levels off when increased further to 1 L/min. Theoretically an increase in oxidising agent pushes the reaction forward due to increased reactant concentration. Despite this, burns off rates were seen to slow down when the flow rate was increased to 1 L/min albeit with the CTC continuing to rise. Carbon dioxide is known to produce a very microporous carbon [González, Molina-Sabio *et al*. 1994] and the similar burn off, but higher CTC, could be due to

additional narrow micropore formation deep within the particle which requires small mass removal. This theory is aided by Figure 4:16 where a very microporous carbon is produced.

The flow meter used allowed a maximum of 1 L/min CO_2 flow. However, with carbon dioxide being relatively expensive it is seen that keeping the flow rate down to a minimum will be crucial for an economically viable process. It can be seen from Table 4-9, that carbon dioxide activation produces an activated carbon with a much lower CTC compared to steam under the same conditions (800 ^oC, 60 minutes). The result with steam produced a CTC of around 60 compared to a CTC of around 25 with carbon dioxide activation. The flow rate of water/steam was at 1.5 ml/min and the max flow of carbon dioxide used was 1 L/min due to equipment limitations. The best way to compare both oxidising agents is on a molar basis due to Reaction 1 and Reaction 2 resulting in 1 mole of H_2O or CO_2 reacting with 1 mole carbon. Over 1 hour the difference in moles entering the system of both oxidising agents are shown:

$$\text{Moles } H_2O = \frac{\text{Mass}}{Molar\ Mass} = \frac{90}{18} = 5 \text{ moles/hr} \qquad \textbf{Equation 4-2}$$

$$\text{Moles } CO_2 \text{ (STP)} \quad n = \frac{Pv}{RT} = \frac{101325 \times 0.06}{273.15 \times 8.314} = 2.68\ moles/hr \qquad \textbf{Equation 4-3}$$

The molar flow of CO_2 is almost half of the molar water flow under these conditions. Taking results from Chapter 5, under the same molar flow, temperature and residence time the steam activation produced a carbon with a CTC of 45. This is still significantly higher than the value produced by CO_2. The burn off for the carbon activated by steam was 31.6% whereas the burn off for this carbon with CO_2 activation is between 19% and 20%. This is also shown by González, Molina-Sabio *et al*., [1994], Román, González *et al*., [2008] and Marsh, and Reinoso, [2006] that steam is more reactive than CO_2, with steam activation reaction rate being much faster. This is also backed up by Roman *et al*., [2007] who report that steam shows a quicker onset of pore development and by Koresh *et al*., [1980] who state 'For a given porosity, the effective diffusivity of steam is estimated to be around 50% higher than that of carbon dioxide'. This 50% increase appears to be accurate in accordance to these results.

With Figure 4:11, as with steam activation, CTC value increased with an increasing temperature up to 900 ^oC. Raising the temperature further to 1000 ^oC caused a further decrease in yield whilst also producing a lower CTC value. This is likely to be because of pore destruction due to the enhanced reaction rate causing micropores to collapse and lowering the overall surface area and/or external burn off. This is also seen with steam activation in Chapter 5 with high

temperature activation trials which concluded that external burn off was the main reason for this occurrence.

Nitrogen was kept at 1 L/min for the first three experiments. However, it was then turned off for experiment 4. As shown in Table 4-9 the CTC remained similar, even with partial pressure of CO_2 increasing and the yield decreasing by around 5%. With no nitrogen entering the system, there is a chance that further external burn off could occur and could be the reason for the slight decrease in yield. The other possibility is that when reducing the gas flow, the smaller the cooling effect the gas entering the system has. As seen, a slight change in temperature within the system can have a big effect on burn off. Reducing the nitrogen flow had similar effects with steam activation (4.10) yet the CTC also changes based upon burn off following the usual trend shown in Figure 5.2.

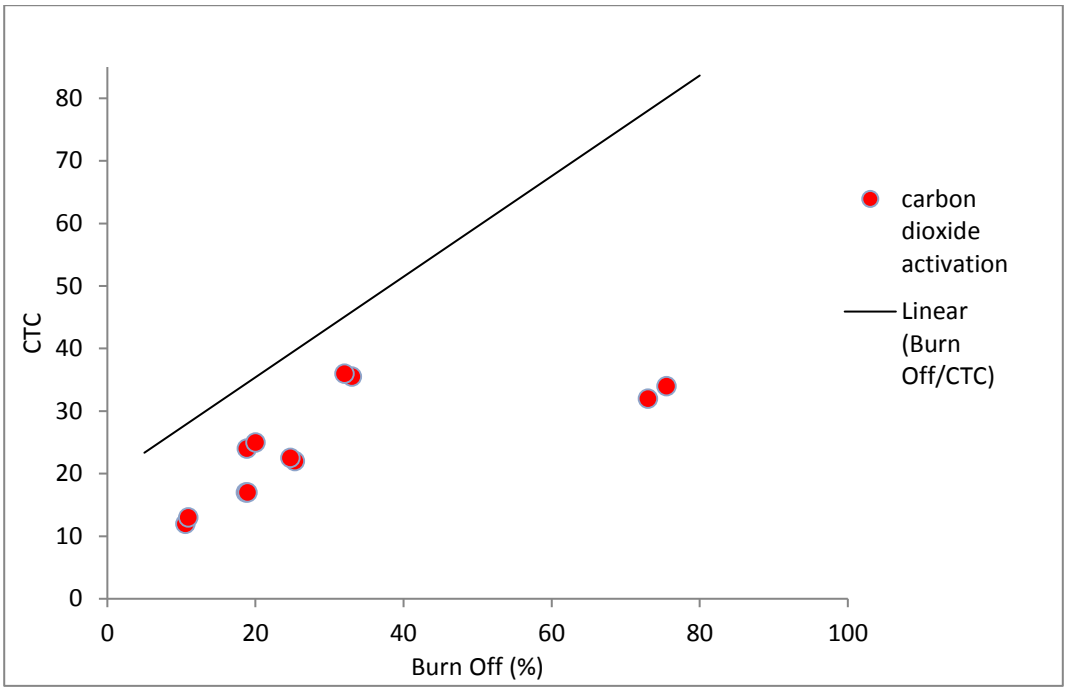


Figure 4:12 How CO_2 activation compares to steam activation in regards to Burn off (%)/CTC relationship.

Figure 4:12 linear trend line is taken from Chapter 5 Figure 5:2 olive stone steam activation optimum ratio between burn off and CTC values. The CO_2 data points have been added. The CO_2 data points all fall below this optimum trend line. This means at a given burn off the CTC value of the activated carbon is lower, and as Chapter 5 proves, CTC analysis proves a very good overall test for carbon quality and has strong correlations with total pore volume, surface area and methylene blue numbers etc.

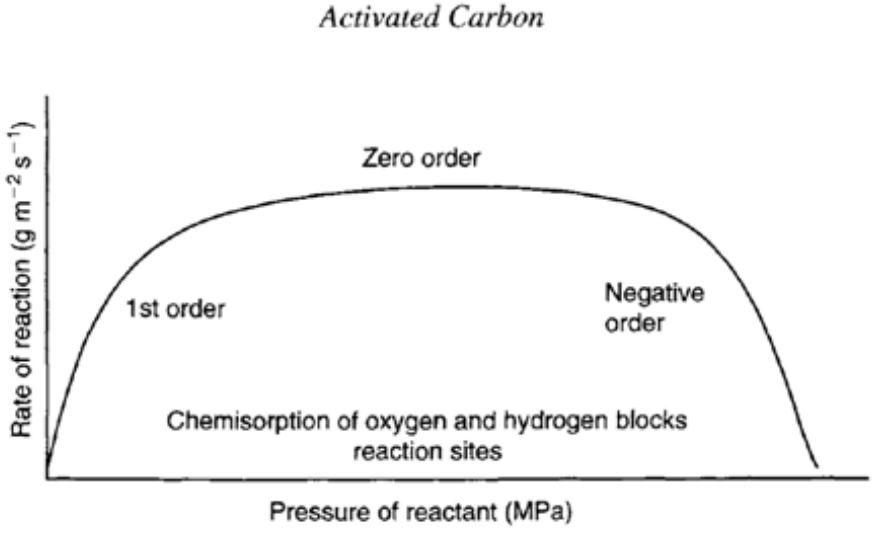
4.8 Carbon Dioxide and Steam Combination

Table 4-10 CO_2 and H_2O activation trials results.

No.	CO_2 flow L/minute	Temperature (°C)	H_2O flow ml/minute	Carbon Yield + Ash (%)	CTC
1	0.2	800	1.5	31	60.5
1	0.2	800	1.5	32	59.0
2	0.5	800	1.5	36	60.5
2	0.5	800	1.5	35	61.0
3	1.0	800	1.5	45	64.0
3	1.0	800	1.5	44	64.0

The next step was to look at CO_2 activation in addition with steam to see what effect two oxidising agents had when used simultaneously. In these three experiments the water flow rate was kept constant at 1.5 ml/min. The first thing to notice is the decrease in yield compared to the yield from both CO_2(g) and H_2O(g) individual activation across all three experiments, but in particular trials 1 and 2.

Unexpectedly the results show that yield starts to increase as CO_2 flow is increased to 1 L/min. It may be assumed that an increase in CO_2 flow at constant temperature would lead to additional burn off as in section 4.7. However, yield increase of around 15% is observed from increasing CO_2 flow from 0.2 L/min to 1 L/min. An answer to this could be explained by the kinetic rates of reaction [Marsh and Reinoso, 2006].



Variation of order of reaction with increasing pressure of carbon dioxide or steam to illustrate inhibition of rates of reaction (g $m^2 s^{-1}$).

Figure 4:13 Impact on reaction rate when increasing partial pressure of CO_2 and/or H_2O [Marsh and Reinoso, 2006]

Figure 4:13 would suggest with an increased flow of CO_2 at 1 L/min and steam flow 1.5 ml/min the kinetic reaction rate reaches a negative order rate of reaction. This is also backed up and seen again in Chapter 5 when steam flow rate is increased with olive stone and pine wood steam activation. This phenomenon is discussed by Marsh and Reinoso, [2006] who report the reason for this is because the reaction products (CO and H_2) act as inhibitors to the forward reaction. When too many products are created at once the forward reaction becomes less favourable as the products can bind to carbon atoms. For instance, the then required temperature to break a C(H) bond is 1500 K [Marsh and Reinoso, 2006]. This shows that once these bonds form, the carbon atoms become less reactive and hence are less likely to be removed from the graphene layer.

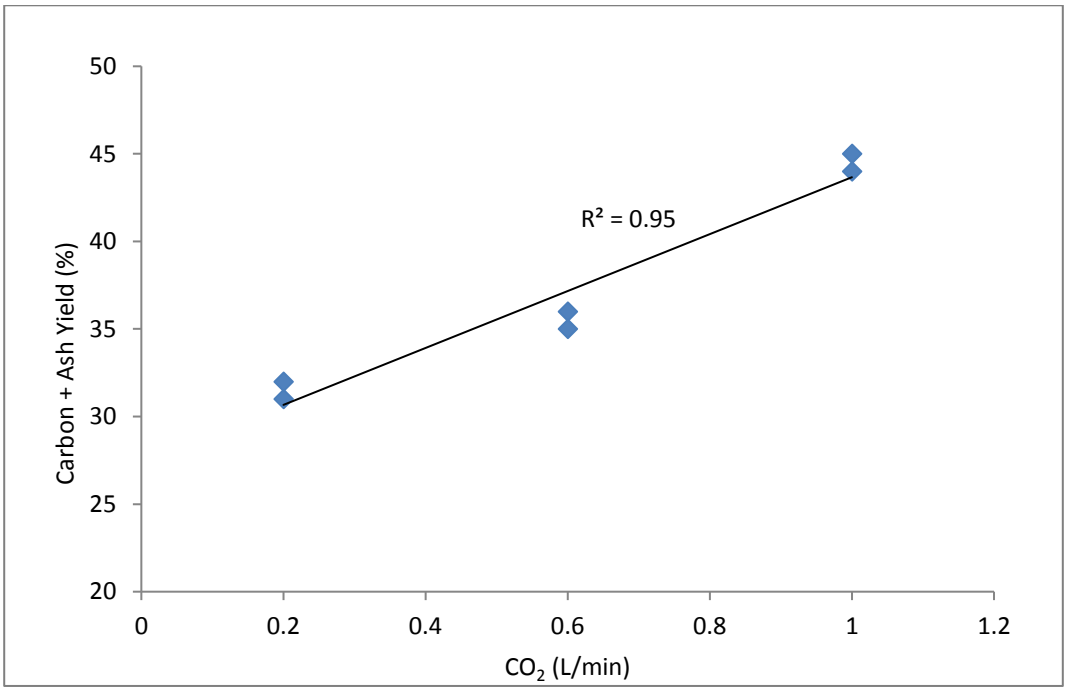


Figure 4:14 How increasing CO_2 flow increases the carbon yield when combined with steam.

Table 4-10 shows that as the CO_2 flow rises from 0.2 L/m to 0.5 L/m there is no change in the CTC value. The CTC rises slightly as the CO_2 flow is increased again to 1 L/m, but still negligible. Adding a small amount of CO_2 appears to increase burn off significantly compared to solely using steam for activation under the same temperature and residence time. This would initially suggest adding CO_2 drastically increases external particle burn off due to no increase or decrease in CTC value compared to steam activation. Increasing CO_2 flow further may cause the oxidising agents (CO_2 and H_2O) concentration to become too extreme and a reaction rate of negative order occurs for the reasons mentioned above by Marsh and Reinoso, [2006] preventing external burn off. Again these points can be added to the trend line produced in Figure 5:2 shown in Figure 4:15

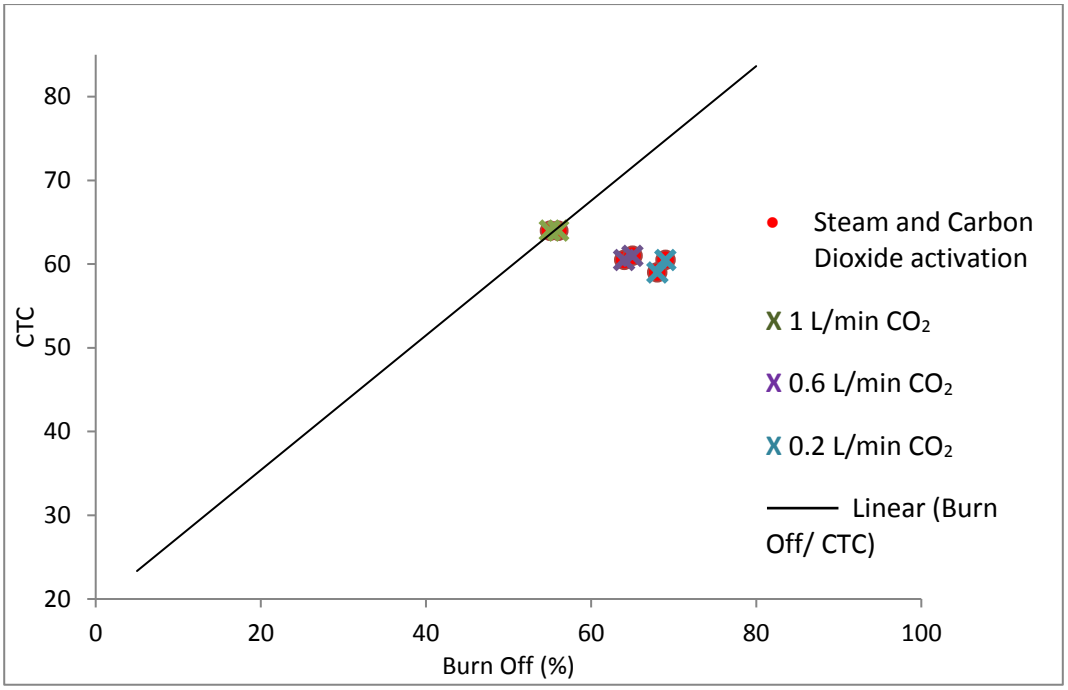


Figure 4:15 Simultaneous steam and carbon dioxide activation against steam activation.

The results show how experiments no.1 and no.2 fall below the optimum ratio (Figure 5:2). However, experiment no.3 data points obtained by using 1 L/min (CO_2) fit perfectly to the optimum correlation. Basing the carbon on CTC value alone, this shows how using CO_2 in addition as an oxidising agent maybe not be a worthwhile exercise as would just add further expense to the process for no porosity gain. On the other hand, literature reports that CO_2 activation produces a very microporous carbon that contains many narrow micropores [Molina-Sabio, Gonzalez *et al*. 1996]. Additionally, Marsh and Reinoso, [2006] report that it would seem water molecules within the porous structure react less selectively than carbon dioxide creating a wider pore size distribution. Therefore CO_2 activation could become important if the required carbon specification requires a large number of narrow micropores in the diameter range < 0.7 nm. A carbon produced via the CO_2 route therefore could perform better with certain applications for example carbon dioxide adsorption [Wie *et al*, 2012].

4.9 Pore Analysis of CO_2 Activation Trials

Table 4-11 From top to bottom as seen in Figure 4:16.

Temperature (°C)	Residence Time (mins)	CO_2 Flow (L/min)	H_2O Flow (ml/min)	Mesopore (%)
800	60	0.5	1.5	41.3
800	60	0.2	1.5	38.2
800	60	1.0	1.5	37.3
900	60	1.0	0	15.0
800	60	1.0	0	13.5
800	60	0.6	0	13.4
800	60	0.2	0	9.5

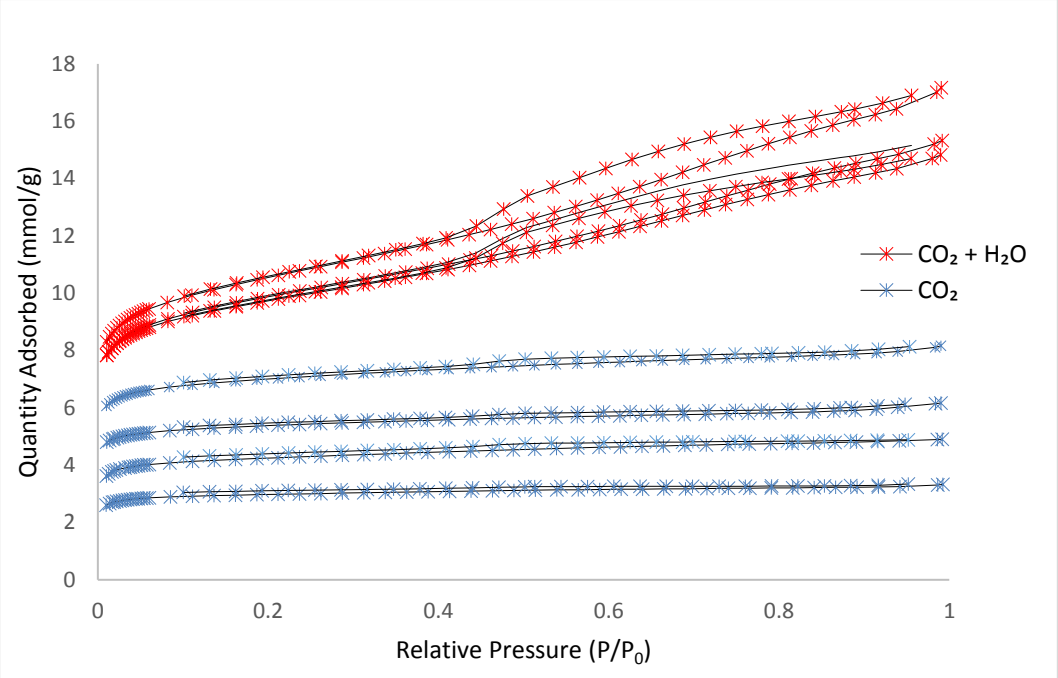


Figure 4:16 Nitrogen isotherms of samples shown in Table 4-11.

Figure 4:16 gives an insight into how steam and CO_2 act as oxidising agents by producing different pore structures within the carbons. CO_2 activation produces a carbon which is mainly microporous with small pore size distribution [Reinoso *et al*., 1994]. The raw data tables (Appendix A-3) show this and also in Table 4-11 where the mesopore percentage values can be seen with 9% to 15% for CO_2 activation as opposed to 37% to 42% with simultaneous CO_2 and H_2O activation. This shows that adding the two oxidising agents together creates a wider pore size range and creates a more mesoporous carbon. Looking at the steam only activated olive stone isotherm curve in Figure 4:7, the mesopore percentage for this carbon is 22% to 23% and also fits in with further results seen in Chapter 5. This is around double to solely CO_2 activation under the same conditions. The isotherm shapes also shows this with CO_2 only activation are very flat whereas after 0.2 p/p_0 the carbons produced via CO_2 and H_2O activation continue to rise. The desorption curves also shows mesopores are present in the carbon with a hysteresis loop being detected. The CO_2 only activation shows no clear sign of a hysteresis loop being detected.

4.10 Changing the Nitrogen Flow

This set of experiments looked into the effect of either increasing or decreasing nitrogen flow from the standard 1 L/min.

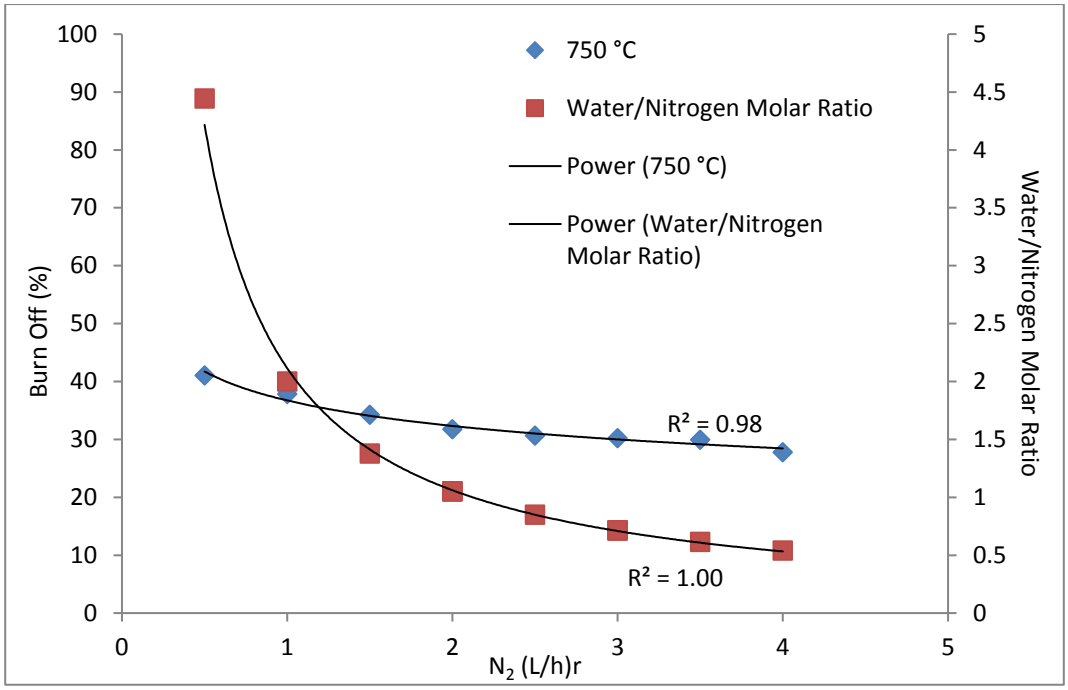


Figure 4:17 Effect of increasing the nitrogen flow and reducing the partial pressure of steam on the burn off (%), olive stone.

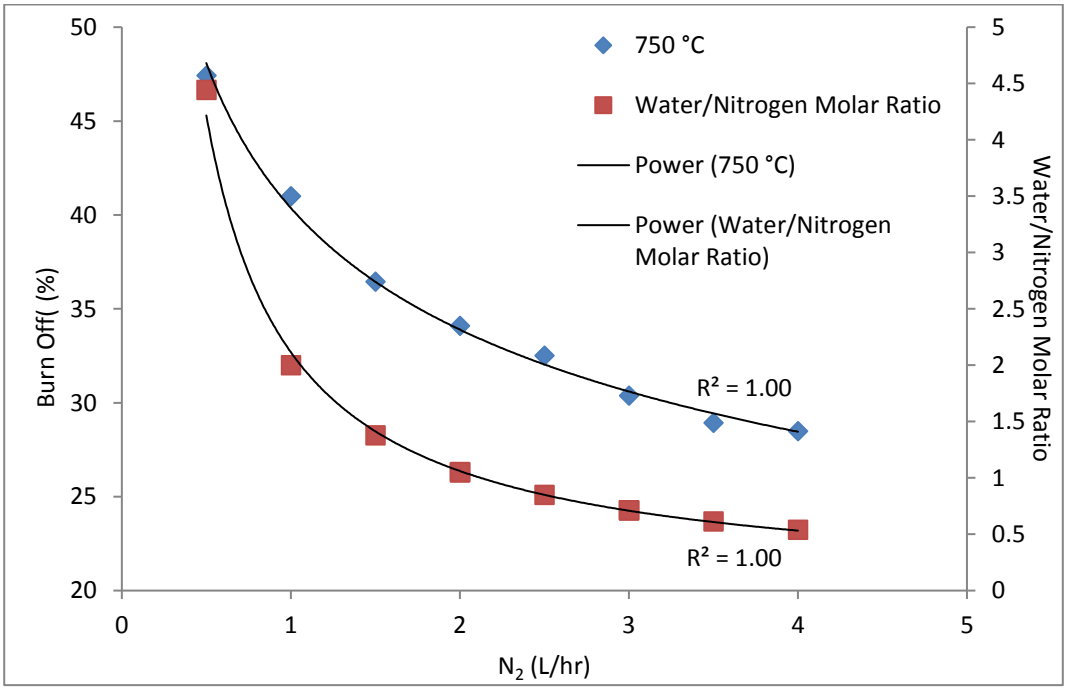


Figure 4:18 Effect of increasing the nitrogen flow and reducing the partial pressure of steam on the burn off (%), pine wood.

Figure 4:17 and Figure 4:18 show that as nitrogen is increased burn off percentage decreases. Repeats were done on 1, 2, 3 and 4 (L/min) trials and the averages used in the figures above (see results Table A-4 in Appendix). The burn off percentage and CTC values still correlate just as before seen in Figure 5:2. There is a bigger decrease in burn off when using pine wood compared

to olive stone. With increased nitrogen flow the result is a decrease in steam partial pressure. Figures 4:17 and 4:18 show the effect of the water/nitrogen molar ratio that represents this change in partial pressure. The produced power trend line with high R^2 values on both figures increases confidence that there is a clear direct relationship between steam, nitrogen molar ratio and burn off percentage. Therefore, nitrogen gas is essentially diluting steam concentration in the quartz tube during activation causing the reaction rate (Reaction 1) to slow.

4.11 Conclusion

1. Increasing activation temperature leads to an increased carbon burn off. This increased burn off increases porosity shown by the increasing CTC value across the biomass feedstocks analysed.
2. Olive cake is the exception to point 1. This is due to olive cake experiencing excessive burn off even under mild activation conditions. The reason for the witnessed excessive burn off, as proved in literature, is due to high alkali alkaline metal content catalysing the activation reaction. This therefore means that the reaction rate is too high with the carbon burnt off before a highly porous structure is formed.
3. Over 30 biomass feedstocks have been tested, some novel and some that have been investigated previously. The biomass feedstocks produced different carbons (powdered or granular) and differing adsorption results under the same activation conditions showing how selection of biomass precursor is an important decision when developing an activated carbon product for a specific industrial application.
4. The six biomass feedstocks taken forward for further analysis produced individual (N_2) isotherms leading to a more micro or mesoporous carbon being produced under the same activation conditions.
5. Across the six biomass feedstocks there is a direct correlation between micropore volume (cm^3/g) and BET surface area (m^2/g) shown by N_2 adsorption isotherms.
6. Carbon dioxide is less reactive than steam under same molar flow and activation temperature. This means to achieve the same burn off the activation temperature when using carbon dioxide needs to be increased. Carbon dioxide produced a highly microporous carbon compared to steam activation as stated in current literature.

   Carbon dioxide negatively impacts the optimum CTC burn off ratio found with steam activation in Chapter 5.
7. Simultaneous steam and carbon dioxide activation leads to increased mesoporosity, however, external burn off is significant. Increasing carbon dioxide flow further reduces forward reaction due to increased produced of reaction inhibitors.
8. Increasing nitrogen flow and therefore decreasing steam partial pressure resulted in a lower burn off. However, the CTC burn off relationship remains unchanged.

4.12 References

A. Aho, N. DeMartini, A. Pranovich, J. Krogell, N. Kumar, K. Eränen, B. Holmbom, T. Salmi, M. Hupa, D.Yu. Murzin, January 2013, Pages 22–29 Volume 128, "*Pyrolysis of pine and gasification of pine chars – Influence of organically bound metals*" Bioresource Technology

Anon, 2014. *Chemicool.* [Online]
Available at: http://www.chemicool.com/definition/equilibrium_constant.html
[Accessed November 2015].

Ayhan, D., 2006. "*Production and Characterization of Bio-Chars from Biomass via Pyrolysis"*. 28(5).

Aysel T. Atimtay, Murat Varol, 2008. "*Investigation of co-combustion of coal and olive cake in a bubbling fluidized bed with secondary air injection"*. Fuel*.*

Brownsort, P. A., 2009. "*Biomass Pyrolysis Processes; Review of Scope, Control and Variability",* UK Biochar Research Centre.

EC Okoroigwe, CM Saffron, 2012. "*Determination of Bio-energy Potential of Palm Kernel Shell by Physicochemical Characterization*". Nigerian Journal of Technology*,* Volume 31.

Faraco, Vincenza & Hadar, Yitzhak, 2011. "*The potential of lignocellulosic ethanol production in the Mediterranean Basin*". Renewable and Sustainable Energy*,* Volume 15.

Gaspard and Ncibi, 2014. "*Biomass for sustainable application pollution and remediation energy".*RSC Green Chemistry.

Harry Marsh and Francisco Roriguez Reinoso, 2006. "*Activated Carbon"* Elsevier Science & Technology Books.

Kiyoshi Okada, Nobuo Yamamoto, Yoshikazu Kameshima, and Atsuo Yasumori, 2003. "*Porous Properties of Activated Carbons from Waste Newspaper Prepared by Chemical and Physical Activation"*. Colloid and Interface Science*.*

Klemn, D., Philipp, B., Heinze, T., Heinze, U., Wagenknecht , 1998. "*Comprehensive cellulose chemistry". Fundamentals and analytical methods.* Vol 1 ed. Germany: Wiley-VCH.

Koresh J, Soffer A. , 1980. "*Study of molecular sieve carbons. Part I. Pore structure, gradual pore opening and mechanism of molecular sieving*". Volume 1;76:2457-2471..

Maty J Tatsuki Ohji, Gary Pickrell, Winnie K. Wong-Ng, Raghunath Kanakala 2015 Advances in Materials Science for Environmental and Energy Volume 253 pg 100

Michael Jerry Antal, Jr, Stephen G. Allen , Xiangfeng Dai ,Brent Shimizu , Man S. Tam ,and Morten Grønli, 2000. "*Attainment of the Theoretical Yield of Carbon from Biomass*". Volume 39.

Rodríguez-Reinoso, F., M. Molina-Sabio, M.T. González, 1995. "*The use of steam and CO2 as activating agents in the preparation of activated carbons*". Carbon*,* 33(1).

S. Román, J.F. González, C.M. González-García, F. Zamora, 2007. *"Control of pore development during CO2 and steam activationof olive stones*". Fuel Processing Technology.

Tancredi, C. R.-M. a. R., 1996. "*Activated carbons from Uruguayan eucalyptus wood".* Fuel.

Varol M, 2006 *"Combustion and Co-Combustion of Olive Cake and Coal in a Fluidized Bed"*, Thesis Submitted to Natural and Applied Sciences of Middle East Technical University

Venugopal Mendu Anne E Harman-Ware Mark Crocker Jungho Jae Jozsef Stork Samuel MortonIII Andrew Placido George Huber and Seth DeBolt, 2011. 2011 "*identification and thermochemical analysis of high-lignin feedstocks for biofuel and biochemical production*". Biotechnology for Biofuels.

Wei H, Deng S, Hu B, Chen Z, Wang B, Huang J, Yu G., 2012. "*Granular bamboo-derived activated carbon for high CO(2) adsorption: the dominant role of narrow micropores*".

Wen-Yang Wen 2006 *"Mechanisms of Alkali Metal Catalysis in the Gasification of Coal, Char, or Graphite"* Catalysis Review Science and Engineering *pg 1-28*

Chapter 5 Lab Scale Olive Stone and Pine Wood Analysis

The main variables in physical activation within a single system consist of the activation temperature, residence time and the characteristics of the oxidising agent in both total amount used and the flow parameters during the activation period. Oxidising agent and carbon contact is crucial as shown in this chapter. Steam is the chosen oxidising agent for reasons given in Chapter 4. This chapter focuses heavily on these variables expanding on the work conducted by González, Reinoso and Sabio [1980, 1995, 1997] on olive stone carbons. Using scots pine wood wood as a precursor is investigated in depth with the comparisons between the two biomasses made. Scots pine wood is one of three common types found in the UK and Europe [Woodland Trust, 2016].

Olive stone and pine wood are the two selected biomasses based on criteria discussed in Chapter 4 that have potential to be a viable commercial product. The two precursors are compared using numerous analytical methods. Olive stone is a granular carbon whilst pine wood is a powdered carbon. Olive stones were used as received; with a crushed particle size of approx. 1 to 4 mm. Raw pine wood chips were milled using a 3 mm mesh for lab scale trials. However, the pine wood was not milled before being placed in the pilot kiln and was in the form of chips as shown in Figure 5:1. The char from the pilot kiln was then milled using a 3 mm sieve mesh used for activation trials on lab scale and kept as produced for pilot scale trials. The images of all 6 can be seen below in addition with the bulk densities presented in Table 5-1. Olive stone was sourced from Spain through Garcia-Munte Energia, and pine wood sourced through Forest Fuels.



Figure 5:1 Raw olive stone, olive stone char, raw pine wood (lab), pine wood char (lab), raw pine wood (pilot), pine wood char (pilot).

Table 5-1 Bulk density differences for both olive stone and pine wood and their associated chars produced at 700 °C for 30 minutes.

Material	g/dm^3
Raw Olive Stone (lab and pilot)	750
Olive Stone Char(lab and pilot)	420
Raw pine Wood (lab)	190
Pine Wood Char (lab)	130
Raw Pine Wood (pilot)	190
Pine Wood Char (pilot)	215

The difference in physical characteristics and pore networks found in this chapter means the two biomasses will suit specific applications depending on the need for either a more microporous or mesoporous carbon.

This chapter shows how changing the main stated primary production variables, along with other additional secondary variances affect the carbons both in burn off and pore structure. The porosity and carbon quality can be tested via different techniques, the main ones used are CTC analysis for microporosity, which prove to provide a good scope for overall quality, methylene blue tests for decolouring efficiencies and pore analysis; mainly N_2 isotherms but also CO_2 isotherms for pore structures. Other analytical techniques are used such as Ion chromatography, XPS, SEM, pH, ultimate and proximate analysis.

The possibility of pre biomass treatment is covered by removing some alkali alkaline metals before pyrolysis and activation steps. Single step production is investigated where pyrolysis and activation are conducted simultaneously with both washed and unwashed biomass along with activation of chars produced via different heating rates.

5.1 CTC, Burn Off Percentage Correlations

For evaluation purposes Figure 5:2 and Figure 5:4 below show one of the major findings from this chapter in the overall correlation between CTC and burn off percentage for both olive stone and pine wood activated carbons. The figures below are the results of tests covered in this chapter that will be covered individually and in more detail further on. The figures are the results of many trials under different conditions that show the optimum CTC and burn off correlation line; this trend line will be used throughout this chapter to compare other production conditions against that fall significantly below. Investigating production boundaries is crucial when establishing conditions to produce carbons on large scale.

5.1.1 Olive Stone

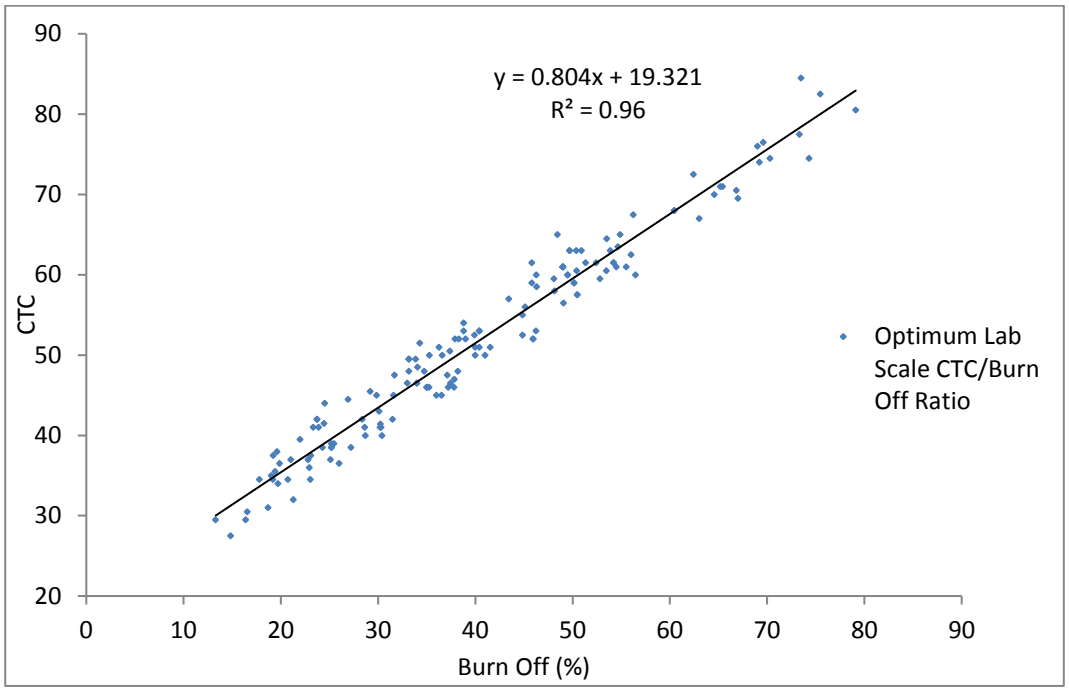


Figure 5:2 Optimum CTC, burn off (%) ratio correlation for olive stone activated carbon.

Figure 5:2 above shows over 160 laboratory trials conducted under different conditions ranging from 650 ºC to 850 ºC, 15 minutes to 6 hours residence time and 0.125 ml/min to 1.5 ml/min water flow to form the optimum linear relationship between CTC and burn off percentage. These conditions produced data points that fit this optimum line whereas deviating from these production ranges meant the performance of the carbon dropped for any given specific burn off. The production boundaries are elaborated upon further on in this chapter.

Figure 5:2 shows the burn off percentage, CTC relationship up to 80% char burn off. After this burn off point is reached the CTC begins to fall as burn off continues to increase. Figure 5:3 shows the results after this burn off point.

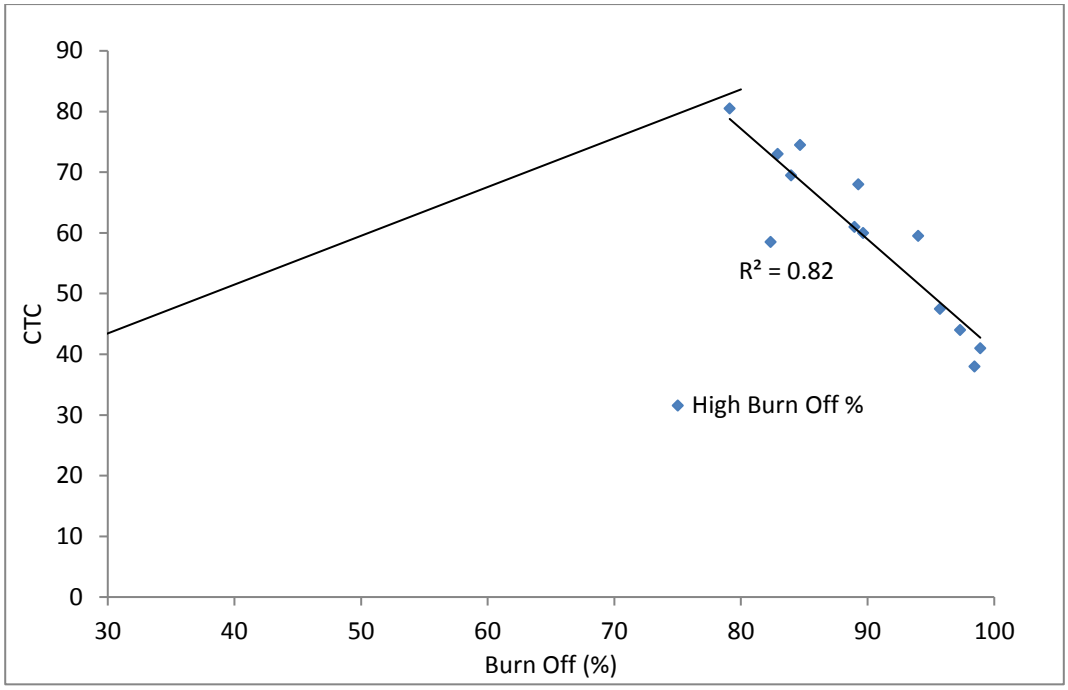


Figure 5:3 Data points after 80% burn off for olive stone carbons. Compared to the positive gradient trend line taken from Figure 5:2 from 30% to 80% burn off.

Evidence from the lowering of the CTC value suggests that the pore structure changes and adsorption potential of the carbon begin to decrease after 80% burn off. Excessive activation can cause pore damage as the pore walls thin and begin to collapse as further carbon is burnt off thus weakening the structure [Mopoung, *et al*., 2015]. Further external ablation of the particle can also damage porosity and reduce yields without increasing porosity at the same time [Demiral, *et al.*, 2010; Okada, *et al*., 2003]. Chang *et al*., [2000] state "Destruction of high porosity by external ablation of carbon particles is more pronounced than development and widening of microporosity" and "Prolonged activation may cause over activation, accelerating surface erosion more than pore formation". However, this is not always reported and it can be the micropore region that gets destroyed initially as pores widen to the point of collapse [Mrozowski, 1963]. It would appear from this data that the olive stone carbon peak CTC value produced via steam activation is approx. 80 at around 80% burn off. A commercial carbon (coal based) was tested at a CTC of 60 to 65 this points to initial signs that olive stone shows the potential necessary to be a commercially viable carbon.

With high burn off the ash percentage is higher as a ratio to remaining carbon, this is, assuming no ash is lost during the pyrolysis and activation process which is not the case with pine wood as shown in section 5.8.6. The inorganic matter is non porous and inhibits adsorption [Khambali, *et al.*, 2015]. To test this biomass was pre washed and trials conducted as shown in section 5.8.9.

5.1.2 Pine Wood

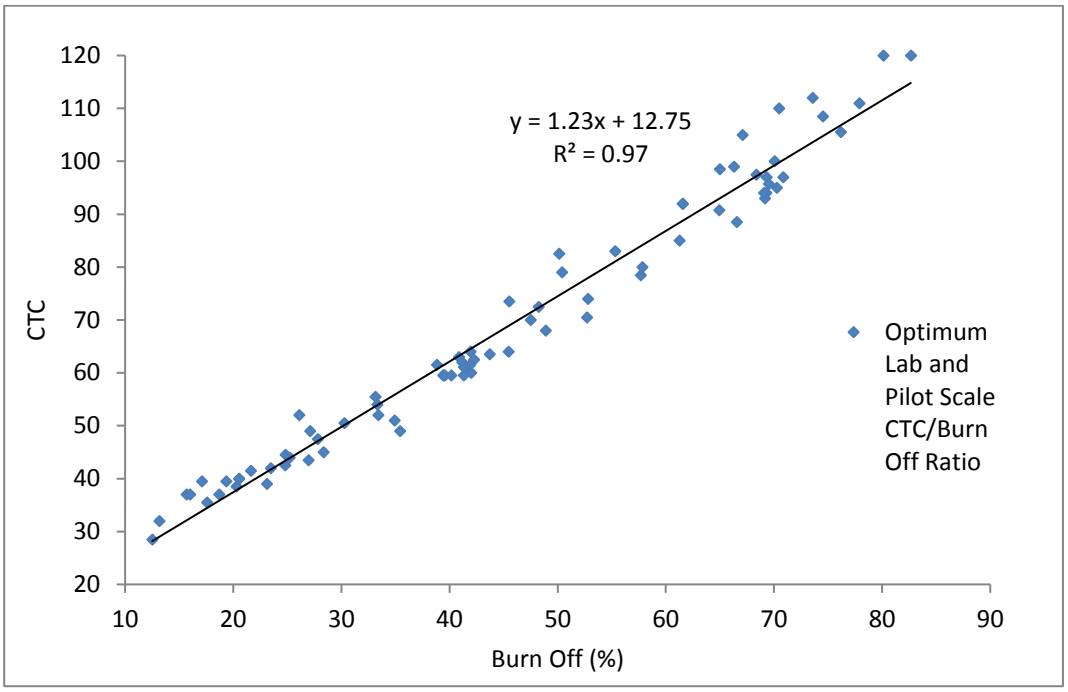


Figure 5:4 Optimum CTC, burn off (%) ratio correlation for pine wood activated carbons.

Figure 5:4 shows a similar pattern as Figure 5:2, with burn off percentage and CTC value having a linear correlation. The peak CTC found with pine wood activated carbon is approx.120 which is a 50% increase from the peak olive stone carbon CTC value of 80 shown in Figure: 5:2.

For both biomasses, whilst there is a linear relationship, doubling the burn off percentage does not double the CTC value. The linear gradient of Figure 5:4 is greater than in Figure 5:2. However, at low burn off percentages the burn off CTC relationship is similar for both biomass types. A graph showing the trend lines side by side is shown (Appendix Figure A:7).

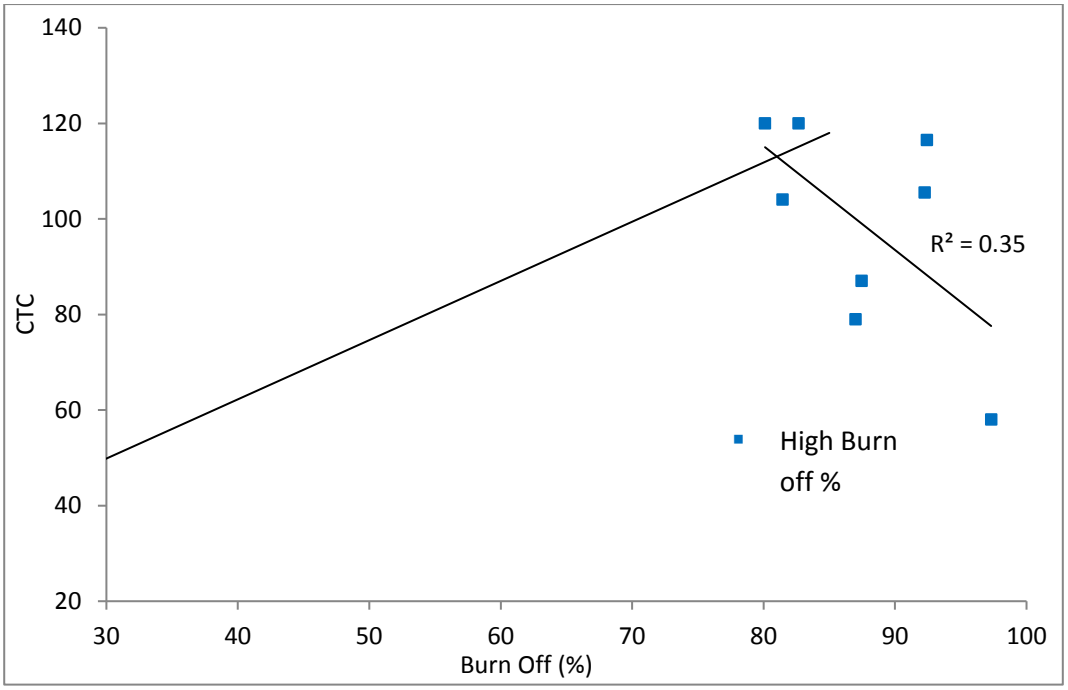


Figure 5:5 Data points for excessive burn off (%) for pine wood carbons. Compared to the positive gradient trend line taken from Figure 5:4 from 30% to 80% burn off.

As with Figure 5:3, Figure 5:5 using data points from pine wood carbons are shown for burn offs > 80%. Whilst there is a drop off there is no true correlation in the drop off. The data points shown are produced under different conditions. It therefore appears to be the specific production variables that are the main influence on the destruction of the pine wood carbons rather than solely the high burn percentage as over 90% burn off still yields very high CTC in some instances. The point with the highest burn off (near 100%) is predictably lower because the ash point is almost reached.

5.2 Overall Pore Analysis

5.2.1 Olive Stone

The figures below show data points from two-step lab scale production.

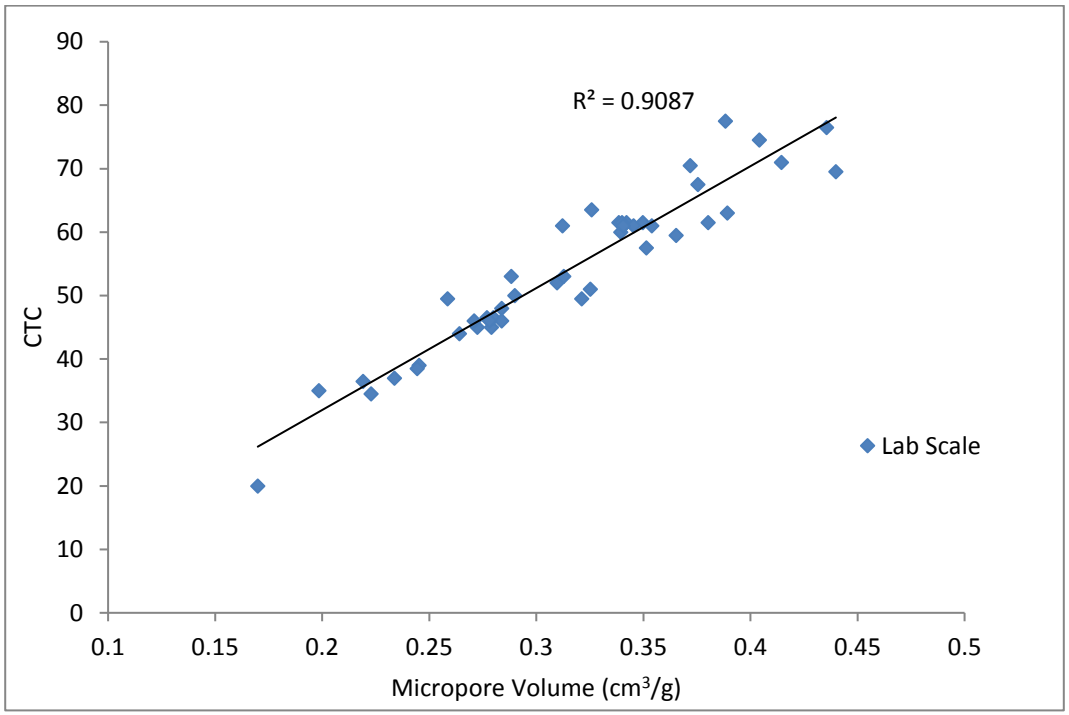


Figure 5:6 CTC against micropore volume (cm^3/g) for olive stone activated carbon samples.

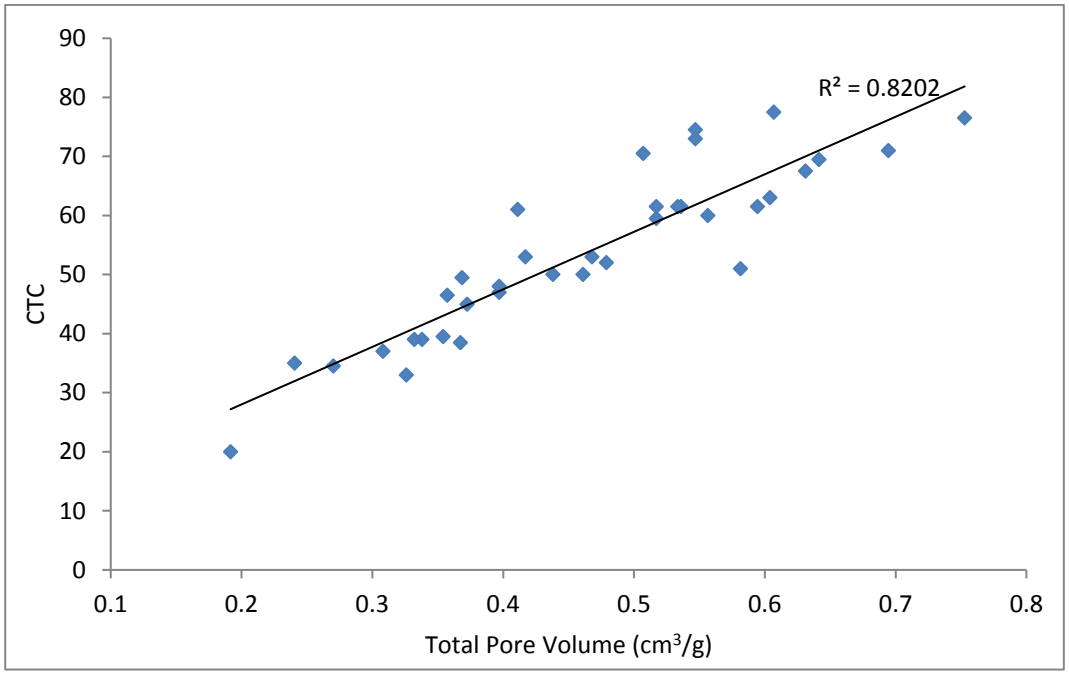


Figure 5:7 CTC against total pore volume (cm^3/g) for olive stone activated carbon samples.

Figure 5:6 and Figure 5:7 show the pore analysis data points taken from samples that were produced within the optimum production boundaries. The strongest correlation comes from micropore volume against CTC rather than total pore volume and CTC. This implies that with olive stone the micropores are the main pore region in which butane is adsorbed - this is expected as micropores provide the highest energy binding sites for adsorption to take place.

5.2.2 Pine Wood

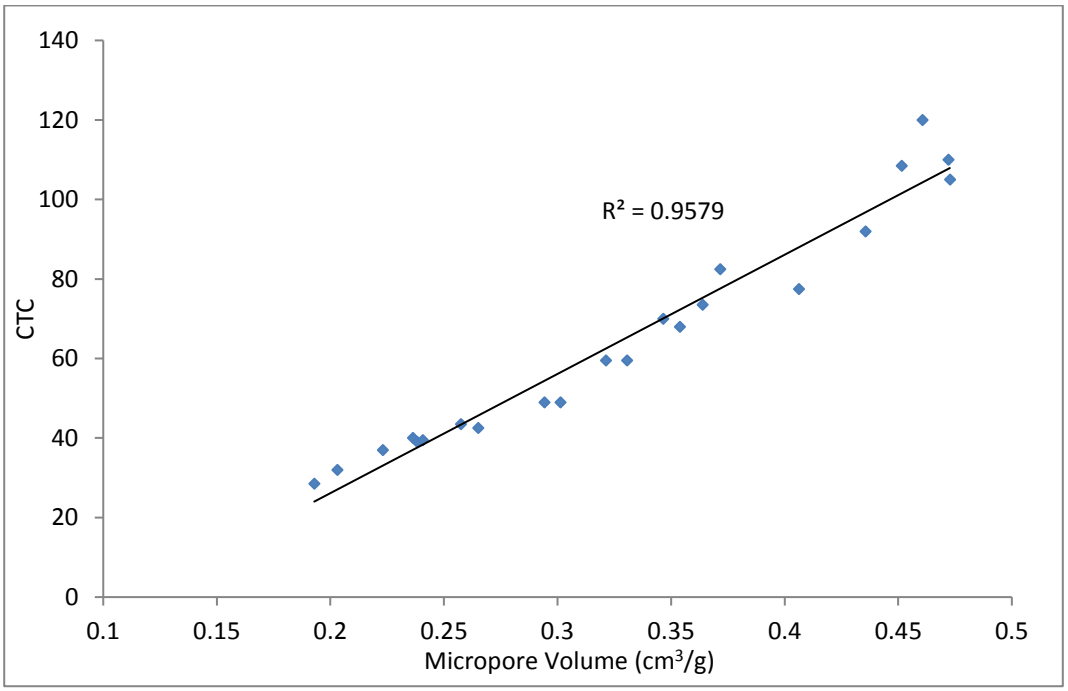


Figure 5:8 CTC against micropore volume (cm^3/g) for pine wood activated carbon samples.

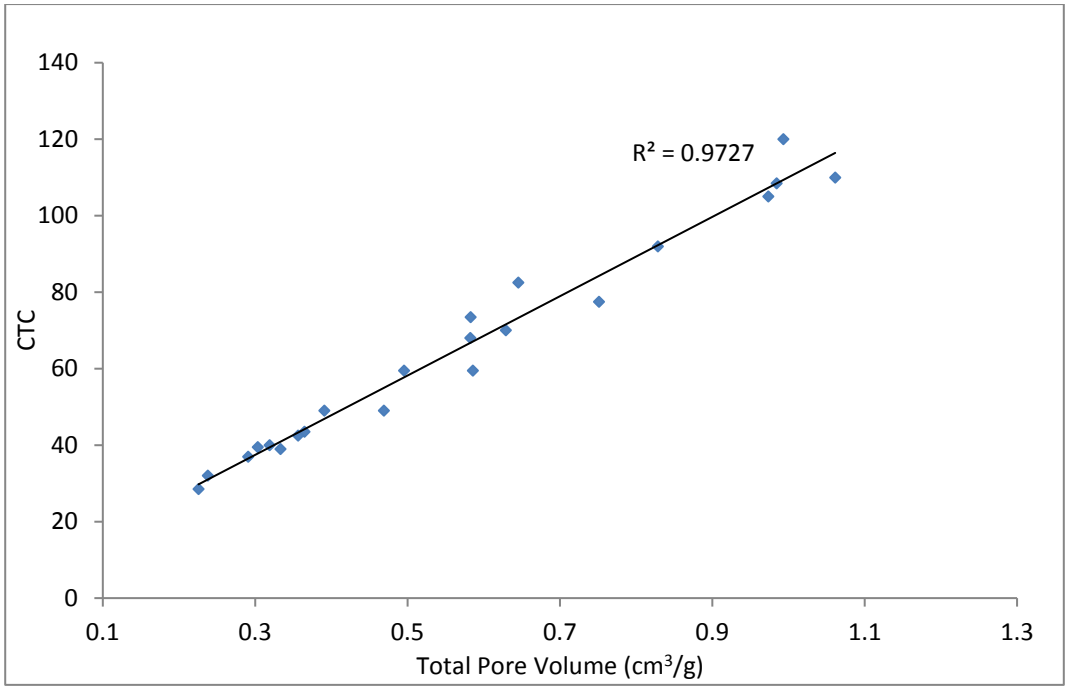


Figure 5:9 CTC against total pore volume (cm^3/g) for pine wood activated carbon samples.

Figure 5:8 and Figure 5:9 show how the results of the pine wood carbons are slightly different compared to the findings with olive stone derived carbons. Here both micropore and total pore volume provide a strong correlation with CTC results. As pine wood activated carbon is generally more mesoporous than olive stone activated carbon, (proved in this chapter) the observed trend cannot be simply associated to the micropore volume making up a very high percentage of total pore volume. This likely means butane is not just being adsorbed into the micropore region but also smaller mesopores.

5.3 Overall Methylene Blue Results

5.3.1 Olive Stone

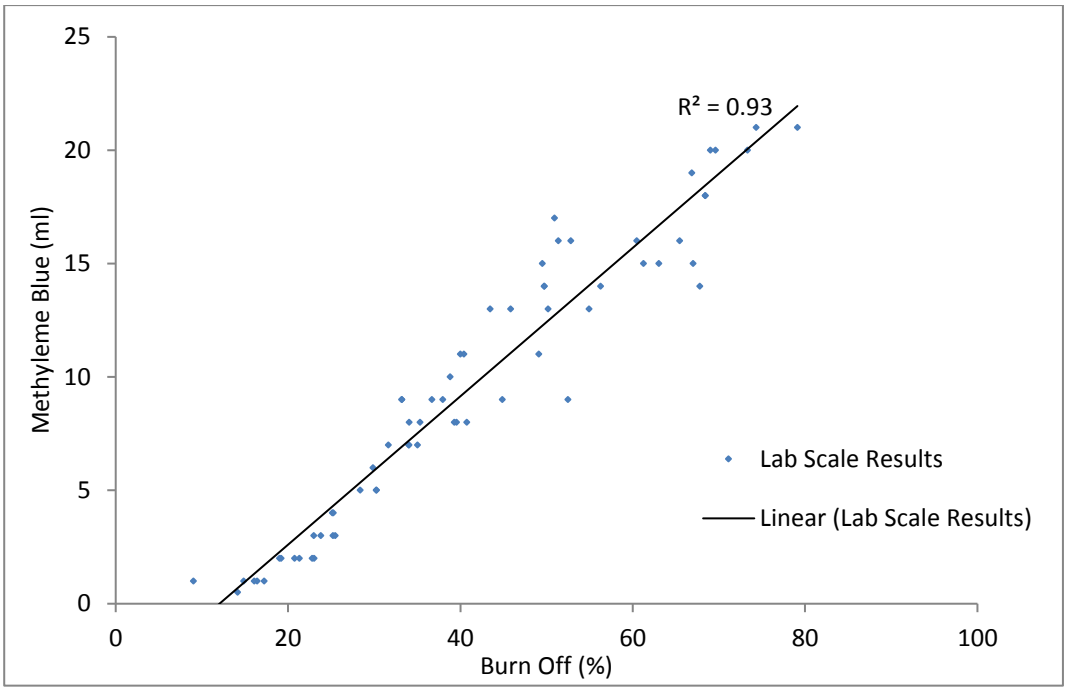


Figure 5:10 Overall lab scale results of burn off (%) against methylene blue number, olive stone.

5.3.2 Pine Wood

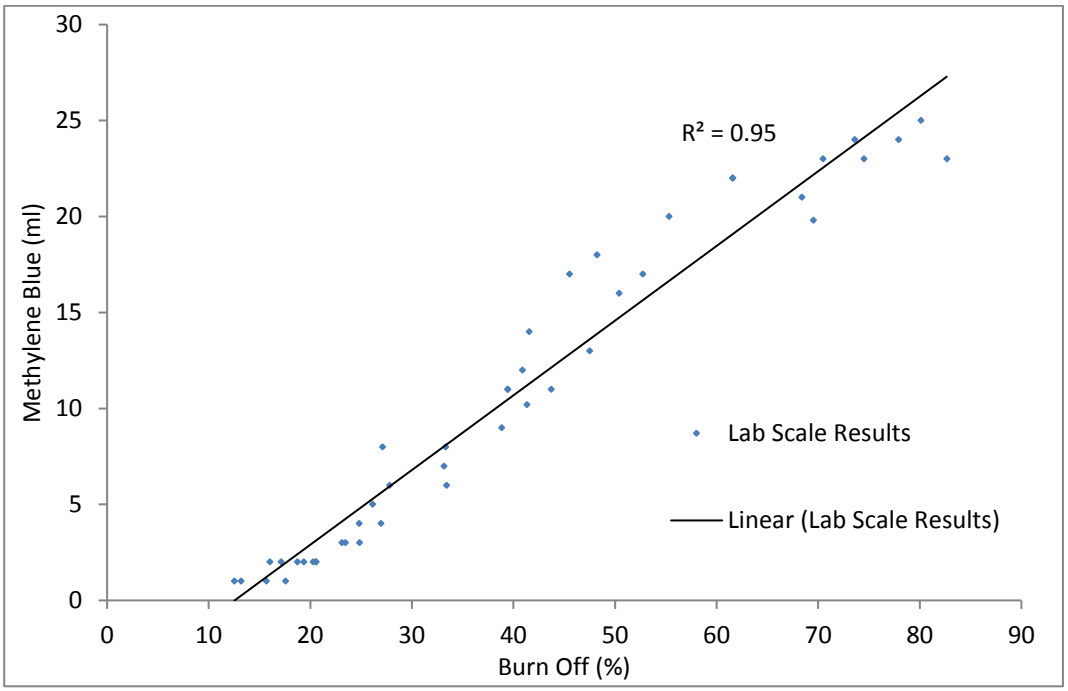


Figure 5:11 Overall lab scale results of burn off (%) against methylene blue number, pine wood.

As with CTC values both biomass derived carbons show a direct correlation between burn off and methylene blue value. This is expected as burn off has proven to increase porosity within both carbons. Methylene blue is investigated further with findings going against expected results.

5.4 SEM Images

5.4.1 Olive Stone Char

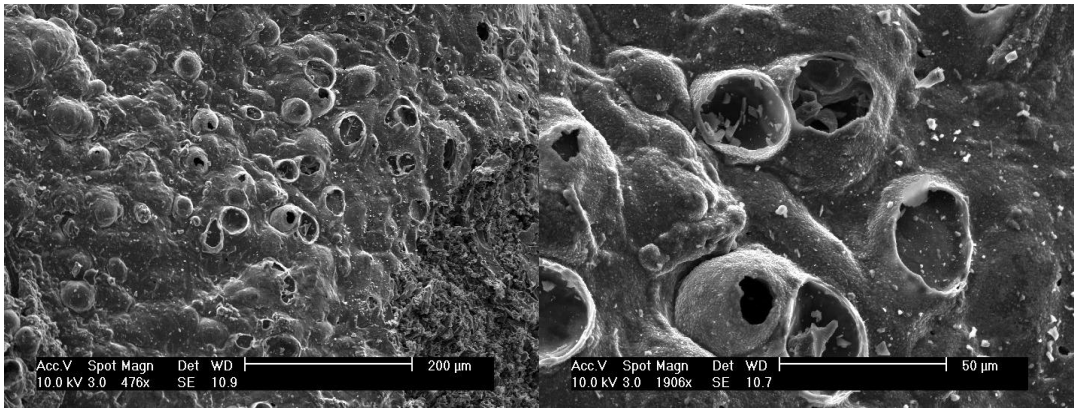


Figure 5:12 and Figure 5:13 Olive stone char surface.

5.4.2 Olive Stone Activated Carbon

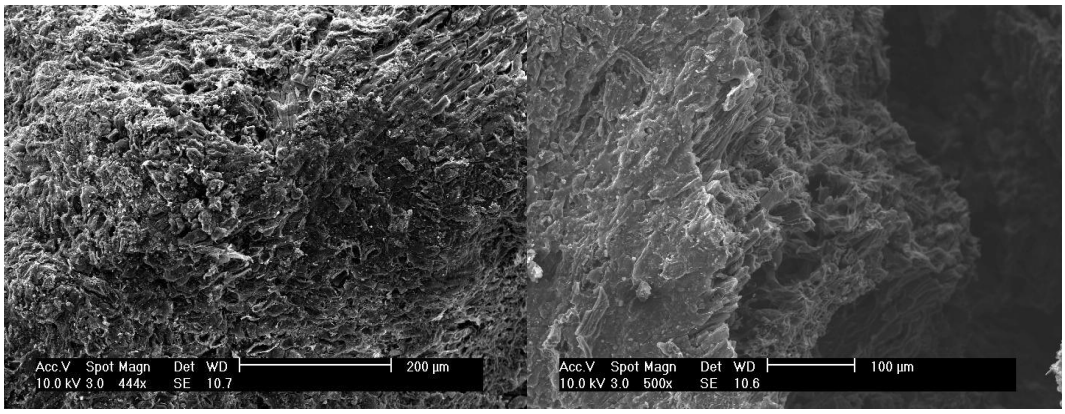


Figure 5:14 and Figure 5:15 Olive stone activated carbon surface.

The SEM images of the olive stone char and activated carbons allow for surface morphology comparisons. Figure 5:12 and Figure 5:13 show olive stone char produced at 700 ^{o}C with a residence time of 30 minutes in a pilot scale rotary kiln. From evidence in 5.8.5 this is a char produced via slow pyrolysis. As can be seen on the char surface, there is evidence of volatile evolution with craters present and the onset of a porous material shown in the corner of Figure 5:12. At this stage the surface porosity is low in comparison to Figure 5:14 and Figure 5:15 which show the char surface after activation at 800 ^{o}C for 1 hour. The surface shows much rougher texture than the char. Steam has reacted with outer ring carbon atoms present on the surface, as reported by Marsh and Reinoso, [2006]. The surface structure looks more disordered. Large

amounts of surface erosion, as shown in earlier studies, is an unwanted property as reduces carbon yields.

The char surface carbon atoms are subjected to highest steam contact compared to the carbon atoms within the centre of the particle as there is no other surrounding carbon atoms to provide "shelter". This can help to explain why macropores tend to open up on the particle surface [Bansal, 2005]. Micropores are likely to be formed deeper within the carbon particle. Mesopores, and macropores are known as the transport pores as adsorbates travel through these sized pores to the highest binding energy sites (micropores). Macropores usually at the surface lead to mesopores which then lead to the micropores in the centre of the carbon particle [Bansal, 2005].

The type of pores that can be observed with these images are likely to fall in the macropore region. These sized pores allow transportation of adsorbents to higher energy sites for surface adsorption: usually the smallest pores the adsorbent can physically fit into.

5.4.3 Pine Wood Char

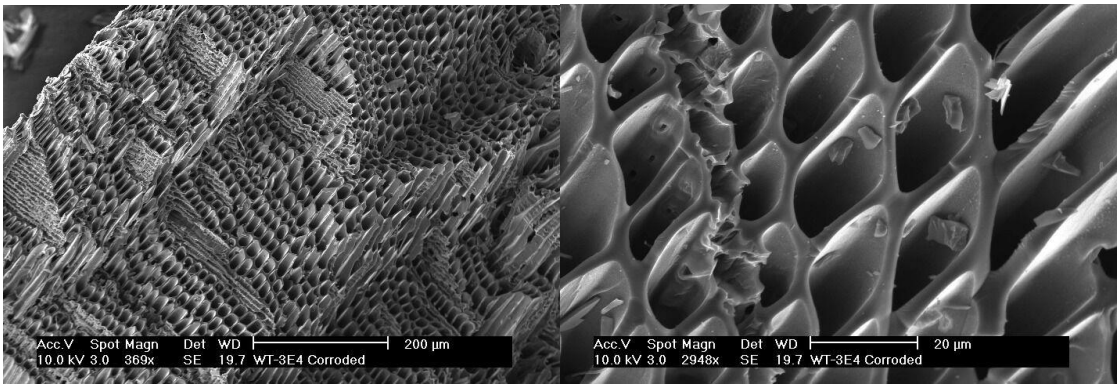


Figure 5:16 and Figure 5:17 Pine wood char surface.

5.4.4 Pine Wood Activated Carbon

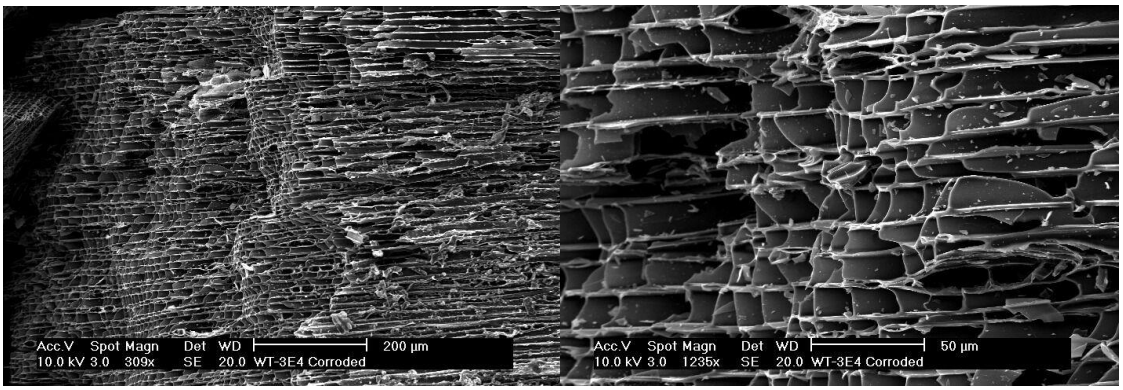


Figure 5:18 and Figure 5:19 Pine wood activated carbon surface.

The pine wood char was produced at 700 °C for 30 minutes in the pilot scale rotary kiln. The pine wood char SEM image shows a naturally porous fibrous material differing from the harder, higher density olive stone char. The morphology of the pine wood char helps to bring visual understanding as to why diffusion through this char structure can occur at faster rates and reach activation to certain porosity quicker than with olive stone. Section 5.7.2 shows that increasing steam flow causes external burn off with the olive stone char particle but not with pine wood at the flows used (3 ml/min). The natural porosity of the pine wood is likely to be the reason why higher concentrations of steam can pass through the particle without causing additional external ablation. Using Figure 5:16 and Figure 5:17 the surface of the char appears relatively smooth.

Figure 5:18 and Figure 5:19, show a pine wood activated carbon sample that has been produced at 750 °C for 105 minutes which has a similar burn off to the olive stone sample used. The surface morphology, as with olive stone, has been changed after activation with a much rougher texture observed. Carbon burn off can be clearly seen occurring through the fibrous cell walls creating a damaged appearance. This burn has helped to create a pore network with the pores forming an interconnect "maze" as discussed by Marsh and Reinoso, [2006] in Chapter 2.

5.5 Primary Production Variables – Activation Temperature

5.5.1 Temperature - Olive Stone

As shown in Chapter 4 increasing the activation temperature increases char burn off and in result increases CTC value up to a point. The increased temperature increases the reaction rate based upon the Arrhenius equation (Equation 5-1) and in this case the activation energy required for carbon water reaction.

$$K = Ae^{-Ea/(RT)} \qquad \textbf{Equation 5-1}$$

Considering Reaction 1 an increased temperature increases the frequency of collisions between the H_2O (g) molecule and C (s) atom and increases the reactivity of steam and carbon. From Chapter 2 Marsh and Reinoso [2006] report that on average around 10^7 collisions are required before a successful reaction takes place. This means the time taken for this number of collisions is lower at a higher temperature. An increased temperature increases the collision energy between steam and carbon. This means the average number of collisions required before a steam-carbon reaction occurs decreases as the increased temperature leads to a higher percentage of the collisions having sufficient activation energy to push the reaction forward. This increases the kinetic rate constant as shown in Appendix Figure A:1 and pushes the reaction forward.

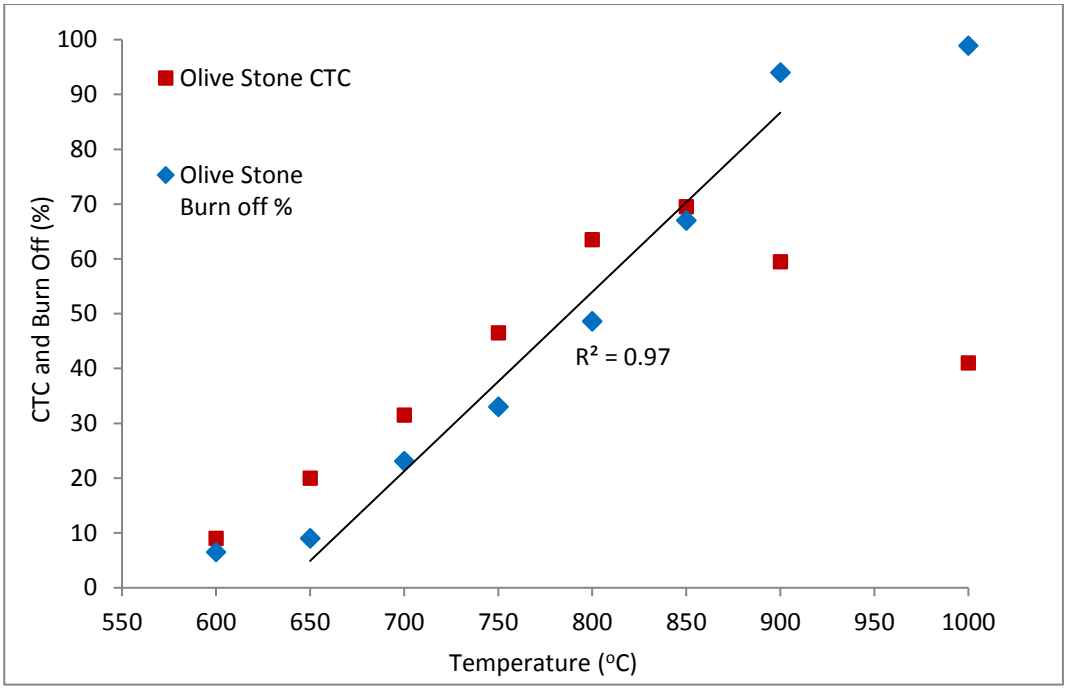


Figure 5:20 Olive stone activated carbon burn off (%) and CTC produced at different temperatures with 1 hour residence time and 1.5 ml/min water flow.

From Figure 5:20 it is clear as activation temperature is increased burn off percentage increases, and the CTC value increases in line with this trend until an activation temperature of 900 °C is used. At this point burn off is above 90% and the CTC value starts to drop. As the activation temperature is increased further to 1000 °C burn off approaches the ash point and the CTC falls further. At high burn off it is important to take into account that the remaining solid fraction is likely to be made up of a high percentage of inorganic material (ash) which is non porous.

The linear trend line (R^2 0.97) shown in Figure 5:20 represents points from 650 °C and 950 °C. Points at 600 °C and 1000 °C have been discounted. This is due to the 600 °C data point being affected by any char moisture and remaining volatiles present and 1000 °C due to ash point almost reached at 950 °C and so final ash point is reached somewhere between 950 °C and 1000 °C. The data points in between this range show how increasing temperature produces a linear burn off trend. Each degree Celsius increase from 650 °C to 950 °C results in an increased burn off of 0.0327 g/hr at this specific water flow rate and initial char mass.

5.5.1.1 Pore Analysis data - Olive Stone Carbons

Pore analysis was conducted on samples from 650 °C to 850 °C. Above this there was not sufficient sample to analyse. High temperature > 900 °C pore analysis can be seen in section 5.5.5.2.

Table 5-2 Pore analysis data from Figure 5:21.

Temperature (°C)	Residence Time (minutes)	BET (m^2/g)	Vmi (cm^3/g)	Vme (cm^3/g)	Vtot (cm^3/g)	Vme (%)	Burn off (%)	CTC
650	60	435	0.1699	0.0217	0.1916	11.3	8.9	20.0
700	60	508	0.1984	0.0421	0.2405	17.5	19.1	35.0
750	60	709	0.2769	0.0803	0.3572	22.4	32.9	46.5
800	60	823	0.3123	0.0987	0.4110	34.0	49.3	61.0
850	60	1118	0.4399	0.2015	0.6414	31.4	67.1	69.5

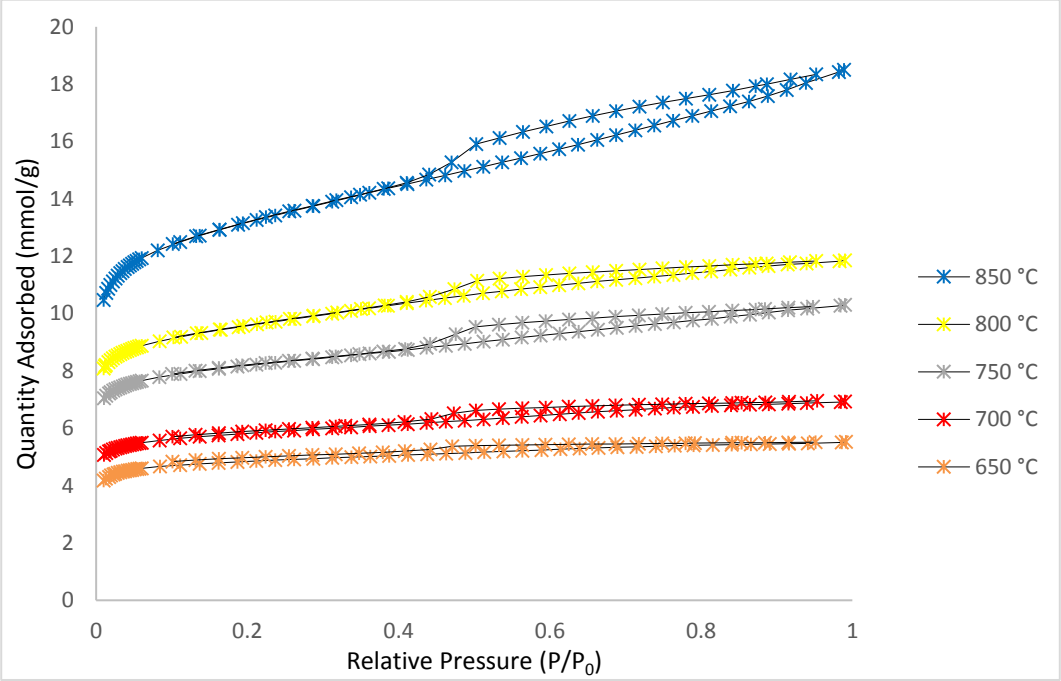


Figure 5:21 N_2 isotherms for olive stone activated carbons produced at 650 °C to 850 °C.

Evidence from Table 5-2 and Figure 5:21 suggests that increasing the activation temperature from 650 °C to 850 °C on olive stone char increases the BET surface area and has a significant effect on the porosity of the carbon both for micropore and mesopore volumes this is also shown by Gonzalez and Reinoso [1980]. The isotherms move from Type-I towards Type-IV at 850 °C. This change implies that the carbon is becoming more mesoporous as activation temperature is increased. This is backed up in Table 5-2 where mesopore volume and mesopore percentage increases with increasing temperature. Above 0.2 p/p_0 mesopore filling occurs and explains why the adsorption capacity from the sample produced at an activation temperature of 850 °C continues to rise whereas samples produced at lower activation temperatures result in a flatter isotherm. Reports show that lower activation temperatures favour micropore creation opposed to mesopore creation and this is shown in Table 5-2 with low mesopore percentage at the lower temperatures. [Marsh and Reinoso, 2006; Pastor *et al* 1999; Rodriguez Reinoso 2000]

Additionally the desorption curves on the isotherms provides evidence on porosity. With increased temperature the hysteresis loop becomes more apparent leading to a conclusion that the mesoporosity is increasing with temperature. Depending on pore structure a specific amount of condensed N_2 is contained by the material via capillary condensation at a given bulk pressure and so the quantity adsorbed on desorption curve is more than the adsorption curve at the same relative pressure. This indicates a failure of the system to equilibrate [Naumov, 2009]. This is a common occurrence in mesopores due to the nature of their sometimes "bottle neck" shape which can block desorption.

For microporosity the isotherm starting point on the Y-axis and the subsequent steepness of the initial rise relate to micropore volume. It can be seen that the carbon produced at 850 ^oC has the steepest gradient from 0 to 0.2 p/p_0. The overall position on the y axis indicates total pore volume cm^3/g. The micropore volume and BET surface area provide a perfect correlation shown Figure 5:22.

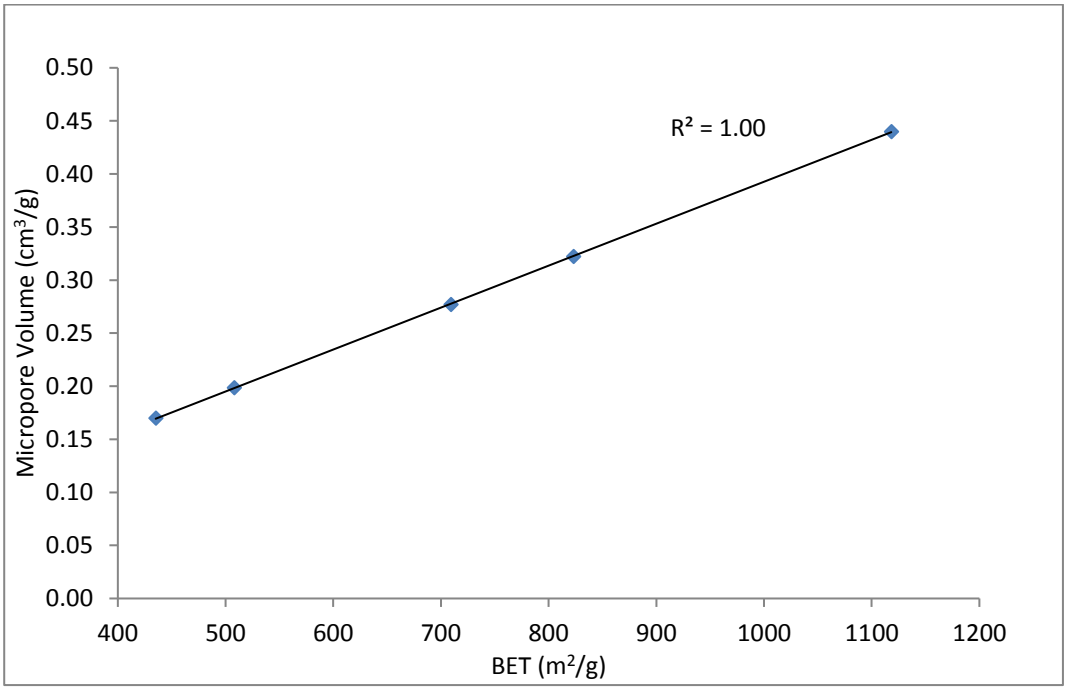


Figure 5:22 Correlation between micropore volume (cm^3/g) and BET surface area (m^2/g).

This shows that the micropore volume is directly linked to the BET surface area and the majority of the surface area is found within the micropore region due the large number of micropores present. Micropore surface areas can reach several thousand m^2/g whereas mesopores and macropores are usually in the region of 50 m^2/g to 200 m^2/g [Bansal and Goyal 2005]. More BET analysis is conducted further in this chapter with much larger data sets examined where this correlation is maintained. Figure 5:23 shows the micropore volume and CTC correlation of the five carbons tested.

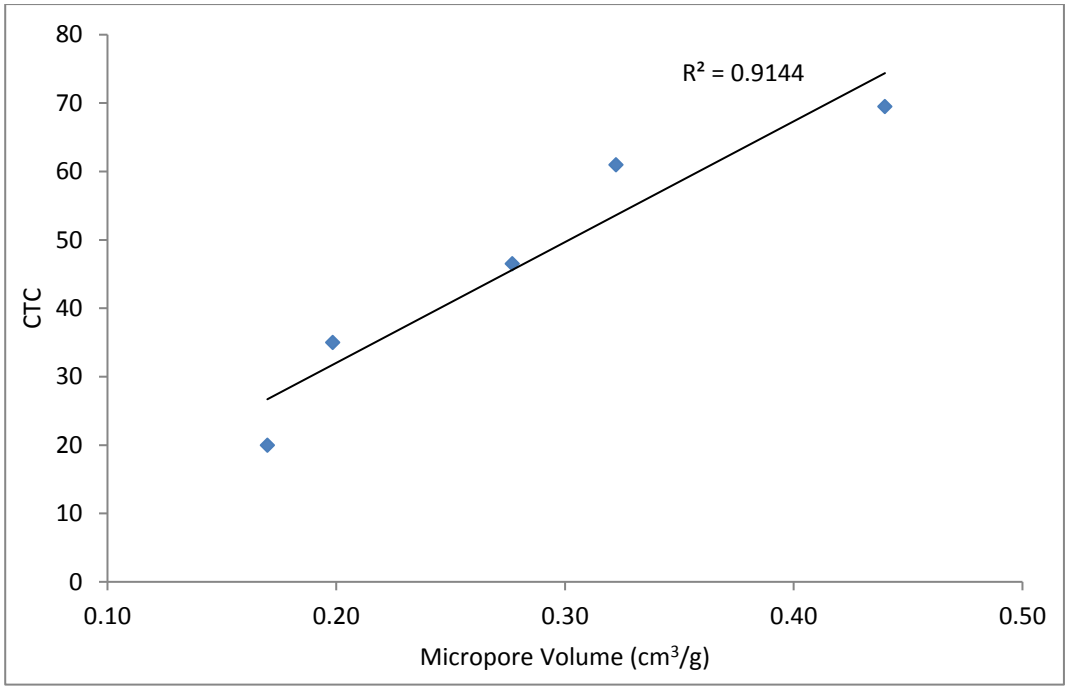


Figure 5:23 Correlation between micropore volume (cm^3/g) and CTC values.

Figure 5:23 linear trend line has an R^2 value of 0.91 however this is relatively strong taking into consideration the error in both CTC value and BET analysis shown in Chapter 3. The butane molecule is small 0.43 nm in diameter [Mohanty and Purkait, 2012] and fits within the micropore region (< 0.2 nm). Micropore regions have the highest energy binding sites [Mangun *et al* 1997], therefore this pore size is filled first if the molecule dimensions are acceptable.

5.5.2 Temperature – Pine Wood

Below are the trials conducted using pine wood. The residence time and water flow remained at 1 hour and 1.5 ml/min respectively as with the olive stone trials.

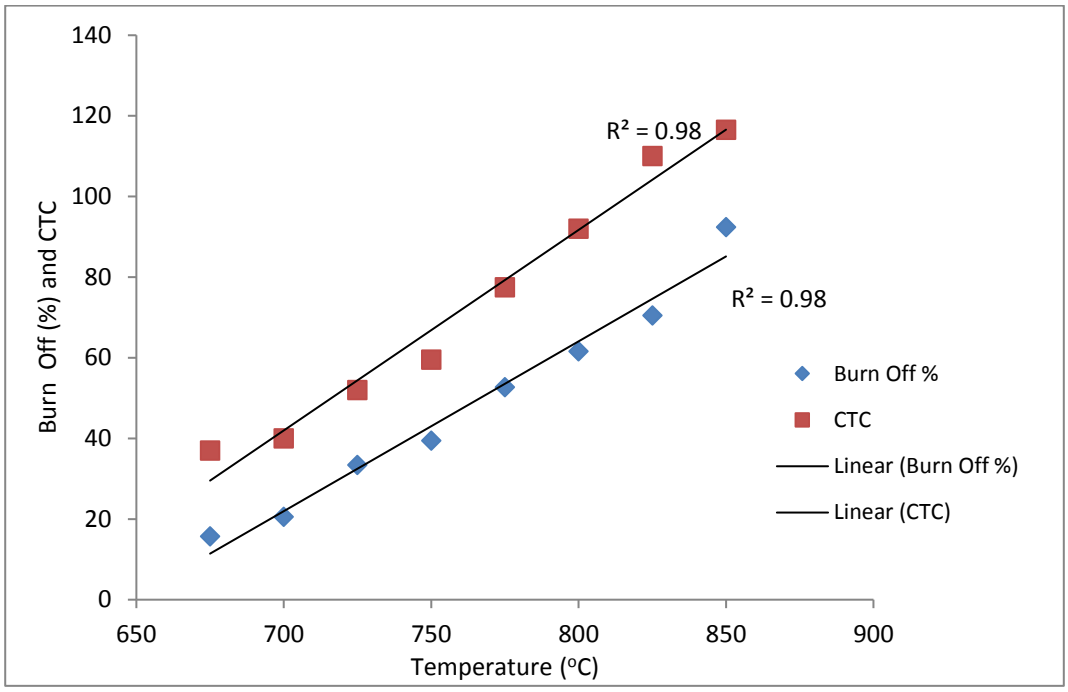


Figure 5:24 Pine wood activated carbon burn off (%) and CTC produced at different temperatures with 1 hour residence time and 1.5 ml/min water flow.

The activation temperature range for the trials using pine wood ranged from 675 °C to 850 °C with trials conducted at every 25 °C under the standard reaction conditions (residence time of 1 hour and water flow of 1.5 ml/min). Using an activation temperature of 850 °C only ash remained. Shown in Figure 5:24 is that the trend line initially follows the same pattern as Figure 5:20. However at the higher burn off percentage, 80% and above, there is no sudden drop in the CTC value as there is with olive stone activated carbon. The CTC continues to rise, albeit at a slower rate as the char approaches ash point. At this point there is a high ash to carbon ratio. High inorganic content as Bandosz, [2006] state is an unwanted property for activated carbon as it lowers overall activity and appears to be the case in these trials.

As stated across literature increasing temperature of steam activation increases carbon burn off and therefore increases porosity in terms of "creating void space" however, it becomes more complex as to what size pores are created. What is not reported on is the effect on the CTC value on these two biomass precursors and the temperature at which both carbons start fall away from the optimum CTC, burn off ratio.

5.5.2.1 Pore Analysis Pine Wood

Table 5-3 Pore analysis data for pine wood activated carbons

Temperature (°C)	Residence Time (mins)	BET (m^2/g)	Vmi (cm^3/g)	Vme (cm^3/g)	Vtot (cm^3/g)	Vme (%)	Burn off (%)
700	60	603	0.2363	0.0827	0.3190	25.9	20.5
750	60	817	0.3212	0.1741	0.4953	35.2	39.4
775	60	1030	0.4063	0.3449	0.7512	45.9	52.7
800	60	1101	0.4355	0.3929	0.8284	47.4	61.6
825	60	1190	0.4720	0.5893	1.0613	55.5	70.5
850	60	1169	0.4650	0.5624	1.0274	54.7	92.4

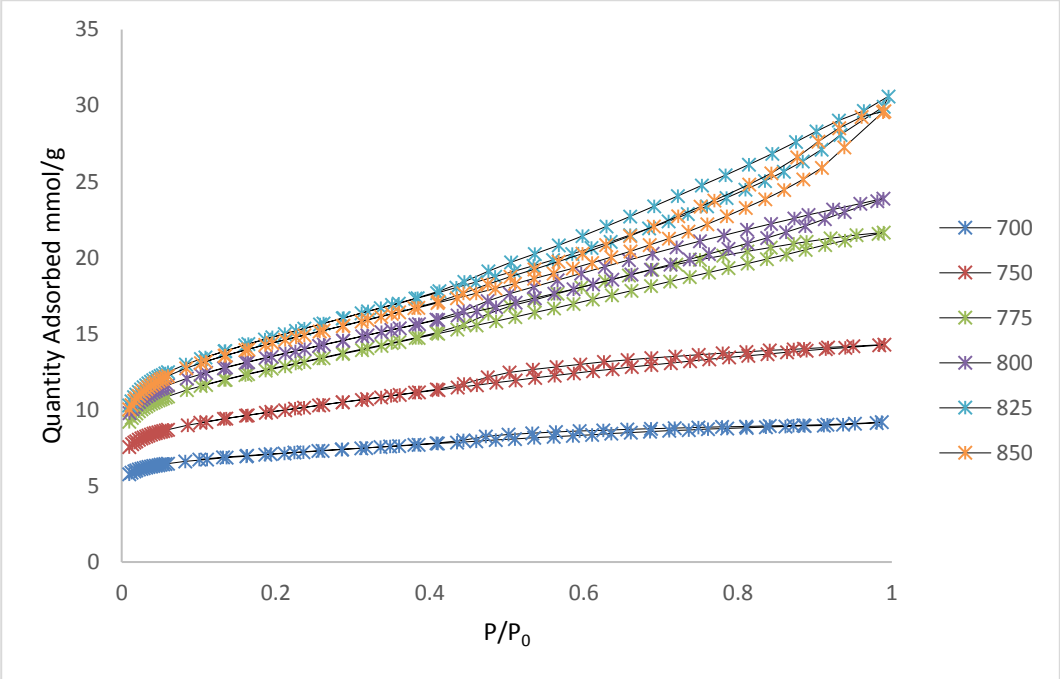


Figure 5:25 N_2 isotherms for pine wood activated carbons conducted at different temperatures.

The isotherms obtained for the carbons produced at different temperatures follows the same pattern as with the olive stone activated carbons shown in Figure 5:21. As activation temperature rises from 700 °C to 850 °C the isotherms go from Type-I to Type-IV as the carbons become more mesoporous. This is backed up in Table 5-3 showing that as temperature and burn off increase as does the mesoporosity of the carbons. Once the temperature reaches 850 °C a slight decrease in porosity is observed. Additionally this carbon has a very high burn off with a burn off increase of 12% from the carbon produced at 825 °C with no porosity gain. This means producing at this high temperature would seem not to be the most efficient or economical route to go as the carbon porosity is becoming damaged due to excessive burn off, losing yield and quality.

5.5.3 Comparison of Olive Stone and Pine Wood

Pore size change on temperature can be seen by the analysis below

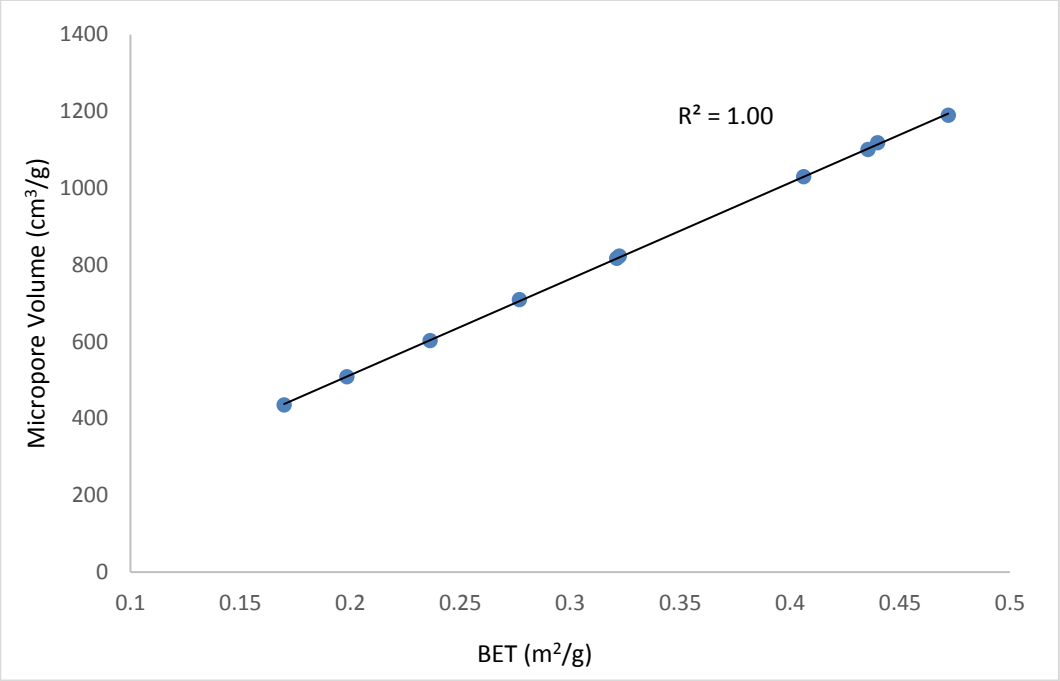


Figure 5:26 BET surface area (m^2/g) against micropore volume (cm^3/g) for both pine wood and olive stone activated carbons.

Figure 5:26 shows the relationship between micropore volume and BET surface area which form a perfect correlation across different biomass types.

As seen in Figure 5:2 Figure 5:4 burn off correlates to CTC for both biomasses, the figures below use burn off to show how pore size relates to both carbons produced at different temperatures.

The sample produced at 850 ^{o}C was excluded from the following figures due to excessive burn off leaving ash in the sample and a reduction in pore volume as seen in Figure 5:25. The set of figures shown below are all looking at how burn off affects pore structure by using different activation temperatures.

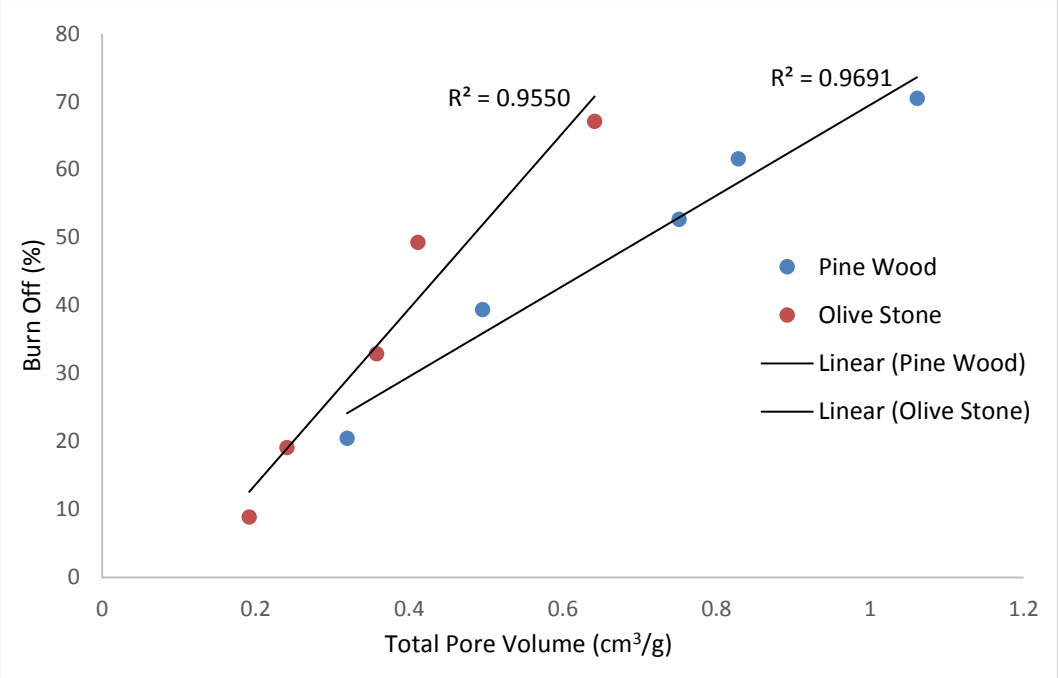


Figure 5:27 Total pore volume (cm^3/g) against burn off (%) for both olive stone and pine wood activated carbons.

Figure 5:27 to Figure 5:30 are produced to show how olive stone and pine wood micropore and mesopore volume changes with increasing burn off.

In Figure 5:27 the burn off percentage is plotted against the total pore volume. There is a strong correlation between the burn off percentage and total pore volume for both carbons - demonstrated by the high R^2 values. The gradient of the slope produced by olive stone is steeper than that produced by pine wood. This shows how less burn off is required with pine wood to achieve a higher overall porosity. The total pore volume is made up from micropores and mesopores in this analysis. Moving on to Figure 5:28 it can be seen how micropore volume correlates to burn off.

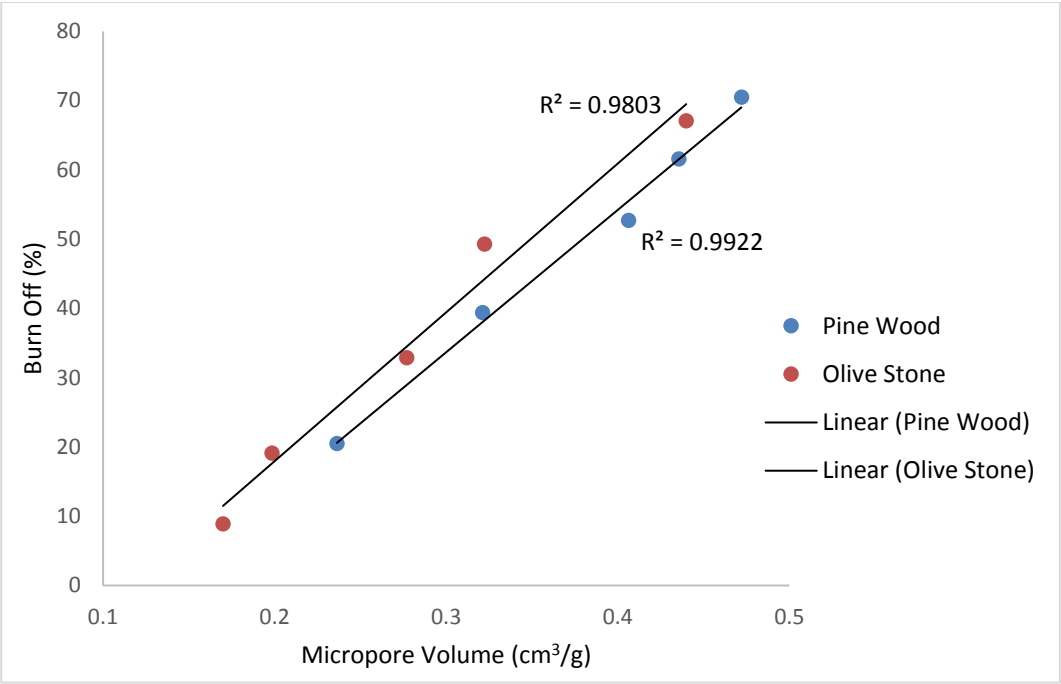


Figure 5:28 How burn off (%) effects the micropore volume (cm^3/g) with pine wood and olive stone carbons.

Before pore destruction take places at higher temperatures it can be seen that micropore volume increases linearly with increasing burn off with both carbons. Compared to Figure 5:27 the gradients of both slopes are similar in Figure 5:28. This implies that the micropore volumes at a similar burn off percentage are relatively close between the two biomasses. Conversely, with increasing burn off percentage, a larger increase in mesoporosity is predicted within the pine wood carbon compared to olive stone carbon. Evidence to this statement can be seen in Figure 5:29.

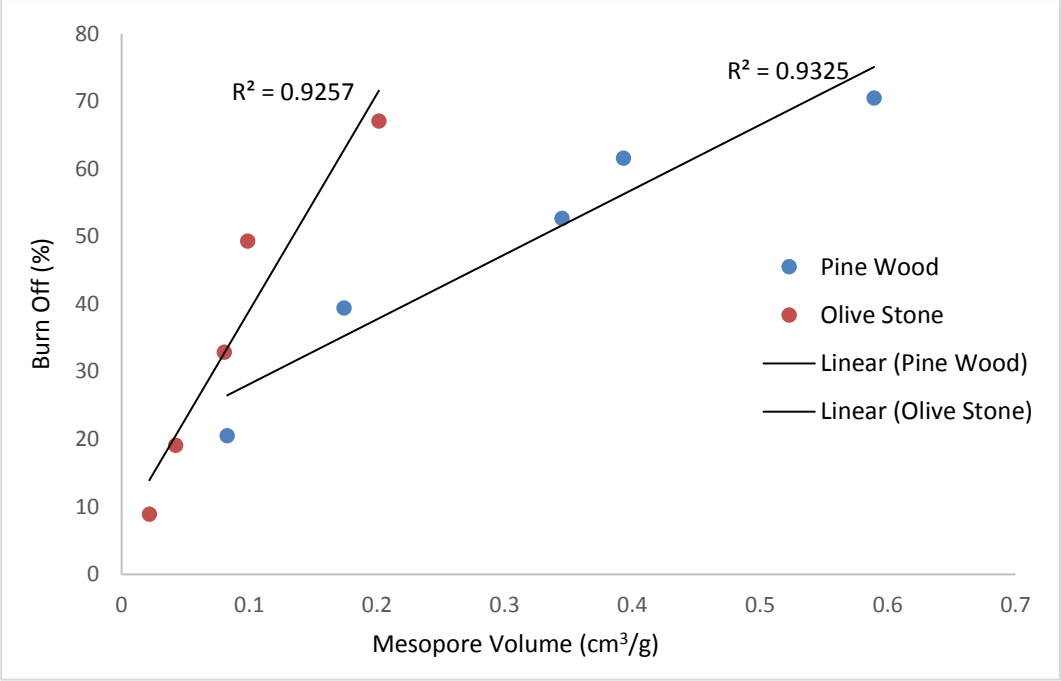


Figure 5:29 How mesopore volume (cm^3/g) changes with increased burn off for both pine wood and olive stone carbons.

From previous figures it can be seen how mesopore volume increases significantly faster with pine wood than olive stone as burn off increases. For example, at around 65% to 70% burn off for both carbons pine wood yields a threefold increase in mesopore volume over olive stone.

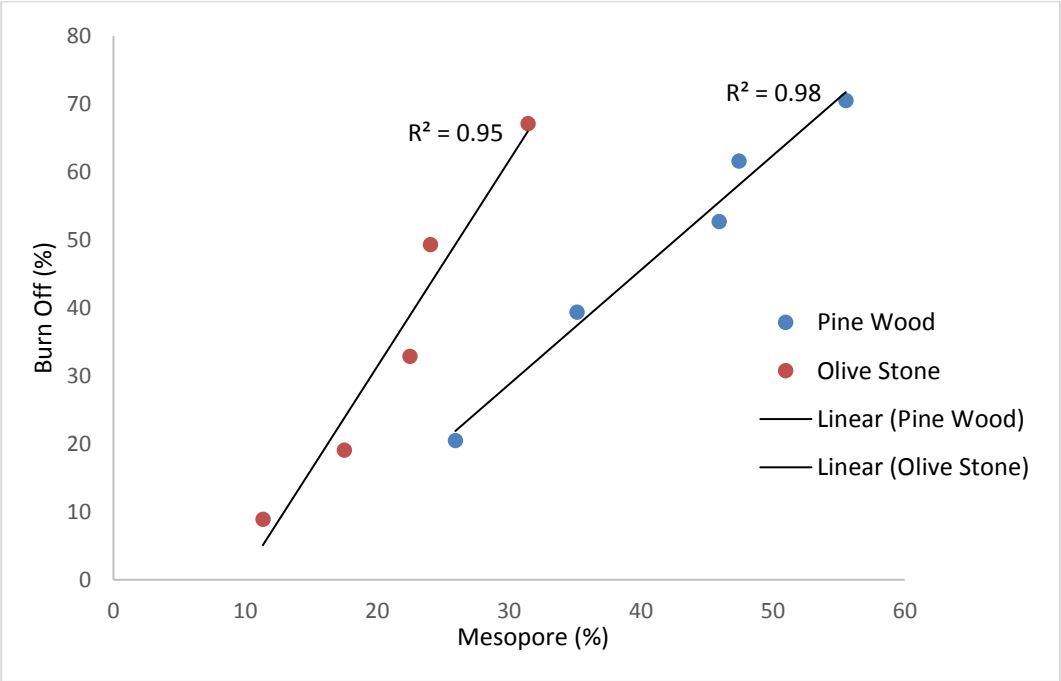


Figure 5:30 Mesopore (%) changes with increased burn off for pine wood and olive stone carbons.

The overall mesopore percentage for pine wood carbons is higher than with olive stone carbons. This is expected with results from previous figures.

5.5.4 Methylene Blue Adsorption

Whilst CTC tests are designed to analyse a carbons adsorption performance in the gas phase methylene blue tests are conducted to analysis the carbon adsorption performance in the- liquid phase.

The below trials were conducted at a range of activation temperatures, 60 minutes residence time and 1.5 ml/min water flow rate. Each ml of methylene blue solution adsorbed equates to 15 mg of methylene blue dye.

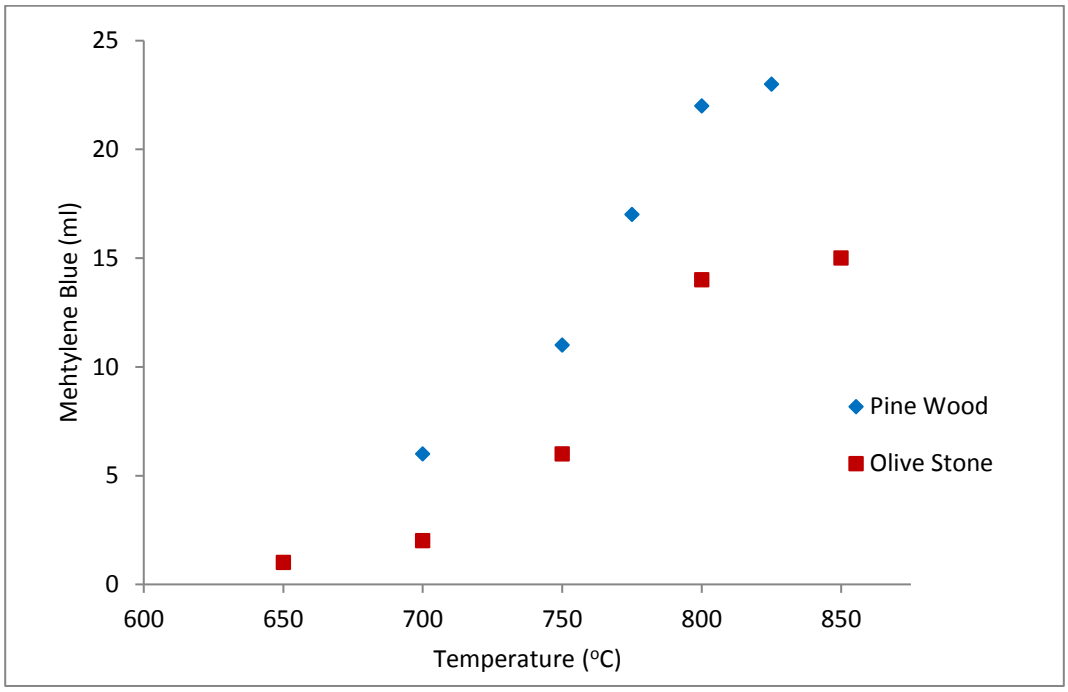


Figure 5:31 Methylene blue adsorption value (ml) against activation temperature (°C) for both pine wood and olive stone carbons.

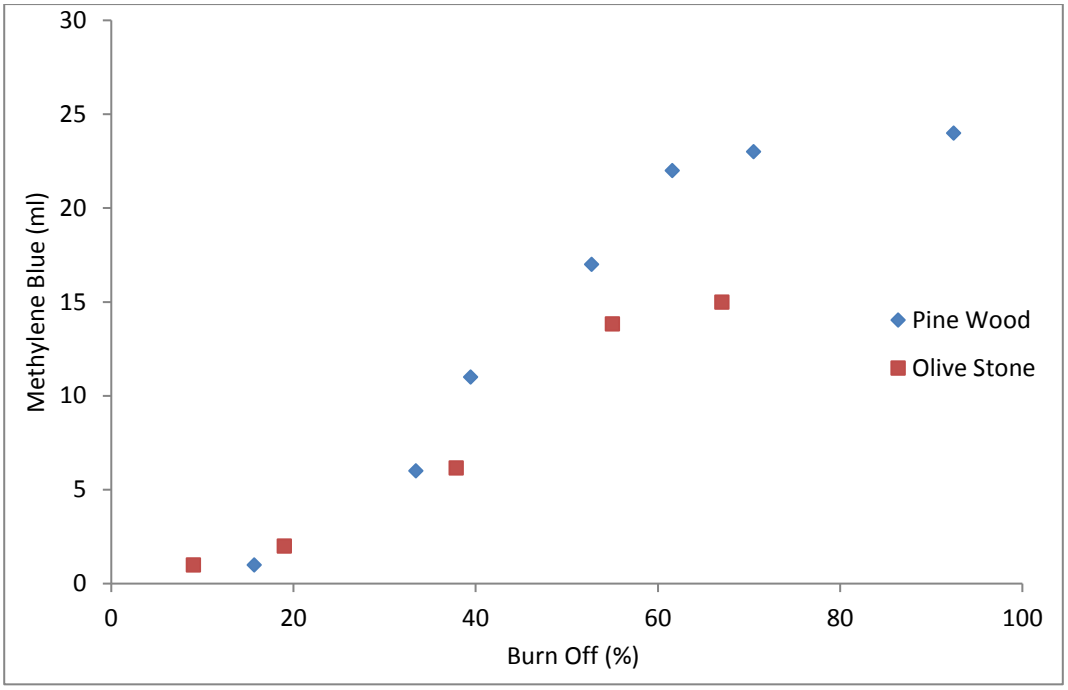


Figure 5:32 Methylene blue (ml) adsorption values against burn off (%) for both pine wood and olive stone carbons.

Figure 5:31 and Figure 5:32 show that methylene blue adsorption increases with activation temperature and the subsequent burn off. Initially the increase is gradual until around 20% burn off, where a rapid increase in adsorption initiates: between 20% and 60% for olive stone and 20% and 70% for pine wood. After this point the increase slows down with adsorption levelling off.

5.5.4.1 Methylene Blue and Pore Analysis

Methylene blue is known to be a mesoporous analysis technique however Figure 5:33 below shows the best fit is with micropore volume. This phenomena is a reported occurrence and is elaborated upon in 5.6.10. The mesopore volume and total pore volume to methylene blue correlation can be seen in Appendix Figures A:8 and A:9 respectively.

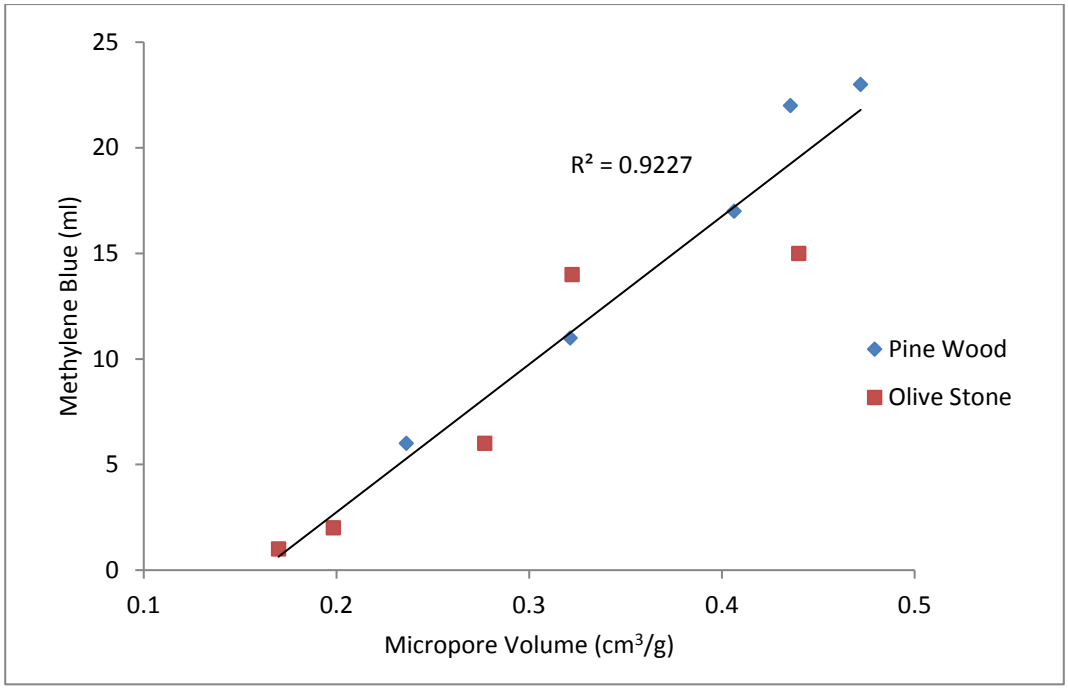


Figure 5:33 Micropore volume (cm^3/g) against methylene blue (ml).

There appears to be a correlation between micropore volume and methylene blue adsorption for the two biomass types. This correlation is unexpectedly stronger than the mesopore volume and methylene blue correlation shown in the Appendix Figures A:8 and A:9. Although at the higher micropore volumes pine wood has higher adsorption values than olive stone with the same micropore volume, the possible reason for this is covered in section 5.8.12, provided by CO_2 isotherms.

5.5.5 High Temperature Trials

5.5.5.1 Olive Stone Char High Activation Temperature

For olive stone activated carbon produced at ≥ 900 °C the carbon's adsorption performance reduces shown by a decreased CTC value but this can be misleading due to excessive burn off > 80%. To observe what effect temperature alone is having, the residence time and water flow rate were reduced to prevent excessive burn off taking place.

Olive Stone trials were conducted as shown in Table A-8 in the Appendix.

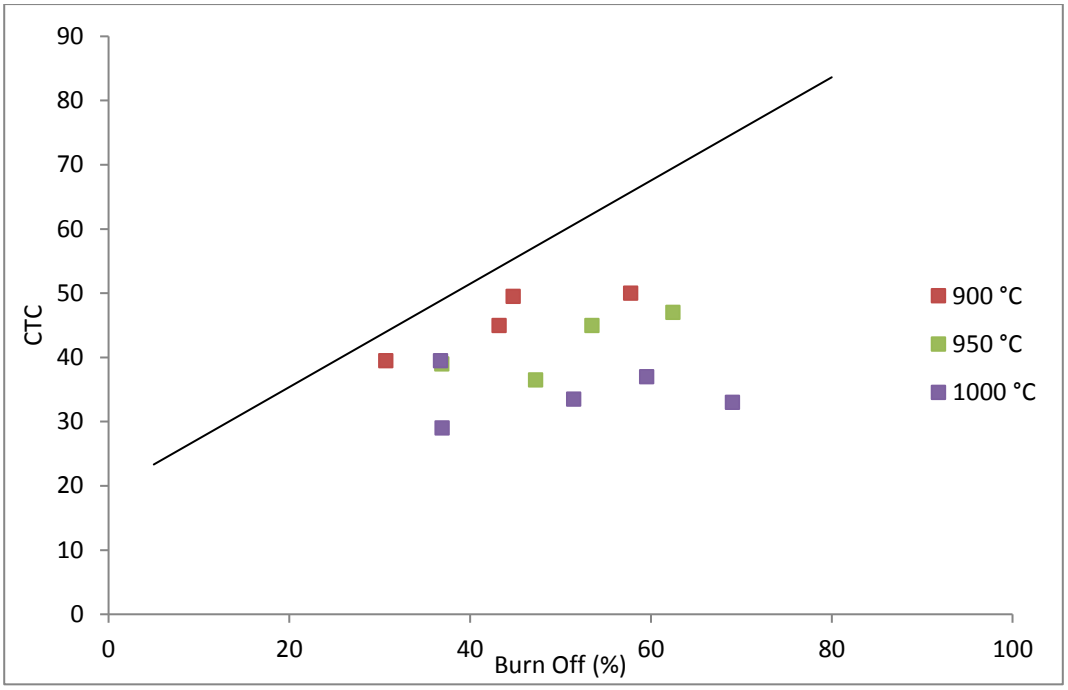


Figure 5:34 Burn off (%), CTC relationship when increasing temperature from 900 °C to 1000 °C.

The linear trend line shown is taken from Figure 5:2 and can be viewed as the optimum burn off CTC ratio. What can be ascertained from these results is that as activation temperature increased from 900 °C to 1000 °C the further the data points fall from this optimum ratio. Higher temperatures increase rate of diffusion, therefore rate of steam through the particle is increased at these raised temperatures causing an increased reaction rate between the steam and carbon. However, the reaction rates can become too fast. This means high external ablation of the particle can occur as discussed earlier in this chapter. External burn off is an unwanted property as carbon is burnt off at the surface as opposed to inside the particle where porosity can be developed.

Pore analysis was conducted on certain samples below:

5.5.5.2 Pore Analysis

Table 5-4 Pore analysis on high activation temperature samples.

Temperature (°C)	Residence Time (mins)	Total Water Flow (ml)	BET (m^2/g)	Vmi (cm^3/g)	Vme (cm^3/g)	Vtot (cm^3/g)	Vme (%)	Burn Off (%)	CTC
900	30	45	846	0.333	0.128	0.461	27.8	57.7	50.0
900	60	15	609	0.239	0.125	0.364	34.3	43.2	45.0
900	60	30	620	0.244	0.118	0.362	32.6	44.8	49.5
950	15	22.5	636	0.250	0.088	0.338	26.0	36.8	39.0
950	30	45	728	0.286	0.111	0.397	28.0	62.4	47.0
950	60	15	534	0.210	0.103	0.313	32.9	47.2	36.5
950	60	30	687	0.270	0.126	0.396	31.8	62.4	47.0

1000	15	22.5	644	0.254	0.100	0.354	28.3	36.7	39.5
1000	30	45	548	0.216	0.110	0.326	33.7	69.0	33.0
1000	60	15	368	0.145	0.088	0.233	37.8	36.9	29.0
1000	60	30	265	0.105	0.252	0.357	70.6	59.5	37.0

The N_2 isotherms generated can be seen in Appendix Figures A:10 to A:12

Table 5-5 Showing colours for the production conditions and shapes for temperatures for the below figures.

15 minutes/ 1.5 ml/min	30 minutes/ 1.5 ml/min	60 minutes/ 0.125 ml/min	60 minutes/ 0.25 ml/min
□	○	△	
900 °C	950 °C	1000 °C	

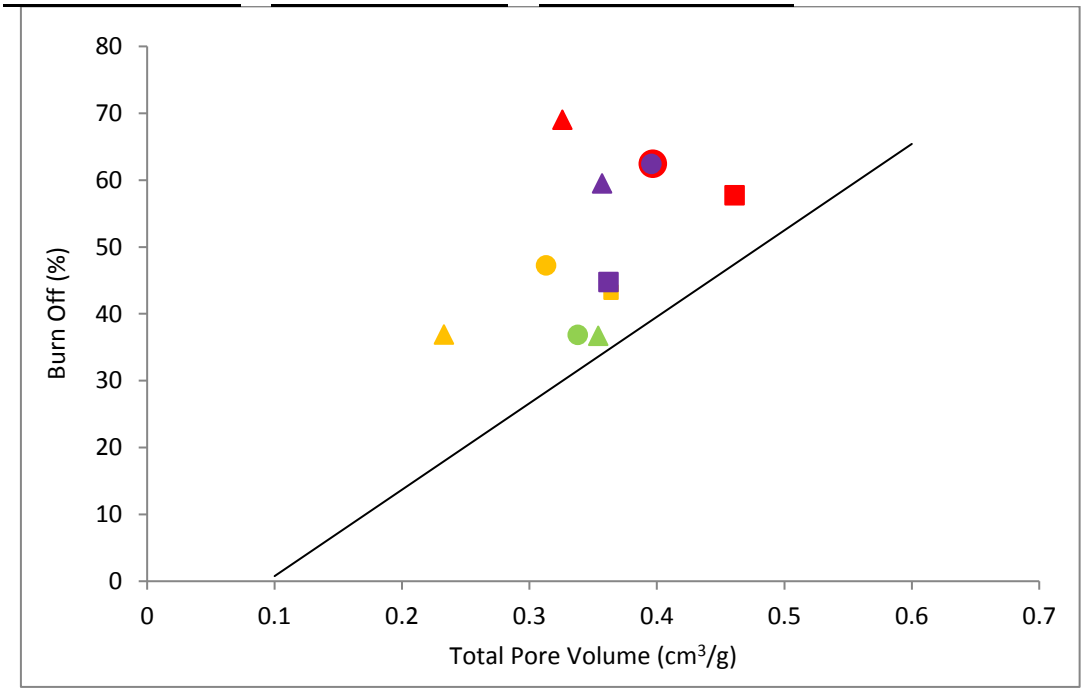


Figure 5:35 Total pore volume (cm^3/g) against burn off (%) for high activation temperature trials plotted against linear correlation shown in Figure 5:27, olive stone

Figure 5:35 shows what is happening to total pore volume as temperature is increased further from 900 °C to 1000 °C under four different production conditions - as shown in Table 5-4 all data points fall above the linear trend first shown in Figure 5:27. Therefore at a specific burn off percentage the total pore volume is lower than the data shown by activation temperatures < 850 °C. This shows at these raised activation temperatures significant external erosion is taking place during activation due to too harsh conditions. Increased burn off without further pore development is an unwanted occurrence in a commercial environment where products are sold on a weight basis.

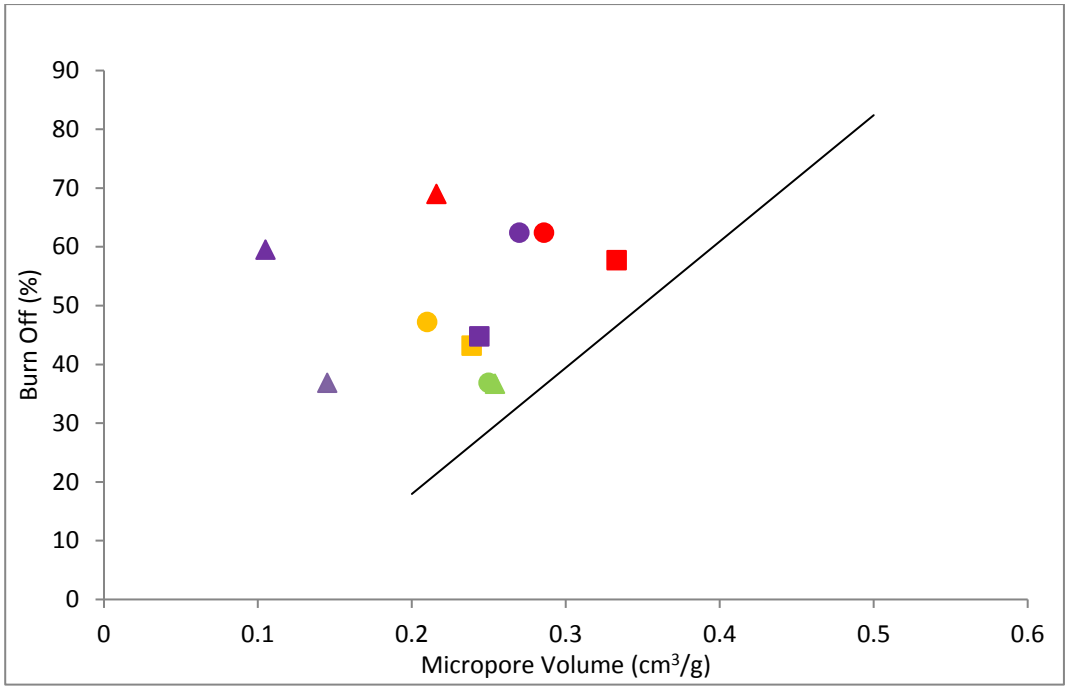


Figure 5:36 Micropore volume (cm^3/g) against burn off (%) for high temperature activation trials plotted against linear correlation from Figure 5:28, olive stone

As with Figure 5:35 all points fall above the linear trend line produced in Figure 5:28. This shows that the micropore volume with high activation temperature trials is lower than expected at a given burn off percentage than trials conducted at < 850 ºC. Gonzalez *et al* [1994] work with olive stones back this finding up by stating "increasing activation temperature means a reduction of the volume of total microporosity especially when going from 850 ºC to 900 °C". Additionally in literature, the higher activation temperatures widen micropores into mesopores [Tascón, 2012; Lua and Yang, 2004]. Figure 5:37 address this.

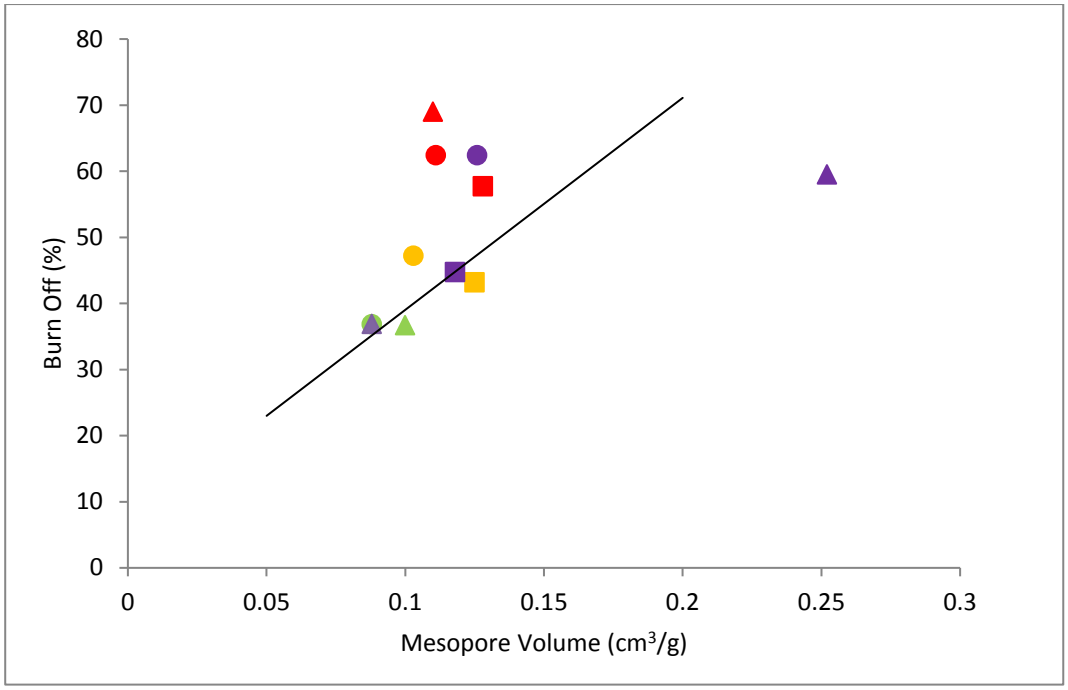


Figure 5:37 Mesopore volume (cm^3/g) against burn off (%) for high activation temperature trials plotted against linear correlation from Figure 5:29, olive stone

The figure above shows how the data points produced are either side of the trend line produced in Figure 5:29. It would appear mesopore volume decrease is not as significant as micropore volume loss at a given burn off percentage and why mesopore percentage is higher. This is likely to be because although high temperatures cause external particle burn off there is still widening of micropores creating mesopores.

Using evidence from the three figures it would seem the main cause of drop in performance is that carbon is being burnt off whilst porosity is not further increasing as expected. This is a clear sign of external ablation and backs up the work reported earlier [Demiral, *et al*., 2010; Okada, *et al*., 2003] and Chang, *et al*., [2000] who state external ablation is more significant than micropore widening.

5.6 The Effect of Residence Time on Olive Stone Activated Carbons

Residence time of activation needs to be carefully considered and can be divided into two areas:

Part 1: Where activation time increases or decreases under a constant temperature and water flow. This however means the total water flow over the given residence time is changing due to a constant flow rate.

Part 2: Increasing or decreasing the activation time but keeping the total water flow the same over the activation period. Whilst the total water flow remains constant the water flow rate is either reduced or increased.

5.6.1 Change in Activation Residence Time with Constant Water Flow

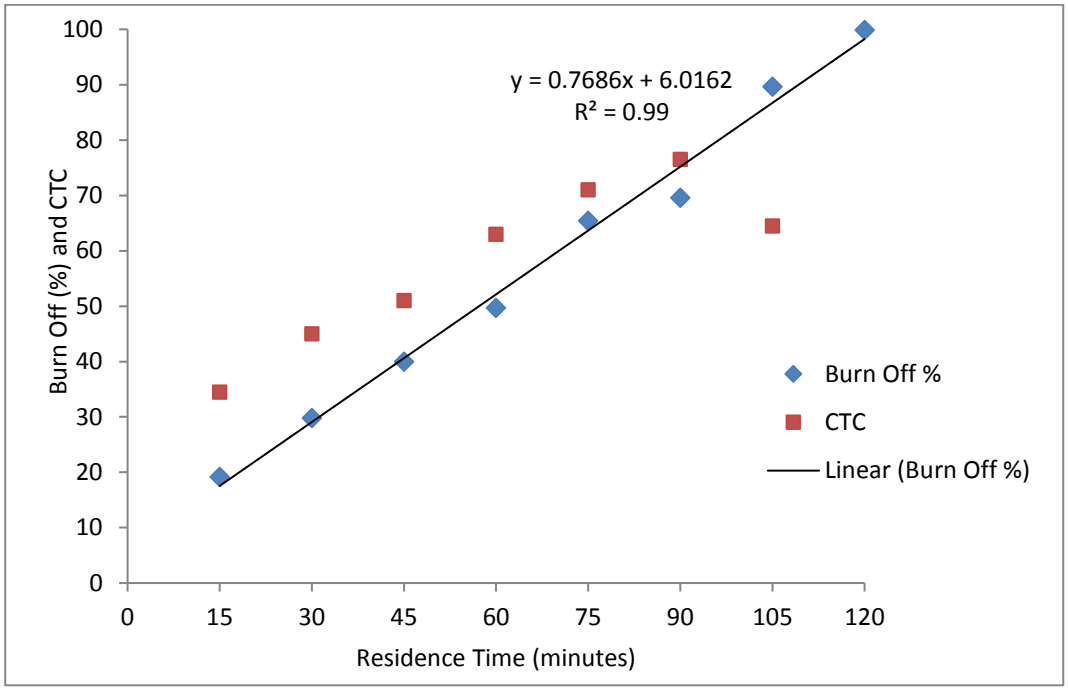


Figure 5:38 The effect of changing the activation residence time on olive stone char (10g) at 800 °C and a flow rate of 1.5 ml/min.

Evidence from Figure 5:38 shows a linear relationship between activation time and burn off rate. This implies that under the same temperature and constant water flow the burn off rate remains constant throughout the activation period. The rate of carbon (mass) evolution remains constant even though carbon is being continuously burnt off and total mass reducing throughout the activation. The main difference occurs in the first 15 minutes of activation, which exhibits a larger burn off, however this can be accounted for by remaining volatiles and moisture content within the char. Using the equation from the linear trend line in Figure 5:38 the average burn off from the 10 g of char used between 15 and 120 minutes is 0.0767 g/min (0.77 %/min). The same pattern in terms of increasing residence time is reported in literature [Gonzalez, *et al* 2007],

however, the report does not mention the linear relationship that forms under the same steam flow rate.

The same set of data was carried out at 750 °C under the same water flow and time periods (every 15 minutes) this is shown in Figure 5:39.

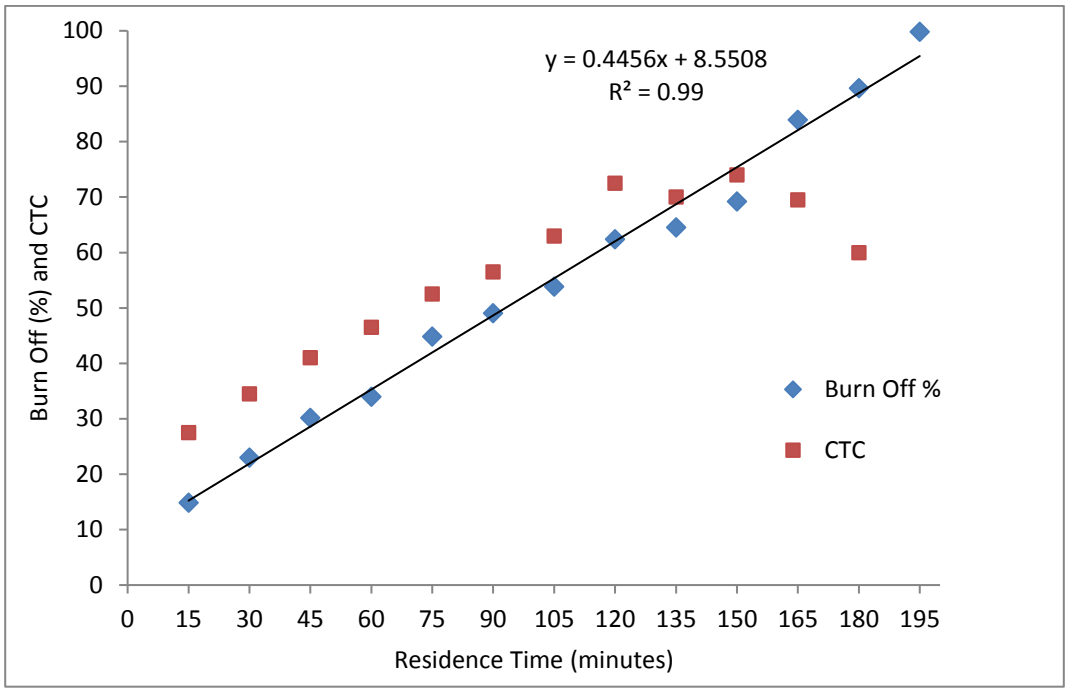


Figure 5:39 The effect of changing the residence time with olive stone activated carbon at 750 °C and a flow rate of 1.5 ml/min.

Figure 5:39 differs from Figure 5:38 in that it has taken more time for the activation to reach ash point due to the lower temperature used. This was 195 minutes compared to 120 minutes in Figure 5:38. Again a linear relationship is shown between residence time and burn off. Using the same method the average burn off calculated was found to be 0.0447 g/min (0.45 %/min).

Regarding the CTC values in both Figure 5:38 and Figure 5:39 the same pattern is observed: A linear increase in CTC with an increase in burn off, up to 80%, at which the CTC begins to reduce significantly.

Data points were collected using an activation temperature of 850 °C up to 60 minutes, (see Appendix Figure A:13) but much the same can be seen with a linear relationship with an average burn off of 0.104 g/min (1.04 %/min)

What can be taken from these sets of results is that increasing residence time increases burn off in a linear fashion as does increasing temperature > 650 °C as proven in section 5.5.1.

When considering commercial scale production, to achieve the desired burn off it must be calculated whether it is cost effective to increase the temperature or to increase the residence

time. This can be done by considering energy balances for the process whilst taking into account the efficiency of the production equipment.

For example, on lab scale under the same water flow to achieve a burn off of 50% (5g)

750 ^{o}C = $\frac{5g}{Burn\ off\ g/min} = \frac{5}{0.04456}$ = 112.2 minutes

850 ^{o}C = $\frac{5g}{Burn\ off\ g/min} = \frac{5}{0.1044}$ = 47.9 minutes

A difference of 64.3 minutes can be seen between these two temperatures to achieve a 50% burn off. The next calculation when designing the operating conditions must show if it is economically and operationally beneficial to increase the residence time by this amount or the temperature by 100 ^{o}C. Thermal efficiency/retention, source of heating and kiln size required are the main dictators in this decision; however there are also other areas to be considered which are elaborated on further in the chapter.

5.6.2 Pore Analysis of Residence Time Trials

Table 5-6 Pore analysis data from olive stone activated carbon produced at different residence times at 800 ^{o}C and 1.5 ml/min water flow.

Residence Time (minutes)	BET (m^2/g)	Vmi (cm^3/g)	Vme (cm^3/g)	Vtot (cm^3/g)	Vme (%)
15	571	0.2228	0.0473	0.2701	17.5
30	696	0.2725	0.1000	0.3725	26.8
45	846	0.3253	0.2562	0.5815	44.1
60	894	0.3421	0.2522	0.5943	42.4
75	1049	0.4145	0.2799	0.6944	40.3
90	1103	0.4356	0.3172	0.7528	42.1

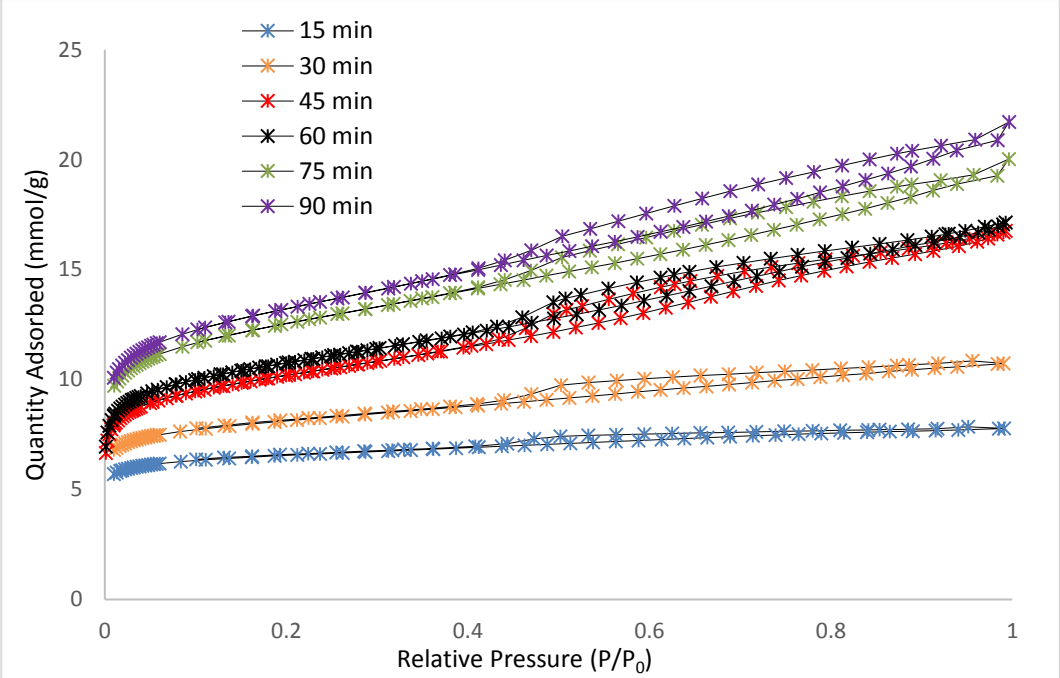


Figure 5:40 N_2 isotherms of data presented in Table 5-6.

The pore analysis results show that as residence time increases from 15 minutes to 90 minutes as does the overall porosity of both micropores and mesopores. With micropore volume increase, the BET surface area also increases in a direct correlation (see Appendix Figure A:14). The mesopore percentage increases initially to around 40% to 45% after 45 minutes. This is shown by the shapes of the isotherms – at 15 and 30 minutes the isotherms are relatively flat (Type-I). After 30 minutes they begin to change into Type-IV showing a higher mesoporosity. This value then remains constant for the other results showing that mesopore pore volume and micropore volume are increasing at a similar rate. As a result, micropores are likely widened to form mesopores and further new micropores are formed throughout the activation.

5.6.3 Residence Time Pine Wood

Similar set of experiments were carried out using pine wood as the precursor.

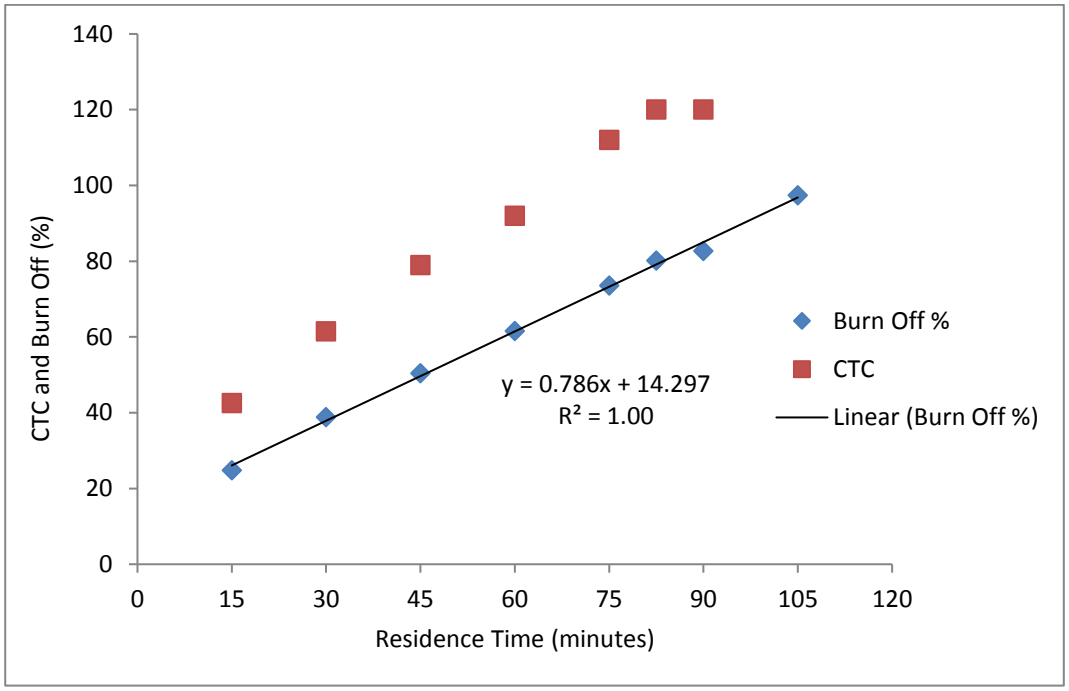


Figure 5:41 The effect of changing the activation residence time on pine wood activated carbon at 800 °C and a flow rate of 1.5 ml/min.

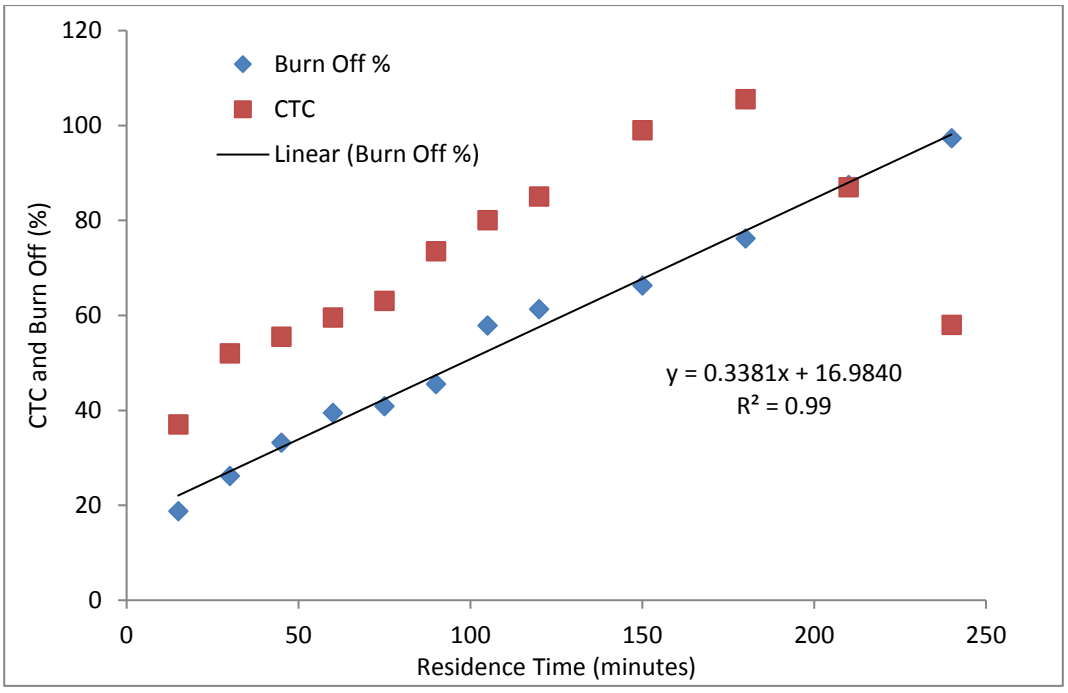


Figure 5:42 The effect of changing the activation residence time on pine wood activated carbon at 750 °C and a flow rate of 1.5 ml/min.

Looking at both Figure 5:41 and Figure 5:42, they show identical patterns to Figure 5:38 and Figure 5:39 with a linear relationship seen between residence time and burn off.

Figure 5:41 at 800 ºC shows a 0.0275 g/min (0.79 %/min) burn off rate, whilst Figure 5:42 at 750 ºC shows a 0.012 g/min (0.34 %/min) burn off rate.

Therefore when using pine wood char an increase in activation temperature of 50 ºC results in a burn off increase of 232% - this is half the increase seen with olive stone carbons when increasing the activation temperature by 50 ºC. This demonstrates that when increasing activation temperature the steam-carbon reaction is more sensitive to change, resulting in a faster reaction rate when using pine wood compared to olive stone. Conversely increasing residence time increases olive stone char burn off at a faster rate than when using pine wood char.

5.6.4 Comparison of Olive Stone and Pine Wood Derived Carbons

Olive stone (10 g) and pine wood (3.5 g) were placed in the crucible to fill the same volume (the difference in initial mass being due to density differences).

Using both sets of data, olive stone and pine wood at 800 ºC, average burn off rate is 0.0767 g/min and 0.0275 g/min respectively. This follows Le'Chatliers principle and Reaction 1 with the higher mass of olive stone char (C) available the reaction is pushed forward to produce more product species (CO and H_2). However, comparing both in terms of burn off percentage g/min of char the values are 0.77% and 0.79% for olive stone and pine respectively.

At 750 ºC there is a greater difference in burn off percentage for olive stone and pine wood. The figures show how the pine wood burn off per gram is lower than that of the olive stone at a temperature of 750 ºC. An increase in temperature to 800 ºC for pine wood activation therefore has a bigger effect on burn off than it does for olive stone.

Results show that to achieve ash point at 750 ºC with pine wood it takes 240 minutes, as opposed to olive stone char where it takes 195 minutes. Conversely, at 800 ºC it takes less time to achieve full burn off with pine wood (105 minutes) compared to olive stone (120 minutes). This may be due to the composition of the lignocellulosic biomasses. Lignin decomposes at a higher temperature range (160 ºC to 900 ºC) than both hemi-cellulose (220 ºC to 315 ºC) and cellulose (315 ºC to 400 ºC) [*Yang et al., 2006*], it is also reported in literature that pine wood can have a higher lignin content with values reported between 25% and 35% [Hayes, 2016], whereas olive stone values are reported between 20.6% and 26.5% [Mendu *et al* 2011]. The higher lignin content of pine wood may cause a higher increase in burn off with increasing temperature compared with olive stone carbon.

This project shows a specific burn off percentage provides an overall indication of the quality of carbon produced, which is carried over to large scale production (see Chapter 6). The effect of altering temperature and residence time is shown in the previous figures as a linear relationship

against burn off percentage - increasing the temperature whilst decreasing the residence time (and vice versa) produces the same yield and a similar carbon.

In large scale production energy efficiency is important. An energy efficient process reduces the carbon footprint, as well as reducing operational costs. These lab trials provide evidence of how biomass char reacts to changing conditions. Increasing activation temperature by 50 ºC with pine wood from 750 ºC to 800 ºC has the same burn off increase as from 750 ºC to 850 ºC with olive stone. This means that it is beneficial to increase the activation temperature for pine wood as opposed to increasing residence time compared to olive stone carbon production. With olive stone it is beneficial to increase residence time as opposed to increasing the temperature if an increase in burn off is required.

It must be noted external factors such as operating equipment efficiency has an influence, but it demonstrates that different production conditions are preferential for each biomass.

A linear relationship between burn off rate and time is easily scaled up to large operations. Burn off is a significant factor in terms of overall quality, therefore it is important that the burn off level can be predicted for a large scale process.

5.6.5 Change in Residence Time with Altered Water Flow to Allow Same Total Water Volume Flow into the System

5.6.5.1 Olive Stone

The second part of the residence time trials involves reducing flow to keep the total flow of steam the same whilst altering the residence time.

Trials were conducted at 750 ºC, 800 ºC and 850 ºC degrees with two different residence times of 30 minutes and 120 minutes. The flow rates used for these two times were 1.5 ml/min and 0.375 ml/min respectively. This meant over the two different residence times the total water flow was equal.

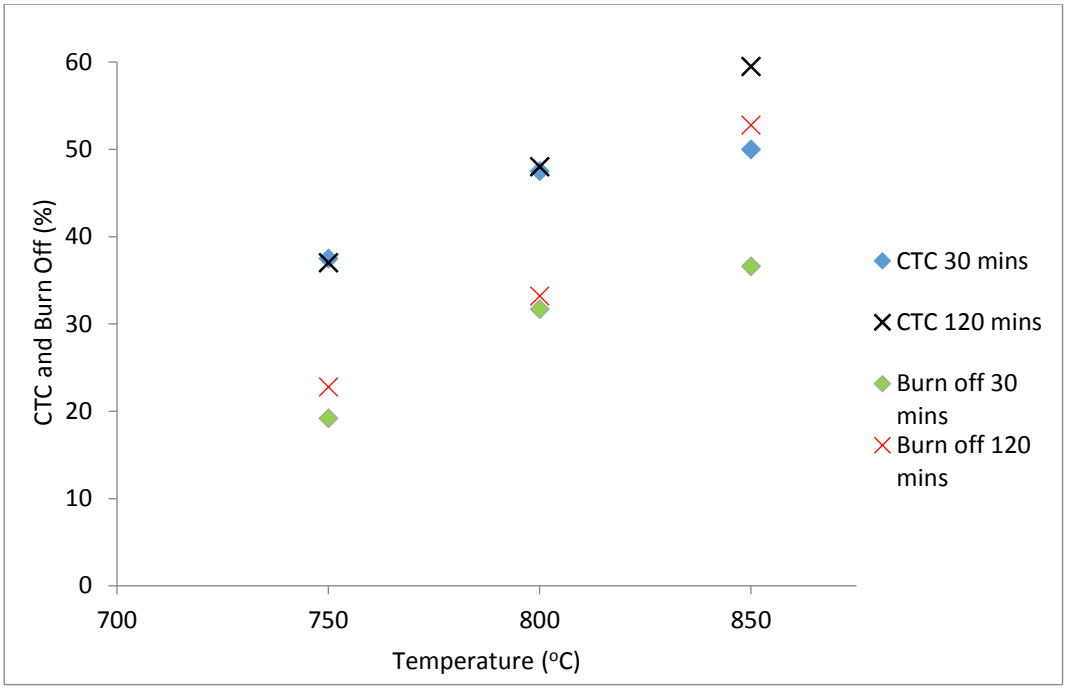


Figure 5:43 Results of the two different residence times with the same total water entering the system.

For activations temperatures (750 °C and 800 °C) the residence time change has a small effect on the burn off with the longer residence time achieving only a slightly higher burn off. Therefore the results show that total water flow appears to be the determining factor. In contrast, there is a significant increase in burn off when the temperature rises to 850 °C. This implies that the longer but reduced flow rate at higher temperatures result in a higher burn off. Using knowledge from previous trials, higher activation temperatures result in a quicker burn off rate along with a higher chance of a successful steam carbon reaction; therefore, over the 120 minute period there is more chance for this to occur. The next step was to see if this observation was carried over at the two lower activation temperatures by increasing residence time further.

Table 5-7 Raw data results represented in Figure 5:44.

800 °C Total Water Flow (ml)	45		67.5		90		112.5	
Residence Time / (Burn Off %)	1 hour	(31.6)	1 hour	(43.4)	1 hour	(49.7)	1 hour	(61.2)
Residence Time / (Burn Off %)	2 hours	(35.0)	3 hours	(50.2)	4 hours	(60.4)	5 hours	(89.3)

750 °C Total Water Flow (ml)	45		67.5		90		112.5		135	
Residence Time / (Burn Off %)	1 hr	(25.1)	1 hr	(30.2)	1 hr	(34.0)	1 hr	(39.5)	1 hr	(39.5)
Residence Time / (Burn Off %)	2 hr	(25.2)	3 hr	(33.2)	4 hr	(40.4)	5 hr	(55.9)	6 hr	(55.9)

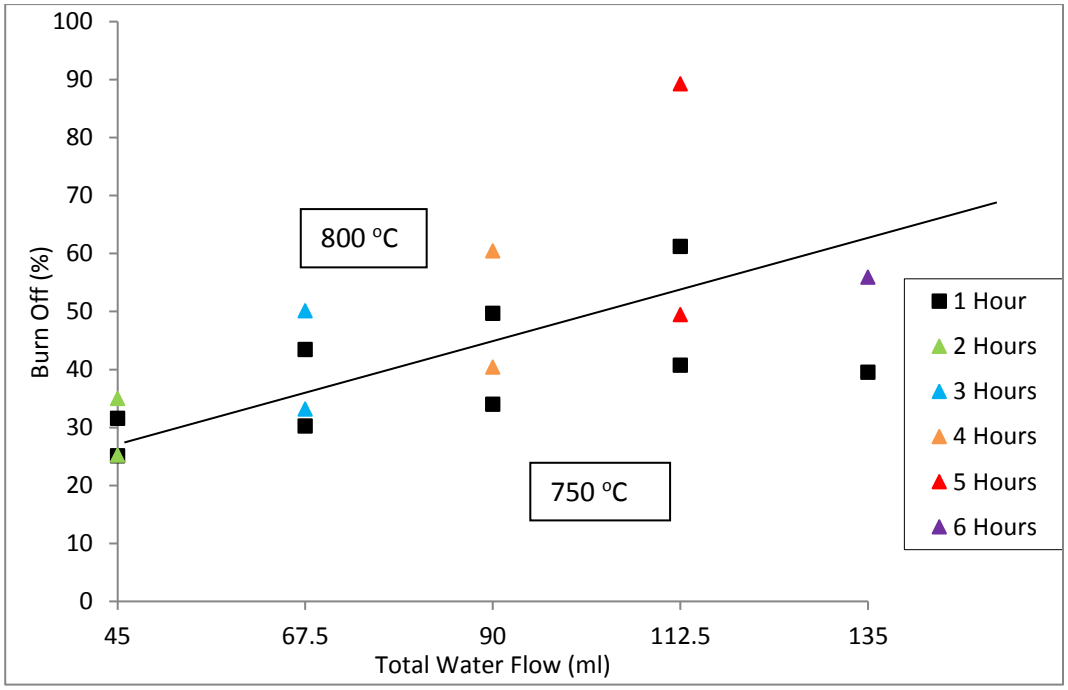


Figure 5:44 Olive stone trials conducted at both 750 °C and 800 °C (separated by the dividing line) at different residence times.

Using both Table 5-7 and Figure 5:44 the effect of having different residence times, yet same total water entering the system is seen. A longer residence time with the reduced water flow rate results in an increased burn off compared to a shorter residence time with higher water flow rates, thus meaning more steam has reacted with the char.

As the residence time between the two points is increased the effect becomes more apparent. The reason being as residence time is longer there is more time for a successful reaction to occur even though the partial pressure of steam is lower during the course of the activation. The results show the point at which reaction time becomes a more dominant factor in activation than steam partial pressure. With the lower water flow rate there is less excess steam passing over the carbon bed at any one time, this results in a higher percentage of the total water reacting with the carbon over the longer period.

This information can be beneficial to the large scale production as it means longer residence times with lower water flow rates could be the most efficient way to achieve the burn off desired.

5.6.5.2 Pine wood

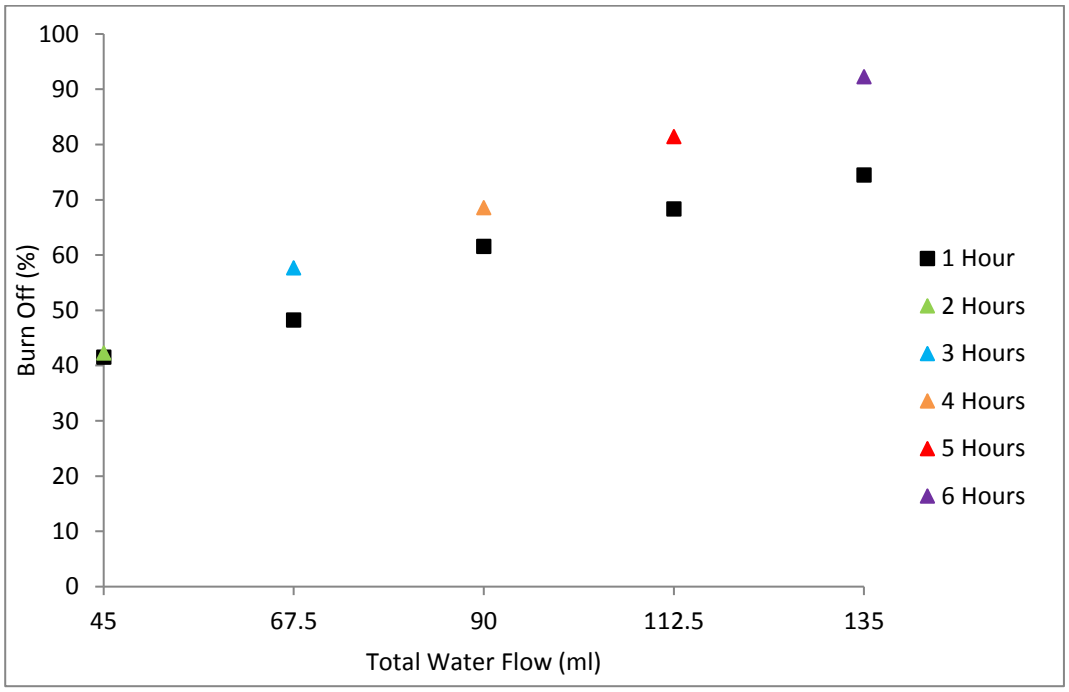


Figure 5:45 Pine wood trials conducted at 800 °C at different residence times.

Figure 5:45 shows similar correlations to Figure 5:44. Just like the olive stone, carbon burn off increases with same total water entering the system but over a longer residence time with the overall difference becoming larger.

5.6.6 Long Residence Time Trials

5.6.6.1 Olive Stone

Table 5-8 Long residence time trials for olive stone activated carbon.

	Residence Time (mins)	Temperature (°C)	Flow Rate (ml/min)	Burn Off (%)	CTC
800 °C	120	800	0.375	35.0	46.0
	180	800	0.375	50.2	59.0
	240	800	0.375	60.4	68.0
	300	800	0.375	89.3	68.0
750 °C	120	750	0.375	25.2	38.5
	180	750	0.375	33.2	49.5
	240	750	0.375	40.4	53.0
	300	750	0.375	49.5	60.0
	360	750	0.375	55.9	60.0
	420	750	0.375	56.9	61.5
	420	750	0.375	62.2	62.5
	480	750	0.375	72.1	63.5

The water flow for both the following olive stone and pine wood trials was reduced to 0.375 ml/min. This was done to prevent excessive burn off and destruction, but allow up to 8 hours of activation. The activations temperatures used were 750 ºC and 800 ºC for both olive stone and for pine wood.

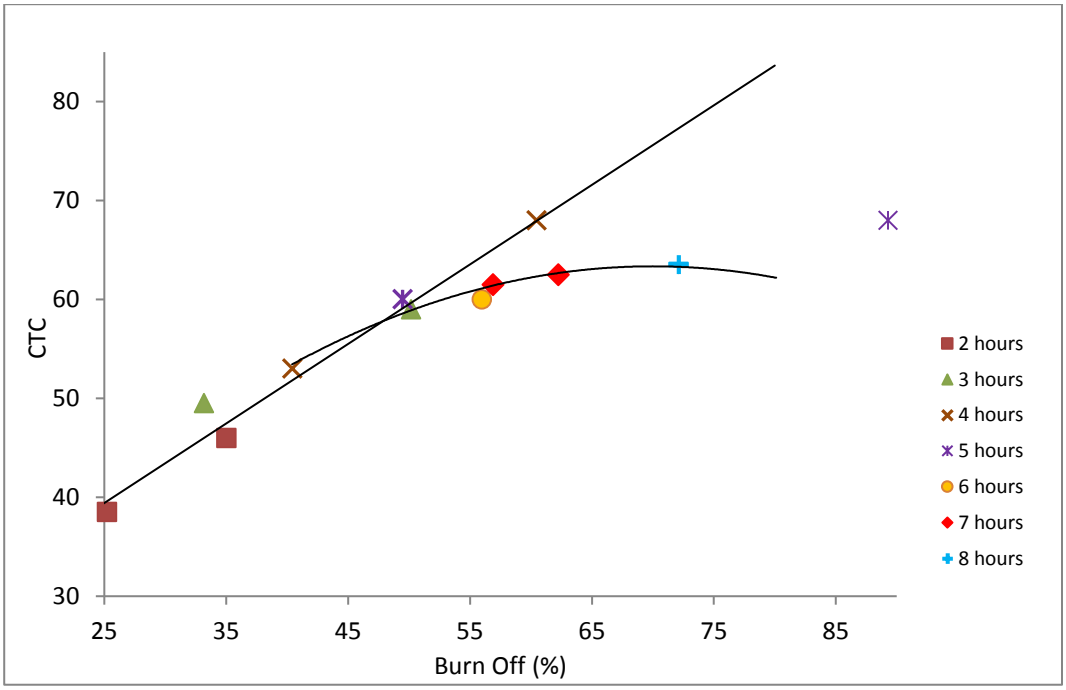


Figure 5:46 Long residence times at both 750 ºC and 800 ºC trials shown in Table 5-8.

Findings show how activating olive stone over a long period leads to a drop off in performance compared to the optimum CTC burn off ratio after the six to seven hour mark. According to Okada, *et al*., [2003] prolonged activation may cause over activation, accelerating surface erosion more than pore formation; this data appears backs up this statement. An activation temperature of 800 ºC was used first, however, only five hours under this flow was achieved before excessive burn off had occurred. For this reason a lower activation temperature of 750 ºC was used, this was to enable an activation time of eight hours to be possible.

A drop off in performance at a given burn off is an unwanted property as previously stated additionally another disadvantage of activating for a prolonged time comes in the terms of capital costs. The rotary kiln will have to be of sufficient length to accommodate such a time. A possible but unfavourable way round this is to reduce the rpm of the heat tube within the kiln but this hinders mixing potential. It is crucial that good mixing of the steam and carbon is maintained and this means a reasonable rpm of the heat tube is required. Very slow rates are expensive to maintain and in addition favour micropore formation [Marsh and Reinoso 2006]. Pore analysis has been conducted on certain samples as shown in section 5.6.6.3

5.6.6.2 Pine Wood

Table 5-9 Long residence time trials for pine wood activated carbon.

	Residence Time (mins)	Temperature (°C)	Flow Rate (ml/min)	Burn Off (%)	CTC
800 °C	60	800	0.375	27.1	49.0
	120	800	0.375	42.3	62.5
	180	800	0.375	57.7	78.5
	240	800	0.375	68.6	88.5
	300	800	0.375	81.5	104.0
	360	800	0.375	92.3	105.5
750 °C	60	750	0.375	19.3	39.5
	120	750	0.375	25.2	44.0
	180	750	0.375	34.9	51.0
	360	750	0.375	52.8	74.0
	420	750	0.375	63.5	88.5
	480	750	0.375	67.0	98.0

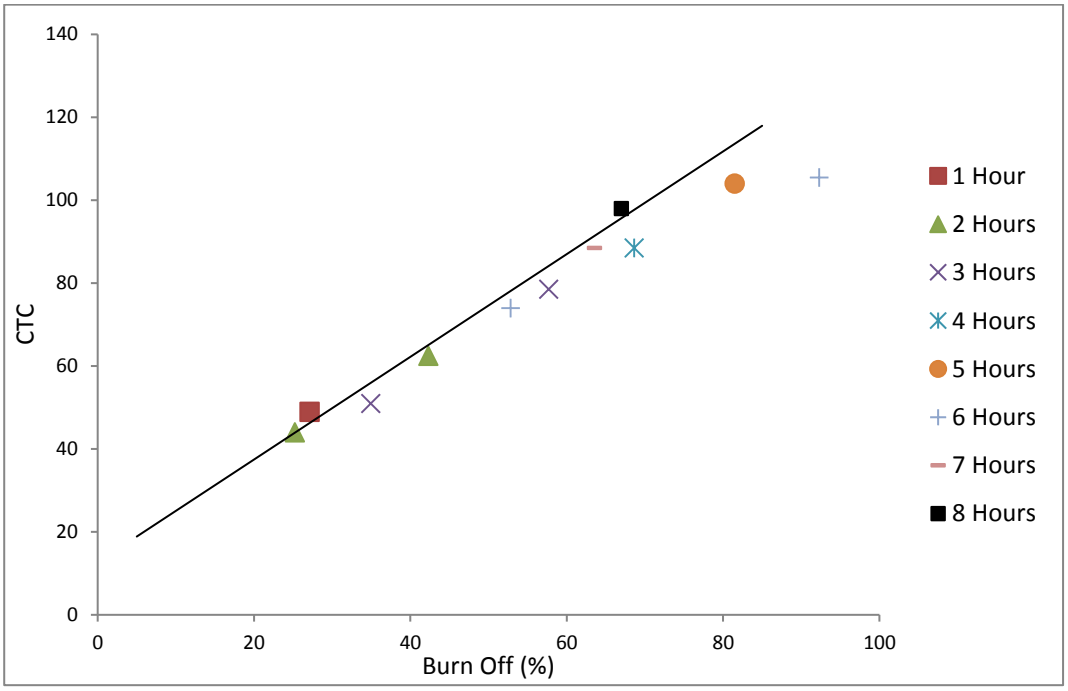


Figure 5:47 Long residence times at both 750 °C and 800 °C trials shown in Table 5-9.

As before lowering the activation temperature to 750 °C was required to reach the longer residence times before excessive burn off took place. Unlike with olive stone, an activation time of seven/eight hours does not seem to affect the burn off, CTC relationship with no drop in performance seen before 90% burn off, where, at this point natural destruction and high ash to carbon ratio is taking place. This would lead to the assumption, as with increasing the water flow

seen previously, that external erosion of the pine wood char does not occur to the same extent as with olive stone char under these production conditions.

5.6.6.3 Pore Analysis for Long Residence Time Activation

Table 5-10 Pore analysis for long residence time olive stone activated carbons.

Temperature (°C)	Residence Time (hours)	BET (m^2/g)	Vmi (cm^3/g)	Vme (cm^3/g)	Vtot (cm^3/g)	Vme (%)	Burn Off (%)	CTC
750	2	627	0.2443	0.1230	0.3673	33.5	25.2	38.5
750	3	661	0.2586	0.1099	0.3685	29.8	33.2	49.5
750	4	744	0.2883	0.1286	0.4169	30.9	40.4	53.0
750	5	884	0.3395	0.2169	0.5564	39.0	49.5	60.0
750	6	878	0.3386	0.1949	0.5335	36.5	55.9	61.5
750	7	1080	0.4276	0.2771	0.7047	39.3	62.2	62.5
750	8	1088	0.4311	0.2558	0.6869	37.2	72.1	63.5

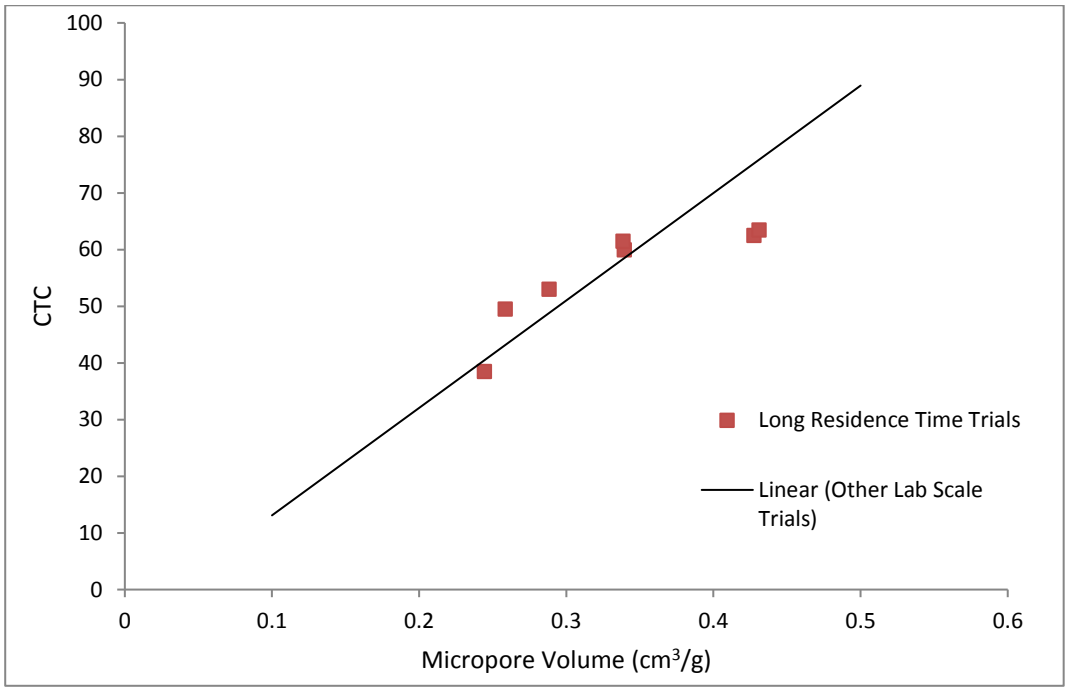


Figure 5:48 Long residence time micropore (cm^3/g) against CTC results, olive stone.

Firstly from Table 5-10 it would seem that whilst micropore volume increases as residence time increases the mesopore percentage also increases but does not go above 40%, this would seem to go against the statement from Marsh and Reinoso, [2006] which states that 'longer activation times showed bias towards micropore formation'. However, the exact time of activation in the statement is not expanded upon. Figure 5:48 shows how the micropore volumes fit in with other lab scale trials. It can be seen how micropore formation is still occurring at the longer residence times, interestingly, the results show that the CTC is expected to be higher for the given micropore volumes at the seven and eight hour residence time trials. This would lead to the

assumption that either the micropore shape has deformed allowing entry to a nitrogen molecule but not a butane molecule or that the longer residence time has caused a change in surface chemistry less favourable to butane adsorption.

5.6.7 Steam Flow

In the following trials the molar ratio between the water entering the system over a two hour period and moles char (olive stone) present was used. Two hour residence time trials were used to allow a higher molar ratio of 6:1 which is the maximum achievable in an hour with the older stop start system. Raw table results (see Appendix Table A-9)

Molar ratio calculation

$$\frac{\left(\frac{Water(g)}{Mr\ \mathrm{g\ mol^{-1}}}\right)}{\left(\frac{Carbon(g)}{Mr\ (\mathrm{g\ mol^{-1}})}\right)}$$

Equation 5-2

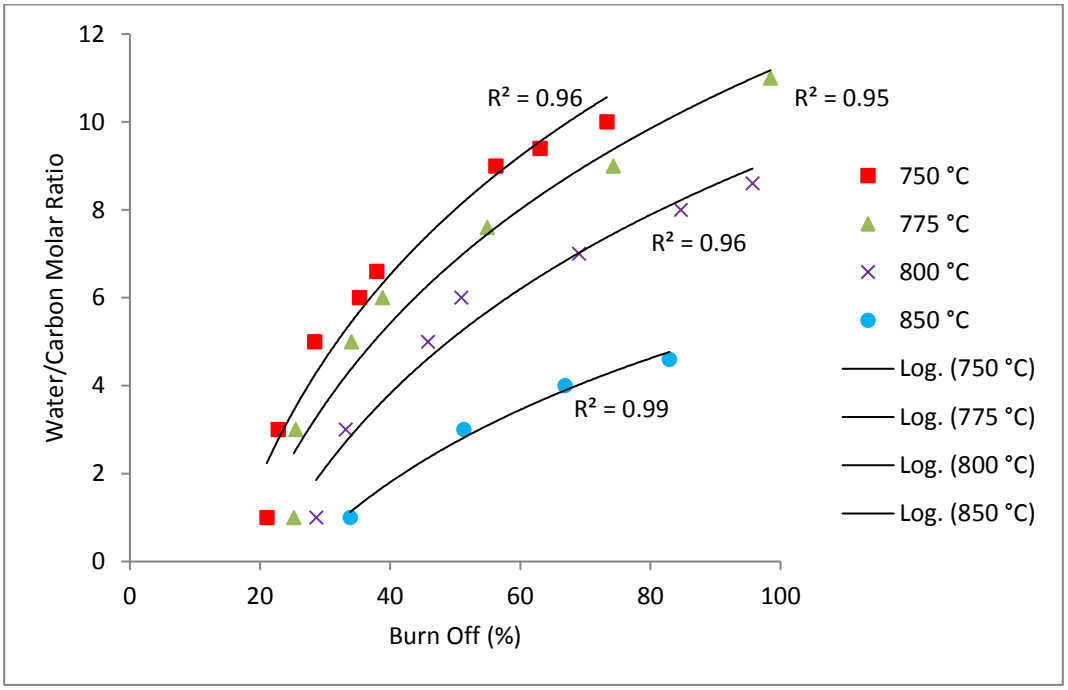


Figure 5:49 Olive stone char subject to changing amount of steam over a two hour period expressed as molar ratio.

As expected increasing activation temperature immediately increases burn off. Additionally, increasing the steam/carbon molar ratio over the two hour period has the same affect. The results provide a strong correlation to a logarithmic trend line. This shows how burn off is directly related to the amount of steam entering the system during the two hours as the mass of carbon is kept constant. This coincides with literature results [Asadullah, 2007; Kang Sun, 2010] and others who all report that increasing water flow increases burn off at any given temperature. The

maximum water flow used in these two hour trials was 1.375 ml/min (11:1 ratio) which is lower than the standard 1.5 ml/min. As the water is increased up to the higher ratios the burn off rate accelerates as shown by the levelling off of the curves. This shows how changing the overall amount of water into the system does not follow the same linear trend seen when increasing residence time and temperature in 5.5.1and **Error! Reference source not found.**. Increasing the xidising agent over a set amount of time will push the reaction forward (more products). The burn off rate increases as more water is added to the system. This coincides with the increase in steam partial pressure along with the overall increase in steam/carbon molar ratio. This continues to rise during carbon burn off through the activation trial.

The implication of getting to the high steam/carbon molar ratios on a larger scale means a significant amount of steam is required. The cost of producing steam is an energy intensive process due to the latent heat value of water (2257 kJ/kg). When considering changing variables, increasing the steam quantity is likely to be the most expensive. However a steam excess is still required as there will always be un-reacted steam in the open system.

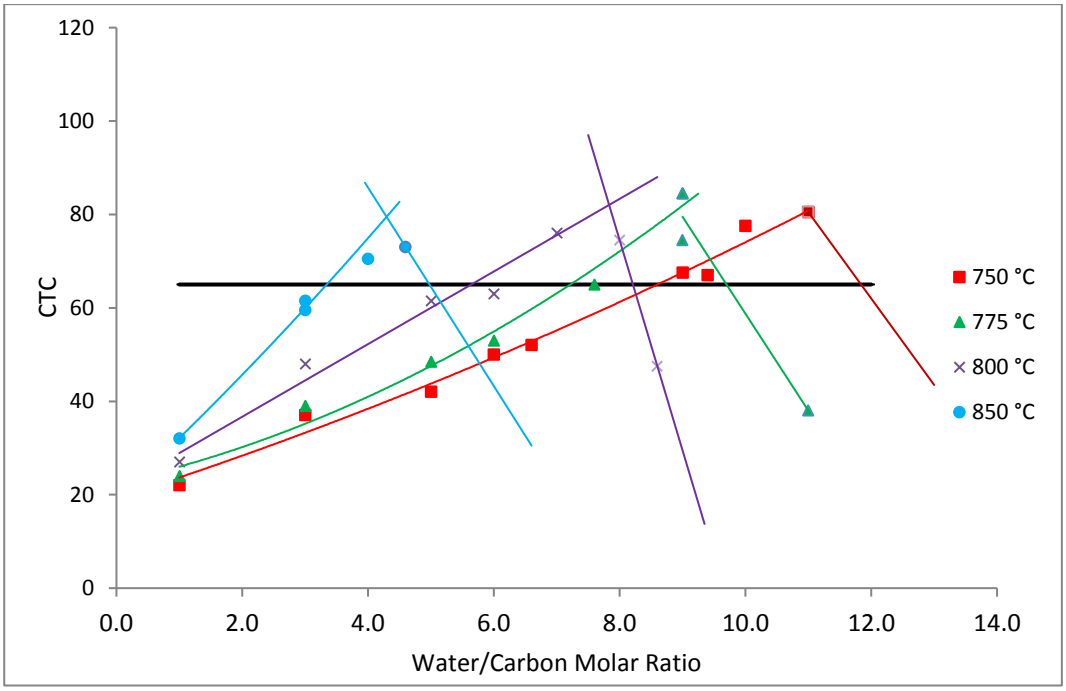


Figure 5:50 Water carbon molar ratio effect on CTC values.

Figure 5:50 above shows the carbon's CTC results in relation to the water carbon molar ratio used in these trials. The linear trend lines have been extended to help represent what is happening across the results using information from Figure 5:3 involving a drop in performance at over 80% burn off. As activation temperature is increased the required steam reduces to achieve the same burn off, yet, the burn off CTC correlation remains. These results reinforce the finding that there is a trade off in process conditions to achieve a similar quality carbon determined by CTC

tests. The chosen process route comes down to the specific porosity required and which out of the three main variables is cheaper to adjust.

The black horizontal line on Figure 5:50 shows the CTC result of a commercial carbon for comparative representation of where the olive stone carbons fit in respect to carbons currently in the market.

5.6.8 Methylene Blue Results

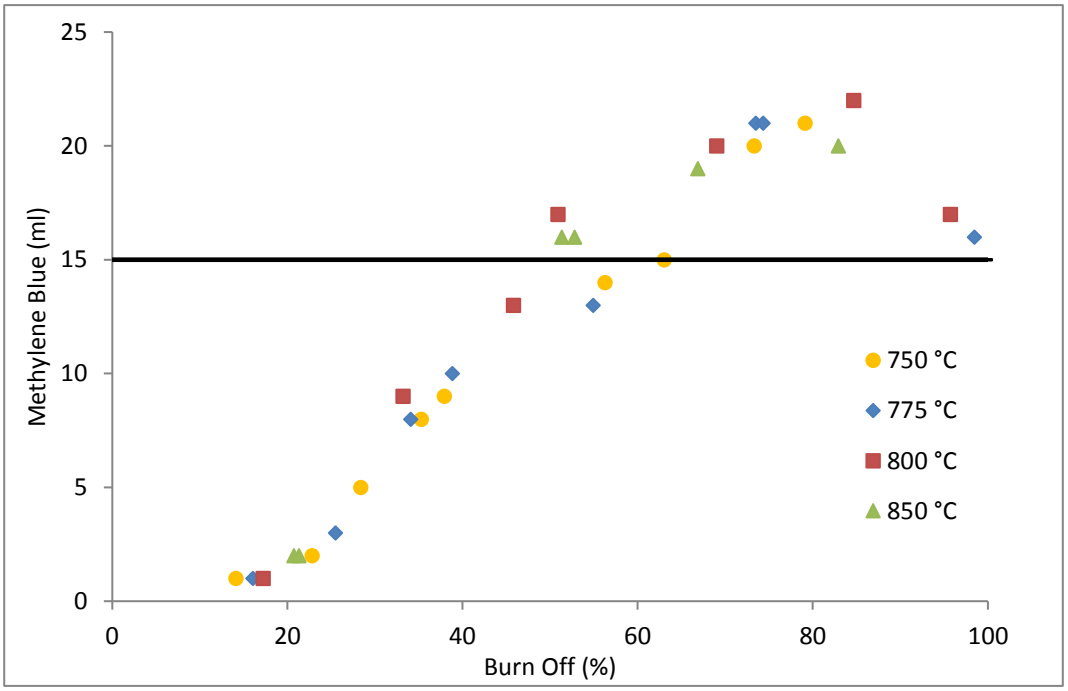


Figure 5:51 Methylene blue adsorption (ml) values for results above and shown in Table A-9 in the Appendix.

Figure 5:51 shows the methylene blue adsorption from the same carbons produced in Figure 5:49 and Figure 5:50. Any points above the horizontal black line show an increase in adsorption potential than the current commercially available carbon that can be used for liquid phase applications. After 20% burn off there is a linear increase in adsorption across the four activation temperatures. At approx. 40% burn off methylene blue no. becomes more disperse with the carbons produced by higher temperatures (850 °C and 800 °C) showing an increase in adsorption. Olive stone appears to peak at around 21/22 ml with these production parameters at around 85% burn off. At just over 90% burn off methylene blue adsorption begins to lower. This is slightly higher than the drop of seen with CTC values.

5.6.9 Pore Analysis of Two Hour Residence Time Trials.

Pore analysis data table from these trials can be seen in Table A-10 in Appendix. Comparing the results to results taken previously (Table 5-2 and Table 5-6) the mesopore percentage and volume are low in comparison. The main difference with this data set is the reduced steam flow rate and

the resultant reduced steam partial pressure - as the residence time was increased to two hours the steam flow was reduced resulting in a slightly more microporous carbon.

This would start to imply that the flow rate and total steam entering the system has a major influence on mesopore development, this is backed up by results from Gonzalez *et al* [2007], who showed that mesopore volume increased when steam flow increased. The two data points that show the highest mesopore volumes are both at 750 °C (the lowest temperature) with the highest amount of total steam and highest flow rate. However, all the results don't follow this correlation; increasing the temperature along with increasing the water flow creates a drop off in mesopore volume. This can be seen in Figure 5:53.

Mesopore volume and mesopore percentage is not solely governed by steam flow as looking at the high temperature data set (Table 5-4) 900 °C to 1000 °C results showed a high mesopore volume with reduced flow rate, again this would imply that a point is reached where temperature becomes the dominant force in mesopore formation.

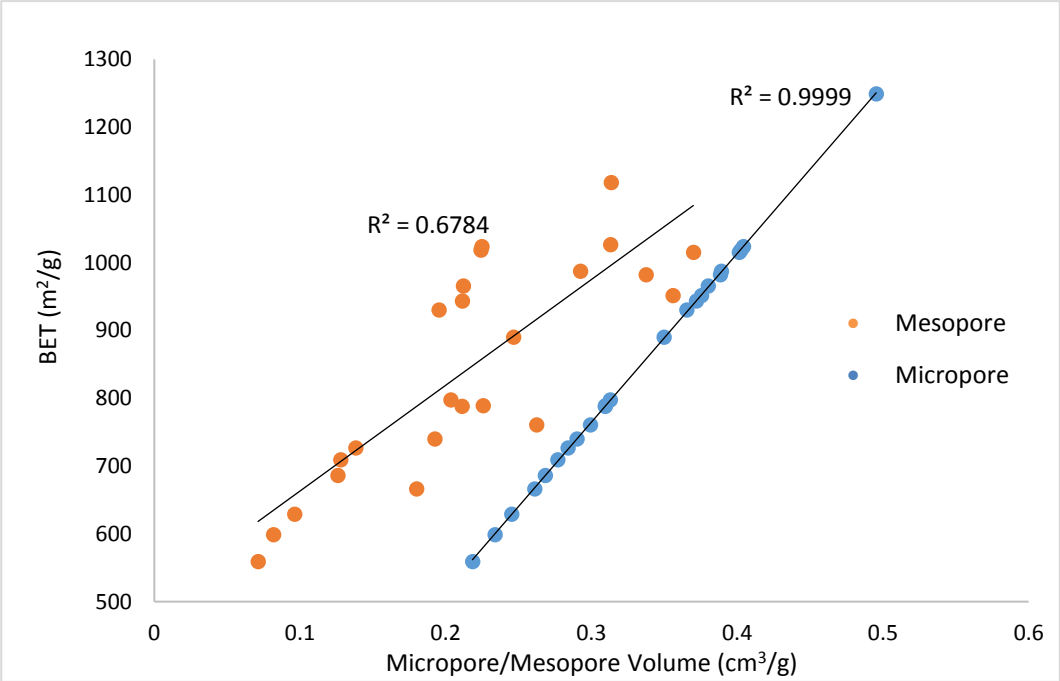


Figure 5:52 Relationship between micropore and mesopore volume (cm^3/g) with surface area (m^2/g).

Figure 5:52 shows the clear correlation between micropore volume and BET surface area just as previous BET analysis has. Conversely, whilst mesopore volume increases with increased surface area the correlation is much weaker. M. T. Gonzalez, [1995] also studied the relationship between micropore volume and BET surface area and found strong correlations for activated carbons.

A highly mesoporous carbon tends to have a lower BET surface area, however, the carbon may still suit a specific application better than a highly microporous carbon. This usually depends on the impurity wanting to be adsorbed, for this reason BET surface area should not govern whether a carbon is of sufficient quality. Pore volumes are important in regards to the particle size of the species being adsorbed. This is a reason why coconut shell activated carbon is mainly used in purifying gases as opposed to liquid phase contaminants that have a larger particle size. Coconut shell is a well-known highly microporous carbon [Ello *et al*, 2013] as shown in Chapter 4 that has been used for many years. Coconut shell, due to its high microporosity, has been used for years in the respiratory sector.

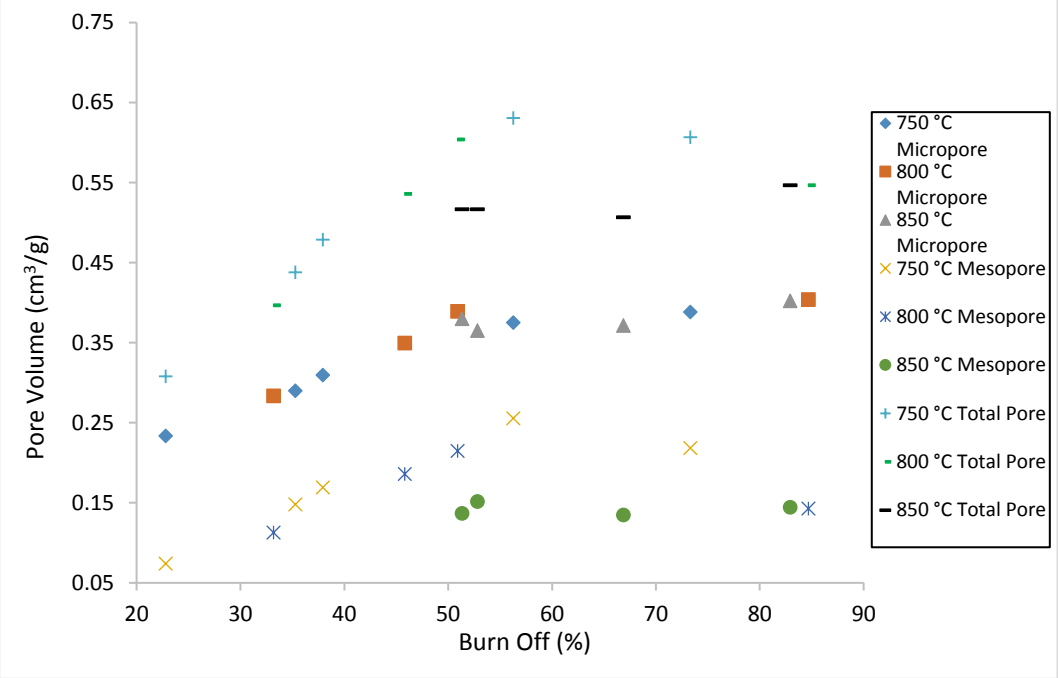


Figure 5:53 Burn off (%) against pore volume (cm^3/g) for micropore and mesopores at 750 °C, 800 °C and 850 °C.

Figure 5:53 shows the micropore volume, mesopore volume and total pore volume for the given temperatures and flow rates. An increased burn off represents an increased flow rate for each temperature in Figure 5:53 that can be found in the results Table A-10 in Appendix.

Examining total pore volume at activation temperatures of 750 °C and 800 °C show a very similar trend in regards to total pore volume. An initial linear rise is followed by a levelling off between 60% and 75%. After this point a reduction in total pore volume is seen. At 850 °C the total pore volume remains constant across all burn off range. This means that additional burn off is not increasing total porosity of the carbons. Although, CTC and methylene blue numbers continue to follow the same burn off adsorption ratio and continue to rise showing that adsorption isn't solely down to total porosity available.

Micropore volumes, for all three activation temperatures used, follow a similar trend and temperature alone seems to have little effect in altering the microporosity. Instead burn off appears to be the dominant factor, after 50% burn off micropore volume remains relatively constant. Under these conditions and across the shown burn off range no clear destruction of the micropore region is evident. It has been reported that micropore widening is a common occurrence where micropores widen into mesopores [Inagaki *et al*., 2013]. However, analysing the mesopore volumes in this set of results show this may not be occurring here.

Mesopore volumes, as with total pore volumes and activation temperatures (750 ºC and 800 ºC) follow the same trend: an initial increase followed by a decrease. Unlike the micropore volume, mesopore volume sees a reduction in volume. This goes against some reports that state widening of micropores is likely to cause a reduction in micropore volume first and a potential increase in mesopore volume [Reinoso and Sabio, 1992]. This is not seen with olive stone activated carbon in these trials. At 850 ºC the mesopore volume remains constant in the burn off ranges produced.

In summary 750 ºC and 800 ºC show the same pattern across micropores and mesopores. When temperature is increased to 850 ºC the micropores and mesopores volumes appear to remain relatively constant across the burn off range. However it must be noted that the difference in water flow was also the smallest as a small increase resulted in a large increase in burn off.

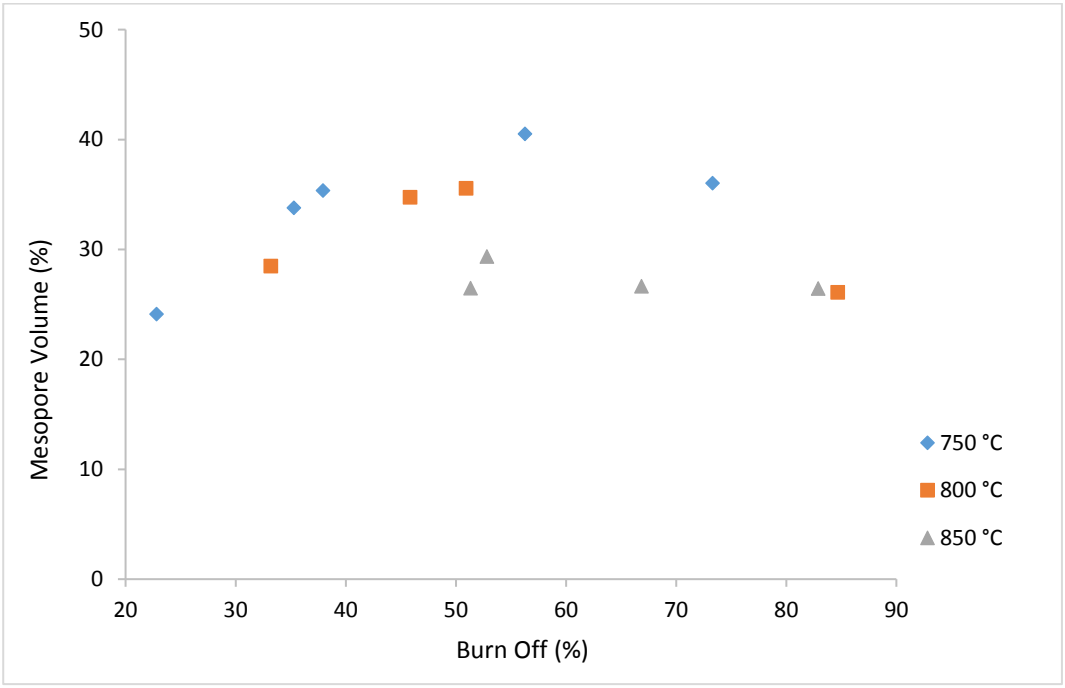


Figure 5:54 Burn off (%) against mesopore (%) at 750 ºC, 800 ºC and 850 ºC.

Figure 5:54 shows that an activation temperature of 850 ºC produces a higher number of micropores compared to mesopores. This ties in with the theory that an increased water flow

enhances mesoporosity as the trials conducted at 850 °C used less water. Although, the answer may not be that simple as Figure 5:55 below shows.

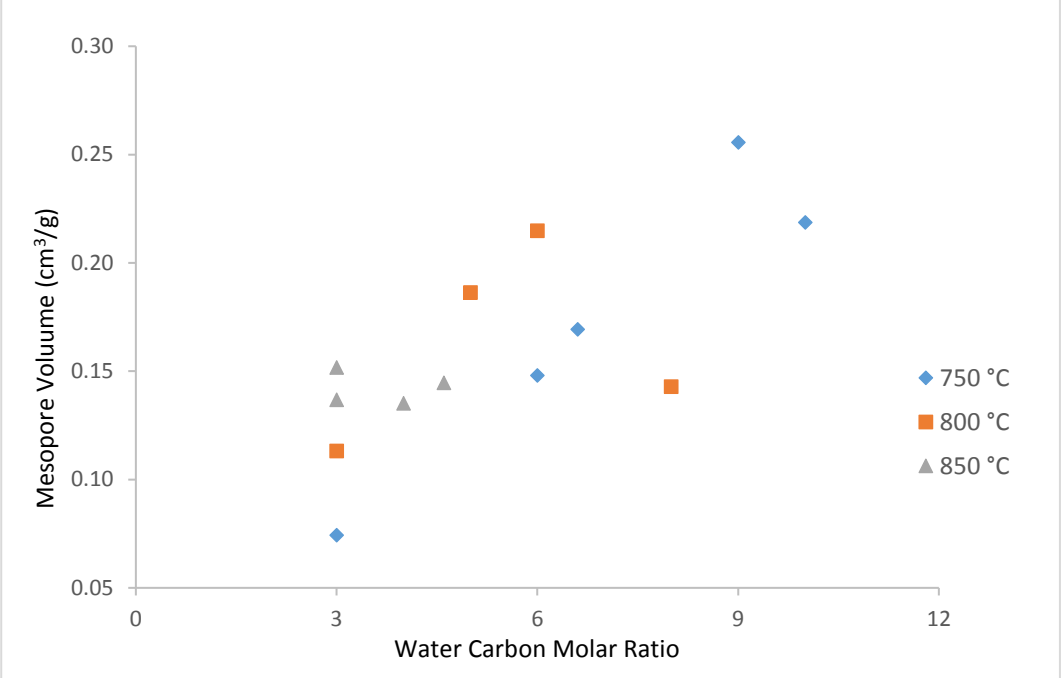


Figure 5:55 Water carbon molar ratio against mesopore volume (cm^3/g) at 750 °C, 800 °C and 850 °C.

Figure 5:55 shows that a lower activation temperature can reach a higher mesopore volume at a higher flow rate before destruction takes place. Yet, initially in early stages of activation a higher temperature is the dominant factor in mesopore creation. This data suggests both the temperature and flow rate have a significant impact on mesopore volumes with mesopore volume being lower with a higher burn off (> 80%).

5.6.10 Methylene Blue and Pore Analysis

Methylene blue tests were conducted on the olive stone samples produced in section 5.6.7. Methylene blue tests are assumed in industry to give a good indication of mesopore volume adsorption due to surface dimensions of the methylene blue molecule, [Nunes and Guerreiro 2011]. The surface area of a methylene blue molecule is 197.2 $Å^2$ [Graham, 1955] and a cross sectional area of 0.9 nm meaning it cannot enter into pores less than 1.3 nm in diameter [Wang, 2005].

The adsorption mechanism of methylene blue adsorption within a porous solid happens in three main steps. Firstly, mass transfer of the solute to the surface of the carbon, secondly, mass transfer to the centre of the particle and then finally adsorption to the highest energy site that it can bind to i.e. the smallest pore into which it can fit. This information is vital when viewing the next set of figures. Temperature also is a factor in adsorption kinetics.

This is based upon Freundlich adsorption isotherm

$$\frac{\chi}{M} = Kp^{1/n}$$ **Equation 5-3**

χ = mass of adsorbate

M = mass of adsorbent

P = equilibrium pressure of adsorbate

K and n represent adsorbate constants which are specific for a given temperature.

In these trials the temperature was kept around 25 ^{o}C for comparative purposes.

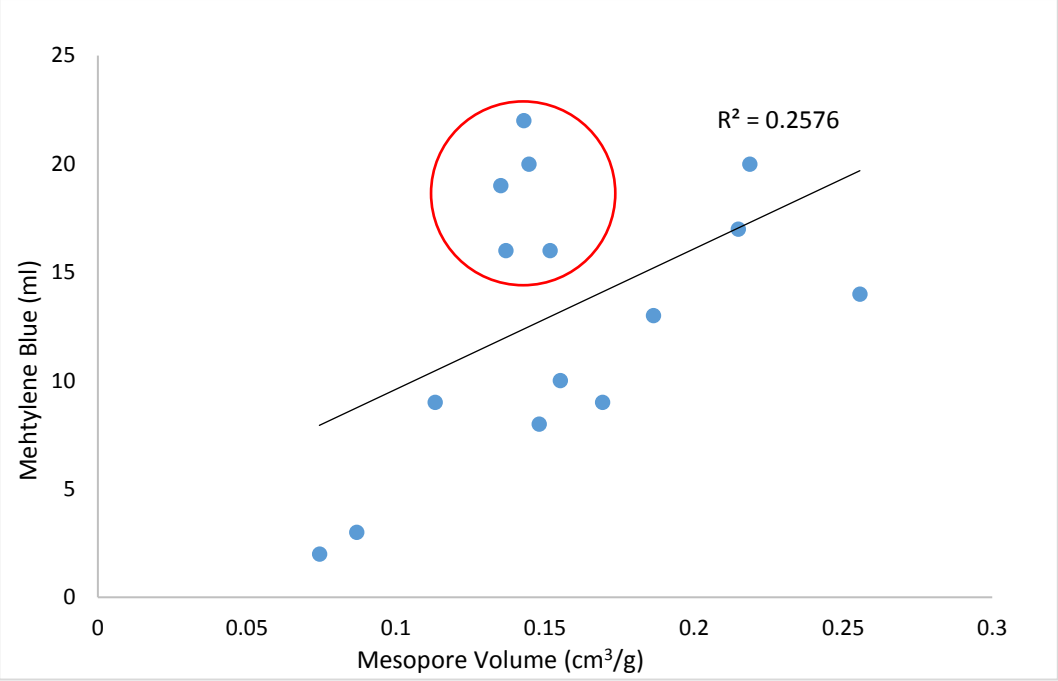


Figure 5:56 Mesopore volume (cm^3/g) against methylene blue number (ml).

Figure 5:56 shows the correlation between methylene blue uptake and mesopore volume of the carbons. The evidence suggests there is practically no direct correlation between mesopore volume and methylene blue adsorption. The data points shown within the red circle are the carbons produced by the higher activation temperatures 850 ^{o}C and one point from 800 ^{o}C with the highest water flow used. This shows at higher activation temperatures the same mesopore volume results in a higher methylene blue adsorption than the carbons produced by lower activation temperatures. The conclusion from Figure 5:56 is that, in the case of olive stone, the mesopore volume is not the dominant factor in terms of methylene blue adsorption.

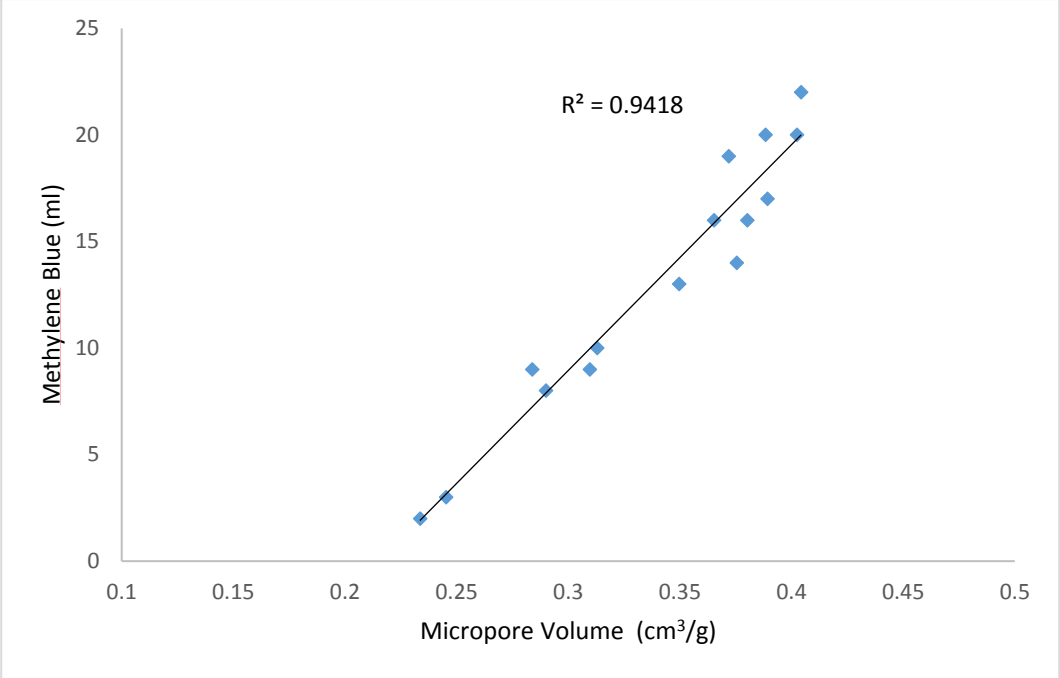


Figure 5:57 Micropore volume (cm^3/g) against methylene blue number (ml).

Figure 5:57 shows the strong correlation between micropore volume and methylene blue adsorption, especially taking into consideration error from both methylene blue tests and pore analysis shown in Chapter 3. The R^2 value of 0.94 compares to the mesopore volume R^2 value of 0.26 shown in Figure 5:56. This suggests the majority of the methylene blue adsorption is occurring in the micropore region < 2 nm. However, as shown from literature [Graham 1955; Nunes and Guerreiro 2011; Wang *et al.*, 2004], the methylene blue molecule will be unable to fit in small micropores due to the molecular dimensions but can fit into larger micropores. Micropores are higher energy sites than mesopores so, if accessible, are likely to fill up first at a faster rate.

Nunes and Guerreiro [2011] and Wang *et al.*, [2004] both report the same phenomena with their carbons: methylene blue adsorption correlation is much stronger with micropore volume than with mesopore volume. Additionally from previous literature González, [2007] concludes that steam produces wide/large micropores from the onset of activation when comparing to CO_2 activation. The data points found within the red circle in Figure 5:56 begin make further sense - concurring with literature and previous results that higher activation temperature leads to additional micropore widening, in this case creating larger micropores but not going quite as far as to produce further mesopores at 850 ^oC. Additionally discussed in Chapter 2, Zhu, Gao *et al.*, [2012] report finds that higher activation temperature using steam causes larger micropores to form and would seem to follow this conclusion.

Methylene blue adsorption can also be dependent on the number of acid surface groups present on the carbon surface; due to methylene blue being a cationic dye and having attraction to carbon with negatively charged sites along with adequate pore size to accommodate the molecule. Not all micropores in the carbons are accessible for methylene blue adsorption. Therefore depending on shape the methylene blue molecule may be able to fit into certain shaped micropores [Bansal, 2005]. The pH of the tested carbons in this project were approx. 9.5-9.8 which aids adsorption backed up by Wang, [2004] who reports that a higher pH of solution results in the higher adsorption capacity for basic dye.

Another answer could well be provided by Shafeeyan, [2015] who states "low temperature oxidations lead to formation of strong acidic groups (e.g. carboxylic) while high temperature oxidations can be used to create a considerable amount of weak acid groups (e.g. phenolic)". Methylene blue dye does not need strong acidic groups for attraction due to being a cationic dye and therefore will be attracted to phenolic surface groups due to the negative charge formed in solution. During higher activation temperature, a higher number of these weak acidic surface groups may be present on the carbon and explains why Figure 5:56 shows more methylene blue adsorption on the carbons produced at a higher activation temperature with similar mesopore volumes than carbons produced at lower temperatures. The mesopores are there simply to facilitate methylene blue adsorption - not the reason or preference for adsorption.

The same findings were seen with pine wood carbons: methylene blue and micropore volume having a strong correlation see Appendix Figure A:15.

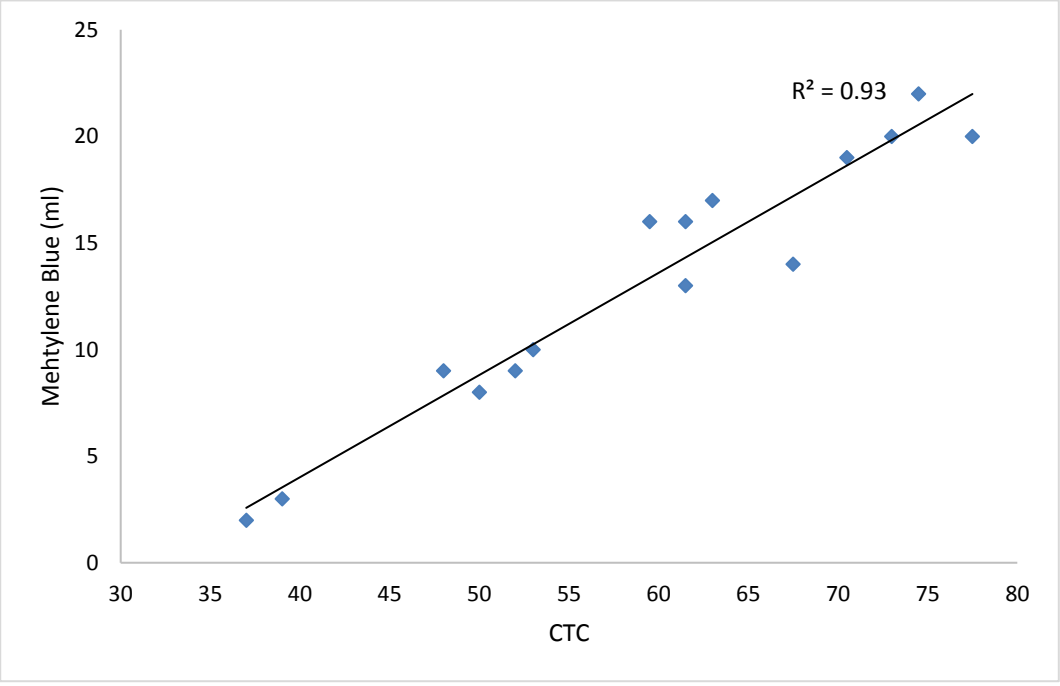


Figure 5:58 Correlation between CTC values and methylene blue adsorption (ml).

Methylene blue correlates well with CTC values of olives stone activated carbon. With olive stone CTC values correlate best with micropore volumes but also appear to give an indication of overall porosity. Methylene blue adsorption potentially can do similar for liquid phase adsorption.

5.6.11 Two Hour Residence Time Trials Conclusion

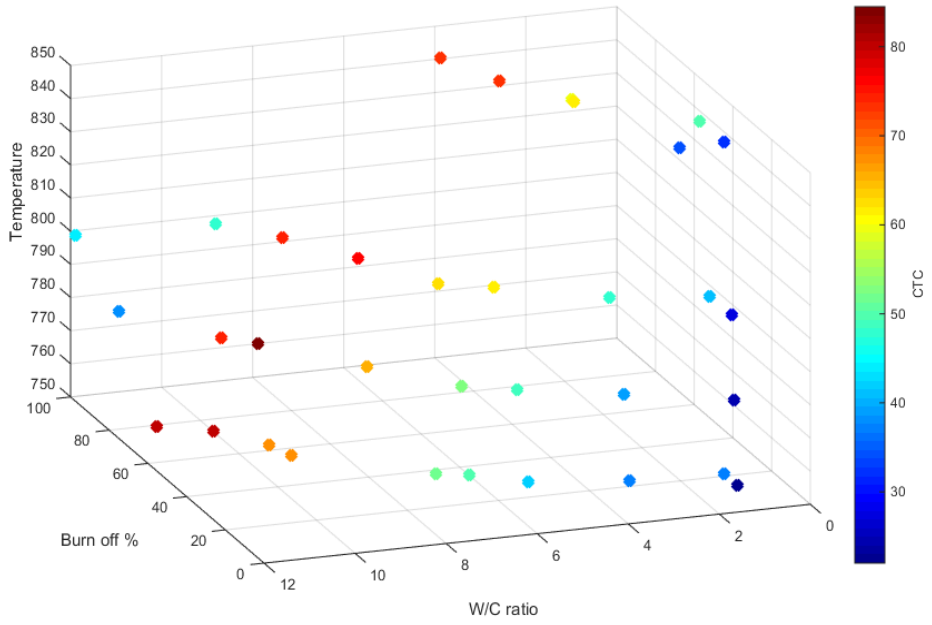


Figure 5:59 Trade-off between temperature and water carbon molar ratio.

Figure 5:59 shows the two variables from this trial, water carbon molar ratio and temperature, and how they affect the burn off percentage and the proceeding CTC value. The figure presents a clear path in how to get high CTCs values with olive stone carbons. The red data points show the high CTCs and these were achieved by either having a high water to carbon molar ratio or using a high temperature as the CTC drops to the lowest where both a low temperature and low water to carbon molar ratio was used.

This information gained within these trials can be used on large scale equipment that contains a fixed residence time.

5.7 Steam Percentage Reacting During Activation

5.7.1 Olive Stone Trials

Reaction 1 shows how one mole of steam reacts with one mole of carbon to produce a single mole of carbon monoxide and hydrogen. For this purpose it is assumed the char is 100% carbon, the moles of water reacted can be calculated. The below figures shows steam reacted over a 60 minute residence time period with differing flow rates. The water reacted is expressed as a molar percentage of the total moles water entering the system during the hour.

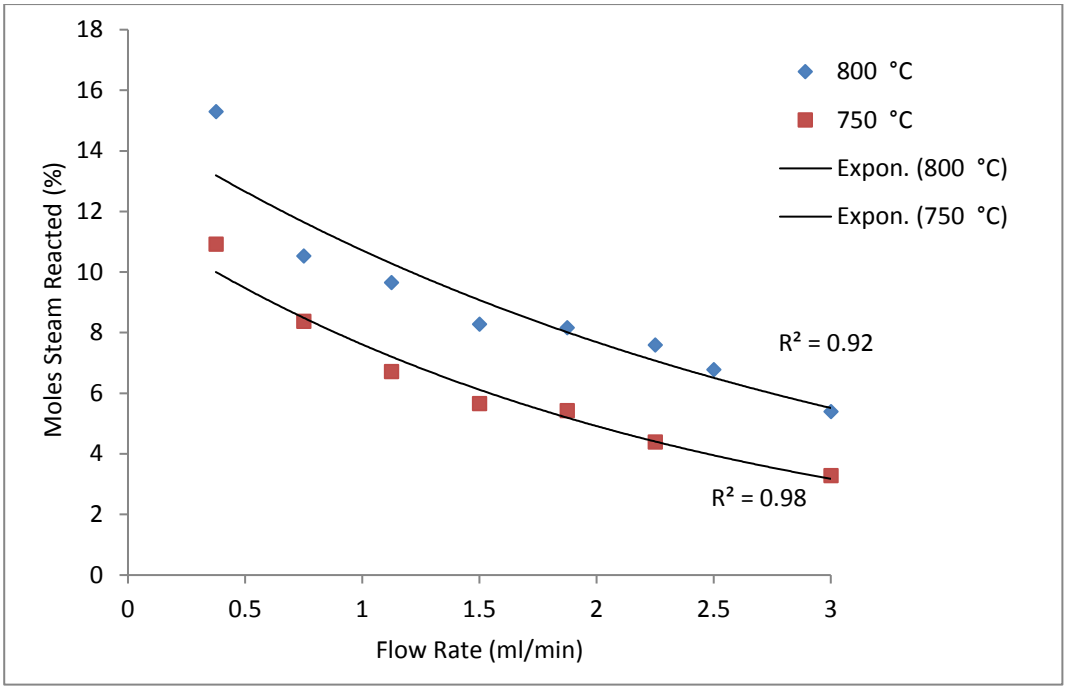


Figure 5:60 Moles steam reacted as a percentage of total steam at different flow rates at 750 °C and 800 °C.

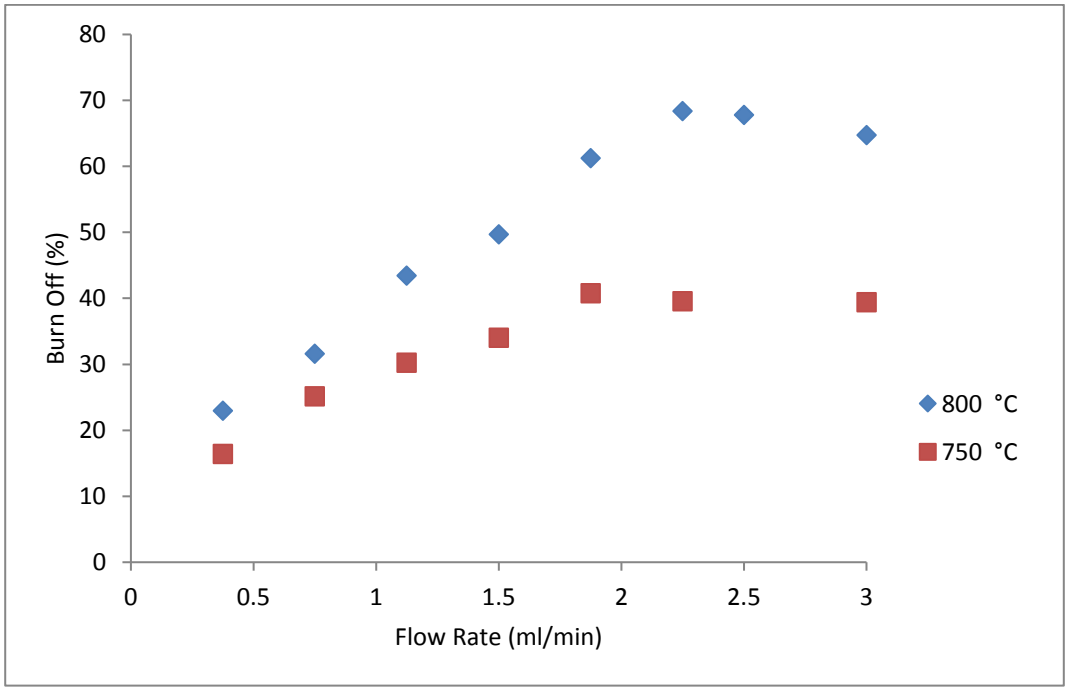


Figure 5:61 Burn off (%) at different flow rates (ml/min).

Figure 5:60 shows as water flow increases the moles of steam reacted as a percentage of total moles in the system lowers (steam excess is increased). Steam and nitrogen are the two gases present in the open system meaning steam partial pressure increases as steam flow increases and nitrogen flow kept constant. As this is an open system and gas in equals gas out, the pressure in the quartz tube will remain close to atmospheric pressure. With the increased flow the Reynolds

no. will increase as shown in Chapter 6 yet the flow always remains laminar with these conditions. With olive stone char, increasing water flow starts to show a possible mass transfer limitation occurring. Figure 5:60 shows how increasing the water flow does not produce a linear burn off relationship and this can be seen clearer in Figure 5:61

Figure 5:61 shows the burn off percentage, that can also represent burn off rate (shown in Figure 5:63) as the residence time is kept constant, reaches a peak at 1.875 ml/min at 750 ^{o}C and 2.25 ml/min at 800 ^{o}C. This implies mass transfer limitation is taking place and that has reached a diffusion maximum at the given temperatures and flow rates. As the temperature increases, the amount of energy available for diffusion is increased and allows a higher rate of diffusion [Brooke Roberts 2015]. Marsh and Reinoso [2006] state "increasing temperature would enhance penetration". However, it would appear that with olive stone char there is a clear limitation that has been reached at a specific flow rate for each temperature.

Marsh and Reinoso, [2006] go onto report a reason why this pattern is observed as shown which was first shown in Chapter 4.

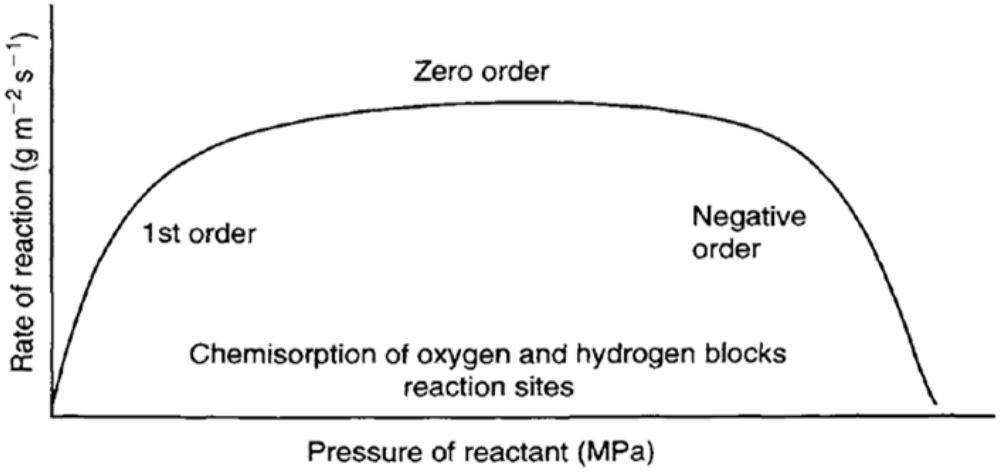


Figure 5:62 (Marsh and Reinoso, 2006).

- With an increase in steam flow the higher the reaction rate until a certain point is reached (1st order).
- At this point the reaction rate levels off because both oxygen from carbon monoxide and hydrogen (the two main products) can bind to the hexagonal planar carbon atoms increasing stability and inhibiting the reaction, hydrogen more so than oxygen. (Zero order).
- Increased further, the reaction is slower as higher concentrations of inhibitors are formed from early stages of the reaction (negative order).

Changing the units in Figure 5:61 using Daltons law of partial pressures (Equation 5-4) and changing burn off percentage to a burn off rate (g s^{-1}) a similar figure can be produced (Figure 5:63)

$$Pi = P_{total}\chi_i \qquad \textbf{Equation 5-4}$$

P_{total} = 0.1 MPa

Using total molar flow over 60 minutes residence time:

$$\chi_i = \text{mole fraction} = \frac{H_20\ (mol)}{H_20\ (mol)+N_2\ (mol)} \qquad \textbf{Equation 5-5}$$

Where,

$$H_2O \text{ moles} = \frac{mass\ (g)}{Molar\ mass} \qquad \textbf{Equation 5-6}$$

$$N_2 \text{ moles} = n = \frac{PV}{RT} \qquad \textbf{Equation 5-7}$$

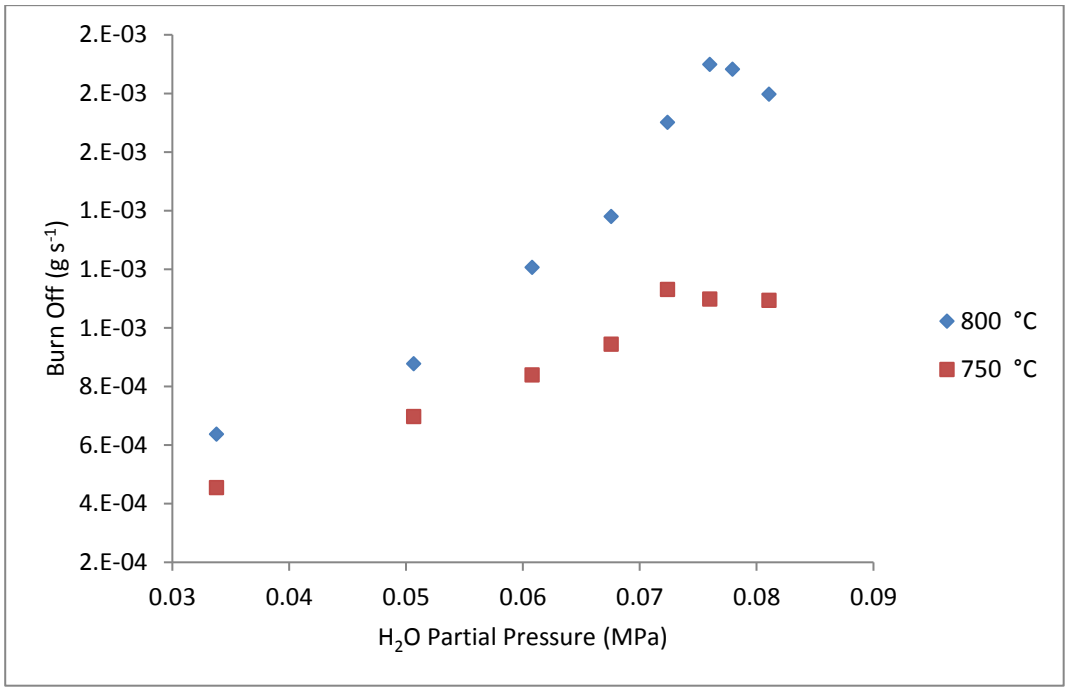


Figure 5:63 Partial pressure of H_2O in system and the associated burn off rates (g s^{-1}).

Figure 5:63 shows the same pattern as Figure 5:62, however, the peristaltic pump maximum rate is 3 ml/min and so more data cannot be taken in this area as the results move towards a reaction rate of negative order. Initially, as steam partial pressure increases, burn off rate increases (1st order). Once the burn off peak is reached increasing the steam further has no further impact on burn off which remains constant and zero order can now be seen. This reason is helped by the

explanation provided by Marsh and Reinoso, [2006] thus being too high an initial reaction rate produces high concentration of inhibitors from early stages of the reaction that bind on to carbon atoms. These inhibitors (H, CO) require large amounts of energy to remove this theory is also discussed by Walker, [1996].

5.7.2 High Water flow Rate Trials

Table 5-11 Increased flow rate with different process conditions, olive stone.

No.	Residence Time (mins)	Temperature (°C)	Char Mass (g)	Flow Rate (ml/min)	Total Flow (ml)	Burn Off (%)	CTC
1	15	800	10	3	45	22.5	32.5
2	30	800	10	3	90	36.3	44.0
3	45	800	10	3	135	50.3	49.0
4	60	800	10	3	180	64.7	57.5
5	15	750	10	3	45	15.9	29.0
6	30	750	10	3	90	23.5	36.5
7	45	750	10	3	135	30.2	41.0
8	60	750	10	3	180	39.4	44.5

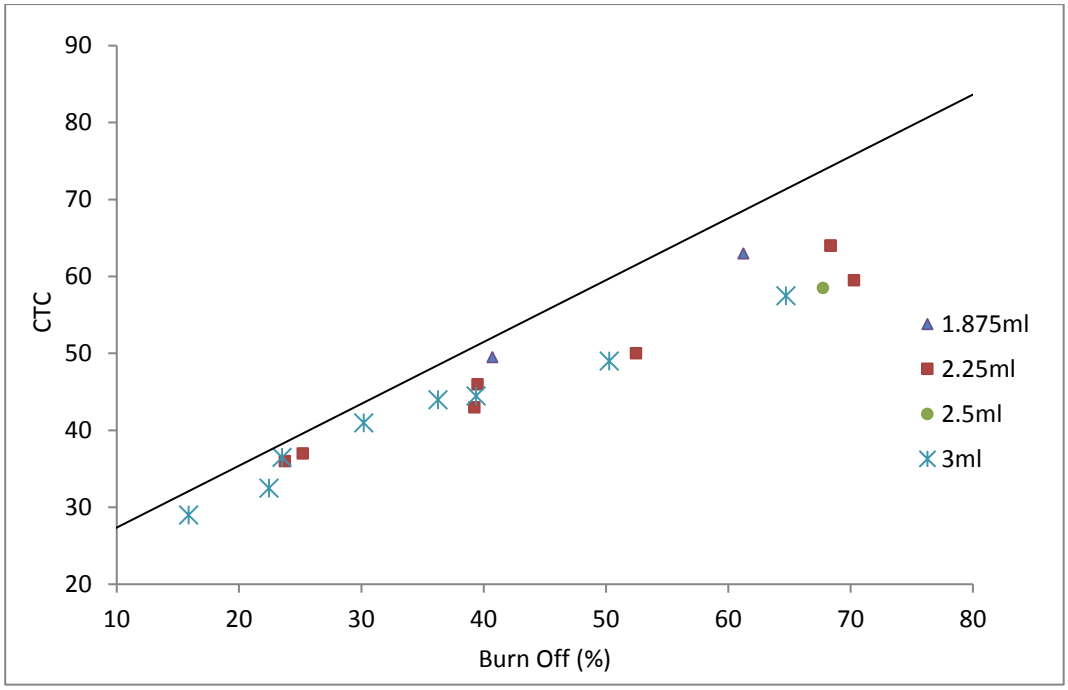


Figure 5:64 Results from Table 5-11 and other results using high (> 1.5 ml/min) water flow rates.

The first theory discussed, mass transfer limitation, where the maximum rate of steam diffusion is reached with the olive stone char is evident. Once this has reached, significant external ablation appears to have initiated causing a drop off in CTC for the given burn off percentage. Evidence is provided in Figure 5:64. This is backed up by Marsh and Reinoso [2006] who state "very high

rates are not producing porosity, as rates become diffusion controlled and burn-off is restricted to external surfaces". Diffusion limitation can be dominant in controlling the reaction. In Figure 5:64 at higher burn offs (> 40%) this can be seen when steam flow rate is increased from 1.5 ml/min (which makes up the trend line shown in Figure 5:2) to 3 ml/min where the points begin to fall further away from this optimum line. At 1.875 ml/min the points can be seen to fit within the error range but at 3 ml/min at the higher burn offs the points fall further away. At burns offs (< 40%) the points do not fall too far from the optimum line. This can be attributed to the fact these trials shown in Table 5-11 have shorter residence times meaning less reaction time available for external burn off to take place.

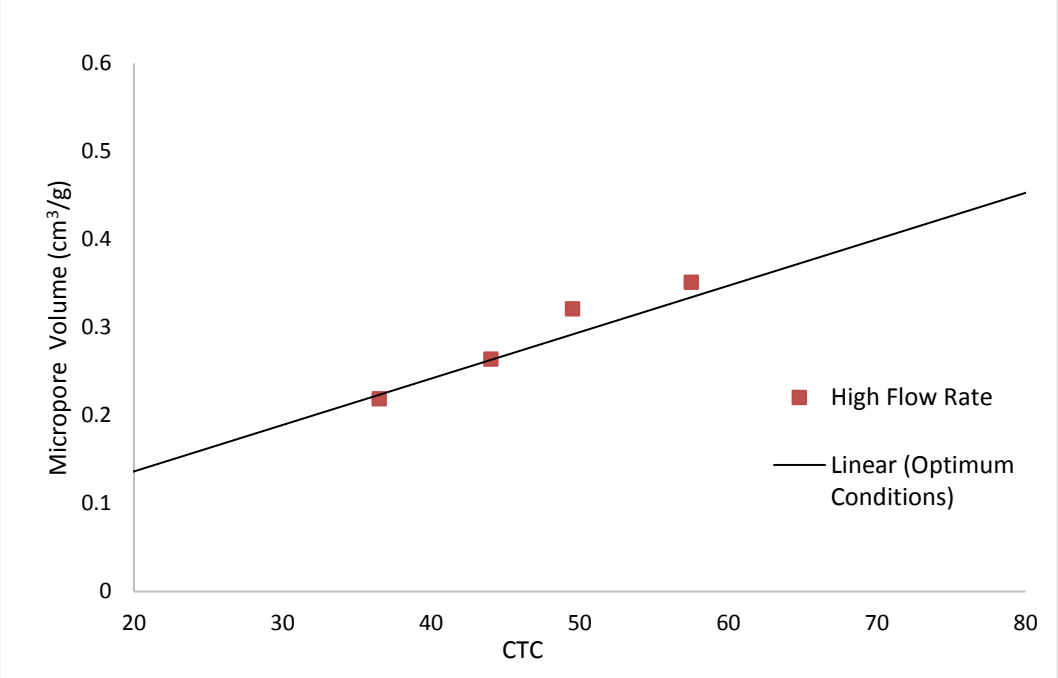


Figure 5:65 Micropore volume (cm^3/g) against CTC for sample 2, 4, 6 and 8 from Table 5-11 against other results shown using optimum conditions shown by the linear trend line.

Using Figure 5:65 it is clear to see that micropore volume has been unaltered in terms of micropore volume to CTC correlation. Therefore porosity change is not the reason for the drop in CTC value at a given burn off shown in Figure 5:64. Through deduction this leads to the conclusion that external burn off is the reason for these findings. This is an important factor to consider when thinking about pilot scale production as too much steam can hinder production efficiency for olive stone carbons.

5.7.2.1 Pine wood Trials

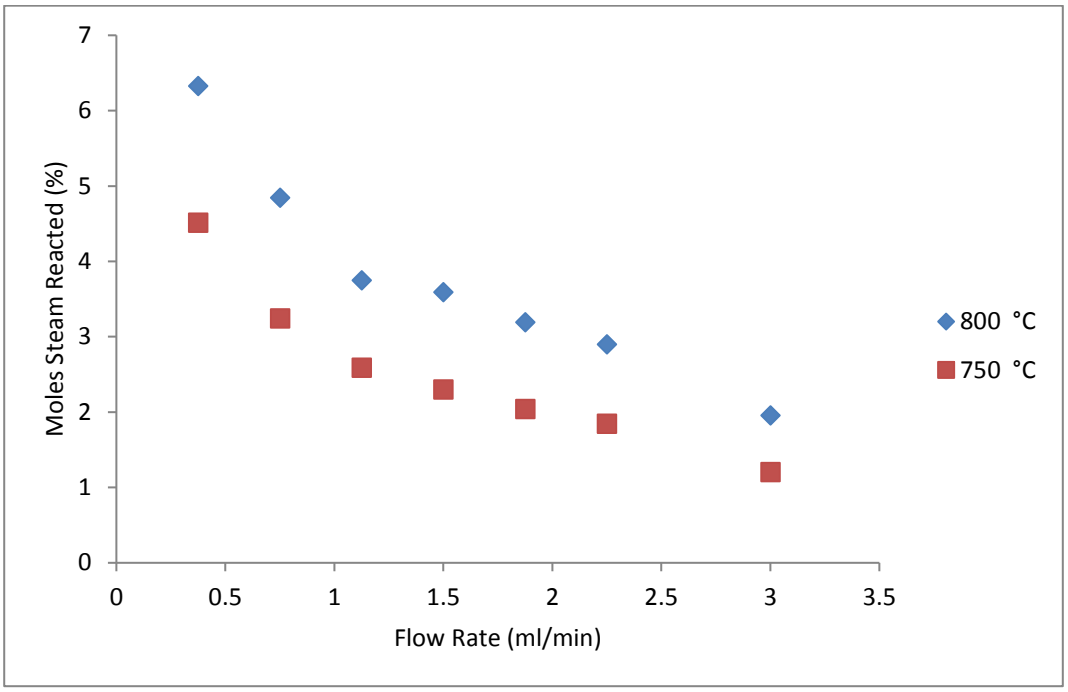


Figure 5:66 Molar percentage of steam reacting with pine wood char at different flow rates (ml/min).

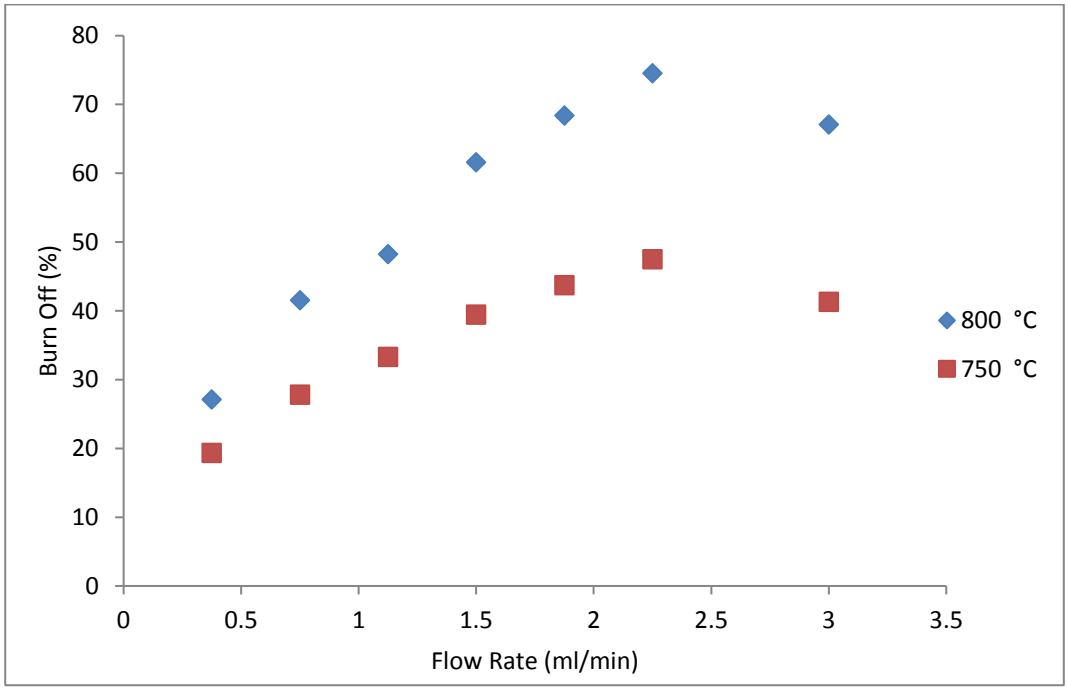


Figure 5:67 Burn off (%) against flow rate (ml/min) for pine wood char.

As with the olive stone char pine wood char follows the same trend: as steam flow increases the moles of steam reacted as a percentage of total moles reduces.

In Figure 5:67 burn off percentage and burn off rate peak occurs up to a flow of 2.25 ml/min before decreasing at both temperatures. Initially, as with olive stone, a linear trend is observed.

When the peak burn off rate point is reached there is no longer additional burn off to the point where a slight reduction in rate is observed, moving to zero and negative order.

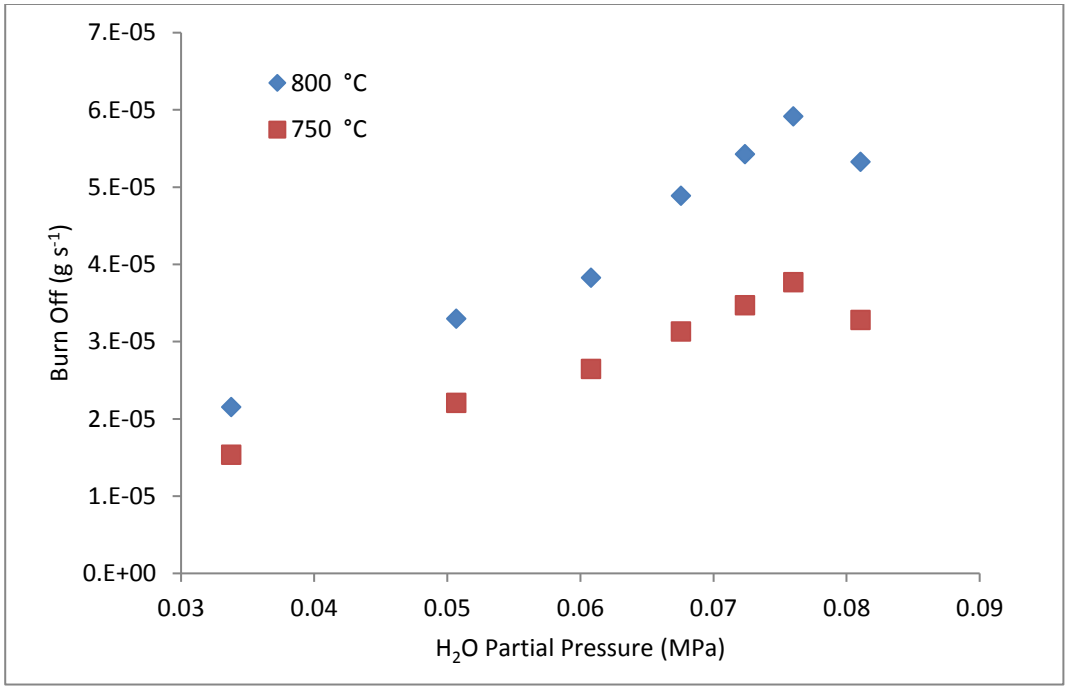


Figure 5:68 H_2O partial pressure against burn off rate (g s^{-1}) for pine wood carbon.

As with olive stone, the pine wood matches well with Figure 5:62. Meaning once steam flow is increased to a certain point no further burn off is observed for the same reasons as given for Figure 5:63.

Table 5-12 Increased flow rate with different process conditions.

No.	Residence Time (mins)	Temperature (°C)	Mass char (g)	Flow Rate (ml/min)	Total Flow (ml)	Burn Off (%)	CTC
1	15	800	10	30	45	30.3	50.5
2	30	800	10	30	90	48.9	68.0
3	45	800	10	30	135	65.0	98.5
4	60	800	10	30	180	67.1	105.0
5	15	750	10	30	45	21.6	41.5
6	30	750	10	30	90	28.3	45.0
7	45	750	10	30	135	35.4	49.0
8	60	750	10	30	180	41.3	59.5
9	75	750	10	30	225	45.3	64.0
10	90	750	10	30	270	50.1	82.5

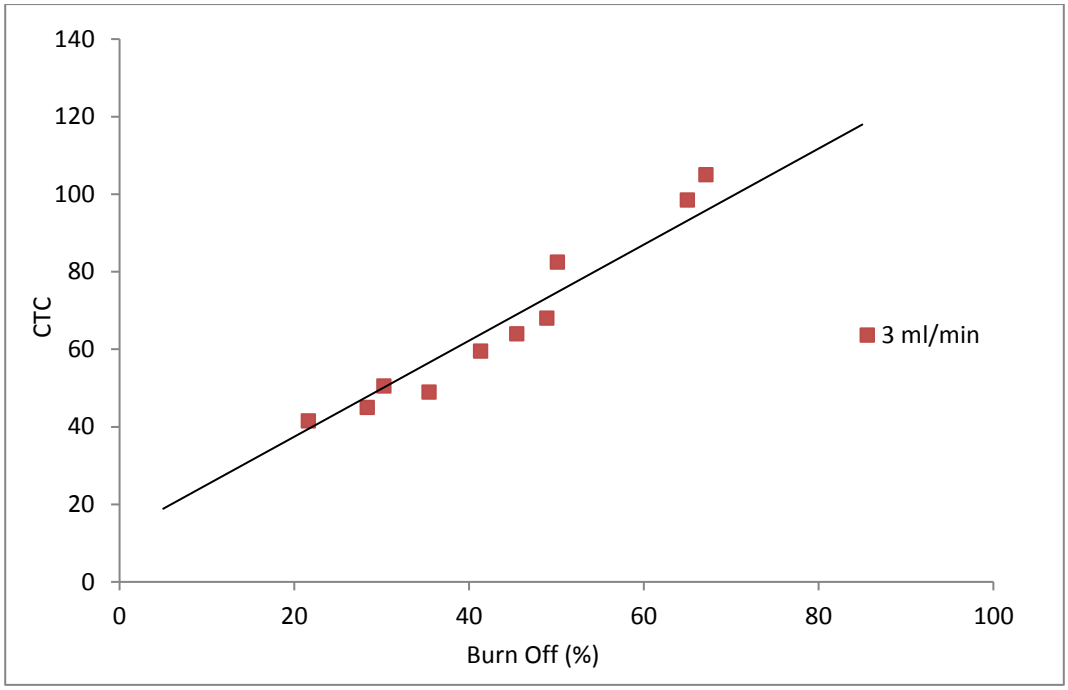


Figure 5:69 Increased flow rate (ml/min) effect on burn off (%), CTC relationship for pine wood activated carbon.

With pine wood it would seem that no extensive external ablation is taking place as the data points, as shown in Figure 5:69 at a flow of 3 ml/min, still fit the optimum trend line.

Thus, on comparing both biomass precursors they follow the same trend i.e. increasing the flow rate to a point where no extra burn off is taking place. With pine wood this comes at no additional cost other than a reduction in burn off rate, conversely, with olive stone not only more steam is being used than necessary it is also having adverse effects in regards to the burn off CTC optimum ratio. This information again points towards the difference in potential diffusion rates of steam through each biomass. Pine wood is a lower density material that is a naturally more porous as shown by SEM images in section 5.4.

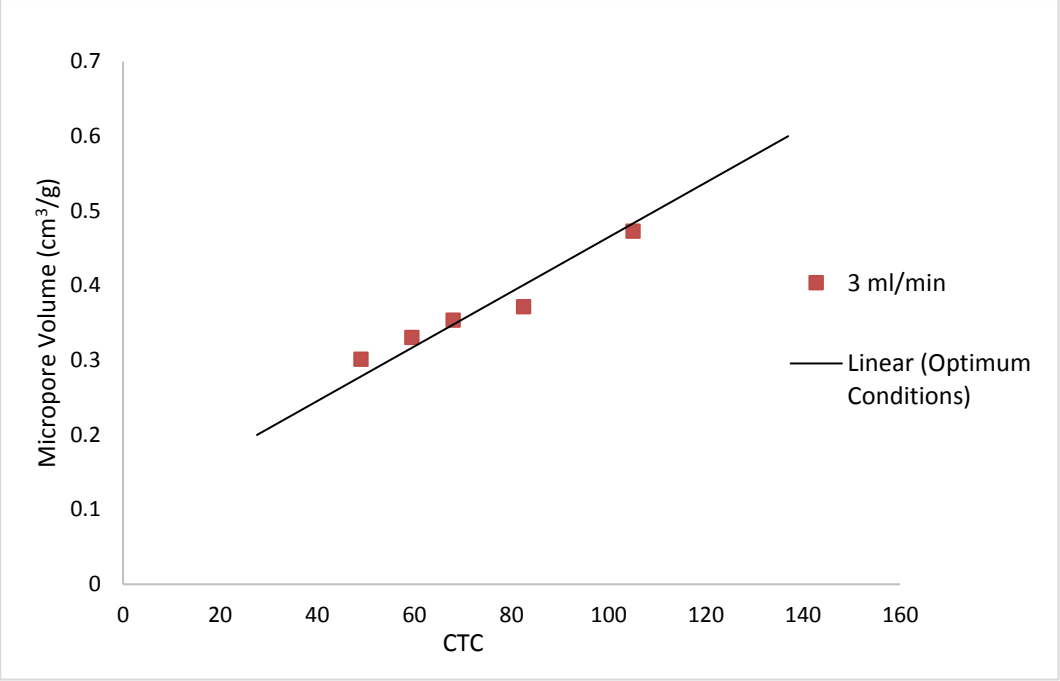


Figure 5:70 CTC against micropore volume (cm^3/g) for pine wood activated carbon samples 2, 4, 7, 8, 10.

Pine wood activated carbon samples produced by high steam flow rates underwent pore analysis to see if any changes had occurred in porosity. This was not the case, the CTC and micropore volume maintained a strong correlation.

5.8 Secondary Production Variables

5.8.1 Steam Carbon Contact

After the high temperature trials were completed the crucible began to warp. This led to lower than expected burn off percentage values. A new crucible was produced with the same dimensions as the original crucible before warping. The dimensions are shown in Table 5-13 along with the associated burn off and CTC values.



Figure 5:71 Warped and new crucible.

Table 5-13 Crucible dimensions and results at 800 °C, 1 hour dwell, 1.5 ml/min water flow rate.

	Surface Area (cm^2)	Crucible Height (mm)	Bed Depth (mm)	Burn Off (%)	CTC
Original crucible	31.5	14	10	49.0	61.0
Original warped crucible	22.9	14	11	38.9	52.0
New deep crucible	31.5	14	10	51.0	63.0

The CTC values maintain the burn off percentage correlation as they have throughout under these conditions. Looking at the surface areas of the crucibles this appears to have an impact on the burn off percentage. A decrease in surface area, with the closed warped original crucible, has a 10% lower burn off percentage than the crucible before warping. Preventing steam contact by covering the carbon with warped crucible meant the carbon was subject to less steam contact over the hour activation period. This shows how contact area available for steam carbon contact is important in the burn off process.

The original and new crucibles produced very similar results and were exactly the same dimensions.

Tests were completed on each layer of the carbon bed with the warped crucible by carefully scrapping off the upper surface carbon. The top layer carbon gave a CTC of 56 whereas the two bottom layers gave a CTC of 52. This was also done with the new crucible which was more uniform with a CTC value of 62 at the top followed by 61 for the bottom two layers. There seems to be a slight increase in burn off from the carbon surface with the warped crucible. This is as expected as the bottom two layers are sheltered from both the warped crucible and the top layer carbon. However the differences are still minor. Using Figure 5:2 it can be seen this CTC difference is resultant of a 4% to 5% burn off difference. More importantly the bottom of the bed had a similar CTC value as the top and middle layer showing that at this bed depth steam easily diffused through the bed of olive stone char.

5.8.2 Reaction Rates- Changing Char Mass

Another variable that was conducted on laboratory scale was changing the amount of char in the crucible to see if this affected the burn off and burn off rate per mass of char present. Olive stone was used to conduct these trials. The trials were conducted at 750 °C, 800 °C and 850 °C for 30 minutes with a flow rate of 1.5 ml/min. The different initial char mass ranged from 2.5 g to 15 g as 15 g was the maximum that could be placed in the crucible (see Appendix Table A-11).

The first stage involved increasing the initial char mass in the crucible whilst keeping water flow constant

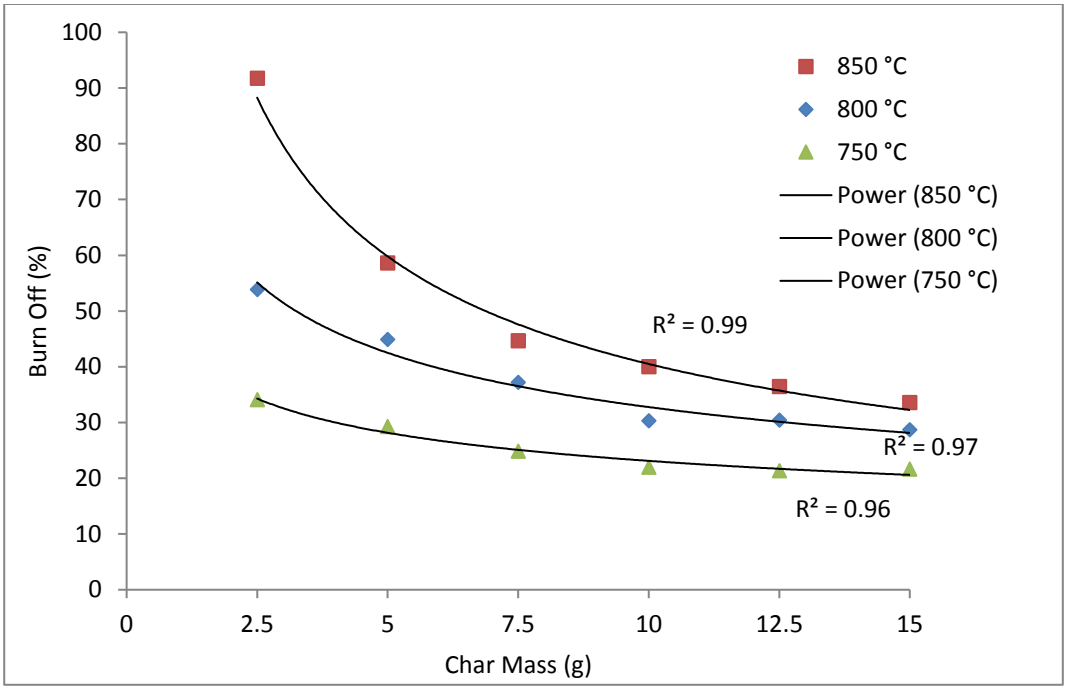


Figure 5:72 How changing char mass affects burn off (%).

Initially by increasing the mass in the crucible the burn off percentage is decreased. This decrease begins to plateau at around 7.5 g to 10 g. At the lowest mass and highest temperature (850 ºC, 2.5 g) the increase in burn off is the largest as expected from 2.5 g to 5 g. All three data sets fit the power trend line well showing the percentage mass change is the dominant factor with a logarithmic scale showing a clear linear trend.

This graph also resembles burn off rate (g s/g) and also moles H_2O reacted per g of carbon present. Calculating the water carbon molar ratio shows an interesting correlation to the shape of the graphs as does the decreasing bed depth. However, from section 5.8.1 bed depth at these levels is proved to be having minimal effect.

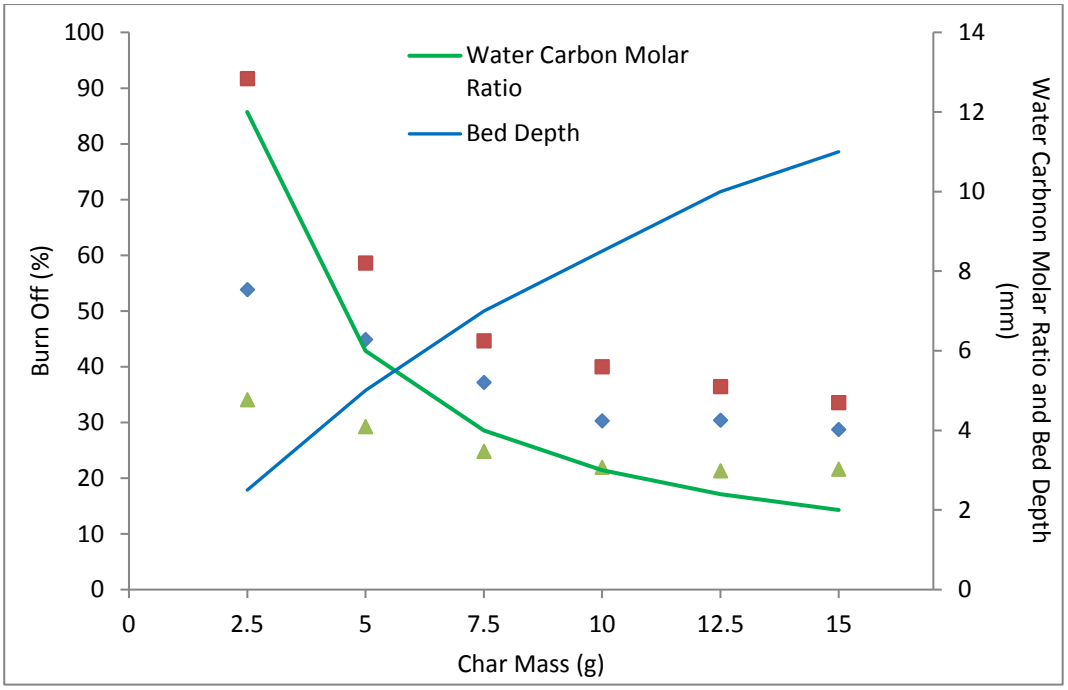


Figure 5:73 How an increase in mass has an effect on the water carbon molar ratio and the subsequent burn off (%) for olive stone.

Calculating the water carbon molar ratio and bed depth produces the curves shown in Figure 5:73. With a reduced char mass with same water flow there is a higher water to carbon ratio. Likewise, the variation in bed depth also increases or decreases depending on the mass of char.

To see the effect of the water flow, the water flow was reduced to keep the same water carbon molar ratio when increasing or decreasing the initial char mass.

With the figure below, the trials were conducted at 800 ^{o}C - the same figure with same findings were produced with activation temperatures of 850 ^{o}C and 750 ^{o}C (see Appendix Figure A:16)

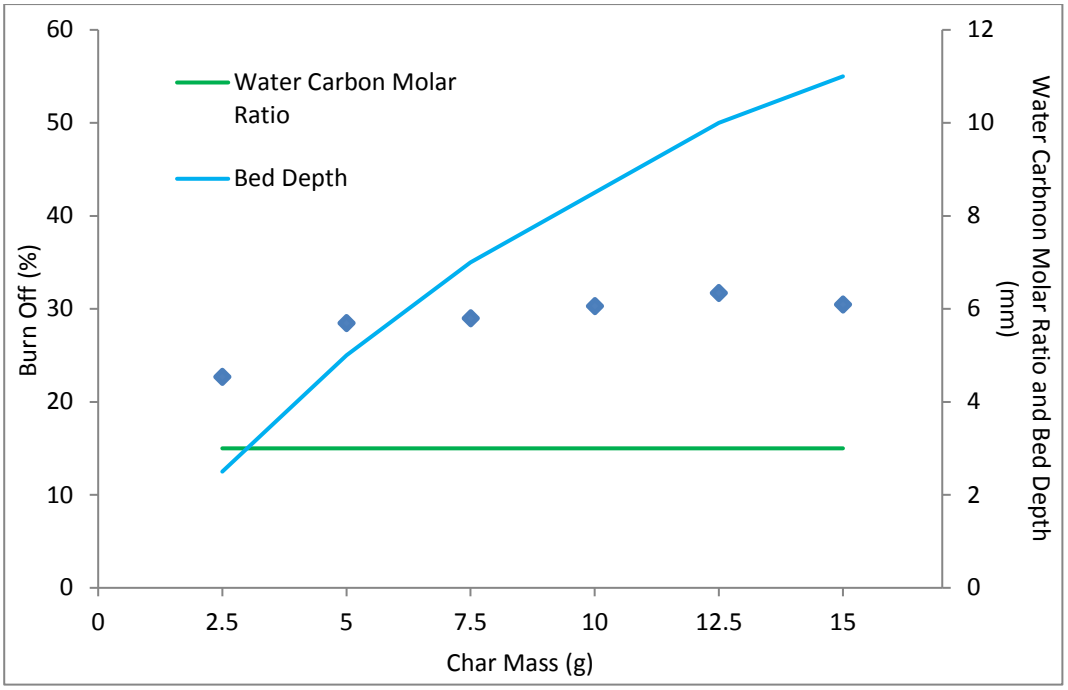


Figure 5:74 Effect of changing char mass but with water carbon molar ratio kept the same has on burn off (%) for olive stone.

When the water carbon molar ratio is kept constant the burn off percentage becomes relatively linear and constant, compared to Figure 5:72. This shows that when the char mass is low, the increased water carbon molar ratio is having an effect. However, this impact weakens as the char increases. Repeats were conducted at 750 ^{o}C with 60 minutes residence time where the same patterns were observed with CTC results again following the burn off relationship (see Appendix Table A-12). Figure 5:74 shows how the char bed depth at these levels is having little to no effect on burn off and so can be ignored in these trials.

The mass of char was also altered for pine wood trials which were conducted at 750 ^{o}C for 1 hour with 1.5 ml/min water flow rate.

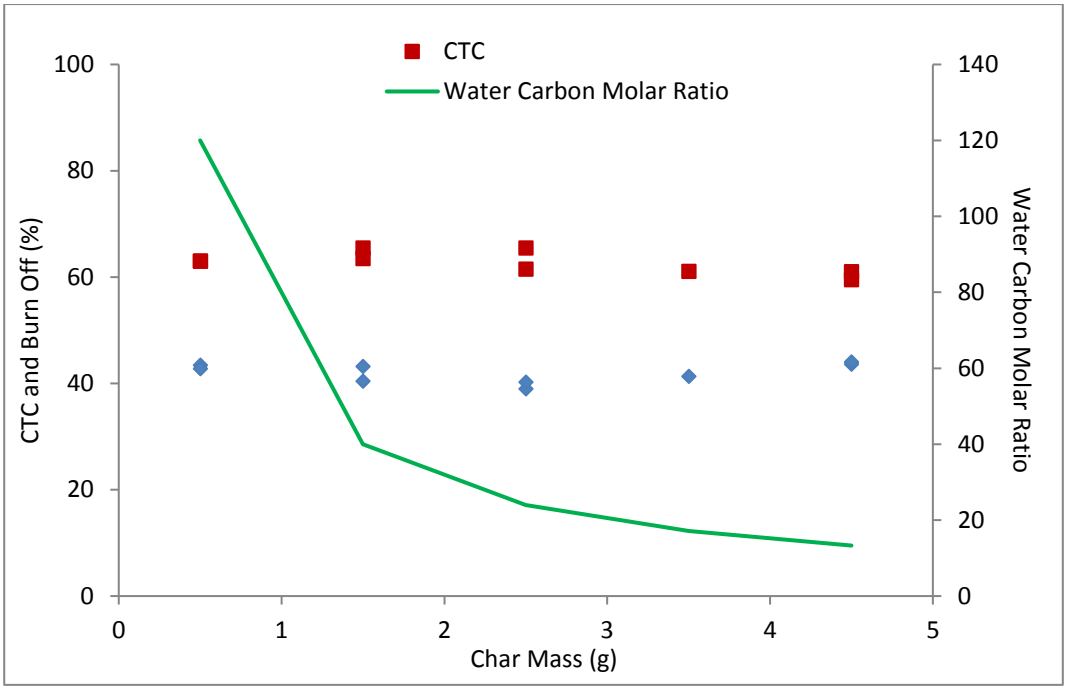


Figure 5:75 How an increase in mass has an effect on the water carbon molar ratio and the subsequent burn off (%) for pine wood.

Figure 5:75 is showing how burn off is independent of initial char mass. This is unlike olive stone, shown in Figure 5:73, where a lower mass increases burn off percentage. The burn off (g s^{-1}/g) is constant with pine wood which implies that mass loss rate is dependent on only the three main variables: temperature, residence time and oxidising agent.

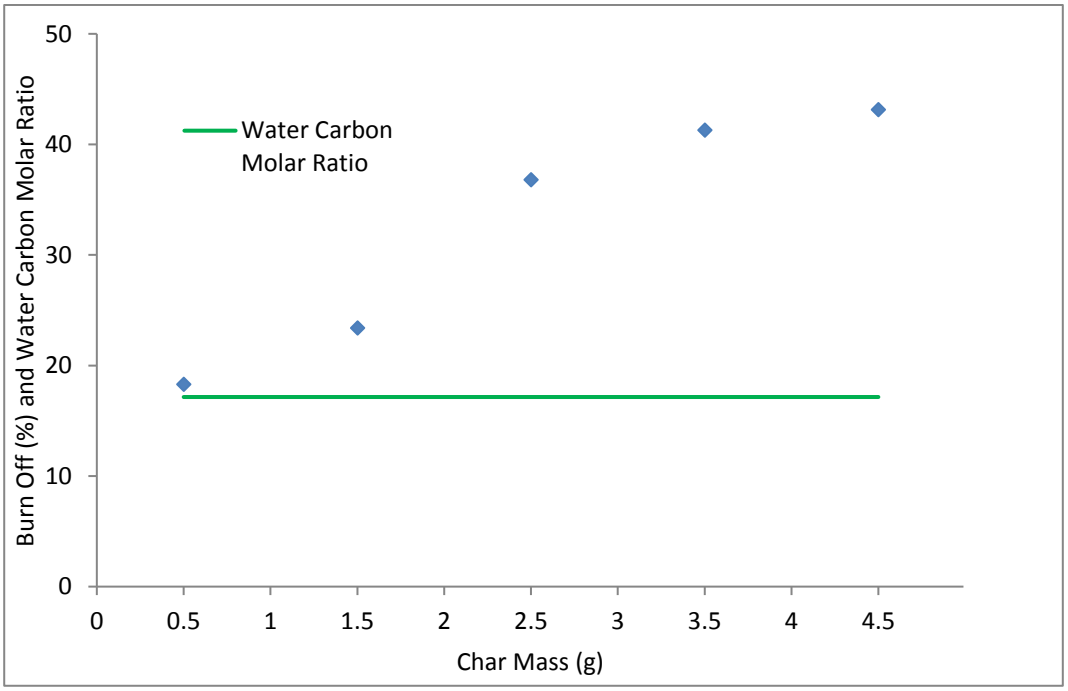


Figure 5:76 Effect of changing char mass but keeping water carbon molar ratio the same has on burn off (%) for pine wood.

Figure 5:76 shows the average points from Table A-13 in Appendix. Keeping the same water carbon molar ratio produced a significant difference when compared to how olive stone char behaved under the same conditions. Olive stone burn off percentage remained constant whilst keeping the same water carbon molar ratio, whereas pine wood burn off percentage increased with increased mass and flow.

This again points to how mass transfer limitation is occurring during activation with olive stone. Pine wood burn off percentage appears to be centred upon steam flow rate, as at constant flow rate the burn off percentage also remains constant, whereas when the flow is increased or decreased (Figure 5:76) the burn off percentage moves accordingly with the change.

Below the burn off rates are considered:

5.8.3 Burn Off Rates

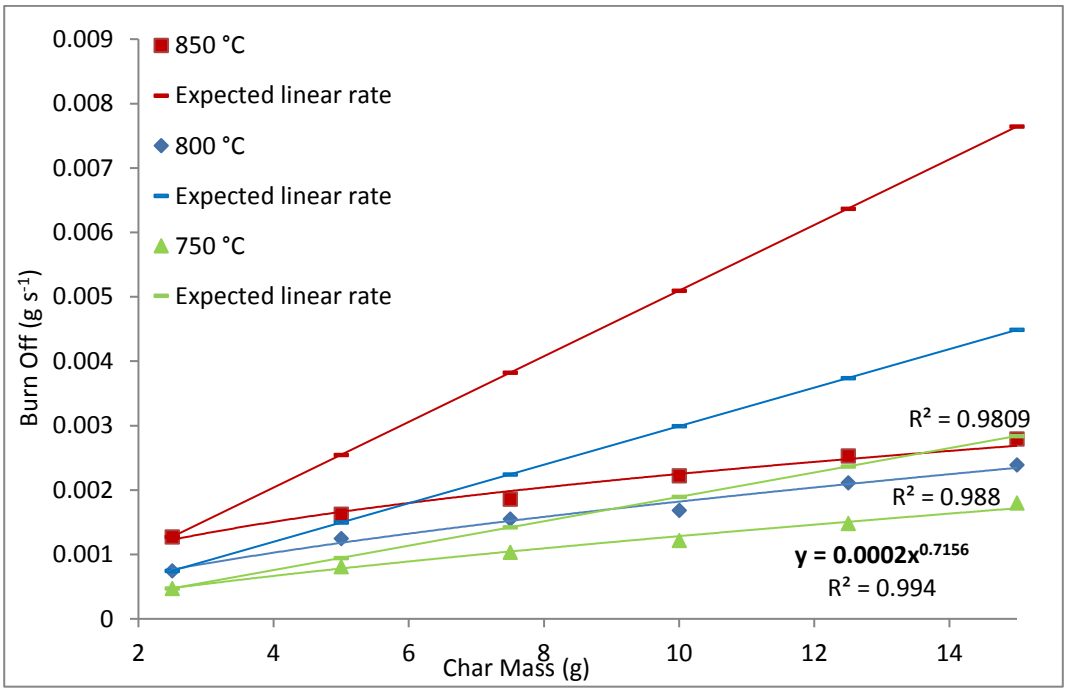


Figure 5:77 How doubling char mass does not double burn off rate with olive stone char, trials conducted at a water flow of 1.5 ml/min for 30 minutes.

Doubling the initial mass does not double the burn off rate (g/s) which is seen with pine wood char in Figure 5:78. This points towards the initial mass of olive stone char being the dominant variable controlling burn off in these trials; with increased char mass slowing burn off rate per gram of initial char present. The expected linear trend lines have been placed on Figure 5:77 yet, the actual data points fit the power trend line emphasising how burn off and burn off rate is controlled by the amount of initial char. Using Figure 5:77, assuming the power trend was to continue, the burn off rate can be predicted for further increases in mass:

For example, calculating the predicted burn off of from 100 g char at 750 °C using the graph equation the predicted burn off percentage would be 9.7% over a 30 minute period calculated by:

$$y = 0.0002x^{0.7156}$$

$$\frac{y \times T}{Mi} \times 100 \qquad \textbf{Equation 5-8}$$

y = Burn off rate (g/s)

T = Activation time (s)

Mi = Initial Char mass

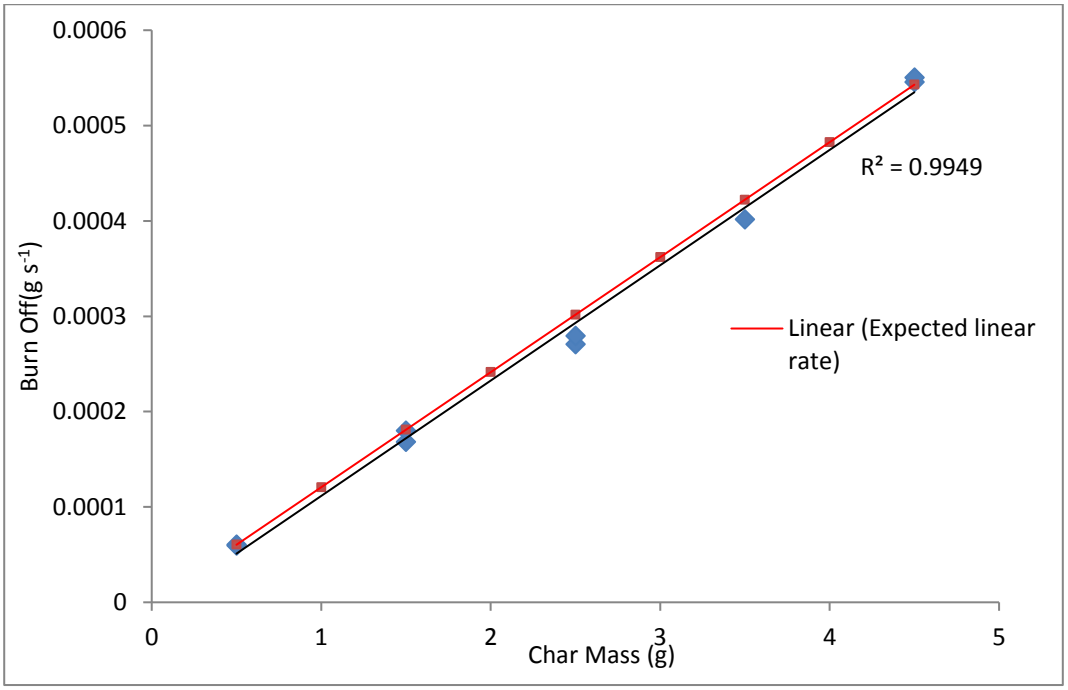


Figure 5:78 Doubling the char mass now doubles the mass burn off rate with pine wood char. 750 °C 60 minutes, 1.5 ml/min flow rate.

Unlike with Figure 5:77, Figure 5:78 shows that now a linear trend is seen with burn off rate whilst increasing char mass. Doubling the mass now doubles the burn off rate as shown by the red trend line – demonstrating that extra mass is having no effect on burn off rate per gram char.

With doubling the char mass leading to a doubling in burn off rate leads to the conclusion that mass transfer limitation has not been reached with these pine wood trials. The naturally more porous nature of the pine wood allows burn off rate to remain the same when the initial mass is being altered.

The rate is determined by the three main variables in this instance 750 ºC, 60 minutes residence time and flow rate of 1.5 ml/min. Being able to estimate the burn off, and thus the quality of carbon, can be seen as a significant advantage without the necessity of going through a trial and error method approach on commercial scale. This allows the burn off to be calculated by changing these variables based on a few sets of results.

5.8.4 Single Step Lab Trials

Single step activation involves pyrolysis and activation occurring simultaneously. The set of experiments were designed on lab scale to compare this single step process to the original two-step process. The potential benefits behind a single step process are that it can significantly reduce CAPEX costs, production time, reduce energy consumption and, in doing so, reduce carbon footprint. Conversely the disadvantages come in the form of a more complex production process with steam and volatiles mixing potentially causing equipment issues and reducing energy recovery efficiency. Additionally during equipment downtime neither char nor activated carbon can be produced unlike the two-step process that would usually utilise two kilns: one for pyrolysis and one for activation.

The experiments were set up to see if the production had any effect on quality of the carbon or yields. To compare the yields fast pyrolysis was conducted on olive stone and pine wood and repeated 5 to 7 times to produce an average result that will be used in the single step burn off percentage as shown in Table 5-16. The char produced was then activated at 5 different conditions, the final yield was taken. The raw biomass was placed inside the kiln and activation begun at 700 ºC rising to the final temperature as stated in Chapter 3, the final yields and CTC values were compared.

Table 5-14 Single step and comparative two-step activation trials for olive stone.

	OS	Activation Temperature (ºC)	Residence Time (minutes)	Water Flow (ml/min)	Initial Raw Olive Stone (g)	Burn Off (%)	Total Yield (%)	CTC
1	2 Step	800	30	1.5	20	53.5	10.6	64.5
	Single Step	800	30	1.5	20	59.0	9.5	64.0
2	2 Step	750	60	1.5	20	56.8	11.4	62.5
	Single Step	750	60	1.5	20	54.2	10.6	61.5
3	2 Step	750	60	1.0	20	45.9	12.3	52.0
	Single Step	750	60	1.0	20	46.2	12.4	53.0
4	2 Step	750	60	0.5	20	23.7	17.5	42.0
	Single Step	750	60	0.5	20	23.3	17.7	41.0
5	2 Step	700	60	1.5	20	23.1	17.7	37.5
	Single Step	700	60	1.5	20	27.2	16.7	38.5

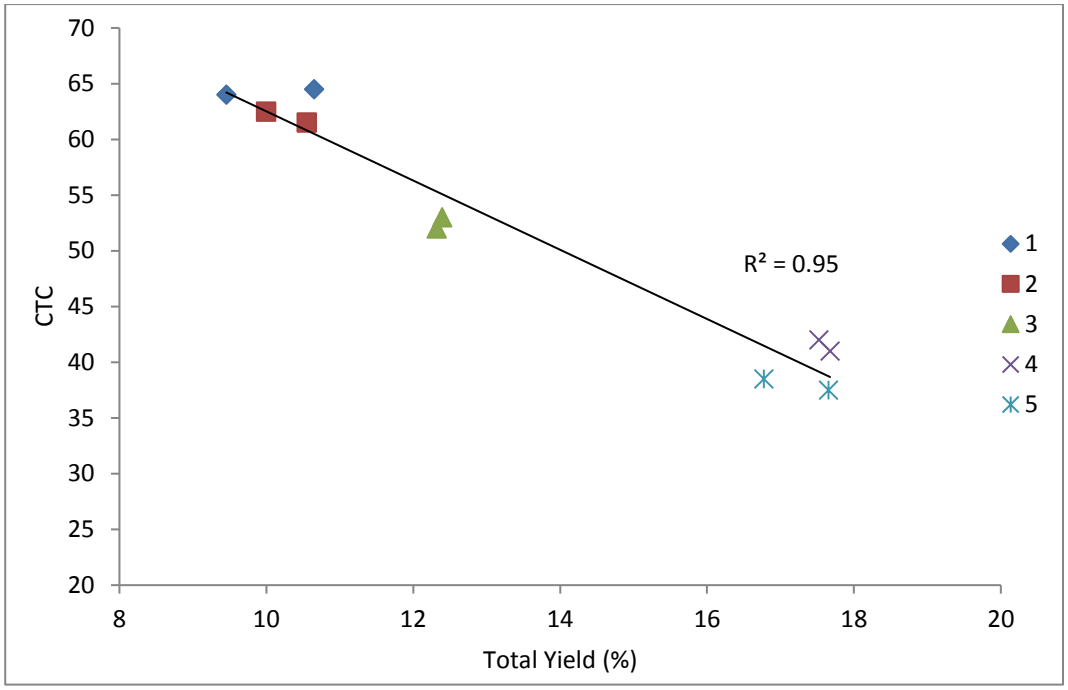


Figure 5:79 CTC against total yield (%) for single step and two-step process shown in Table 5-14.

Table 5-15 Single step and comparative two-step activation trials for pine wood.

	PW	Activation Temperature (°C)	Residence Time (minutes)	Water Flow (ml)	Initial Raw Pine Wood (g)	Burn Off (%)	Total Yield (%)	CTC
1	2 Step	800	30	1.5	6.5	61.6	7.1	90.0
	Single Step	800	30	1.5	6.5	66.3	6.4	89.5
2	2 Step	750	60	1.5	6.5	59.9	7.7	80.0
	Single Step	750	60	1.5	6.5	58.9	7.9	79.0
3	2 Step	750	60	1.0	6.5	53.7	8.8	76.0
	Single Step	750	60	1.0	6.5	56.2	8.3	76.5
4	2 Step	750	60	0.5	6.5	34.2	12.6	57.0
	Single Step	750	60	0.5	6.5	37.2	11.9	60.0
5	2 Step	700	60	1.5	6.5	22.3	14.6	48.5
	Single Step	700	60	1.5	6.5	27.7	13.7	54.5

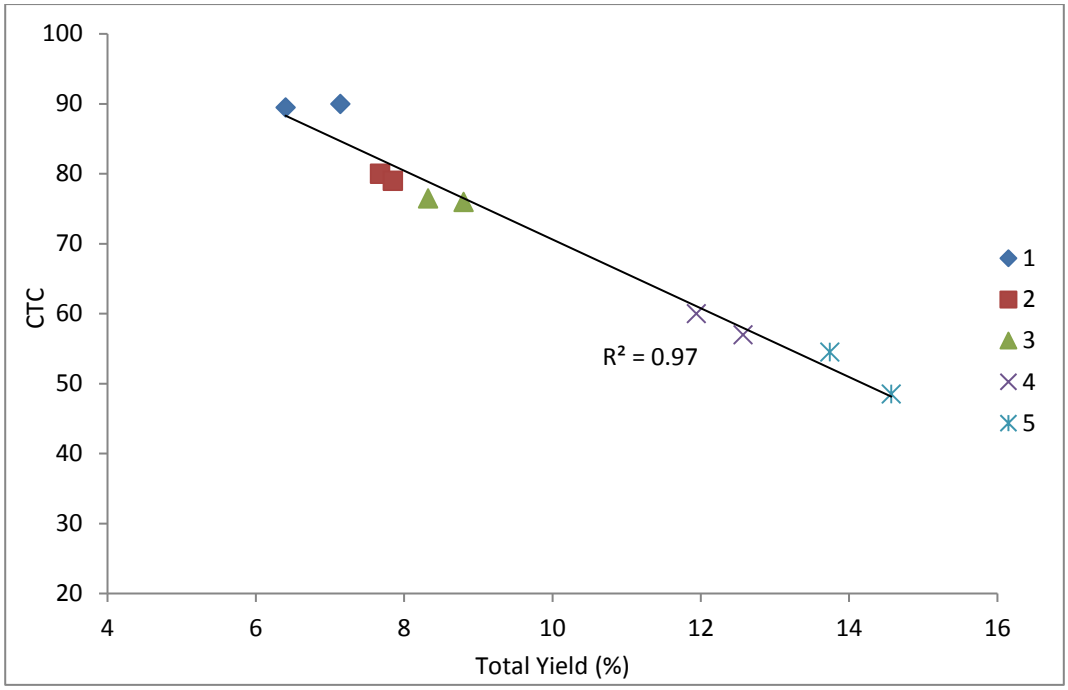


Figure 5:80 CTC against total yield (%) for single step and two-step process shown in Table 5-15.

The burn off percentage shown for single step represents the burn off from char to the activated carbon product and uses the average value obtained by the fast pyrolysis runs shown in Table 5-16. Figure 5:79 and Figure 5:80 above for olive stone and pine wood respectively show the same correlation. Single step activation produces a carbon with an almost identical char burn off and total yield under the same activation conditions as the carbon produced via a two-step method. This means the volatile evolution during the single step activation is having little to no effect on the end product. The yield, CTC relationship still follows the same pattern as all the other trials have shown thus far.

Single Step process will be discussed further in this chapter using biomass that has been washed and also in Chapter 6 where runs are conducted on pilot scale.

5.8.5 Fast Pyrolysis Vs Slow Pyrolysis

Table 5-16 Fast and slow pyrolysis yields from olive stone (20 g) at 700 °C for 30 minutes.

No.	Fast Pyrolysis Yield (%)	Slow Pyrolysis Yield (%)
1	23.65	27.88
2	22.95	27.35
3	22.79	27.34
4	22.98	27.37
5	22.91	27.60
Average	23.05	27.50

Table 5-17 Fast and slow pyrolysis yields from pine wood (6.5 g) at 700 °C for 30 minutes.

No.	Fast Pyrolysis Yield (%)	Slow Pyrolysis Yield (%)
1	19.51	23.98
2	19.09	24.11
3	18.98	23.74
4	18.75	23.86
5	18.60	23.98
Average	18.99	23.94

Slow pyrolysis on average gave an increase yield of approx. 4.5% higher for olive stone and 5% for pine wood. This seems like a small increase yet a 5% char yield increase followed by; 50% burn off during activation can increase the final yield by 2.5%. Activated carbon can sell for over £1000/ton so the accumulative effect of the 2.5% increase is significant. Throughout literature similar findings are observed with a slow heating rate producing higher percentage of char and a fast heating rate producing a higher percentage of liquid and gas yields Brownsort, [2009] However, reports there are exceptions dependant on feedstock.

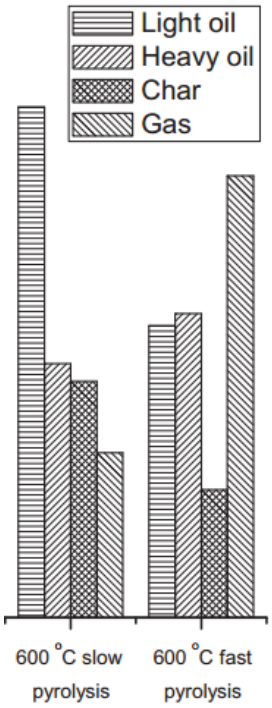


Figure 5:81 Fast and slow pyrolysis products [Ben and Ragauskas, 2013].

Ben and Ragauskas, [2013] Studied in depth fast and slow pyrolysis of pine wood and found that fast pyrolysis produced more gas than slow pyrolysis and that fast pyrolysis could be improving decomposition of lighter oils into gases. Additionally more heavy oil is produced during fast pyrolysis. When using ^{13}C NMR the significant difference between fast and slow pyrolysis oil is the content of methoxyl groups. This content decreased by 76% for pine wood when using fast pyrolysis.

The below trials compared the burn off percentages between using slow pyrolysis char and fast pyrolysis char with different activation conditions.

Table 5-18 Activation of fast and slow pyrolysis olive stone chars.

Activation Condition No.	Pyrolysis	Activation Temperature (°C)	Residence Time (minutes)	Water Flow (ml)	Char Mass (g)	Burn Off (%)	Total Yield (%)	CTC
1	Fast	800	30	45	4.58	53.5	10.7	64.5
	Slow	800	30	45	5.52	38.3	17.0	52.0
2	Fast	750	60	90	4.61	56.8	11.4	62.5
	Slow	750	60	90	5.57	45.1	15.3	56.0
3	Fast	750	60	60	4.56	50.5	12.3	57.5
	Slow	750	60	60	5.47	36.3	17.4	51.0
4	Fast	750	60	30	4.60	23.7	17.5	42.0
	Slow	750	60	30	5.47	19.6	22.0	38.0
5	Fast	700	60	90	4.59	23.1	17.7	37.5
	Slow	700	60	90	5.47	17.8	22.5	34.5

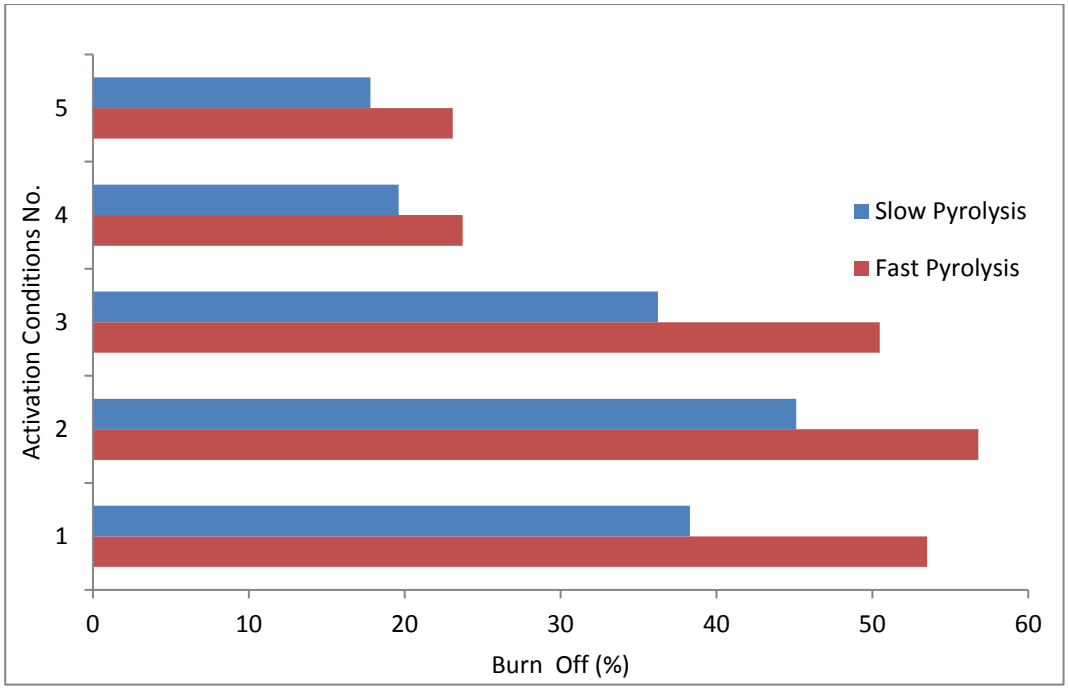


Figure 5:82 Burn off (%) of fast and slow pyrolysis chars conducted in a range of activation conditions shown in Table 5-18.

Olive stone results show that burn off percentage is higher when using char produced via fast pyrolysis. However, how significant the change in yield is hard to quantify as previous trials have suggested that changing the initial amount of char in the crucible alters the burn off percentage. As the pyrolysis results show there is an extra 4.5% (0.9 g) in yield with slow pyrolysis and so the char used for each trial was slightly different. This is not the case with pine wood, as the change in char in the crucible did not affect burn off. The results are shown below.

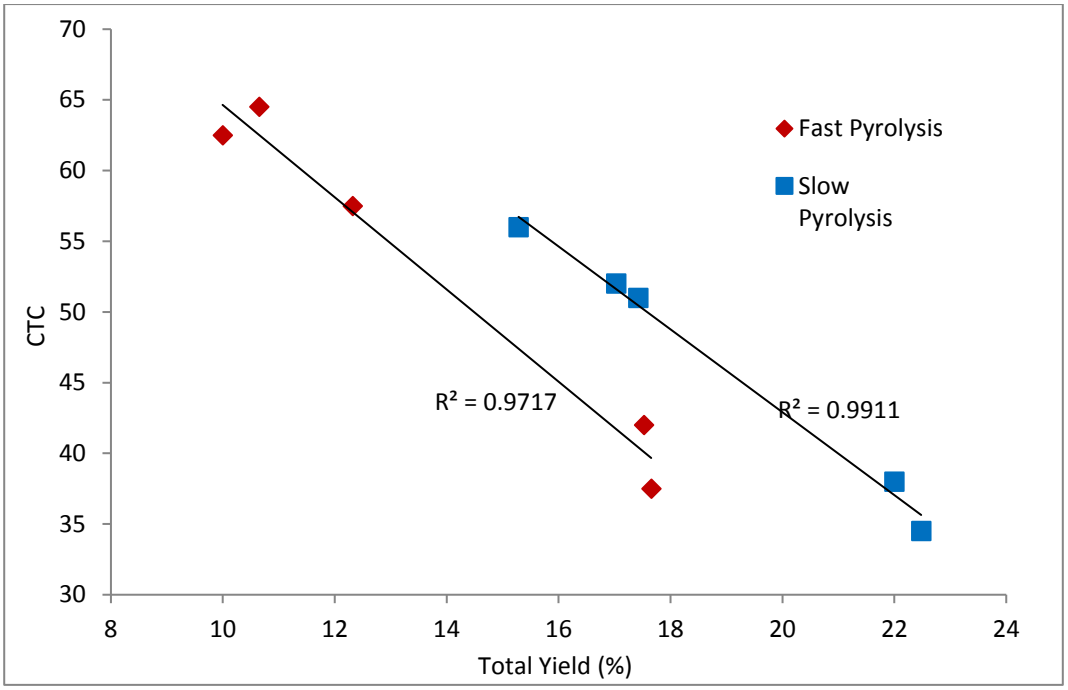


Figure 5:83 Final yield (%) against CTC for both fast and slow pyrolysis chars.

Whilst char burn off data with olive stone cannot be relied upon for reasons above, the total yields produced under the same conditions can. Figure 5:83 shows the total yields compared to the CTC values. The results shows using char that has been produced via slow pyrolysis has a higher total yield to CTC ratio than using char produced via fast pyrolysis. The burn off, CTC ratio however remains the same and fits the trend line shown on Figure 5:2.

Increasing yield is crucial for commercial scale production however; there are disadvantages of using the char produced via the slow pyrolysis route. Firstly design of equipment to ensure that the biomass is heated at a slow rate. Secondly, and most importantly, is that a more reactive char means a lower temperature, short residence time and lower amount of oxidising agent is required to achieve the same burn off and therefore general quality of the carbon.

Table 5-19 Activation of fast and slow pyrolysis pine wood chars.

Activation Condition No.	Pyrolysis	Activation Temperature (°C)	Residence Time (minutes)	Water Flow (ml)	Char Mass (g)	Burn Off (%)	Total Yield (%)	CTC
1	Fast	800	30	45	1.21	53.5	7.1	90.0
	Slow	800	30	45	1.56	45.2	13.1	70.5
2	Fast	750	60	90	1.27	50.5	7.7	80.0
	Slow	750	60	90	1.56	43.0	13.7	68.5
3	Fast	750	60	60	1.23	45.9	8.8	76.0
	Slow	750	60	60	1.54	37.5	14.8	64.5
4	Fast	750	60	30	1.24	34.2	12.6	57.0
	Slow	750	60	30	1.57	27.4	17.5	52.5
5	Fast	700	60	90	1.22	23.1	14.6	48.5
	Slow	700	60	90	1.55	17.9	19.6	39.5

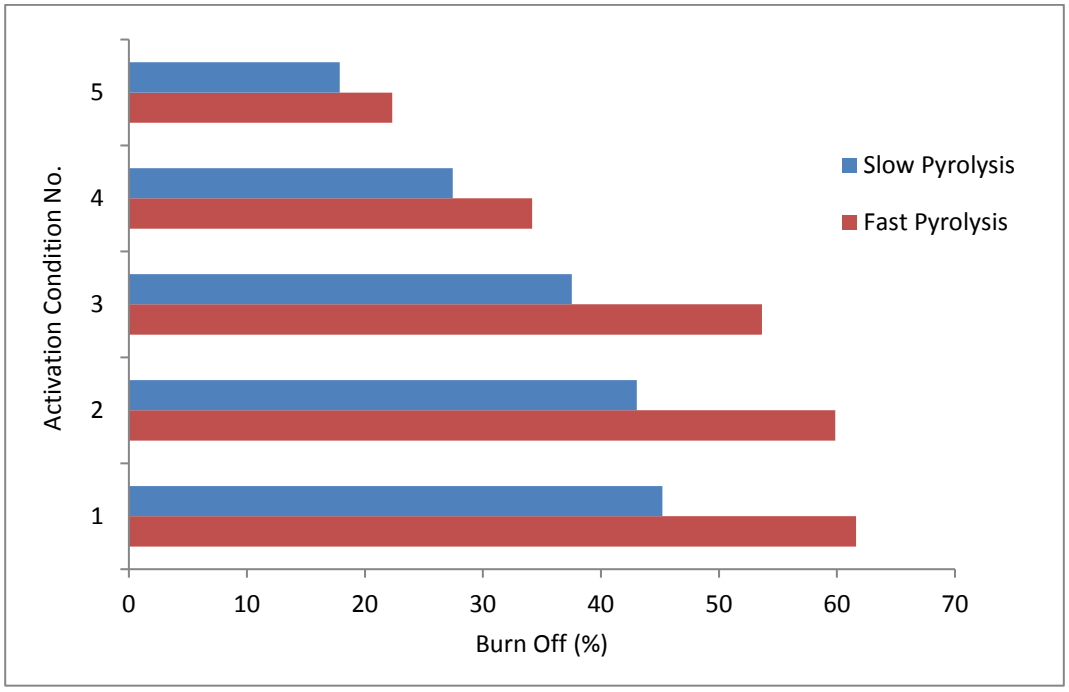


Figure 5:84 Burn off (%) of fast and slow pyrolysis chars conducted in a range of activation condition shown in Table 5-19.

The pine wood results and observations can be taken with more confidence as a small change in char in the crucible results in no real change in burn off. Figure 5:84 shows how char produced by fast pyrolysis is more reactive than char produced via slow pyrolysis. This phenomena is backed up by Chen *et al*, [1996] who researched char reactivity of birch wood when pyrolysed with fast heating rate compared to a slow heating rate and found a similar occurrence. They state "chars obtained from rapid pyrolysis possessed higher reactivities in the reaction with carbon dioxide or steam compared with chars from slow pyrolysis"

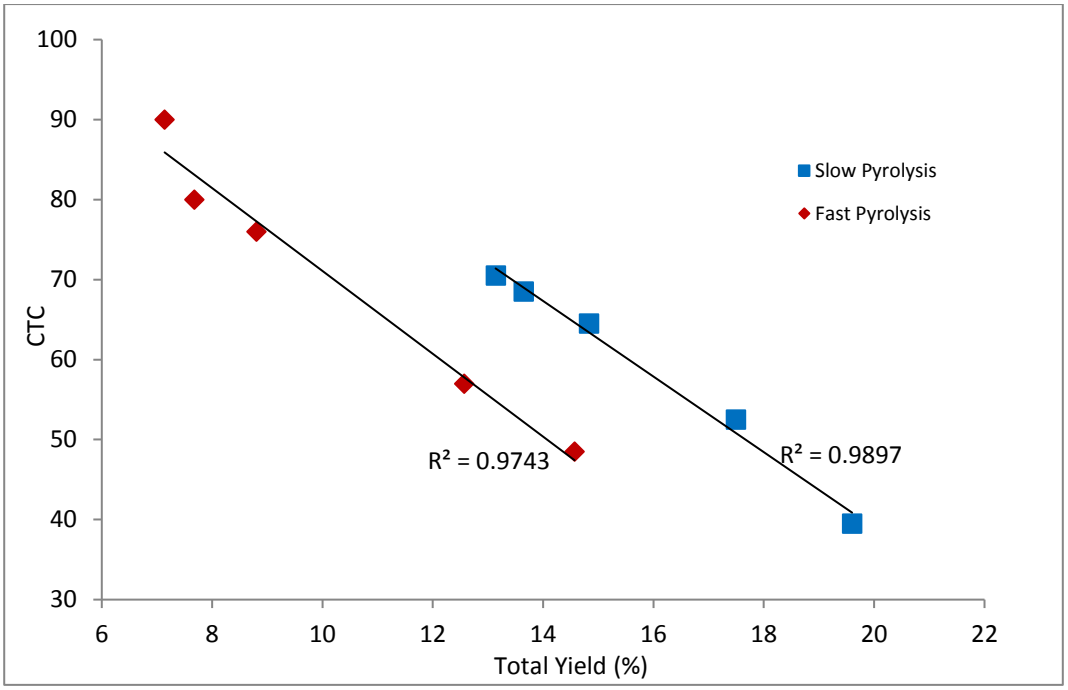


Figure 5:85 Total yield (%) against CTC for both fast and slow pyrolysis chars.

Just as with olive stone, pine wood in Figure 5:85 shows the same pattern. The burn off, CTC relationship is the same for both slow and fast pyrolysis but the end yield shows how they differ with the overall yield being higher for char generated by the slow pyrolysis route.

5.8.6 Impact of Ash with Ion Chromatography Analysis

Table 5-20 Pine Wood [Tony Hansen, 2003] and Olive Stone [Miranda, *et al* 2008].

Ash composition	Pine Wood	Olive Stone
CaO	41.10%	7.52%
MgO	8.21%	1.51%
K2O	10.96%	39.61%
Na2O	0.77%	0.95%
P2O5	4.67%	3.43%
SiO2	2.00%	12.98%
Fe2O3	0.07%	0.91%

The samples used by this analysis were produced on lab scale

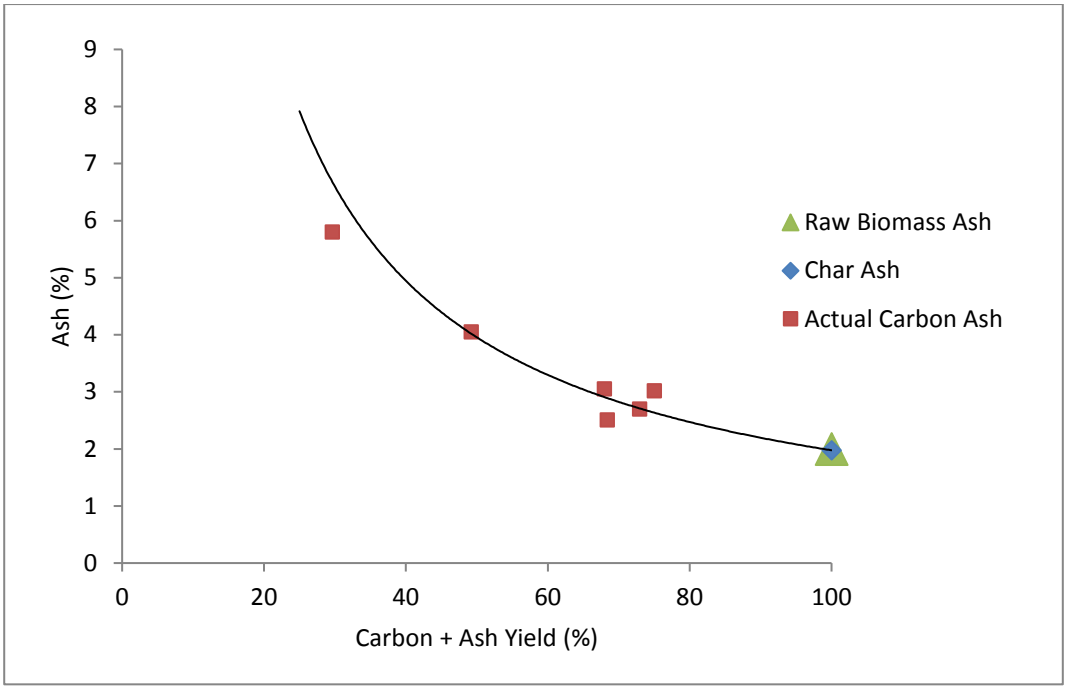


Figure 5:86 Actual ash measured in activated carbon and expected ash (%) based upon ash results in raw and charred olive stone.

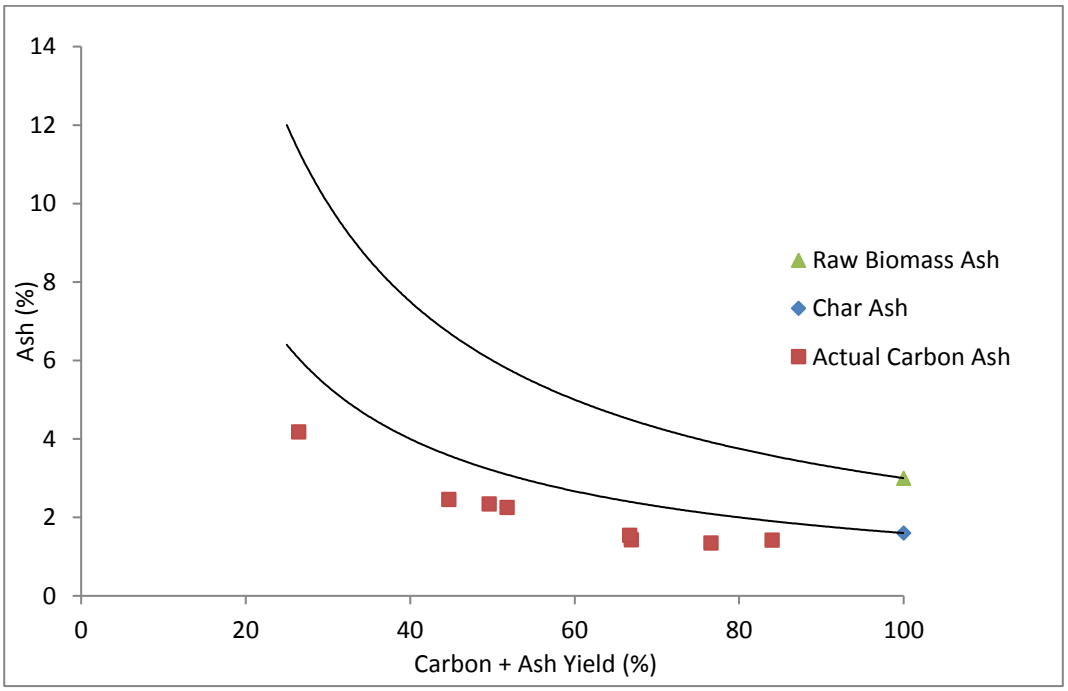


Figure 5:87 Actual ash measured in activated carbon and expected ash (%) based upon ash results in raw and charred pine wood.

Ash tests were conducted on a number of activated carbon samples produced from both olive stone and pine wood. Ash tests were also conducted on the raw material and subsequent char. The values from the raw material and char were then extrapolated by using the expected ash at the final activated carbon yield assuming no ash is lost during pyrolysis and activation. The actual ash was produced by running ash tests on a range of activated carbons with different yields.

Figure 5:86 shows olive stone ash results and how the ash from the activated carbon samples matches up with the expected ash content based on the raw material and char samples which were near identical. This implies that the ash level does not change throughout pyrolysis and activation and the expected ash content can be calculated based on the raw material value alone. Conversely in Figure 5:87 (pine wood) ash results from the char and more significantly the activated carbon samples fall much lower than the expected values based from the raw material ash content. This implies something within the ash is either reacting or being removed during the pyrolysis and again during activation.

Using Table 5-20 pine wood naturally has a higher calcium oxide content that olive stone and by deduction this would appear to be the main component being removed during activation. To see this in greater detail pH tests were completed and then ion chromoatography analysis (IC) was completed on the samples.

pH tests

- Olive stone (OS1) = 9.8 after second wash = 9.1
- Pine wood =(PW1) 10.1 after second wash 9.3

After testing the pH is was decided to see if the alkali alkaline metals were present in solution and causing the high pH and this was tested with ion chromatography. [Marsh and Reinoso, 2006]; [Tascon, 2012] state that inorganic matter increases the pH of the solution so the results are expected.

Table 5-21 IC data from 1st and 2nd washes of olive stone (OS) and pine wood (PW) with (2) next to the carbon signalling values from the 2nd "wash".

	PW 1	PW 1 (2)	PW 2	PW 2 (2)	PW 3	PW 3 (2)	OS 1	OS 1 (2)	OS 2	OS 2 (2)	OS 3	OS 3 (2)	Raw PW	Raw OS
Na (mg/g)	0.16	n.a.	n.a.	n.a.	n.a.	n.a.	0.13	n.a.	n.a.	n.a	n.a.	n.a.	0.45	0.44
K (mg/g)	18.56	3.26	22.71	3.72	26.50	5.87	33.71	2.99	40.10	6.35	32.0	3.20	1.38	3.64
Mg (mg/g)	n.a.	1.55	n.a.	n.a.	n.a.	n.a.	n.a.	1.56	n.a.	n.a	n.a	n.a.	n.a.	n.a.
Ca (mg/g)	0.02	0.00	0.36	n.a.	n.a.	n.a.	0.07	n.a.	n.a.	n.a	n.a	n.a.	4.05	n.a.

The samples used for IC testing were produced on the pilot scale kiln. The same method used for the pH testing (see Chapter 3) was used to produce the solution used for IC analysis. The concentration of Sodium (Na^{+}), Potassium (K^{+}), Magnesium (Mg^{+2}) and Calcium (Ca^{+2}) cations were investigated. It must be noted that Na and K are much more soluble than Mg and Ca

[Tascon, 2012] but as Tascon, [2012] goes onto report even small amounts of Mg and Ca can have an impact on the basicity.

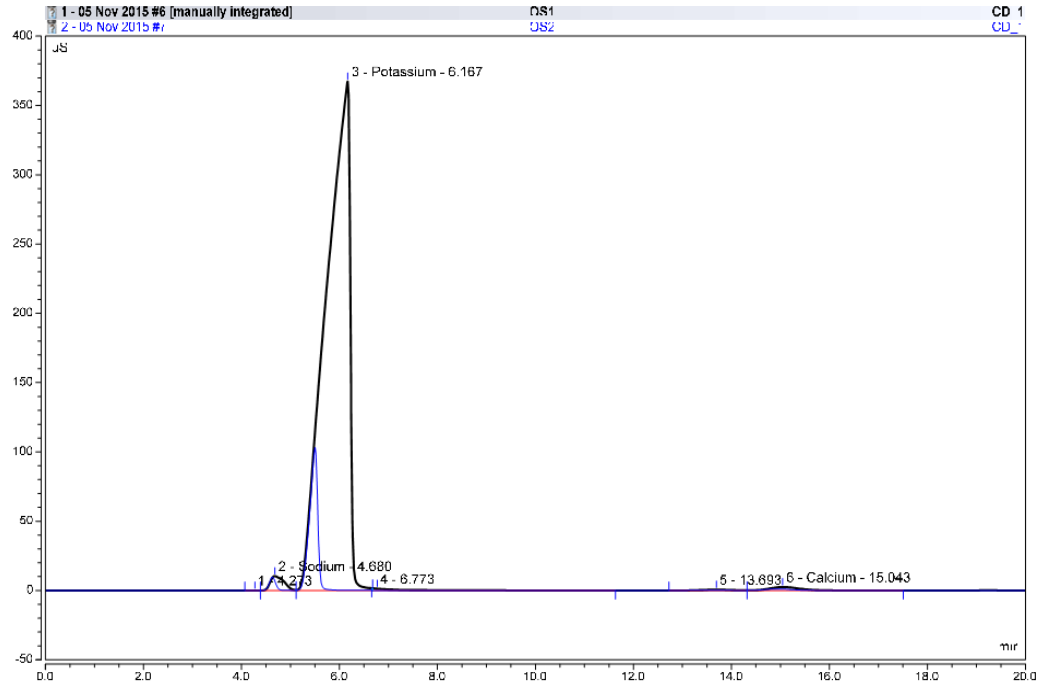


Figure 5:88 Ion chromatography graph produced by olive stone activated carbon after first and second washes.

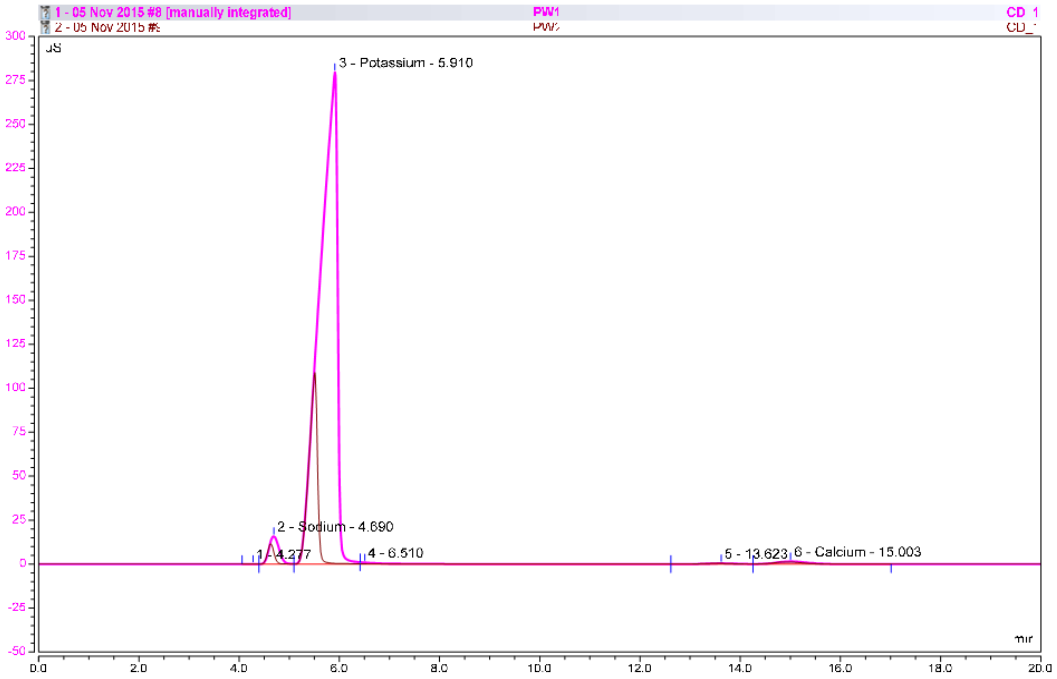


Figure 5:89 Ion chromatography graph produced by pine wood activated carbon after first and second washes.

Using the same method for pH testing stated in Chapter 3 can be seen to remove alkaline, alkali metals from the activated carbons and raw biomasses proved by IC analysis (Figure 5:88 and Figure 5:89). Removing these metals can be beneficial in certain applications that require

minimal leaching during the process. These metals raise the pH of the solution as shown by the pH results.

Washing the carbons a second time shows that the metals in the solution lowers from the previous wash. The main decrease during washing is potassium. The exception is that magnesium appears in two of the samples that have gone through two washes. This may point towards magnesium being more difficult or slower to remove from the carbons as stated by Tascon [2012].

Converting results from ppm to mg/g for the carbon or raw biomass can give a clearer indication for comparable purposes. This is due to different masses of raw biomass and carbon being used to produce the solution for IC analysis to make sure the concentration was high enough.

The raw biomass values have to be carefully considered when comparing (mg/g) to the activated carbon samples as total carbon yield has to be taken into account. This due to lower mass used in producing the solution for IC analysis and so the metal concentration (mg/g) should be higher. By changing the values to match final activated carbon yields it can be seen what metal concentrations are expected to be present in the final activated carbon product.

Initially the values can be expressed in terms of yield of activated carbon produced. The carbon yields used and can be found in Chapter 6 and in these cases 1 g of raw biomass produces 0.07g or 0.115-0.165 g of activated carbon for pine wood and olive stone respectively based on the sample trials completed.

Table 5-22 Theoretical values when taking into account carbon yields.

	Raw PW	Raw OS	PW yield correction	OS yield correction
Na (mg/g)	0.45	0.44	6.40	2.68- 3.84
K (mg/g)	1.38	3.64	19.72	22.09-31.69
Mg (mg/g)	n.a.	n.a.	n.a.	n.a
Ca (mg/g)	**4.05**	n.a.	**57.87**	n.a.

The estimated value of potassium for pine wood activated carbon is 19.72 mg/g based on the results from raw pine wood. This fits well in the range of 18.56 mg/g to 26.51 mg/g shown in Table 5-21. The estimated value for olive stone falls slightly below the carbon values of 22.09-31.69 mg/g to 32- 40.13 mg/g observed in Table 5-21. This can be explained by two possible reasons. Firstly, as shown with previous results and SEM images, olive stone is naturally less porous than pine wood and so metal leaching from the raw olive stone would likely be more difficult via simple hot water washing. In addition the yields used are the overall yields not the batch yields for each sample as they are unknown on large scale due to discussed limitation in Chapter 3. Sodium appears to disappear from both pine wood and olive stone, with the greater

loss occurring in pine wood. The main loss is with calcium which is found in the large quantities in the raw pine wood and despite the fact that calcium is less soluble than the other metals [Tascon, 2012] it is the same for both carbon and raw biomass and quantities can still be compared. Looking at the activated carbon samples minimal amounts are seen (4.05 mg/g) compared to the large amounts predicted based on the raw biomass data of 57.87 mg/g.

This begins to piece together which part of ash is "disappearing" during activation. Calcium oxide (CaO) is the major component of pine wood ash [Tony Hansen, 2003] and would seem to be reacting or being driven off during the two-steps of the process.

Once the samples had been washed and the substrate tested with IC analysis ash tests were conducted on the samples to see if ash levels had indeed reduced during hot water washing. The results are shown below.

Table 5-23 Ash (%) of the carbon after 1st and 2nd washing.

Sample	PW3	PW4	OSR6	OSR7
Activated Carbon	2.92	3.87	3.76	2.59
1st 'Wash'	2.22	1.83	1.90	1.57
2nd 'Wash'	1.52	1.47	1.72	0.83

Table 5-23 shows that the ash content lowers as expected as parts of the ash are being removed from hot water washing as the IC data shows. This can be seen as an important property: for example, in applications such as water filtration in fish tanks the leaching of ash components into solution is an unwanted property as it can increase the pH which could be harmful to inhabitants. Hot water washing rather than a full acid wash is a possibility to remove some inorganics from the carbons. Acid washing is more effective at removing inorganics opposed to water washing but can add large costs to production [Marsh 2001]. Marsh, [2001] also reports how each specific acid is better at removing certain impurities.

5.8.7 Acid Washing to Reduce Iron Content

Acid washing was conducted to remove iron content of the olive stone activated carbon for a certain application that requires no yellow colour leach into the solution. The method used to conduct this is given in Chapter 3 acetic acid (2M) was used rather than the usually more utilised HCl. HCl is usually used due to it being cheaper and a stronger acid. For example using [chemicals.co.uk, 2016] the cost of HCl is £2.02/L for compared to £2.70/L for acetic acid. The reaction between iron (III) oxide Fe_2O_3 and acetic acid $6CH_3COOH$ produces Ferric acetate $2(CH3COO)_3Fe$ and H_2O. Whereas the HCl route in this case will produce Iron (III) Chloride $FeCl_3$.

The iron content maximum for the application was 100 mg/kg and the rescored value of the carbon was 69 mg/kg which meant the carbon met the required specification. The Fe content tests were conducted by Warwick Analytical 2015.

5.8.8 XPS Analysis

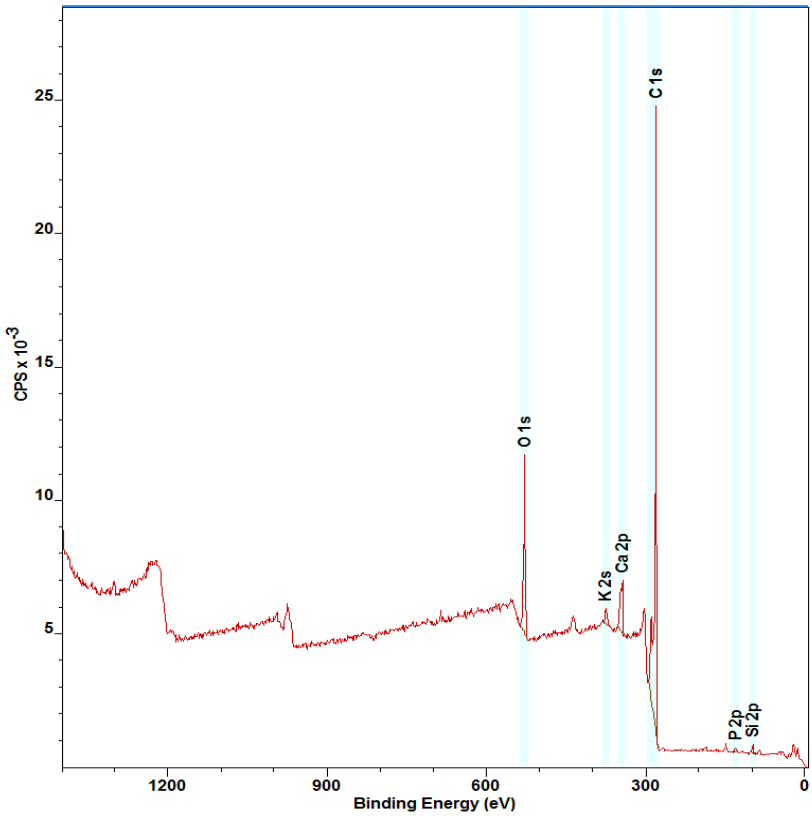


Figure 5:90 Example wide spectra of olive stone activated carbon produced via single step production.

The figure above shows an example of the wide spectrum produced by XPS for olive stone activated carbon. The carbon is mainly made up from carbon atoms and this can be seen in Figure 5:91 below, where in this case carbon makes up over 80% of the surface structure. This also ties in with the ultimate analysis results which showed a carbon percentage of 84% for a carbon with a similar burn off.

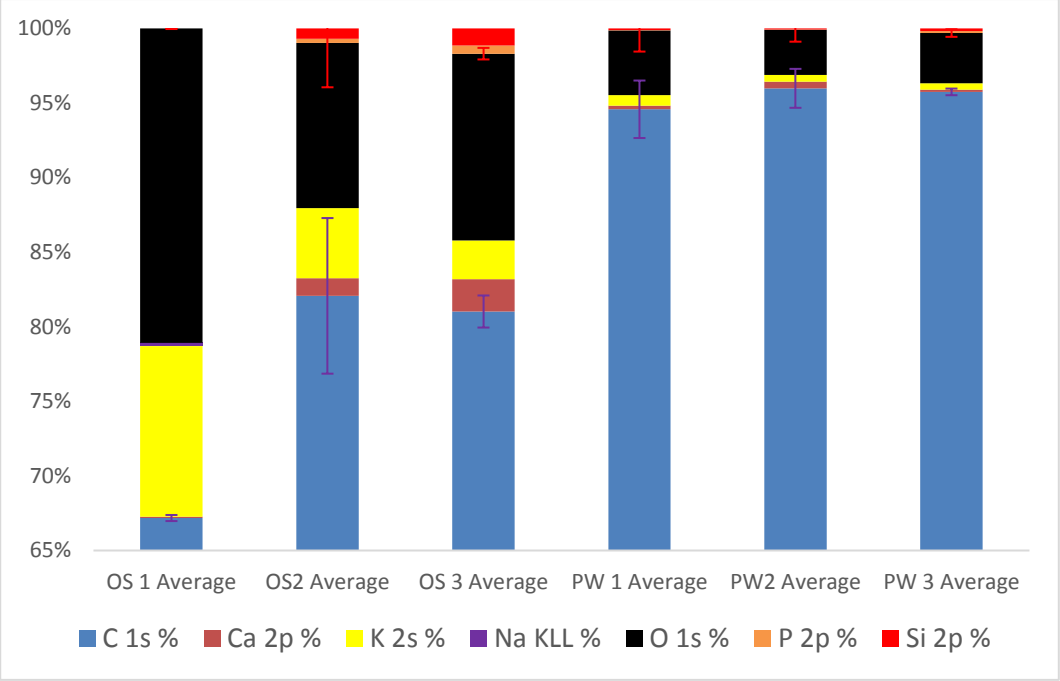


Figure 5:91 Average data collected by XPS analysis on the olive stone and pine wood samples with error bars (SD) for carbon and oxygen components. OS 1 and PW 1 represent char samples. OS 2 and PW 2 represent the two stage pyrolysis and activation with OS 3 and PW 3 representing single step production.

XPS analysis was conducted to analyse the surface chemistry on the carbons. The surface penetration is approx. 10 nm. The results are shown in Figure 5:91 -. What can be seen is that olive stone contained more oxygen surface groups than pine wood. With the char containing the largest amount of oxygen on the surface, oxygen surface groups are elaborated upon further on. Inorganic components although present in the pine wood carbon proved by IC analysis are clearly not located on the surface compared to olive stone. The pine wood char to activated carbon remains uniform on the surface. Olive stone undergoes the greatest change, with a higher percentage of carbon being seen with a reduction in potassium and oxygen. Also seen is the exposure of silicon and calcium after activation.

5.8.8.1 Oxygen Surface Groups.

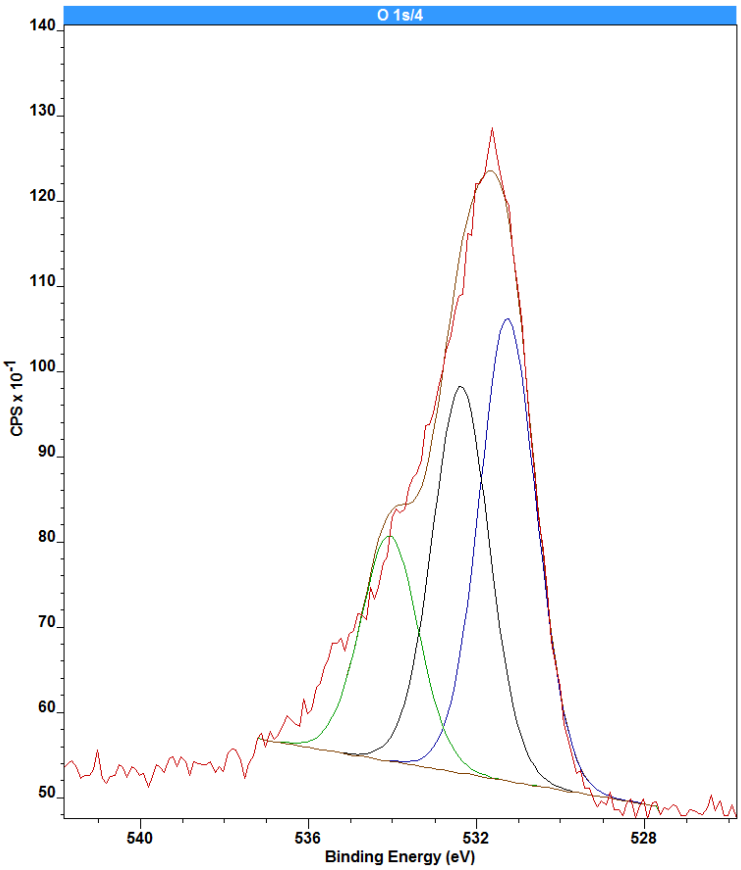


Figure 5:92 O1s XPS peaks for olive stone single step sample showing different oxygen containing compounds with different binding energies.

The range of binding energy form from 531-534 (eV) the peak is broad that implies slightly different compounds are being seen. Here using CasaXPS software components can be made and the peak split up.

Around 531.2-532 (ev) is known for organic C-O and 533 (ev) for organic C=O

These bonds are reported across literature in terms of activated carbon oxygen surface groups. The main ones found include carbonyls, lactones and phenols. Along with others such as ethers, anhydrides, quinones and pyrenes.

Also with the carbons containing a small amount of silicon it is also possible SiO_2 can be seen within this region with a binding energy of 532.9 [Thermo Scientific, 2016] and [G Beamson and D Briggs, 2012].

5.8.9 Hot Washing Biomass

The next step was to see what effect the alkaline alkali metals have on both pyrolysis and activation yields. Across literature it reports that the presence of metals increase pyrolysis yield but conversely decreases gasification yield [J Huyghe, 2014]. J Huyghe, [2014] also states "They

(alkali alkaline earth metals) induced a decrease in the absolute amount pyrolysis products formed, accompanied by an increase of non-condensable gases and char" also that they can reduce primary decomposition of cellulose by inhibiting the glycosidic bond breakage. An example for gasification effects is reported by C Di Blasi, [2009] who state "The oxides and salts of alkaline (Na, K) and alkaline earth (Ca, Mg) metals are also good catalysts for steam gasification of carbon". Calcium oxide (CaO) influences the activity significantly which is found in high quantities within pine wood [Liu and Zhu 1986].

Removing some of these metals via hot washing produced the following results:

The pyrolysis stages were first looked into to see what effect this had. Fast and slow pyrolysis were repeated 5 times each.

Table 5-24 Results for fast and slow pyrolysis using washed biomass, olive stone.

No.	Fast Pyrolysis Yield (%)	Slow Pyrolysis Yield (%)
1	21.4	26.78
2	21.38	26.71
3	21.21	26.62
4	21.19	26.21
5	21.22	26.63
Average	21.28	26.59

When comparing these values to the unwashed fast and slow pyrolysis yields shown in Table 5-16 (23.05% and 27.5%) there is a difference of 1.77% and 0.91% respectively. It therefore would suggest that fast pyrolysis yield was most affected with the removal of metals.

The chars were then activated under the conditions used in section 5.8.5

Table 5-25 Activated carbon produced by washed and unwashed olive stone followed by fast pyrolysis.

No.	Fast Pyrolysis	Activation Temperature (°C)	Residence Time (minutes)	Water Flow (ml)	Initial Raw Olive Stone (g)	Burn Off (%)	Total Yield (%)	CTC
1	washed	800	30	45	20	51.0	10.5	58.5
	unwashed	800	30	45	20	53.5	10.7	64.5
2	washed	750	60	90	20	55.2	9.6	59.0
	unwashed	750	60	90	20	56.8	10.0	62.5
3	washed	750	60	60	20	46.5	11.4	52.0
	unwashed	750	60	60	20	45.9	12.3	52.0
4	washed	750	60	30	20	22.1	16.5	39.0
	unwashed	750	60	30	20	23.7	17.5	42.0
5	washed	700	60	90	20	24.6	16.0	38.5
	unwashed	700	60	90	20	23.1	17.7	37.5

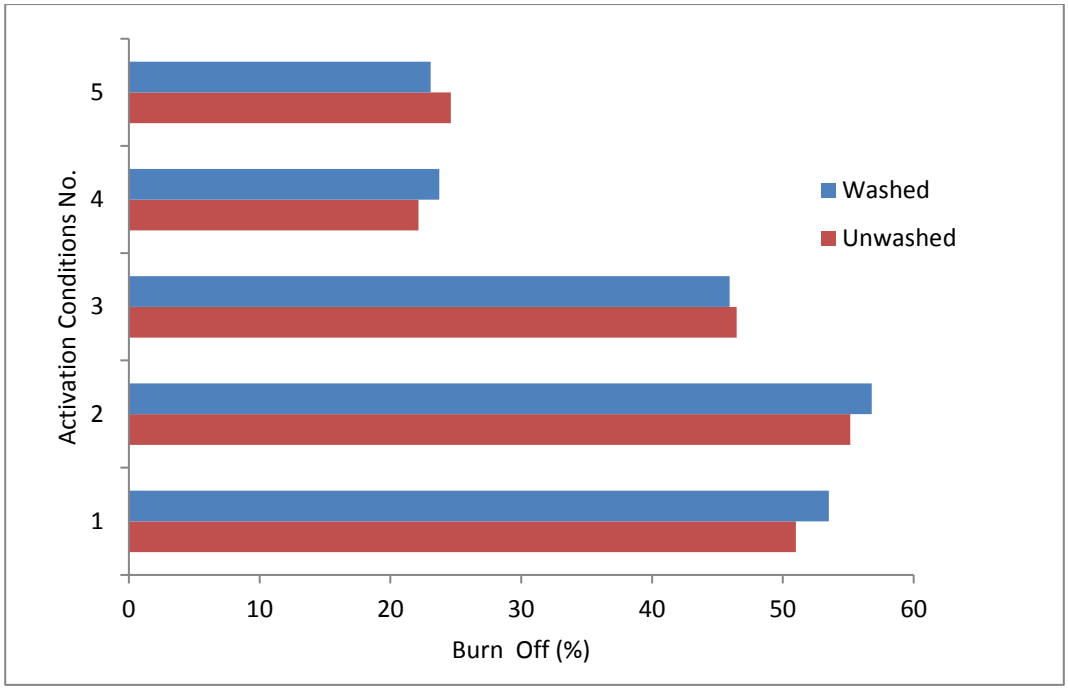


Figure 5:93 Burn off (%) for the activation trials for the washed and unwashed (fast pyrolysis) samples of olive stone.

When activating with fast pyrolysis char, from washed and unwashed samples, burn off percentages are very similar. The only difference being pyrolysis yield is slightly lower with the washed samples resulting in a slightly lower total yield. The CTC results are similar and follow the general trend (shown in Figure 5:95) with no great difference is seen between the two carbons.

Table 5-26 Activated carbon produced by washed and unwashed olive stone followed by slow pyrolysis.

No.	Slow Pyrolysis	Activation Temperature (°C)	Residence Time (minutes)	Water Flow (ml)	Initial Raw Olive Stone (g)	Burn Off (%)	Total Yield (%)	CTC
1	washed	800	30	45	20	30.5	18.6	45.5
	unwashed	800	30	45	20	38.3	17.0	52.0
2	washed	750	60	90	20	37.0	16.9	48.0
	unwashed	750	60	90	20	45.1	15.3	56.0
3	washed	750	60	60	20	27.4	19.3	41.5
	unwashed	750	60	60	20	36.3	17.4	51.0
4	washed	750	60	30	20	15.0	22.3	32.5
	unwashed	750	60	30	20	19.6	22.0	38.0
5	washed	700	60	90	20	17.3	22.0	33.0
	unwashed	700	60	90	20	17.8	22.5	34.5

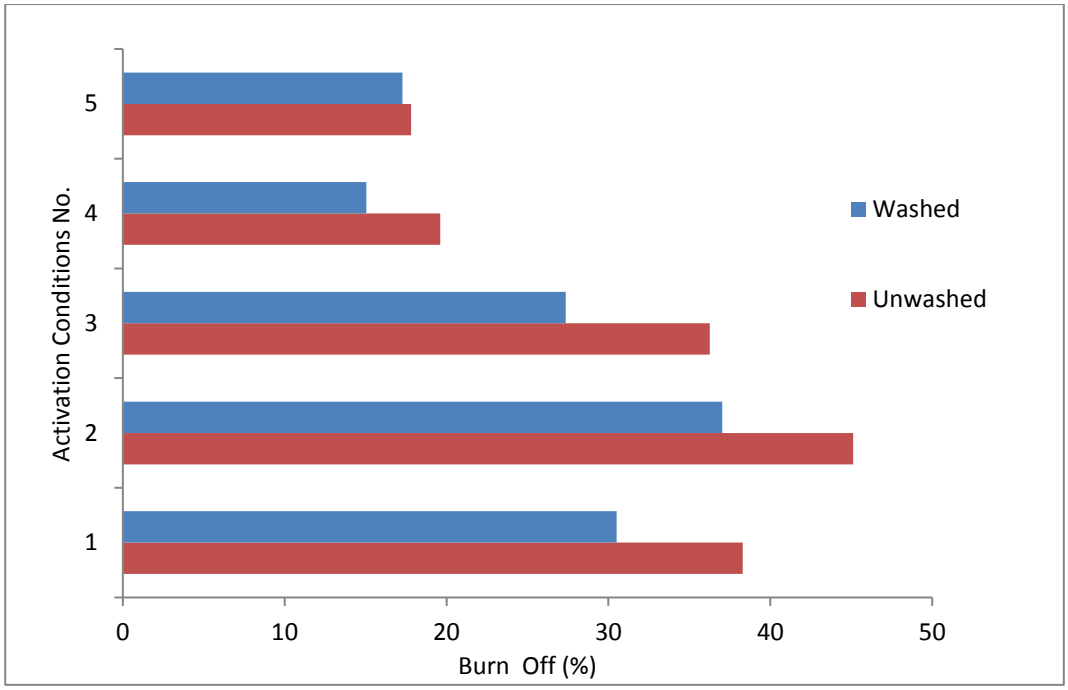


Figure 5:94 Burn off (%) for the activation trials for the washed and unwashed (slow pyrolysis) samples of olive stone.

Conversely, whilst there was no major difference when using char produced via fast pyrolysis this is not the case when using char produced via slow pyrolysis. Washed biomass samples using this produced char, with the exception of the 700 ^{o}C trial, shows a significant reduction in burn off meaning the char has become further un-reactive. Although the pyrolysis yield with the washed samples is lower, than unwashed samples via slow pyrolysis, the end yield is still higher due to the significant decrease in burn off. This implies that the metals removed from this type of char has a large role to play in the char-steam reactivity, whereas with an already reactive char the effect is negligible.

The slow pyrolysis char is already less reactive than the fast pyrolysis char and washing the biomass has meant that this has become less reactive still. For example the difference in burn off at 800 ^{o}C using fast pyrolysis char compared to washed slow pyrolysis char at 800 ^{o}C char is 20.5%.

Removing some of the alkali alkaline metals has no effect on the CTC values with the same burn off, CTC trend shown in Figure 5:95 being seen.

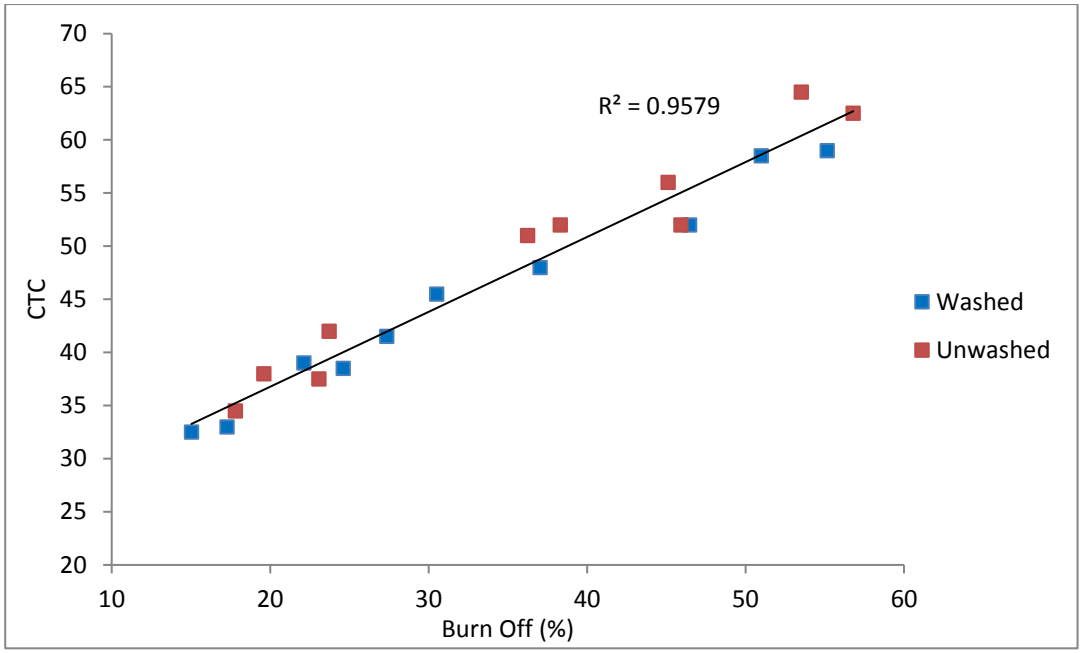


Figure 5:95 CTC and burn off (%) correlation is unaffected by pre washing olive stone.

The above figure shows how the washed and unwashed samples still form a strong correlation between burn off percentage and CTC. This shows the uptake in butane is not significantly changed when washing the biomass prior to pyrolysis and subsequently activation.

Table 5-27 Fast and slow pyrolysis from washed pine wood.

No.	Fast Pyrolysis	Slow Pyrolysis
1	16.29	22.23
2	17.43	22.12
3	17.15	22.22
4	16.35	21.62
5	15.92	21.43
Average	16.63	21.92

As with fast and slow pyrolysis of unwashed pine wood there is a large difference in yields between the two. An average difference of 5.3% is observed. Comparing these washed values to the unwashed values shown in Table 5-17 a difference in yield for fast and slow pyrolysis is 2.36% and 2.02% respectively with a decrease again being found in the washed samples, same occurrence as seen with olive stone. The difference in yield between washed fast pyrolysis and an unwashed slow pyrolysis is 7.3% showing how pyrolysis yields can be easily manipulated by conditions and basic treatments.

Table 5-28 Activated carbon produced by washed and unwashed pine wood followed by fast pyrolysis.

No.	Fast Pyrolysis	Activation Temperature (°C)	Residence Time (minutes)	Water Flow (ml)	Pine Wood (g)	Burn off (%)	Total Yield (%)	CTC
1	washed	800	30	45	6.5	49.1	8.9	73.0
	unwashed	800	30	45	6.5	61.6	7.1	90.0
2	washed	750	60	90	6.5	38.0	10.1	66.0
	unwashed	750	60	90	6.5	59.9	7.7	80.0
3	washed	750	60	60	6.5	35.5	11.1	68.0
	unwashed	750	60	60	6.5	53.7	8.8	76.0
4	washed	750	60	30	6.5	30.8	11.1	58.0
	unwashed	750	60	30	6.5	34.2	12.6	57.0
5	washed	700	60	90	6.5	18.3	13.0	50.5
	unwashed	700	60	90	6.5	22.3	14.6	48.5

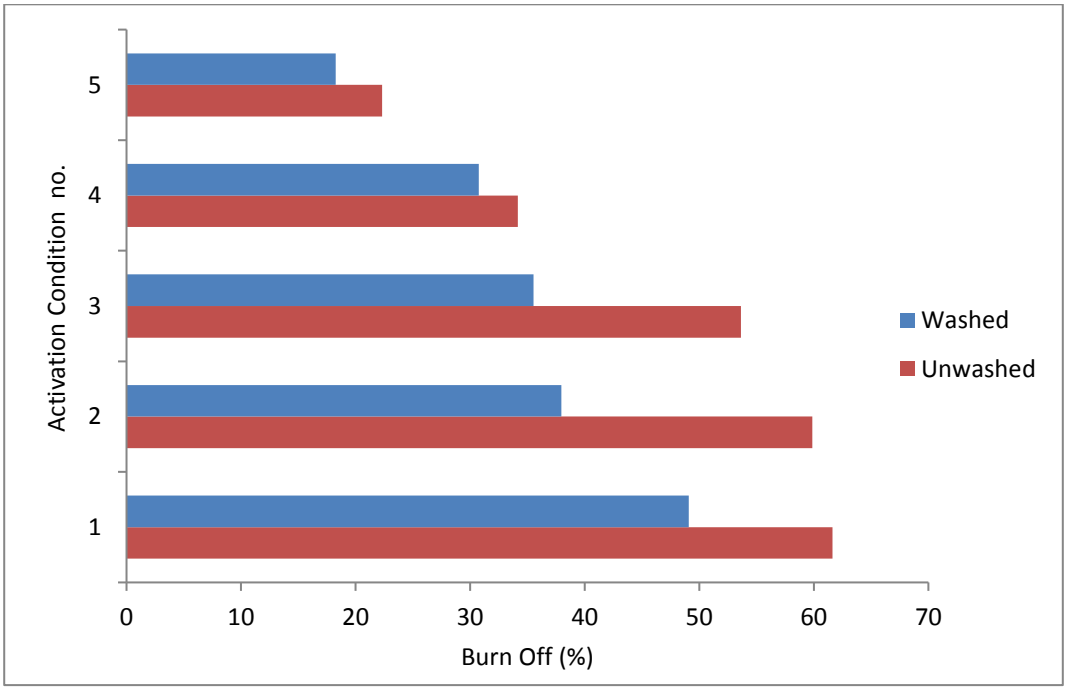


Figure 5:96 Burn off (%) for the activation trials for the washed and unwashed (fast pyrolysis) samples of pine wood.

Conversely, unlike olive stone where burn off was not affected when using char from fast pyrolysis, there is a significant difference with pine wood char. The washed samples achieve a lower burn off under the same conditions by using fast pyrolysis char. The removal of metals once again appears to lower the reactivity of char during activation. The difference is greater here than seen with slow pyrolysis char samples which are shown below.

Table 5-29 Activated carbon produced by washed and unwashed pine wood followed by slow pyrolysis.

No.	Slow Pyrolysis	Activation Temperature (°C)	Residence Time (minutes)	Water Flow (ml)	Pine Wood (g)	Burn Off (%)	Total Yield (%)	CTC
1	washed	800	30	45	6.5	38.0	13.7	64.0
	unwashed	800	30	45	6.5	45.2	13.1	70.5
2	washed	750	60	90	6.5	30.2	15.5	52.0
	unwashed	750	60	90	6.5	43.0	13.7	68.5
3	washed	750	60	60	6.5	27.0	16.2	58.0
	unwashed	750	60	60	6.5	37.5	14.8	64.5
4	washed	750	60	30	6.5	21.2	17.0	44.5
	unwashed	750	60	30	6.5	27.4	17.5	52.5
5	washed	700	60	90	6.5	13.8	18.5	37.5
	unwashed	700	60	90	6.5	17.9	19.6	39.5

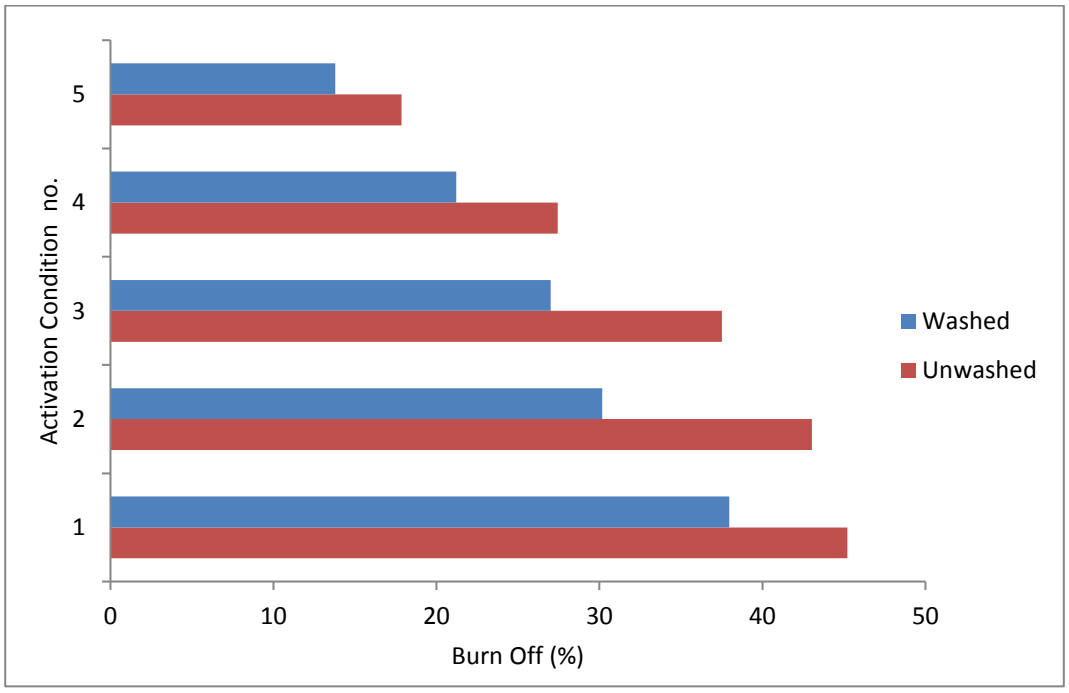


Figure 5:97 Burn off (%) for the activation trials for the washed and unwashed (slow pyrolysis) samples of pine wood.

Similar to olive stone, slow pyrolysis char burn off once again is reduced during activation under the same conditions with the washed samples. Although findings show this phenomena does not occur to the same extent as with fast pyrolsis char, there is still a significant reduction in burn off with pre washing of biomass.

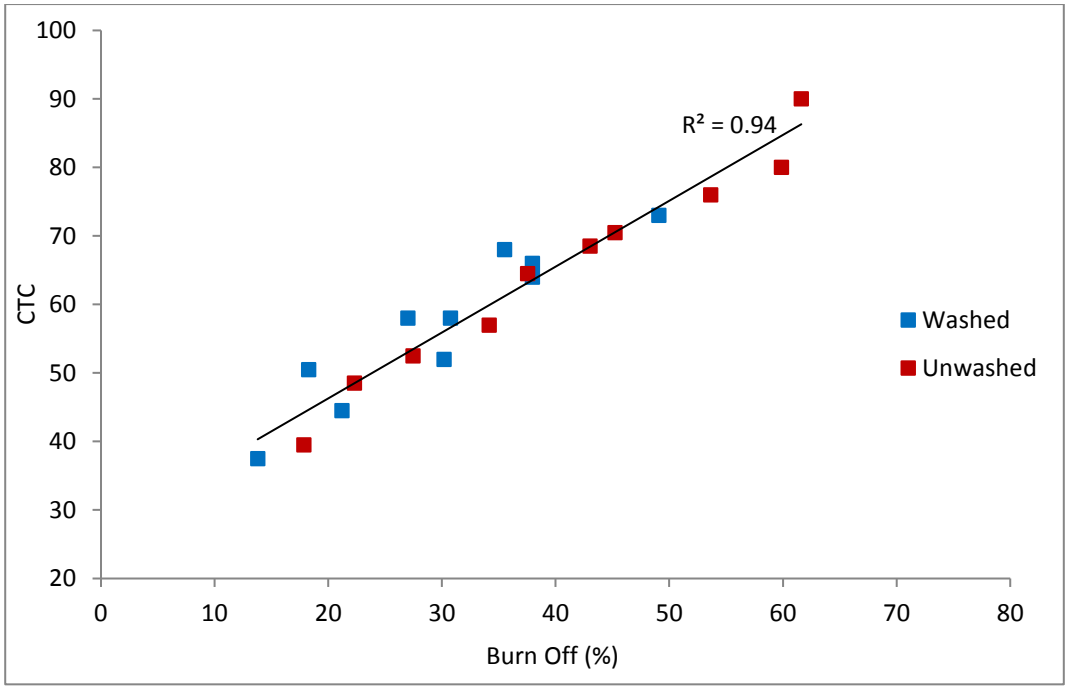


Figure 5:98 CTC and burn off (%) correlation is unaffected by pre washing pine wood.

As with olive stone, pine wood washed and unwashed does not deter from a strong correlation between burn off percentage and CTC value. Again showing how the removal of inorganic material prior to pyrolysis and activation is having little impact on butane adsorption.

5.8.10 Single Step Process Using Washed Biomass.

The next set of single step trials involved activating both biomasses in a single pyrolysis and activation step after being hot water washed to remove some of the alkali alkaline metals. From previous trials it is known that the washing decreased pyrolysis yields but increased activation yields. The table below shows results from both olive stone and pine wood.

Table 5-30 Olive stone single step activation from washed biomass.

Temperature (°C)	Residence Time (mins)	Total Water Flow (ml)	Olive Stone (g)	Burn Off (%)	Total Yield (%)	CTC
800	30	45	20	51.9	10.2	60.5
750	60	90	20	58.9	8.8	65.5
750	60	60	20	54.6	9.7	62.0
750	60	30	20	26.0	15.7	44.5
700	60	30	20	28.5	15.2	45.5

Table 5-31 Pine wood single step activation from washed biomass.

Temperature (°C)	Residence Time (mins)	Water Flow (ml)	Pine Wood (g)	Burn Off (%)	Total Yield (%)	CTC
800	30	45	6.5	55.0	7.5	80.0
750	60	90	6.5	46.2	9.0	77.0
750	60	60	6.5	41.0	9.8	72.0
750	60	30	6.5	34.4	10.9	57.0
700	60	30	6.5	21.6	13.0	47.0

The results above are now compared to the two-step washed fast pyrolysis followed by activation trials.

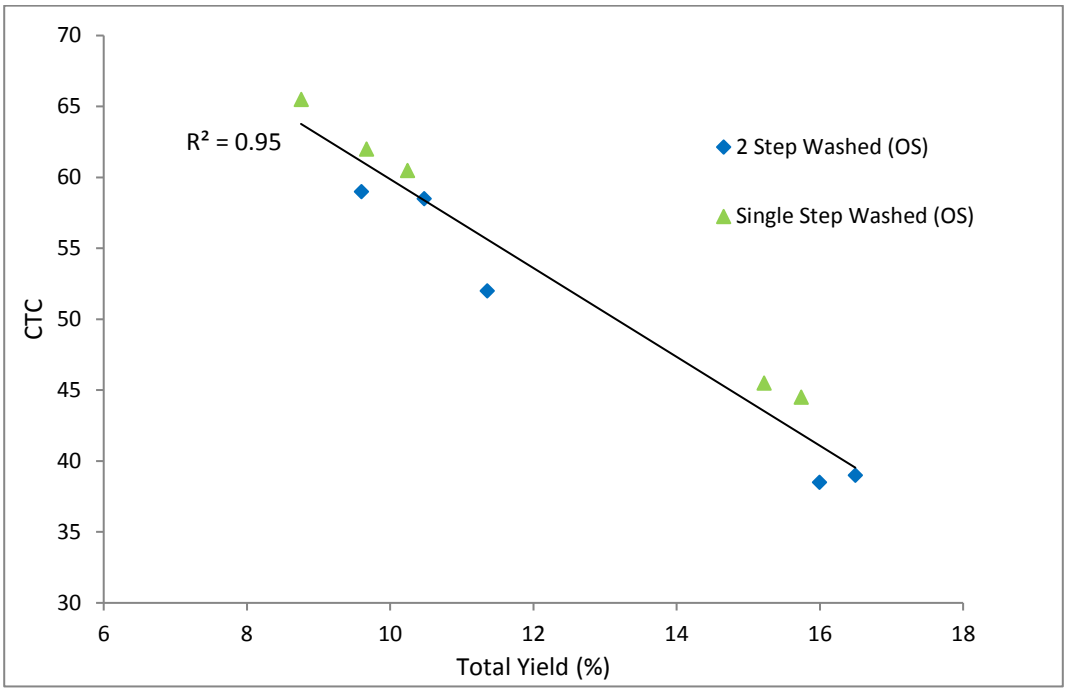


Figure 5:99 Total yield (%) against CTC for both washed and unwashed single step trials, olive stone.

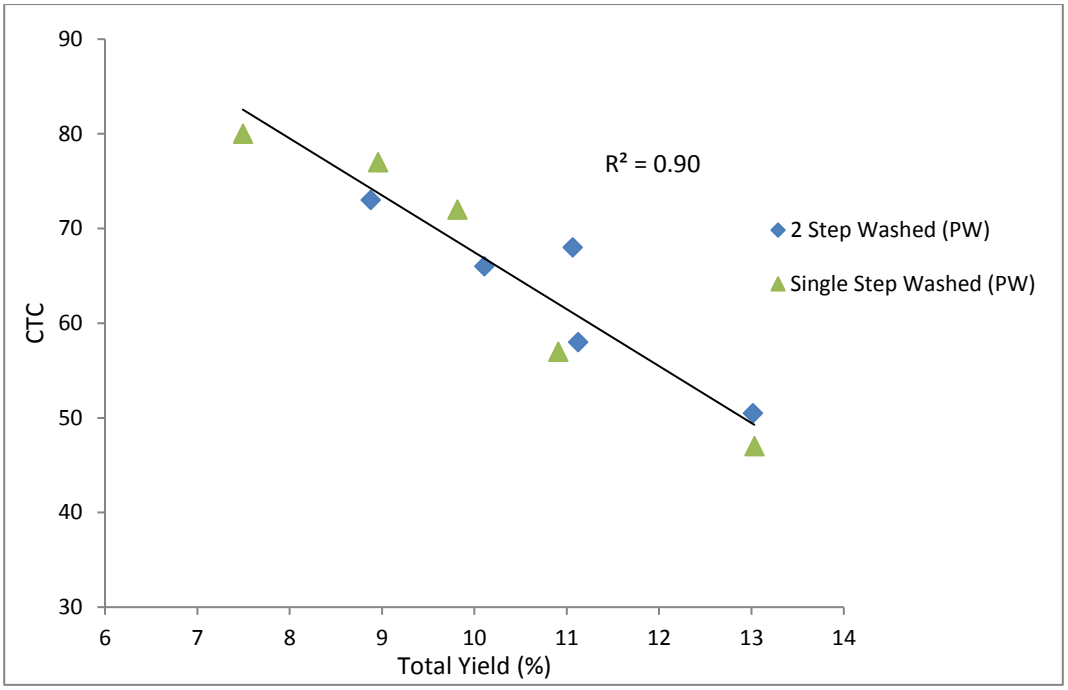


Figure 5:100 Total yield (%) against CTC for both washed and unwashed single step trials, pine wood.

As Figure 5:99 and Figure 5:100 show, although washing the carbon and changing the pyrolysis and activation yields the two processes yield very similar carbons once again independent of a one or two-step process. This is based upon the CTC results which have proven to be very good indicators of overall quality.

The next stage was to compare these results to the previous single step trials that used unwashed biomass. In the tables below the final yield results are shown:

Table 5-32 Olive stone single step trials washed and unwashed final yields.

Temperature (°C)	Residence Time (mins)	Water Flow (ml)	SS unwashed Final Yield (%)	SS washed Final Yield (%)
800	30	45	9.5	10.2
750	60	90	10.6	8.8
750	60	60	12.4	9.7
750	60	30	17.7	15.7
700	60	90	16.8	15.2

Table 5-33 Pine wood single step trials washed and unwashed final yields.

Temperature (°C)	Residence Time (mins)	Water Flow (ml)	SS unwashed Final Yield (%)	SS washed Final Yield (%)
800	30	45	6.4	7.5
750	60	90	7.9	9.0
750	60	60	8.3	9.8
750	60	30	11.9	10.9
700	60	90	13.7	13.0

Seen with both biomasses, although more evident with pine wood, is that to begin with at the lower burn off conditions the washed yield is lower than the unwashed yield. However, as the activation conditions become harsher the yield becomes higher for the washed biomass. This is expected due to an increase in yield during activation with washed biomass. Initially with the washed biomass the resultant lower pyrolysis yield is keeping the total yield lower for the carbon samples with low burn off: where weak activation conditions are only responsible for little loss in mass. However, when activation is responsible for a larger loss of mass (harsher activation conditions) the lower alkali alkaline metal content is having a lower catalytic effect keeping the total yield higher.

Comparing the burn off between the washed and unwashed single step trials (Table A-14 and A-15 in Appendix) show that the burn off for the washed samples as before are lower than the unwashed samples. However the end yields are quite similar due to the trade-off between pyrolysis and activation yields. Burn off percentage and CTC again remains constant throughout the trials with a correlation with an R^2 value of 0.96 for olive stone and R^2 value of 0.93 for pine wood (see Appendix Figures A:17 and A:18).

Trials in this area using butane adsorption as a quality indicator for the carbons show that a pre hot wash does not improve the carbon in terms of quality. It does however affect the pyrolysis and activation yields, firstly by reducing pyrolysis yields and increasing activation yields. The overall end yields are not too dissimilar between the washed and unwashed samples. It would therefore appear the additional cost of pre washing the carbons is not a worthwhile task with these two biomass precursors. However, if minimising inorganic leaching is important when being used in liquid phase applications, then it could still have a place in production.

More important is the trade-off between using fast and slow pyrolysis, with a slow pyrolysis producing a higher yield but fast pyrolysis producing a more reactive carbon meaning lower temperature, residence times and steam flow rates can be used to achieve the same burn off.

5.8.11 Pore Analysis of Single Step and Washed Biomass

A selection of single step and fast and slow washed and unwashed carbons were chosen to undergo pore analysis. The chosen trials and raw data tables can be seen in Appendix Table A-16. The two figures below take the micropore volume data from the chosen samples and the associated CTCs for each sample and are compared to previous two-step lab scale trials (under the optimum conditions).

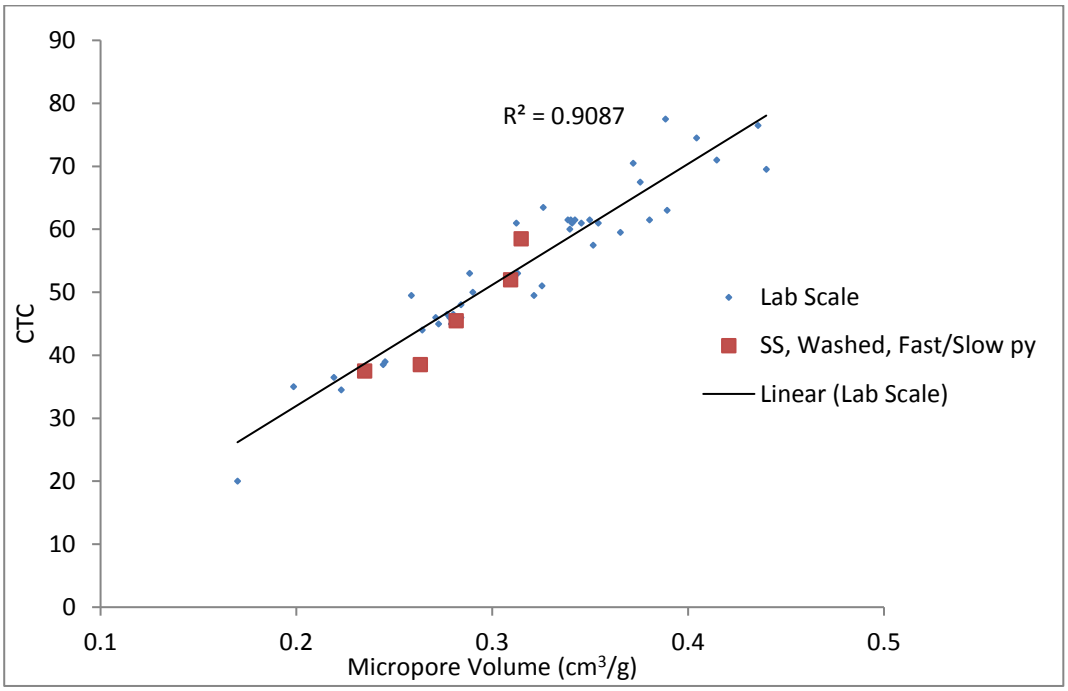


Figure 5:101 Micropore volume (cm^3/g) and CTC of single step, washed and fast and slow pyrolysis. Linear trend line used from Figure 5:6, olive stone.

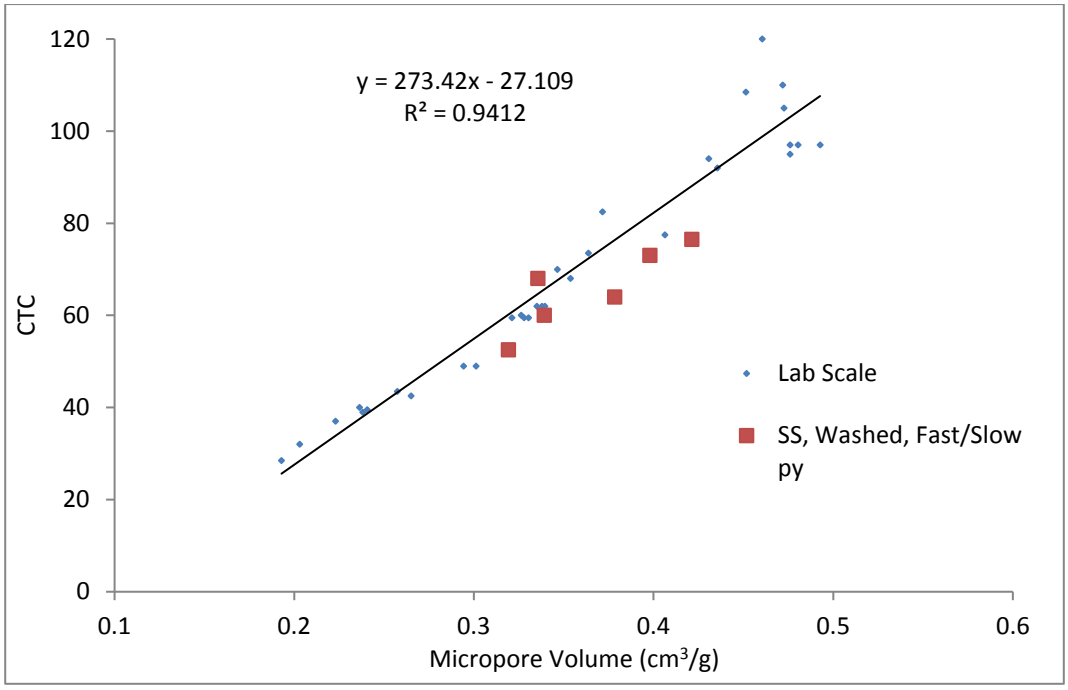


Figure 5:102 Micropore volume (cm^3/g) and CTC of single step, washed and fast and slow pyrolysis, pine wood.

Figure 5:101 and Figure 5:102 show that even though the production has changed significantly the micropore volume and CTC correlation still remain for both biomasses. This again shows how single step or pre washing has no negative effects solely on butane adsorption and only has effects on the burn off and overall yield of the biomass. The rest of the results shown in the Appendix Table A-16 also appears very similar to other previous lab trials.

5.8.12 Carbon Dioxide Isotherms

Carbon dioxide isotherms were completed alongside and joined to nitrogen isotherms for a selection of samples shown in Table 5-34. Carbon dioxide has been used in addition to nitrogen to get accurate pore size distribution (PSD) within the micropore region, joining both isotherms together gives a clearer, more detailed, full pore analysis of a carbon due to CO_2 being easier and quicker to adsorb into ultra-microporous regions (< 0.7 nm). By using CO_2 it overcomes the problems of activated diffusion effect of nitrogen adsorption [Marsh and Reinoso, 2006]. This is because CO_2 adsorption occurs at higher temperature (273K) as opposed to N_2 (77K), additionally CO_2 is a linear molecule and can fit into small slit pores more easily. These factors allows CO_2 to be adsorbed a lower pressures in a realistic time frame.

Table 5-34 Showing pore analysis data from CO_2 and N_2 joined isotherms.

Biomass	Temp (°C)	Dwell (mins)	H_20 (ml/min)	CO_2 L/min	Vmi_{ultra} (cm^3/g)	Vmi (cm^3/g)	Vmi_{ultra} (%)	Vme (cm^3/g)	Vme (%)	Vtot (cm^3/g)
OS	800	60	1.5	0.2	0.1742	0.2763	63.1	0.2765	50.0	0.5528
OS	800	60	1.5	0.5	0.1767	0.2969	59.5	0.3140	51.4	0.6109
OS	800	60	1,5	1	0.1746	0.2881	60.6	0.2795	49.2	0.5676
OS	800	60	0	0.2	0.0801	0.1203	66.6	0.0140	10.4	0.1342
OS	800	60	0	0.6	0.0676	0.0876	77.2	0.0147	14.4	0.1023
OS	750	60	1.5	0	0.1599	0.2466	64.9	0.2202	47.2	0.4667
OS	750	60	1.5	0	0.1652	0.2527	65.4	0.2381	48.5	0.4908
OS	800	60	1.5	0	0.1725	0.2935	58.8	0.2790	48.7	0.5725
OS	800	60	1.5	0	0.1693	0.2914	58.1	0.2709	48.2	0.5623
PW	750	60	1.5	0	0.1648	0.2954	55.8	0.2450	45.3	0.5404
PW	750	60	1.5	0	0.1569	0.2783	56.4	0.2591	48.2	0.5374
PW	800	60	1.5	0	0.1610	0.3395	47.4	0.5779	63.0	0.9174

Table 5-34 shows the two highest ultra micropore percentages belong to the two trials that were activated using CO_2 only. The ultra micropore percentage is a percentage against total micropore volume. Using only steam and steam with CO_2 produced similar ultra micropore percentages; showing that steam has the dominant effect in porosity formation with pore widening from early stages of the reaction which was also seen in Chapter 4 section 4.8. The pine wood samples, activated with steam, show the lowest ultra micropore volume percentages. This is expected as pine wood has been proved to be more mesoporous that olive stone in previous trials. However, the two pine wood samples conducted at 750 °C show a comparable mesopore volume percentage to some olive stone samples in these trials. This means that pine wood carbons contain a higher percentage of larger micropores (0.7 nm to 2 nm). This finding may initially explain why Figure 5:33 shows pine wood samples adsorbing slightly increased amounts of methylene blue dye at the larger micropore volume ranges: as methylene blue dye can fit into larger micropores (> 1.3 nm) [Wang, 2005]. However, joining together, Figure 5:57 and Figure A:15 from the Appendix, Figure 5:103 is produced below. This shows that whilst pine wood may have wider micropores there is not enough conclusive evidence to state that this aids further methylene blue adsorption, as both carbons appear very similar with micropore volumes up to approx. 0.45 cm^3/g.

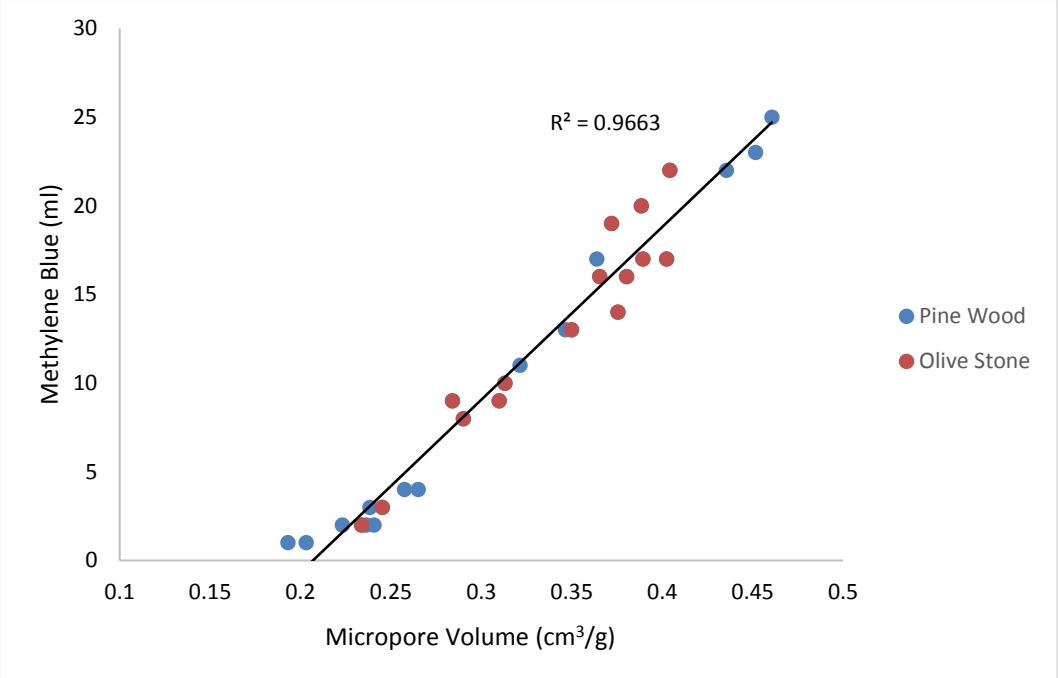


Figure 5:103 Micropore volume (cm^3/g) against methylene blue adsorption for both olive stone and pine wood carbons.

An example of the CO_2 and N_2 isotherm and joined NLDFT pore size distribution can be seen below:

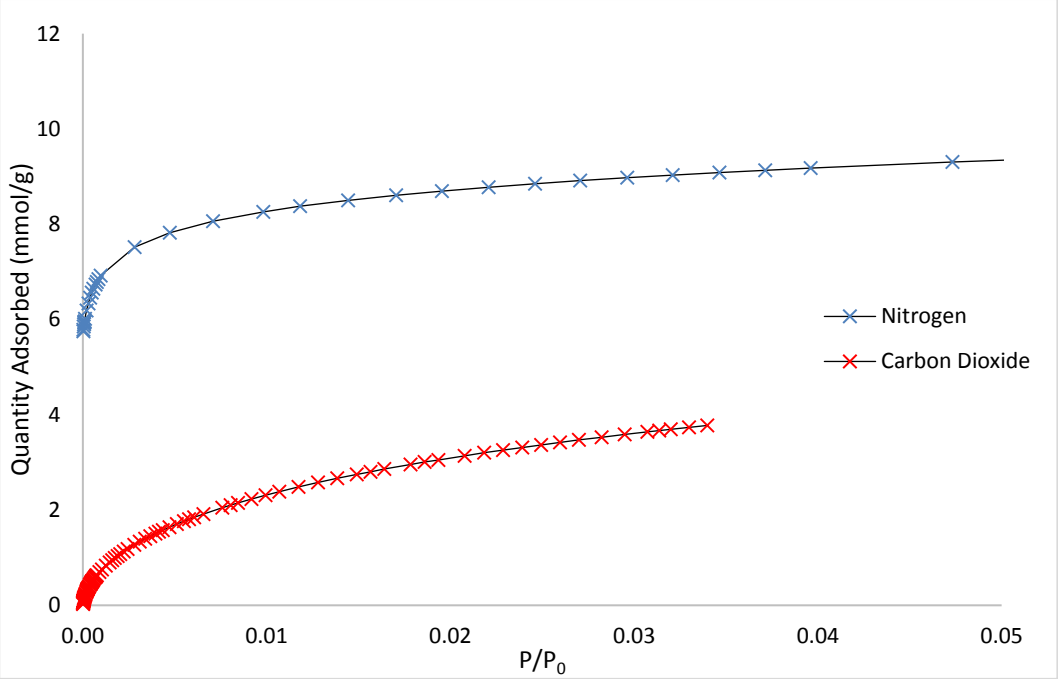


Figure 5:104 Carbon dioxide and nitrogen isotherm for olive stone carbon produced at 800 °C, 60 minutes with water flow of 1.5 ml/min.

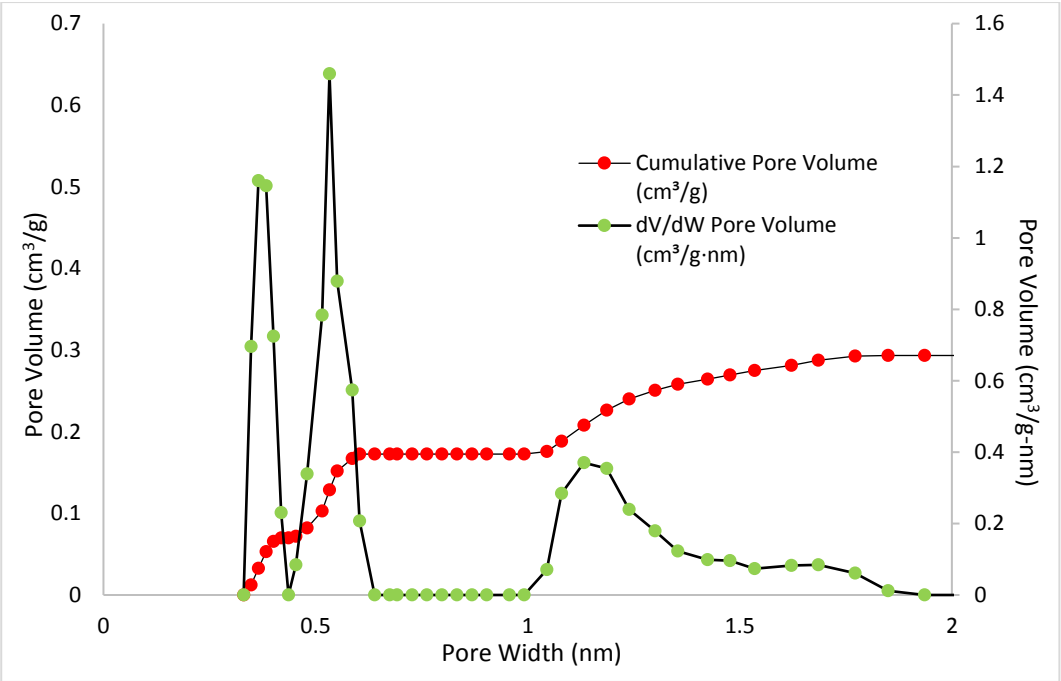


Figure 5:105 Cumulative pore volume isotherm for olive stone carbon produced at 800 °C, 60 minutes with water flow of 1.5 ml/min produced by joining both isotherms.

5.9 Conclusions

1. A strong correlation between burn off percentage and CTC values for both biomass carbons under a large range of production conditions. Pine wood provides a higher CTC value compared to olive stone for a given burn off percentage, however when pyrolysis yields are taken into account, olive stone provides a higher value for the total overall yield**.**
2. Pine wood activated carbon peak individual CTC value was found to be 120 whilst olive stone activated carbon was 84.5, showing butane adsorption per weight much higher for pine wood activated carbon.
3. Using olive stone as the biomass feedstock a char burn off of over 80% and likewise approx. 85% for pine wood sees carbon pore destruction along with a high ash to carbon ratio causing a drop in CTC value due to reducing amounts of site for butane adsorption.
4. A strong micropore volume, CTC correlation for olive stone carbon, and a strong micropore and total pore volume, CTC correlation with pine wood carbon is seen. With carbon derived from pine wood being more mesoporous this would lead to the conclusion that butane is also being adsorbed into some smaller mesopores.
5. Methylene blue adsorption corresponds to micropore volume as opposed to the expected mesopore volume for both carbons due to possible reasons discussed in the chapter.
6. Increasing activation temperature produced a linear burn off percentage increase for both biomass chars under constant steam flow rate and residence times. Activation temperature limits were found for both chars before negatively impacting the carbons: > 850 ^{o}C and > 825 ^{o}C for olive stone and pine wood respectively.
7. High activation temperature trials, at relatively low burn offs using olive stone as the biomass feedstock, show at these raised temperatures external particle burn off is taking place and lowering the CTC, burn off ratio. High activation temperature using pine wood causes total char destruction.
8. Increasing residence time produces a linear char burn off rate for both biomass chars under constant activation temperature and steam flow rate.
9. Long residence time trials showed that after approx. 6 hours additional external burn off was seen with olive stone char. No such negative impact was seen with pine wood during long activation times.
10. Increasing activation temperature increases the carbon burn off rate faster with using pine wood char compared to olive stone char, yet increasing residence time increases burn off rate with olive stone char more so than pine wood char.
11. Increasing steam flow rate produced an exponential increase in burn off for both biomass chars. When steam flow rate increased to approx. (> 1.875 ml/min) there was a negative

impact on the olive stone carbons due to external burn off, no negative impact was seen with pine wood up to the maximum flow rate (3 ml/min). Additionally at increased flow rates the burn off rate reached zero and negative order due to an initial increase of reaction inhibitor concentration produced at early stages of the reaction for both chars.

12. Changing char mass affected burn off with olive stone, with evidence pointing towards mass transfer limitations. This was not seen with pine wood activation as burn off remained constant despite changing char mass. Olive stone burn off percentage was determined by amount of steam entering the system as a ratio to initial char. Under constant activation temperature and residence time olive stone char mass was the dominant factor in burn off, whereas with pine wood, steam flow was the dominant factor.
13. Single step activation trials showed no significant difference in yields and adsorption properties from the two-step activation process.
14. Fast and slow pyrolysis had a significant effect on burn off and the associated CTC value, with fast pyrolysis producing a much more reactive char. A more reactive char meant lower yields but less harsh activation conditions required to reach a certain burn off. The CTC, burn off relationship remained throughout despite using more or less reactive char.
15. Ash loss for pine wood during pyrolysis and activation was seen. Using ion chromatography analysis it was determined that the calcium content of the pine wood had significantly reduced.
16. Hot washing biomass to remove alkali/alkaline metals reduced pyrolysis yield but increased activation yield. There was little to no change in CTC value between washed and unwashed biomass. The same effect was seen with washed single step production with the harsh activation conditions yielding an increased yield but the gentle activation conditions producing a lower yield than using unwashed biomass.
17. CTC analysis strongly correlates with other more expensive analysis techniques showing the potential of a quick 20 minute test to estimate results from these techniques.
18. Carbon dioxide isotherms show additional pore volume information within the ultra micropore region, with CO_2 activation producing a higher percentage of ultra micrpore volumes as expected. Pine wood appears to have a larger percentage of wider micropores, as expected, as it is a generally more mesoporous carbon at higher burn off percentages.
19. The highest surface area of 1118 m^2/g and a micropore volume of 0.434 cm^3/g for olive stone activated carbon was produced at 850 ^oC, 60 minutes residence time at a water flow rate of 1.5 ml/min, whereas the highest surface area (1190 m^2/g) and micropore volume (0.472 cm^3/g) seen with pine wood carbon was produced at an activation temperature of 825 ^oC, 60 minutes residence time at a flow rate of 1.5 ml/min. Pine wood activated carbon produced a more mesoporous carbon with a peak mesopore volume of 0.589 cm3/g compared to the olive stone carbon peak of 0.317 cm^3/g.

5.10 References

A.V. Bridgwater, D. B., 1997. "*Developments in Thermochemical Biomass Conversion" Vol 1/Vol 2*. s.l.:s.n.

Aik Chong Lua, Ting Yang, 2004. "*Effect of activation temperature on the textural and chemical properties of potassium hydroxide activated carbon prepared from pistachio-nut shell". Colloid and Interface Science.*f*shell-based microporous carbons for CO2 capture". Microporous and Mesoporous Materials.*

Anon, 2013. *Thermo Scentific.* [Online]
Available at: http://xpssimplified.com/elements/oxygen.php
[Accessed February 2016].

Anon, 2016. *Chemicals.* [Online]
Available at: http://www.chemicals.co.uk/hydrochloric-acid and
http://www.chemicals.co.uk/acetic-acid accessed
[Accessed April 2016].

Anon, 2016. *Woodland Trust.* [Online]
Available at: https://www.woodlandtrust.org.uk/visiting-woods/trees-woods-and-wildlife/british-trees/native-trees/scots-pine/
[Accessed June 2016].

Bandosz, 2006. "*Activated Carbon Surfaces in Environmental Remediation".*

Ben Haoxi, Arthur J. Ragauskas, 2013. "*Comparison for the compositions of fast and slow pyrolysis oils by NMR*". *Bioresource Technology.*

Blasi, Colomba Di, 2009. "*Combustion and Gasification Rates of Lignocellulosic Chars*". *Progress in Energy and Combustion Science.*

Brownsort, P. A., 2009. "*Biomass pyrolysis Processes: Review of Socpe, Control and Variability UKBRC" Working Paper 5*.

C.L. Mangun, M.A. Daley, R.D. Braatz, J. Economy, 1997. "*Effect of pore size on adsorption of hydrocarbons in phenolic-based activated carbon fibers". Carbon.*

Chiung-Fen Chang, Ching-Yuan Chang, and Wen-Tien Tsai, 2000. "*Effects of Burn-off and Activation Temperature on Preparation of Activated Carbon from Corn Cob Agrowaste by CO2 and Steam". Colloid and Interface Science.*

D Briggs and G Beamson , 2012. "*XPS of Polymers Database".*

F. Rodríguez-Reinoso, M. Molina-Sabio, 1992. "*Activated carbons from lignocellulosic materials by chemical and/or physical activation: an overview*". *Carbon.*

Francisco. Rodriguez-Reinoso, Jose Miguel. Martin-Martinez, Celia. Prado-Burguete, Brian. McEnaney, 1987. "*A standard adsorption isotherm for the characterization of activated carbons". Physical Chemistry .*

Graham, D., 1955. "*Separate effects of pore size upon adsorbentcapacity of activated carbon*". *Physical Chemistry.*

Guanxing Chen , Qizhuang Yu, Krister Sjostrom, 1996. "*Reactivity of char from pyrolysis of birch wood". Analytical and Applied Pyrolysis.*

Guerreiro, Cleiton A. Nunes e Mário C., 2011. "*Estimation of Surface Area and Pore Volume on Acitvated Carbons by Methylene Blue and Iodine Numbers*". *Química Nova.*

Haiping Yang, Rong Yan Hanping, Chen Dong Ho, Lee Chuguang Zheng, 2006. "*Characteristics of hemicellulose, cellulose and lignin pyrolysis*". *Fuel.*

Hakan Demiral , Ilknur Demiral, Belgin Karabacakoglu, Fatma Tümsek, 2010. "*Production of activated carbon from olive bagasse by physical activation",* Eskisehir, Meselik Campus: s.n.

Hanson, 2003. *Ceramic Materials.* [Online]
Available at: https://digitalfire.com/4sight/material/pine_wood_ash_1119.html accessed May 2015[Accessed May 2015].

Harry Marsh and Francisco Roriguez Reinoso, 2006. "*Activated Carbon".* Elsevier Science & Technology Books.

Hayes, D., 2016. *Advanced Biomass Research for Beyond the Petroleum Age.* [Online]
Available at: http://www.carbolea.ul.ie/wood.php
[Accessed March 2016].

Huyghe, J., 2014. "*The role of alkali and earth alkaline metals as intrinsic catalysts in the fast pyrolysis of biomass constituents".*

Isabel M. Lima, Kyoung S. Ro , G. B. Reddy , Debbie L. Boykin and Kjell T. Klasson, 2015. "*Efficacy of Chicken Litter and Wood Biochars and Their Activated Counterparts in Heavy Metal Clean up from Wastewater*". *Agriculture.*

Kang Sun, Jian Chun Jiang, 2010. "*Preparation and characterization of activated carbon from rubber-seed shell by physical activation with steam*". *Biomass and Bioenergy.*

Kaustubha Mohanty, Mihir K. Purkait, 2012. "*Membrane Technologies and Applications".*

Khambali Setiawan Sukiran Al Jauhari, 2015. *"Activated Carbon Adsorption Effectiveness in Coconut Shell*". *Environment and Earth Science,* 5(22).

Kiyoshi Okada, Nobuo Yamamoto, Yoshikazu Kameshima, and Atsuo Yasumori, 2003. "*Porous Properties of Activated Carbons from Waste Newspaper Prepared by Chemical and Physical Activation". Colloid and Interface Science.*

L. Gonzalez and F. R Reinoso, 1980. *"Preparation and characterization of active carbons from olive stones". Carbon.*

M.T. González, M. Molina-Sabio, F. Rodríguez-Reinoso, 1995. "*Steam Activation of Olive Stone Chars, Development of Porosity*". *Carbon.*

Marsh, H., 2001. "*Activated Carbon Compendium": A Collection of Papers from the Journal Carbon ,*

Michio, Feiyu Kang, Masahiro Toyoda, Hidetaka Konno, 2013. "*Advanced Materials Science and Engineering of Carbon".*

Mohammed Asadullah, Muhammad Anisur Rahman, Mohammad Abdul Motin and Mohammed Borhanus Sultan, 2007. "*Adsoprtion studies on Activated Carbon Derived from Steam Activation of Jute Stick Char*". *Surface Science Technology.*

Mrozowski, S., 1963. "*Proceedings of the Fifth Conference on Carbon", Volume 2.*

Naumov, S., 2009. "*Hysteresis Phenomena in Mesoporous Materials",* Leipzig: s.n.

P.L Walker, JR L.G Austin and S.P Nandi, 1966. "*Activated Diffusion of Gases in Molecular-Sieve Materials*". In: *Chemistry and Physics of Carbon Vol 2 257-371.* s.l.:s.n.

Roberts, B., 2015. "*The Effect Temperature Has on the Rate of Diffusion".*

S. Román, J.F. González, C.M. González-García, F. Zamora, 2007. "*Control of pore development during CO2 and steam activationof olive stones*". *Fuel Processing Technology.*

Sebastian Rojas, Irene Montero, Antonio Ruiz, 2008. "*Combustion Analysis of Different Olive Residues*". *Molecular Sciences* .

Shaobin Wang, Z.H. Zhua, Anthony Coomes F. Haghseresht, G.Q, 2004. *"The physical and surface chemical characteristics of activated carbons and the adsorption of methylene blue from wastewater*". *Colloid and Interface Science.*

Sumrit Mopoung, Phansiri Moonsri, Wanwimon Palas, and Sataporn Khumpai, 2015. "*Characterization and Properties of Activated Carbon Prepared from Tamarind Seeds by KOH Activation for Fe(III) Adsorption from Aqueous Solution*". *The Scientific World.*

Tascón, J. M. D., 2012. *Novel Carbon Adsorbents.* , Oviedo Spain, Elsevier

Venugopal Mendu, E HarmanWare, Mark Crocker, Jungho Jae, Jozsef Stork, Samuel MortonIII, Andrew Placido, George Huber and Seth DeBolt, 2011. "*Identification and thermochemical analysis of high-lignin feedstocks for biofuel and biochemical production*". *Biotechnology for Biofuels.*

Wang S a,∗, Z.H. Zhua, Anthony Coomes b, F. Haghseresht c, G.Q. Luc (2005) "*The physical and surface chemical characteristics of activated carbons and the adsorption of methylene blue from wastewater*" Journal of Colloid and Interface Science 284 (2005) 440–446
Elsevier

Zuo-Liand Liu, He-hui Zhu, 1986. "*Steam gasification of coal char using alkali and alkaline-earth metal catalysts*". *Fuel.*

Zhu, Y., J. Gao, et al. (2012). "*Preparation of activated carbons for SO2 adsorption by CO2 and steam activation.*" Journal of the Taiwan Institute of Chemical Engineers **43**(1): 112-11

Chapter 6 Pilot Scale Activation

6.1 Pilot Scale Kiln Introduction

This chapter includes all pilot scale investigations; majority of trials were conducted with olive stone as the precursor however, trials using pine wood and coconut shell were also conducted. Additionally, a single step process was tested with olive stone and pine wood. Pilot scale equipment allowed the production of kilograms rather than grams of carbon seen on lab scale which allowed an accurate estimation of scalability to industrial commercial quantities.

The pilot scale test conditions were determined by data from lab scale trials. Lab scale results with olive stone and pine wood showed how increased temperature, residence time and steam flow rate increased burn off and therefore porosity - within given boundary limits.

6.2 Lab and Pilot Scale Differences.

The main difference in addition to quantity produced between lab scale on a horizontal tube furnace and a pilot scale rotary kiln is that lab scale is a batch process whereas pilot scale is a continuous process. As such an average residence time was calculated for the continuous pilot scale. Mean residence time is an important factor when analysing the data and was calculated as shown in Chapter 3 7.1.2.

6.2.1 Reynolds Number

Reynolds number was calculated to distinguish steam flow characteristics within the kiln. Theoretically a turbulent flow would increase steam carbon mixing efficiency which is a wanted parameter. Increased mixing of steam and carbon leads to increased steam carbon contact which pushes the steam carbon reaction forward. This has been proved in Chapter 5. This increase in contact means less excess steam is required for activation to produce a certain burn off.

Calculating the Reynolds number of both systems - Lab scale at 1.5 ml/min and pilot scale at 300 ml/min.

$$Re = (\rho u^2) / (\mu u / L) \qquad \text{Equation 6-1}$$

$$= \rho u L / \mu$$

$$= u L / \nu$$

Re = Reynolds Number

ρ = density (kg/m^3, lbm/ft^3)

u = velocity based on the actual cross section area of the duct or pipe (m/s, ft/s)

μ = dynamic viscosity (Ns/m^2, lbm/s ft)

L = characteristic length (m, ft)

$\nu = \mu / \rho$ = kinematic viscosity (m^2/s, ft^2/s)

At these two respective water flows (1.5 ml/min and 300 ml/min), and their associated corresponding nitrogen flows, the total flow can be analysed to see whether it is either laminar (Re < 2300), transition (Re 2300 to 4000) or turbulent (Re > 4000).

The results show that both flows are laminar with a Reynolds number of 14 and 857 for lab and pilot scale respectively. The larger number is associated with pilot scale but, without heat tube lifters present, there remains a large void space above the carbon bed. The other benefit of having lifters, in addition to aiding mixing, is they can increase flow turbulence. In Chapter 5 the importance of steam carbon contact was shown, and turbulent flow increases mixing potential.

The first pyrolysis stages were completed with olive stone, with an aim to produce a similar char as seen in the lab scale trial. The temperature across the heat tube was set to 700 ^{o}C and a residence time of around 30 minutes was achieved by adjusting the heat tube speed. The resultant char went under proximate analysis (results below).

Table 6-1 Proximate analysis results of olive stone char (yield 32%).

Component	Raw (%)	Char (%)
Moisture	10.7	0.1
Ash (dry basis)	0.5	2.3
Volatile (dry basis)	79.0	5.5
Fixed Carbon (dry basis)	20.5	92.2

The proximate results show at 700 ^{o}C, 30 minutes a char is produced with a low volatile percentage, in line with lab scale results. This is important when comparing activation conditions and the subsequent effects as it maximises char uniformity. A portion of this generated char was used for all lab scale trials from this point (April 2014, char yield 32%). The char yield ranged from 27% and 32% depending on batch of olive stone at slightly varying moisture contents.

When sufficient char had been generated, activation trials began without the use of the steam generator; instead a supply of cold water was flowed through the kiln at different rates. One disadvantage of this method was that there was a temperature discrepancy in varying areas of the kiln. The temperature in the initial part of the kiln was lower as heat energy was being used in

the endothermic reaction, changing the phase of water to steam, which is high due to the latent heat energy requirement. This caused the first of the three heater elements on the pilot kiln to struggle and a lower temperature was needed to be set on the HMI. The other two elements were set to 850 ^{o}C. However, it must be noted the thermocouples measured the temperature at the outside surface of the heat tube. Therefore, the exact temperature of the carbon bed is unknown. The CTC results from this trial peaked at 30 meaning burn off was very low. The residence time in the kiln was around 1 to 1.5 hours with a water flow of 300 ml/min and a char feed rate of 7.25 kg/hour. This means on average there was 10.875 kg of char inside the kiln with 27 dm^3 of water entering the kiln. This gave a water/carbon molar ratio of 1.7:1. When reducing the water flow down to 100 ml/min, the CTC value remained very similar with a value of around 25.

However, the first element temperature could be raised due to less water entering and cooling the system; there are a number of possible reasons why this caused little change in the quality of activated carbon produced.

When the water flow rate was 18 dm^3/hr the first element could not provide adequate heat energy and the temperature had to be lowered. This meant that inside the heat tube the cold water was having a significant cooling effect. In addition, reducing the water flow by 200 ml/min means a large energy saving as shown below:

Table 6-2 Energy requirement at different water flows.

Energy	18 dm^3/hr	6 dm^3/hr
0-100 ^{o}C kJ	6048	2016
Evaporation kJ	40680	13560
100-800 ^{o}C kJ	26964	8988
kWh	**20.47**	**6.82**

The energy required across the kiln for the two conditions differed widely, as shown in Table 6-2. Additionally, with a higher water flow, the final steam temperature will have taken longer to reach. Whilst there was more steam in the first trial, leading to a higher chance of a successful reaction (as shown above with results and Le'Chatliers principle) in the second trial the steam will be produced quicker and reach the set temperature faster, leading to an increased reaction rate. This is why results were very similar across the two trials as a negating effect was taking place.

The next stage was to use a steam generator. The steam generated allowed up to around 300 ml/min of water flow, and the steam was directly injected into the heat tube through the hollow feed screw. Using steam instead of water allows the set temperature of the first heating element to be raised as the latent heat energy requirement of the water does not have to be

accounted for. With no latent heat energy required for evaporation from the kiln, the first section of the kiln remained hotter and at a more consistent temperature. The kiln raised the temperature of the steam from 110 °C to 800 °C which is approx. one third of the total energy required previously, as shown in Table 6-1 using the same calculations.

6.3 Reference Trial with Coconut Shell

Coconut shell char activation was used for a reference material due to being commonly available and used in the carbon market.

Coconut shell pyrolysis was conducted at 700 °C for 30 minutes and proximate analysis was carried out on the produced char.

Table 6-3 Proximate analysis results coconut shell char (yield 23%).

Component	Raw (%)	Char (%)
Moisture	8.5	0.8
Ash (dry basis)	0.7	2.2
Volatile (dry basis)	76.3	4.5
Fixed Carbon (dry basis)	23.0	93.3

Table 6-4 Results from the coconut activation trials carried out on the pilot kiln for a reference point.

Temperature (°C)	Water Flow (ml/min)	Nitrogen Flow (L/min)	Reynolds Number	Char Mass (kg)	Heat Tube RPM	Mean Residence Time (hrs)	Feed Rate (kg/hr)	Total Burn Off (%)	CTC
675-875-875	300	20	857	10.0	0.40	3.5	5.0	39.3	53.0
675-875-875	300	20	857	10.0	0.40	3.5	5.0	39.3	67.0
675-875-875	300	20	857	20.0	0.40	3.5	16.7	26.1	41.0
675-875-875	300	20	857	20.0	0.40	3.5	16.7	26.1	54.0

The coconut char was activated in the pilot kiln aided by the use of the steam generator. Changing the conditions slightly showed the possibilities of activation. The coconut char peak activation produced a CTC of 67 - this correlates with commercial carbon available today and, therefore, olive stone and pine could be activated under similar conditions.

6.4 Olive Stone Pilot Scale Activation

At this point a steam generator was now introduced for olive stone char activation. The results can be seen below in Table 6-5. Total yield and burn off are presented along with a CTC average that was calculated from a number of samples taken from each trial. Samples were taken once an hour after the initial residence time (see Chapter 3) and dried at 125 °C for 12 hours.

The experimental results are split as the first batch was conducted with old heating elements and second batch with new more insulated elements.

Batch 1

Table 6-5 Olive stone activated carbon pilot trials using old heating elements.

Temperature (°C)	Water Flow (ml/min)	Nitrogen Flow (L/min)	Reynolds Number	Char Mass (kg)	Heat Tube RPM	Mean Residence Time (hrs)	Feed rate (kg/hr)	Total Burn Off (%)	Average CTC
650-875-875	100	20	255	20.0	1.20	1.0	7.4	24.2	35.0
800-875-875	125	5	274	20.0	0.40	3.5	7.4	28.0	43.0
625-875-875	300	20	675	20.0	0.40	3.5	7.4	43.3	56.0
625-875-875	300	20	675	10.0	0.40	3.5	4.3	46.5	59.0
625-875-875	300	20	675	10.0	0.30	-	-	-	78.5
675-875-875	280	20	599	30.0	0.40	3.5	10.0	30.5	45.0

Batch 2

Table 6-6 Olive stone activated carbon pilot trials using new heating elements.

Temperature (°C)	Water Flow (ml/min)	Nitrogen Flow (L/min)	Reynolds Number	Char Mass (kg)	Heat Tube RPM	Mean Residence Time (hrs)	Feed Rate (kg/hr)	Total Burn Off (%)	Average CTC
675-800-800	300	20	675	15.0	0.50	2.5	5.0	34.9	45.5
675-800-800	100	20	255	15.0	0.50	2.5	5.0	30.4	41.5
675-800-800	200	20	465	15.0	0.50	2.5	5.0	33.7	43.5
675-875-875	300	20	255	20.0	0.36	3.5	5.0	47.7	59.0
675-875-875	100	20	255	20.0	0.36	3.5	5.0	42.5	51.0
675-875-875	200	20	465	25.0	0.36	3.5	5.0	11.8	21.5
675-875-875	200	20	465	17.5	0.36	3.5	5.0	46.6	57.5
600-700-700	300	20	675	17.0	0.36	3.5	5.0	23.8	28.5
700-875-875	300	20	675	18.5	0.50	2.5	5.0	41.7	57.0

The CTCs were placed on the optimum burn off, CTC correlation graph first seen in Chapter 5.

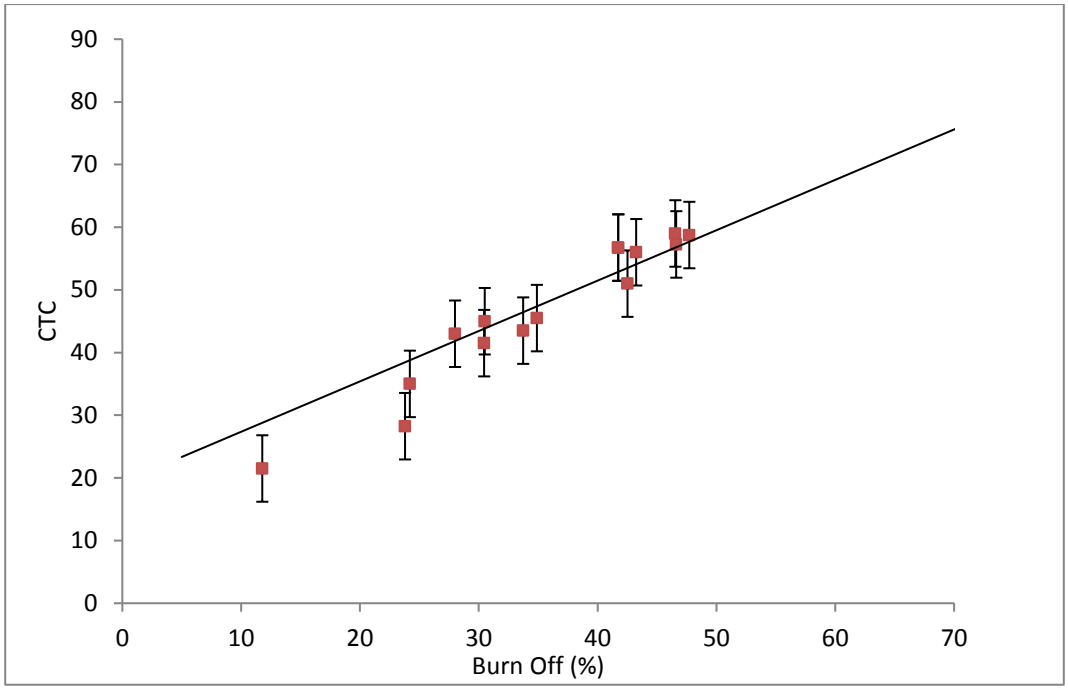


Figure 6:1 Pilot scale activation of olive stone char in comparison to optimum CTC, burn off (%) correlation from Figure 5:2. Error bars (SD).

Individual CTCs ranged higher than shown in Figure 6:1, the data points used were averages with the associated error bars (SD). Samples were collected at different stages throughout the day and different burn offs were occurring, this was due to initial heating of the kiln and then the subsequent cooling once the kiln was turned off towards the end of the day. The samples at steady state were used for CTC testing. The trial that produced the highest CTC (78) in batch 1 could not have the associated yield calculation due to the feed rate and kiln speed being too slow with the kiln having to be turned off before completion (as shown in Table 6-5). The average CTC values for completed trials fell well in regards to the optimum CTC burn off relationship observed on lab scale.

These set of results give credence to the finding that there is a direct correlation with CTC and burn off with olive stone carbons on larger scales. The lower burn off trials meant the results fell further way from the optimum trend line but as stated; commercially viable carbons tends to have a CTC of > 40 and after this point the correlation with lab scale results is strong.

6.5 Pilot Scale Activation of Pine Wood Char

Initially pine wood biomass was charred under the same conditions as with olive stone pyrolysis, the exception an increased feed rate due to the difference in densities and produced the following proximate analysis results. The char yield ranged from 17% to 20% depending on batch and moisture content.

Table 6-7 Proximate analysis results pine wood char (yield 17.1%).

Component	Raw (%)	Char (%)
Moisture	15.7	0.8
Ash (dry basis)	0.6	1.6
Volatile (dry basis)	81.9	3.3
Fixed Carbon (dry basis)	17.5	95.1

This char was then activated as shown below.

Table 6-8 Pine wood activation results.

Temperature (°C)	Water Flow (ml/min)	Nitrogen Flow (L/min)	Reynolds Number	Char Mass (kg)	Heat Tube RPM	Mean Residence Time (hrs)	Feed rate (kg/hr)	Total Burn Off (%)	Average CTC
700-840-840	200	20	465	8.3	0.50	2.50	2.5	64.9	91.0

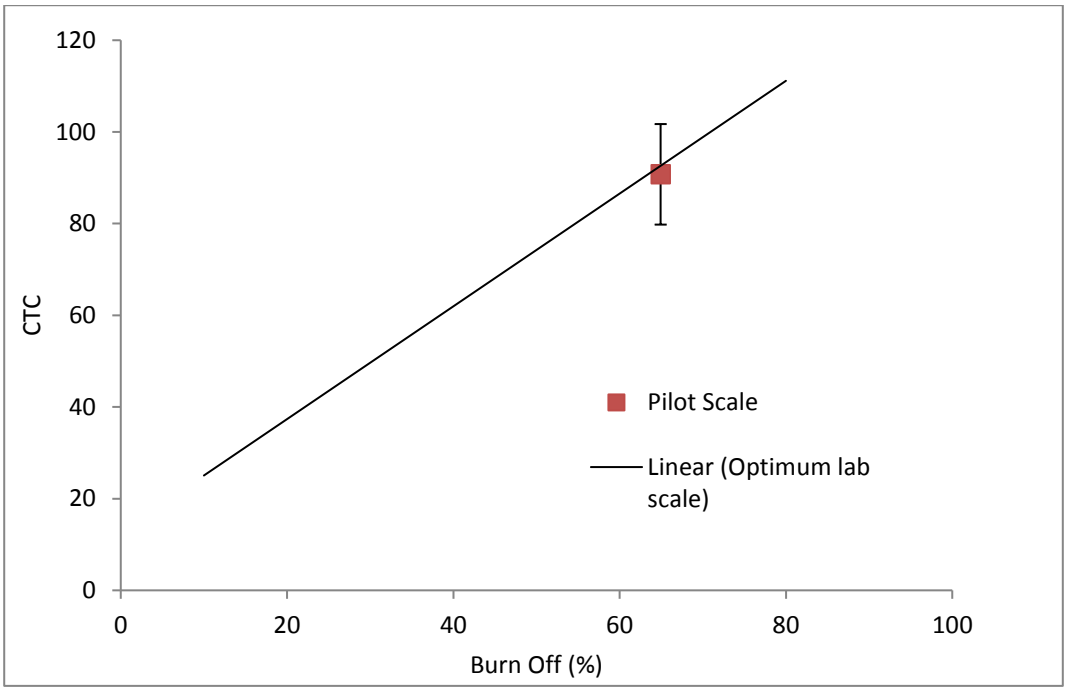


Figure 6:2 Pilot scale activation of pine wood char in comparison to optimum CTC, burn off (%) correlation from Figure 5:4. Error bars (SD).

As with olive stone char activation, pine wood char activation was carried out in a similar way with an exception to feed rate and heat tube speed (rpm) which were increased and temperature decreased. As Chapter 5 lab scale results showed, at an activation temperature of 800 °C pine wood required less residence time to achieve a specific burn off compared to olive stone, because of this pilot scale pine wood activation was carried out with a residence time of 2.5 hours as opposed to 3.5 hours used for olive stone activation. The activation temperature was reduced

slightly as lab scale results showed how pine wood char not only requires a lower activation temperature to achieve a specific burn off but also destruction initiates at lower temperatures compared to olive stone. Although only a single data point was taken, it still fits well within the CTC burn off optimum lab scale trend line.

6.6 Single Step Pilot Scale

Two single step trials were completed on pilot scale with olive stone and pine wood similar to the lab scale single step trials where pyrolysis and activation occur simultaneously.

6.6.1 Olive Stone Single Step Activation

With olive stone, the rotary kiln has produced similar char yields to those obtained from lab scale "slow" pyrolysis as shown in Chapter 5. As there wasn't time to conduct another pyrolysis run on the pilot kiln with the new batch of olive stone (also used for the lab scale single step trials) it was assumed that the char yield would be the similar (approx. 27.5% dry basis). The moisture content was measured to be 14.5%. Therefore an expected char yield for single step production is 23.5%; this char yield value is used to calculate the burn off percentage in Table 6-9.

Table 6-9 Results table for single step trial of olive stone activation.

Temperature (°C)	Water Flow (ml/min)	Nitrogen Flow (L/min)	Reynolds Number	Char Mass (kg)	Heat Tube RPM	Mean Residence Time (hrs)	Feed rate (kg/hr)	Total Burn Off (%)	Average CTC
750-875-850	200	20	465	24.8	0.40	3.5	5.0	75.6	74.0

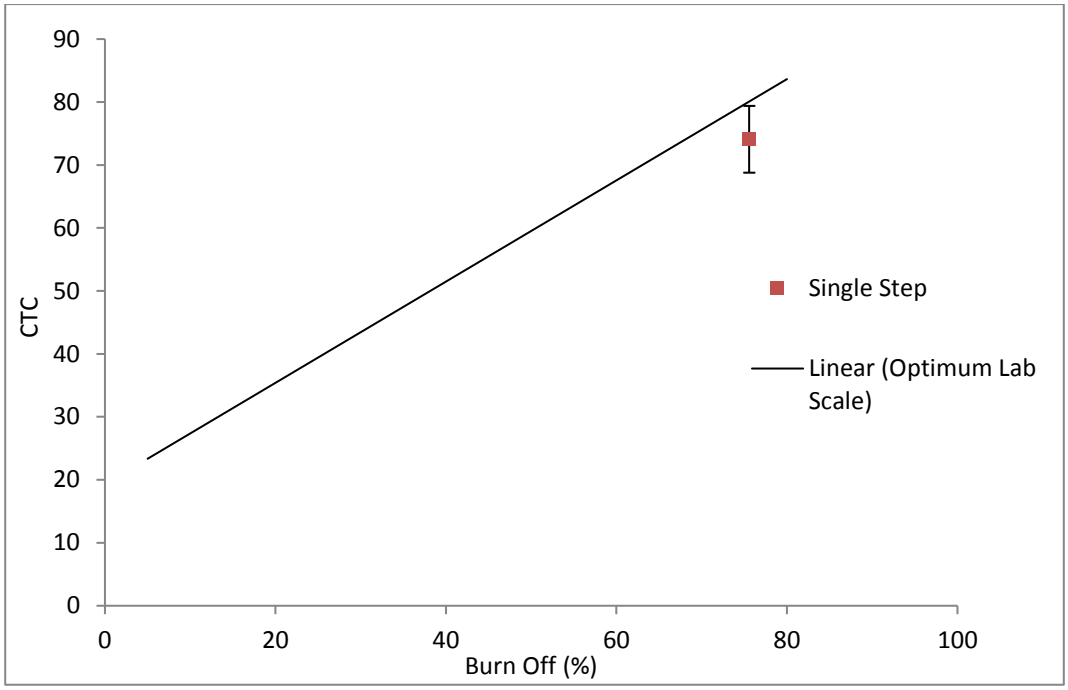


Figure 6:3 Single step data point of olive stone compared to optimum CTC, burn off (%) correlation Figure 5:2 Chapter 5. Error bars (SD).

Two sample batches were collected at set time intervals and dried for 12 hours. From this CTCs tested three times on each sample. An overall mean was calculated with standard deviation error bars shown in Figure 6:3. As with the two-step trials the average CTC value fell close to the optimum trend line from lab scale results. More trials must be done in this area to prove this to be conclusive. However, the initial signs are that it also follows the trend. The next trial involved using pine wood in the same fashion.

6.6.2 Pine Wood Single Step Activation

Unlike with olive stone single step trials, pyrolysis was conducted on the biomass batch that was used for single step production. This yield was used to calculate the burn off percentage in Table 6-10. The pyrolysis yield for this given batch was found to be 19.9% with an initial moisture content of 17.5% which again fits into the "slow" pyrolysis results found on lab scale trials in Chapter 5.

Table 6-10 Results table for single step trial of pine wood activation.

Temperature (°C)	Water Flow (ml/min)	Nitrogen Flow (L/min)	Reynolds Number	Char Mass (kg)	Heat Tube RPM	Mean Residence Time (hrs)	Feed rate (kg/hr)	Total Burn Off (%)	Average CTC
700-850-800	200	20	465	30.3	0.80	1.5	2.5	38.6	59.3

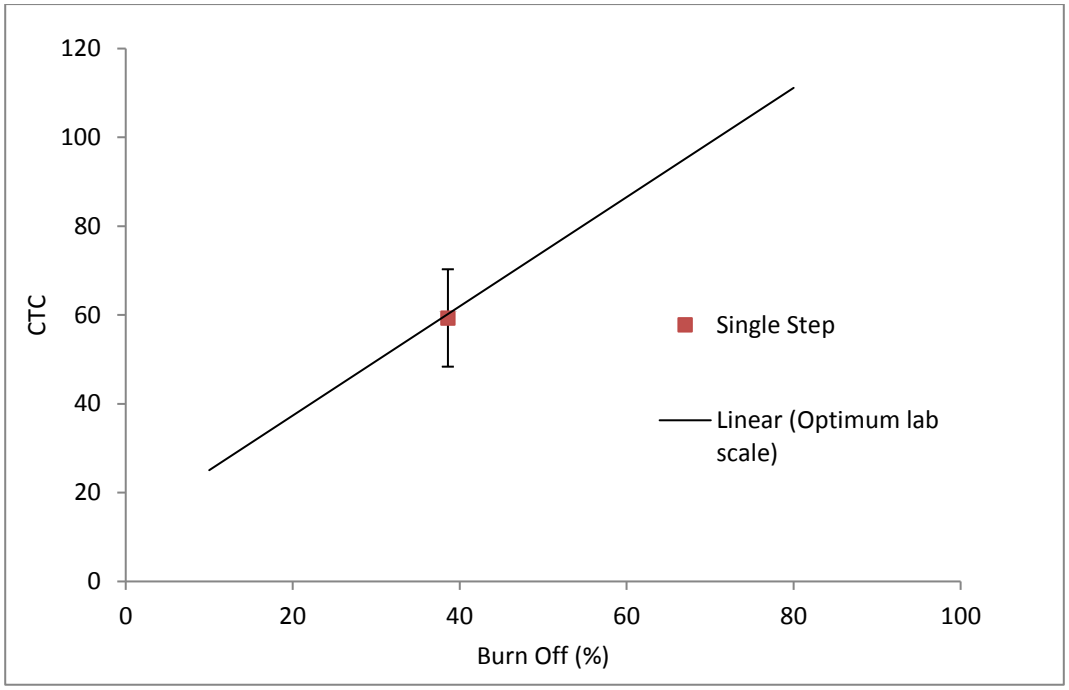


Figure 6:4 Single step data point of pine wood compared to optimum CTC, burn off (%) correlation Figure 5:4 Chapter 5. Error bars (SD).

Pine wood activated carbon produced via the single step method also produced a carbon that fits well to the optimum burn off CTC ratio produced on lab scale. Again further trials are needed along the burn off range. However, the single step approach showed little difference between lab and pilot scale. As previously mentioned in Chapter 5, single step production does not come without design issues yet both CAPEX and OPEX cost savings can be significant if the obstacles can be overcome.

6.7 Additional Analysis

Hardness tests were conducted on olive stone, which came out as 86 %. This percentage was exactly the same as a commercial carbon that was tested on the same apparatus following the method stated in Chapter 3.

Iodine numbers were conducted on three samples of olive stone carbons that had CTC values of 78, 65 and 52. The iodine numbers found were 1150 mg/g, 960 mg/g and 740 mg/g respectively. The iodine number for the commercial carbon also came out at 940 mg/g proving the carbons produced here are comparable to carbons currently in the market.

6.8 The Importance of Steam Carbon Contact

Steam production can be expensive and so it is beneficial to utilise a maximum amount of this steam produced. In doing this the process efficiency is increased meaning reduced process and energy requirement costs. Therefore to achieve this, the mixing efficiency is crucial when it comes to designing a suitable rotary kiln. In addition it is important for the char particle size to

be uniform with the smallest char particle size used for activation, this can be determined by the specified end product particle diameter. This is because the smaller the particle the easier and quicker the diffusion of steam into the centre of the particle. This was studied by [Huo, 2014] who states their results show that the pore diffusion resistance increases with increased particle size. Also it was found that gasification rates of these three chars decreased as the particle size increased. The end application must be considered however, as there may be a minimum particle size required.

A uniform end product is also desired and therefore it is beneficial for each char particle to be exposed to the same amount of steam during activation. On small scale experiments the material is placed into a crucible with a bed depth of (10 mm), however the top layer of char will theoretically be more exposed to the passing steam than the lower "sheltered" layers. An experiment was conducted to see if this had a significant impact on uniformity and, although it did not in that case (see Chapter 5), a deeper bed depth than 10 mm is likely to have impact. On a commercial scale rotary kiln there is likely to be lifters present in the heat tube to help prevent this occurrence. The lifters long with heat tube rotation are required to ensure steam carbon contact. One design that is currently used is during rotation the char is picked up by the lifters and held till it reaches the top of the tube, the char then falls back to the char bed utilizing the void space in the heat tube and passing through the steam flow. This process happens throughout the length of the heat tube. An image of this type of mixer is shown below:



Figure 6:5 Rotary kiln heat tube mixers (zcrusher 2015).

If this project were to continue, testing these types of mixers on pilot scale may be beneficial in ways to improve process efficiency.

6.8.1 A Single Step Process Kiln Concept.

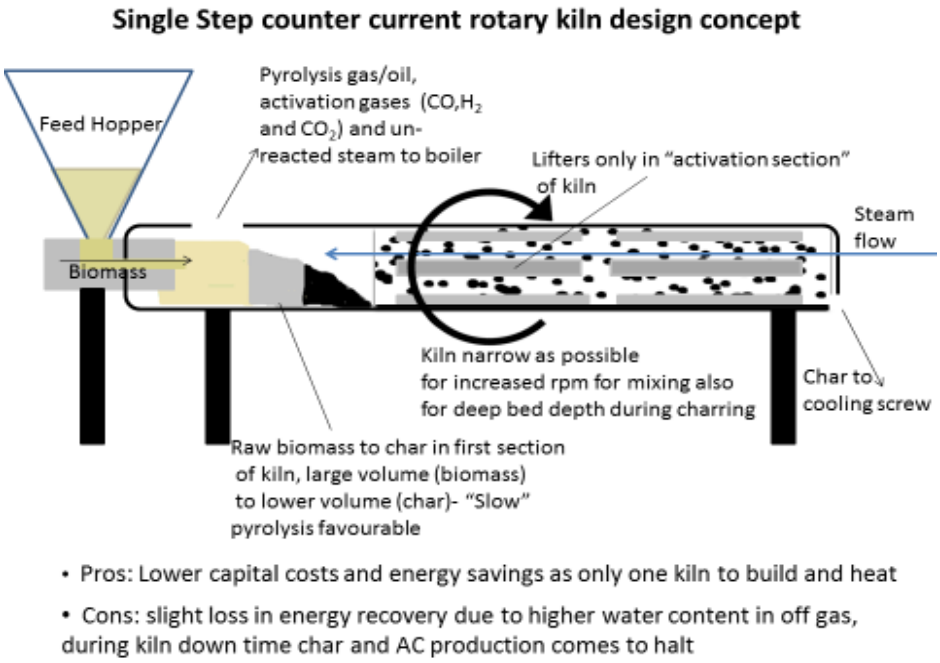


Figure 6:6 Single step rotary kiln process concept.

Data from both Chapter 5 and Chapter 6 show that a single step process produces a similar carbon for both olive stone and pine wood. As mentioned there are design obstacles to overcome e.g. a second stage is required to separate water and volatile components released during pyrolysis. However, a kiln concept is shown in Figure 6:6. Knowing that the single step yields similar carbons, the pyrolysis and activation steps can be undertaken simultaneously on one kiln, saving on capital expenditure. In literature counter-current activation kilns are usually employed such as by Ortiz *et al.* [2003, 2007] who worked on rotary kiln optimisation for eucalyptus wood activation. This is different to the co-current pilot kiln used in this project. A counter-current system maximises contact between the gas and solid phases. Similarly mixers increase contact and have been discussed above and are used within industry to produce carbons as well as for regeneration purposes.

Another design to increase contact is to have a narrow but long kiln - as long as the minimum throughput can be reached. A narrow long kiln allows an increased rpm of the heat tube, leading to more mixing as the carbon will be lifted and dropped at an increased rate. The length is important to facilitate residence time of the steam carbon contact whilst maintaining a higher rpm. The pyrolysis stage does not require lifters as mixers are likely to reduced secondary pyrolysis that can happen through a deep bed of biomass. A deep bed results increased pyrolysis yields as reported by [Boroson *et al.*, 1989]

6.9 Pore Analysis on Pilot Scale Material

A selection of pilot kiln produced carbons (olive stone) were tested and the results can be seen in the figure below and in Table A-17 in Appendix

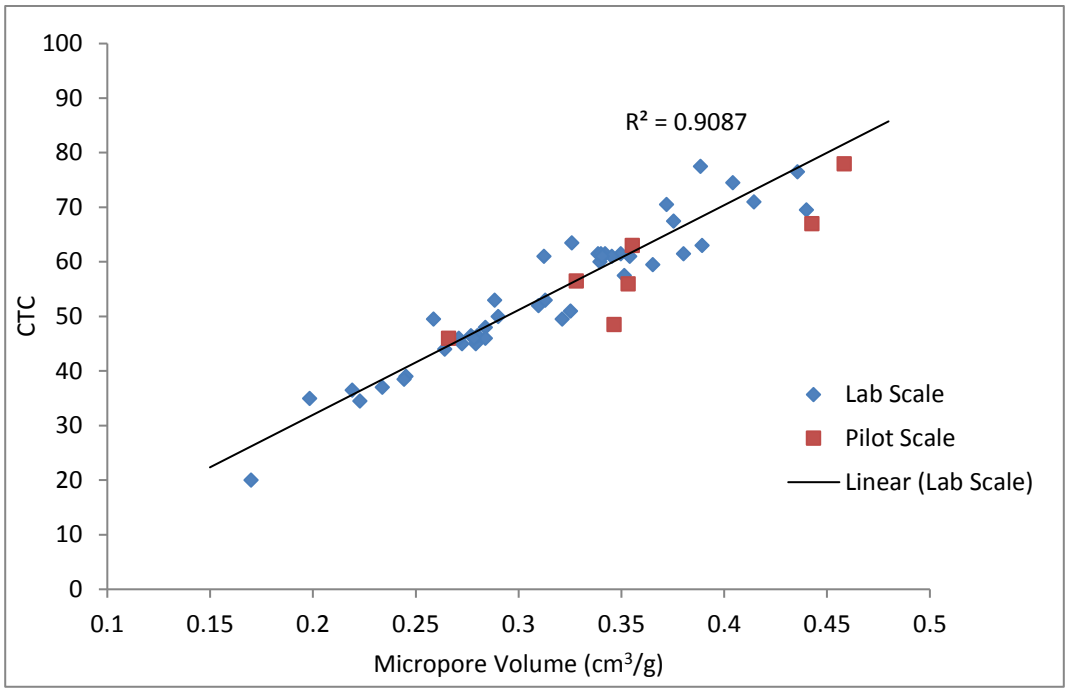


Figure 6:7 Pore analysis (micropore cm^3/g) of both lab and pilot scale olive stone activated carbons.

The pilot scale carbons are less uniform than the lab scale carbons due to the nature of how they are produced on pilot scale as shown by the error bars seen in this chapter. However, the results show they are not too far away from the lab scale olive stone activated carbons and they follow the same pattern in terms of micropore volume relationship with CTC results. The mesopore volume were also comparable to lab scale produced carbons shown in Table A-17.

6.10 Conclusions

1. Similar highly porous olive stone and pine wood carbons were produced on the pilot scale rotary kiln compared to lab scale production despite stated differences between the lab and pilot scale production. Results match lab scale results with burn off percentage and CTC correlation strong proving scalability of the carbons.
2. The drawback of the large scale production was that the rotary kiln produced less uniform carbon than lab scale with higher error due to nature of production, such as a thicker carbon bed and no lifters within the heat tube to enhance steam carbon mixing.
3. As with lab scale production without mixers present incorporated in the heat tube steam flow still laminar reducing maximum mixing potential of the steam and carbon.
4. Single step carbon production for both olive stone and pine wood was successful by following the CTC, burn off percentage correlation seen throughout the lab scale and pilot scale two step production process.
5. Pore analysis results for olive stone activated carbons tested show near identical results regarding micropore volume and CTC correlation. This shows that the CTC test can provide a clear indication of micropore volume across different production scales.
6. The peak CTC value observed with an olive stone activated carbon sample on pilot scale production was 78 and with the peak value of a pine wood carbon sample being 91.
7. Olive stone activated carbon produced on pilot scale produced surface areas up to 1157 m^2/g which was approximately the same peak value seen on lab scale production with a micropore volume of 0.458 cm^3/g. This peak performing carbon was produced at 675-875-875 ^oC across the three heating elements, with an approx. 240 minutes residence time and 300 ml/min water flow.

6.11 References

Anon, 2015. *FDM.* [Online]
Available at: http://www.zcrusher.com/rotary-kiln.html
[Accessed April 2015].

Michael L. Boroson, Jack B. Howard, John P. Longwell, William A. Peters 1989 **"***Heterogeneous cracking of wood pyrolysis tars over fresh wood char surfaces Energy and Fuels" 3* (6), pp 735–740

O. A. Ortiz, N. D. Martinez, C. A. Mengual and P. M. Abally, 2007. "*Optimal Operation Profit of a Pilot Kiln for Charcoal Activation".*

Oscar A. Ortiz Nora D. Martínez, Carmen. A.Mengual and Pablo M. Aballay Instituto de Ingeniería Química – Universidad Nacional de San Juan, 2003. "*Optimisation Study of Pilot Rotary Kiln for Activated Carbon Production*". *Enpromer.*

Wei Huo, Zhijie Zhou ⇑, Fuchen Wang, Yifei Wang, Guangsuo Yu, 2014. "*Experimental study of pore diffusion effect on char gasification with CO2 and steam". Fuel,* p. Pages 59–65.

Chapter 7 Cost Analysis Model

7.1 Process Overview

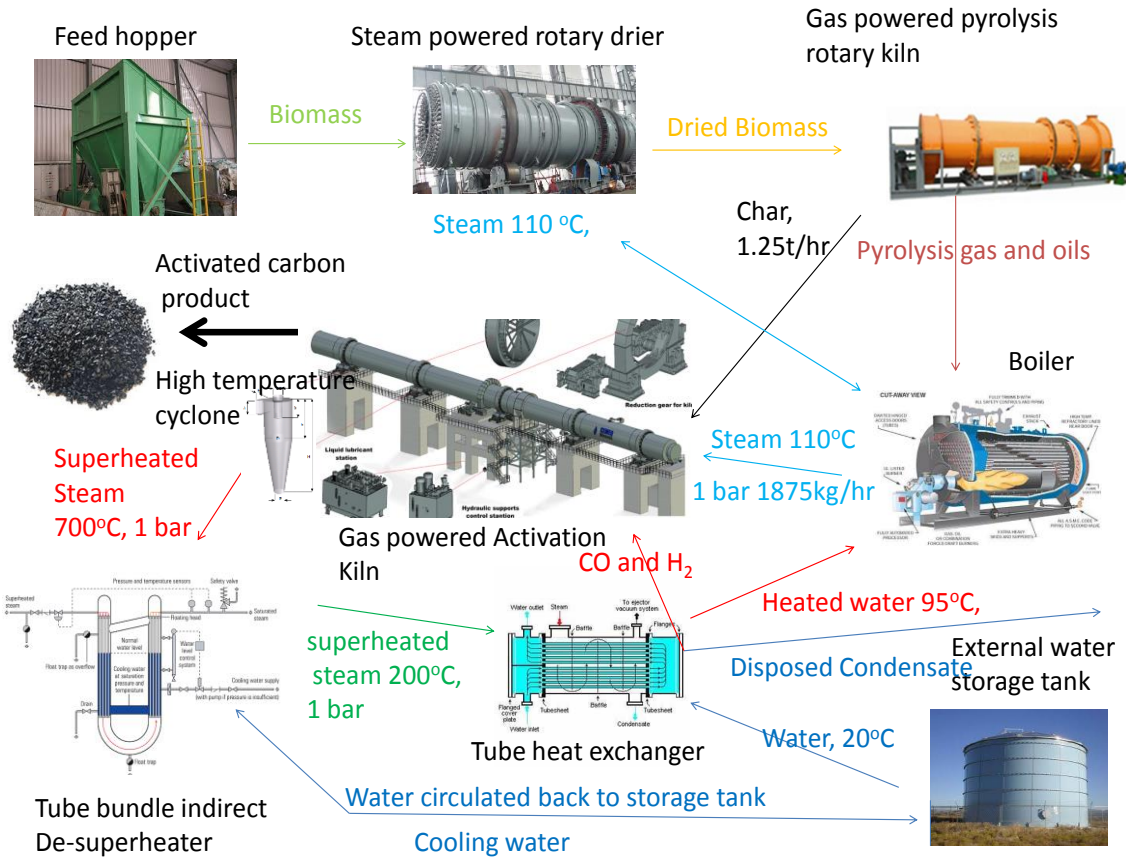


Figure 7:1 A possible production process, used in the given examples in Chapter 7.

Figure 7:1 shows a possible production process to produce both granular (olive stone) and powdered (pine wood) activated carbons. The model contains a two-step production, first being pyrolysis followed by steam activation. There is an option to use a steam powered pre drier to dry the biomass or simply can place raw biomass straight into the pyrolysis kiln. Energy recovery is included in the form of a heat exchanger and boiler that reduces the amount of natural gas required to power the process and heat water. Additionally, water recovery is integrated to reduce the amount of fresh water required. This along with energy recovery will help to reduce the carbon footprint of the process.

7.2 Introduction

The below financial model has been made on a theoretical plant design (Figure 7:1) taking results provided from both lab and pilot scale. Capital costs have been calculated based on previous studies. [RK Sinnott, 2005].

The cost analysis model has been made using Microsoft Excel for two different biomass types: olive stone and pine wood. Both have different characteristics in regard to product yield, carbon quality and selling price due to their physical characteristics and possible application uses. The selling price has been taken from alternative carbons available from information gained at the Biogas and AD Exhibition at the Birmingham NEC, 2016. The production plant has a specific chosen process for this model. However, there are many options and alternatives that can be used.

7.3 Application Examples

During this chapter two examples are used to show how the financial and process model works. This is an olive stone activated carbon with a CTC of 60 and pine wood activated carbon of a CTC of 70. The moisture contents used are 20% and 30% respectively which goes in accordance with the initial moisture contents seen during this project with the two biomasses.

The chosen olive stone carbon was selected for this example as it is of similar specification to a tested commercial activated carbon that is currently used for removal of H_2S (purifying biogas). The pine wood activated carbon (powdered) application example would be either decolouring in a liquid phase and/or for use in the pharmaceutical industry where the powdered carbon is more commonly used for removal of hazardous chemicals where pressure drop is not an issue. Powdered carbons are generally cheaper as they cannot be used for as many industrial applications and cannot be reactivated.

7.4 Option 1 Drying and Pyrolysis

At the start of the model produced in Microsoft Excel the chosen biomass can be selected from the drop down menu

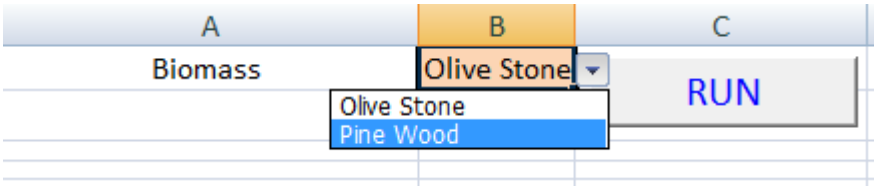


Figure 7:2 Initial required biomass selection.

Once the biomass has been selected the VBA code can run by pressing "RUN" within the spreadsheet to calculate drying and pyrolysis energy requirements for the desired biomass type.

When “RUN” is selected the seven spreadsheets are updated including the activation, capital costs, break even analysis etc.

The first sheet is titled pyrolysis and consists of two Options.

Option 1: The biomass is dried in a pre-drier (steam powered) before entering the pyrolysis rotary kiln.

Option 2: The biomass is directly placed into the rotary kiln at the given moisture percentage.

Initially the yearly char production target (tonne) is chosen and inputted in the spreadsheet. For this written example, 10,000 tonnes of char was required. The plant is assumed to be running for 8,000 hours per year which takes into account down time and equipment maintenance, this is the standard operating hours targeted by typical industrial plants [Mahadevan, 2009]. This means that an average char production of 1.25 t/hr is required.

From pilot scale results the char yield is known for both biomass types. The yield was calculated based on a dry basis. The used yields (dry basis) for olive stone and pine wood were 35.83% and 20.24% respectively. This is based on pyrolysis at 700 ^{o}C for 30 minutes with specific batches of raw material.

The box titled “moisture %” as shown in Figure 7:3 must be altered according to the current stored biomass moisture content prior to production

Yield dry (%)	35.83
Moisture (%)	**20.0%**
Pyrolysis yield (%)	28.66

Figure 7:3 Pyrolysis yield (%) of olive stone and the moisture content inputted to the financial model.

Figure 7:3 shows the values for olive stone, at 20% moisture (the maximum percentage that can be selected is 60% for both biomasses) the char yield is 28.7%. Figure 7:4 below shows the values for pine wood using the chosen examples.

Yield dry (%)	20.24
Moisture (%)	**30.0%**
Pyrolysis yield (%)	14.17

Figure 7:4 Pyrolysis yield (%) of pine wood with the selected moisture content.

Pine wood pyrolysis yield (14.2%) under the chosen moisture content is much lower.

The next step was to calculate the energy required to remove the moisture if using Option 1 above. For this the following information was required:

1. The specific heat capacity of biomass. 2.5 kJ/kg was used for both biomass types. This is based on the pine wood biomass value which is readily available and the highest value was chosen.
2. The specific heat of water, 4.2 kJ/kg.
3. The latent heat of water, 2257 kJ/kg.

All values were taken from [Engineering Toolbox, 2015].

$$Q = mC\Delta\mathrm{T} \qquad \textbf{Equation 7-1}$$

The assumed biomass initial temperature (T_1) was 20°C.

The moisture content (kg) and solid content (kg) was calculated per tonne of biomass.

Therefore to heat both the liquid fraction and solid fraction to 100 °C: (Following example calculations will assume 1 tonne of olive stone at 20% moisture). Using Equation 7-1:

Solid fraction:

$$Q = 800 \times 2.5 \times (100 - 20) = \frac{160{,}000\ \mathrm{kJ/kg}}{3600\ s} = 44.44\ kWh$$

Liquid fraction:

$$Q = 200 \times 4.2 \times (100 - 20) = \frac{67{,}200\ \mathrm{kJ/kg}}{3600\ s} = 18.67\ kWh$$

Both the values in the model were expressed as kWh - to get this both values are divided by 3600 (number of seconds in an hour)

The next step was to calculate the energy requirement to evaporate the 200 kg of water present:

$$Q = M\ (kg) \times L\ kg/kJ \qquad \textbf{Equation 7-2}$$

$$\frac{200\ (\text{kg}) \times\ 2257(\text{kg/kJ})}{3600\ (s)} = 125.39\ kWh$$

Total kWh was multiplied by £/kWh. The average industrial price paid for gas was selected at 0.025p/kWh. [DECC, 2015]

Total energy requirement to dry:

$$44.44\ +\ 18.67\ +\ \ 125.39 = 188.5\ kWh$$

The total cost to dry 1 tonne at 100% efficiency would be £4.71. However, the actual efficiency needs to be considered.

The next step was to calculate the energy cost of using the drier both £/hr and £/t. To do this the required throughput was calculated. On a dry basis the amount of biomass required to produce 1 tonne of char:

$$\frac{1}{\text{dry yield }\%}$$ **Equation 7-3**

Taking into account moisture percentage:

$$\frac{1}{\text{Actual yield }\%}$$ **Equation 7-4**

As 10,000 tonnes of char are required in 8000 hours this value was multiplied by 1.25.

Using Equation 7-4 to calculate the throughput of raw biomass needed to produce 1 tonne of char (example olive stone at 20% moisture):

$$\frac{1}{28.66\ \%} = 3.49\ t/hr.$$

Throughput required per hour =

$$3.49\ \times \frac{mass\ char\ t/yr\ (10000)}{Working\ hrs/yr\ (8000)}$$ **Equation 7-5**

$$= 4.36\ t/hr$$

This can be calculated from the cost to dry 1 tonne as above (£4.71). At 100% efficiency the energy £/hr for olive stone biomass to be dried at 20% moisture:

$$Drying \quad £/t \quad \times Throughput \quad t/hr \qquad \textbf{Equation 7-6}$$

$$£4.71/t \times 4.36 \text{ t/hr} = £20.54/\text{hr}$$

The drier efficiency was selected at 40%. Industrial drier efficiencies usually fall below just 50% [Kemp, 2012]. For this purpose a contingency of 10% was selected.

The energy £/hr in the drier was calculated by:

$$\frac{£/hr \; Efficiency \; (100\%)}{Actual \; Efficiency \; (40\%)} \qquad \textbf{Equation 7-7}$$

In this case the cost is calculated at £51.38/hr at 20% moisture.

Using the same method, the cost for the rotary drier at any given moisture percentage can be calculated for both energy cost (£/kWh) per tonne of char produced and cost on an hourly basis (£/hr). The yearly cost (£/yr) was also calculated by multiplying by 8000 hours.

As the model is mainly based on cost per tonne, the cost per tonne of produced char in this example worked out to be £41.10/t

It must be noted that as the moisture percentage rises, the drier needs to facilitate the higher biomass throughput which increases capital costs due to an increase in drier size required.

Continuing with Option 1, the next step is the pyrolysis stage of the dried material, example using pre dried olive stone:

The known dry yield of olive stone is 35.83% from trials conducted on pilot scale. From this the feed rate of biomass into the kiln can be calculated so that 10,000 tonnes of char are produced per year.

This 10,000 tonnes is to be produced in the 8,000 operating hours. This means that the required char production rate is 1.25 t/hr requiring 3.49 t/hr of dried biomass as previously calculated.

Based on an experiment conducted by S Russell [May 2015] on pine wood, the make-up of products during pyrolysis is as follows:

Table 7-1 Pyrolysis gas, oil and char percentages of pine wood.

Component	%
Pyrolysis gas	50.00
Pyrolysis oil	29.76
Char	20.24

For olive stone it is assumed that the ratio of gas to oil remains the same from the char yield.

Table 7-2 Pyrolysis gas, oil and char percentages of olive stone.

Component	%
Pyrolysis gas	40.23
Pyrolysis oil	23.94
Char	35.83

Large weight loss occurs between 300 ^{o}C and 500 ^{o}C during olive stone pyrolysis on a rotary kiln [P. Sanginesa *et al*., 2013]. As such, 350 ^{o}C was chosen as the main weight loss stage. This is the assumed point at which volatiles are given off and the specific heat for each fraction changes.

The first part of the calculation assumes that the biomass stays as a solid up to 350 ^{o}C at which point the gas and liquid components evolve. It is also assumed the biomass enters at 50 ^{o}C directly from the drier.

Using Equation 7-1:

$$\frac{3.49 \times 10^{3} \times 2.5 \times (350-50)}{3600} = 726.8\ kWh$$

The solid is assumed to have reached its final yield at 350 ^{o}C. However, volatile matter evolves over a large range in temperature depending on the composition of cellulose, hemi-cellulose and lignin components (as discussed in previous chapters). Nevertheless, for this initial cost analysis, this temperate is used for comparative purposes.

The three fractions solid, liquid and gas, now must reach the final pyrolysis temperature of 700 ^{o}C. For this, the specific heat energy requirements for each fraction must be known:

Table 7-3 Specific heats for each fraction [engineering toolbox, 2015].

Component	kJ/kg
Solid	2.5
Liquid	1.8
Gas	1.2

Next the required energy (kWh) calculation was completed taking into account the weight of the solid, liquid and gas components using the percentage yields of the three fractions shown in Table 7-2

Table 7-4 Associated energy cost to heat the three fractions to 700 °C.

Component	kWh
Solid	303.8
Liquid	146.2
Gas	163.7
Total	1340.5

The total energy shown in Table 7-4 is based on 100% efficiency. Rotary kilns operate at a much lower efficiency than this and are usually at between 50% to 60% efficiency [L.Goovaerts, *et al*, 2001]. In this instance 45% efficiency will be used to include contingency or worst case scenario for the calculations, again 10% lower than the mean stated value.

Actual kiln energy requirement:

$$\frac{total\ energy\ required\ (kWh)}{efficiency\ \%} \qquad \textbf{Equation 7-8}$$

In this case the total kiln energy requirement is 2978 kWh at a cost of £74.47/hr and £59.58/t.

Option 1 which consists of a pre drier and pyrolysis kiln energy OPEX per tonne:

$$Drying\ Cost + Pyrolysis\ Cost\ (£) = \boldsymbol{£100.68/t}$$

7.5 Option 2 Pyrolysis

Option 2 consists of no drier, only a rotary kiln for pyrolysis. Using olive stone at 20% initial moisture the yield is 28.7%. The same oil and gas ratios are used as before except now the solid fraction is lower due to the 20% moisture content.

The amount of biomass needed at different moisture levels for the pyrolysis kiln is calculated within the model. For example (olive stone 20% moisture) the biomass required throughput is 4.36 tonnes per hour. This is an increase of 0.87 tonnes per hour compared to the dry biomass.

Solid = 3.49 t/hr

Water (20%) = 0.87 t/hr

The energy required to bring the solid and liquid fractions to 100 ºC was carried out using to using Equation 7-1. Values of the solid and water component are 193.8 kWh and 81.4 kWh respectively. Subsequently the same calculations as Option 1 were carried out for solid, liquid and gas fractions. However, now there is a fourth added fraction, moisture. This unwanted moisture adds to total energy requirement for char production. The water requires energy for heating to boiling point followed by vaporisation. The steam produced will reach the final pyrolysis temperature requiring further energy. The vaporisation for 0.87 t takes 546.8 kWh followed by a further 305.3 kWh to reach 700 ºC.

This is added to the values calculated for the solid which is heated up to 350 ºC and then to the solid, oil and gas up to 700 ºC which are 605.7 kWh, 303.8 kWh, 163.7 kWh and 146.2 kWh respectively.

With a kiln efficiency of 45% the total energy required:

= 5214.9 kWh

Cost per tonne char produced using biomass at 20% moisture = **£104.30 /t**

The energy required for Option 2 is higher than Option 1 during the pyrolysis stage at this moisture content because the moisture in the biomass requires heating, vaporising and then heating to final pyrolysis temperature.

The pros and cons of having a pre-direr are shown below in Table 7-5

Table 7-5 Pros and cons of having the biomass dried.

Pro	Con
• lower CAPEX of pyrolysis kiln • Lower or no moisture to heat up to final temperature • biomass dried can be stored longer, lowers risk of mould growth • higher char production rate at same kiln size • Boiler efficiency (energy recovery) higher with no moisture	• CAPEX of drier • higher maintenance cost • more room needed for two units • another operator potentially required • May not be worth it a lower moisture %

In this example Option 2 is slightly more expensive per tonne char produced. The graph below shows this across moisture percentage range (0-60%) for both olive stone and pine wood

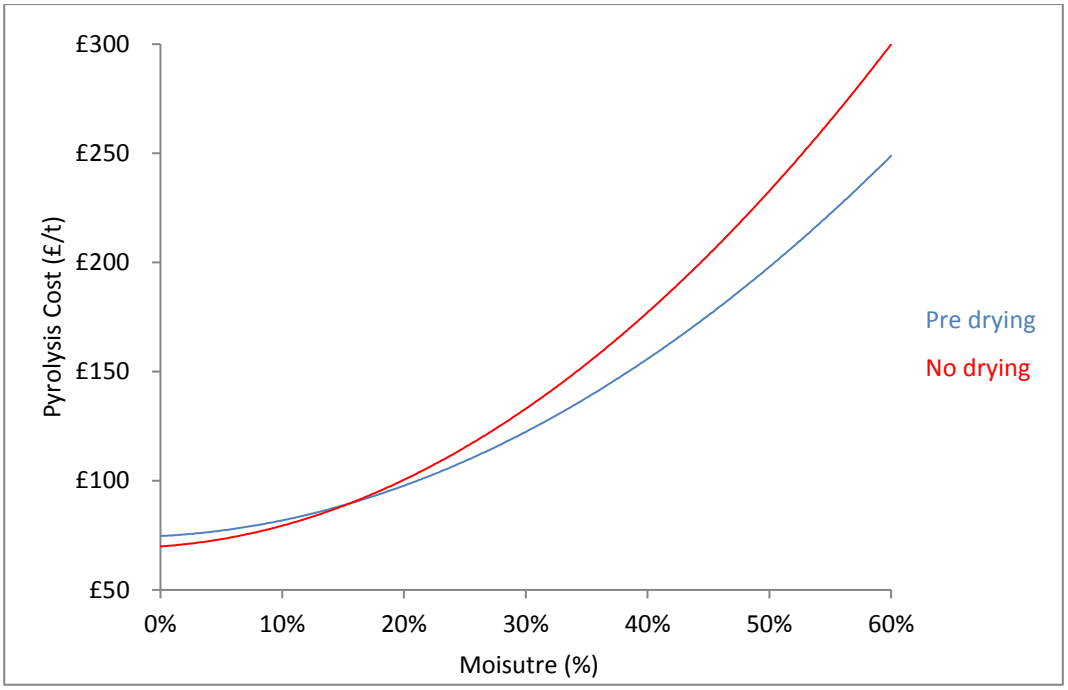


Figure 7:5 Energy OPEX (£/t) difference between Option 1 and Option 2 for olive stone.

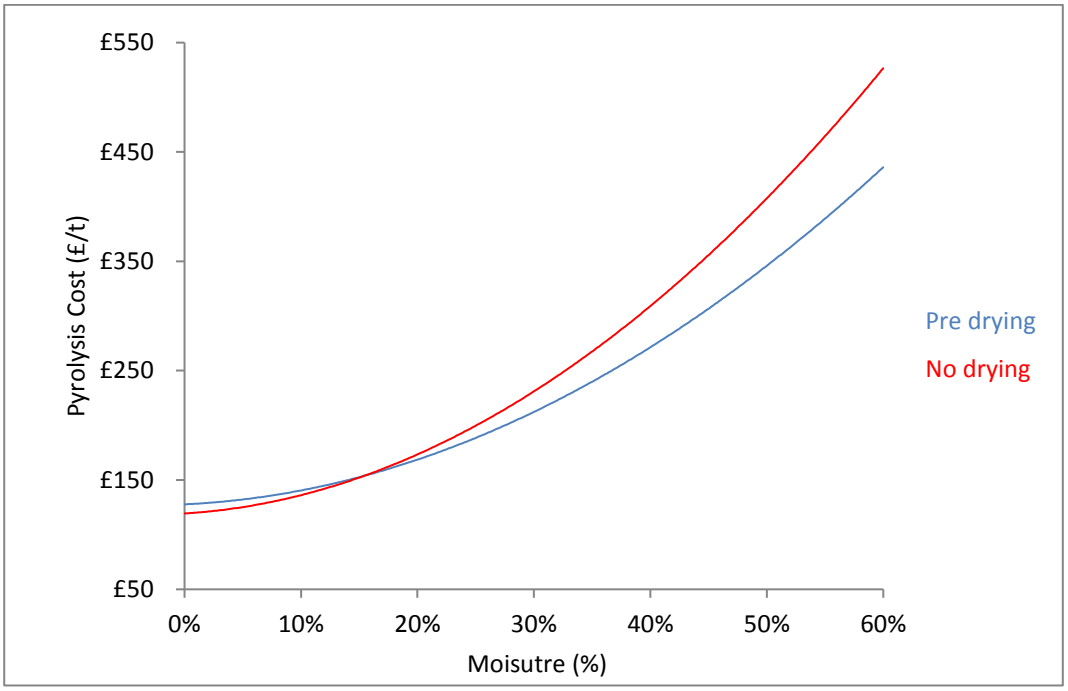


Figure 7:6 Energy OPEX (£/t) difference between Option 1 and Option 2 for pine wood.

When moisture content reaches approx. 15% Option 1 becomes favourable. It is common for wood biomass moisture content to be over 15%. Olive stone can vary as seen in this project and be below this figure; 10% moisture was received in the first large batch of olive stone. However, as shown in Table 7-5, the pros and cons must be considered when making any decision. The other thing to deduce from Figure 7:5 and Figure 7:6 is that, per tonne of char produced, olive

stone is much cheaper to carbonise than pine wood. This is due to the higher yields allowing throughput to be lowered to achieve the same char production rate as pine wood.

7.6 Activation Stage

The next part of the model is activation and follows directly from pyrolysis. It is assumed that the full 10,000 tonnes a year have been produced during the pyrolysis stage. There are two parts of the activation model labelled "Olive Stone Activation" and "Pine Wood Activation"

The desired carbon is selected as shown in Figure 7:2 along with the desired CTC of the carbon. The CTC has been proven to be a very good indicator of overall quality in terms of BET surface area and pore volume, along with general adsorption qualities proven as shown in previous chapters.

The CTC is selected as shown in Figure 7:7. The CTC range that can be selected in the model for olive stone is 40 to 80: 80 is the approximately the highest CTC achieved and around 40 is seen as the minimum that can be sold for most purposes [Paul Rogers, CPL Industries, 2012]. Pine wood can achieve a much higher CTC and so the range selectable is 40-100. Pine wood trials have shown CTC value to go much higher than 100 but most applications today do not require a CTC value that high and it is not in the commercial interests of the production company to produce a better quality carbon than required due to the associated lower yields and costs. The graphical equations shown in Figure 7:8 and Figure 7:9 are used to calculate the burn off and overall yield for biomass chars. These figures are taken from Chapter 5 where all lab and pilot scale data have produced an optimum CTC, burn off ratio.

Char tonnes produced/yr	10000
Desired CTC (range 40-80)	**60**
Burn off %	50.60
Char yield %	49.40
Activated carbon produced t/yr	4940.30
Graph equation	1.2438x - 24.031
Tonnes producer/ hr	0.62
Overall yield	14.16%
Tonnes char thoughput/ hr	1.25
Tonnes produced per year	**4940.3**

Figure 7:7 Chosen CTC required for olive stone carbon, burn off (%), char yield (%), tonnes per year produced and tonnes per hour using graph equation provided in Figure 7:8.

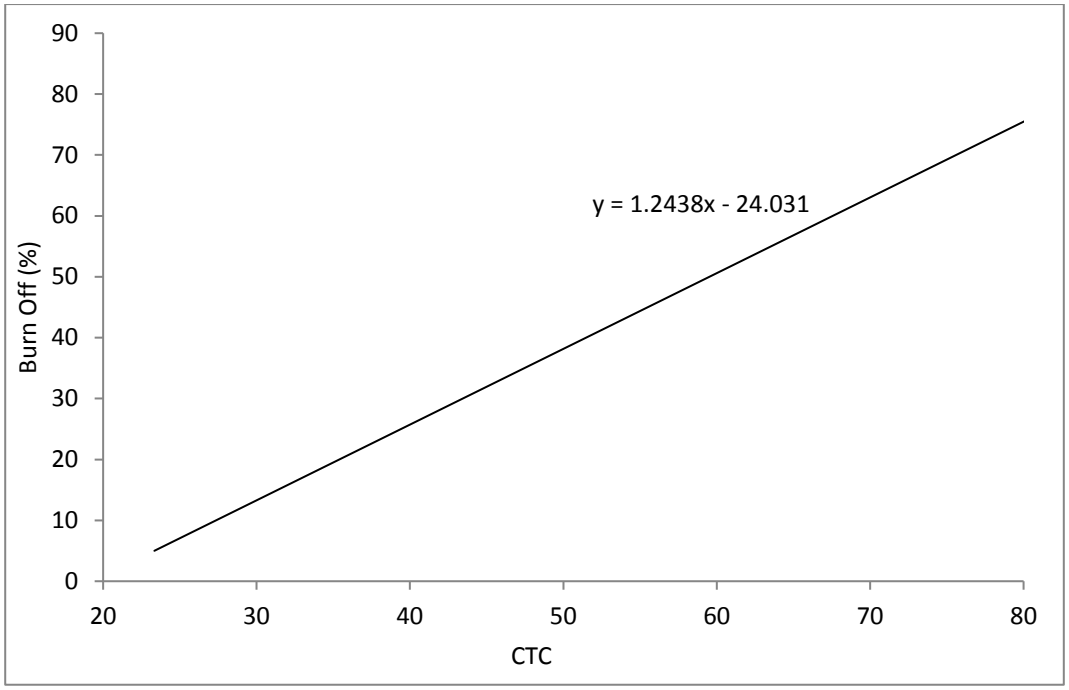


Figure 7:8 Graph equation used in model for olive stone activated carbon taken from Figure 5:2.

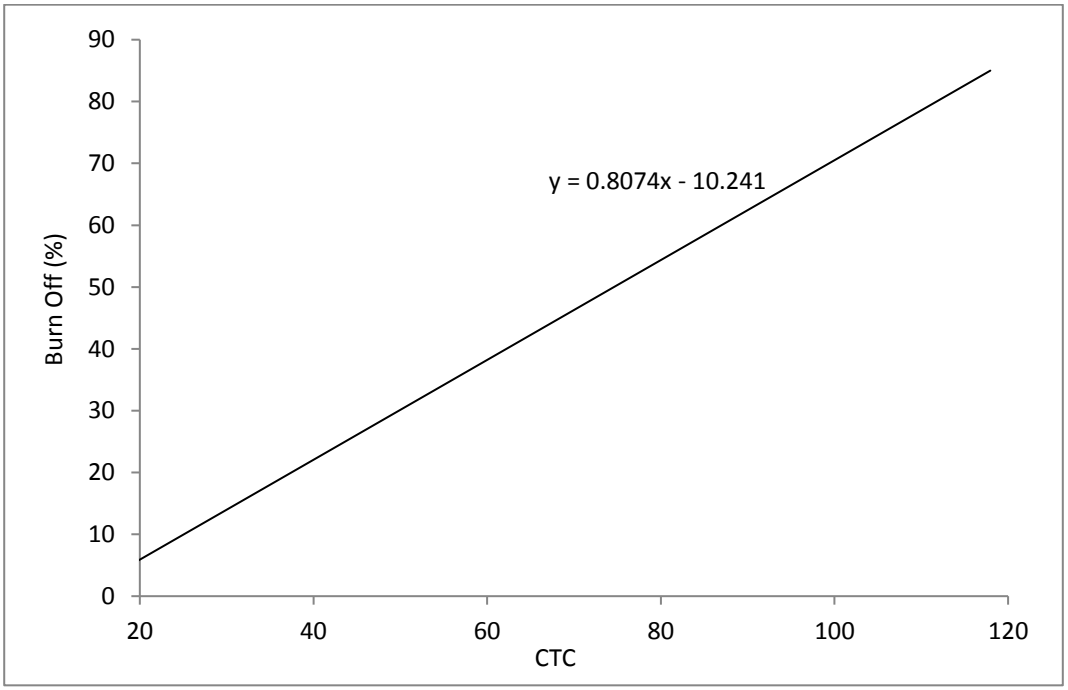


Figure 7:9 Graph equation used in model for pine wood activated carbon taken from Figure 5:4.

The data from the above figures has been generated both on lab and pilot scale.

The model provides an additional method; the user can select a certain amount of required carbon of a specific CTC value. The model then provides the amount of char needed for this task as shown in Figure 7:10 below:

Desired CTC (range 40-100)	70	Target t/yr	1000
Burn off %	46.28	Char required t/yr	1861.40

Figure 7:10 Showing example of pine wood 70 CTC.

The throughput per hour depends on the amount of char produced per year as this is the limiting factor. In this theoretical plant 10,000 tonnes of char has been produced and requires processing within 8,000 working hours. This results in a 1.25 t/hr feed rate into the activation kiln, this is important to know for sizing and flexibility to meet changes in demand.

The next part of the model was to decide on the steam flow rate. The main variables in lab and pilot scale trials have been temperature, residence time, and steam flow. For this financial model example temperature has been selected as the one variable that will be changed to alter the burn off, with steam flow rate and residence time being kept constant. Using both small and pilot scale results the water, carbon molar ratio was chosen to be 3:1. This means as 1.25 t/hr char enters the system 1.875 t/hr of steam enters. This is a 1:1 molar ratio on entry however as residence time is selected to be 3 hours, similar to pilot scale tests, the overall ratio is 3:1 as each 1.25 t of char is subject to three times 1.875 t/hr of steam. This is the same principle that has been used in both lab and pilot scale results.

As mentioned, presently temperature has been chosen as the only variable in this model. This can be altered in the future to include the other two main variables, but before these variables can be added to the model more data on large scale heat tubes containing lifters is required. On large scale equipment mixing efficiency should be improved significantly with design reducing required steam and residence time.

Figures using lab scale results have been generated to show how temperature affects the burn off and CTC of both the biomass carbons, the graph equations are then used (see Figure 7:11 and Figure 7:12).

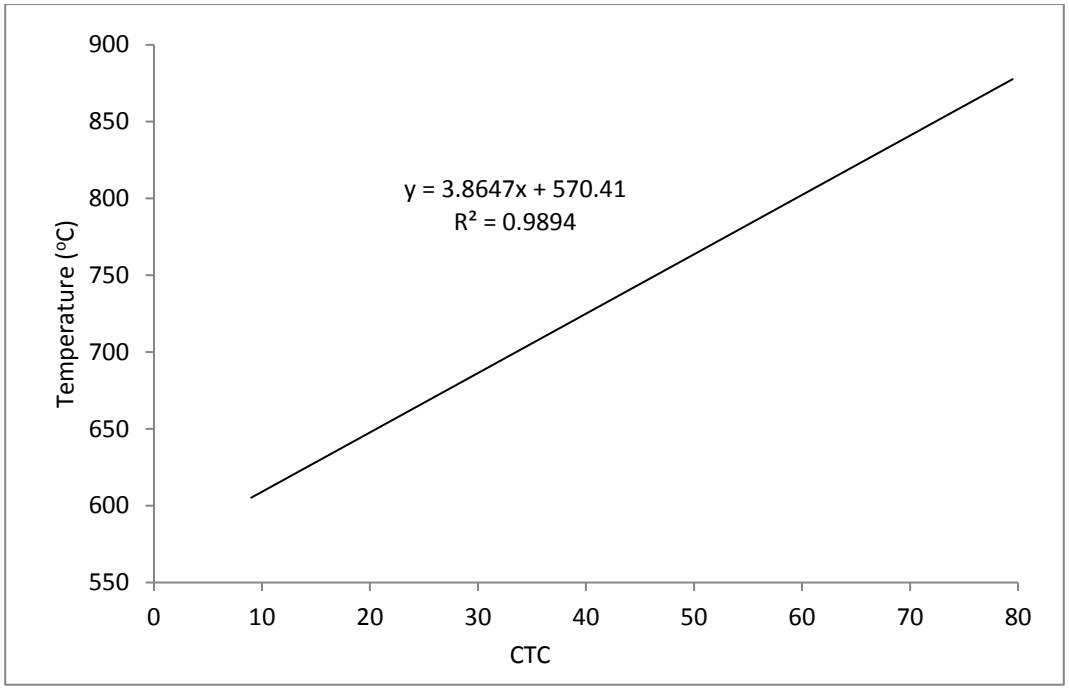


Figure 7:11 How a change in activation temperature changes CTC of olive stone carbon, taken from Figure 5:20

.

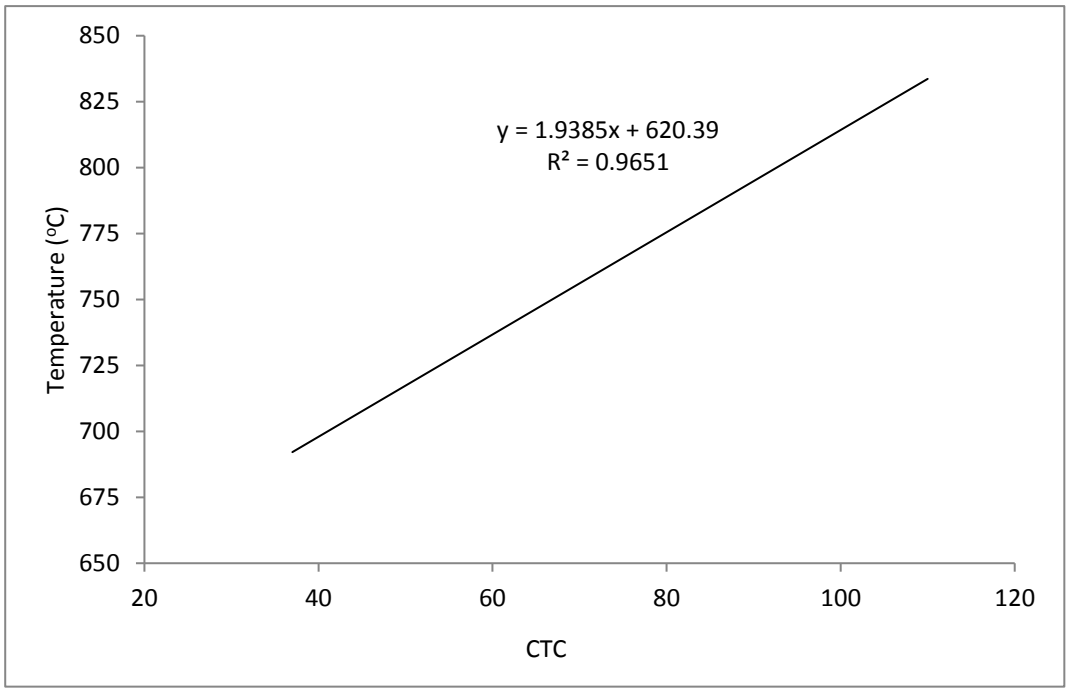


Figure 7:12 How a change in temperature changes CTC of pine wood carbon, taken from Figure 5:24

Once the desired CTC is selected the model then uses information provided by these two figures in addition to Figure 7:8 and Figure 7:9 to calculate the activation temperature required to result in a specific burn off percentage. For example if olive stone and pine wood desired CTC value is 60 and 70 respectively:

Char tonnes produced/yr	10000
Desired CTC (range 40-80)	**60**
Burn off %	50.60
Char yield %	49.40
Activated carbon produced t/yr	4940.30
Graph equation	1.2438x - 24.031
Tonnes producer/ hr	0.62
Overall yield	**14.16%**
Tonnes char thoughput/ hr	1.25
Tonnes produced per year	**4940.3**
Graph equation	3.8647x + 570.41
Desired temperature °C	**802**

Figure 7:13 Olive stone activation temperature to achieve a carbon with a CTC of 60 (20% moisture).

Char tonnes produced/yr	10000
Desired CTC (range 40-100)	**70**
Burn off %	46.28
Char yield %	53.72
Activated carbon produced t/yr	5372.30
Graph equation	0.8074x - 10.241
Tonnes producer/ hr	0.67
Overall yield %	**7.61%**
Tonnes char thoughput/ hr	1.25
tonnes produced per year	**5372.3**
Graph equation	1.9385x + 620.39
Desired temperature °C	**756**

Figure 7:14 Pine wood activation temperature to achieve a carbon with a CTC of 70 (30% moisture).

As shown in previous chapters, pine wood carbon requires a lower activation temperature to produce a carbon with a CTC value of 70 than olive stone does for a CTC of 60.

7.6.1 Energy Balance for Activation

For this example calculation pine wood with a CTC of 70 is used.

The following specific heat capacities will be used [engineering toolbox, 2015]

Average char cp = 2.0 kJ/kg

Average superheated steam (100 °C to 850 °C) cp = 2.1 kJ/kg

The proceeding calculations are based on water entering the system with no energy recovery present.

Using Equation 7-1: $Q\ (kWh) = \frac{MC(Tf-Ti)}{3600}$

$$\text{Water to 100 °C} = \frac{1875\ \text{kg} \times 4.2\ \text{kJ/kg} \times (100\ ^{\circ}\text{C} - 20\ ^{\circ}\text{C})}{3600\ s} = 175.0\ kWh$$

$$\text{Char to 100 °C} = \frac{1250\ \text{kg} \times 2\ \text{kJ/kg} \times (100\ ^{\circ}\text{C} - 20\ ^{\circ}\text{C})}{3600\ s} = 55.6\ kWh$$

$$\text{Evaporation of water} = \frac{1875\ \text{kg} \times 2257\ \text{kJ/kG}}{3600\ s} = 1175.5\ kWh$$

On large scale without knowing exact product gas evolution rate at given temperatures, it is assumed char remains unaltered until the final temperature is reached for comparative purposes.

Char to final temperature (756 °C)

$$= \frac{1250\ \text{kg} \times 2 \times (756 - 100)}{3600\ s} = 455.6\ kWh$$

Steam to final temperature (756 °C)

$$= \frac{1875\ \text{kg} \times 2.1 \times (756 - 100)}{3600\ s} = 717.5\ kWh$$

Total activation energy requirement = **2579.3 kWh**

This above value is taken at 100% efficiency. An efficiency of 40% is assumed for the activation kiln. An extra 5% efficiency reduction has been chosen in comparison to the pyrolysis kiln. The reason being as residence time is longer, the kiln will be longer resulting in a larger surface area for heat loss.

Actual energy required for the activation kiln in this example (using Equation 7-8):

$$\frac{total\ energy\ (kWh)}{40\ \%} = 6448.2\ kWh$$

Using the same cost (0.025p/kWh) the cost per hour works out to be £161.2

This equates to a yearly cost (8000 hours) of £1,289,641

From this, the cost per tonne can be calculated. Figure 7:14 shows how much carbon would be produced at a CTC value of 70 (30% moisture). At 10,000 tonnes of char the activated carbon produced works out at 5372.3 tonnes per year. This leads to a cost per tonne of £240.05. The model can provide the cost per tonne of a mixture of carbon qualities. The tonnes of char produced/used for each CTC need be altered. The costs per tonne is added up and the mean calculated. For example:

5000 tonnes of char were used to produce a carbon with a CTC of 60. The carbon output from this char comes out at 3089.85 tonnes at a cost of £205.9/t

Another 5000 tonnes of char were then used to produce a carbon with a CTC of 80. The carbon output from this char comes out at 2282.45 tonnes at a cost £286.3/t

The average price per tonne across the year =

$$\frac{\textit{Total cost per tonne}}{\textit{Total tonnes produced}} = \frac{(205.9 \times 3089.85) + (286.3 \times 2282.45)}{5372.3} = £240.1 \qquad \textbf{Equation 7-9}$$

Activation costs prior to energy recovery were produced for both biomass types

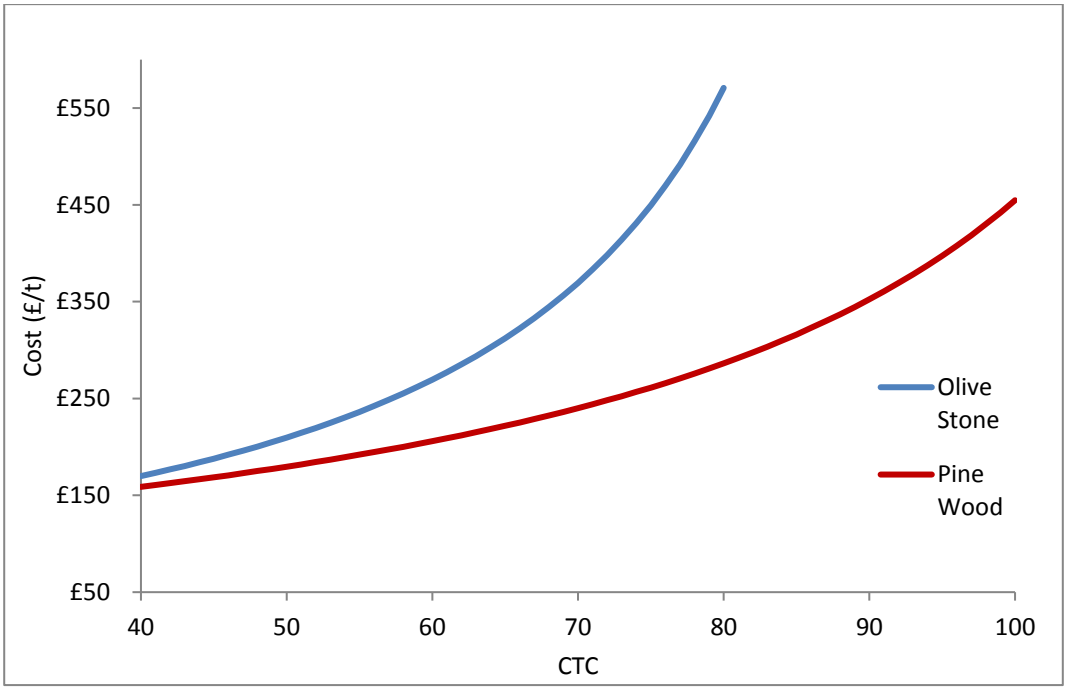


Figure 7:15 Activation costs only for both biomass types.

What can be seen in Figure 7:15 is that olive stone activation requires higher energy input to yield the same CTC. This has been shown throughout the chapters as a higher temperature is required to achieve a specific quality carbon. However, this extra cost may be offset by the physical characteristics of the granular carbon that has a higher selling price than the powdered carbon.

7.7 Pore and Methylene Blue number Estimates

In addition to predicting burn off and end yields the pore network and methylene blue number can be predicted within the model. This was done by using figures generated in Chapter 5

Table 7-6 Results from the model for pine wood CTC 70, (30% moisture).

Estimate of pine wood BET (m^2/g)	**879**
Estimate of micro pore v (cm^3/g)	**0.36**
Estimate of total pore v (cm^3/g)	**0.62**
Estimation of mesopore v (cm^3/g)	**0.26**
Mesopore (%)	**42.0**
Methylene blue number (ml)	**13**

The above results were calculated using figures from Chapter 5 in this example BET surface area was calculated from Figure 5:9, micropore volume from Figure 5:67, total pore volume from 5:68 and methylene blue number from Figure 5:13. With high R^2 values given in these figures stated confidence can be taken from the values shown in Table 7-6. This provides a very useful comparison when deciding what carbon to produce as the estimates provided can give a clearer picture as to what characteristics the carbon will have. The same was inputted in the model for olive stone.

7.8 Energy Recovery

For a plant to run efficiently energy recovery is vital and can save a large percentage of OPEX costs. Energy recovery requires extra initial capital investment but is likely to repay this cost quickly and is important for long term profitability and sustainability whilst also lowering the carbon footprint of the process.

In this financial model a boiler was chosen as the main energy recovery method along with heat exchangers. Many other options and possibilities are available to recover energy from the process, such as a gas engine, steam turbine etc. However, because steam is needed in this process, the model incorporates a boiler to produce steam for both activation and the drier.

7.8.1 Boiler Potential

The first part of energy recovery in this model covers the boiler. The boiler combusts the oils and gases from the pyrolysis stage and uses this energy to heat water. An industrial steam boiler usually has efficiency between 80% and 90% [Sinnott, R.K., 2005]. In this model the efficiency of 80% has been used.

In order to work out the amount of energy available for recovery, the calorific value must be known for both the gas and oil of pyrolysis. Using literature the values are given below:-

Wood gas LHV 5.7 MJ/kg [Taylor and Fayette, 1985]

Pyrolysis oil LHV 17.2 MJ/kg [M.Ringer *et al*., 2006]

The percentage make up of these fractions have already been discussed during the pyrolysis stage

Taking Option 1, with drier, the amount of gas and oil is shown below (pine wood):-

Gas = 3087.94 kg/hr

Oil = 1837.94 kg/hr

$$\text{Gas (kWh)} = \frac{3087.94 \times 5.7}{3.6} = 4889.3\ kWh$$

$$\text{Oil (kWh)} = \frac{1837.94 \times 17.2}{3.6} = 8781.3\ kWh$$

This is how much energy is produced assuming 100% complete combustion.

Taking into account boiler efficiency (80%) the combined energy for steam production

= (energy gas + energy oil) × 80% = **10936.43 kWh**

At atmospheric pressure steam saturation point is approx. 100 ^{o}C. The boiler is outputting this steam to 10 ^{o}C above saturation point in order to prevent saturation in insulated piping. The water enters the boiler at 95 ^{o}C via the heat exchanger (this area is discussed in section 7.7). The energy required to produce steam is calculated below. The steam is sent directly to the activation kiln.

Required steam flow, 1875 kg/hr

Water flow into boiler has been heated by heat exchangers at a rate of 1875 kg/hr and 95 ^{o}C

Q (kWh) to 100^{o}C $\frac{mCw\Delta T}{3600} = 10.94\ kWh$

Q, Evaporation (kWh) = $\frac{mL}{3600} = 1175\ kWh$

Q (kWh) to 110^{o}C = $\frac{mCs\Delta T}{3600} = 10.94\ kWh$

Where,

m =1875 kg

Cw = 4.2kJ/kg

Cs = 2.1 kJ/kg

L = 2257 kJ/kg

Total energy for steam production requirement (1875 kg of water) for activation =

1197.4 kWh

The boiler has more potential energy to produce more steam and this steam can be utilised in the steam powered drier, in which the latent heat energy is given up during condensation of the steam and used to dry the biomass.

For example (pine wood 70 CTC) "spare energy" remaining

$$Potential \text{ Boiler energy } - \text{energy for activation steam } = 9739.03 \text{ kWh}$$

The burn off percentage must be taken into account during activation. As the amount of steam reacting during activation changes depending on the quality of carbon produced i.e. burn off. Therefore, an increased burn off, and hence an increased reaction, reduces the excess steam left over. This steam will then pass through the heat exchanger that provides the latent heat energy to heat cold water before entering the boiler. The below calculations provide a step by step guide to the process for both pine wood and olive stone activated carbon energy recovery.

The heat exchanger, discussed in further detail below, shows that it is possible for the total water to be heated up to 95 ^{o}C is 11107.75 kg/hr for pine wood when the chosen CTC is 70. From this 1875 kg/hr is used for the activation oxidising agent (constant) leaving a potential 9232.75 kg/hr to be sent off to the steam drier.

The energy requirement to heat this excess water up to 110 ^{o}C, using the same calculations used previously, is 5896.14 kWh

There is still 3842.90 kWh available to produce further steam for the drying process if needed. The below process calculates the amount of water that can be heated up to 110 ^{o}C in the energy recovery system.

The condensed steam used from the drier can also be re-circulated to pass back through the boiler to be evaporated once more. It is assumed this condensate is to be approx. 95 ^{o}C.

The next step was to calculate the percentage of the energy requirement for heating to 100 ^{o}C, vaporisation and then heating further to 110 ^{o}C, the results were shown in Table 7-7 below

Table 7-7 Total boiler steam production (110 ^{o}C) along with activation requirement and availability for drier, pine wood.

Liquid to Gas	%
To 100 ^{o}C	0.91
Evaporation	98.17
To 110 ^{o}C	0.91

These percentages are then multiplied by the remaining kWh potential from the boiler to get the following shown in Table 7-8

Table 7-8 Energy (kWh) required for the 3 stages.

Liquid to Gas	kWh
To 100 °C	494.0
Evaporation	3318.1
To 110 °C	30.9
Total	3842.9

Now by re-arranging the Equation 7-1, m can be calculated by converting kWh back into kJ/kg

$m = \frac{Q}{cp\Delta T}$ and $m = \frac{Q}{L}$

All three stages should yield the same mass and in this example 5485.78 kg/hr

This means the total boiler potential, in the case of pine wood, with the aid of the heat exchanger can provide 17125.34 kg/hr of steam at 110 °C atm (5485.78 kg/hr + 11639.55 kg/hr from heat exchanger) however from this 1875 kg/hr is required for activation.

Table 7-9 Total boiler steam production (110 °C) along with activation requirement and availability for drier, pine wood.

	Kg/hr
Total boiler steam production	17125.34
Activation requirement	1875
Total available for drier	15250.34

For olive stone the boiler works in the same way with the above calculations but with different values. As the yield is higher, and lower throughput required per hour, there is less energy recoverable with olive stone pyrolysis.

The same amount of energy is required to heat the steam required for activation energy but what is remaining after this ("spare energy") comes out at 3503.28 kWh which is much lower than the pine wood value of 9739.03 kWh.

This excess energy will be used to heat up the water arriving from the heat exchanger as with the pine wood process. However, now there will not be enough excess energy to heat up all the water required for drying at high moisture content.

To work out how much steam can be generated the following calculations were done.

Again, the percentages were calculated based on water entering the boiler at 95 °C

Table 7-10 Percentage energy requirement to produce steam.

Liquid to gas	%
To 100°C %	0.91
Evaporation %	98.17
To 110°C %	0.91

These were multiplied with the "spare energy" as before.

Using m = $\frac{Q}{cp\Delta T}$ and m = $\frac{Q}{L}$

The mass of 95 °C water than can be turned into 110 °C steam atm = 5908.05 kg/hr

This means (example olive stone CTC 60) excess or waste water from the heat exchanger: 10291.43 kg/hr – (1875 kg/hr + 5908.05 kg/hr) = 2508.38 kg/hr

Summary for olive stone at CTC 60

Table 7-11 Total boiler steam production (110 °C) along with activation requirement and availability for drier, olive stone.

	Kg/hr
Total boiler steam production	7783.05
Activation requirement	1875
Total available for drier	5908.05

Now steam kg/hr has been calculated for both biomass types it is possible to see what maximum moisture percentage can be dried in the drier utilising the energy recovery of the process.

The energy requirement at each moisture percentage is known for the drier. Taking into account the stated 40% efficiency and using steam flow rate (mass) and the latent heat, it can be calculated how much energy has been transferred.

It can also be calculated what kg/hr of steam is required to dry the material to 0% moisture

This was done by:

$$\frac{energy\ of\ drier\ required\ (40\%\ eff)\ kJ/hr}{Latent\ heat\ kJ/kg} \qquad \textbf{Equation 7-10}$$

For example pine wood at 40% moisture:

$$\frac{29778079.71\ kJ/hr}{2257\ kJ/kg} = 13193.66\ kg/hr\ steam$$

This means at 40% moisture the pine wood can be dried as 15250.34 kg/hr steam is available and the requirement is 13193.66 kg/hr

Figure 7:16 and Figure 7:17 show the results of this for the different biomass types.

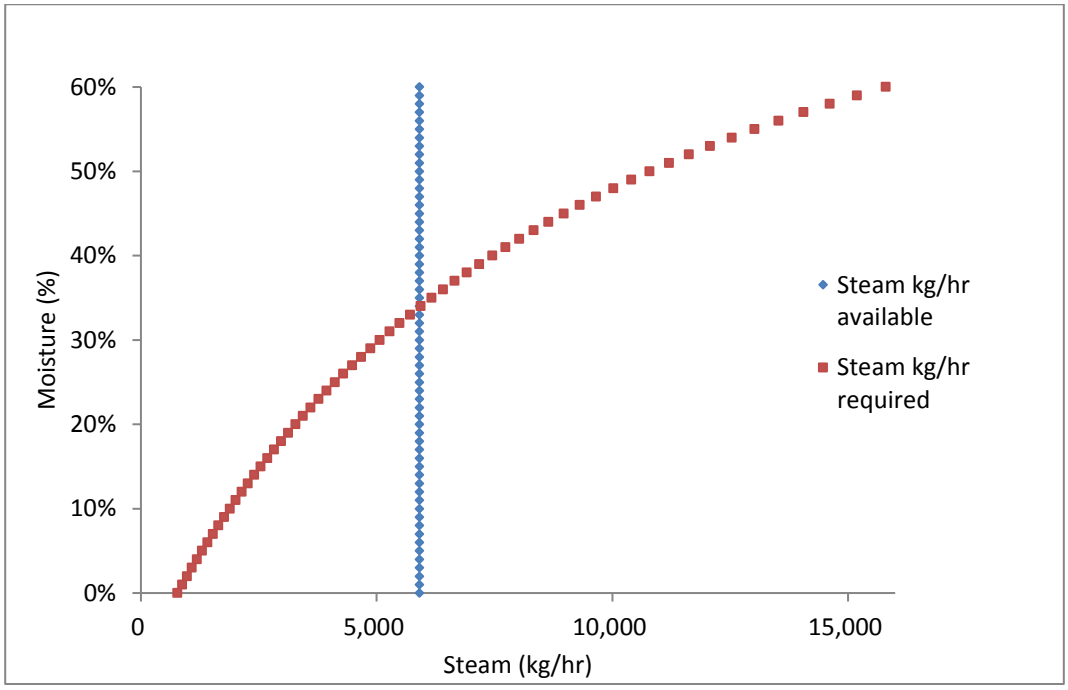


Figure 7:16 Steam available for drying against steam required, olive stone CTC 60.

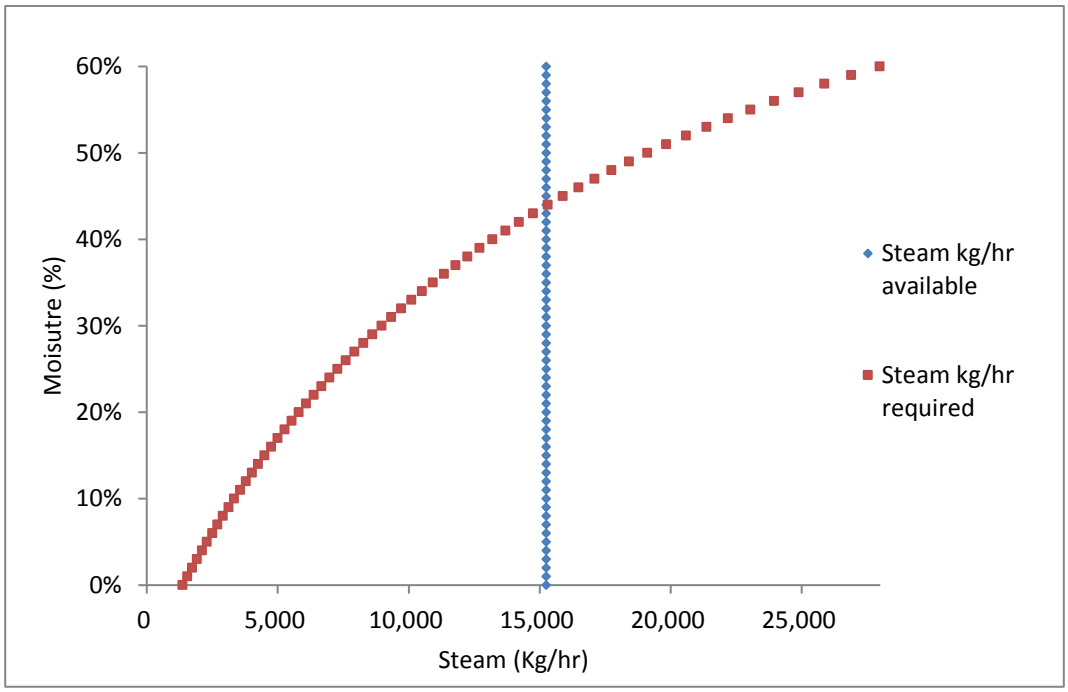


Figure 7:17 Steam available for drying against steam required, pine wood CTC 70.

Looking at both the figures, the steam generated from the boiler can dry pine wood of up to 43% moisture and olive stone up to 33% moisture.

Possible steam production from pine wood production is much higher than from olive stone due to the higher amount of volatiles being released during pyrolysis; because of the lower char yield and a higher throughput. This is offset slightly by less biomass per hour to dry for olive stone due to resultant higher yields. For example to dry both biomasses at 25% moisture requires 4113 kg/hr and 7281 kg/hr of steam for olive stone and pine wood respectively. However the higher volatile gas and oil yields from pine wood pyrolysis more than compensate for this.

Whilst olive stone can only be fully dried up to 33% moisture compared to 43% moisture with pine wood both maximums are very unlikely to be exceeded as long as the biomass is stored correctly.

It must be noted that olive stone energy recovery remains constant when altering the desired CTC level (spec) due to only affecting how much excess water must be disposed as;

Cold water heated in heat exchanger > boiler potential.

This means that even if there is greater excess steam available from activation to heat the cold water in the heat exchanger the energy provided by the boiler by pyrolysis product combustion is not enough to turn this amount into steam at 110 ^{o}C

This is not the case for pine wood. The required specification of pine wood affects the energy recovery for the following reasons;

1. Higher burn off means less un-reacted steam remaining in the system.
2. This results in less steam giving up providing the latent heat energy in the heat exchanger unit.
3. In turn less water is being heated to 95 ^{o}C prior to the boiler.
4. More cold water (20 ^{o}C) is thus required to make up to the boiler maximum output which requires more energy to heat than water at 95 ^{o}C.

7.8.2 Heat Exchanger and De-Superheater

The heat exchanger has already been discussed above and values used in determining the requirement for the boiler and drier. The below calculations will show how it can be designed and how the values given previously were calculated.

Pine wood CTC 70 example:

The kg/hr of un-reacted steam in the system: moles C burn off = Moles H_2O reacted based on Reaction 1:

$$H_2O_{(g)} + C_{(s)} \rightarrow CO_{(g)} + H_{2\,(g)}$$

$$\text{Steam un-reacted} = \quad \text{Steam in} - \left(\frac{Moles\ burn\ off/hr\ \times\ Mr}{1000 \times\ 3}\right) \qquad \textbf{Equation 7-11}$$

Moles burn off = moles water reacted (t/char) = 38564.17

For 1.25 t, 48205.2 moles of water react per hour

$Mr_{(H_2O)} = 18$

$$\text{Mass} = \text{Moles} \times \text{Mr} \qquad \textbf{Equation 7-12}$$

= 867.69 kg of water reacted per 1.25 tonne of char over 3 hours

Therefore 289.23 kg/hr water reacted with the char

3 = residence time in hours (assuming 1.25t of char are subject to 3 × 1875 kg/hr water)

Steam kg/hr un-reacted = 1585.28 kg/hr

Steam kg/hr reacted = 1875 kg/hr – un-reacted = 289.71 kg/hr

So in this reaction one can assume that 289.71 kg/hr steam is reacting to form both CO and H_2

This steam has been cooled by a de-superheater down to 200 ^oC at atmospheric pressure. The calculations and reason for this will be provided:

Mcw = Mass flow rate of cold water kg/hr

Ms = Mass flow rate of superheated steam 1585.28 kg/hr

H_1 = Enthalpy of steam (assuming around 700 ^oC) 3928.29 kJ/kg

H_2= enthalpy of steam at 200 ^oC 2869.92 kJ/Kg

Hcw = enthalpy of cooling water (20 ^oC) 83.95 kJ/kg

$$\mathbf{Mcw = Ms}\left(\frac{(\boldsymbol{H1-H2})}{(\boldsymbol{H2-Hcw})}\right) \qquad \textbf{Equation 7-13}$$

$$= 1585.77\ \text{kg/hr}\left(\frac{(3928.29-2869.92)}{(2869.92-83.95)}\right) = 602.2\ \text{kg/hr}$$

Turn down ratio =

$$\frac{\textbf{Max flow}}{\textbf{Min flow}} \qquad \textbf{Equation 7-14}$$

$$= \frac{1710.52}{1344.71} = 1.27$$

Based on flow needed at range of excess steam left over

The same applies to olive stone.

The reasons to use de-superheater: [spirax sarco, 2015]

- "The coefficient of heat transfer when using superheated steam as the heating medium is variable, low and difficult to quantify accurately. This makes accurate sizing and control of heat transfer equipment difficult and will also result in a larger and more expensive heat exchanger.
- Once the superheated steam is cooled to saturation temperature, the heat transfer coefficient increases dramatically, and the temperature at which the steam condenses back into water is constant. This greatly assists accurate sizing and control of heat transfer equipment.
- The presence of high heat transfer coefficients associated with saturated steam leads to smaller and cheaper heat exchangers than those which utilise superheated steam.
- Some processes (for example, distillation columns) perform less efficiently when supplied with superheated steam.
- The higher temperatures of superheated steam may mean that higher rated, and hence more expensive, equipment is required.
- The higher temperature of superheated steam may damage sensitive equipment.''

Now the steam temperature entering the heat exchanger is known, 200 ^{o}C, the heat transferred to the water heading towards the boiler can be calculated. The aim is to get the water to around 95 ^{o}C before it enters the boiler.

Using $Q = mC\Delta T$ and $Q = mL$

The steam provides energy when cooling from 200 ^{o}C to 100 ^{o}C but the main heat transfer is at steam saturation point where latent heat energy is transferred. This is the reason for having a de-superheater to make sure the steam is cooled sufficiently:

$Q = -1585.28 \times 2.1 \times (200-100) = -332909$ kJ

$Q = -1585.28 \times 2257 = -3577980$ kJ

Total 1 = -3910888.84 kJ

$M = \frac{Q}{cp\Delta T} = 11{,}639.55$ kg/hr

The flow rate above is the required flow rate of cold water to increase from 20 ^{o}C to 95 ^{o}C and to cool down the steam to saturation point when the latent heat is given up. To make sure the balance is met:

Total 2, Q = 11639.55 × 4.2 × 80 = 3910888.84

And, Total 1 +Total 2 = 0

The flow rate seen here is used when calculating the boiler output in the section above for pine wood CTC 70. Olive stone calculations are calculated in the same way.

The final piece of energy recovery comes during the condensation of the steam inside the heat exchanger. It is assumed the reaction solely follows Reaction 1. In reality this reaction will not be the only reaction occurring for example the water gas shift will be also to varying levels. The water gas shift reaction for a detailed analysis requires more data during and after activation to be placed in this model. It will be possible to increase production of hydrogen with a catalyst such as a copper-zinc aluminium catalyst that promotes the production of hydrogen from CO and H_2O as [A. Andreev *et al*., 1991]. In this model it is simply assumed that the products produced during activation stay at the same concentration throughout and can be used as syngas once the steam has been condensed from the off gas.

The following calculations were completed:

The burn off percentage was used to calculate moles of CO and moles H_2 produced per tonne of char. Using the same example (pine wood CTC 70) the burn off is 46.36%. Using Equation 7-12:

Moles burn off = $\frac{mass\ burn\ off\ (g)}{12}$ = 38629.17

Therefore from the reaction equation we know moles carbon burn off = moles H_2 and moles CO

The next step was to find the mass in kg of these fractions again using Equation 7-2:

Mass kg = $\frac{Moles \times Mr}{1000}$

Mass H_2 = 69.53 kg/t

Mass CO = 1081.62 kg/t

Below are the calorific values for the two gases [engineering toolbox, 2015]

H_2 MJ/kg	119.96

CO MJ/kg	10.16

The kWh when both gases are combusted can be calculated assuming 100% combustion.

$H_2 = \frac{(Mass \times 1.25) \times \frac{MJ}{kg}}{3.6}$ = 10426.40 MJ/hr

CO = $\frac{(Mass \times 1.25) \times \frac{MJ}{kg}}{3.6}$ = 13736.49 MJ/hr

Total = 6711.9 kWh

Savings are worked out assuming that this syngas was going to help power one of the kilns.

Saving/hr = Total kWh × kiln efficiency % × cost/kWh = £67.12

This means the savings per tonne of activated carbon produced = $\frac{Savings/hr}{Tonne\ /hr}$ = **£53.70**

7.9 Part 4 Raw Material Costs

The largest part of the OPEX costs are due to the raw materials. Raw material costs are usually the bulk of the operating costs and with over 50% a normal occurrence [Sinnott, R.K., 2005].

Material purchase costs are difficult to predict. Using costs associated with this project along with literature references the costs used are shown below.

Dried pine wood £40/t [Bio Boost, 2013].

Dried Olive stone £100/t however depends more on harvest. [Parenti *et al*., 2014].

Using the price on dry basis the raw material cost can be calculated at any given moisture percentage.

Two figures were generated using the costs of the precursors at given CTC values using the known burn off percentages from lab and pilot scale. The equations produced from these graphs were used in the model to calculate the cost at the chosen CTC of either olive stone or pine wood and added to the OPEX. Figure 7:18 and Figure 7:19 were generated by knowing the total yield on dry basis and plotted against their corresponding CTC values.

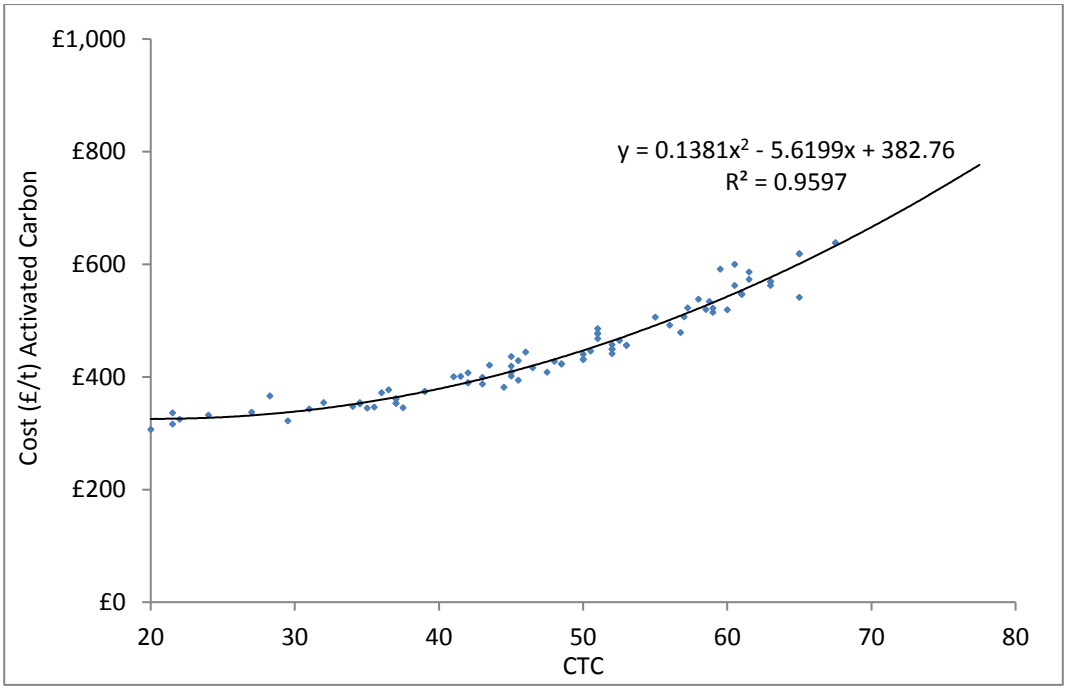


Figure 7:18 Used to calculate olive stone precursor cost.

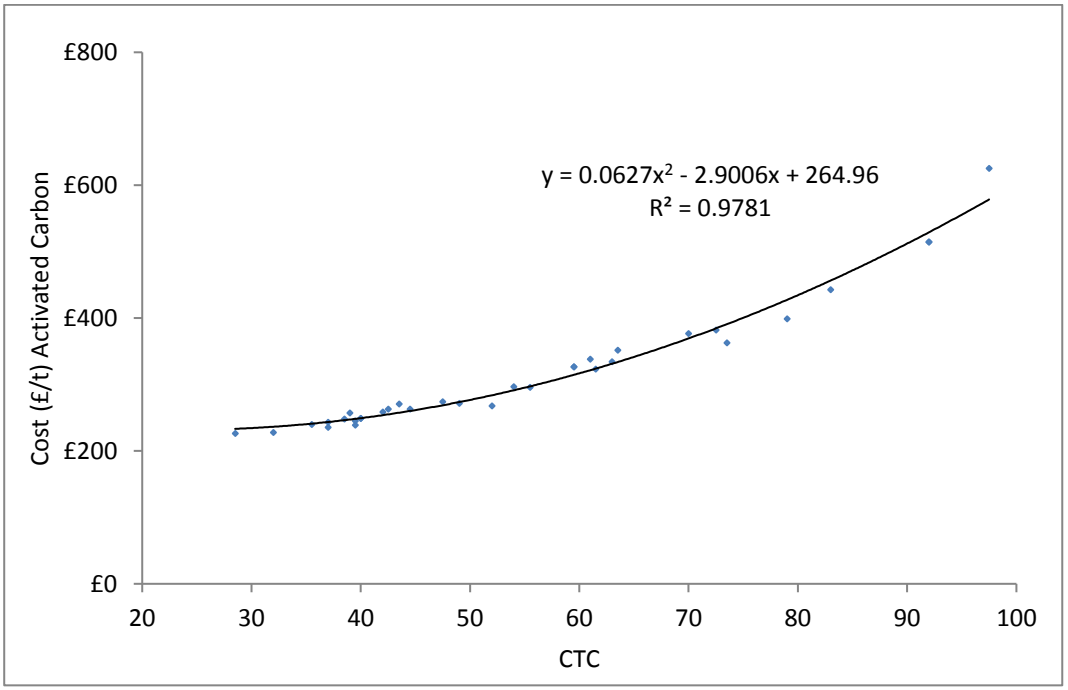


Figure 7:19 Used to calculate pine wood precursor cost.

Raw material cost is likely to fluctuate both up and down depending on the yearly harvest quality for olive stone. For example 2015 was a particularly bad year for olive stone harvests as Tracy McVeigh [2015] pointed out in her report found in the Guardian newspaper. In contrast, pine wood availability is likely to remain more consistent with growth and supply more

predictable. Sensitivities have been included in the model and allow for such circumstances where the material becomes more expensive.

7.10 Part 5 Additional OPEX Costs and Selling Price

So far OPEX costs consist of drying, pyrolysis, activation and raw material cost. Other OPEX costs need to be considered such as labour, maintenance and rent costs.

Effluent treatment can also be required but in this model it is assumed that it doesn't alter the costs of the current effluent stream at the plants facilities. The condensed water from the steam drier is either returned to the boiler or is simply transported outside to a large water storage tank. The water is assumed to be cooled enough during transportation that it has no effect on the temperature of the water inside the storage tank. However, this is likely to fluctuate with external temperature. The water that requires treatment will likely contain contaminants in the remains of the condensate from the heat exchanger that has been used during activation. This water will be disposed of and replaced with fresh inside the water storage tank, again this cost is ignored as the amount of water required ranges between 1.4 t/hr and 1.7 t/hr and can be considered negligible in terms of the overall process cost. However, to compensate for this cost, the maintenance value calculation was based on the highest potential value.

Firstly, we consider the additional cost of labour. It is assumed that the drier is in operation and requires an operator. The table below shows the costs associated with the employees:

Table 7-12 Labour costs. Example Pine wood (CTC 70, 30% moisture).

Labour costs	£
3 engineers	135,000
7 shift	160,000
Total year	295,000
Cost per tonne	**54.99**

It is assumed, that each engineer earns £45,000 a year and that each shift worker earns just under £23,000 a year [Sinnott, R.K., 2005]. The cost per tonne is calculated by:

$$\frac{\text{Total labour costs/ yr}}{Tonnes\ AC\ produced/yr} \qquad \textbf{Equation 7-15}$$

In respect of maintenance costs, it is suggested that maintenance costs per year fall between 3-5% of ISBL (inside battery limits) of capital costs. The chosen value for this was 5% [Sinnott, R.K., 2005]

To calculate £/t, example, using pine wood at CTC 70 (30% moisture):

$$\frac{Total\ maintainance\ cost/yr}{total\ AC\ produced/yr}$$ **Equation 7-16**

$$= \frac{£211{,}234.29}{5364.5\ t} = £39.38/\text{t}$$

For land rent, using the same reference it is suggested that land rent falls between 1-2% of the ISBL capital costs. Rent value of 2% is used:

$$\frac{Total\ rent\ £/yr}{total\ AV\ produced\ t/yr}$$ **Equation 7-17**

$$= \frac{£84{,}493.71}{5364.5\ t} = £15.75/\text{t}$$

The cost per tonne of carbon produced goes up with increasing moisture content due to a larger drier required and also carbon with higher CTC values as fewer tonnes produced each year.

7.11 Selling Price

The selling price has been assumed by rough estimates and this is both increased and decreased in the sensitivities section. The values are based on current market knowledge and compared to specific carbons that are in the market place today - knowledge gained at (Biogas and AD at Birmingham NEC 2016). Granular activated carbon is worth much more than powdered activated carbon at the same CTC. Pine wood produces powdered activated carbon and olive stone granular and this has been reflected in the rough selling price estimates. As the CTC goes up the selling price accelerates due to niche markets that can be entered, such as the respiratory sector that requires high quality activated carbon. Two figures were produced: one for olive stone and the other for pine wood with rough selling prices. The selling price could be calculated within the model at any given specification. The graph data points were produced by selecting an overall operating profit per year. In this example £1m was used but can be simply altered within the model for more accurate selling prices to be used.

Selling price calculation:

$$\frac{£1m}{t/yr\ produced\ at\ given\ CTC} + OPEX\ cost$$ **Equation 7-18**

7.12 Summary of OPEX and Profitability

With the main OPEX areas covered and the selling price determined results were generated in graphical form to show the process summary.

Table 7-13 Summary of the total OPEX for pine wood (CTC 70, 30% initial moisture).

CTC	70
Pine wood pyrolysis cost/t	£101
Activation cost /t	£240
Using activation gas saving/t	-£54
Boiler savings activation steam /t	-£126
Raw material cost/t based on £40t/dry	£356
Maintenance and rent /t	£55
Drier cost/t	£112
Boiler savings drier	-£112
Labour cost/t	£55
Total OPEX/t AC	**£628**

From this table a pie chart is produced showing the costs and savings associated with OPEX before energy recovery.

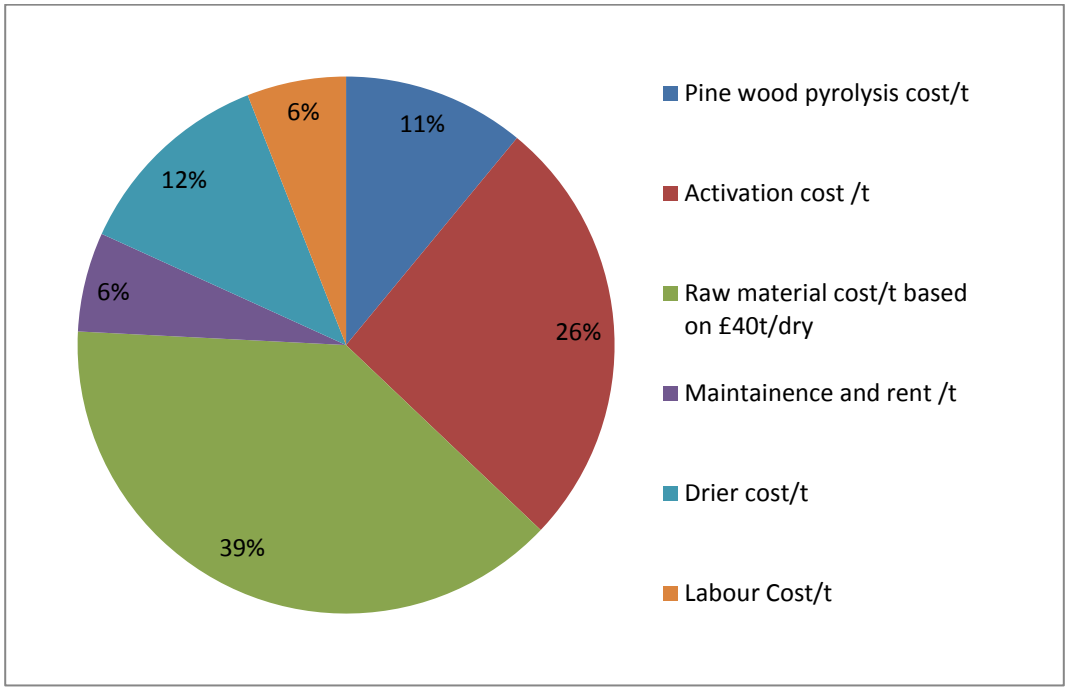


Figure 7:20 Total OPEX for Pine Wood CTC 70, (30% moisture).

Total OPEX without savings in this example: £919

Total OPEX savings via energy recovery: 292

Percentage saved via energy recovery: 32%

Approx. a third of the OPEX costs are recovered through energy savings in this example.

With the total OPEX known, the pre-tax profit margin can be shown per tonne of activated carbon produced at different specifications.

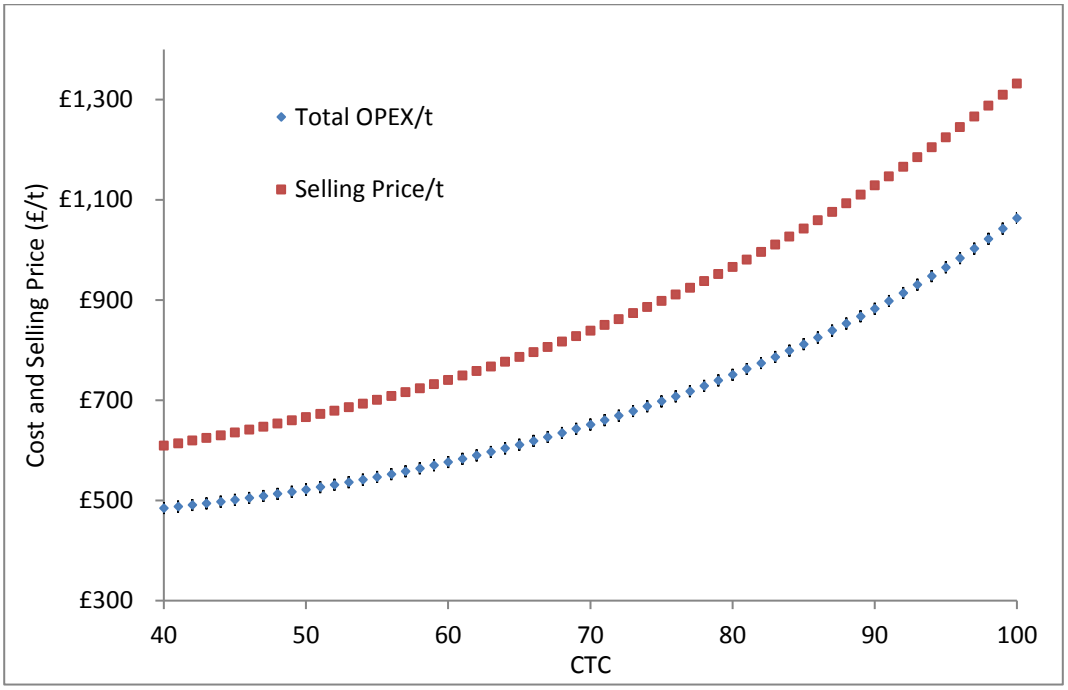


Figure 7:21 Pine wood selling price and OPEX per tonne activated carbon.

The pre-tax profit per tonne is calculated by finding the value in between the two lines shown in Figure 7:21

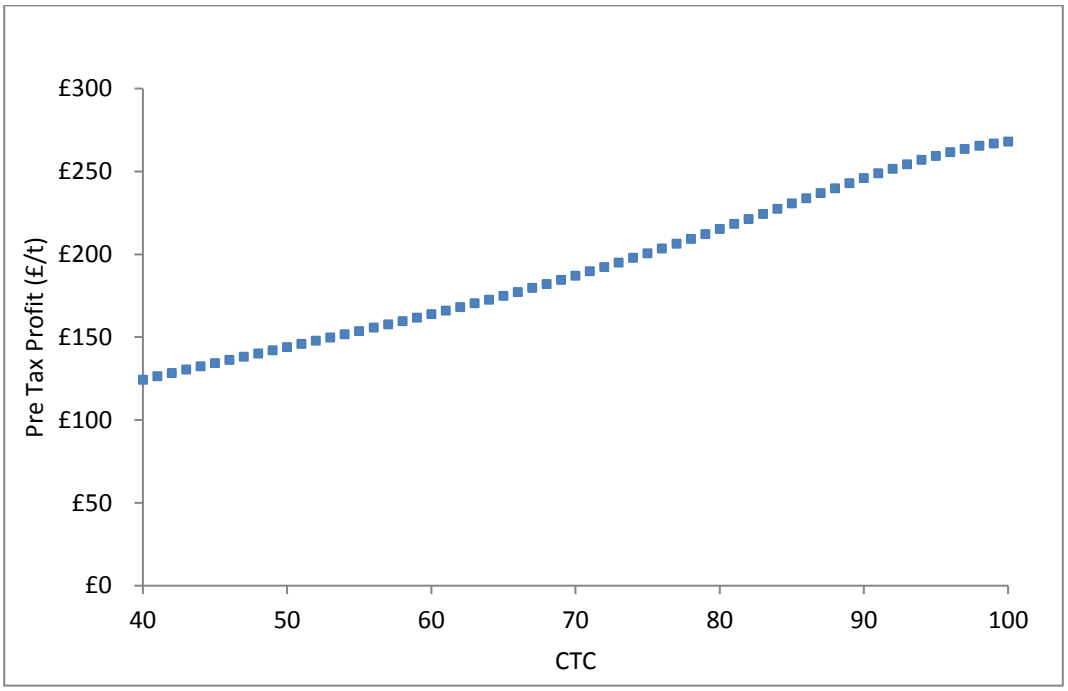


Figure 7:22 Pine wood pre-tax profit per tonne of carbon produced.

Olive stone example CTC 60, initial moisture 20%

Table 7-14 summary shows the total OPEX for olive stone CTC 60, (20% moisture).

CTC	60
Pine wood pyrolysis cost/t	£60
Activation cost /t	£270
Using activation gas saving/t	-£61
Boiler savings activation steam /t	-£132
Raw material cost/t based on £40t/dry	£543
Maintenance and rent /t	£51
Drier cost/t	£41
Boiler savings drier	-£41
Labour cost/t	£60
Total OPEX	**£785**

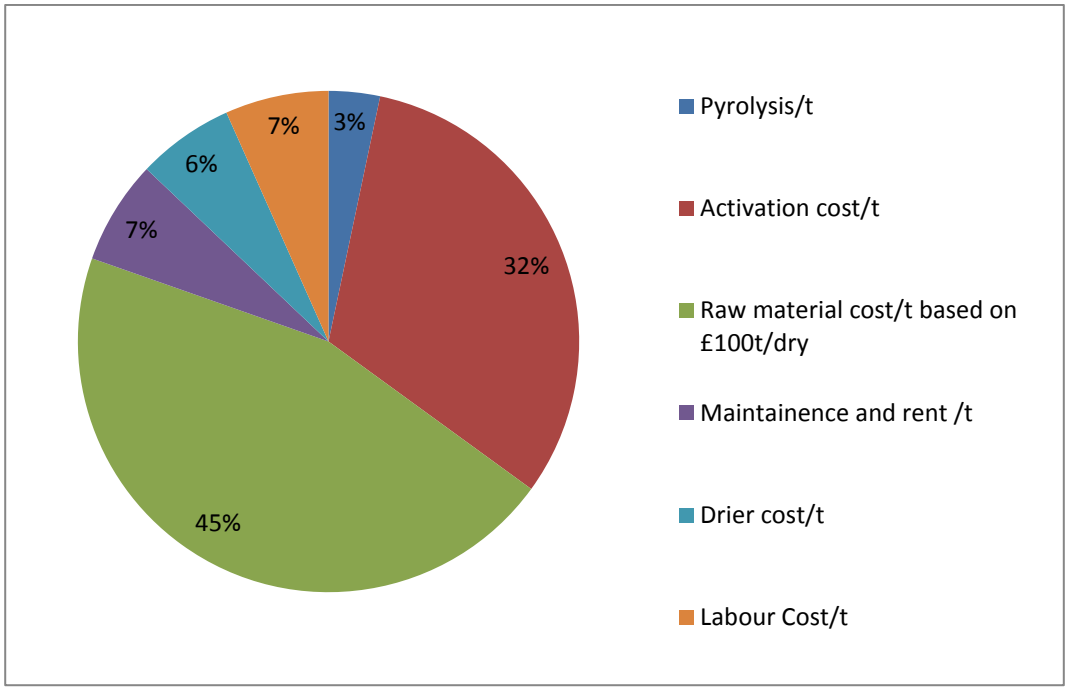


Figure 7:23 Total OPEX for olive stone (CTC 60, 20% initial moisture).

In this example for olive stone the raw material cost contributes to over 50% of the total OPEX.

Total OPEX without savings in this example: £1,024

Total OPEX savings via energy recovery: £239

Meaning energy savings account for 23% of the total OPEX costs.

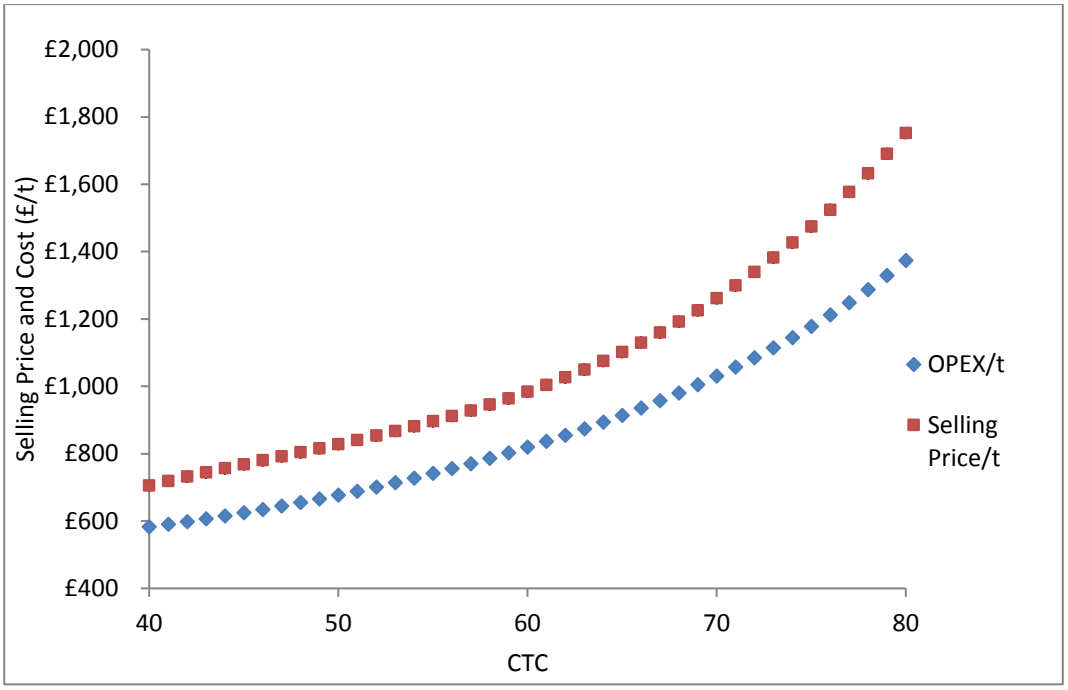


Figure 7:24 Olive stone selling price and OPEX per tonne activated carbon.

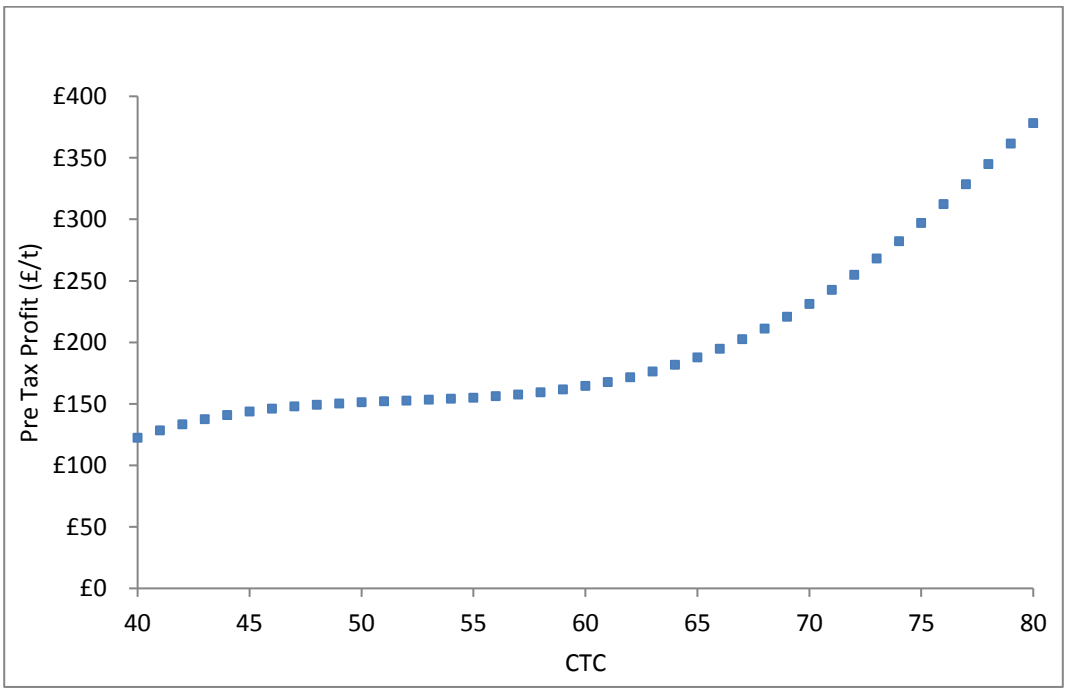


Figure 7:25 Olive stone pre-tax profit per tonne of carbon produced.

This profit is purely based on OPEX and pre-tax. Tax levels for industry are approx. 20-21% depending on how much profit is generated for the taxable year. [HM Revenue & Customs, 2015]

7.13 Capital Costs

The way capital costs were calculated were in line with the method provided by Sinnott, R.K., [2005]. Capital costs were required for the main equipment used in the process. When the equipment price could not be found directly or in literature the costings were assumed to a reasonable value.

The water tank (500 tonnes) has a quoted price of £15,665 [Direct Water Tanks, 2015]

Boiler cost was calculated by using Equation 7-19 provided by [Sinnott, R.K., 2005].

$$Ce = a + bS^n \qquad \textbf{Equation 7-19}$$

$Ce = (106000) + (8.7 \times 5000^{1})$

= USD 149,500 = **£95,360**

Using Sinnott, R.K., [2005] a drier can be calculated with Equation 7-20

$$13000 + 9100 \times A^{0.9} \qquad \textbf{Equation 7-20}$$

Example Olive Stone at 20% moisture

A= the area of the drier (m^2)

To calculate A

$$Q = UAdT \qquad \textbf{Equation 7-21}$$

Q has been calculated previously in kWh and this is then converted into J/s

U= 1160 W/(m^2K). Taken from [engineering tool box, 2015] steam value at saturation point. Temperature change is assumed to be around 80 ^{o}C.

$A = \frac{2055060.35}{1160 \times 80} = 22.15\ m^2$

$Cost = 13000 + 9100 \times 22.15^{0.9}$

= £160,839

Heat exchanger:

Using Olive Stone CTC 20% moisture as example, again using Equation 7-19

$Ce = a + bS^n$

b= area which had to be calculated

$$\text{Area} = \frac{Q}{U\Delta Tm} \qquad \textbf{Equation 7-22}$$

Tm = Mean Temperature Difference

U = Heat transfer coefficient ($W/m^{2\circ}C$)

Q = Mean heat transfer rate (W)

Q= 921500.523 (at given example)

U = 1160 at steam saturation point [engineering toolbox, 2015]

$$\Delta TM = \left(\frac{(Ts - T2) - (Tc - T1)}{ln\frac{(Ts - T2)}{(Tc - T1)}} \right) \qquad \textbf{Equation 7-23}$$

Ts = Temperature of steam 200 ^oC

T1 = Temperature of cold water 20 ^oC

T2 = Temperature of water out 95 ^oC

Tc = Temperature at saturation 100 ^oC

$\Delta Tm = 91.9$

Area = $\frac{921500.52}{1160 \times 91.9} = 8.64\ m^2$

Ce =$24000 + (8.64 \times 46^{1.2}) = £24{,}855$

Pyrolysis kilns approximate cost - estimates provided by heat systems and by P Riley (CPL, 2014):

Pyrolysis Kiln size 2.1m diameter **£429,000**

Activation Kiln 1.5m diameter × 1.5 = **£330,000 × 1.5 = £495,000.**

The cost of the activation kiln is assumed to be 150% of the regular cost of this size kiln due to the length of heat tube that will be required to produce a long enough residence time but high enough rotation per minute to promote steam carbon mixing, this has been proved to be vital in activated carbon production.

De superheater assumption **£40,000**

Cyclone assumption **£30,000 [**R. Allen, 2012]

Table 7-15 below is taken from Sinnott, R.K., [2005] it is an assumption of further capital costs. Each part of these additional costs is a percentage of the initial capital cost.

Table 7-15 Example Olive stone 60 CTC 20% moisture

Other Associated Costs	£
Total	**£1,290,719**
Installation	£645,360
Controls	£258,144
Contingency	£129,072
Design costs	£387,216
Lagging paint	£64,536
Civil	£258,144
Structures and buildings	£129,072
Electrical	£193,608
Piping	£258,144
Outside Battery limits	£516,288
Maintenance +rent /yr	£252,981
Total cost	**£4,130,301**

In this example the total cost is shown to be £4,130,301. This money would be loaned by investors and repaid at either a set amount or a percentage of the operating profit each year.

7.14 Sensitivities

Sensitivities are important when thinking what effect sudden market changes can have on the business. The three main sensitivities looked at are the following [Sinnott, R.K., 2005]:

Utility price change: 50% to 200% of original cost

Raw material price change: 90% to 130% of original cost

Selling price change: 80% to 120% of original cost.

For each one the best and worst scenarios are shown, with a corresponding drop or rise in profit per tonne activated carbon.

Examples below include olive stone at 60 CTC, 20% moisture and pine wood at 70 CTC, 30% moisture.

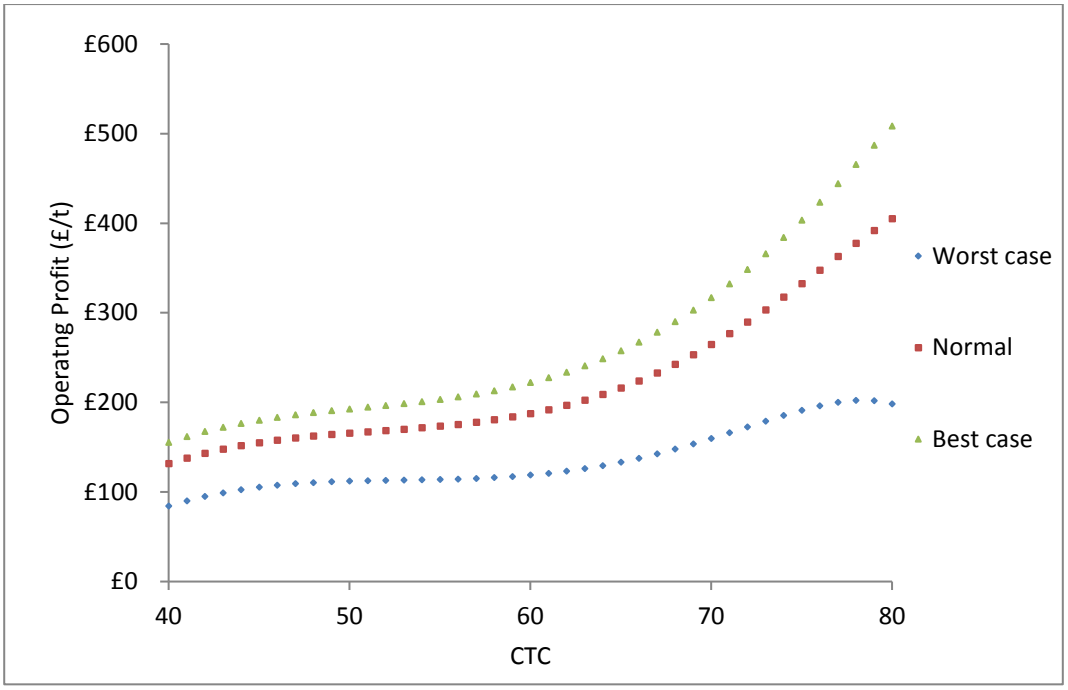


Figure 7:26 Fuel utility price best and worst case effect on profit for olive stone.

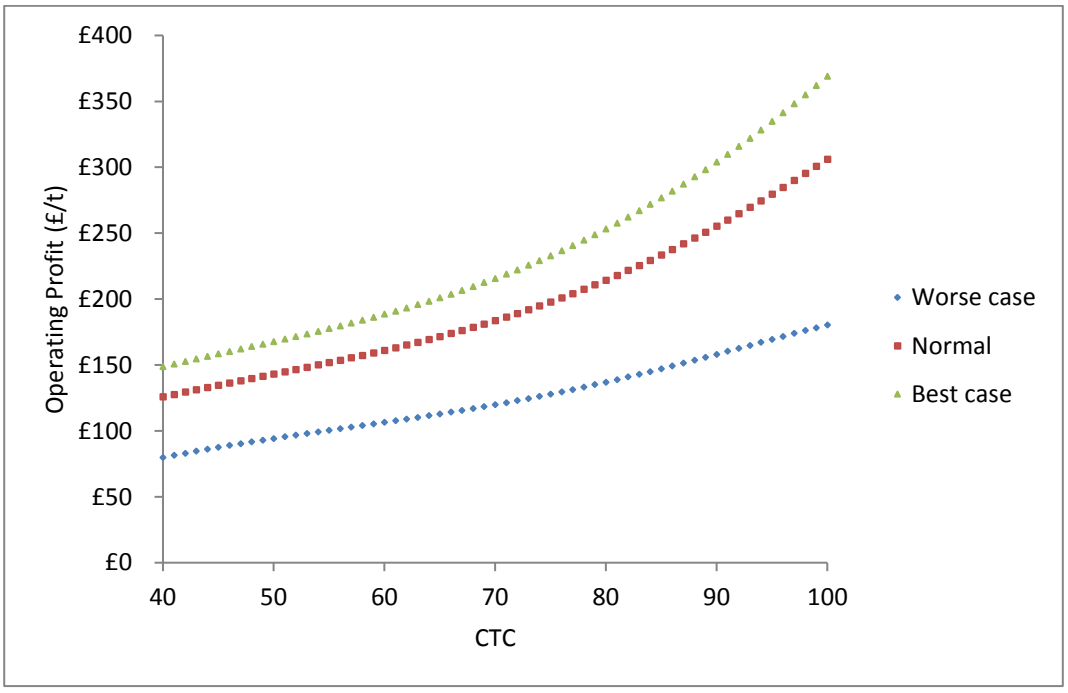


Figure 7:27 Fuel utility price best and worst case effect on profit for pine wood.

Figure 7:26 and Figure 7:27 above show the effect on pre-tax operating profit if utility costs double or half. Gas and electricity prices can fluctuate significantly and, therefore, it must be shown what effects these changes have on the business model. If this is the only change, then pine wood and olive stone stay in profit in the worst case scenario but the profit is lowered significantly.

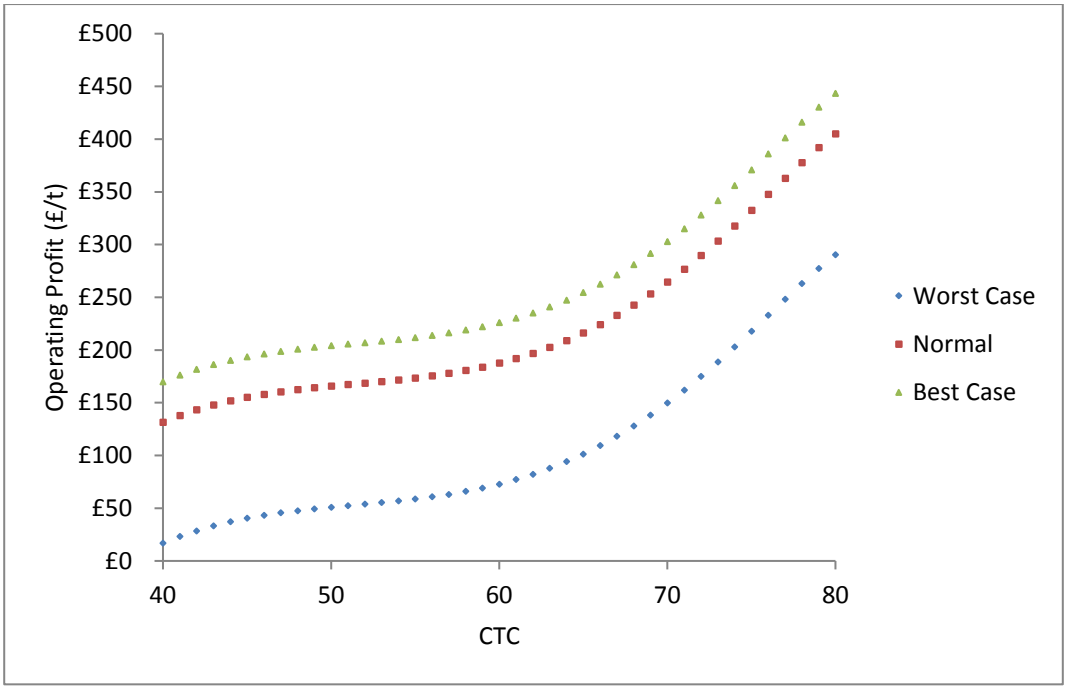


Figure 7:28 Raw material price best and worst case effect on profit for olive stone.

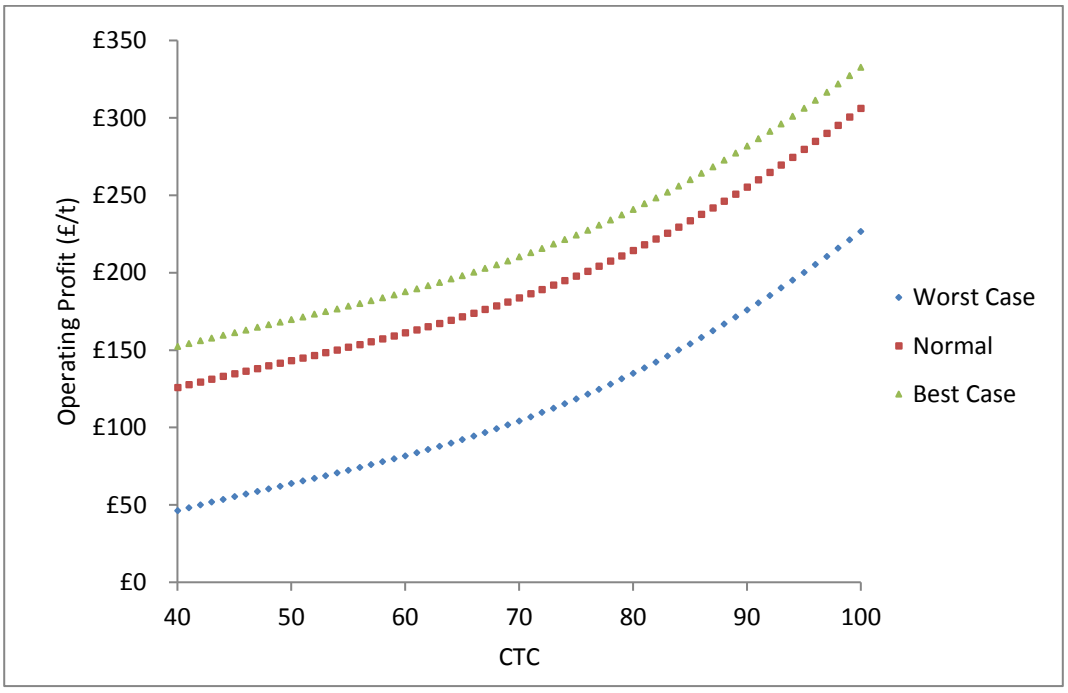


Figure 7:29 Raw material price best and worst case effect on profit for pine wood.

Precursor cost is shown to be the main cost during the production process with olive stone costing more than pine wood. This correlates with Figure 7:28 and Figure 7:29 that show the effect in change of precursor costs from 10% lower in best case to 30% higher in the worst case scenario. Again both remain in profit at the worst case scenario although, as before, with the profit for

both lowered significantly. This is more so in the case of olive stone as raw material costs are greater.

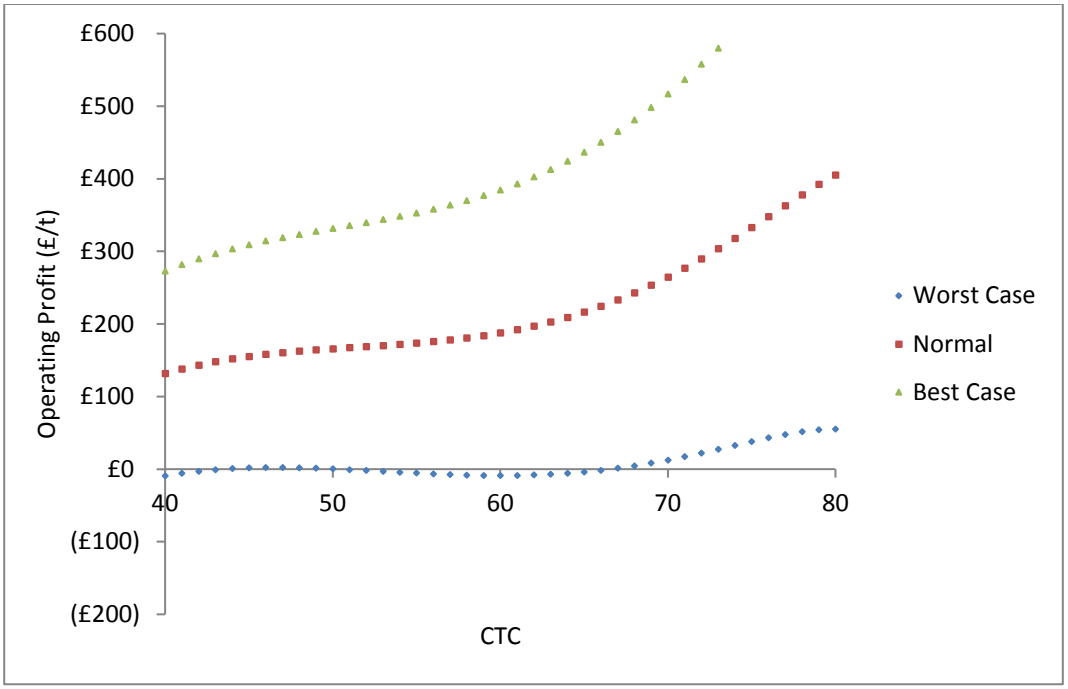


Figure 7:30 Selling price best and worst case effect on profit for olive stone.

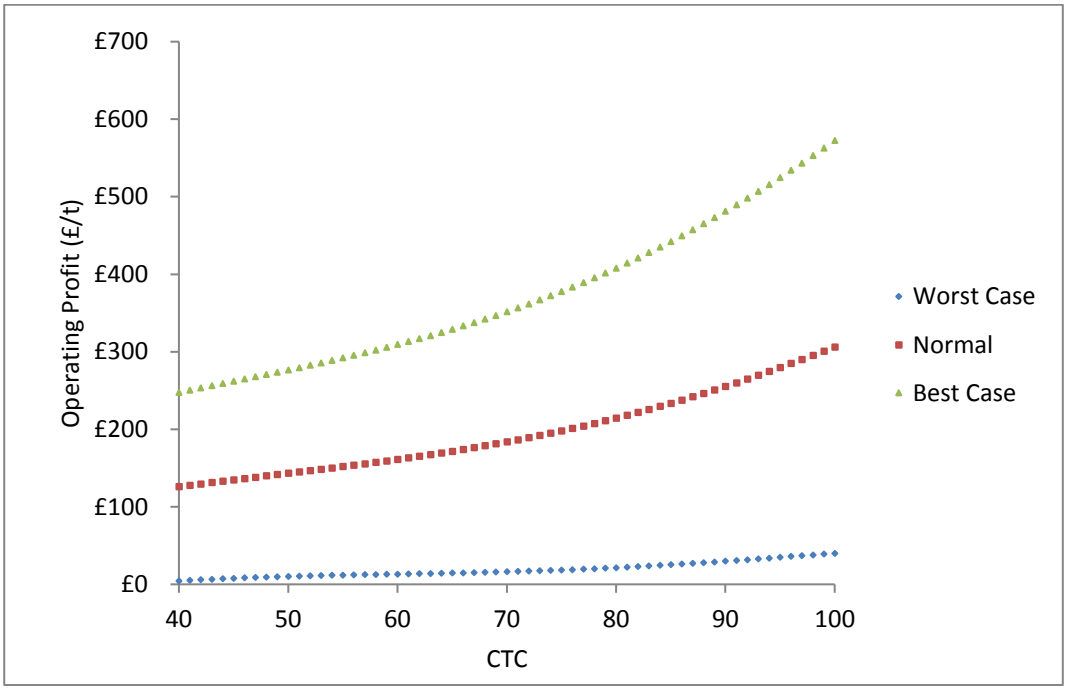


Figure 7:31 Selling price best and worst case effect on profit for pine wood.

The selling price can change too and needs to be considered. It may be that there becomes increasing competition in the market which would decrease the attainable selling price, or decreased competition and alternatives that would enable the selling price to be increased.

Assuming everything else were to remain the same, then Figure 7:30 and Figure 7:31 show how changing the selling price by 20% either way affects overall operating profit. Pine wood manages to stay in profit but olive stone starts to incur an operating loss. This is due to olive stone having a higher selling price as the same quality of pine because of its harder nature allowing it to be sold as granular activated carbon. Therefore the price decreases more significantly with the worst case scenario.

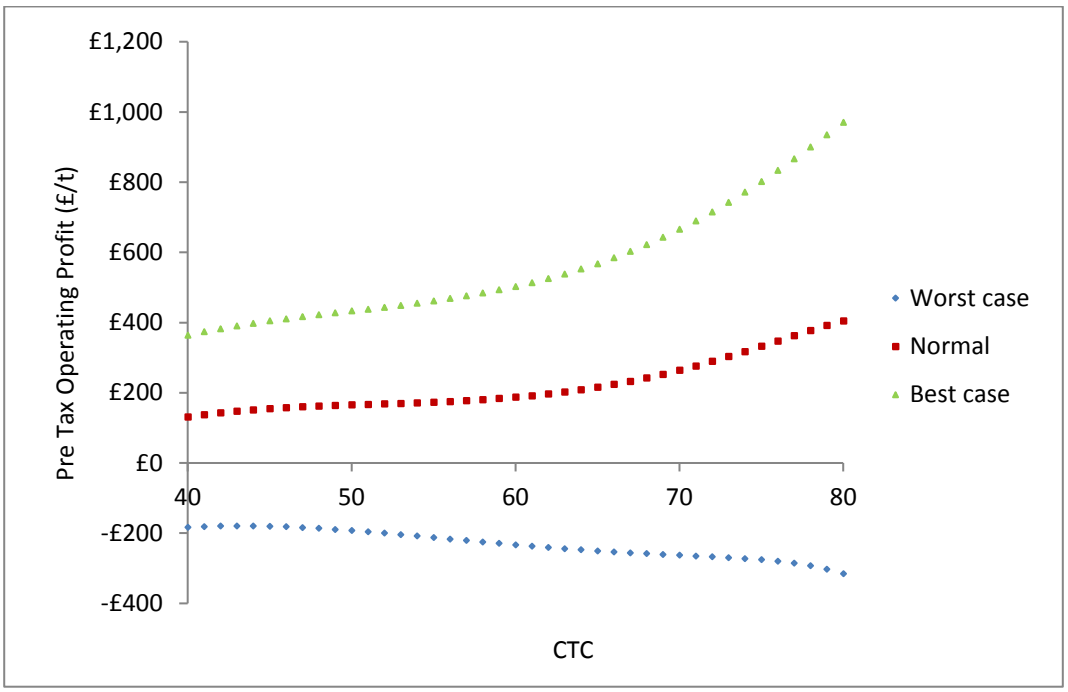


Figure 7:32 Showing overall sensitivities for olive stone activated carbon.

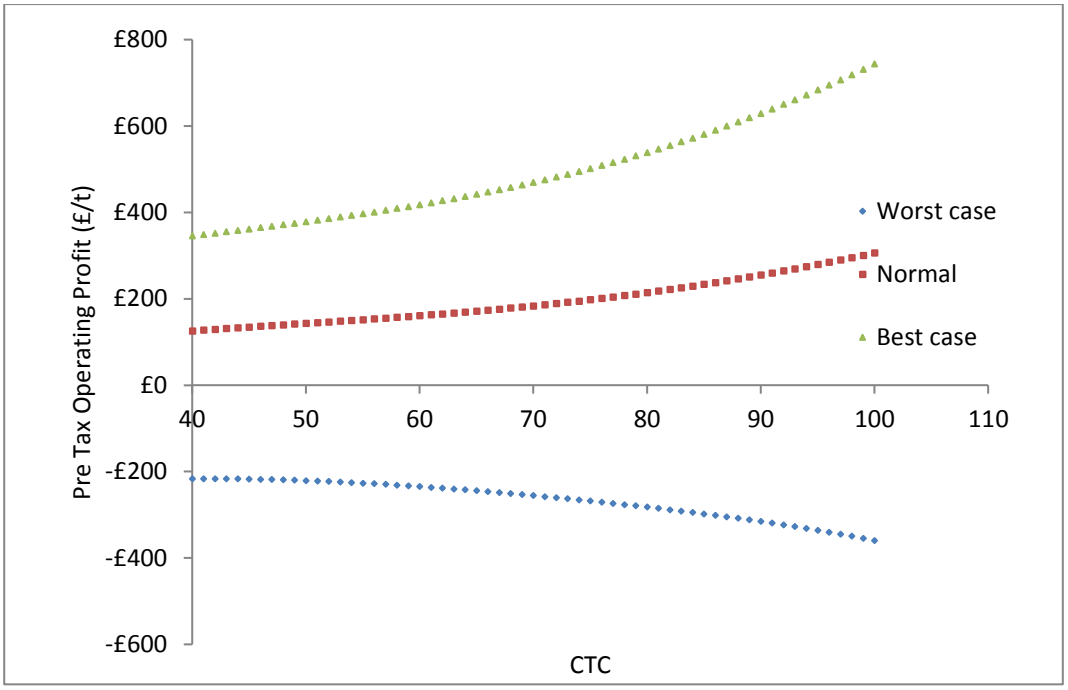


Figure 7:33 Showing overall sensitivities for pine wood activated carbon.

Figure 7:32 and Figure 7:33 above show the total best and worst case scenarios from the sensitivities above. Both carbons on all worst case scenarios provide an operating loss. However, the best case scenarios show very strong business models, as do normal conditions. Operating profit is important but also the capital expenditure needs to be brought into the equation as repayment of loans is required.

7.15 Break Even Analysis

For this part tax at 21% has been taken into account.

Here it is assumed that all char produced during pyrolysis is turned into activated carbon and then 100% of this is then sold at the stated selling price for the given CTC.

Table 7-16 CAPEX payback period for olive stone CTC 60 initial (20 % moisture).

Profit after tax per/t using chosen CTC	**£162**
Average tonnes sold (yr)	**5120**
Average operating profit forecast(yr)	**£830,570**
Capital cost	**£4,130,301**
Payback period in years before interest	**4.97**

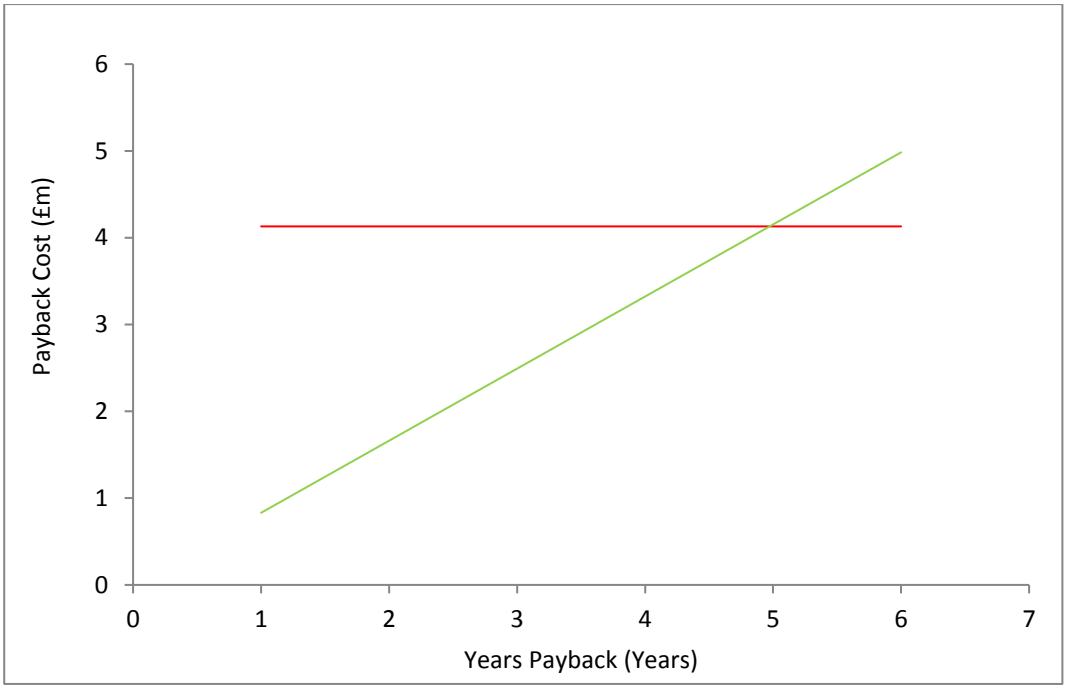


Figure 7:34 The payback period taking assuming no interest on loan is approx. 4.97 years.

If many different carbons were produced during the year then the using the same method before the average years pay back can be calculated. Different carbons maybe needed throughout the year to meet market need.

7.16 Conclusions

1. Depending on the initial moisture content it is either advantageous to go through a pre-drying stage or straight into a pyrolysis kiln. The results show that when the initial moisture content reaches approx. 15% it is more beneficial to pre dry the biomass.
2. Required activation temperatures are calculated to achieve a specific burn off based on lab scale results. Activation temperature is the main changeable variable incorporated in the model.
3. Activation and pyrolysis steps provide potential for energy recovery that can offset significant percentage of OPEX costs 23% and 32% for olive stone and pine wood respectively.
4. Lab scale and pilot scale production results used to predict surface area, pore analysis and methylene blue number for given carbons depending on conditions chosen.
5. Energy recovery calculations show steam production provided by combustion of pyrolysis gas and oils can dry up to moisture contents of 33% and 43 % for olive stone and pine wood respectively.
6. Sensitivities conducted show how losses only occur on cumulative worst case scenarios.
7. The model shows both carbons can produce a profitable business with carbons of varying quality.
8. The model provides a good comparison between granular (olive stone) and powdered (pine wood) carbons and how the pyrolysis, activation and energy recovery stages differ for both. Total OPEX lower for pine wood carbons across the CTC range.
9. Pine wood activated carbon is cheaper to produce but selling price is lower. Olive stone can produce higher revenue at high CTC values as selling price much higher for niche markets that require high quality granular carbon: such as the respiratory sector.
10. With the examples used: olive stone at a CTC value of 60 and initial moisture content of 20% yields a pre-tax operating profit of approx. £160/t. Pine wood with a CTC of 70 and 30% moisture yields a pre-tax operating profit of approx. £185/t.

7.17 References

A. Andreev, V. Kafedjiiski, T. Halachev, B. Kunev, M. Kaltchev, 1991. "*Raney type copper-zinc-aluminium catalyst for water-gas shift reaction".* Applied Catalysis.

Alessandro Parenti Piernicola Masella Lorenzo Guerrini Antonio Guiso Paolo Spugnoli, 201*4. 9 "Energetic and Economic Viability of Olive Stone Recovery as a Renewable Energy Source: A Southern Italy Case Study".* Agricultural Engineering.

Allen, P. R., 2012. "Particulate Emissions"..

Anon, 2015. Direct Water Tanks. [Online]
Available at: http://www.directwatertanks.co.uk/500000-litres-coated-steel-water-tank-with-liner-and-cover&currency=GBP&language=en?gclid=COKe08SjxMcCFQmdGwodurUKOA
[Accessed July 2015].

Anon, 2015. Engineering toolbox. [Online]
Available at: http://www.engineeringtoolbox.com/
[Accessed September 2015].

Anon, 2016. Bioboost. [Online]
Available at: http://bioboost.eu/uploads/files/bioboost_d1.1-syncom_feedstock_cost-vers_1.0-final.pdf
[Accessed July 2016].

DECC, 2015. *"Quarterly energy prices", Department for Business,* Energy & Industrial Strategy.

*Kemp, I. C., 2012. "Modern day drying technology" - F*undamentals of Energy Analysis of Dryers. Volume 4 e*d.*

L.Goovaerts, Y.veys, P.Meulepas, P.Vercaemst, R. Dijkmans,, 2001. *"Beste beschikbare technieken voor de gieterijen".*

M. Ringer, V. Putsche, and J. Scahill, 2006. *"Large-Scale Pyrolysis Oil Prodcution, A technology Assessment and Economic Analysis":* National Renewable Energy Laboratory.

Mahadevan, B., 2009. Operation Management*: "Theory and Practice". 1* ed. India: Business & Economics.

McVeigh, T., 2015. Price of olive oil soaring after worst harvest in over a decade. [Online]
Available at: https://www.theguardian.com/lifeandstyle/2015/jan/03/olive-oil-price-rise-feared
[Accessed November 2015].

P. Sanginés, M. P. Domínguez, F. Sánchez and G. San Miguel, 2015. *"Slow pyrolysis of olive stones in a rotary kiln: Chemical and energy characterization of solid, gas, and condensable products".* Renewable and Sustainable Energy.

Revenue, H., 2015. Quarterly energy prices. [Online]
Available at: https://www.gov.uk/government/organisations/hm-revenue-customs
[Accessed July 2015].

Sinnott, R., 2005. *"Coulson and Richardson's Chemical Engineering" Volume 6* - Chemical Engineering Design. 4th Edition ed.

Taylor, C. F., 1995. *"Internal Combustion Engine in Theory and Practice: v. 1 (Internal Combustion Engine in Theory & Practice. In: Thermodynamics, Fluid Flow, Performance"*. Cambridge: , p. pp. 46–47.

Chapter 8 Key Conclusions and Future Work

8.1 Key Conclusions

1. Initial findings from the preliminary trials show how biomass feedstock choice is crucial in determining how the final carbon product performs. Each biomass feedstock produces a carbon with different physical and pore characteristics. This means for an activated carbon to meet the requirements of an industrial application the right type of precursor must be selected before reaching the activation stage. So although primary and secondary activation variables can influence pore structure initial precursor choice the most important when deciding the type of carbon required.
2. Steam is more reactive with carbon then carbon dioxide at the same activation temperatures. Not only is steam production usually cheaper than using carbon dioxide it also means milder activation conditions can be used to achieve the same burn off between the two physical activation oxidising agents. However, this depends on the final application requirements - Steam activation produced a much more mesoporous carbon whereas if an ultra-microporous carbon is required then CO_2 activation has the advantage.
3. Linear burn off rates are observed with increasing activation temperature and residence time, yet exponential increase seen with increasing water flow rate. This was the same for olive stone and pine wood chars. These trends can be of major advantage when prediction of burn off is required when changing the production variables.
4. Direct linear correlation between burn off and CTC values for both olive stone and pine wood activated carbon. This correlation can be a significant help in planning large scale carbon production as the burn off being achieved will give a clear indication as to the current quality of the carbon.
5. CTC analysis provides an excellent correlation to micropore volume, methylene blue number and surface area. CTC values provide a relatively good estimate of total pore volume in particular with pine wood. CTC analysis (a 20 minute test) proves to be a very good overall indicator of a carbon's quality and correlates well to more expensive analysis techniques.
6. CTC values begin to curtail over 80% and 85% burn off for olive stone and pine wood respectively due to high ash to carbon ratio and destruction. At this point either the activation temperature or residence time of the reaction is too high, too long or a combination of both. A reduction in carbon adsorption performance along with a yield reduction is an unwanted outcome for the carbon producers.

7. High activation temperature causes external particle burn off from early stages of the reaction as reaction rate too high. This high reaction rate offers no carbon performance enhancement and only lowers product yield.
8. Methylene blue number correlates better with micropore volume than mesopore volume with both carbons. This is an unexpected finding as although it has been reported in literature methylene blue adsorption is more commonly known as a mesopore volume indicator.
9. In comparison to olive stone carbons, pine wood carbons can reach higher mesopore volumes, this difference escalates as carbon burn off increases. At low burn offs both carbons micropore and mesopore volumes are very similar. This means that pine wood carbons with burn off > 50% will potential be better suited to industrial applications that requires more adsorption in the mesopore region.
10. Primary variable production boundaries on lab scale were found. For olive stone activated carbon production (> 850 ^{o}C, > 6 hours, > 1.875ml/min). Activation temperature limit found for pine wood carbons (> 825 ^{o}C). Anything over these boundaries had adverse effects on the carbon whether in terms of adsorption performance, yield or a combination.
11. Olive stone char burn off rates dependant on amount of char present during the activation reaction with the increasing char mass leading to a decrease in burn off per gram of char. Pine wood char burn off rate remained constant throughout trials. Mass transfer limitation observed with olive stone char during activation again signalling the importance of maximising steam carbon contact.
12. Single step production shows no negative effects on the carbon product, pore structure and carbon adsorption properties compared to a two-step production process. This finding can have a significant impact on large scale production with large capital expenditure savings being met due to the requirement of only one rotary kiln for simultaneous pyrolysis and activation.
13. Fast pyrolysis produces a more reactive char meaning lower activation temperature, residence time and water flow rate required to achieve desired burn off, but at the cost of final yield.
14. Cost analysis proves that carbon production using both pine wood and olive stone biomass feedstocks can yield a profitable business plan with an energy recovery system implemented.

8.2 Future Work

1. Lab Scale future work: Investigating in depth chemical activation, using the same two biomass feedstocks used in the majority of this project. This would enable a direct comparison to be made between chemical and physical activation of pine wood and olive stone carbons. Conducting the same analysis techniques would allow a direct comparison of pore structure and size distributions along with adsorption performance of butane and methylene blue. Chemical activation can bring added performance to carbons as certain chemicals can be added during the activation stage or before that can increase carbon performance, for example the addition of K_2CO_3 during activation aids in the adsorption of CO_2.

2. Pilot Scale future work: further pilot scale experimental trials can be completed with different pilot kilns and design. This is to be able to produce the most cost efficient design that produces a high quality carbon whilst minimising activation thermal input, residence time and the amount of oxidising agent required. Further work should be done on the exact benefits of lifters and what effects they have within the heat tube in terms of additional mixing, allowing less steam to be used.

3. End application carbon performance is crucial and although CTC and methylene blue adsorption tests give an idea of the quality of the carbon it can't be taken with 100% confidence that the carbon will perform the same in an industrial application. End user applications trials are the next important step before producing these carbons on a commercial scale as there are many external factors that can affect how the carbon performs. An example of these external factors include the concentration of the unwanted impurity or the environmental condition in which the unwanted contaminant is wanted to be removed. Carbons are continuously finding new markets and meeting the needs of new industries with continuous stricter environmental regulations being put in place. Tests can be carried out within industries in which carbons are, as of yet, not used and would provide valuable information to both producers and potential customers on how to optimise the use of activated carbons.

4. The cost analysis model can be enhanced further with more information gained by additional pilot scale trials. Currently the cost analysis model is based around changing activation temperature to achieve different levels of burn off. Additional information would allow both residence time and steam flow rate change being incorporated into the financial model. This would enable the user to find the cheapest method to produce

a carbon of a specific burn. CFD can also be incorporated into the work to analyse flow dynamics. With chemical activation also investigated the cost analysis model can reflect this type of activation where a clearer indication would be given as to which route to go down if both physically and chemically activated carbons meets the application specification requirements.

A. Appendix

Physical activation reactions were considered both thermodynamically and kinetically

$$\boldsymbol{H_2O + C \rightarrow CO + H_2}$$ **Reaction A-1**

And,

$$\boldsymbol{CO_2 + C \rightarrow 2CO}$$ **Reaction A-2**

A.1 Gibbs Free Energy Analysis of Reaction 1 and Reaction 2

Reaction 1

Enthalpy of reaction

$$\sum H = \sum Hfo\ (products) - \sum Hfo\ (reactants)$$ **Equation A-1**

∑(-110.5+ 0) – (-241.8 + 0) = +131.3 kJ/mol. Endothermic reaction

Therefore, to convert 1 mole of water to 1 mole of each H_2 and CO requires 131.3 kJ of energy. Increased water in the system increases H_2 production in accordance with Le Chatelier's principle, i.e. an increase in concentration on one side of the equilibrium results in an increase in concentration on the other side.

To calculate the Gibbs free energy of the reaction the entropy must also be calculated using Equation A-1 however, this time using entropy values:

∑(197.66+ 130.59) – (5.69 + 188.72) = 133.84 j k^{-1} mol^{-1} = 0.13384 kJ mol.

Because the entropy is positive, a reversible reaction is possible but would take a significant amount of time.

Gibbs free energy

$$G = \Delta H - T\Delta S \qquad \textbf{Equation A-2}$$

A negative value is needed for a spontaneous reaction to occur.

Example - activation temperature of 800 °C (1073K)

$\sum (131.3) - (1073 \times 0.13384)$

=131.3 – 143.6304 = **-12.33 KJ**

At around 700°C (973.15K) Gibbs free energy is 0 meaning the forward reaction is no longer spontaneous and requires further energy.

This aids understanding as to why there is a significant increase in burn off found from 700°C to 800°C

Reaction 2

Enthalpy of formation

Using Equation A-1:

$2(-110.525) - (-393.509)$

Enthalpy of formation = **172.459 kJ mol. endothermic**

$\sum 2(197.66) - (5.69 + 213.79) = 175.84$ J k^{-1} mol. = 0.17584 kJ mol.

Entropy = **0.17584 kJ mol.**

Gibbs free energy at 800°C

Using Equation A-2:

$(172.459) - (1073.15 \times 0.17584)$

= 172.459 – 188.703

Gibbs = **-16.24 kJ = spontaneous**

Increasing temperature means the reaction moves forward as per Le Chatelier's principle due to the reaction being endothermic. In this case more hydrogen and carbon monoxide will be produced.

Changing pressure has no effect in this reaction equilibrium due to same number of moles present on each side of the equilibrium. If the moles weren't balanced, then increasing pressure would result in movement to the side with the fewest moles.

A.2 Equilibrium Rate constant

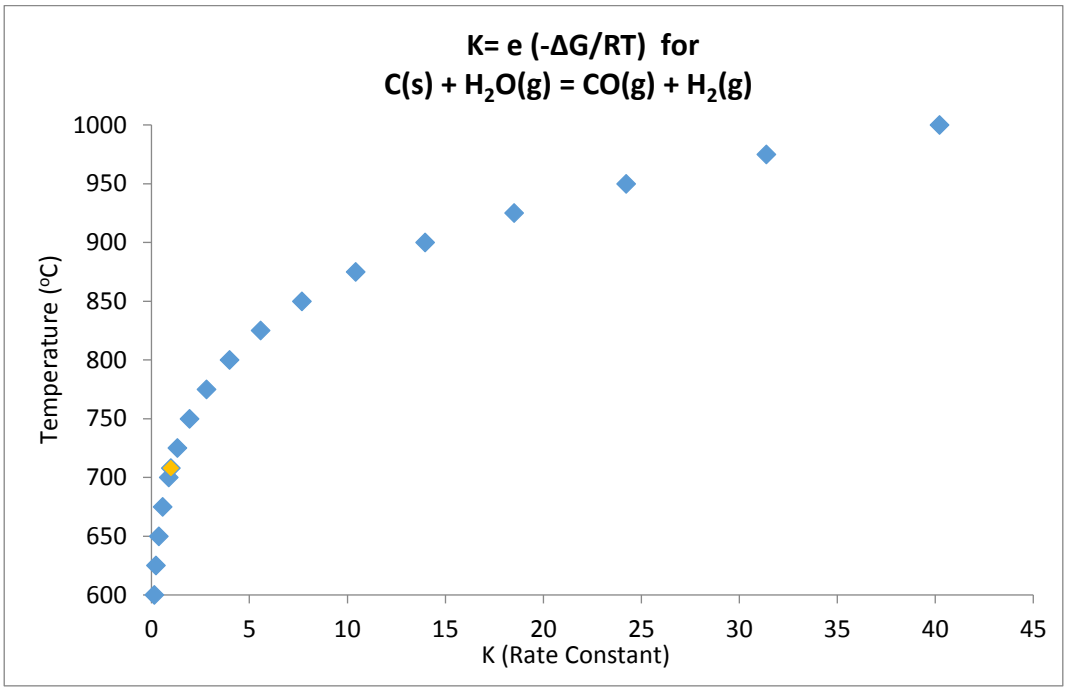


Figure A:1 Equilibrium constant (K) against temperature.

A reaction's equilibrium constant, K, measures the extent to which reactants are converted to products by the reaction [Chemicool, 2014]. The equilibrium constant is important to understand what is occurring during the activation process. The kinetic rate of reaction increases as temperature increases as it is solely temperature dependent. When the rate constant (K) is above "1" the forward reaction is favoured. This occurs at precisely 709.7 °C as shown by the yellow data point on Figure A:1. As the temperature increases beyond this point the graph shows how the rate of reaction increases rapidly before the increase begins to slow. This shows that, as the temperature during activation increases, the faster the reaction happens and so, in theory, the quicker the desired activated carbon product can be produced.

Therefore, commercially speaking, this is beneficial as faster the carbon can be produced the higher the productivity. However, it is not as straightforward as this and, as the results in this project show, too high a temperature can have other negative effects on the carbon.

This research aided the decisions as to what temperature ranges to look at during activation

A.3 Tables and Figures

Table A-1 Biomass Database.

Column1	Carbonisation Temperature (°C)	Carbonisation Dwell Time (mins)	Carbonisation Yield %	Sample used for Activation (g)	Activation Temperature (°C)	Activation Residence Time (mins)	Water flow rate (ml/min)	Nitrogen flow rate for Carb/Act (L/min)	Heating rate for Carb/Act (°C)	Mass of sample after activation (g)	Carbon Yield (%)	Activated carbon yield from raw biomass %	CTC
Almond Shell	700	30	22.57	5.06	800	60	1.5	1	15	2.89	57.11	**12.89**	**55**
Palm Kernel Shell	700	30	28.33	6.03	800	60	1.5	1	15	4.5	74.63	**21.14**	**44**
Waste Wood	700	30	23.54	4.98	800	60	1.5	1	15	2.79	56.02	**13.19**	**46.5**
Olive Cake pellets	700	30	25.29	7.08	725	60	1.5	1	15	3.05	43.08	**10.89**	**25**
Eucalyptus Wood	700	30	18.1	0.733	800	60	1.5	1	15	0.164	22.37	**4.05**	**93**
Olive Stones	700	30	28.1	3.37	800	60	1.5	1	15	2.68	79.53	**22.35**	**54**
Coconut Shell	700	30	25.24	3.4	800	60	1.5	1	15	2.2	64.71	**16.33**	**65**
Peach stones	700	30	22.57	3.19	800	60	1.5	1	15	2.24	70.22	**15.85**	**51**
Avocado pits	700	30	21.73	1.7	800	60	1.5	1	15	0.41	24.12	**5.24**	**37**
Miscanthus pellets	700	30	28.74	3.89	700	60	1.5	1	15	2.12	54.50	**15.66**	**29**
Grape Seed	700	30	31.2	2.11	800	60	1.5	1	15	0.921	43.65	**13.62**	**64**
Cherry stones	700	30	25.63	1.58	800	60	1.5	1	15	0.446	28.23	**7.23**	**83**
Coffee grinds	700	30	22.5	2.44	800	60	1.5	1	15	0.882	36.15	**8.13**	**54.5**
Oat Husk	700	30	23.34	0.88	800	60	1.5	1	15	0.49	55.68	**13.00**	**9**
Coco Peat	700	30	41.97	4.08	800	60	1.5	1	15	1.71	41.91	**17.59**	**5**
Micanthus	700	30	24.72	0.754	600	60	1.5	1	15	0.733	97.21	**24.03**	**25**
Miscanthus Pellets	700	30	28.74	3.89	800	60	1.5	1	15	Ash	**N/A**	**N/A**	**N/A**
Avocado	700	30	21.73	1.7	800	60	1.5	1	15	0.1	**N/A**	**N/A**	**9**
Wood coarse char	N/A	N/A	N/A	6.01	800	60	1.5	1	15	3.68	61.23	**N/A**	**60**
Wood fine char	N/A	N/A	N/A	6.5	800	60	1.5	1	15	3.6	55.38	**N/A**	**55**
Straw	700	30	21.94	2.22	800	30	1.5	1	15	0.068	3.06	**0.67**	**2.00**
Castus Hard wood	700	30	11.87	2.863	800	30	1.5	1	15	1.728	60.36	**7.16**	**42**
Coconut shell char	N/A	N/A	N/A	15	800	60	1.5	1	15	9.184	61.23	**NA**	**47.5**
Brown Coal	700	30	45.36	11.331	800	60	1.5	1	15	5.727	50.54	**22.93**	**45**
Grape seed	700	30	34	7.584	800	60	1.5	1	15	1.898	25.03	**8.51**	**71.5**
Brazil nut case	700	30	24.02	3.598	800	60	1.5	1	15	0.95	26.40	**6.34**	**68**
Tucuma	700	30	26.27	5.163	800	60	1.5	1	15	3.945	76.41	**20.07**	**39.5**
Tucuma char	**N/A**	**N/A**	**N/A**	12.421	800	60	1.5	1	15	9.394	75.63	**N/A**	**34**
Palm fruit bunch	700	30	24	5.736	800	60	1.5	1	15	0.869	15.15	**3.64**	**37**
Anthracite	700	30	78.39	16.54	800	60	1.5	1	15	15.024	90.83	**71.21**	**7**
Pine Wood Illiotii dried	700	30	20.8	3.072	800	60	1.5	1	15	1.72	55.99	**11.65**	**70**
Pine wood Tibea dried	700	30	20	2.562	800	60	1.5	1	15	1.207	47.11	**9.42**	**99**

The pyrolysis conditions set as 'standard' for these trials were 700 ºC for half an hour, with a heating rate of 15 k/min and nitrogen flow rate of 1 L/min. The activation conditions chosen as 'standard' were 800 ºC for 1 hour, with a water flow rate of 1.5 ml/min and nitrogen flow rate of 1 L/min. These activation conditions were only altered if these standard activation conditions were too 'harsh' to yield a carbon. For example with miscanthus pellets the activation temperature had to be reduced in order to obtain sufficient sample to analyse, otherwise the only material left in the crucible was ash. How much raw biomass used was decided upon by a given volume within the crucible, as each biomass has a different associated density.

Table A-2 Proximate analysis of biomass as received

Biomass	Moisture %	Ash %	Volatile %	Carbon %
Almond shell	7.9	0.9	80.1	11.1
PKS	7.7	1.3	75.8	15.2
Pine wood	15.7	0.8	72.9	10.6
Olive cake pellets	12.3	5	74	8.7
Eucalyptus wood	4.6	1	81	13.4
olive stones	10.7	0.5	79	9.8
Coconut shell	8.5	0.7	76.3	14.5
Peach stones	19.7	0.7	77.9	1.7
Miscanthus pellets	9.2	7.8	72.2	10.8
Grape seed	10.9	4	69.8	15.3
Coffee grinds	8.3	2.4	78.7	10.6
Oat husk	8.1	4.6	78.1	9.2
Coco Peat	13.3	10	68.1	8.6
Waste wood Coarse char	1.1	15.2	3.2	80.5
Waste wood fine char	0.7	33.9	5.5	59.9

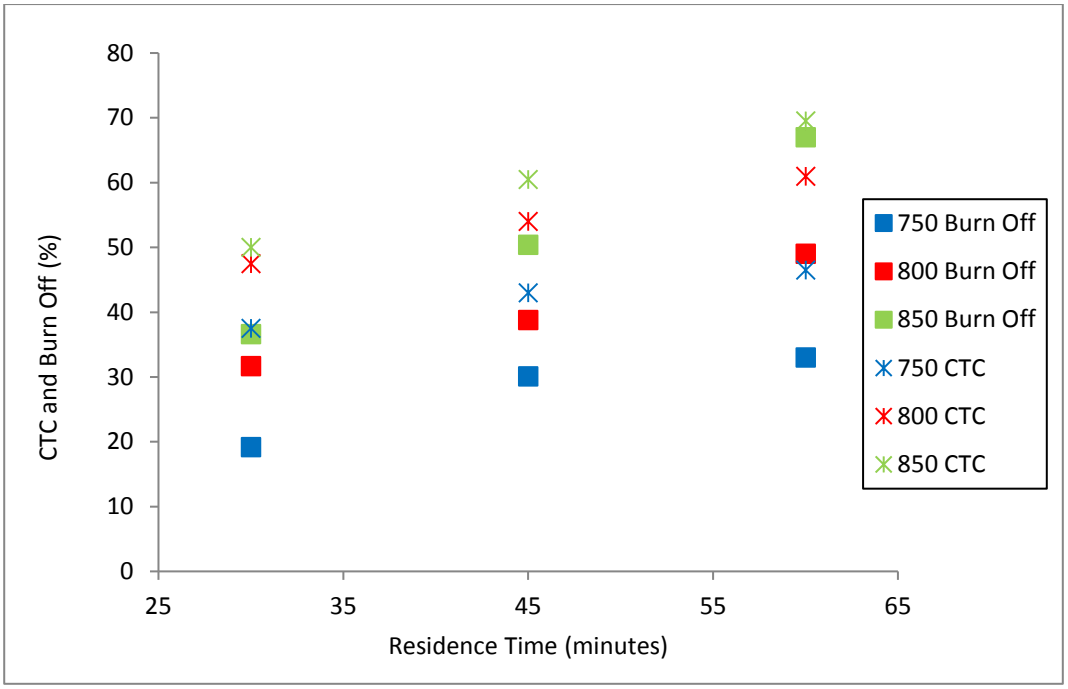


Figure A:2 CTC, temperature and burn off relationship of olive stone activated carbon.

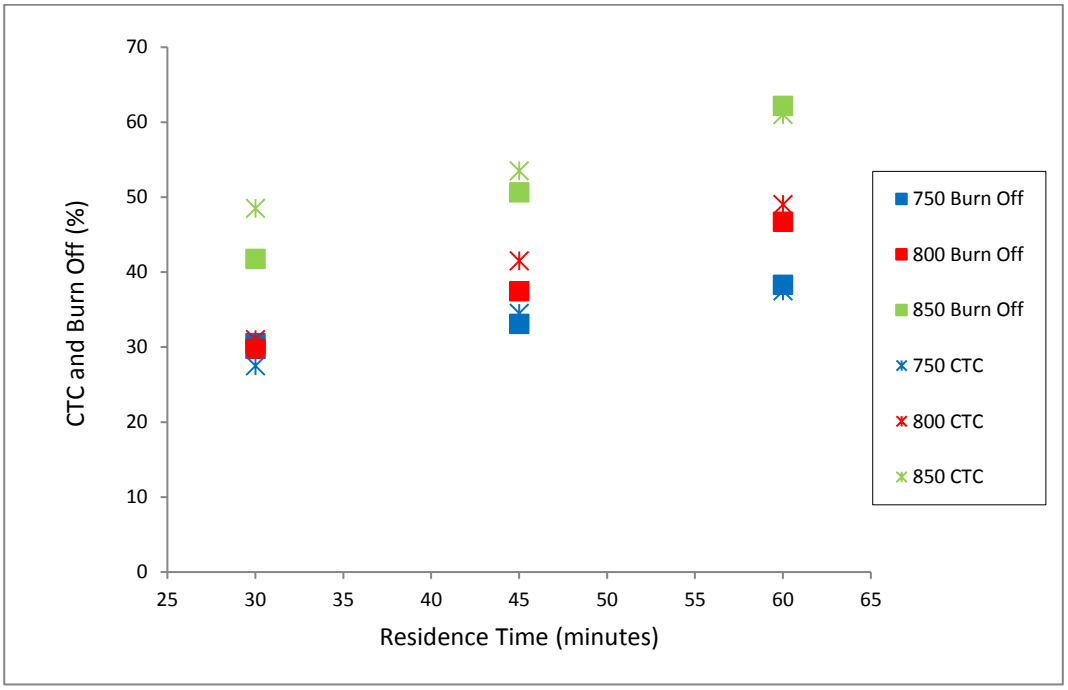


Figure A:3 CTC, temperature and burn off relationship of Almond Shell activated carbon.

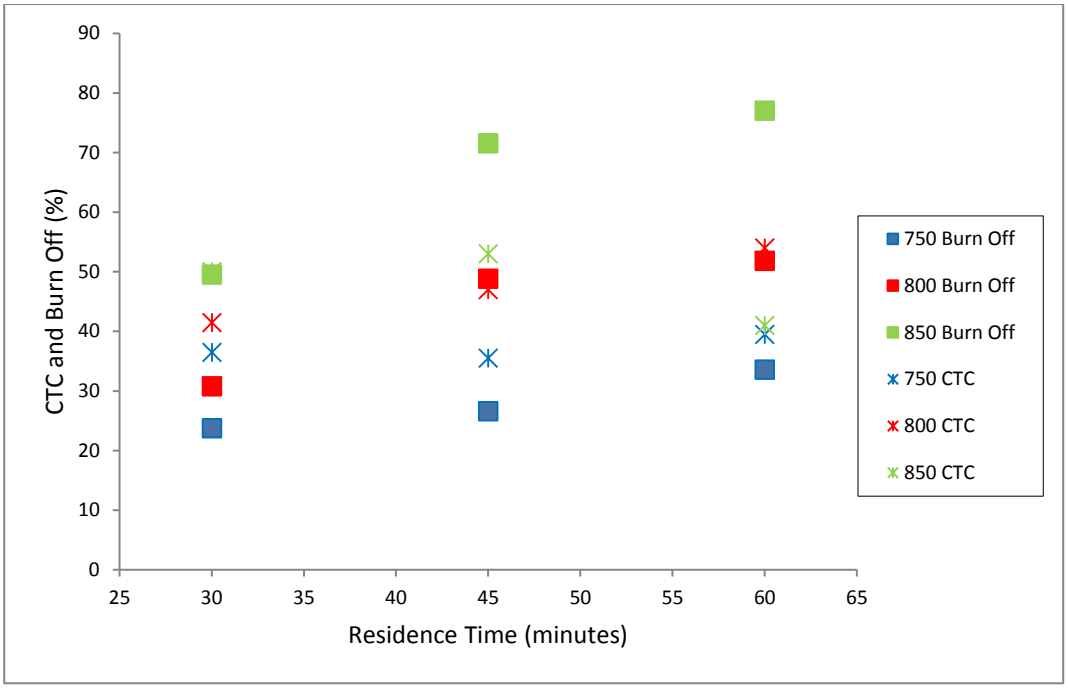


Figure A:4 CTC, temperature and burn off relationship of grape cake activated carbon

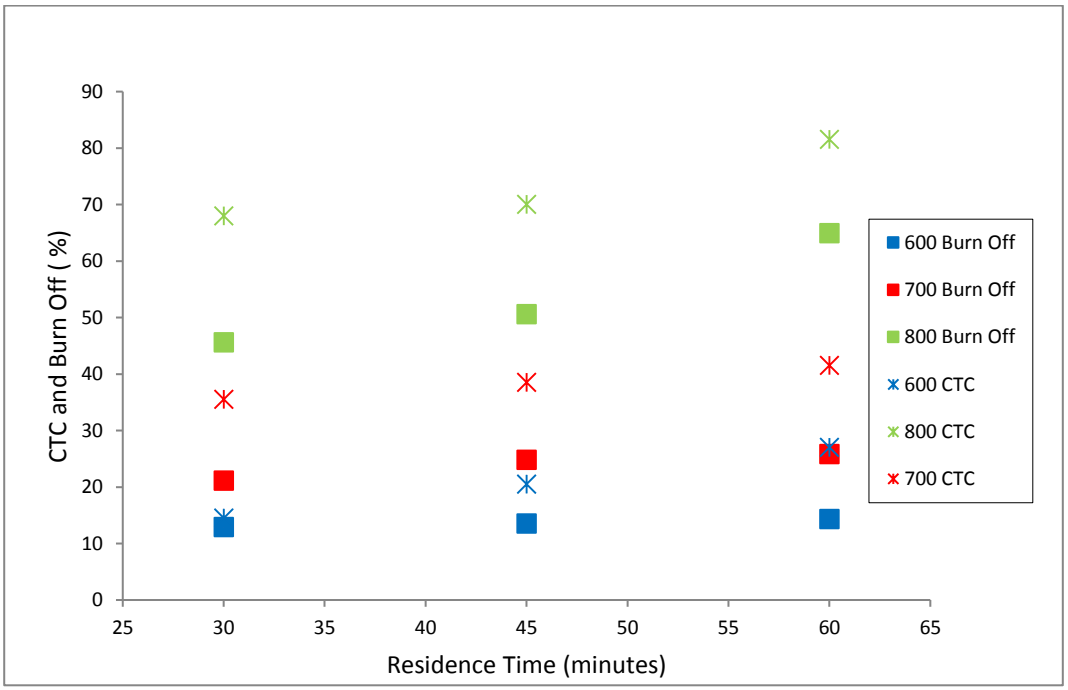


Figure A:5 CTC, temperature and burn off relationship of eucalyptus wood activated carbon.

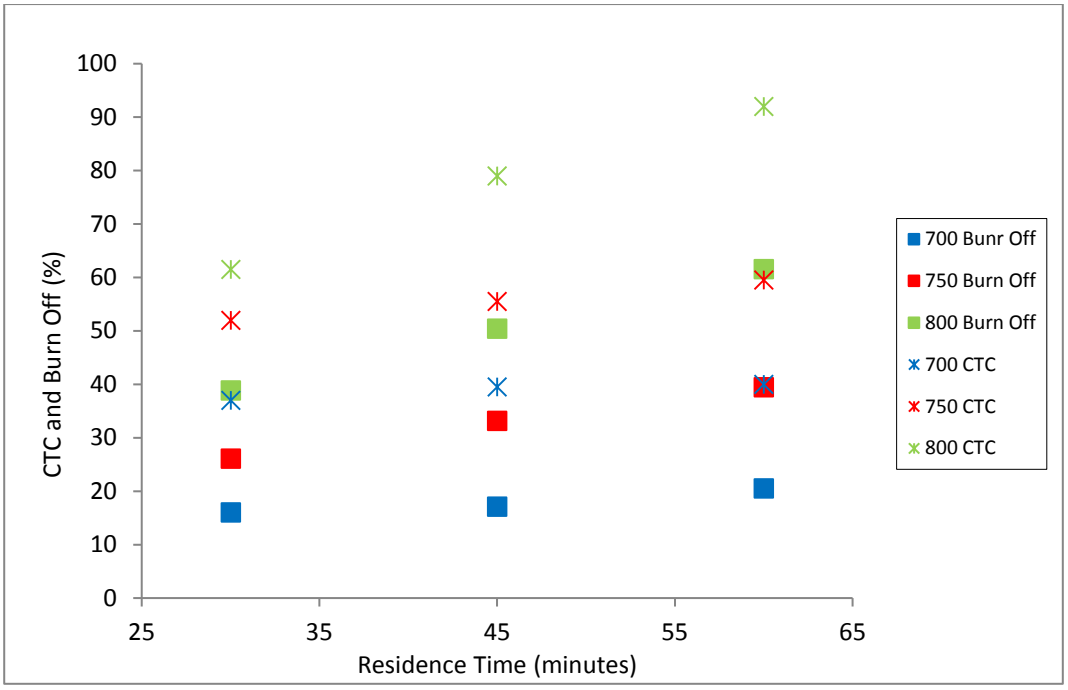


Figure A:6 CTC, temperature and burn off relationship of pine wood activated carbon.

Table A-3 Carbon dioxide and steam/carbon dioxide pore analysis.

CO_2 L/min (800°C)*	Vmi (cm^3/g)	Vme (cm^3/g)	Vtot (cm^3/g)	Vme (%)	BET SA (m^2/g)
0.2L	0.1045	0.0109	0.1154	9.45	263.8
0.6L	0.1472	0.0228	0.17	13.41	372.3
1L	0.1851	0.0288	0.2139	13.46	474
* 900 1 L	0.2405	0.0425	0.283	15.02	607.6
0.2L/ H_20 1.5ml/min	0.3285	0.2029	0.5314	38.18	833.1
0.5L/H_20 1.5ml/min	0.3491	0.2459	0.595	41.33	885.7
1L/H_20 1.5 ml/min	0.3223	0.1914	0.5137	37.26	823.9

Table A-4 Nitrogen flow rates.

	Temp (°C)	Residence Time (mins)	Water Flow (ml)	Nitrogen (L/min)	Moles N_2	Moles H_2O	W/N Molar Ratio	Burn Off (%)	CTC
OS	750	60	90	1	2.5	5	2.0	37.8	47.0
	750	60	90	0.5	1.1	5	4.4	41.0	48.5
	750	60	90	1.5	3.6	5	1.4	34.2	44.0
	750	60	90	2	4.8	5	1.1	32.2	40.5
	750	60	90	2	4.8	5	1.1	31.4	42.0
Average	**750**	**60**	**90**	**2**	**4.8**	**5**	**1.1**	**31.8**	**41.25**
	750	60	90	2.5	5.9	5	0.9	30.6	41.0
	750	60	90	3	7.0	5	0.7	30.1	40.0
	750	60	90	3	7.0	5	0.7	30.3	41.0
Average	**750**	**60**	**90**	**3**	**7.0**	**5**	**0.7**	**30.2**	**40.5**
	750	60	90	3.5	8.1	5	0.6	30.0	39.0
	750	60	90	4	9.3	5	0.5	28.1	38.0
	750	60	90	4	9.3	5	0.5	27.5	37.0
Average	**750**	**60**	**90**	**4**	**9.3**	**5**	**0.5**	**27.8**	**37.5**
PW	750	60	90	1	2.5	5	2.0	41.0	61.0
	750	60	90	0.5	1.1	5	4.4	47.4	69.5
	750	60	90	1.5	3.6	5	1.4	36.5	59.0
	750	60	90	2	4.8	5	1.1	34.3	55.5
	750	60	90	2	4.8	5	1.1	33.9	56.0
Average	**750**	**60**	**90**	**2**	**4.8**	**5**	**1.1**	**34.1**	**55.75**
	750	60	90	2.5	5.9	5	0.9	32.5	53.0
	750	60	90	3	7.0	5	0.7	29.3	50.5
	750	60	90	3	7.0	5	0.7	31.4	50.5
Average	**750**	**60**	**90**	**3**	**7.0**	**5**	**0.7**	**30.4**	**50.5**
	750	60	90	3.5	8.1	5	0.6	28.9	50.5
	750	60	90	4	9.3	5	0.5	27.9	49.0
	750	60	90	4	9.3	5	0.5	29.1	48
Average	**750**	**60**	**90**	**4**	**9.3**	**5**	**0.5**	**28.5**	**48.5**

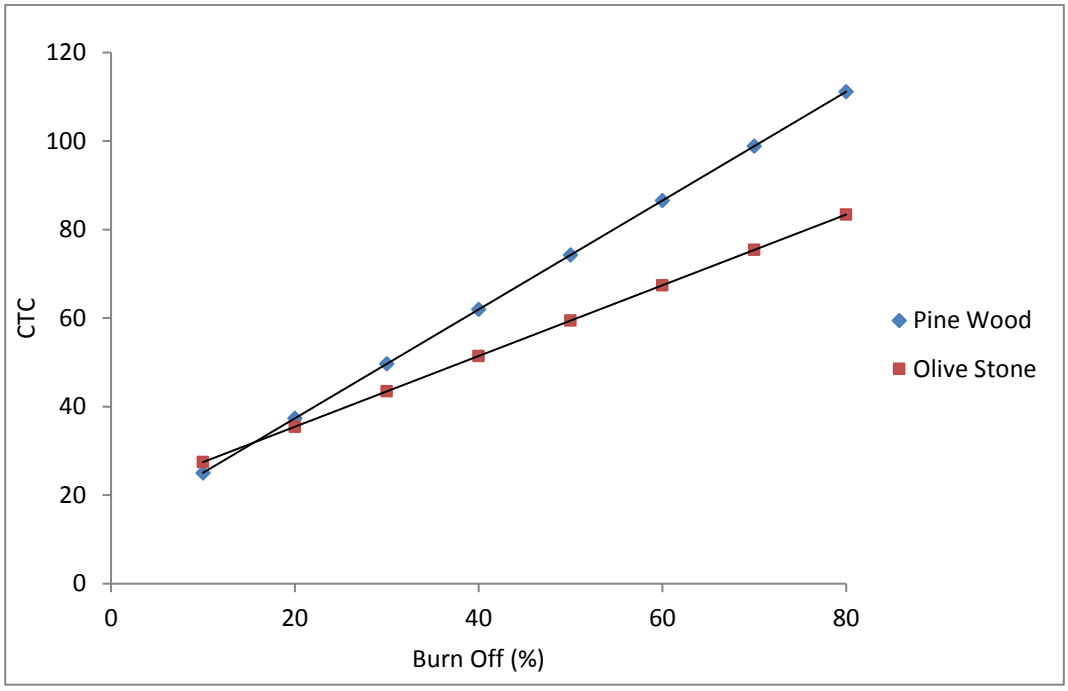


Figure A:7 Burn off (%) and CTC relationship for both carbons side by side.

Table A-5 Olive stone repeats.

Dwell Time (mins)	Temperature (°C)	Char Mass (g)	Water Flow (ml/min)	Total Water Flow (ml/min)	Burn Off (%)	Yield % from Biomass (10.7% M)	Yield (%) on dry basis	CTC	Methylene Blue (ml)
60	750	10	1.5	90	37.1	20.1	22.5	47.5	7
60	750	10	1.5	90	36.5	20.3	22.7	45.0	6
60	750	10	1.5	90	37.5	20.0	22.4	46.5	6
60	750	10	1.5	90	37.8	19.9	22.3	46.0	7
60	750	10	1.5	90	38.2	19.8	22.2	48.0	8
60	750	10	1.5	90	40.0	19.2	21.5	50.0	6
60	800	10	1.5	90	55.5	14.2	15.9	61.0	13
60	800	10	1.5	90	54.2	14.7	16.4	61.5	15
60	800	10	1.5	90	54.5	14.6	16.3	61.0	14
60	800	10	1.5	90	56.0	14.1	15.8	62.5	13
60	800	10	1.5	90	56.5	14.0	15.6	59.0	14
60	800	10	1.5	90	54.7	14.5	16.2	63.5	14

Table A-6 Pine wood repeats

Dwell Time (mins)	Temperature (°C)	Char Mass (g)	Flow (ml/ min)	Total Water Flow (ml)	Burn Off (%)	Yield (%) from Biomass (15.7% M)	Yield (%) on dry basis	CTC	Methylene Blue (ml)
60	750	10	1.5	90	41.9	18.6	20.8	64.0	11
60	750	10	1.5	90	41.2	18.8	21.1	62.0	11
60	750	10	1.5	90	42.0	18.7	20.8	60.0	9
60	750	10	1.5	90	41.9	18.6	20.8	61.5	10
60	750	10	1.5	90	39.6	19.3	21.7	59.5	10
60	750	10	1.5	90	40.2	19.2	21.5	59.5	-
60	800	10	1.5	90	69.2	9.9	11.1	93.0	20
60	800	10	1.5	90	69.3	9.8	11.0	94.0	18
60	800	10	1.5	90	70.3	9.5	10.7	95.0	21
60	800	10	1.5	90	69.3	9.8	11.0	97.0	19
60	800	10	1.5	90	70.9	9.3	10.4	97.0	21
60	800	10	1.5	90	69.1	9.9	11.1	94.0	-
60	800	10	1.5	90	70.1	9.6	10.7	100.0	-

Table A-7 Repeat pore analysis results.

	Temp (°C)	Dwell (mins)	BET SA (m^2/g)	Vmi (cm^3/g)	Vme (cm^3/g)	Vtot (cm^3/g)	Vme (%)	Burn Off (%)	CTC
OS 750 60 2	750	60	712.2	0.2791	0.1462	0.4253	34.4	36.5	45.0
OS 750 60 3	750	60	715.9	0.28	0.1361	0.4161	32.7	37.5	46.5
OS 750 60 4	750	60	724.0	0.2839	0.1441	0.428	33.7	37.8	46.0
OS 750 60 4 (2)	750	60	709.0	0.2782	0.1467	0.4249	34.5	37.8	46.0
OS 750 60 4 (3)	750	60	692.3	0.271	0.114	0.385	29.6	37.8	46.0
Average			**710.7**	**0.27844**	**0.13742**	**0.41586**	**33.0**	**37.5**	**45.9**
SD			11.7	0.004693	0.013767	0.017823	2.0	0.5	0.55
OS 800 60 1	800	60	828.4	0.3259	0.1873	0.5132	36.5	54.7	63.5
OS 800 60 3	800	60	863.9	0.34	0.1821	0.5221	34.9	54.2	61.5
OS 800 60 4	800	60	875.6	0.3454	0.2065	0.5519	37.4	54.5	61.0
OS 800 60 4 (2)	800	60	898.1	0.354	0.215	0.569	37.8	54.5	61.0
OS 800 60 4 (3)	800	60	862.0	0.3407	0.2093	0.55	38.1	54.5	61.0
Average			**865.6**	**0.3412**	**0.20004**	**0.54124**	**36.9**	**54.5**	**61.6**
SD			25.3	0.010213	0.014452	0.022987	1.3	0.2	1.08
PW 750 60 2	750	60	859.4	0.338	0.2036	0.5416	37.6	41.2	62.0
PW 750 60 2 (2)	750	60	851.1	0.3351	0.2125	0.5476	38.8	41.2	62.0
PW 750 60 2 (3)	750	60	863.2	0.3396	0.2106	0.5502	38.3	41.2	62.0
PW 750 60 3	750	60	828.5	0.3264	0.2214	0.5478	40.4	42.0	60.0
PW 750 60 5	750	60	836.6	0.3279	0.1926	0.5205	37.0	39.6	59.5
Average			**847.8**	**0.3334**	**0.20814**	**0.54154**	**38.4**	**41.0**	**61.1**
SD	.		14.8	0.005953	0.010759	0.012182	1.3	0.9	1.24
PW 800 60 2	800	60	1087.5	0.4308	0.5308	0.9616	55.2	69.3	94.0
PW 800 60 3	800	60	1206.9	0.476	0.5964	1.0724	55.6	70.3	95.0
PW 800 60 5	800	60	1241.3	0.4927	0.5715	1.0642	53.7	70.9	97.0
PW 800 60 4	800	60	1196.5	0.4761	0.6098	1.0859	56.2	69.3	97.0
PW 800 60 4 (2)	800	60	1208.6	0.4804	0.6072	1.0876	55.8	69.3	97.0
Average			**1188.2**	**0.4712**	**0.58314**	**1.05434**	**55.3**	**69.8**	**96.0**
SD			58.7	0.023591	0.032941	0.052741	1.0	0.7	1.41

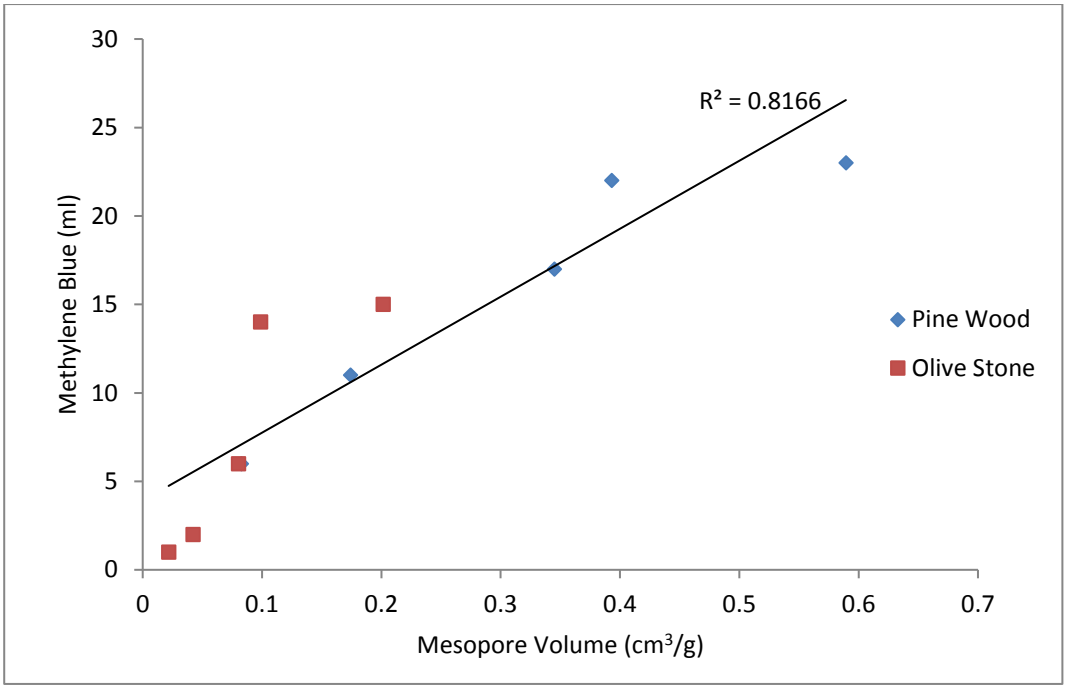


Figure A:8 Mesopore volume (cm^3/g) against methylene blue (ml) at different activation temperatures.

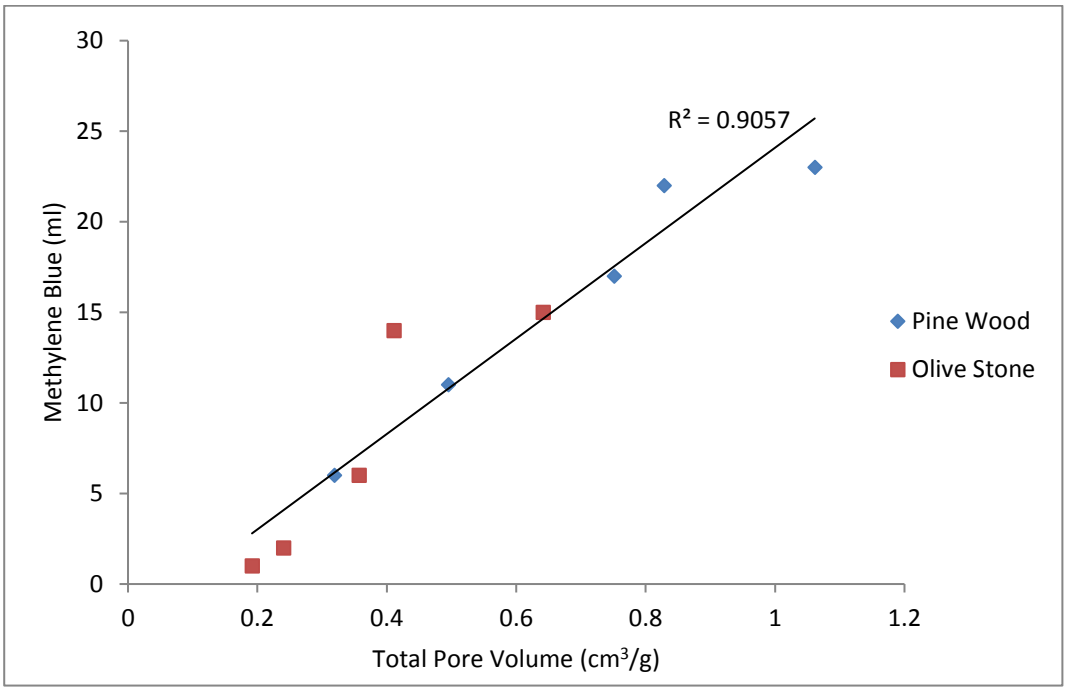


Figure A:9 Total Pore volume (cm^3/g) against methylone blue (ml) at different activation temperatures.

Table A-8 Raw data table for olive stone high temperature trials.

Temperature (°C)	Residence Time (mins)	Char Mass (g)	Water Flow (ml)	Flow (ml/min)	Water/Carbon Molar Ratio	Char Yield (%)	Burn Off (%)	CTC
900	120	10	15	0.125	1:1	56.8	43.2	45.0
950	120	10	15	0.125	1:1	52.8	47.2	36.5
1000	120	10	15	0.125	1:1	63.1	36.9	29.0
1000	120	10	30	0.25	2:1	48.6	51.4	33.5
900	120	10	30	0.25	2:1	55.3	44.8	49.5
950	120	10	30	0.25	2:1	46.5	53.5	45.0
1000	120	10	30	0.25	2:1	40.5	59.5	37.0
900	30	10	45	1.5	3:1	42.3	57.7	50.0
950	30	10	45	1.5	3:1	37.6	62.4	47.0
1000	30	10	45	1.5	3:1	31.0	69.0	39.5
900	15	10	22.5	1.5	1.5:1	69.4	30.7	39.5
950	15	10	22.5	1.5	1.5:1	63.2	36.8	39.0
1000	15	10	22.5	1.5	1.5:1	63.3	36.7	33.0

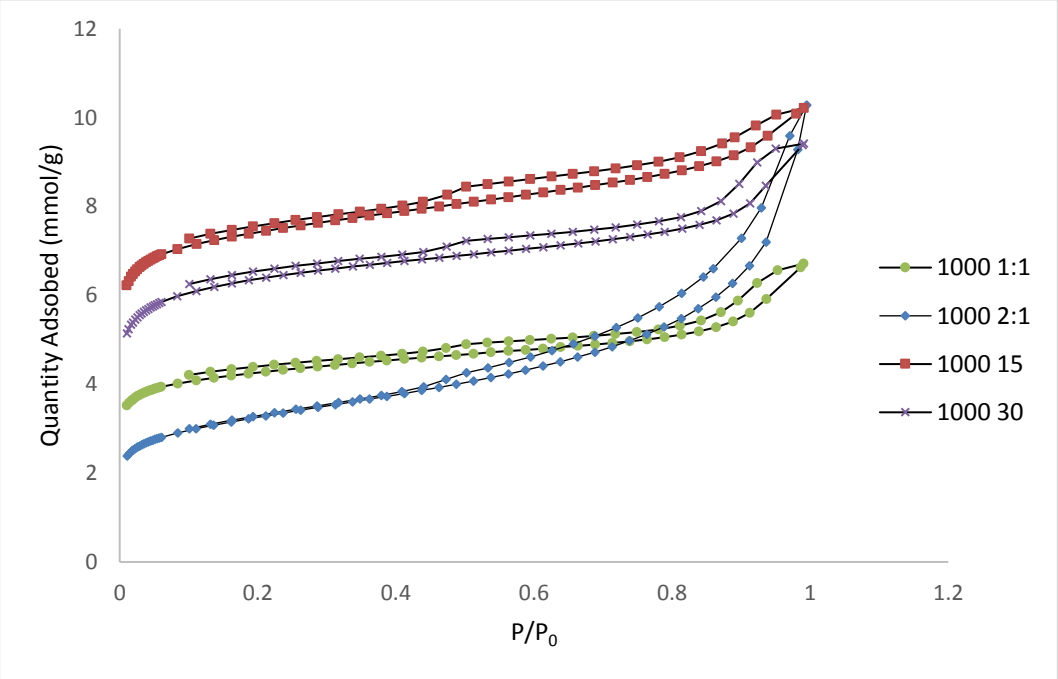


Figure A:10 High activation temperature isotherms, 1000 °C.

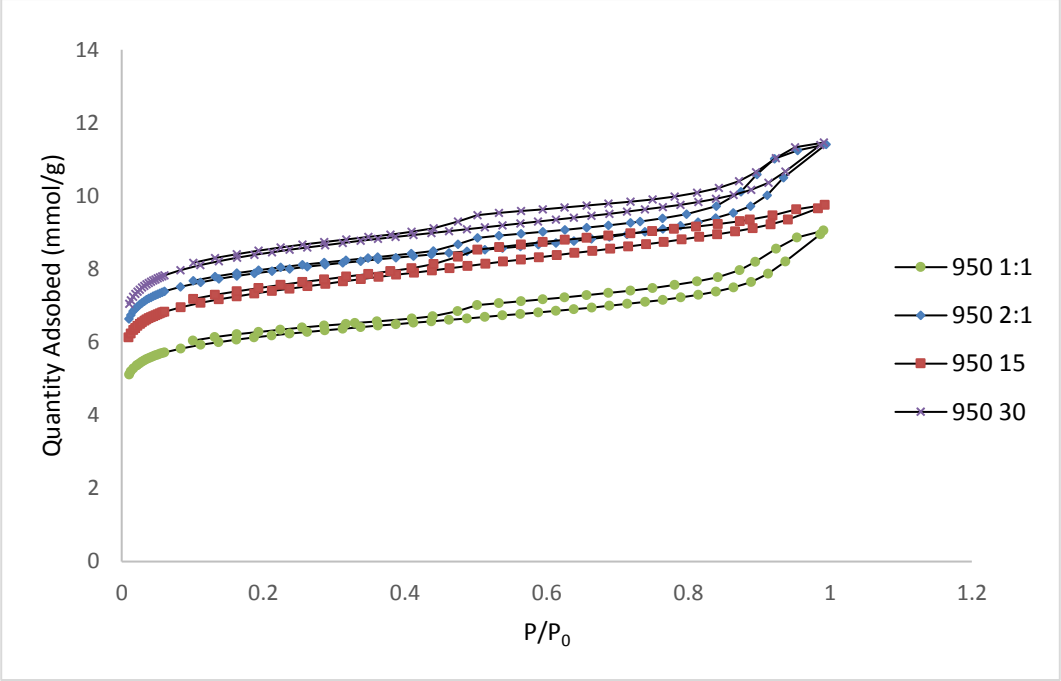


Figure A:11 High activation temperature isotherms, 950 °C.

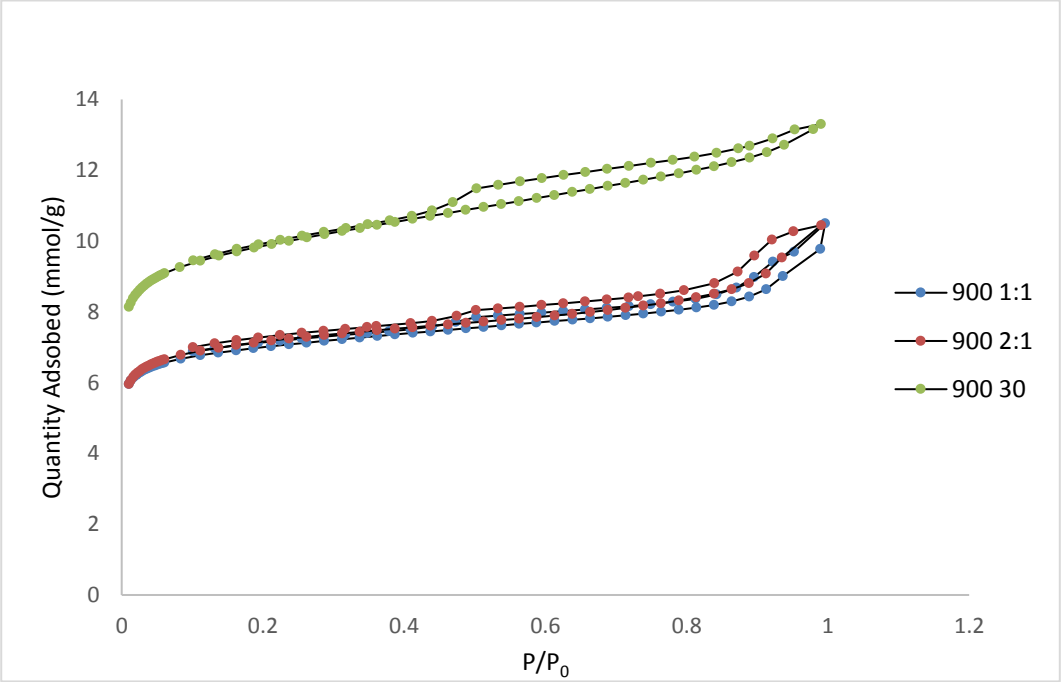


Figure A:12 High activation temperature isotherms, 900 °C.

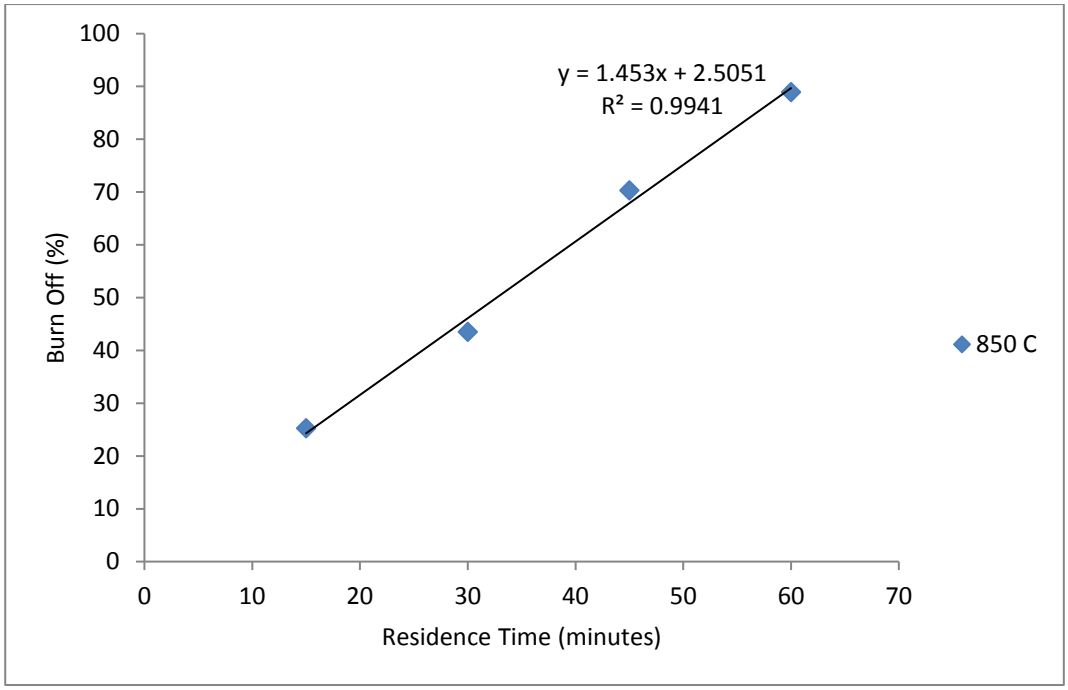


Figure A:13 850 °C burn off (%) linear relationship with increasing residence time.

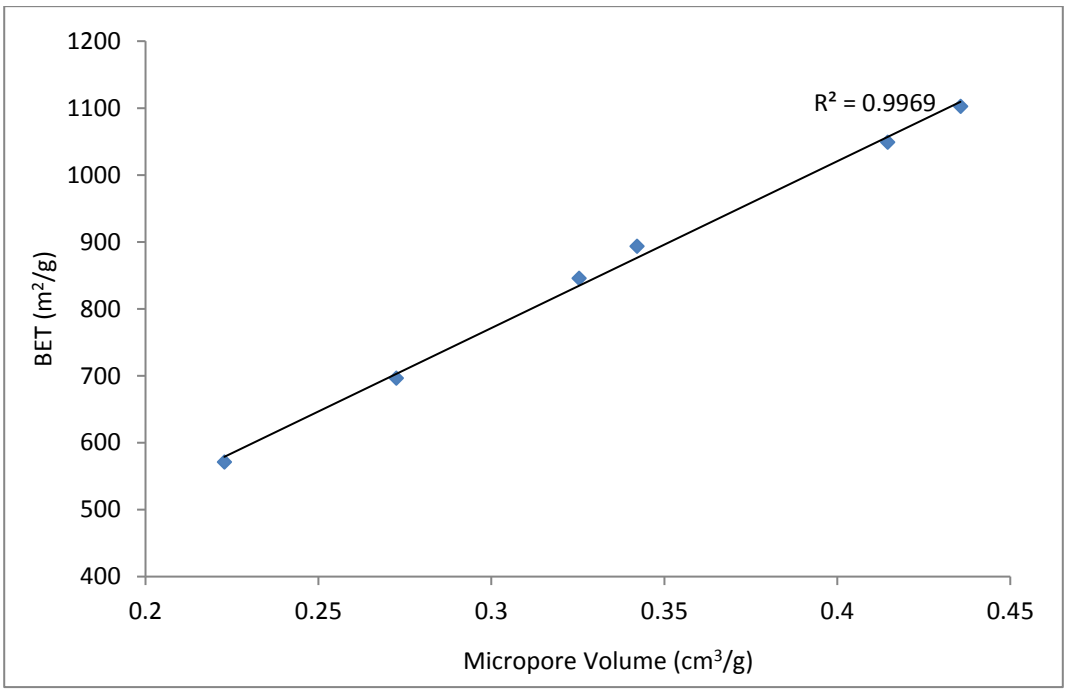


Figure A:14 Micropore volume (cm^3/g) against BET surface area (m^2/g) for residence time trials.

Table A-9 Results for two hour trials (olive stone).

Dwell Time (mins)	Temperature (°C)	Char Mass (g)	Water/Carbon Molar Ratio	Burn Off (%)	CTC	Methylene Blue (ml)
120	750	10	3.0	22.8	37.0	2
120	750	10	5.0	28.4	42.0	5
120	750	10	6.0	35.3	50.0	8
120	750	10	6.6	37.9	52.0	9
120	750	10	9.0	56.2	67.5	14
120	750	10	9.4	63.0	67.0	15
120	750	10	10.0	73.3	77.5	20
120	750	10	11.0	79.1	80.5	21
120	750	10	1.0	21.0	37.0	2
120	775	10	3.0	25.5	39.0	3
120	775	10	5.0	34.0	48.5	8
120	775	10	6.0	38.8	53.0	10
120	775	10	7.6	54.9	65.0	13
120	775	10	9.0	73.5	84.5	-
120	775	10	9.0	74.3	74.5	21
120	775	10	11.0	98.4	38.0	-
120	800	10	3.0	33.2	48.0	9
120	800	10	5.0	45.8	61.5	13
120	800	10	6.0	50.9	63.0	17
120	800	10	7.0	69.0	76.0	20
120	800	10	8.0	84.7	74.5	22
120	800	10	8.6	95.7	47.5	17
120	800	10	1.0	28.6	41.0	-
120	850	10	1.0	33.8	49.5	-
120	850	10	4.6	82.9	73.0	17
120	850	10	4.0	66.8	70.5	19
120	850	10	3.0	51.3	61.5	16
120	850	10	3.0	52.8	59.5	16
120	850	10	2.0	20.7	34.5	2

Table A-10 Pore analysis results for two hour dwell time trials.

Temp (°C)	Dwell (mins)	BET SA (m^2/g)	Vmi (cm^3/g)	Vme (cm^3/g)	Vtot (cm^3/g)	Vme (%)	Burn Off (%)	CTC	Methylene Blue (ml)
750	2	598.8	0.2337	0.0743	0.3080	24.1	22.8	37.0	2
750	2	740.2	0.29	0.148	0.4380	33.8	35.3	50.0	8
750	2	951.6	0.3754	0.2556	0.6310	40.5	56.3	67.5	14
750	2	982.3	0.3884	0.2186	0.6070	36.0	73.3	77.5	20
750	2	789.1	0.3097	0.1693	0.4790	35.3	37.9	52.0	9
775	2	629.2	0.2452	0.0868	0.3320	26.1	25.5	39.0	3
775	2	797.5	0.3129	0.1551	0.4680	33.1	38.8	53.0	10
800	2	726.8	0.2839	0.1131	0.3970	28.5	33.2	48.0	9
800	2	890.4	0.3497	0.1863	0.5360	34.8	45.8	61.5	13
800	2	987.67	0.3892	0.2148	0.6040	35.6	50.9	63.0	17
800	2	1024	0.4042	0.1428	0.5470	26.1	84.7	74.5	22
850	2	930.5	0.3653	0.1517	0.5170	29.3	52.8	59.5	16
850	2	965.7	0.3802	0.1368	0.5170	26.5	51.3	61.5	16
850	2	943.5	0.3719	0.1351	0.5070	26.6	66.9	70.5	19
850	2	1018.9	0.4024	0.1446	0.5470	26.4	82.9	73.0	17

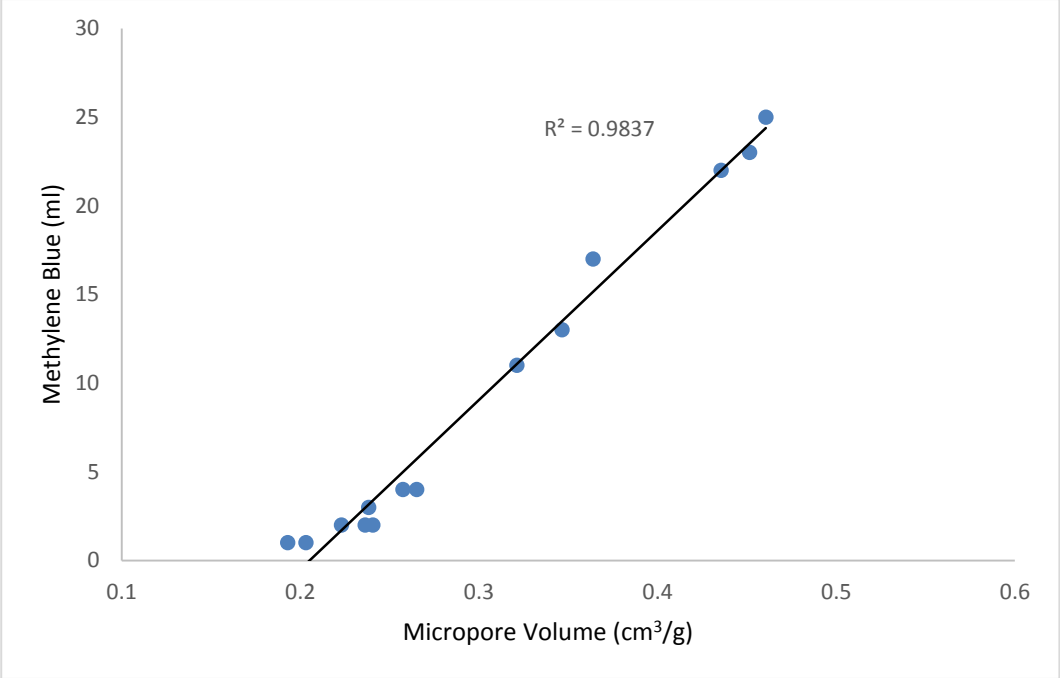


Figure A:15 Micropore volume (cm^3/g) correlation with methylene blue number (ml), pine wood.

Table A-11 Reaction rates with different char masses

Bed Depth (ml)	Dwell (mins)	Temp (°C)	Steam (ml)	Mass (g)	Burn Off (%)	Carbon Burn Off (g)	Moles Burn Off	Moles loss per g	Moles H_2O	(%) H_20 reacted	W/C Molar Ratio
2.5	30	800	45	2.5	53.8	1.35	0.112	0.045	0.112	4.5	12
5	30	800	45	5	44.9	2.24	0.187	0.037	0.187	7.5	6
7	30	800	45	7.5	37.2	2.79	0.233	0.031	0.233	9.3	4
8.5	30	800	45	10	30.3	3.03	0.253	0.025	0.253	10.1	3
10	30	800	45	12.5	30.4	3.80	0.317	0.025	0.317	12.7	2.4
11	30	800	45	15	28.7	4.31	0.359	0.024	0.359	14.4	2
2.5	30	850	45	15	33.6	5.03	0.419	0.028	0.419	16.8	2
5	30	850	45	12.5	36.4	4.55	0.380	0.030	0.380	15.2	2.4
7	30	850	45	10	40.0	4.00	0.333	0.033	0.333	13.3	3
8.5	30	850	45	7.5	44.6	3.35	0.279	0.037	0.279	11.2	4
10	30	850	45	5	58.6	2.93	0.244	0.049	0.244	9.8	6
11	30	850	45	2.5	91.7	2.29	0.191	0.076	0.191	7.6	12
2.5	30	750	45	15	21.6	3.24	0.270	0.018	0.270	10.8	2
5	30	750	45	12.5	21.3	2.67	0.222	0.018	0.222	8.9	2.4
7	30	750	45	10	21.9	2.19	0.183	0.018	0.183	7.3	3
8.5	30	750	45	7.5	24.8	1.86	0.155	0.021	0.155	6.2	4
10	30	750	45	5	29.3	1.46	0.122	0.024	0.122	4.9	6
11	30	750	45	2.5	34.1	0.85	0.071	0.028	0.071	2.8	12

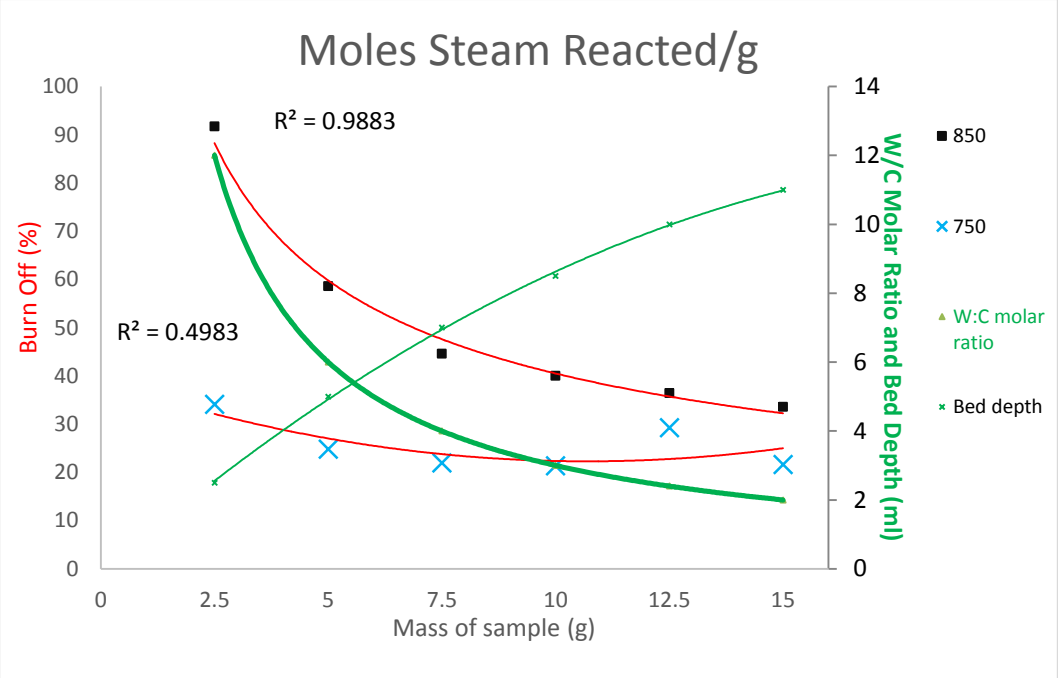


Figure A:16 Results for 750 °C and 850 °C.

Table A-12 Olive stone activation with different initial char mass at 750 °C.

Temperature (°C)	Residence Time (mins)	Water Flow (ml)	Olive Char (g)	Burn Off (%)	CTC
750	60	90	5	48.1	59.5
750	60	90	7.5	41.0	50.0
750	60	90	10	37.8	47.0
750	60	90	12.5	35.2	46.0

Table A-13 Pine wood activation with different initial char mass at 750 °C.

Temperature (°C)	Residence Time (mins)	Water Flow (ml)	Olive Char (g)	Burn Off (%)	CTC
750	60	90	0.5	43.4	63.0
750	60	90	0.5	42.8	63.0
750	60	90	1.5	40.4	63.5
750	60	90	1.5	43.2	65.5
750	60	90	2.5	39.0	61.5
750	60	90	2.5	40.2	65.5
750	60	90	3.5	41.3	61.1
750	60	90	4.5	43.6	61.0
750	60	90	4.5	44.0	59.5

Table A-14 Olive Stone washed and unwashed single step production.

Temp (°C)	Residence Time (mins)	Water Flow (ml)	SS end Yield (%) unwashed	SS end Yield (%) Washed	Burn Off (%) unwashed	CTC unwashed	Burn Off (%) washed	CTC washed
800	30	45	9.46	10.24	58.98	64.0	51.9	60.5
750	60	90	10.55	8.755	54.23	61.5	58.9	65.5
750	60	60	12.40	9.67	46.23	53.0	54.6	62.0
750	60	30	17.68	15.74	23.32	41.0	26.0	44.5
700	60	90	16.78	15.22	27.22	38.5	28.5	45.5

Table A-15 Pine Wood washed and unwashed single step production.

Temp (°C)	Residence Time (mins)	Water Flow (ml)	SS end Yield (%) unwashed	SS end Yield (%) Washed	Burn Off (%) unwashed	CTC unwashed	Burn Off (%) washed	CTC washed
800	30	45	6.40	7.49	66.29	89.5	54.9	80.0
750	60	90	7.85	8.95	58.68	79.0	46.2	77.0
750	60	60	8.32	9.82	56.17	76.5	41.0	72.0
750	60	30	11.94	10.91	37.13	60.0	34.4	57.0
700	60	90	13.74	13.03	27.65	54.5	21.6	47.0

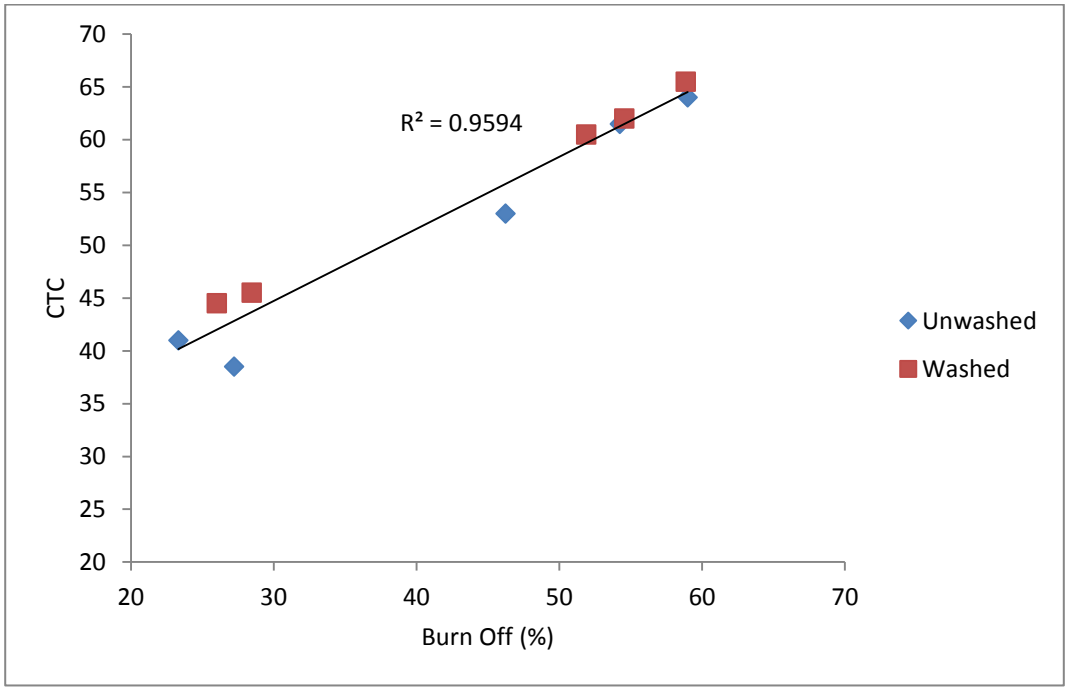


Figure A:17 Olive stone single step washed and unwashed follow same burn off (%) CTC relationship.

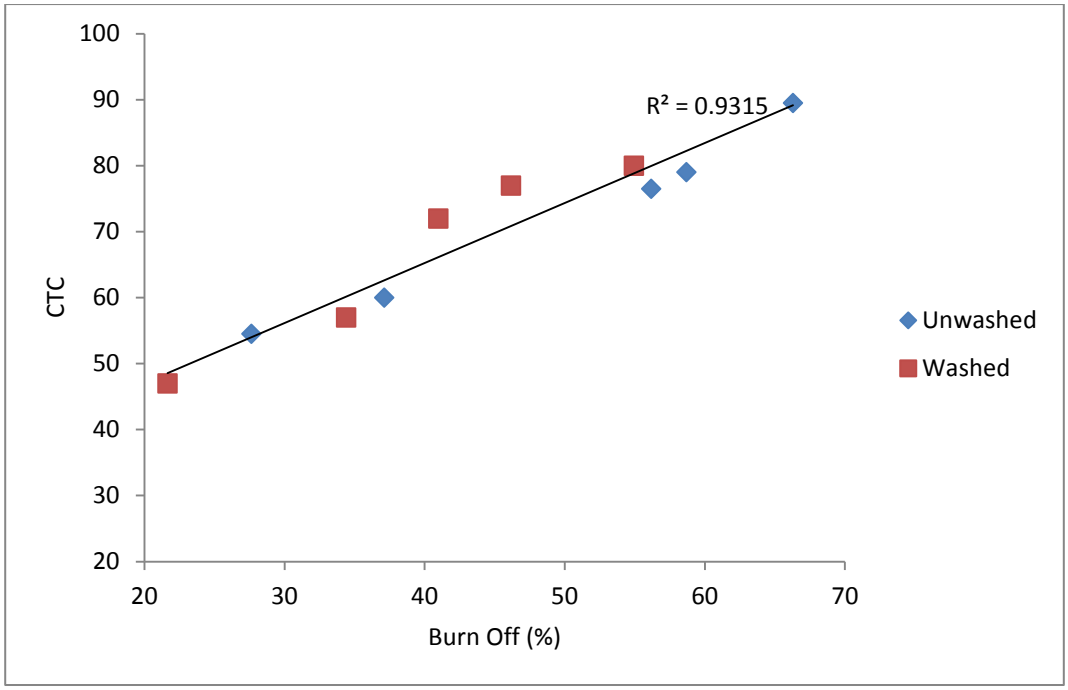


Figure A:18 Pine wood single step washed and unwashed follow same burn off (%) CTC relationship.

Table A-16 Pore analysis of single step, washed and fast/slow pyrolysis.

Char/Biomass used	Temp (°C)	Dwell (min)	Water Flow (ml)	BET (m^2/g)	Vmi (cm^3/g)	Vme (cm^3/g)	Vtot (cm^3/g)	Vme (%)	CTC
OS Single Step	700	60	90	672.0	0.2632	0.1098	0.373	29.4	38.5
OS Washed SLOW-PY	700	60	90	599.7	0.2348	0.0866	0.3214	26.9	37.5
OS SLOW- PY	800	30	45	788.3	0.3093	0.1557	0.465	33.5	52
OS WASHED FAST-py	800	30	45	799.1	0.3147	0.3269	0.5416	41.9	58.5
OS WASHED SLOW-py	800	30	45	718.7	0.2815	0.1626	0.4441	36.6	45.5
PW Washed FAST PY	700	60	60	856.6	0.3357	0.1097	0.4454	24.6	68
PW Single Step	750	60	60	1066.8	0.4214	0.2562	0.6776	37.8	76.5
pw Single Step	750	60	30	863.3	0.3392	0.1344	0.4736	28.4	60
PW SLOW-py	750	60	30	816.6	0.3193	0.0832	0.4025	20.7	52.5
PW WASHED SLOW-py	800	30	45	964.1	0.3784	0.1254	0.5038	24.9	64
PW WASHED FAST-py	800	30	45	1010.7	0.3979	0.2066	0.6045	34.2	73

Table A-17 Pilot scale pore analysis.

Sample	BET (m^2/g)	Vmi (cm^3/g)	Vme (cm^3/g)	Vtot (cm^3/g)	Vme (%)	CTC
LBOS56	899.5	0.3532	0.0887	0.4419	20.1	56.0
LBOS67	1114.1	0.4426	0.2188	0.6614	33.1	67.0
LBOS78	1157.3	0.4583	0.1986	0.6569	30.2	78.0
LBOS46	679.2	0.266	0.0785	0.3445	22.8	46.0
OS RUN5-3	879	0.3464	0.0636	0.4100	15.5	48.5
OSRUN4-4	900.6	0.3553	0.0676	0.4229	16.0	63.0
OSRUN6-3	834.6	0.328	0.0647	0.3927	16.5	56.5